Advanced Methods for Air Distribution in Occupied Spaces for Reduced Risk from Air-Borne Diseases and Improved Air Quality

Bolashikov, Zhecho Dimitrov

Publication date:
2010

Document Version
Publisher's PDF, also known as Version of record

Advanced Methods for Air Distribution in Occupied Spaces for Reduced Risk from Air-Borne Diseases and Improved Air Quality

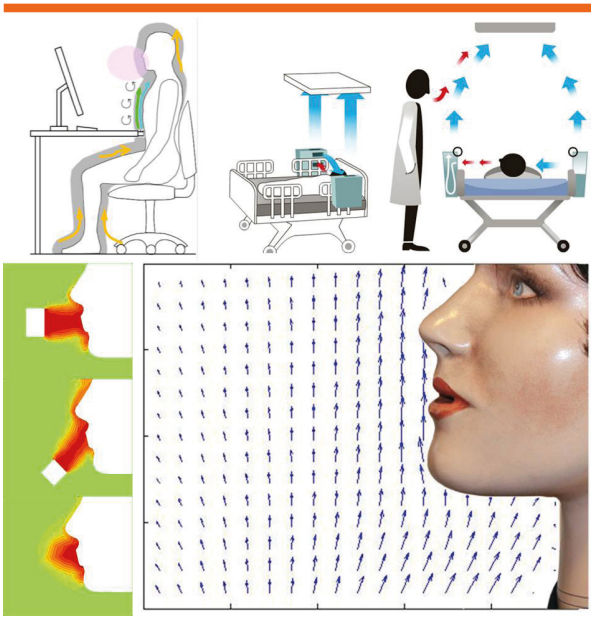

Zhecho Dimitrov Bolashikov

PhD Thesis

Department of Civil Engineering

2010

DTU Civil Engineering Report R-239 (UK)
May 2010

DTU Civil Engineering
Department of Civil Engineering

Declaration

I hereby declare that the submitted dissertation was completed by myself and no other. I have not used any sources or materials other than those enclosed. Moreover, I declare that the following dissertation has not been submitted further in this form or any other form, and has not been used to obtain any other equivalent qualifications at any other organization/institution.

Additionally, I have not applied for, nor will I attempt to apply for any other degree or qualification in relation to this work.

Zhecho D. Bolashikov

15/03/2010

International Center for Indoor Environment and Energy,
Department of Civil Engineering, Technical University of Denmark,
2800 Kgs. Lyngby, Denmark

Claims

Methods for control of airflow interaction at the breathing zone to improve inhaled air quality and decrease the risk of airborne cross-infection are developed and studied. The present Ph.D. thesis claims the following points:

New methods for controlling the strength of the free convection layer at the breathing zone of a seated occupant in an office environment, by locally blocking or exhausting the boundary layer at the groin and upper chest region, are developed. It is documented that the methods improve significantly the performance of personalized ventilation with regards to air quality and can help reduce the risk from airborne cross-infection.

New methods for controlling the airflow interaction at the breathing zone, by inserting the PV flow within the boundary layer of a seated occupant and close to the breathing zone, or by substituting the free convection layer by a jet of PV air directed towards the breathing zone, is studied. It is documented that these strategies improve significantly the air quality and can help reduce the risk from airborne cross-infection.

A novel ventilation method that is able to evacuate the coughed air from a sick person and to provide improved protection to the medical staff and the other patients in a hospital ward from getting infected with airborne diseases is developed and its efficient performance is documented. The novel ventilation method and the corresponding device are part of patient in Europe (EP 09165736.1) and in the United States of America (US 61/226,542).

Preface

This Ph.D. thesis sum up the work carried out at the Technical University of Denmark (DTU), Department of Civil Engineering, International Centre for Indoor Environment and Energy, Kgs. Lyngby, Denmark, for the period September 2006 - February 2010. The work was composed under the DTU Ph.D. program and was funded by the Ministry of Science, Technology and Innovation. Supervisor during this Ph.D. study was Associate Professor, Ph.D. Arsen K. Melikov from the International Centre for Indoor Environment and Energy, Department of Civil Engineering at the Technical University of Denmark.

I would like to express my deepest gratitude to my supervisor and good friend Arsen for being next to me, guiding, helping and supporting me throughout the whole study. He was always available when needed, even in the hardest moments of my life, inspiring me with his thirst for knowledge, high morals and unending energy to pursue and find answers to existing problems.

I would like to express also my gratitude to the late Professor P. Ole Fanger who ignited the interest in the field of Indoor Climate and recommended me for doing this Ph.D. study.

I would like also to thank to Professor Bjarne Olesen, the head of the International Center for Indoor Environment and Energy, for his helpfulness, patience and understanding.

My gratitude goes to all the people who helped me in accomplishing my work and inspired me with their ideas and professional attitude: special thanks to Hideaki Nagano, Shengwei Zhu, Clara Marika Velte, Knud Erik Meyer, Professor David Wayon, Professor Zbigniew Popiolek, Miroslav Krenek, Marek Brand, Michal Spilak, Viktor Djartov, Pawel Wargocki, Lei Fang, Inesse Nagla.

My heartiest gratitude to my closest friends who helped me overcome the loss of my late mother and were always next to me sharing good and bad moments, pushing me and inspiring me never to give up: Katia Jankova, Kiril and Antonia Naydenov, Velichka Borova, Angela Simone, Velina Ljubenova.

Also I would like to thank to my colleagues Angela Simone, Rune Vinther Andersen, Daria Zukowska and Peter Strøm-Tejsen for their helpfulness, support and extreme patience towards me.

Last but not least I would like to express my thanks to the technician Peter Simonsen at the International Center for Indoor Environment and Energy, for his help and thorough understanding.

My love and special thanks goes to my sister Raina Kapitanova and my niece Vania Kapitanova, who are the two dearest persons that love me truly and dearly for what I am and who never, even for a second, stopped believing in me.

I would like to ask for forgiveness all those who felt offended and insulted by my actions or my behaviors as well as I forgive all those who involuntarily or voluntarily caused me any inconvenience in my personal or professional life.

Finally I would like to dedicate this work to my late mother, Ivanka, who did not manage to witness the end of this project. She has always been with me in my heart through the toughest times of my work and the memory of her always gave me the will and energy to push forward.

Thank you!

Abstract

The current Ph.D. thesis deals with new advanced methods of air distribution in occupied places aimed to improve the inhaled air quality and to reduce the risk from airborne cross infection among the occupants.

The existing ventilation strategies nowadays are not able to provide enough clean air to the occupants and can even enhance the risk from cross-infection from airborne diseases indoors. Clearly new advanced methods are needed to improve the current situation. The subject is especially important because of the energy issue as well as the increased possibility of random mutations of known airborne pathogens. The threat from possible bio-terrorist attacks in the last decade makes the topic quite important.

So far the existing methods of indoor air cleaning rely on several basic strategies: dilution, filtration and Ultra Violet Germicidal Irradiation (UVGI). Dilution utilizes ventilation at high flow rates to reduce the concentration of pollutants/pathogens to levels that would not deteriorate the air quality or be harmful for the occupants. It is also connected to certain energy limitation issues. Filtration and UVGI are efficient in protecting occupants provided the sources are located outdoors. However, these methods are not very efficient, if the contaminant sources are indoors and especially if the source is a sick individual.

The current thesis focuses on two ways to provide reduced risk from airborne infections: by providing personal protection of each individual in an office environment and by protecting medical staff, patients and visitors from cross-infection in hospital wards.

The first part of the thesis focuses on improvement of inhaled air quality and thus reduction in the risk from cross-infection by advanced ventilation, providing clean air close to the occupants with personalized ventilation (PV) by applying control over the airflow interaction at the breathing zone. Two new control methods, namely control over the free convection layer around the human body and control over the personalized flow are studied when applied for different PV designs. The first method aims to reduce the strength of the free convection layer via blocking or local exhausting, and thus make possible its penetration by the personalized flow at low velocity (low flow rate). The second method aims to control the way the PV flow is supplied so that it is less affected by the flow interaction around the human body: by immersing it within the convection flow or by simply substituting the boundary layer with a PV flow adjacent to the body. Both methods helped greatly increase the performance of the employed PV systems with respect to the amount of clean air supplied into the breathing zone of the occupant compared to the case when the PV was used alone. These methods also show great potential for energy savings, due to the reduced PV flow rate. The suggested designs are easy for implementation in occupied spaces, where people spend most of the time seated, e.g. offices, theaters, cinemas, busses, trains, airplanes, etc.

The second part of the thesis focuses on a novel ventilation strategy for reduction the risk of cross-infection for medical staff, visitors, and patients in hospital wards. The novel ventilation strategy is implemented by a specially developed device, named Hospital Bed Integrated Ventilation Cleansing Unit (the device is part of a patient application in Europe (EP 09165736.1) and in the United States of America (US 61/226,542). The HBIVCU helped to provide improved protection to doctor and other patients, present in a space, from a sick individual with highly

contagious airborne transferred disease, by locally evacuating the air coughed by the sick patient. Apart of increased protection the use of the HBIVCU leads to decrease of the background ventilation rate. This technique of local exhaust and cleaning of the coughed air can provide solution to the existing problems in a hospital environment related to control and, handling the spread and treating patients with contagious airborne diseases, as well as problems with insufficient space in hospital wards in times of epidemics and pandemics.

Resume

Denne Ph.d. afhandling beskæftiger sig med nye avancerede metoder til luftfordeling i lokaler. Formålet er at forbedre den inhalerede luftkvalitet og mindske risikoen fra luftbåren krydsinfektion blandt dem der opholder sig i lokalet.

De eksisterende ventilationsstrategier nu til dags er ikke i stand til at yde tilstrækkelig ren luft til brugerne og kan endda øge risikoen for krydsinfektion af luftbårne sygdomme indendørs. Det er tydeligt at nye avancerede metoder er nødvendige for at forbedre den nuværende situation. Emnet er særligt vigtigt på grund af spørgsmålet om energiforbrug samt den øgede mulighed for tilfældige mutationer af kendte luftbårne patogener. Truslen fra mulige biologiske terrorangreb i det seneste årti gør emnet meget vigtigt.

Hidtil har de eksisterende metoder til indendørs luftrensning bygget på flere grundlæggende strategier: Fortynding, filtrering og Ultraviolet Bakteriedræbende Bestrålingen (Ultra Violet Germicidal Irradiation – UVGI). Fortynding benytter ventilation ved høje strømningshastigheder til at reducere koncentrationen af forurenende stoffer / patogener til et niveau, der ikke forringer luftkvaliteten eller er til skade for de mennesker der opholder sig i bygningen. Fortynding er også forbundet med visse energimæssige begrænsninger. Filtrering og UVGI er effektive til at beskytte personer, forudsat at kilderne er placeret udendørs. Men disse metoder er ikke særlig effektiv, hvis de forurenende kilder er indendørs, især hvis kilden er en syg person.

Afhandlingen fokuserer på to metoder der nedsætter risikoen smittespredning af luftbårne sygdomme ved at yde personlig beskyttelse af den enkelte i et kontormiljø, og ved at beskytte medicinsk personale, patienter og besøgende fra krydsinfektion i sygehusafdelinger.

Den første del af afhandlingen fokuserer på forbedring af inhaleret luftkvalitet og mindskelse af risikoen for krydsinfektion gennem et avanceret ventilationsprincip som giver renere luft tæt på brugerne. Princippet er opkaldt personlig ventilation (PV) og anvender kontrol med luftstrømmes interaktion tæt på vejrtrækningszonen. To nye kontrolmetoder, nemlig kontrol over det frie konvektive lag omkring den menneskelige krop og kontrol af det personlige flow er undersøgt, når de anvendes til forskellige PV design. Den første metode har til formål at reducere styrken af det frie konvektive lag via blokering eller lokal udsugning, hvilket dermed muliggør indtrængen af luftstrømninger fra PV med lav hastighed (low flow rate). Den anden metode går ud på at kontrollere måden hvorpå PV strømmen leveres, så denne er mindre påvirket af strømmeningssamspillet omkring den menneskelige krop: Ved at nedsænke strømningen i den konvektive strømning eller ved blot at udskifte grænselaget med en PV strømning som støder op til kroppen. Begge metoder bidrog i høj grad til at øge effektiviteten af de anvendte PV systemer med hensyn til mængden af ren luft, der leveres i indåndingszonen i forhold til da PV blev anvendt uden nogen form for kontrol. Disse metoder viser også stort potentiale for energibesparelser, som følge af nedsat PV strømningshastighed. De foreslåede design er lette at implementere i rum, hvor folk for det meste sider ned, fx kontorer, teatre, biografer, busser, tog, fly, etc.

Den anden del af afhandlingen fokuserer på en ny ventilationsstrategi der reducerer risikoen for krydsinfektion af medicinsk personale, besøgende og patienter på hospitalsafdelinger. Den nye ventilationsstrategi er implementeret ved hjælp af specielt udviklet udstyr, som er opkaldt

’Hospital Bed Integrated Ventilation Cleansing Unit (HBIVCU)’ (udstyret er en del af en patient ansøgning i Europa (EP 09165736,1) og i USA (US 61/226, 542). Ved at udsuge den luft som patienten udsender ved host bidrog HBIVCUen til at beskytte læger og andre patienter mod luftbåren smitte. Udover øget beskyttelse fører brugen af HBIVCUen til fald i baggrunden ventilationsraten. Denne teknik til lokal udsugning og rensning af luft fra host kan løse de eksisterende problemer der er relateret til håndtering af spredningsrisiko under behandling af patienter med luftbårne smitsomme sygdomme i et hospital miljø i perioder med epidemier og pandemier.

Contents

Chapter 1 : Airborne Transmission of Pathogens and Existing Methods for Protection from Airborne Cross-infections Indoors

Nowadays people live, work and recreate in close proximity, making them vulnerable to spreading of commutable diseases. Merriam-Webster online dictionary gives the following definition for a disease: "*a condition of the living animal or plant body or of one of its parts that impairs normal functioning and is typically manifested by distinguishing signs and symptoms*". The condition of sickness has strong negative effect on the society and if uncontrolled and spreading, it could lead to huge financial losses, heavy psychological impact and even death tolls. Therefore ways for reducing the risk from emergence and spreading commutable diseases among humans need to be studied. Increased mobility permits the rapid dissemination of new diseases and elevates the risk of further pandemics, e.g. of Severe Acute Respiratory Syndrome (SARS), as well as the emergence of old and well-known diseases that have developed resistance to existing drug treatment, e.g. tuberculosis (Shah et al. 2007). Another threat imposes the rapid mutation of some microorganisms and their adaptation as a cause of human diseases, e.g. Ebola, the H5N1 strain of avian flu, the recent outbreak of swine flu, etc.

Most of our indoor occupied places are not designed to prevent the spread of airborne pathogens. Furthermore, air distribution systems may even enhance transmission. In order to solve this multidisciplinary problem successfully, knowledge in different fields needs to be combined: the type of pathogen, its generation and survival mechanism before affecting the host, possible disinfection methods to eradicate it, and transmission mechanisms among people. Engineering solutions can be proposed in order to efficiently reduce the pathogen loads released in air, disable their virulence, and make them harmless for healthy inhabitants. The methods applied should be neither life nor health threatening, nor should they reduce in any way occupants' perceived air quality or thermal comfort. They should also be user friendly (if people are to operate them), with low noise emission, energy efficient, highly ergonomic and aesthetic. This is discussed in detail in **Paper I**, **Appendix I** and is summarized in the following discussion of this chapter.

1.1. Airborne transmission of human infectious pathogens

We are surrounded by air and our lungs process 10-25 m^3 of this air per day (Hinds 1999). This makes the airborne route of transmission quite important and plausible to be studied. Some of the most dangerous diseases with high death tolls in human history have the airborne transmission route as predominant: measles, varicella and tuberculosis (Qian et al. 2006). Furthermore recent studies show connection between the airborne route of infection and the spread of diseases such as SARS (Li et al. 2007) and influenza (Tellier 2006). This is truly alarming considering the fact that we need to breathe in order to exist, making the humans extremely vulnerable to the airborne route of transmission.

1.1.1. Classification and nature of pathogens

The causatives of a disease are termed pathogens and in most cases these include

unicellular organisms such as viruses, bacteria or other microorganisms (fungi, protozoa, etc.). The size of a single pathogen can vary greatly, ranging from 22 nm up to over 15 μm, the smallest in size being the viruses and the bacteria. Each pathogen has a preferred environment in the host it infects and cannot reproduce unless it finds its natural habitat, e.g. tuberculosis cannot initiate an infection unless it enters the upper lung regions of a healthy human.

1.1.2. Airborne transmission mechanism

Airborne route of infection is the air transportation of pathogens, released as fine aerosols from the infected to the susceptible host. After generation of the aerosol, the small particles evaporate fast and form a residue known as droplet nuclei that hosts the pathogen (Wells 1936). Due to their small size (less than 5 μm in diameter) the nuclei remain airborne for long periods of time and when ingested could initiate disease in the susceptible host. Only limited number of pathogens could become airborne and this depends on their size as well as on the nuclei droplet diameter. Another factor is the shedding location of the pathogen. There are 4 parts in the respiratory tract where microorganisms may multiply and be dispersed in exhaled air: nose, oral cavity, throat and lungs. The shear stress created by the exhaled air from respiratory activities on the bronchia and trachea causes aerosolisation and droplet formation. Dispersal may take place through the nose and the mouth. When coughing, sneezing, talking or breathing, people generate particles of different sizes and air jets with different initial characteristics. Nicas et al. (2005) summarized the scarce data on the particle size distribution of respiratory aerosols. Evaporative water loss was also taken into account. After evaporation is complete the particle retains half of its original diameter. The small particles (geometric mean of 9.8 μm and geometric standard deviation of 9 μm) constitute 71% of all particles emitted by coughing. Also, particles with a diameter of 10 μm and less are able to penetrate into the lungs (Hinds 1999). Thus generated droplets with diameters below 20 μm should be considered as possible initiators of airborne cross-infection, because after full evaporation of the water content in them they attain a diameter of 10 μm or less.

Xie and Li (2006) showed that expelled droplets move more than 6 m when sneezing (initial velocity of 50 m/s), more than 2 m when coughing (initial velocity of 10 m/s), and less than 1 m when breathing (initial velocity of 1 m/s) in a still environment. However the effect of ambient velocity and different air distribution techniques, as in the case of ventilation, may affect the evaporation, heat and mass transfer and Brownian motion which in turn would affect the droplet dispersal in ambient air indoors. Wan et al. (2009) and Sze To et al. (2009) investigated the dispersion and deposition of particles as a result from cough in a mock aircraft cabin and the consequent infectious disease transmission. They both concluded that setting higher supply airflow rates led to better dilution but also enhanced the dispersion to expiratory aerosols. Those passengers closer to the sick patient had lower exposures to the expiratory aerosols due to dilution. However, the enhanced dispersion effect also took more aerosols to those passengers seated further away, leading to higher exposures at those locations. This let them conclude that higher supply airflow rate may result in more infections provided the pathogens are highly infective, but it may reduce the number of cases in case of low infectivity. Dispersion of aerosols was found to be size dependent.

1.1.3. Survival of pathogens and infection initiation

Once generated in order to initiate infection the pathogens need to survive the unfavourable conditions outside of the body of the source person and end up in the body of the new host (the recipient). Pathogens which actually replicate on or in the human body must be able to grow and reproduce within the temperature range 20 – 40 ^{o}C (Greenwood et al. 2002). In other words this is the temperature range of human indoor habitats worldwide and it also includes surface and deep core body temperature: from 33 ^{o}C up to 38 – 39 ^{o}C. This makes factors like ambient air temperature and relative humidity important. So far, knowledge on the influence of relative humidity on pathogens is scarce. In general, mid-range humidity conditions (40–60%) have been shown to be more lethal to non-pathogenic bacteria (Hatch and Wolochow 1969). Viruses with more lipids (orthomyxoviruses member of whom is the influenza virus, Figure 1.1a) tend to be more persistent at lower relative humidity, while viruses with less or no lipid content (coronaviruses of whom SARS is a representative, Figure 1.1b) are more stable at higher relative humidity (Assar and Block, 2000). Studies also report that the effects of relative humidity on virus survival can be influenced either positively or negatively by temperature (more details provided in **Paper I, Appendix I**). Microorganisms occluded in salt have greatly enhanced resistance to oxidation. Also the presence of blood or other organic materials (sputum, saliva, semen, etc.) reduces the effectiveness of chlorine-based disinfectants. (Greenwood et al. 2002).

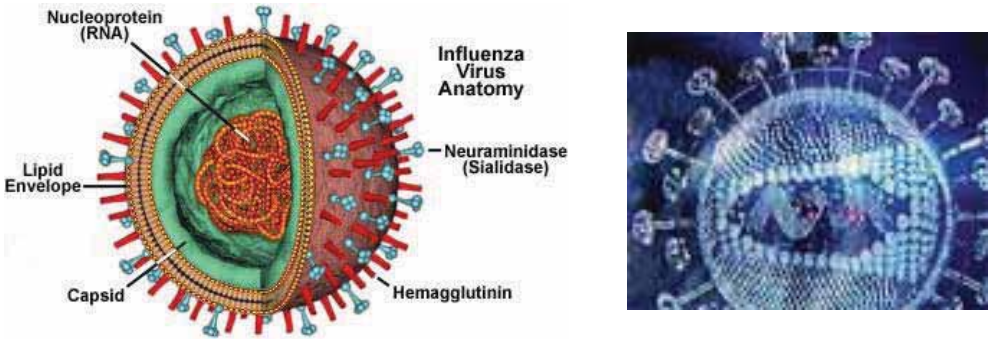

a) b)

Figure 1.1 *Structure of some viruses a) Influenza virus b) SARS virus.*

When entering the body the pathogen needs to establish an infection in order to cause a disease. The initial interaction occurs with host tissue at a mucosal lined surface (mouth cavity, nose cavities and eyes in case of airborne contamination). If the pathogen is bacteria, adhesion (establishment of infection focus) followed by invasion and in some cases dissemination to other body sites takes place. If the pathogen is virus the first interaction is by random collision and depends on the relative concentration of virus particles and cells (Greenwood et al. 2002). Therefore to initiate an infection of viruses high concentrations are needed close to "favorable" cells. The next barrier in initiating an infection is the natural defense mechanism of the host and the ability of the pathogen to "hide" or avoid the host immune response. This is dependent on the pathogen physiology, including presence of capsule to make it resistant to ingestion by phagocytic cells, masking infected cell regions to avoid antibody contact, secretion of inhibitors that slow or prevent

immune response from the host etc. (Greenwood et al. 2002). Another point of importance is the infective dose: sometimes a single organism can cause a disease. But this factor is strongly dependent on the immune system and/or age of the host: immuno-compromised people as well as old and very young are more susceptible.

1.2. Methods for protection from airborne cross-infections indoors

A great effort has been made to find engineering techniques to keep airborne pathogens away from occupants in buildings, or at levels low enough to be unable to cause a disease: dilution, filtration, Ultra Violet Germicidal Irradiation (UVGI), etc. The airborne pathogens might originate from a sick person, from the building itself (infected/polluted HVAC system, infected building materials, etc.) or from an intentional release, i.e. a terrorist attack.

1.2.1. Dilution

Dilution of room air with clean disinfected air is one of the easiest and best known methods to remove pathogens and to decrease the risk of infections in rooms. Natural, mechanical and hybrid ventilation are often used to supply clean air in rooms. However, as discussed in **Paper I, Appendix I**, this method has its limitations, related to air distribution pattern, occupants' thermal comfort, etc. Moreover, if one assumes perfect mixing, a reduction of contaminants' concentration by a factor requires an increase of the air change rate by the same factor. Chapter 2 of this thesis is focused on the role of the present air distribution methods for decrease the risk of airborne cross-infection.

1.2.2. Filtration

A method widely used today is the filtration of air in HVAC systems. Classifications and guidelines exist for applying filtration as part of the ventilation system (ASHRAE 52.2-1999, ISO 14644-1-1999). Studies show that filtration is a good method to prevent outside pathogens from penetrating the building envelope through the mechanical ventilation. Kowalski and Bahnfleth (1998, 2002) showed that 80 and 90% filters can produce air quality improvements that approach those achieved with HEPA filters, but at much lower cost. Another finding is that microorganisms capable of penetrating HEPA filters are predominantly nosocomial infections (HEPA filters remove 99.97% of all particles 0.3 μm or larger in diameter). Enzyme filters eradicate microbes by attacking the microbial cell membrane, but this assumes that they come into close contact with the microbes. Yamada et al. (2006) studied the performance of such an enzyme filter. They used two filters: with and without enzymes, and found out that the performance of the enzyme filter did not differ much from that of a control filter, due to adhesion of particles over time on the filter surface, preventing close contact between the enzymes and any microbes retained by the filter. For further details about filter application as air cleansing unit in an HVAC system refer to **Paper I, Appendix I**.

1.2.3. UVG Irradiation

UVGI utilizes the UVC light emitted at wavelength of 253.7 nm by low-pressure mercury vapour arc lamps. UVGI damages the DNA of pathogens by breaking the bonds of thymine

dimmers and thus makes them harmless: they cannot reproduce once they have entered their host. There are two ways to use UVGI application in practice: ceiling/wall mounted or in-duct application. Disinfection of air by ceiling/wall mounted UVGI started in the 30 s in USA (Wells 1936, Wells 1955). The inactivation process occurs when the pathogens enter the UVGI zone: minimum 1.8 m above the floor (the minimum height above which UVGI systems should be installed to avoid any health risks for occupants). The inactivation rate of UVGI in rooms could be enhanced by increasing the intensity of light, by promoting better mixing in rooms, or by generating an upward flow to help the upward transport of pathogens (Riley and Permut 1955, Riley et al 1971, Riley et al 1971a). Another important factor for UVGI efficiency is the level of relative humidity; increased humidity in the environment gives the pathogens better chance to survive the germicidal effect of the UVGI lamp (Peccia et al. 2001, Xu et al. 2005). The UV radiation should be evenly distributed and good room air mixing should be provided. Room relative humidity should be kept around 50%. Values above 75% significantly reduce UVGI performance (Xu et al. 2005). Due to its damage on the DNA the UVGI has adverse health effects on humans, which include a mild form of reddening of the skin (erythema) and painful photokeratitis of the eyes (sensitization to light, as in snow blindness). UVGI lights are therefore mounted in deep louver enclosures to prevent overexposure at eye level or excessive reflection from ceilings, but such casings absorb a large amount of the useful UV energy, making the unit less efficient. The effectiveness of the upper room UVGI depends on factors such as the position of the supply and exhaust vents, the position of the UVGI devices, the irradiation dose as well as the position of the pathogen source (Minki et al. 2009). In buildings with ceilings lower than 2.4 m duct UVGI irradiation must be applied. The problems of direct eye contact or skin contact are not relevant here, so the systems could be operated at even higher intensities. Good mixing and the use of reflective surfaces is an economical way to increase the effectiveness of the induct UVGI systems (Kowalski and Bahnfleth 2000, 2001). The UVGI application for indoor air purification is further discussed in **Paper I, Appendix I**.

1.2.4. Photocatalytic oxidation (PCO)

Photocatalysis is the acceleration of a photoreaction by the presence of a catalyst (TiO2, WO3, ZnS, etc.). In photogenerated catalysis the photocatalytic activity depends on the ability of the catalyst to create electron–hole pairs, which create free short-lived radicals able to undergo secondary reactions. Photocatalytic oxidation (PCO) could be achieved by either using fluorescent or UV light. PCO is an emerging technology in the HVAC industry, especially in purging airborne bacteria, which is performed by utilizing short-wave ultraviolet light (UVC). However only small portion of the pathogens will be absorbed on the catalyst and chemically attacked from a single pass system. Also with time there will be accumulation of ‘‘dead’’ pathogens on contact surface, which will reduce the effectiveness of the method as the UV light will be stopped from activating the catalyst layer and killing the pathogens. Details on PCO application as air cleansing technique are discussed in **Paper I, Appendix I**.

1.2.5. Other techniques

Other methods used for air purification include techniques such as desiccant rotors,

plasmacluster ions, essential oils and silver nanoparticles. These are referred in details as air purification methods in **Paper I, Appendix I**.

Chapter 2 : Protection by Ventilation

The current awareness of new emerging diseases comes to emphasize the need to design such indoor conditions that would reduce the risk from cross-infection and exposure to airborne transmission. A simple way to limit the spread of pathogens is by supplying clean outdoor air, reducing the harmful concentrations indoors by dilution. The review article of Li et al. (2007) shows strong evidences demonstrating the association between ventilation and control of airflow directions in occupied spaces and transmission and spread of infectious diseases. Depending on the airflow pattern, the ventilation process of supplying fresh air indoors may decrease the risk of airborne cross-infection, or it may even enhance the spread of diseases in occupied volumes. The following discussion, on the importance of airflow distribution in rooms for the airborne transmission of diseases, is limited to mechanically ventilated rooms only. The first part of this chapter is based on a peer review publication that contains more relevant details on the matter (**Paper I, Appendix I**).

2.1. Office environment

2.1.1. Total volume air distribution

Two main principles of room air distribution are commonly used in practice: mixing and displacement air distribution. Mixing air distribution aims to create a homogeneous environment in the whole ventilated volume. The clean air is supplied at high velocity to promote better mixing with the room air, and thus with the pathogens generated by any sick occupant. Displacement ventilation introduces the clean air at a slightly lower temperature (3–6 ^{o}C lower than room temperature), through floor or wall mounted diffusers. The cold air, supplied at relatively low velocity, spreads over the floor and moves upwards, entrained by flows generated from heat sources (people, equipment etc.), and then it is exhausted close to the ceiling from the better-mixed upper region of the ventilated space. Under these conditions airborne cross-infection between occupants (who are not too close to each other) will be low since the warm exhaled air, which may carry pathogens will rise upwards to the ceiling due to buoyancy. The problem arises in a dynamic environment, i.e. when people move, cough or use source of forced convection (table fans, etc.) and the boundary layer around their bodies is disturbed. The airflow pattern in a displacement type of ventilation is much dependent on local disturbances because air velocity is quite low (except near the floor and in thermal plumes generated by people, office equipment, etc.). A walking person (with speed of more than 1 m/s) in room with displacement ventilation may promote air pattern close to that of mixing type ventilation (Bjørn et al. 1997, Matsumoto et al. 2008, Halvonova and Melikov 2010). Mundt (2001) studied particle resuspension at 2 and 4 air changes per hour (ACH) in a room with displacement ventilation. The results indicated elevated levels of particles in the room and within the free convection flow of the heated cylinders used to simulate the occupants. Therefore, when a person walks in a room with displacement ventilation the dispersion of resuspended particles (with diameter from 0.5 μm to 25 μm) resembles that of mixing ventilation. This is valid for those particles for which the settling velocity is smaller than the velocity of the free convection flow. The settling velocities (Stoke's Law) reported by Mundt (2001) for talcum powder

particles with a density of 2700 kg/m^3 and diameter 0.5 μm, 5 μm and 10 μm was respectively 2 x 10^{-5} m/s, 2 x 10^{-3} m/s and 8 x 10^{-3} m/s. With the density of 1746 kg/m^3 for talcum broken, these velocities will be respectively 1.3 x 10^{-5} m/s, 1.3 x 10^{-3} m/s and 5.1 x 10^{-3} m/s. The diameters of resuspended particles of respiratory origin calculated for these settling velocities and the dry density of nonvolatile species in saliva (Na^+, K^+, Cl^-, lactate and glycoprotein) of 88 kg/m^3 (suggested by Nicas et al. 2005) corresponds respectively to 2.2 μm, 22 μm and 45 μm. The latter two diameters, after evaporation and taking into account only nuclei diameter, are outside the penetration range for the human lungs (only particles with a diameter less than 10 μm can penetrate the lungs) and are easily resuspended by human activities indoors. Therefore particles of respiratory origin, resuspended from the floor, could increase the risk of infection if they carry viable pathogens.

Wan and Chao (2005) compared four different types of supply-exhaust positions in regard to dispersion of droplet aerosols indoors: ceiling (supply and exhaust located in the ceiling), floor-return (both supply and exhaust placed in the floor), upward (supply in floor, exhaust in ceiling) and downward (supply in ceiling, exhaust in floor). It was found that the downward system performed best in controlling the transmission of infection by exhaled droplets by achieving the best dilution and reducing lateral dispersion indoors. However, no heat sources were present in the room. The convection flow above heat sources would definitely influence the airflow interaction in the room and the dispersal of droplets indoors.

Underfloor ventilation has been shown to provide air quality similar to that achieved by displacement ventilation when supplied air was discharged vertically upwards and not horizontally (Cermak and Melikov 2006). The inhaled air quality was found to deteriorate when increasing the throw of the supply jet from the floor diffuser.

Dilution could solve to some extend the problem of controlling the level of pathogens in rooms with total volume ventilation but the limiting factor here would be local thermal discomfort: both mixing and displacement ventilation can cause draught problems. Another issue could be the low cost effectiveness of this approach, due to increased energy use and increased initial costs (larger ducts, more powerful fans, over-sizing of the HVAC unit etc.). In densely occupied spaces, like theaters, aircraft or vehicle cabins, etc., dilution does help to some extend but the risk of transmission of diseases by contact and by droplet transmission, remains high due to proximity of people.

To avoid some of the associated problems of increased dilution, UVGI technology could be used instead. Mounted at the ceiling level, a UVGI unit with louvers would work quite well with mixing ventilation (Minki et al. 2009). The enhanced air mixing would transport any pathogens more rapidly to the upper part of the room, where they would be inactivated, but this approach would clearly be less effective when applied to displacement ventilation. Once they had been transported by the warm convection flow around humans, the pathogens would be exhausted close to the ceiling. This would be the case when the gravity forces acting on the droplets are smaller compared to the velocity of the free convection flow, or they would leave the jet and be deposited in the room. The appropriate UVGI technology here is in-duct installation, provided recirculation is available. This approach is therefore useful for large halls with displacement ventilation, where people spent most of the time seated: theaters, concert halls, offices, etc. (Buttolph 1948, Menzies et al. 2003). Filtration could also be used to control the pathogen levels in such buildings. However

filters are not efficient in protecting occupants if pathogens are generated inside the occupied space. In duct installation they are effective at removing the microorganisms or toxins present in the outside air. Sometimes filters themselves can become a source of bacterial growth and thus contribute to high pathogen levels in the respirable range: less than 1.1 μm, especially at elevated humidity, higher than 80% RH (Möritz et al 2001). As mentioned above, PCO may generate by-products, which can reduce perceived indoor air quality or in themselves are hazardous. Economy is another important point for consideration: filters need to be regularly changed, as does the catalytic coating of the PCO unit and both types of unit add additional flow resistance to the HVAC system, resulting in a requirement for more powerful fans. In rooms with mixing ventilation an alternative solution can be the usage of chilled-beams or convectors, recirculating part of the room air through a heat exchanger and a local HEPA filter or a UVGI unit.

2.1.2. Advanced air distribution

There is a need for new air distribution systems that reduce to a minimum the airborne route of pathogens in occupied volumes and protect occupants from cross-infection to occur. One possible solution is personalized ventilation (PV) that provides clean air to the breathing zone of each occupant, and thus improves perceived air quality. Improved thermal comfort, by providing individual control of velocity, temperature and direction of the personalized flow to each occupant, is another benefit of PV, thus increasing occupants' satisfaction, decreasing SBS symptoms, and increasing work performance (Melikov 2004). When properly applied, PV has greater potential than total volume air distribution to protect occupants from airborne pathogens. Research in this area started only recently but there is already evidence that PV in conjunction with mixing ventilation can protect occupants from airborne pathogens and is superior to mixing air distribution alone (Cermak and Melikov 2007). Cermak and Melikov (2007) applied the model for prediction of the risk of airborne transmission of diseases suggested by Rudnick and Milton (2003) to compare the performance of mixing ventilation, underfloor ventilation and personalized ventilation in conjunction with background mixing ventilation. An air terminal device installed on a movable arm and supplying clean air to the face from front was used. The comparison was based on the reproductive number calculated for influenza in case of a quantum generation rate of 100 quanta per hour. The reproductive number represents the number of secondary infections that arise when a single infectious case is introduced into a population where everyone is susceptible. The calculation was made when one of 30 persons occupying the same room for eight hours was infected. The results indicate that in the case of mixing ventilation and a supply rate of 10 L/s per person, it is likely that 7 out of 30 occupants will contract influenza in the course of one working day. The number of possibly infected persons decreases to just two (one already infected and one secondarily infected), if either the ventilation rate is increased to 40 L/s per person, or an under floor system (UFAD) with a short throw is employed. The use of PV is shown to reduce the risk of any cross-infection to a very low level.

Apart from protecting occupants, PV may also facilitate the transport of exhaled pathogens, in the case where the host individual uses PV while the other occupants do not use any PV. In rooms with displacement ventilation, PV promotes mixing of the exhaled air with room air (Melikov et al. 2003, Cermak et al. 2004). This is also true for rooms with underfloor ventilation

(Cermak and Melikov 2007, Cermak and Melikov 2004, Cermak and Melikov 2003, Cermak et al. 2004). There is therefore a risk of transmission of airborne infections to occupants, who are not protected by PV, e.g. occupants who are not at their work places. PV has been reported to improve the perceived air quality when applied with downward ventilation in rooms with textile air terminals (Nielsen et al. 2007c).

Most of existing PV designs are for desk mounted air supply devices. Bolashikov et al. (2003) reported on an air terminal device (named Round Movable Panel, RMP) for installation on a desk, providing nearly 100% clean air for inhalation. A solution that incorporates the PV air supply diffusers into the headrest of the user's chair has recently been proposed Melikov et al. (2007). In this case, over 90% of the inhaled air was clean air at PV flow rates above 8 L/s per person. The performance of this system was found to be dependent on the position of the head relative to the diffusers, the angle of the diffusers themselves, the clothing insulation of the occupant, the thermal insulation of the seat and the ambient air temperature. Niu et al. (2007) studied a chair-based adjustable personalized air supply nozzle attached to the armchair and providing upward flow when adjusted in front of the chest. Eight different nozzles conically shaped, four circular and four rectangular with different dimensions, were studied in terms of their effectiveness in reducing exposure to pollutants and personalized air utilization efficiency (the proportion of actual personalized air in inhaled air to the total supplied personalized air). The best nozzle managed to achieve 80% of clean PV air in the air inhaled but when the thermal manikin was not heated, i.e. in the absence of the boundary layer surrounding the human body. Human subject tests were also performed. People found the air quality better, but at high flow rates (1.6 L/s) they felt draught. Nielsen et al. (2007b) proposed a low velocity personalized ventilation system (LVPV) discharging supply air at very low velocities (laminar flow) and relying on the entrainment of this clean PV air from the natural convection around the human body. Their designs were for a person seated in a chair and included: a neck support pillow, a complete seat cover (placed on the seat and backrest of the chair, with the whole surface being the air outlet) and a seat cover which was partially open in areas along the two sides of the seat. The effectiveness of the neck support pillow reached 94% of clean air in the air inhaled and 80% for the seat cover, in both cases for flow rates above 14 L/s. Among other factors, the performance of PV systems installed in desks and chairs depends on their users' activity, body posture and movement. Such designs protect occupants from airborne transmission of infectious agents only when the user is seated at the desk. This narrows their usefulness. Bolashikov et al. (2003) used a headset to supply clean air just in front of the mouth and the nose, in order to overcome the disadvantages described above. They achieved up to 80% clean air in inhalation. The close proximity of the Headset supply orifice to the breathing zone makes it applicable in places where there is high occupation density and hence an elevated risk of airborne infection (theaters, cinemas, airplanes etc.). Zhu et al. (2008) made CFD simulations with the headset incorporated PV studying the effect of positioning and shape of the device on its effectiveness in supplying clean air into inhalation. They showed that within close distance from mouth (0.04 m) those two parameters do not play important role as in all studied cases the amount of clean air into inhalation exceeded 85%.

The positive feature of the advanced air distribution methods discussed above is their feasibility and the relatively small flow rates used, as well as their close proximity to the occupant.

A HEPA filter or UVGI unit can be included in PV systems that use room air to ensure that each occupant receives air that is clean and free from pathogens. This would further improve the efficiency of the PV system. However field studies are required to evaluate the magnitude of this improvement.

2.2. Infectious hospital wards

2.2.1. Total volume ventilation

Hospitals are the places where the sick and the weakened are accepted to be cured and to recover. Therefore they occupy important part in the social well-fare and well-being of humanity. When treating the sick or the injured individuals, the hospitals have to provide conditions that will limit the spread of contagious pathogens released by the infected, as well as ensure healthy environment for rehabilitation of those with reduced immune response and recovering. Due to the different nature of the health care services provided by the hospital, different environmental control strategies are required. For example people undergoing surgical intervention or those immuno-compromised, require special environment to "protect" them from the surroundings by creating a "sterile" place free of pathogens. Those that are sick with contagious diseases, on the other hand, will require certain "isolation" in order to stop the spread of the disease among the healthy population. This is accomplished by the help of well ventilated isolation rooms. In the former case the space is kept over-pressurized by supplying more air than exhausting, while in the latter scenario more air is returned than provided resulting in a negative pressure gradient in the patients' room. Sometimes due to various reasons, the isolation rooms fail to function as required resulting in elevated risk for the patients in them, the health care staff or for the other patients as well as visitors in the hospital. In those cases pathogen laden air spreads uncontrollably resulting in Hospital Acquired Infections (HAI) a.k.a. nosocomial infections (Gustafson et al. 1982, Wel et al. 1996, Decker and Schaffner 1999, Kaushal et al. 2004, Li et al. 2005, Beggs et al. 2008, Cano et al. 2009). In USA twenty thousand people die annually as a direct result from HAI and sixty thousand more deaths are reported where the nosocomial infections are a contributing factor (Kaushal et al. 2004). Nosocomial infections result in elevated risks of infection with contagious disease for the health care staff as well (Wel et al. 1996, Menzies et al. 2000, Qian et al. 2006). During the 2003 SARS epidemic 20% of all infected individuals worldwide were from the health care workers (Qian et al. 2006). Therefore to reduce the risk from HAI resulting from airborne distribution the design of special hospital ventilation is required (Streifel 1999, Kaushal et al. 2004, Beggs et al. 2008). Different guidelines and standards have been established for the ventilation of the health care facilities (ASHRAE 170 2008, CDC guidelines 2005, DS 2451-9 Dansk standard 2003) prescribing the lowest ventilation equivalent of 12 air changes per hour for isolation rooms. The minimum specified pressure difference between the Airborne Infection Isolation (AII) rooms and adjacent spaces should not be lower than 2.5 Pa (ASHRAE 170 2008, CDC guidelines 2005), and as high as 10 to 15 Pa (DS 2451-9 Dansk standard 2003). The effect of different pressure gradients and ventilation flow rates on the performance of the AII room with downward ventilation (supply on the ceiling and exhaust on the wall and close to the patient's head) has been studied by Tung et al. (2009). They showed that the infiltration due to the negative pressure difference into the isolation

room increases with the increase of the pressure drop and this lead to the decrease of the total concentration of contaminants. The ventilation efficiency of the studied mock-up isolation room was best for the 6 times higher pressure difference and doubled ventilation rate above the recommended values, resulting in -15.0 Pa and 24 ACH respectively. Decker (1995) reported on the leakage of pollutants associated with opening and closing the door of the isolation room, as well as when people moved in and out of it. He noticed substantial leakage when the door was left open or when a person moved in or out of the isolation room. Moreover, a moving person out of the AII room appears to cause more contaminant leakage than when entering. This fact should be thoroughly considered into the design process and can be to some extend solved by implementation of anterooms that can compensate for the pressure fluctuations resulting from moving people and opening and closing of doors (Shih et al. 2007). Other factors for the proper functioning of the AII room is also the position of the supply and exhaust vents which would determine the air distribution pattern in the whole space. Studies (Cheong and Phua 2006, Noakes et al. 2009, Tung et al. 2009a) show that the downward ventilation principle: supply on the ceiling or top of the wall and exhaust on the wall close to the patient's head provides the best air dilution and lowest contaminant space distribution for a AII room. This could be explained with the fact that due to the elevated down directed velocities the airborne particles are "pushed" towards the floor and evacuated through the exhaust of the ventilation system not allowing to "scatter" uncontrollably into the room. A comparison of the performance of three ventilation supply systems (mixing, displacement and downward air distribution) was carried out by Qian et al. (2006) in a simulated hospital environment, to determine which was most capable of protecting patients and hospital care workers (HCWs) from cross-infection due to inhalation of droplet nuclei. The downward ventilation performed in a similar way to the mixing ventilation, due to the counter flow from the free convection around the human body but still superior compared to mixing alone. So although it is recommended for clean rooms, infectious wards and operating theaters, downward air distribution may not always protect people from cross-infection. Displacement ventilation performed worse when patient was lying face sideways, because the exhalation jet persisted over a very long distance, assisted by the thermal stratification (Qian et al. 2006). Kao and Yang (2006) show that the dilution efficiency depends strongly on the air change rate in the space and nearly independent of the airflow pattern. However the airflow pattern is a significant parameter influencing the droplet fallout released from the coughing patient. In their work they suggest the parallel flow (supply and exhaust placed on opposite walls) as the best distribution method of all tested by them, able to secure a minimum region of coughed gas diffusion and droplet fallout. The effectiveness of the parallel system in evacuating the contaminants out of the isolation room and providing the occupants with clean unpolluted outdoor air depends on factors such as height of the supply diffuser from floor and position of the patient in the room (Kumar et al. 2008). The higher the supply diffuser is located the more time the released droplets spend in the room resulting in higher risks from airborne infection. To secure "clean" working environment for the HCWs in an AII room or to protect the patient from possible infection (over pressure isolation rooms) the location of the infectious and immuno-compromised patient should be near the exhaust wall and near the supply wall respectively. Qian et al. (2008) studied the effect of locating the return openings on cross-infection risk with downward ventilation in hospital wards with and without partitions between the

beds. The downward flow was provided by a textile ceiling diffuser at low velocities. The lowest pathogen exposure for the HCW and the other patient was achieved when the four return openings were placed close to the ceiling. However the textile partitions introduced between the beds did not manage to decrease the risk of cross infection and even slightly increased the risk for the HCWs. In other numerical study by Ching et al. (2008) the hospital textile curtains reduced the peak concentration of bioaerosols by as much as 65% in the transient dispersion process. However the effect of air distribution inside the isolation room under different supply and exhaust layouts was not investigated.

It is evident that the performance of the isolation rooms on dispersion of airborne contaminants strongly depends on factors like air change rates, air distribution pattern and pressure difference with the surrounding rooms. Therefore good ventilation plays important role in the optimal functioning of such hospital utilities. Based on a field study performed in Hong Kong, Li et al. (2007a) showed that even the newly constructed isolation wards for the SARS outbreak failed to provide the required 12 ACH (28% of all visited isolation wards in hospitals), 90% allowed for air leakage when isolation room door was open, and 60% had the toilets and bathrooms under positive pressure. Regular checks of air flow direction and air change are highly recommended together with specific training of hospital maintenance engineers and HCWs (Decker 1995, Streifel 1999, Li et al. 2007a).

Clearly the traditional air ventilation and distribution techniques are not suited well enough to provide effective functioning of the isolation rooms in allowing control over the airflow distribution throughout the hospital envelope, i.e. uncontrolled leakage of pathogen laden air. The present existing practices aim to dilute as much as possible and then evacuate it successfully out of the hospital envelope. This is a costly strategy as huge amounts of air need to be cleaned and conditioned, so that to be supplied in the occupied zones. Instead of supplying more air and rely on mixing and diluting the pollutants, advanced techniques that would locally control the flow interaction and provide successfully the occupant with clean air as well as evacuate the polluted pathogen laden air away from the occupied zone can be applied. More advanced engineering methods are needed to be implemented and introduced into practice to couple with the background ventilation so as to enhance the performance with respect to airborne bioaerosol removal and overall cross-infection risk reduction.

2.2.2. Advanced air distribution

A possible solution to the problem is to apply the personal ventilation into the isolation room environment as a supplement to the total volume ventilation. This would provide clean air directly to the breathing zone of each patient and reduce the possibility from cross-infection. Ishida et al. (2009) reported on a PV air-conditioning system, installed by each hospital bed, able to accommodate every patient with desirable thermal environment and at the same time to contribute to their mental being. However their work was concentrated on the thermal sensation and did not study the possibility of improving the air quality and thus minimize the risk from cross infection (HAI) among the patients and the HCWs.

Low velocity personalized ventilation, based on a ventilated pillow and a ventilated blanket for application in the hospital environment as a way of limiting cross-infection, was studied

and reported by Nielsen et al. (2007a). The performance of these devices was investigated in regard to protection of the patient and not of the health care workers or visitors. The efficiency of both devices was found to be dependent on the position of the patient: lying on one side or on the back. The highest efficiency was achieved for a patient lying on his side: almost 95% of the inhaled air was clean PV air. When lying on the back less clean air was able to reach the breathing zone of the patient. This was due to the low supply velocities: the entrainment rate of the clean PV air by the natural convection flow was low and it was pushed aside before reaching the nose/mouth. A possible issue with this ventilation could be the increased number of airborne particles due to elevated number of squama (skin flakes) that the convection boundary layer will transport from the body into the room laden with contagious pathogens like *Staphylococcus aureus*, *Acinetobacter*, *Clostridium* etc. being some of the major causatives of nosocomial airborne infections in hospitals (Beggs et al. 2008).

The research on isolation room ventilation and its ability to reduce cross infections from airborne route just started to increase rapidly, especially in the last few years with the emergencies of new contagious diseases such as SARS, avian flu, swine flu, multi drug resistant *Staphylococcus Aureus* (MDRSA) etc., but still more knowledge is needed especially on flow interaction and air distribution.

2.3. Need for improvement

Ventilation aims for providing occupants with fresh and healthy air to breathe free from hazardous matter and contagious pathogens, as well as comfortable thermal environment. However the existing strategies of space ventilation, namely mixing and displacement air distribution, fail to fulfil these goals. Their weak points are especially noted today with the rise of new mutated pathogens responsible for the epidemics and the pandemics like *SARS*, *H5N1* and *H1N1* viruses. In rooms with mixing air distribution all occupants are equally exposed to airborne pathogens and thus those who are with weaker immune system, like the children the elder or the immune-compromised are under greater risk from airborne cross infection. The displacement air distribution also has its weak points: namely, it is very sensitive to movement of people or other moving objects as the supply velocities are very low. When people are moving in a room with displacement ventilation the displacement effect is completely destroyed and the air distribution pattern becomes similar to that of mixing ventilation (Halvoňová and Melikov 2010). Furthermore, as already discussed the displacement ventilation can prolong the exhaled air propagation horizontally by locking it between the stratified zones (Qian et al. 2006). Therefore, the displacement ventilation can also increase the risk from cross-infection as a result from airborne transmission between occupants.

Clearly more understanding is needed about the release of infectious pathogens in air, their transport, survival mechanisms in the ambient environment as well as the ways they end up in a new host/occupant as has already been pointed out in Chapters 1 and 2. For the release of microorganisms and viruses from a sick individual into the ambient air, general everyday pulmonary activities like breathing, coughing, sneezing, talking or even singing are noted as contributors (Cole and Cook 1998, Edwards et al. 2004, Wong and Leung 2004), discussed in Chapters 4 and 5 in details. The released droplets suspended in the air, after being expelled from the lungs, are transported into the ambient air and their fate depends on the flow interaction within the

vicinity of the occupant. This interaction is dominated by many factors such as the nature of the airflow generated by the individual (coughing, sneezing, breathing etc.), the natural convection layer around the human body, the strength of any source of forced convection within the occupied zone, the background ventilation, etc. Though crucial, not much knowledge is available on the flow interaction within the occupied zone, especially close to the breathing zone of the occupant, and clearly more understanding is needed (**Paper I**, **Appendix I**). The existing ventilation strategies and technologies nowadays rely solely on dilution by supplying extra amounts of conditioned clean air. This also makes them energy inefficient and very demanding. In many cases they also create many problems connected with elevated velocities and draught issues. Hence new ways of organizing the ventilation pattern within the occupied zones are required that would try to control the flow interaction locally and reduce the exposure and migration of released airborne pathogen laden droplets indoors. These new advanced techniques should be able to meet the requirements of all occupants for air quality and thermal comfort and prioritise the personal satisfaction and health protection as major goal. At the same time these new ventilation strategies should be user friendly and energy efficient, and result in increased well-being and self-performance of the end users.

Chapter 3 : Objectives

The overall objectives of the present study is to develop advanced methods of air distribution close to occupants in spaces able to improve inhaled air quality and to reduce the risk from cross-infections contamination via the airborne route of transmission.

The specific objectives of the study are:

I. To develop and study methods for control over the airflow interaction in close vicinity to the human body leading to improvement of inhaled air quality and decrease in the risk from airborne cross-infection in office environment;

II. To develop and study advanced methods for air distribution in infectious hospitals wards aiming to decrease the risk of cross-infection for the health care workers and the other patients in the ward.

Chapter 4 : Control of Airflow Interaction around the Human Body

4.1. Airflows at the vicinity of human body

This section gives overview of existing understanding of how different flows around human body develop and interact with each other as well as their impact on the pathogen dispersal indoors.

4.1.1. Free convection flow around human body

Heat transfer in a fluid in the form of energy transport by the moving fluid particles is referred as convection. The motion can be created by external source e.g. pump or fan and in this case it is defined as forced convection. Even in the absence of external factors the motion in a fluid is created as a consequence of existing temperature differences. The resulting motion from the buoyancy forces is known as free convection. In fact these forces sustain the flow.

In calm indoor environment ($v < 0.1$ m/s) around the human body a convection boundary layer is developed resulting from the warmer surface of the skin and the clothing. Within the indoor temperature range specified by present guidelines and standards (CEN CR 1752 - 1998, ISO 7730-2005, ASHRAE 55 - 2004, EN 15251 - 2007) of 20 to 26 ^{o}C, the maximal difference between the skin temperature and the ambient room air temperature is about 13 ^{o}C (the average skin temperature in state of thermal comfort is about 33-34 ^{o}C). The clothing temperature is lower (about 27-28 ^{o}C) and therefore the temperature difference is smaller. Several studies have been performed in order to identify and characterise the free convection layer surrounding the human body (Lewis et al. 1969, Clark and Toy 1975, Homma and Yakiyama 1988, Özcan et al. 2005, Settles 2005, Clark and de Calcina-Goff 2009). One of the first and most informative studies on the nature of the free convection flow around a standing still naked human and its role as an active transport of pollutants and particles (in the form of skin flakes) was reported by Lewis et al. (1969). The boundary layer starts very close to the floor at the dorsa where part of it detaches due to the horizontal nature of the feet. The air that remains attached to the feet (close to the ankles) advances upwards the legs, accelerating and becoming thicker. At the height of the knees it is already 1-2 cm thick and continues accelerating until it reaches the chest. About 1 m from the floor the boundary layer changes between laminar and turbulent and above 1.5 m (mid-chest) becomes fully turbulent. At the shoulders most of it breaks away upwards. When the free convection flow reaches the head its movement upwards becomes strongly modified by the contours of the face: namely the neck, the jaw, the nose and the pinna of the ears. Part of the air follows the convex structure of the jaws upwards, while the remaining follows under the surface of the chin. Some of the air that overcomes the chin passes over the lips and becomes part of the air inhaled, the other flows along the cheeks, over the eyes, the forehead and joins the air that rises up from the sides and back of the head and the shoulders. The result is a plum that persists for a certain distance above the head of the occupant. However there are certain regions of the body where the boundary layer is brought to rest. This

happens when the flow is constrained by a horizontal surface such as the perineum, the axilla, the region under the chin and lobe of the ear and under the nasal septum. A nude standing subject at 20 ^{o}C room temperature, can generate up to 60 L/s of passing air over the head at a maximum velocity of 0.25 m/s , extending up to 2 m above the head and develop a maximum thickness of 0.20 m (Clark 1973, 1976, Homma and Yakiyama 1988, Zhukowska et al. 2008). Hence, the velocities measured within the convection flow are close to the upper limits suggested in the present guidelines and standards (CEN CR 1752-1998, EN 15251 2007) of 0.2 m/s. Therefore the convection plume rising from the human body acts as an active air transport indoors. Due to unsteady flow in the convection boundary layer or by changes of conditions in the plume surroundings, wandering of the thermal plume axis above the occupant appears as a result (Popiolek 1981, Kofoed 1991, Zukowska et al. 2007). Furthermore studies (Clark 1973, 1976, Mierzwinski 1980, Homma and Yakiyama 1988, Zukowska et al. 2008) have documented that the plum above the head of the seated or standing person is comparable to the ventilation flow and therefore affects the flow interaction into an occupied place. In a room with displacement ventilation the convection flow around the body was shown to affect the height of the stratification zone: the border layer between the clean and the contaminated zones in an occupied space (Zukowska et al 2008). Thus the enhanced mixing in the lower zone of the room “pulls” the polluted air downwards and results in higher pollution levels.

However, seldom people stand still, let alone naked in indoor environments. An important parameter contributing to the development of the free convection flow around the occupant’s body is the posture (standing, sitting, lying), the clothing insulation, the physical activity indulged, as well as the presence or absence of objects/furniture. When the occupant is seated part of the back, buttocks and thighs are in contact with the furniture (seat) which limits the development of the boundary layer at the rear side of the body and changing the ratio between convection and radiation heat losses from the body (Zukowska et al. 2007a). The warmed air coming upwards from the legs of a seated person does not flow smoothly as it detaches at the knees and interacts with the flow starting at the abdominal area joining in one flow at the height of the lower chest (Homma and Yakiyama 1988, Zukowska et al. 2007a). The flow above the head of a sitting person was described as a non axis-symmetrical, because velocities were found to be higher above the legs than behind the back, but at a height 1.5 m above the head, profiles become almost axis-symmetrical (Zukowska et al 2007).

Zukowska et al. (2007) studied the thermal plum above a simulated sitting person with different complexity of body geometry. They found out that a dummy comprised of head, torso and legs can be successfully used as a simulator of a sitting person, especially when the air distribution in the room is considered.

In the case of lying body, the boundary layer is generally slower and thinner compared to when standing (Clark and de Calcina-Goff 2009). For lateral air speeds (walking, moving, etc.) above 0.2 m/s the convection layer around the human body ceases to exist. Instead it is swept downstream and forms the aerodynamic wake (Settles 2005, Clark and de Calcina-Goff, 2009). The legs act as two shedding cylinders with flow between them resulting in a faster downstream dissipation compared to that of the torso. Breathing as well as localized motions (hand movements), do not affect significantly the upward thermal plum (Rim and Novoselac 2009).

Clothing is another factor affecting the boundary layer. Increasing the clothing thermal insulation leads to a total reduction of the convection heat loss and hence the strength of the boundary layer (Zukowska et al. 2007a) and its turbulence (Homma and Yakiyama 1988). Also when humans move, clothing creates billowing and pumping action around the rims which combined with the abrasive effect of the fabric on the skin helps the detachment and dispersal of skin flakes via the convection flow into the occupied space (Clark and Cox 1973, Clark 1974).

Studying the convection flow around the human body is in itself important, as it has been shown of being quite active in bringing air into the breathing zone (Nielsen et al. 2002) and in transporting particles entrained either from the air into the room or shed from the skin or close to the floor (Lewis et al 1969, Clark and Cox 1973, Rim and Novoselac 2009, Clark and de Calcina-Goff, 2009). The boundary layer can carry particles with the density of water (close to that of saliva, Nicas et al. 2005) upwards up to a diameter of 80 μm equivalent diameter (skin scales) making it ideal transport for the large droplet dispersion of infectious diseases (Clark and de Calcina-Goff, 2009). Furthermore it has been shown that interaction of the convection flows between people can occur even at body distance as large as 0.5 m (Rim and Novoselac 2009, Datla and Glauser 2009, Clark and de Calcina-Goff, 2009) making it an important factor for airborne disease dispersal indoors among people especially in densely occupied environments.

4.1.2. Transient flow from respiratory activities

Human pulmonary activities, such as breathing, coughing, sneezing etc., contribute to the generation and dispersal of large droplet and airborne particles with attached pathogens (Wells 1936, Loudon and Roberts 1967, Morawska 2005, Nicas et al. 2005, Fiegel et al. 2006, Yang et al. 2007). Therefore the transient flows of exhalation, coughing and sneezing are of major importance for airborne cross-infection in spaces.

Every minute 6 litres of air pass through the human lungs as a result from breathing, at normal sedentary activity, making this natural pulmonary process quite important for the air flow distribution around the human body (Hyldgaard 1994). However, depending on whether exhalation is through the nose or the mouth, different initial conditions are established within the generated jet. Exhalation from nose forms two separate jets at an intervening angle of 30^{o} that do not interact with each other and at 45^{o} below the horizontal direction, with an initial velocity of approximately 2 m/s (Hyldgaard 1994). The exhalation from mouth forms a single jet that due to buoyancy forces rises fast after being expelled (Özcan et al. 2005, Nielsen et al. 2009). Both exhalation from mouth and nose have quite high initial momentum and are able to penetrate the free convection layer surrounding the human body. All pollutants and particulate matter generated from exhalation therefore are pushed away from the body and very little amount is re-inhaled or pulled back by the convection layer (Hyldgaard 1994, Melikov and Kaczmarczyk 2007). One of the most common ways of droplet and sub-micron particles generation is through exhalation. Hersen et al. (2008) showed that there is similarity among exhaled breaths of healthy individuals and difference from those of individuals with symptoms of cold. However no specific size distribution was obtained for those who showed symptoms of being sick. In a recent study Gupta et al. 2010 characterized the exhaled airflow from breathing and talking via human subject experiments with 12 female and 13 male healthy individuals. The parameters described by them via mathematical models were the

respiratory frequency (RF), minute volume (MV) and tidal volume (TV). The study also gave some insight on the initial angles of the exhaled jets from the mouth and nose openings when breathing normally. The average area openings of the nose (0.71 ± 0.23 cm^2 for male and 0.56 ± 0.10 cm^2 for female) and mouth (1.20 ± 0.52 cm^2 for male and 1.16 ± 0.67 cm^2 for female) were also measured to be quite constant during normal breathing. They were shown to depend on the sex of the subject but not on their body surface area. Talking at its nature is quite random and dynamic process, and therefore the flow rate as a result is quite irregular. Thus it can be averaged over the time period it took place. The resultant flow rate from talking was found to depend on the body surface area of the individual: 4.838 to 5.868 L/m^2 for males and 4.421 to 5.160 L/m^2 for female subjects (Gupta et al. 2010). As talking is localised at the mouth the direction of the resulting jet is assumed to be the same as during normal mouth breathing. Gupta et al. 2010 also proposed to use a mean mouth opening (area of 1.8 ± 0.03 cm^2) for talking as the shape changes with time and vocals, and showed no clear trend associated with sex or body surface area of the subject. Melikov 2004a suggested also standardisation of nose and mouth opening of the thermal manikins used in experiments as breathing counterparts of human subjects.

On the other hand sneezing and coughing are processes generating pulsating jets with very high initial momentums. Very little research has been done on sneezing and more attention is paid to coughing due to the fact that it is done through the mouth and this is the most frequent dispersal route for pathogens (Morawska 2005, Fiegel et al. 2006).

Coughing is the most obvious symptom of a respiratory disease. In more details the topic is discussed in Chapter 5, Section 5.1.

4.1.3. PV flow

Personalized ventilation (PV) supplies clean air close to the occupant and directly into the breathing zone, so as to improve the inhaled air quality and to reduce the risk of airborne cross-infection in comparison with total volume (TV) ventilation (Cermak and Melikov 2007). The unique features of PV are the possibility of individual control over the supply flow rate, the temperature, and the direction of the provided clean air. Thus a microenvironment preferred by each occupant can be achieved. Human subject studies have shown that PV significantly improves the inhaled air quality and the thermal comfort and also significantly decreases SBS symptoms compared to TV ventilation (Kaczmarczyk et al. 2004, 2006).

The personalized flow is in most cases a free jet supplied from either a circular or rectangular opening. The first region of such a jet, known as the potential core region, is characterized by constant velocity, low turbulence intensity and hence clean air with a relatively constant temperature, still unmixed with the polluted room air. Non-uniformity of the velocity profile at the air supply, elevated initial turbulence intensity and temperature or density difference between the supplied air and the surrounding air, would enhance the natural process of entrainment and mixing of the supplied clean air with the polluted ambient air and decrease the length of the potential core (Melikov 2004).

The characteristics of the personalized flow depend on the design, size and shape of the air supply nozzle (circular, elliptical, rectangular, etc.). Khalifa et al. 2009 and Russo et al. 2009 used a co-flow PV nozzle to control the characteristics and thus the development of the personalized flow.

They succeeded in increasing substantially the length of the clean air zone of the personalized flow. The initial velocity and turbulence intensity profiles can affect significantly the characteristics of free air jets. As reported in the literature (Nastase and Meslem 2006, Meslem et al. 2008), lobed free jets from nozzles with lobes integrated in the design geometry have completely different characteristics (distribution of velocity, spread of the flow, entrainment ability, etc.). Therefore, the use of lobed jets as personalized flow may be efficient for improving the performance of PV in general and in particular the performance of PV based on inserted jets, such as the headset PV: a smaller nozzle would be able to cover a larger area around the mouth (the inhalation semi-sphere region).

The performance of PV, with regards to occupants' inhaled air quality and thermal comfort, depends on the interaction of the airflows close to the human body: the personalized airflow, the free convection flow around the human body, the transient flow from exhalation and the airflow generated by the background TV ventilation.

4.1.4. Back ground ventilation flow

Nowadays most of the occupied places are equipped with some form of total volume ventilation. As has been discussed in Chapter 2, the type of total volume room air distribution (mixing or displacement), plays an important role in the transmission of airborne diseases indoors. In the present study air distribution pattern with mixing has been applied. It is described later in the thesis, when the obtained results are discussed.

4.1.5. Interaction of flows

Because of the complex aerodynamic environment indoors the interaction of all flows in close proximity to the person should be accounted especially in case of airborne contagious disease transport and likeliness. The interaction of airflows in close proximity to human body, especially at the breathing zone, has been reported only in few studies (Hyldgaard 1994, Melikov and Zhou 1996, Nielasen et al. 2002, Nielsen et al. 2009). In the following the interaction of the flows at the vicinity of the breathing zone is discussed with regard to: 1) protection of occupants, i.e. decrease the risk of inhaling pollution and airborne pathogens and 2) dispersion of pathogens generated during respiratory activities, including exhalation and coughing.

4.1.5.1 Interaction of free convection and PV flow for protection

As already stated (Chapter 2), the aim of the personalized ventilation is to provide fresh air to the occupant and protect from airborne disease infection. Therefore the interaction of the personalized jet with the flows within the occupied zone is of crucial importance for the PV performance (Melikov et al. 2003, Cermak and Melikov 2007, Halvonava and Melikov 2009, Bolashikov and Melikov 2009). The effectiveness of the PV to supply clean air and to penetrate the boundary layer around the human body depends also on the distance between the occupant who uses the PV ATD and the PV nozzle: less polluted air reaches the occupant when decreasing the distance and this results in a reduced risk for acquiring an airborne infection. Therefore, the closer to the body the PV ATD, the less mixing and the better protection, but on the other hand in order to avoid the risk of draft the velocities should be kept low, which makes the flow interaction more

sensitive to the natural motion of the occupant, when seated in front of the PV nozzle. One possible way to solve the problem is as already mentioned: to attach the PV nozzle very close to the head of the person so that it always follows the natural motions of the occupant and provides the necessary amount of clean PV air (Bolashikov et al. 2003).

The direction penetration of the PV flow with respect to the boundary layer around the occupant's body (transverse, assisting or transpose) is another important factor for the PV flow interaction and its effectiveness in protecting people. Transverse and counter PV flows would require much more initial momentum to penetrate and overcome the convection flow and hence reach the breathing zone, while the assisting flow could use the natural acceleration of the convection flow and be transported towards the face.

4.1.5.2 Dispersion of exhaled, coughed air

As already mentioned PV is able to reduce the risk from cross infection for its occupant (Melikov et al. 2003). However the high initial momentum of the flows resulting from exhalation, sneezing or coughing can disturb the personalized air flow and may even result in enhanced airborne spread under certain conditions. With regard to the transport of exhaled air the interaction of the personalized flow, the free convection flow and the background airflow is also important. PV flow can provide occupants with clean air and protection against cross-infection, but it may also enhance the transport of exhaled air (which may contain viruses) between occupants (Melikov et al. 2003, Cermak and Melikov 2007, Halvonava and Melikov 2009).

Tang et al. (2009) showed that surgical masks or even N95 mask cannot fully stop the dispersion of coughed air and due to the high initial momentum the air leaks from the sides of the masks and also through the front. However the leakage is higher with surgical mask. This leakage could be captured by the free convection flow around the body and interact with the total room air. The type of total volume ventilation (mixing or displacement) also affects the dispersion of the exhaled air indoors (Qian et al. 2006, Nielsen et al. 2009, Liu et al. 2009). While mixing ventilation dilutes it after some distance the displacement ventilation can "lock" the exhaled air and prolong its advancement indoors.

Hence other methods are clearly needed: in this case an exhaust opening on the trajectory of the expelled air could be quite beneficial and effective in capturing the released pathogens at the generation point. This would ensure their evacuation and annihilation and better control over pathogen dispersal indoors. It should be taken into account that many of the diseases are asymptomatic in the early incubation stage, when the sick individuals are the most infective and dangerous for the healthy occupants (Greenwood et al 2007).

4.2. Control of free convection flow for improved inhaled air quality

Apparently the free convection flow surrounding the body is a barrier to overcome for the clean PV air on its way to the inhalation zone of the occupant. Moreover, as already mentioned in the previous section, the boundary layer acts as an active transport media for pollutants and particulate matter, which makes its role into the dispersal and cross-infection of airborne diseases quite crucial. Taking into account that the inhaled air by a person at rest is mostly from the upcoming convection layer, and that quite high target velocity is needed for the clean PV air to

penetrate the boundary layer (over 0.2 m/s), it becomes clear that better control over the flow interaction at the breathing zone is needed. One possibility is to reduce the strength of the boundary layer at the face so that more clean personalized air is able to reach the breathing zone of the occupant. Thus, the weakened convection layer would be easier to overcome by personalized flow at reduced target velocity (below 0.3 m/s), i.e. at reduced personalized supply flow rates (energy utilization), resulting also in an improved local thermal sensation (reduced draught).

Several methods of control over the free convection flow at the breathing zone aiming for improvement the performance of two PV units with respect to air quality and cross-infection risk reduction were developed and studied. The first PV unit, named Round Movable Panel (RMP) is shown in Figure 4.1 (Bolashikov et al. 2003). Three of the methods studied with this PV unit focused on thinning out of the free convection layer in front of the seated occupant: 1) by introducing a physical barrier at the abdominal area of a seated occupant on the way of the upcoming boundary layer (passive control), 2) by exhausting part of it (active control) below the table plot, and 3) by combining both active and passive methods (hybrid).

Figure 4.1 *Round Movable Panel incorporated in a workstation and used by an occupant.*

Control over the boundary layer closer to the face was also studied with a chair incorporated PV unit (Melikov et al. 2007) with the help of a pair of control nozzles mounted just below the corresponding pair of PV air supplies (Figure 4.2). In this case the control was achieved: 1) by exhaustion of the upcoming free convection air through the control nozzles (Figure 4.2B); 2) by inserting part of the supplied clean personalized air through the control nozzles into the free convection flow and part supplied from the PV nozzles (Figure 4.2D); 3) by supply of room air through the control nozzles against the free convection flow aiming to "push away" the boundary layer at the upper chest level, just below the shoulders of the seated occupant and to make possible for the clean air supplied from the PV nozzles to reach the mouth/the nose (Figure 4.2C) and 4) inserting the clean PV air without mixing between the chest and the free convection flow at the upper chest/shoulders level (Figure 4.2E). For more details on the methods refer to **Paper II, Appendix II**.

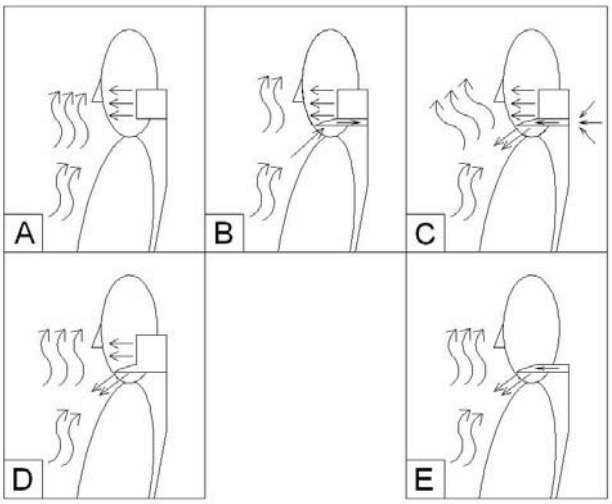

Figure 4.2 *Seat-incorporated personalized ventilation: A) Interaction of the free convection flow with the personalized flow; B) Control of the interaction by exhausting part of the free convection flow air at the upper chest level; C) Control of the airflow interaction by supplying polluted room air to push away the free convection flow at the upper chest/shoulder level; D) Control of the airflow interaction by supplying part of the personalized air at the upper chest/shoulder level to dilute and weaken the free convection flow; E) Control of the airflow interaction by inserting the personalized air without mixing beneath the free convection flow at the chest.*

4.2.1. Method

The experiments studying the control over the free convection layer around an occupant's body (discussed in the following section 4.2) were performed in a full-scale test room (4.70 m × 1.62 m × 2.60 m: W×L×H) with background mixing ventilation (Figure 4.3). Breathing thermal manikin with realistic free convection flow was used. The manikin's body is shaped to resemble accurately the body of an average Scandinavian, 1.7 m in height. The manikin is made of a 0.003 m fiberglass coated polystyrene shell and is divided into 23 segments. Each of these segments is equipped with heating and temperature measuring wiring, controlled by a computer program so as to maintain a surface temperature equal to the skin temperature of a person in a state of thermal comfort at the actual activity level, and thus realistically to recreate the free convection flow surrounding the human body. The control of the manikin is described by Tanabe et al. (1994). However the breathing mode was not used during the measurements as it has been documented that the concentration of tracer gas sampled close to the mouth without breathing is the same as the tracer gas concentration in the inhaled air (Melikov and Kaczmarczyk 2007). The RMP PV supplied the clean air from a round air diffuser (diameter of 0.185 m) positioned at distance 0.4 m from front/above (at 40^{o}) towards the face centring the nose and mouth region. The chair integrated PV units discharged the clean air from nozzles positioned at both sides of the head and at an angle of 45^{o} relative to the symmetry bisecting plane of the manikin body. All the measurements were performed under isothermal conditions with PV air temperature equal to the room air temperature at 20 °C and 26 °C. In all

experiments a tracer gas (Refrigerant R134a) was used to mark the supplied room air simulating pollutants and airborne particulate matter (particles with diameter less than 2μm), while the PV air was kept clean (no tracer gas was dosed into the PV supply). Tracer gas concentration measurements were used to identify the effect of controlling the free convection flow on inhaled air quality and thus on the risk from airborne cross-infection with contagious diseases. To test the effectiveness of the control methods studied, based on the tracer gas measurements, a normalised index known as Personal Exposure Effectiveness (PEE) was used. The PEE represents the portion of clean personalized air in the air inhaled by an occupant. PEE is equal to 1 (or 100%), when only clean personalized air is inhaled, i.e. best performance of the personalized ventilation; PEE equal to 0 (or 0%) means that the inhaled air is polluted room air. Its value is calculated as:

$$\varepsilon_P = \frac{C_{I,0} - C_I}{C_{I,0} - C_{PV}} \times 100 \text{ , (4.2.1)} \qquad \text{, (4.2.1)}$$

where:

ε_p is the personal exposure effectiveness,

$C_{I,0}$ is the pollution concentration if no PV is used,

C_{PV} is the pollution concentration in the personalized ventilation air,

C_I is the pollution concentration in inhaled air.

Prior to all experiments the velocities (speed) was measured at 3 heights 0.1 m, 0.6 and 1.1m from floor in the vicinity of the thermal manikin with an omnidirectional thermal anemometer HT400 and was always below 0.2 m/s (CEN CR 1752 2004, ISO 7730 2005, EN 15251 2007).

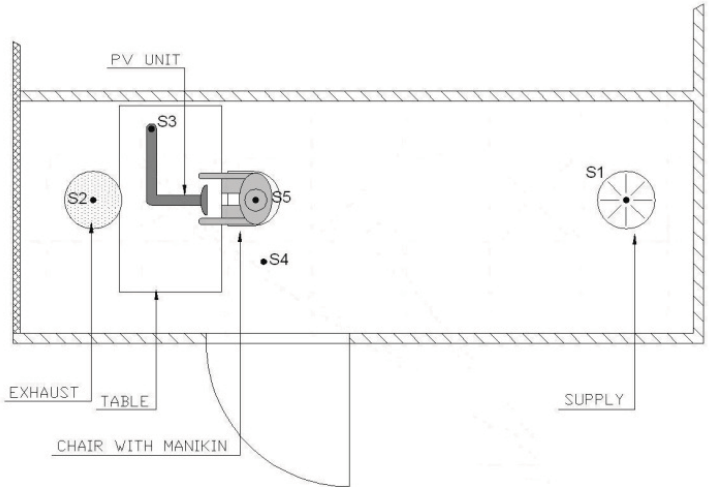

a)

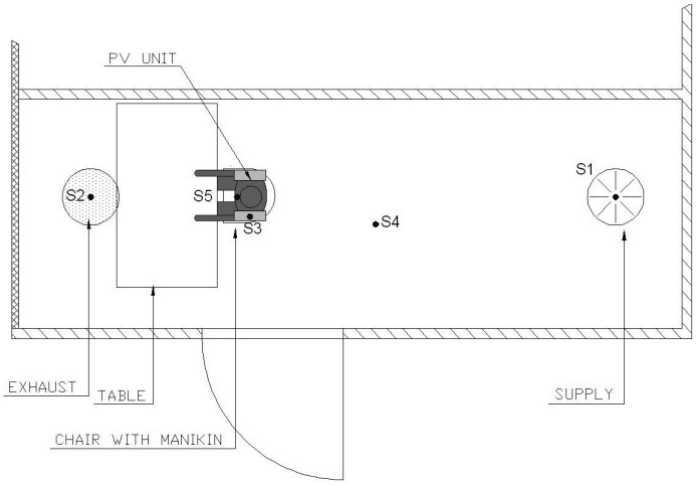

b)

Figure 4.3 *Experimental set-up for control over the free convection layer: a) with RMP PV unit, b) with chair incorporated PV unit. The points S1 to S5 show the measurement points where the tracer gas was sampled: S1 – supply, S2 – exhaust, S3 – PV unit, S4 – room, S5 – mouth of breathing thermal manikin.*

All data obtained were analysed in accordance with ISO guidelines for the expression of the measurement uncertainty (ISO GUIDE 98-3, 2008). The sample standard uncertainty was calculated as the maximum uncertainty of the corresponding measurement (random error). The absolute expanded uncertainty with a level of confidence of 95% (coverage factor of 2) is listed in Table 4.1.

A specially designed tracer gas experiment was performed to account for the uncertainty in determining the normalized PEE index affected by the positioning of the manikin relative to the PV nozzle studied. The same concentration measurement procedure was repeated 3 times in the following order: the manikin was positioned in front of the PV, then after 20 samples it was moved and repositioned again to the same location and new 20 samples were taken. Finally, third measurement (n=20 samples) was repeated without changing the set-up. The maximum difference in the calculated PEE indexes due to repositioning was calculated to be approximately 2%.

Table 4.1 *Sampling frequency, duration of data acquisition, and typical values of the uncertainty with a 95% level of confidence.*

Quantity	**Frequency of Data Acquisition**	**Duration of Measurement Period**	**Uncertainty (Conf. Level 95%)**
Concentrations (inhaled and room)	155 ± 5 sec/6 channels	130 -150 min	1% of reading
Temperature (room)	1 Hz	constant	0.3 °C
Air velocity (room)	5 Hz	3 min	0.03 m/s

4.2.2. Passive control method

This method of control of the free convection layer of a seated occupant was named passive to account for the energy consumption. The method used comprised of a plastic impregnated cardboard, placed in front of the thermal manikin to block the gap between the abdomen and the front edge of the desk, and thus to prevent the warm air generated by the lower body (feet, legs, thighs) from moving upwards towards the breathing zone. Two designs, with round front edge made to fit around the manikin's abdomen – "cut board" (Figure 4. 4a) and with straight front edge – "straight board" (Figure 4. 4b) were tested.

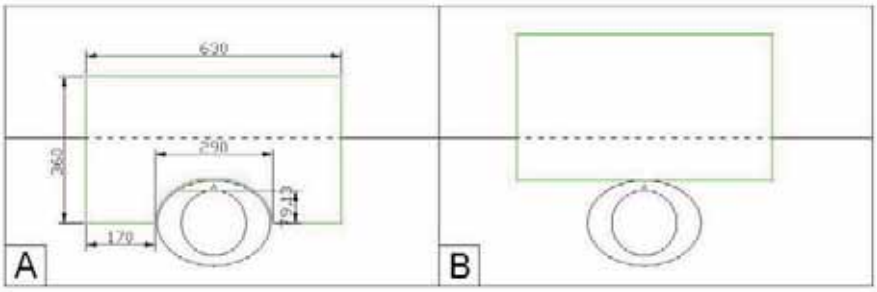

Figure 4.4 *The dimensions and positions of the board: a) with round front edge – "cut board"; b) with the straight front edge – "straight board".*

Figure 4.5 shows the PEE obtained with the RMP when the boards with different shape for passive control of the free convection flow were used. The PEE obtained with the RMP only, i.e. without the boards, is shown in the figures as well. The PEE obtained with and without board increases with the increase of the personalised flow rate. The comparison of the results obtained at 20 ^{o}C and 26 ^{o}C and at all PV flow rates studied show substantially higher PEE obtained with the boards than with RMP alone, i.e. the performance of the PV improved when the boards were used regardless of the shape – "cut" or "straight". Both at 20 ^{o}C and 26 ^{o}C the maximum increase of the PEE with the board is observed already at 6 L/s. The impact of the room air temperature on the strength of the free convection flow can be seen from the results in the figures obtained at 4 L/s and 6 L/s. The increase of the room temperature from 20 ^{o}C to 26 ^{o}C decreased the strength of the free convection surrounding the occupant's body and made its penetration by the personalized flow easier. The differences in the PEE obtained with the two boards at the same personalized flow rate and air temperature were small and could be due to differences in positioning of the boards.

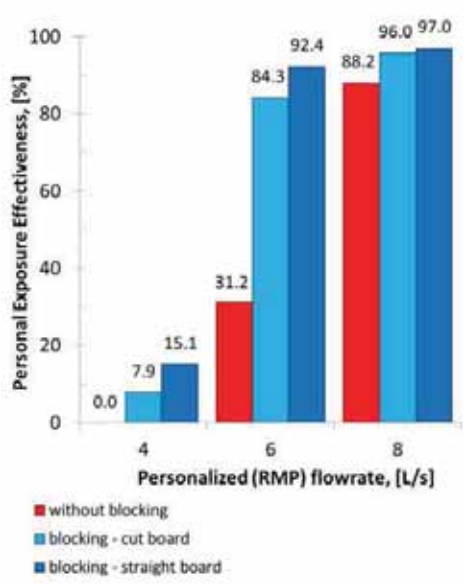

a)

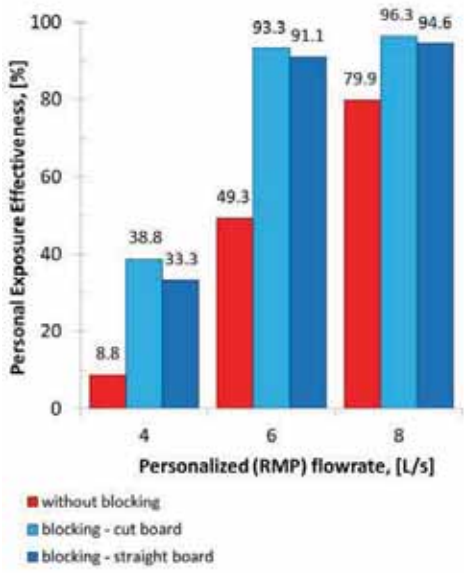

b)

Figure 4.5 *The effect of the board on PEE of RMP: a) at 20 °C, b) at 26 °C.*

4.2.3. Active control method

Like the passive method, the device for active control aimed to reduce the convection flow arising from the lower part of the body and to prevent it joining the flow originating from the lower chest. This appliance consisted of a box with mounted 6 ordinary PC fans of 1.5 W each (in 2 rows of 3 fans per row). The device, named "suction box", was installed below the desk with its front edge aligned to the edge of the table (Figure 4.6). The front and the rear set of 3 fans could be operated separately. The air sucked from the fans was exhausted in the test room more than 1 m away from the manikin in order to avoid disturbances of the personalized flow and the free convection flow.

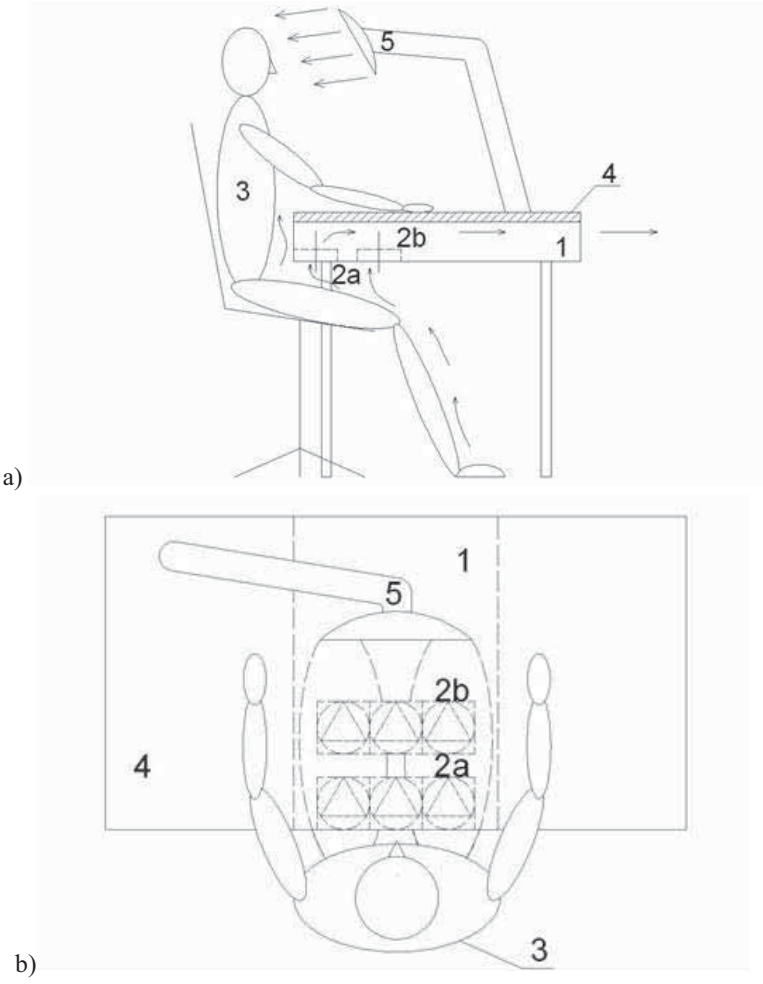

Figure 4.6 *Desk with active control device (the suction box) installed bellow the table; a) Side view; b) Top view. Legend: 1) "suction box"; 2a) front fans; 2b) rear fans; 3) manikin; 4) desk; 5) RMP.*

Figure 4.7 shows the results for PEE when the RMP was used together with the suction box with either front fans or rear fans in operation. The PEE obtained with the RMP only, i.e. without the "suction box" is also shown in the figures as a reference case. The results look quite similar to the results obtained with the board. The PEE obtained with and without fans in operation increases with the increase of the flow rate. The comparison of the results obtained at 20 oC and 26 oC and at all flow rates studied show substantially higher PEE obtained with the fans in operation than with RMP alone, i.e. the performance of the PV improved when the suction box was used. Both at 20 oC and 26 oC the maximum increase of the PEE is obtained at 6 L/s. The effect of the suction box on the PEE is much greater at 20 oC than at 26 oC. This result is in contrast to what was expected and could be due to disturbances by suction. The impact of the room air temperature on the strength of the free convection flow can be seen from the results obtained at 4 L/s and 6 L/s: the increase of the room temperature to 26 oC decreased the strength of the free convection and made its penetration by the personalized flow easier at the lower flow rates resulting in higher values of the PEE. No big difference was noticed between the front or rear fans performance as a whole, although for most of the studied cases slightly better results were achieved with the front group of fans operating, for those were closer to the torso and the thighs, where the convection flow became stronger (formed by joining of the flow emerging from legs and the one originating from groins).

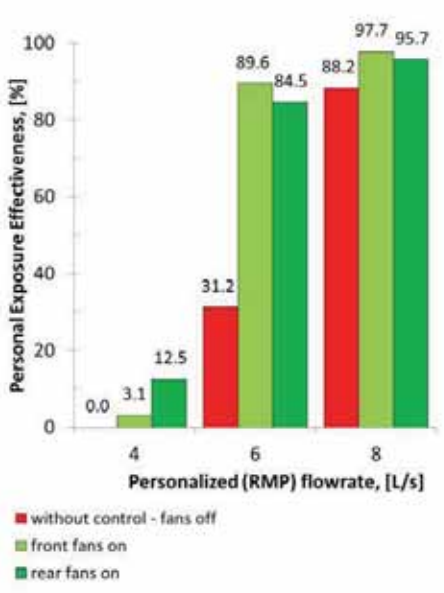

a)

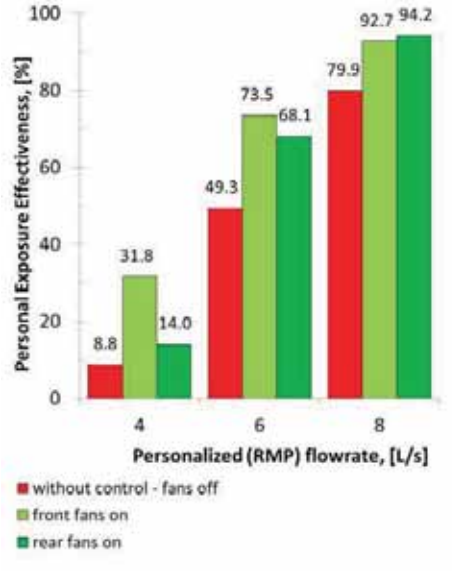

b)

Figure 4.7 *The effect of the fans on PEE of RMP: a) at 20 °C, b) at 26 °C.*

The discussed so far results were obtained when the fans were running at half power (15 V). Figure 4.8 compares the results for the PEE obtained with fans operating at 15 V and 30 V at identical other conditions (personalized flow rate of 8 L/s and air temperature of 26 °C). The PEE was substantially greater when the fans were operated at half power (15 V) than at full power (30 V). One reason for this result can be that the fans operated at full speed create quite strong local suction effect that draws the RMP jet downwards and away from the mouth. This was further investigated by detail measurements of the velocity field performed by Particle Image Velocimetry (PIV). The results of these measurements are discussed later in this chapter.

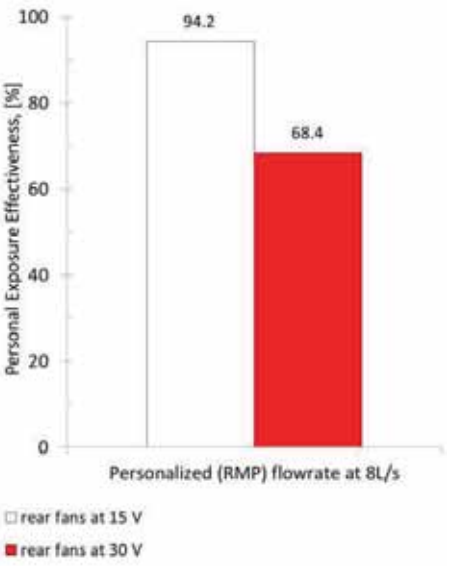

Figure 4.8 *Comparison between half power and full power of the fans.*

4.2.4. Hybrid (active and passive) control method

The results obtained with the "straight" shape board and the "cut" shape board combined with either front or rear fans are shown in Figure 4.9 and Figure 4.10 respectively. At 8 L/s the PEE reached quite high values (above 90%). In almost all studied cases, the simultaneous use of the fans and the boards did not improve the PEE in comparison with the use of the boards alone. For some of the measurements the use of fans and board at the same time led even to a decrease in the PEE. The comparison of the results in Figures 4.9 and 4.10 show that for many of the tested conditions the combination of the boards with the front fans in operation performed slightly better than the combination of the boards with the rear fans.

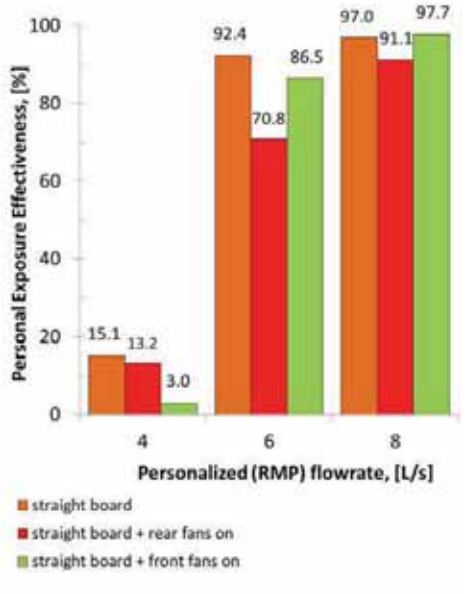

a)

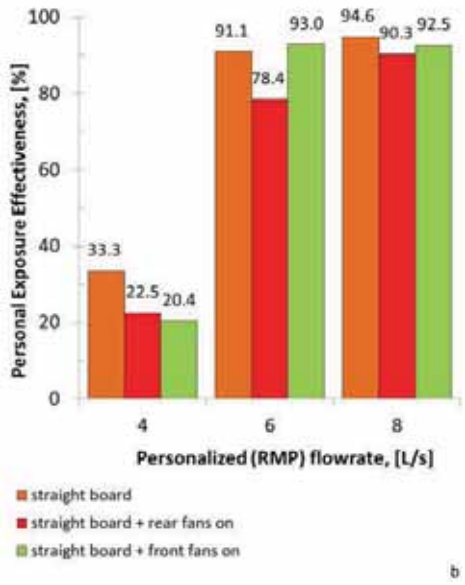

b)

Figure 4.9 *The effect of the fans together with the straight board on PEE of RMP: a) at 20 °C, b) at 26 °C.*

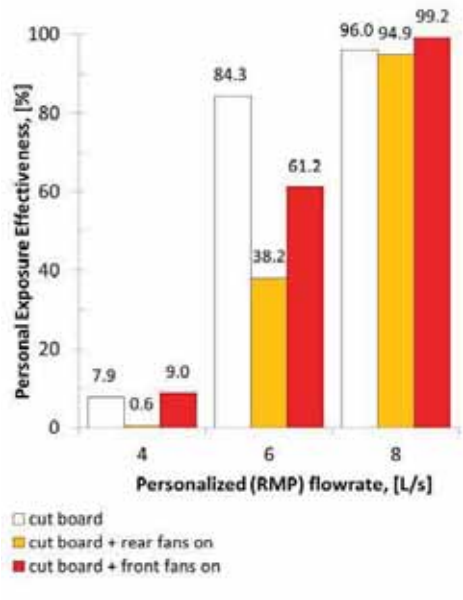

a)

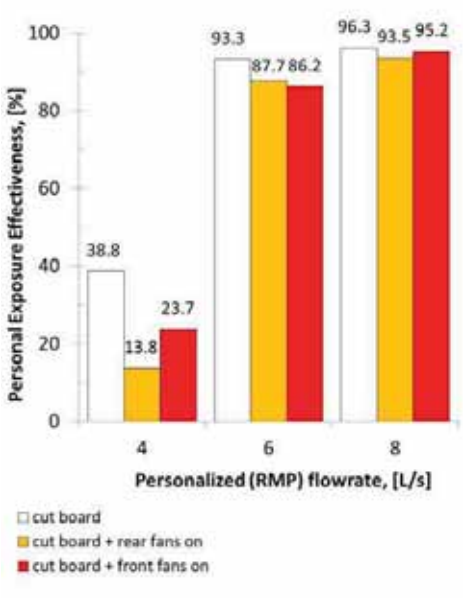

b)

Figure 4.10 *The effect of the fans together with the cut board on PEE of RMP: a) at 20 °C, b) at 26 °C.*

The documented potential of this method to improve the inhaled air quality at reduced amounts of PV air supplied and thus to reduce the risk from airborne cross infection can be easily

implemented in an office environment. A small retractable board, fixed with springs/guides to the desk-top, can gently press against the stomach of a seated person and follow the natural movements back and forth. Such retractable boards exist already and are used to position the keyboard and mouse of a PC. Therefore a slight modification in the design could be applied as mentioned above. The active method (using the fans) can be directly connected to the PV via a plenum box. So the air extracted by the fans could be cleaned and filtered and supplied via the PV nozzle. These two methods can lead to potential energy savings especially the passive as it uses no energy at all. For the active method the energy consumptions of the fans is 1.5 W or 4.5 W in total, so still there might be energy savings as a result from the reduced amount of PV air (less air conditioned) or in the case of room recirculation (as mentioned above) even bigger savings could be achieved. However this needs to be studied in details.

All three methods for control of the free convection flow around the occupant's body combined with the PV unit RMP, i.e. active, passive and hybrid are discussed in details in **Paper II**, **Appendix II**.

4.2.5. Exhausting the free convection layer

The next few methods aimed for control of the free convection flow at the breathing zone. The efficiency of the methods was studied with a seat incorporated PV device similar to that reported by Melikov et al. (2007). In the present design an extra pair of control nozzles was attached below each of the PV units situated at head level at both sides of the head. Two types of nozzle designs were used, i.e. large and small. The dimensions (supply opening area) of the four nozzles were 0.08 x 0.15 m (0.012 m^2) for the large PV nozzle, 0.08 x 0.08 m (0.0064 m^2) for the small PV nozzle, 0.06 x 0.15 m (0.009 m^2) for the large control nozzles and 0.06 x 0.08 m (0.0048 m^2) for small control nozzles (Figure 4.2). The four control strategies as defined in the beginning of this chapter were applied in order to improve the performance of the seat incorporated PV with regards to inhaled air quality.

The results obtained with the use of the large nozzles when strategy 1 was applied, i.e. exhausting part of the free convection layer at the upper chest level, are presented in Figure 4.11. It can be seen that in all cases the "suction" improved the performance of the PV system considerably compared to the reference case noted as "no suction", i.e. only PV air supply from headrest nozzles. The only case where PEE was over 90% was at 26 ^oC, at PV flow rate of 8 L/s and a suction flow rate of 16 L/s. For all conditions studied the results were better when suction was at 16 L/s than at 8.5 L/s, except at the PV flow rate of 8 L/s and 20 ^oC (possibly due to inaccurate positioning of the manikin in relation to the nozzles).

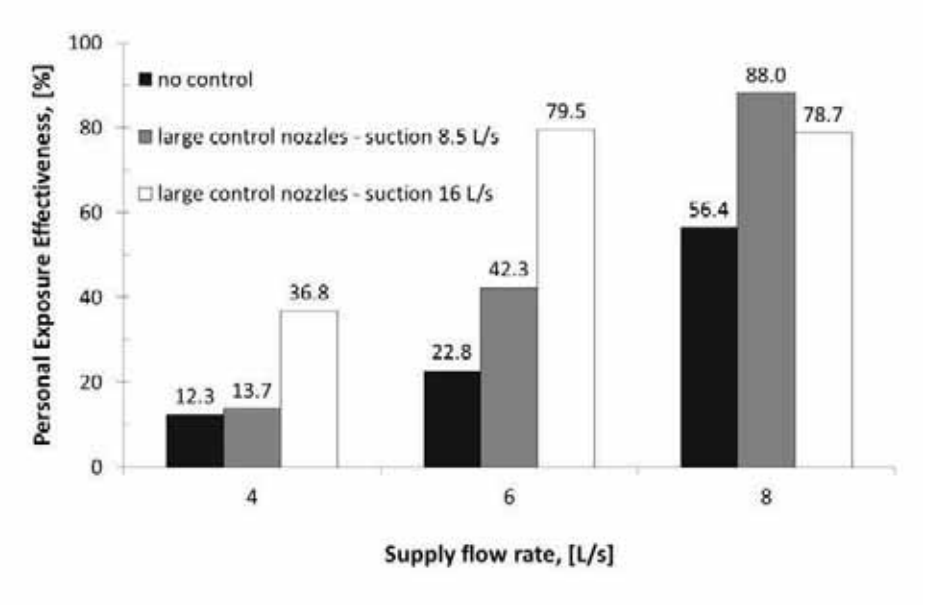

a)

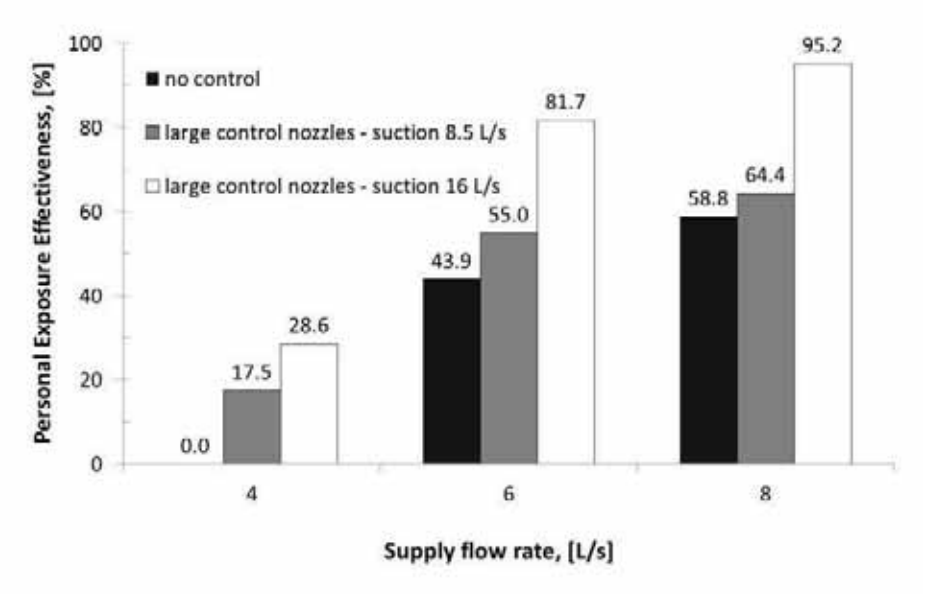

b)

Figure 4.11 *PEE obtained with the large nozzles when control strategy 1 ("suction" mode) was applied: a) at 20 °C and b) at 26 °C.*

Figure 4.12 shows the PEE obtained with control strategy 1 when the small PV nozzles were combined with the corresponding small control nozzles under the "suction" mode. The results

reveal that exhausting part of the free convection air enhances its penetration by the personalized air. The substantial improvement was observed only at 20 ^{o}C and at 4 L/s. In this case the PEE improved substantially from 44.4% to 78% when 8.5 L/s were exhausted through the controlled nozzles and 86.2% when 16 L/s were exhausted. The effect of exhausting the free convection flow with the small control nozzles at 26 ^{o}C was not consistent (Figure 4.11b). In fact at the PV flow rate of 6 L/s and 26 ^{o}C the highest PEE was obtained when the control nozzles were turned off, i.e. when the control strategy was not applied. Due to the weak convection flow, the suction may have affected the discharge of the personalized flow. In general, the results with the small nozzles reveal that control strategy 1 was not so efficient for improving inhaled air quality at a high room air temperature and nozzles with a small cross section area. The discharged personalized flow with relatively high velocity (the cross section of the smaller nozzles being almost half as big as the cross section of the large nozzles) was strong enough to penetrate the free convection flow, even without being weakened by the air suction at the shoulder level. Thus the effect of the suction flow of 8.5 L/s and 16 L/s on inhaled air quality improvement with the small nozzles could mainly be seen when the PV flow was weakest (at the lowest flow rate of 4 L/s) and the free convection flow was strongest (at room air temperature of 20 ^{o}C).

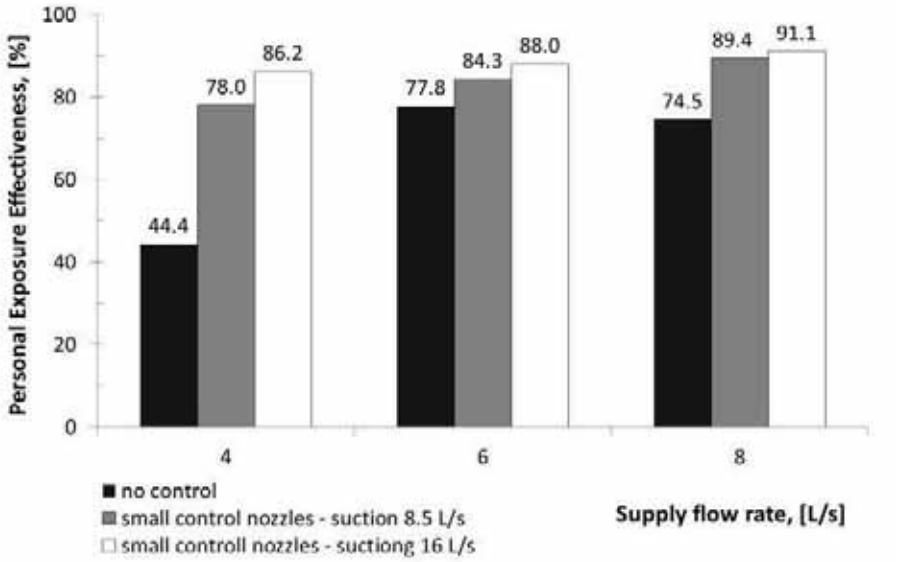

a)

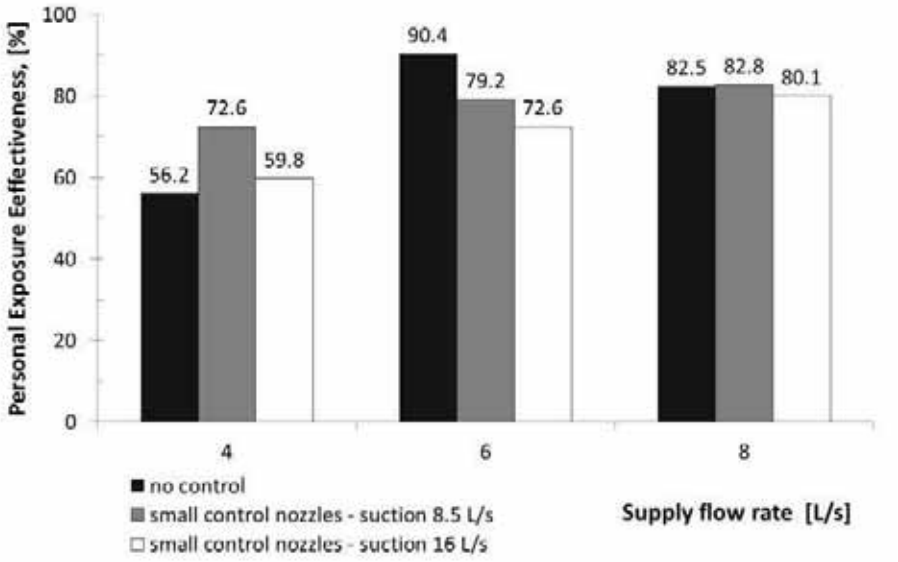

b)

Figure 4.12 *PEE obtained with the small nozzles when control strategy 1 ("suction" mode) was applied: a) at 20 °C and b) at 26 °C.*

4.2.6. Supplying room air from the control nozzles

The room air supplied from the control nozzles against the free convection flow aimed at peeling off the free convection flow and thus making it easier for the personalized air to reach the mouth/nose (control strategy 3). The results from pre-tests performed with the large nozzles at 20 °C, 8 L/s PV flow rate and 8.5 L/s supplied from the control nozzles revealed much higher PEE values when clean air was supplied from the control nozzles, rather than when room air was delivered as can be seen from the comparison in Figure 4.13. The use of control flow of room air to push down and peel off the free convection flow resulted in a decrease of the PEE from 56.4% without control flow to 47.4% with control flow. The control flow of polluted air supplied at shoulder level with relatively high velocity (0.47 m/s at discharge opening) caused mixing and reduced the ability of the personalized flow with lower initial velocity (0.33 m/s) to provide clean air to inhalation. The supply of a controlled flow of clean air caused mixing but also dilution of the polluted free convection flow which resulted in a substantial increase in the PEE, from 56.4% without control flow to 79.7% with the control flow. Therefore it was decided that only supplying clean air through the control nozzles should be studied further. In the following up set of experiments, lower flow rates from the control nozzles were selected, namely 3 L/s and 4.5 L/s, to reduce the total amount of clean air needed. However, control supplying lower flow rates of room air through the control nozzles may prove to be effective as well. This needs to be further studied.

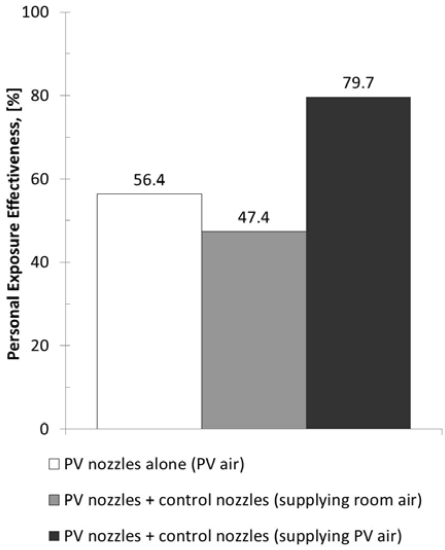

Figure 4.13 *PEE with PV nozzles only for control strategy 2 (to peel off the free convection air by supply of polluted room air) and control strategy 3 (diluting the convection air with clean personalized air supplied from the controlled nozzles). Results obtained with large nozzles, personalized airflow of 8 L/s, airflow supplied from the control nozzle supply 8.5 L/s, air temperature 20 °C (isothermal) are compared.*

4.2.7. Insertion of PV air into the free convection layer

Insertion of part of the clean personalized air in the free convection flow from the control nozzles at the chest level and part of it suplied from the headrest diffusers (control strategy 2) was studied under different conditions. The PEE obtained with the large PV nozzles when clean air was supplied from the large control nozzles is shown in Figure 4.14. At 20 °C, the improvement in the PEE compared to the reference case when clean air was supplied only from the PV nozzles, was dramatic. At a PV flow rate of 4 L/s about 80% PEE was achieved and at 6 L/s PEE exceeded 90%. In fact this was due to the additional amount of clean PV air supplied by the control nozzles. At 26 °C the improvement due to the additionally supplied air from the control nozzles was much smaller (Figure 4.14b) than at 20 °C. At the higher PV flow rates studied, the difference in the PEE with and without redistribution of the PV air decreased as the supply velocity of the personalized flow increased, and thus even without "deflecting" and diluting the convection flow with the control flow the PV flow was able to penetrate and reach the breathing zone of the occupant. At 26 °C the highest PEE achieved was about 71%. The results were slightly better when discharging 4.5 L/s than 3 L/s from the two control nozzles. The buoyancy effect, due to the temperature difference between the supplied PV air and the natural convection flow, was different when the PV air was supplied at 20 °C and 26 °C and this together with the different strength of the free convection flow at the two temperatures may have had an effect on the airflow interaction at the breathing zone.

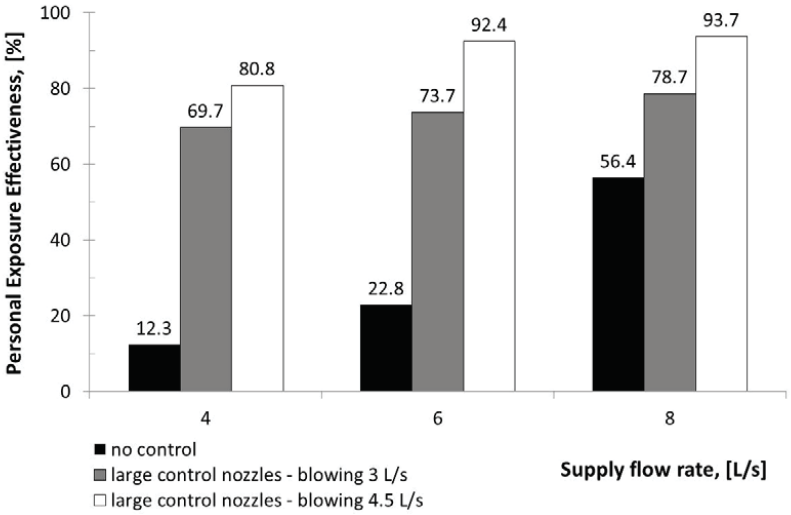

a)

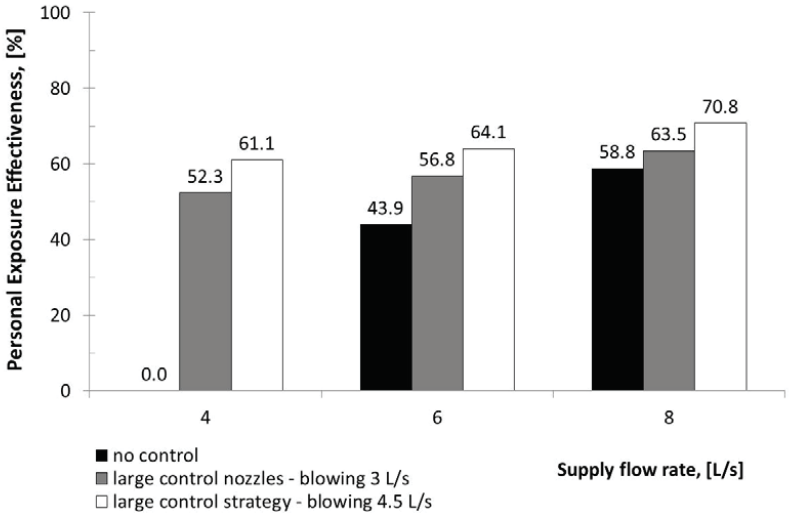

b)

Figure 4.14 *PEE obtained with the large nozzles when control strategy 3 ("blowing" mode) was applied: a) at 20 °C and b) at 26 °C.*

The PEE obtained with this control method when a portion of the clean air was supplied from the small control nozzles is shown in Figure 4.15 for three flow rates supplied from the PV nozzles. At 20 °C the clean air supplied from the control nozzles opposing the free convection flow had a positive effect in all flow rates studied (Figure 4.15a). At 26 °C (Figure 4.15b) the positive effect was achieved only at the PV flow rate of 4 L/s, where PEE increased from 56.2% without

control flow to about 75% when the control flow was applied. At PV flow rates of 6 L/s and 8 L/s the PEE was high (above 82%) and no improvement was achieved when the control flow was supplied. In fact the slight decrease in PEE may be due to the enhanced mixing. In all cases studied (except at 20 °C and PV flow rate of 4 L/s) the change of the control flow rate from 3 L/s to 4.5 L/s had almost no impact on the PEE.

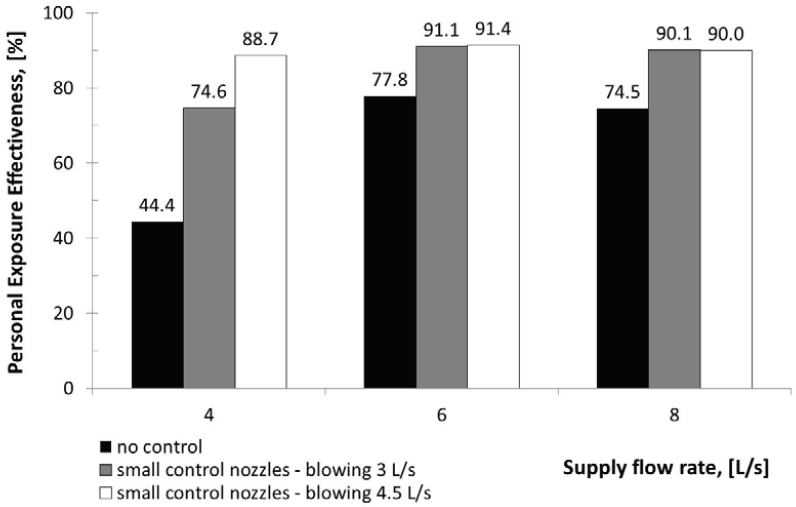

a)

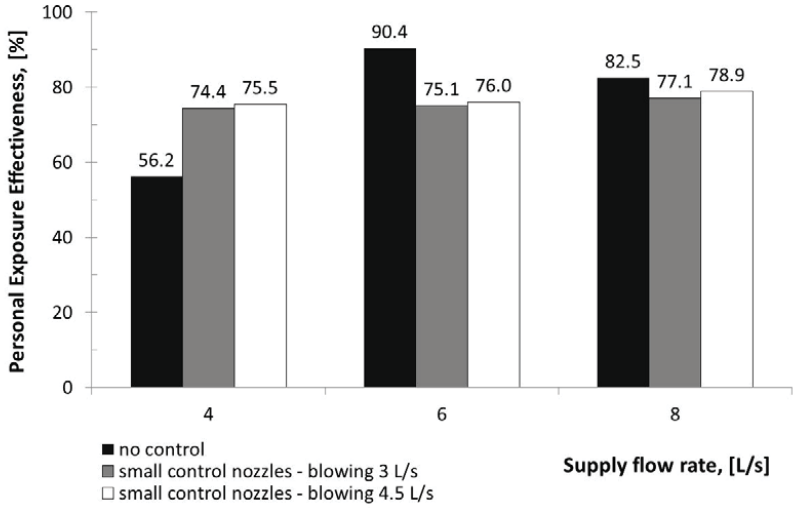

b)

Figure 4.15 *PEE obtained with the small nozzles when control strategy 3 ("blowing" mode) was applied: a) at 20 °C and b) at 26 °C.*

4.2.8. Supplying only through the control nozzles

The fourth control strategy, namely to insert clean air between the free convection flow and the body surface and use the buoyancy to move it upwards to the breathing zone required as less as possible mixing of the supplied clean air with the polluted free convection air. In this respect, the initial velocity of the supplied clean air flow is essential, especially when the free convection flow is weak. During these measurements, the PV flow was switched off. Figure 4.16 shows PEE obtained at 26 ^{o}C, i.e. when the free convection flow was relatively weak and the supplied clean air was warm and light. The results clearly demonstrate that when the supplied flow rate of the control clean air increases (3, 4.5 and 6 L/s) the portion of clean air in inhalation decreases from 36-44% to 16-18%, depending on the nozzle size. The momentum of the inserted flow increased with the increase of the flow rate and enhanced its mixing with the free convection flow. The nozzle size and the shape of the manikin's body (the simulated female shape with large non-uniformity at the chest in comparison with the relatively flat chest of a male body) may play a role as well. The large nozzles covered a larger area of the chest region so the interaction with the convection flow was evenly distributed. With the small control nozzle there may be regions, such as between the breasts, where the interaction was weak and less mixing took place which explains the better performance of the latter.

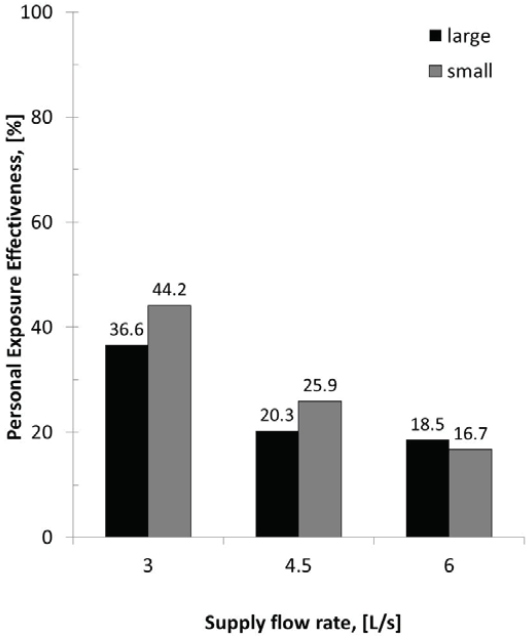

Figure 4.16 *PEE obtained with the large and small nozzles at 26 ^{o}C when control strategy 4 (supply of clean air beneath the free convection flow) was applied.*

The discussed methods can be easily implemented in places where people spend most of

the time seated and do not move much like public transportation sector (buses, planes, cars) or in the entertainment (theaters, cinemas, opera theaters etc.), public or health care sectors (waiting rooms, auditoriums, lecture rooms etc.). They can also be applied in office environment incorporated into the chair design with the back support following the back and forth movement of the person, so that the PV and control nozzles are always within the range of the seated occupant's breathing zone. Furthermore, due to the reduced flow rates some energy savings may result. However this needs to be further studied

All four methods for control of the free convection flow around the occupant's body with the seat incorporated type of PV unit are discussed in details in **Paper III, Appendix III**.

4.3. Control of the Personalized Flow for improved inhaled air quality

As already reported in the previous section, initializing control over the free convection layer by decreasing its strength, helps enhance the air quality at the breathing zone of the occupant at reduced amounts of clean PV air supply, compared to the case with no control. Thus the control diminishes the risk from airborne cross-infection by simply making it possible more clean air to end up into inhalation (Chapter 4, Section 4.2). Another way to improve inhaled air quality is to replace the boundary layer by supplying a stream flow of clean air over the front part of the body directed upward towards the breathing zone. To reduce entrainment of polluted room air the stream of clean air supplied tangentially to the body surface needs to be shielded from the surroundings. For this purpose additional jet of air needs to be added on the outer side of the clean air stream. This system of two jets can be installed in a board similar to the one used in the previous experiments that gently protrude and press the abdominal area of the seated occupant. The performance of this method of personalized air supply, referred in the following as confluent jets, was studied and is discussed in the present section.

Another way to improve the inhaled air quality by supplying the clean personalized air within the free convection layer as close as possible to the breathing zone was examined as well. The idea is to avoid the mixing of the clean personalized jet with the surrounding polluted room air and thus to increase the portion of clean PV air into the air inhaled. Other advantage of this method is that the amount of clean personalized air will be greatly reduced as the PV nozzle with a small size will be immerged into the convection flow just a few centimeters away from the mouth/nose of the user. Bolashikov et al. (2003) incorporated a small nozzle around the microphone of commercially available headset and used breathing thermal manikin to study its performance. Their results showed that more than 80% of the air inhaled by the breathing thermal manikin was clean air supplied by the small nozzle. However the initial conditions of the flow, i.e. shape of opening and initial velocity, as well as positioning from face and direction of the supplied personalized flow were not studied in details.

In this chapter, results obtained from study of the defined above two methods for control of the airflow interaction at the breathing zone for improved air quality are briefly presented and discussed. For more details refer to **Papers IV, V and VI, Appendixes IV, V and VI**.

4.3.1. Confluent jets

4.3.1.1 Method

The experiments were performed in a full-scale test room with dimensions 4.70 m × 2.40 m × 2.60 m (W×L×H). A workplace consisting of a desk with confluent jet device for PV, a light office chair (0.1 Clo) and a seated dressed thermal manikin (clothing thermal insulation of 0.5 Clo) was simulated in the room. Three fixtures (6 W each) located in the ceiling provided the background lighting. The room itself was built in a laboratory hall, 0.7 m above the floor. The walls of the test room were made of particleboard and were insulated by 0.06 m thick styrofoam. One of the walls was made from single thick layer glazing. The mixing type ventilation, used to condition the air in the test room to 26 ^{o}C, supplied 100% clean air (no recirculation) with an air change rate of 2.2 h^{-1}. This flow rate provided good mixing in the room at low velocity (below 0.2 m/s within the occupied zone). A rotation type air supply diffuser and a perforated circular air exhaust diffuser were installed on the ceiling. Air humidity was not controlled but was measured as being relatively constant (30% - 35%). The experimental facilities used in the present measurements with the confluent jets were the same as for the experiments described in the previous section, namely the experiments for control over the convection layer around a seated occupant.

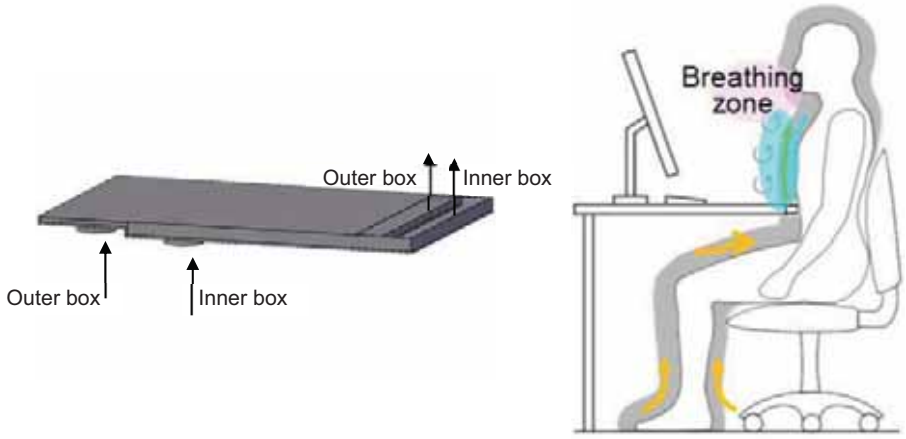

a) b)

Figure 4.17 *Confluent jet design as PV unit a) and its application at a workstation b).*

The air terminal device for the PV ventilation, generating two confluent jets, consisted of two plenum boxes (inner and outer box) nested in each other and placed below the desk top (Figure 4.17). The two boxes had discharge slots with length of 0.5 m and width which could be increased from 0 m up to 0.06 m. The results presented in the following were obtained with two sizes of the discharge slots, namely 0.06 m x 0.5 m (width x length) and 0.03 m x 0.5 m. The two boxes were attached so that the distance between the generated jets was 0.004 m, i.e. almost no distance between the jets. The boxes were pressed firmly against the abdominal area of the thermal manikin (Figure 4.17b). Each box had a separate supply fan to drive the supplied air. The box closer to the

manikin supplied always clean PV air (inner jet) while the outer box (close to table board rim) discharged room air. The fan of the outer jet that was used to drive the room air was placed in the test-room at the opposite corner relative to the manikin at a distance of more than 2.5 m. The temperature of the personalized air was maintained constant to the set value of 26 ^{o}C (same as that of the room) by an electrical heater installed in the PV supply system and a temperature sensor placed in the ducting before the PV supply box (inner jet). The temperuture of the outer jet was not controlled but was measured to be on average 0.5 ^{o}C higher than the room air temperature (due to the heat generated from the fan motor). The humidity of the supplied personalized air was not controlled or measured, but was assessed to be close to that in the room, 30 - 35% (isothermal conditions).

The performance of this method for controlof the airflow interaction for improvement of inhaled air quality was studied by tracer gas concentration measurement as well as PIV measurement of the generated velocity field. In this section the results of the tracer gas measurements are presented and discussed. The PIV measurements are discussed in the following section. The tracer gas (refrigerant R134a) was dosed in the air supplied by the background total volume ventilation system. As already stated the inner jet supplied outdoor clean air free from any tracer. The PEE index (defined in section 4.2) was used to evaluate the performance of the method with respect to inhaled air quality.

4.3.1.2 Results

The results for the air quality performance of the method of confluent jets with width either 0.03 m or 0.06 m as obtained at different supply flow rate are shown in Figure 4.18. Both boxes discharged same amount of air; the inner box supplied only clean PV air, while the outer box operated with recirculated room air mixed with tracer gas.

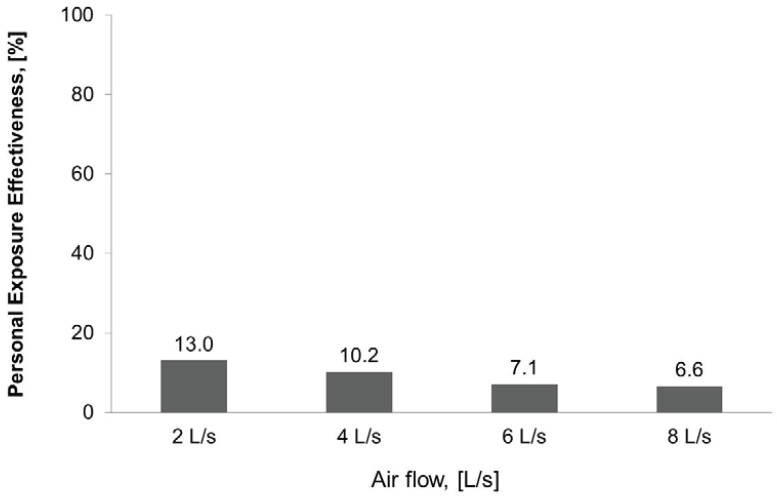

a)

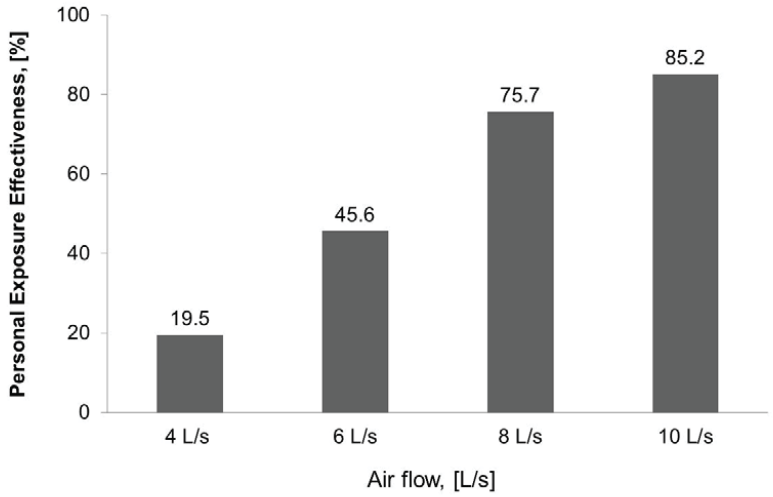

b)

Figure 4.18 *PEE as a function of flow rate. Both inner (PV air) and outer (room air) jets provide same amount of air at a) 30 mm and b) 60 mm width of both openings.*

When the width of both openings was kept at 0.03 m almost no clean air ended into inhalation. The reason is that the initial region of the jet, where it preserves its original characteristics, is two times shorter as compared to the case of jet with 0.06 m width of supply opening. The distance from the box position to the mouth of the breathing thermal manikin was about 0.42 m. Therefore by the time it reaches the mouth the jet is completely mixed with the surrounding room air.

For the big opening of 0.6 m it can be clearly seen that the inhaled air quality improves with the increase of the supplied flow rate. Already at 8 L/s the PEE reaches a value of 76% and 85% at 10 L/s.

The method of confluent jets was also studied when only one of the jets was used to supply the clean air, either the inner or the outer jet (Figure 4.19). When only the inner jet was operational the same amount of clean air into inhalation, 63%, was achieved at width of 0.03 m and 8 L/s as with 10 L/s and 0.06 m discharge width of the supplied jet. However in the latter case the velocity would be one and a half times lower. It is seen that by narrowing the width of the supply opening its effect on air quality can be compensated by increasing the initial velocity of the jet. However this approach is limited by risks from draught and sensation of dry eyes. The maximum PEE of 63% at 8 L/s (0.03 m width of opening) or 10 L/s (0.06 m width of opening), can be explained with the body geometry, the flow pattern of the convection flow around the human body and the face as well as the jet initial conditions.

The performance of the outer jet however with regards to air quality, was much more dependent on the width opening as a factor. With the width of 0.03 m the PEE varied around 23% and was independent of the flowrate. But when the width opening was changed to 0.06 m, and when

the PV air was supplied at the lower flowrate range, i.e. 6 and 4 L/s, the outer box performed much better compared to the inner box. The maximum performance with respect to air quality (PEE=52%) was achieved at 6L/s.

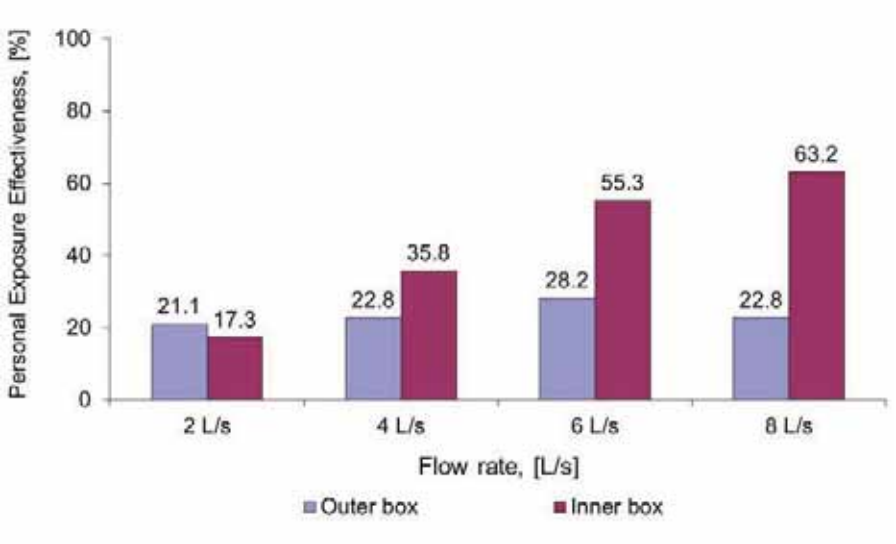

a)

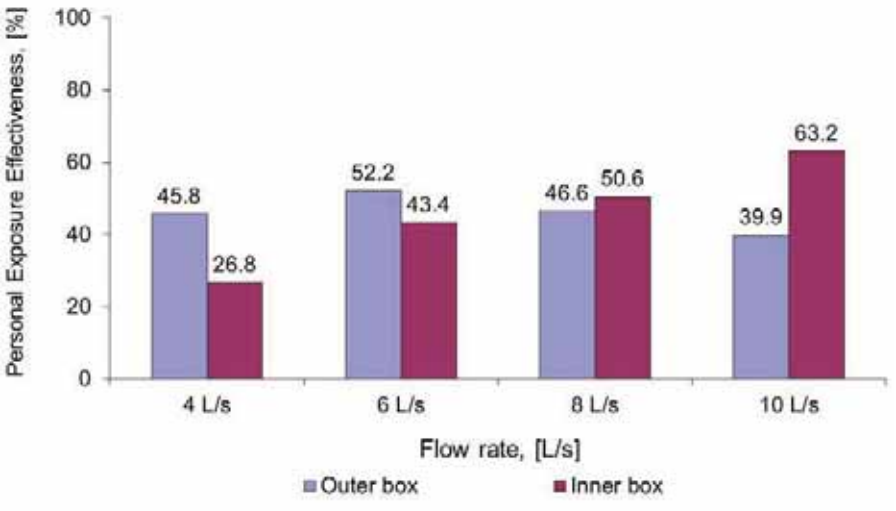

b)

Figure 4.19 *PEE as a function of flow rate. Either the inner or outer opening is working supplying clean air, when both openings are a) at 0.03 m and b) at 0.06 m.*

The effect of different discharge air flows and hence different initial velocities of the inner and the outer jets on PEE was also studied with discharge opening of 0.06 m, as it showed better

results. In these cases the supply flow rate of the inner jet was equal to, two times or half of the air flow from the outer jet. The results of these tests are shown in Figure 4.20.

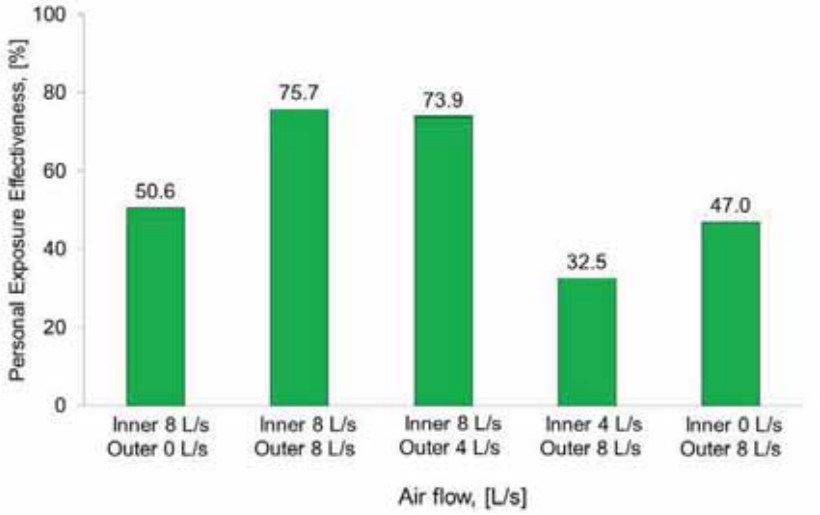

Figure 4.20 *PEE as a function of the difference in the discharge amount of air (air velocity) of the inner and the outer jets at 0.06 m width opening.*

The results in Figure 4.20 show that reducing two times the velocity of the outer jet has no effect on the PEE (74% PV air was inhaled), while in the opposite case, i.e. reducing 2 times the air flow of the inner jet, the amount of clean air in inhalation drops almost 2.5 times. The assisting effect of the outer jet increased the PEE from 51% to 76%.

The impact of body posture on the performance of the method was studied as well. The breathing thermal manikin was positioned backwards or forward (bending it over the table to simulate writing or reading tasks). The results obtained at 0.06 m width of the supply openings (for both inner and outer jets) and at the flow rate of 8 L/s are shown in Figure 4.21.

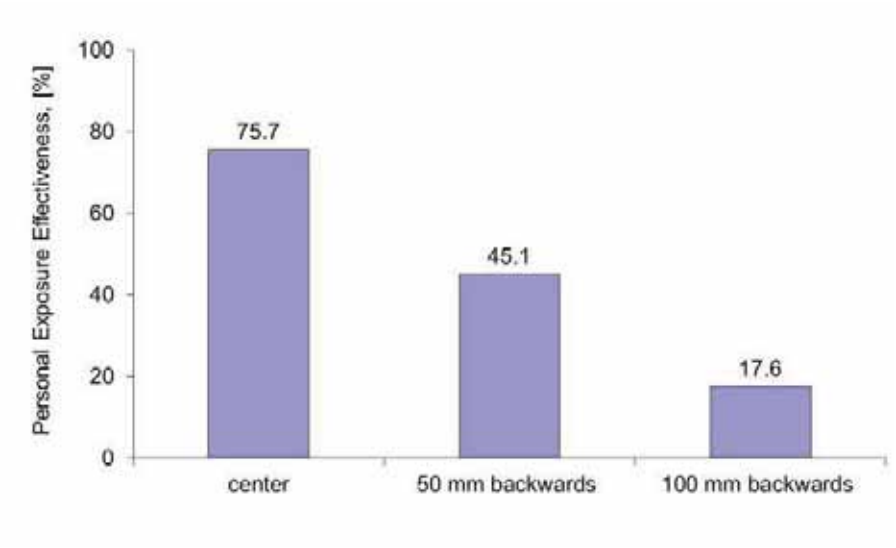

a)

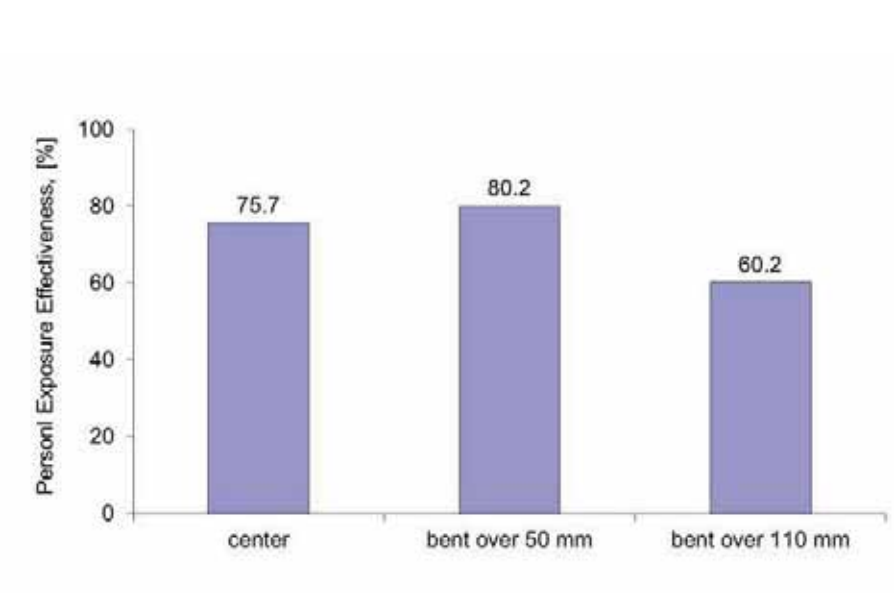

b)

Figure 4.21 *PEE as a function of the positioning of the thermal breathing manikin a) when moving backwards from the table and b) when bending over the table when the width of both jets are at 0.06 m and both supply at 8 L/s.*

As can be seen in Figure 4.21 when moving backwards the effect of the PV on the amount of clean air into inhalation is quickly diminishing and at 0.1m away from the table the PEE is already less than 20%. However when bending over the table initially the PEE keeps relatively constant values (approx. 80%) and decreases to 60% when the tip of the manikin's nose is moved

0.11 m relative to the edge of the table. When tilting slightly the body over the table the angle formed by the jaws and the neck is not as acute as when the manikin is in horizontals direction and therefore, it is much easier for the air to overcome the chin, and end up in the breathing zone.

4.3.2. Inserted Jets

The method of improving the inhaled air quality, by inserting the personalized air into the free convection flow and close to the mouth/nose in order to avoid mixing with the polluted surrounding air, was examined first by CFD simulations and then by physical measurements. The purpose of the CFD simulations was to collect data for better planning of the physical measurements. Some results are presented in **Paper IV** (CFD) and **Paper V** (physical measurements), **Appendix IV** and **Appendix V** respectively. In the following, the main findings of this study are presented.

4.3.2.1 CFD Simulation

4.3.2.1.1 Flow field analyzed

A room with dimensions 3 m×3 m×2.5 m (W x L x H) with a naked male body standing at the centre was simulated. The supply nozzle of the headset was placed 0.04 m away from the mouth. The complex shape of the human body, which was made up of 12,816 surface meshes and very similar to a real one, was adopted to account the impact of the local characteristics of the body shape on the free convection flow at the vicinity of the body. The skin surface area of the CFD human model was 1.46 m^2. The whole room was ventilated by a very slow constant horizontal isothermal flow (0.01m/s, 23 ^oC) from the whole surface of the wall facing the front side of the human body. Therefore, it was considered that the examination on the performance of the personalized airflow was carried out in a calm ambient environment.

4.3.2.1.2 Cases analyzed

In order to examine the impact of the shape and the positioning of the supply nozzle on the performance of the personalized airflow 6 cases were tested (Table 1). The nozzle opening was circular (round) in cases R1, R2 and R3 or ellipsoid in cases E1, E2 and E3. The air discharge area of the openings was identical for both nozzle types, and equalled to 0.0007 m^2 with a depth of 0.02 m. For both nozzle shapes studied, the position was in front of the mouth (Case R1 and E1), bellow the mouth (Case R2 and E2), and sideways relative to the mouth (Case R3 and E3), respectively (Figure 4.22 and Table 4.2). Regardless of the position of the supply nozzle, the distance between the geometric centre of the mouth and of the supply opening was 0.04 m in every case. The personalized airflow was always supplied at an airflow rate of 0.33 L/s (0.48 m/s) and isothermally, i.e. 23 ^oC towards the mouth in each case.

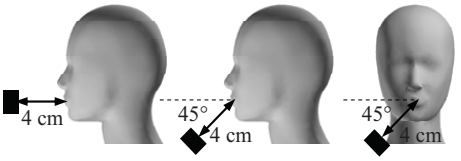

(a) in Case R1 and E1 (b) in Case R2 and E2 (c) in Case R3 and E3

Figure 4.22 *Positions of nozzle in each case.*

Table 4.2 *Measured conditions.*

Case	Nozzle type		Position of nozzle		
	circular	ellipse-like	front	below	side
R1	×		×		
R2	×			×	
R3	×				×
E1		×	×		
E2		×		×	
E3		×			×

4.3.2.1.3 Grid system

For the tested cases, the flow field simulated was made up of 34,700 triangular surface meshes and 665,000 volume cells. Prism-shaped cells were used for the first 4 cell layers placed directly over the skin surfaces and 5 cell layers placed over the other wall surfaces except for the surfaces of the nozzles (Omori et al. 2004). y+, which represents the non-dimensional normal distance (i.e. the wall coordinate) measured from the wall surface to the center of the first fluid cell, was less than 5 over almost all surfaces (Zhu et al. 2007). Previous research on the natural convection from a heated vertical flat board showed that the grid division can ensure sufficient precision for the simulation of the convection flow around the human body (Kato et al. 1993).

4.3.2.1.4 CFD method and boundary conditions

CFD analyses were conducted based on a low-Reynolds-number type k-ε turbulence model (Lien et al. 1996), using the SIMPLE algorithm (Table 4.3). The detailed boundary conditions can be seen in Table 4.4. It was assumed that the human body discharged the heat flux due to convection uniformly at a rate of 23.1 W/m^2 (total 33.8 W) (Zhu et al. 2004). Except for the human body, the other wall surfaces were assumed to be adiabatic. Human respiration was not taken into consideration during any of the simulations performed. The concentration distribution of personalized air was calculated by setting a passive scalar uniformly at the nozzle opening with an initial value of 1: the closer to 1 the concentration calculated at the mouth the better the performance of the PV nozzle. A value of 0 will mean that the air is completely diluted with room air.

Table 4.3 *CFD methods.*

Turbulence model	low-Reynolds-number type k-ε turbulence mode
Algorithm	SIMPLE
Space Scheme	First Order Up Wind
Grid System	Spatial cells: 665,000; surface meshes: 34,700

Table 4.4 *Boundary conditions.*

Ambient Supplying opening (front wall)	Velocity: 0.01m/s, Temperature: 23°C, Turbulence Intensity: 10 %, Turbulence Scale: 0.05m
Ambient Exhaust opening (back wall)	Velocity: free slip, Temperature: free slip
Supplying opening of nozzle	Velocity: 0.476 m/s, Temperature: 23°C, Turbulence Intensity: 10 %, Turbulence Scale: 0.05m
Human body surface	Velocity: no-slip, Uniform heat flux of 23.0W/m2 (quantity of convective heat loss)
Other walls	Velocity, Temperature: no-slip, adiabatic

4.3.2.1.5 Results

The results presented in Figure 4.23 show that although the distribution of personalized air's concentration was affected by the position of the supply nozzle, and was always over 70% around the mouth and nose in each case independent of the position of the supply nozzle. In Table 4.5, the average concentration of the personalized air at the mouth in each case is listed. The average concentration at the mouth was over 0.85 in all of the studied cases. By comparing the concentration values in the cases using the same supply nozzle (circular or elliptical), it was noticed that the value was smallest when the supply nozzle was placed bellow the mouth, and largest when the supply nozzle was put sideways to the mouth. In the case from below the jet glides over the mouth with its natural width, while in the case of side supply it covers better the shape of the mouth, while naturally "spreading".

Table 4.5 *Personalized air's concentration at the mouth surface [-].*

Case	R1	E1	R2	E2	R3	E3
Shape of nozzle	circular	ellipse-like	circular	ellipse-like	circular	ellipse-like
Position of nozzle	in front of the mouth		bellow the mouth		sideways to the mouth	
Concentration	0.969	0.938	0.927	0.856	0.978	0.950

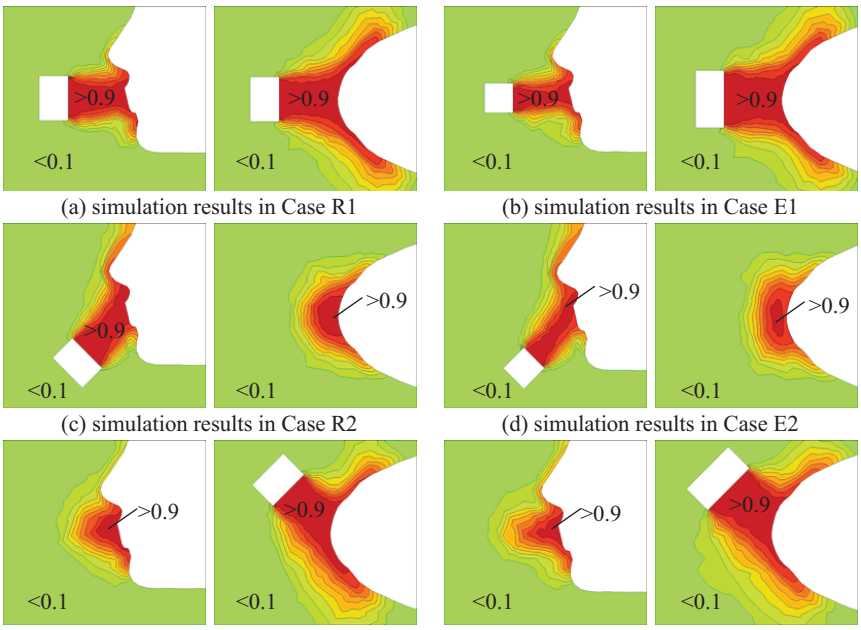

(a) simulation results in Case R1 (b) simulation results in Case E1

(c) simulation results in Case R2 (d) simulation results in Case E2

(e) simulation results in Case R3 (f) simulation results in Case E3

Figure 4.23 *Personalized air's concentration distribution in the area around the face at the vertical section across the middle of body and the horizontal section across the centre of the mouth in each case [-].*

4.3.2.2 Full Scale Physical Measurements

4.3.2.2.1 Method

The experiments were designed and performed in a full-scale test room with dimensions 4.70 m × 1.62 m × 2.60 m (W×L×H). Three ceiling-mounted light fixtures (6 W each) provided the background lighting. A workplace consisting of a desk with a seated breathing thermal manikin, an ordinary light office chair (approximately 0.05 Clo based on contact with the manikin) and personalized ventilation ATD that generated the inserted personalized jet, were used in the set-up (Figure 4.24).

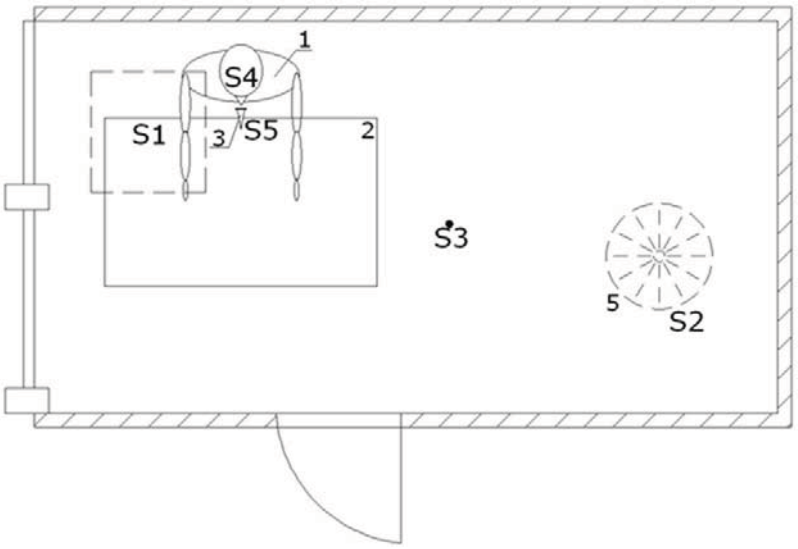

Figure 4.24 *Experimental set-up: 1 – breathing thermal manikin; 2 – desk; 3 – PV with headset ATS; 4 – supply ATD; 5 – exhaust ATD. Tracer gas sampling positions: S1- Supply air; S2 – Exhaust air; S3 – Room; S4 – Artificial lungs; S5 – Personalized air.*

Mixing type background air distribution was used to condition the air in the test room. The air supply diffuser (a rotation diffuser) and the air exhaust diffuser (a perforated circular diffuser) were installed on the ceiling (Figure 4.24). The supplied air was 100% outdoor (no recirculation was used) with a flow rate of 15 L/s, which corresponded to an air change rate of 2.7 h^{-1}. This flow rate provided good mixing in the room with relatively low velocities (less than 0.15 m/s). A slight under-pressure of 1.4 Pa, resulting in 30 L/s at the exhaust, was kept during all the experimental conditions in order to avoid a flow of air from the test room to the tall hall. The supply air temperature (21 ^{o}C) and flow rate (15 L/s), as well as the exhaust flow rate were controlled during all the measurements.

A separate HVAC system was used to supply the personalized air at a specific controlled temperature and flow rate. The temperature of the supplied PV air was controlled by an electric heater installed downstream of the main fan with a temperature sensor placed close to the PV ATD. The humidity of the supplied PV air was not controlled, but was close to that in the room due to the fact that the PV air was supplied at the same temperature as the room air, and both were 100% outdoor air. The flow rate, supplied from the tested ATDs generating the inserted jets, was measured close to the PV nozzle with the help of a Venturi tube with an outer diameter of 0.025 m. The Venturi tube was calibrated prior to the experiments. Nine headset nozzles were chosen to be tested: three with a circular initial cross-section of diameters 0.025 m, 0.03 m and 0.035 m respectively, three nozzles with an elliptic initial cross-section and equivalent diameters of 0.025, 0.030 and 0.035 m (Figure 4.25a) and three lobed jet nozzles with circular, four-leafed clover and six-edged star shapes with a free area equal to the free area of a circular jet of a diameter of 0.025 m (Figure 4.25b). The circular and elliptic nozzles had the shape of a cone with a sloped angle of 7^{o}

and a fine mesh at the end made of copper sheet of thickness 0.0005 m. The lobed nozzles were cut on a plastic hemisphere with a diameter of 0.045 m and a wall thickness of 0.002 m. The circular lobed nozzle was chosen as a reference for the other two lobed nozzles as well as for comparison with the circular jet. The circular and elliptic ATDs were attached to the PV supply system via a 0.50 m long medical silicon pipe of an outer diameter of 0.008 m and wall thickness of 0.001 m. The lobed jet ATDs were attached via a 0.50 m long flexible pipe of 0.035 m diameter. A specially designed mechanism was used to secure firm positioning of the nozzles. The mechanism was attached to a traverse that allowed for fine adjustment in all three coordinates of a Cartesian coordinate system relative to the facial plane of the manikin (Figure 4.25c).

A breathing cycle of an average healthy person performing light physical work was simulated: 2,5 s inhalation, 2,5 s exhalation and 1,0 s break with a respiration flow rate 0,24 L/s (Hyldgaard 1996). The air exhaled by the manikin was warmed to 33.6 °C, in order to ensure a density close to that of air exhaled by a human being.

During these experiments the breathing mode was set to inhalation mouth exhalation nose. Inhalation and exhalation through the mouth may be common for many people when talking. However, breathing only through the mouth was not used, because due to the design of the airway system the uncertainty in measurement of the gas concentration in inhaled air was relatively high. When the exhalation is through the mouth only one jet (with initial velocity of 2.4 m/s for the mouth opening of the used manikin) will result.

The total heat load generated in the test room was 88 W (12 W/m^2). The experiments were performed at an air temperature of 23 ^{o}C (as it is the boundary between winter and summer comfortable room air temperatures recommended in the present thermal comfort standards ISO 7730-2005, ASHRAE 55-2004) and under isothermal conditions, i.e. room air temperature equal to the personalized air temperature. The manikin was positioned with its abdomen at a distance of 0.1 m from the edge of the desk. During the measurements the manikin was dressed with clothing thermal insulation of 0.6 Clo. The manikin was set in comfort mode to resemble an occupant in a state of thermal comfort at light sedentary activity, namely office work, with the corresponding dry heat loss of 1.2 Met, i.e. 69.8W ISO 7730-2005.

The personalized airflow rate was chosen to provide the initial jet velocities of 0.2, 0.4 and 0.6 m/s. Velocity lower than 0.2 m/s might result in full deflection of the jet upwards even though the nozzle is immersed into the boundary layer. The velocity of 0.6 m/s was substantially higher than the velocity of the convection flow. Velocity higher than this could result in an unpleasant sensation and draught for the user, i.e. “too localised effect”, as reported by Kaczmarczyk et al. (2006). The distance between the face of the manikin and the nozzles (0.02, 0.04, 0.06 m) was one of the parameters studied during the experiments as well.

For the headset circular nozzle of diameter 0.030 m, additional measurements were performed that studied the effect of positioning the device relative to the face of the manikin, namely from front, below and side (Figure 4.26)

a)

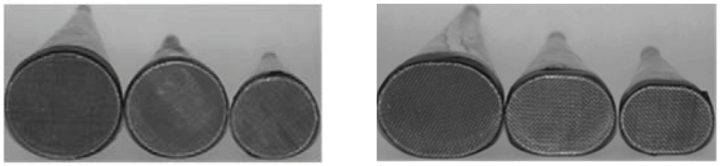

b)

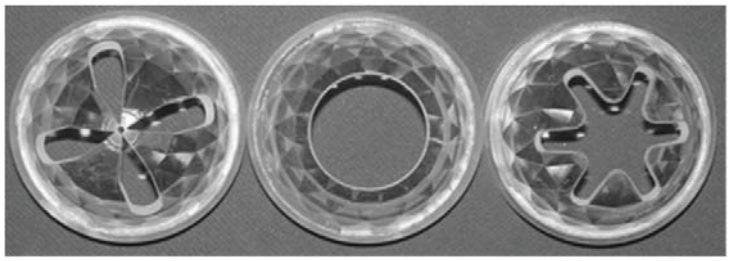

c)

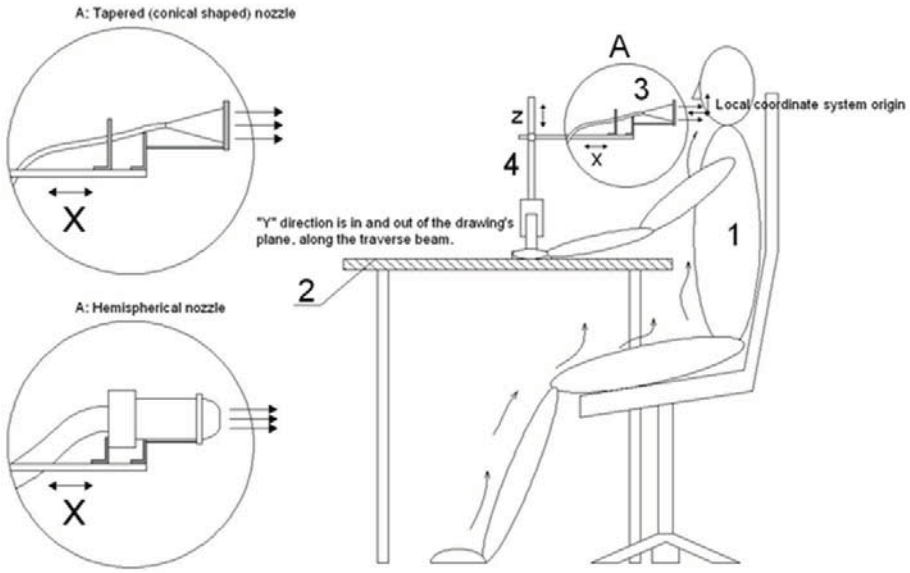

Figure 4.25 *The circular and the elliptical nozzles of the three sizes of 0.035, 0.030 and 0.025 m (a) and the lobed nozzles of 0.025 m equivalent diameter (b) and (c) positioning of the nozzle (3) with respect to the thermal manikin's face (1) as fixed on the support mechanism attached to the traverse (4) and placed on the table (2).*

Tracer gas, Refrigerant R134a, was used to simulate pollution/airborne pathogens laden nuclei (d < 2 μm) in the room air. During the measurements a constant dose of tracer gas was supplied in the duct of the background total volume ventilation system upstream of the ceiling diffuser. The personalized air was free of tracer gas. The air exhaled by the manikin was outdoor clean air with no tracer gas in it. The air inhaled by the manikin, after being analysed, was

exhausted in the TV exhaust system so as to avoid pollution of the tall hall where the climate chamber was situated. During all the measurements the lungs were situated outside of the experimental chamber.

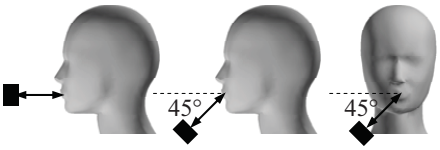

Figure 4.26 *Positioning of the circular nozzle of diameter 30 mm relative to the manikin's face: a) front, b) below, c) side.*

The tracer gas was sampled at 5 points and its concentration was measured by a real-time gas monitor based on the photo-acoustic principle of measurement. The positioning of the 5 sampling points is shown in Figure 4.24. Measurements at Point S3 (Figure 4.24), positioned at 1.1 m above the floor, were used to justify whether or not good mixing in the room was achieved, i.e. when the concentration in the supply, in the exhaust and at the point S3 was close and within 1 – 2 ppm fluctuations.

The inhaled air quality was assessed by the PEE as already described in the above text. The experiments performed at the air temperature of 23 ^{o}C (different flow rates, nozzles, etc.) were completely randomised to avoid biasing. To minimize the error in aligning the nozzle to the centre of the manikin's mouth, a laser beam level meter was used. In more details the experiment is described in **Paper IV, Appendix IV**.

4.3.2.2.2 Results

In Figure 4.27 the results obtained for the PEE with the inserted jet supplied from the nozzles with equivalent diameter of 0.025 m at initial velocity of 0.2, 0.4 and 0.6 m/s, and at the three distances from the mouth, 0.020, 0.040 and 0.060 m, are compared. The results were obtained with nozzles positioned in front of the face and towards the mouth, i.e. with the inserted jets transverse to the free convection layer around the body. The closer the nozzle to the mouth and the higher the velocity, the higher the PEE value measured. The results clearly showed the importance of control of the characteristics of the PV flow for the inhaled air quality. The PEE achieved with the lobed jet of clover nozzle geometry was the lowest and only little or no change in PEE resulted, regardless of the distance of the nozzle from the face and the supplied flow rate. The low performance resulted from the intensive initial mixing in the jet due to the complex initial turbulent structures. The PEE obtained with the star lobed jet was better than the jet from the clover nozzle, but still not as high as the one obtained with the circular or the elliptical nozzles. However, at 0.040 and 0.060 m and velocity of 0.4 m/s the six-star lobed jet performed equally well compared to the circular and elliptic jet, and at 0.6 m/s it became even slightly superior in air quality performance.

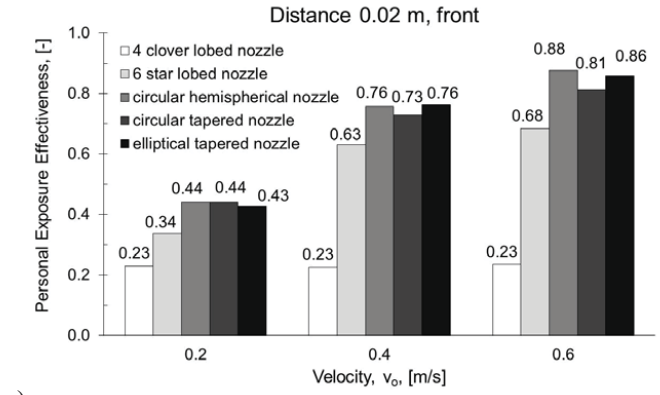

a)

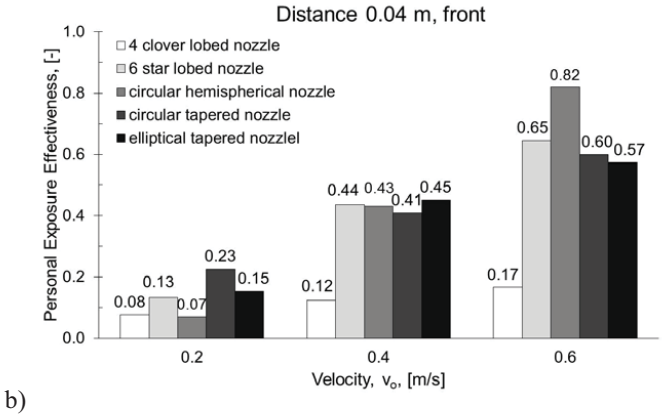

b)

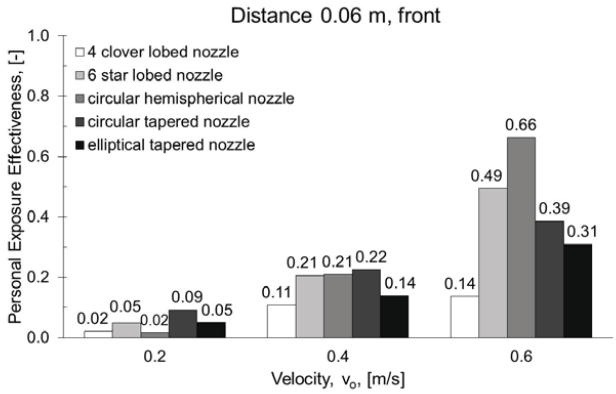

c)

Figure 4.27 *Comparison of air quality performance of the tested PV headset nozzles (diameter 0.025 m) for the three different distances and from front relative to the facial plane: a) 0.02 m, b) 0.04 m, c) 0.06 m.*

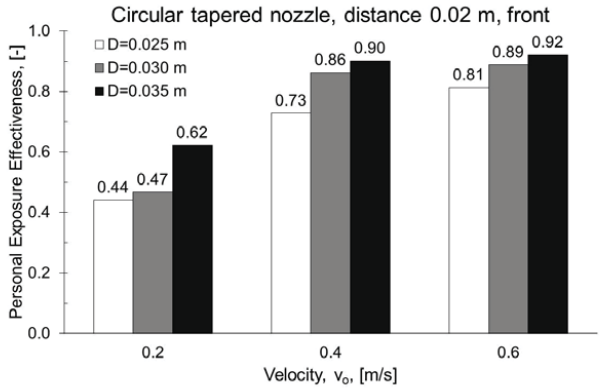

a)

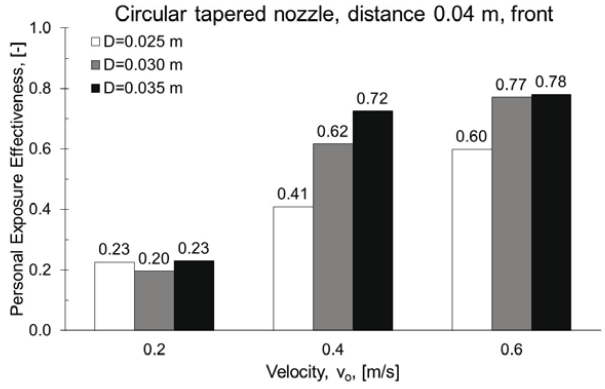

b)

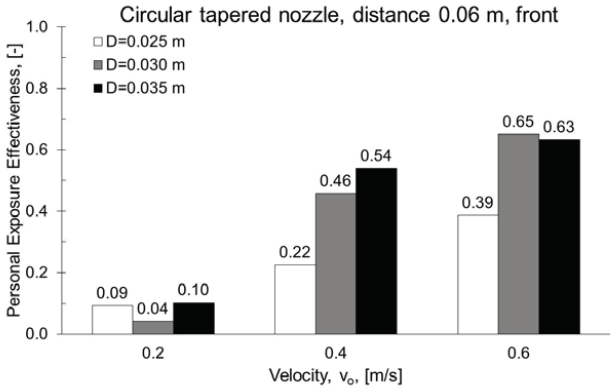

c)

Figure 4.28 *Air quality performance of the circular PV headset nozzles (0.025, 0.030 and 0.035 m diameters) at the three different distances tested and from front relative to the facial plane: a) 0.020 m, b) 0.040 m, c) 0.060 m.*

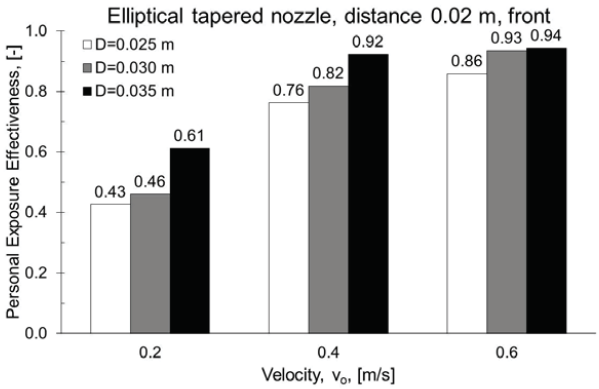

a)

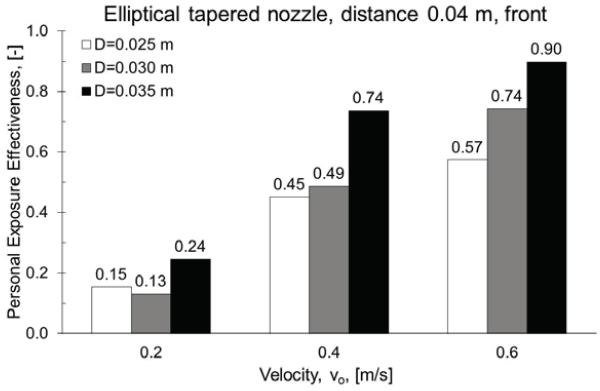

b)

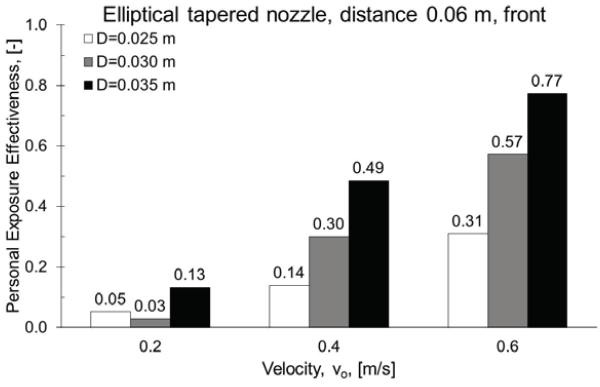

c)

Figure 4.29 *Air quality performance of the elliptical PV headset nozzles (25, 30 and 35 mm diameters) at the three different distances tested and from front relative to the facial plane: a) 0.020 m, b) 0.040 m, c) 0.060 m.*

Figure 4.28 shows the impact of the initial diameter of the inserted jet on the PEE index. The results were obtained with the circular shaped headset nozzles with the three different diameters (D = 0.025, 0.030 and 0.035 m), at the three distances and the three velocities tested. The inserted jets were generated with nozzles positioned horizontally towards the manikin's face. All the circular nozzles showed the same trend of increasing the amount of clean PV air in inhalation with the increment of the supply velocity. Both the initial diameter of the nozzle, the initial velocity and the distance of the nozzle from the face were parameters that influenced the PEE index. The greater the diameter, the more air was supplied to achieve the same initial velocity, and hence more cleaner air into inhalation resulting in a maximum PEE value of 0.92 achieved with the circular nozzle of diameter 0.035 m, initial velocity of 0.6 m/s and a distance of 0.020 m in front of the mouth. The distance was another important factor: the further the nozzle was moved from the mouth the lower the PEE value. The mixing of the PV jet with the free convection flow entraining polluted room air on its way upwards towards the mouth resulted in a PEE below 100% even when the nozzle was just 0.020 m away from the mouth and the supply velocity was as high as 0.6 m/s.

The results obtained with the elliptical nozzles under similar conditions as those for the circular nozzles are shown in Figure 4.29. The PEE values increased either with the increase of the initial velocity (0.2, 0.4 and 0.6 m/s) of the inserted jet, or with the increase of the initial equivalent diameter of the nozzle (0.025, 0.030 and 0.035 m), or with the decrease of the distance between the nozzles and the mouth (0.060, 0.040 and 0.020 m). The maximum PEE=94% was achieved with the largest nozzle (diameter of 0.035 m) at 0.6 m/s initial velocity and 0.020 m frontal distance from the mouth. As the performance of the round jet with a diameter of 0.030 m was slightly better than that of the elliptical jet (Figure 4.28 and Figure 4.29), the former nozzle was chosen for investigating further the effect of directing the inserted jet supply of clean air to inhalation, namely from the front, from the side and from below (Figure 4.30). Only the personalized flow with an initial velocity of 0.4 m/s, strong enough to penetrate the free convection flow at the face region, without causing discomfort due to draught and "dry" eyes", was studied. For the shorter distances of 0.02 and 0.04 m studied, the direction of insertion of the jet had almost no effect on the overall air quality performance. However, at the distance of 0.06 m the best performance was obtained when the inserted jet was directed from the side. When supplied from the side, the inserted jet covered a larger area of the mouth compared to the other two cases from front and below (longitudinal to the mouth). With an increase of the distance between the jet discharge area and mouth the jet also increased its width, covering even better the mouth and the surrounding inhalation zone.

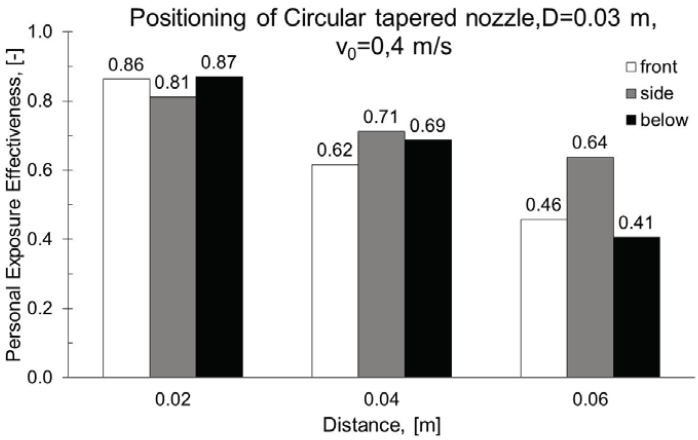

Figure 4.30 *Comparison of the air quality performance of the circular PV nozzle (D=0.030 m), for the three directions of the headset relative to the facial plane, front, side and below.*

4.4. Identification of flow field of the airflow interaction at the breathing zone using PIV measurements

In order to understand the studied complex interaction of flow, detailed Particle Image Velocity (PIV) measurements were performed for most of the studied control methods. Comprehensive large database of velocity and turbulence filed was collected and analyzed. This chapter presents the results of the velocity filed. These results are used to explain the findings reported in the previous section of this chapter. The results on the microstructure of the flow at the breathing zone, i.e. turbulence intensity, micro-scales of turbulence, energy spectra, etc., is not part of this thesis and will be presented in future publications. Peer review paper on the results presented in the following is under preparation.

4.4.1. Method

4.4.1.1 Experiment set-up

The experiment was designed and performed in a full-scale test room with dimensions 4.70 m × 1.62 m × 2.60 m (W×L×H). Three ceiling-mounted light fixtures (6 W each) provided the background lighting. A workplace consisting of a desk with a seated breathing thermal manikin, an ordinary light office chair (approximately 0.05 Clo based on contact with the manikin) and personalized ventilation ATD that generated the inserted personalized jet, were used in the set-up.

The test room itself was built in a laboratory hall, 0.7 m above the floor. The laboratory hall had a separate ventilation system, allowing for temperature control and hence reduced heat transfer (the air temperature of the laboratory hall was kept at the same level as that of the test room itself). The walls of the test room were made of particleboard and were insulated with 0.06 m thick styrofoam plates. One of the walls was made from thick single-layer glazing.

4.4.1.2 Total volume ventilation

Mixing type ventilation was used to condition the air in the test room. The air supply diffuser (a rotation diffuser) and the air exhaust diffuser (a perforated circular diffuser) were installed on the ceiling (Figure 4.3). The supplied air was 100% outdoor (no recirculation was used) with a flow rate of 15 L/s, which corresponded to an air change rate of 2.7 h^{-1}. This flow rate provided good mixing in the room with relatively low velocities (less than 0.15 m/s). A slight under-pressure of 1.4±0.1 Pa, resulting in 30 L/s at the exhaust, was kept during all the experimental conditions in order to avoid a flow of air from the test room to the tall hall. The supply air temperature (19 ^{o}C, or 25 ^{o}C) and flow rate (15 L/s), as well as the exhaust flow rate were controlled during all the measurements.

4.4.1.3 Personalized ventilation

The PV units used to perform the PIV measurements with some of the control strategies studied, were the RMP (Chapter 4, Section 4.2) and the Confluent jet PV (Chapter 4, Section 4.3). Each PV unit tested supplied room air in order to keep up the required seeding for the PIV measurement requirements.

4.4.1.4 Thermal manikin

A thermal manikin with body shape and size of an average Scandinavian woman 1.7 m in height was used to resemble an occupant. Same manikin was used also in the tracer gas experiments and is described in Section 4.2.1. The surface temperature of the thermal manikin was controlled to simulate a person in a state of thermal comfort at light sedentary activity and to realistically recreate the existing around the body convection boundary layer. Some conditions were tested also with the manikin turned off, i.e. absence of boundary layer in order to see its impact on the flow interaction within the breathing zone.

During all PIV measurements the breathing option was disabled, i.e. no breathing.

4.4.1.5 Setup of PIV equipment

The experimental setup is illustrated by a sketch in Figure 4.31. A laser generator was placed frontally, illuminating the face of the breathing thermal manikin from the front and along the axis bisecting the body in two symmetric halves. In additional experiment a radiator panel (0.6 m x 0.7 m, H x L) was illuminated at the middle vertical line. Two cameras were placed on the same side of the light sheet next to each other or above each other (35 mm lenses above the 60 mm lenses CCD cameras). One of the cameras was set normal to the laser sheet, while the other was directed at an angle of 89^{o} relative to the laser sheet. The f-numbers (the focal length divided by the "effective" aperture diameter) were set to between 4 and 5.6 for both cameras to reduce the light budget of the particle scattering and reflections from the face of the breathing thermal manikin. The PIV equipment included a double cavity New Wave Solo 120XT Nd-YAG laser (wavelength 532 nm), capable of delivering light pulses of 120mJ. However the light pulses emitted were up to 60% of the maximal value. The pulse width, i.e. the duration of each illumination pulse, was 10 ns. The light sheet thickness at the measurement position was 2 mm and was created using a combination of a spherical convex and a cylindrical concave lens. The equipment also included two Dantec

Dynamics Hi Sense MkII CCD cameras (1344×1024 pixels) equipped with 35 mm and 60 mm lenses and filters that only pass light with wavelengths close to that of the laser light. A calibration target was aligned with the laser sheet. This target was a metric ruler, which was registered by focusing the two cameras to obtain the geometrical information required for reconstructing the velocity vectors received from each camera. Thus a full description of the velocity components in the laser defined plane was obtained. Calibration images were recorded with both cameras. A linear transform was applied to these images for each camera respectively to perform the reconstruction. This procedure was executed before each set of experiments to assure that no drift had occurred.

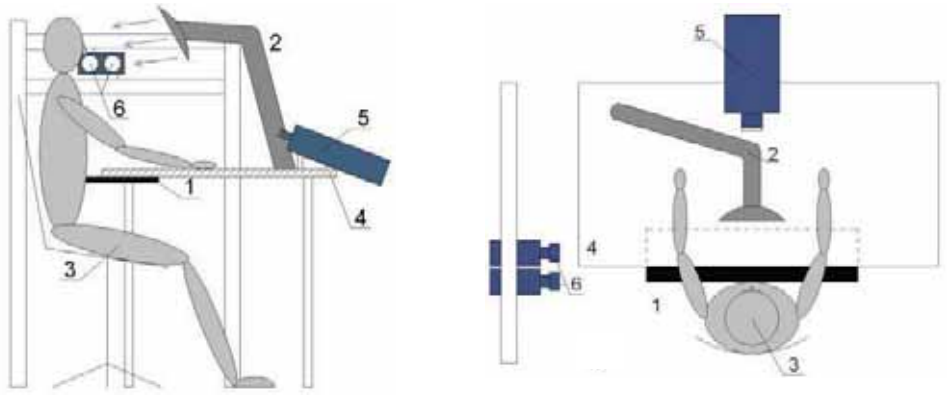

a) b)

Figure 4.31 *PIV set-up of the experiment with the RMP a) side view and b) top view. 1) passive control method – straight board, 2) RMP, 3) thermal manikin, 4) table, 5) laser generator, 6) digital cameras.*

Seeding, consisting of glycerol droplets with a diameter of 2-3 μm, was added to the supplied total ventilation air flow (mixture of water and pure glycerol in volume parts 7 to 3). The seed particles were added before the TV supply plenum box in order to obtain a more homogeneous distribution of the tracers throughout the measurement chamber without significantly disturbing the flow pattern inside. The droplets were produced by blowing pressurized air over a thin-walled pipe with diameter of 0.5 mm. The other end of the pipe was submerged in the glycerol and water solution. The size of the seed particles has been measured by an APS TSI 3320 time-of-flight spectrometer.

The PIV technique was used to study the airflow at the vicinity of the manikin as a result of the methods applied for control of the free convection layer around the manikin as discussed in the previous section, i.e. passive, active and hybrid combined with the RMP and also the board (passive method) with incorporated confluent jets as PV application. The boundary layer over the vertical heated plate (the radiator) was studied for comparison with the free convection development at the front of the manikin as well. In all studied cases with personalized flow, i.e. the RMP and the confluent jet system, the supplied air was taken from the measurement room where the seeding was injected. This was done with the help of a voltage controlled fan in the case of RMP and a pair of the same voltage controlled fans for the confluent pair of PV jets. The set-up assured that the seeding dosed in the room was also introduced into the PV flow. The fans were

placed more than 2 m behind the manikin or the heated radiator and below the supply total volume diffuser in order to avoid any effect of the fans on the velocity field measured by the PIV technique.

4.4.1.6 Data processing

The images were processed using Dantec Flow Manager © software version 4.7. Adaptive correlation was applied using refinement with an interrogation area size of 32×32 pixels. Local median validation was used in the immediate vicinity of each interrogation area to remove spurious vectors between each refinement step. The overlap between interrogation areas was 50%. For each measurement position 1000 realizations were acquired. The recording of image maps was done with time between pulses and trigger rate dependent on the PV flow rate supplied by the RMP or the confluent jets: from 2 700 to 12 000 μs and from 0.2 to 2 Hz respectively. The highest time between pulses corresponds to the cases when only the convection flow was measured and the lowest to the case of PV at 8 L/s. The disparity was typically around 0.05 pixels, i.e., smaller than the optimal measurement accuracy of the PIV system (0.1 pixels). No calibration correction was therefore applied.

4.4.1.7 Spatial resolution and accuracy

The velocity vector maps contain 73 by 63 vectors. The interrogation areas have linear dimensions 0.115 m in the y-direction and 0.173 m in the x-direction for the 60 mm lenses and 0.201 m in the y-direction and 0.258 m n the x-direction for the 35 mm lenses. The spatial resolution of the velocity vector fields is defined by the size of the interrogation area, which also limits the spatial resolution of the estimation of velocity gradients and hence vorticity. In order to resolve the smallest scales in the flow, one needs to fulfill the Nyquist criterion. Therefore, scales smaller than half of the size of the interrogation area cannot be resolved. Since the PIV velocity measurements are local averages over the area of interrogation, one can never obtain measurements closer to the wall than half of the height of the interrogation area size. And even then one needs to be careful in interpreting the measurements, because of the high velocity gradients in this region that are averaged out across the interrogation window.

Table 4.6 *Control parameters for evaluation of correlation noise.*

Control parameters	
$N_I \geq 10 - 20$	Particle image density N_I - mean number of particle images in an interrogation area.
$F_O \geq 0.75$	Loss of particles due to out-of-plane motion F_O - fraction of particles present inside the interrogation area in both images.
$M\lvert\Delta U\rvert\Delta t/d_\tau \leq 0.5$	Velocity gradients M (pix/m) - image magnification ΔU (m/s) - difference in velocity across the interrogation area Δt (s) - time between acquired PIV images d_τ - mean particle image diameter

Several control factors important for evaluation of the correlation noise were considered. They are listed in Table 4.6. The dominating factor is the effect of velocity gradients, which was only altered by changing the image magnification and the time between pulses. If there are large velocity gradients in the flow, variations of particle displacement across the interrogation areas will lead to a broadening of the correlation peak. This will in turn lead to deterioration in the precision of the estimate of the position of the correlation peak. The choice of experimental design will therefore by necessity have to be a trade-off between precision and relative displacement error. If the velocity gradients vary across the measurement plane, one cannot design the experiment so that it is optimized over the entire measurement volume. The number of spurious vectors was always less than 5%, which shows that the effect of large velocity gradients in the flow on accuracy was not unwieldy.

Another source of error, which is not commonly considered, is the ability of the particles to follow the flow. This might be an issue, especially in regions of accelerating flow. This is however discarded from having any significant effect in the flow under consideration because of two reasons; the velocities are very low and the distribution of particles in the PIV images is homogeneous.

4.4.1.8 Reflection reduction

Reflections from the face of the breathing thermal manikin entering the CCD cameras constituted a problem for two reasons. The reflections appeared along the profile of the face in the part of the measurement region, corrupting the signal in this area. If the high power reflections reach the CCD chip, one risks damage to the cameras in the form of dead pixel elements. Reflections were removed by applying a paper tape strip along the reflecting surfaces painted with a mixture of Rhodamine 6G and black non-shiny paint. When the radiator panel was used the front panel was painted: first sprayed with the Rhodamine 6G dye and then painted on top with a black non-shiny paint for ovens. Rhodamine 6G is a fluorescent dye, re-emitting the laser light with the wavelength slightly shifted from the absorbed one. The cameras were equipped with green-pass filters, which only permitted the wavelengths of the laser to pass, allowing the scattering from the particles to pass through and preventing strong reflections from surfaces to reach the CCD chip. Rhodamine 6G has its absorption peak at around 530 nm and emission peak at about 552 nm. This method was successful in reducing most of the unwanted reflections. An additional approach applied in some of the measurement was to slightly shield/move the laser beam, with 1- 2 mm backwards from the body symmetry bisecting plane. The effect of applying Rhodamine 6G made measurements with maximum laser power used close to the face of the manikin and the radiator possible for all measurement positions. The largest reflection reducing effect when measuring with the breathing thermal manikin was, however, obtained by introducing the minute shifting of the laser sheet, removing almost all of the reflections from the face and in particular at the nose and the mouth profile contour. Prior to applying this technique, reflections from the face corrupting the signal were detected as far as up to 0.03 m upstream of the manikin's face profile (at the nose and mouth area).

4.4.2. Results

The results from the PIV measurements are divided into two parts: based on control over the free convection layer and on control over the PV flow. The PIV measurements were done to complement and explain some of the results from the tracer gas measurements. Therefore in the following section the PIV results will be referred and compared to those from the tracer gas experiments.

4.4.2.1 Control over the Boundary Layer

The PIV measurements related to the control over the convection boundary layer in front of the thermal manikin were performed at 20°C isothermal case with the RMP PV nozzle and the control methods mentioned in chapter 4.2, namely the "active" and "passive" control methods. From the passive method the straight board was only selected as no difference based on the board shape was detected with regards to the amount of PV clean air into inhalation (Chapter 4.2.1, **Paper II**, **Appendix II**). From the active method only the front group of three fans was selected to operate either at half or full power in order to explain the lower performance compared to the case when the rear group was working (Chapter 4.2.2, **Paper II**, **Appendix II**). The impact of the hybrid method, comprising of the straight board with the front fans operated at half power only was studied as well.

The results presented and discussed in the following limit to the velocity profiles measured along the plane starting between the lips and away from the breathing thermal manikin (Figure 4.32). The velocities shown are in fact the magnitude (absolute value) of the resultant vector from the x and y component. In some of the graphs the values of the velocities are given as negative. This is done to account for the direction of the flow relative to the manikin attached coordinate system with origin the center point between the two lips (Figure 4.32). The positive "y" direction is upward, i.e. towards the nose, while the positive "x" abscise is in the direction pointed out from the lips and towards the room.

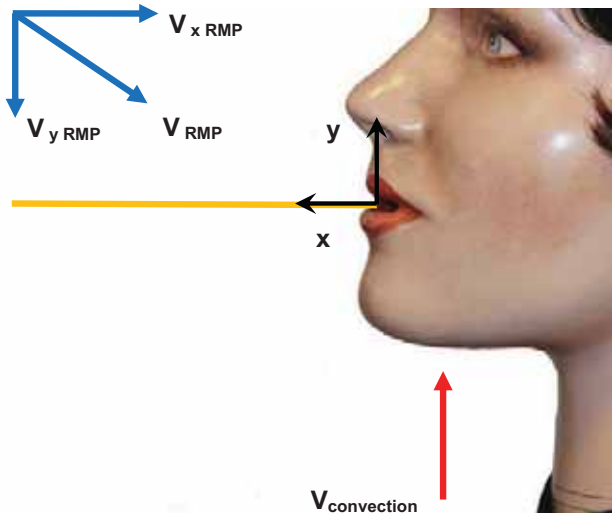

Figure 4.32 *The Measurement plane across the mouth of the thermal manikin with the coordinate system shown from the image made with the 35 mm lenses camera for the RMP.*

Figure 4.33 shows a typical vector diagram and scalar plot of the velocity profiles acquired with the 35 mm lenses camera when no control was applied over the free convection layer. As can be seen the upcoming flow hits the mandible and part of it passes sideways while some part of it continues upwards over the chin and separates from the face at the height of the nose. The region below the jaws and along the nose is characterized by low velocities as has been reported be Lewis 1964. More figures from each condition and with resolution lenses (35 mm) are shown in the **Appendix VII, Part 1**.

Figure 4.34 shows the velocity profile across the free convection layer at the mouth level of the breathing thermal manikin without and with the tested control methods. The applied method of control manages to reduce the peak velocity of the boundary layer close to the mouth almost two times. The presence of the board creates a barrier on the way of the upcoming free convection layer and results in development of "new" boundary layer that is thinner and more sensitive to obstacles and to the human body geometry. Another thing is that the board prevents the part of the free convection layer coming from the legs to join the one starting from the groins of a seated person. This results in deflecting part of the boundary layer away from the face by the mandible as its momentum is not high enough to keep it attached to the body surface (Figure 4.33). Introducing the fans in suction mode and half power, i.e. the active control (Section 4.2.2), resulted in pulling part of the convection layer downwards and explained the slower decay in velocity with distance as compared to the reference case when no control was applied (Figure 4.33 and Figure 4.34). Increasing the power of the fans to maximum ended up in further thinning in the convection layer as a result of the increased suction effect that also lead to the increase in velocity 0.06 m away from the mouth (Figure 4.33 and Figure 4.34). Combining the two methods, the passive and active (fans at half power), was very much the same as applying the fans at full power: the blocked free convection layer was subsequently sucked by the fans.

a)

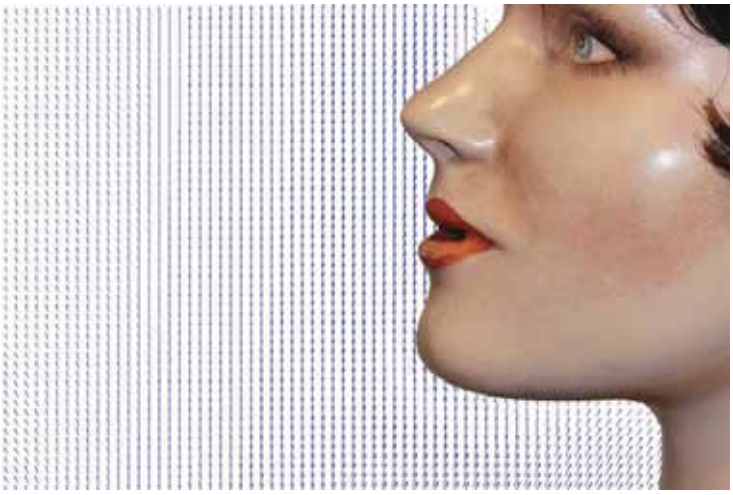

b)

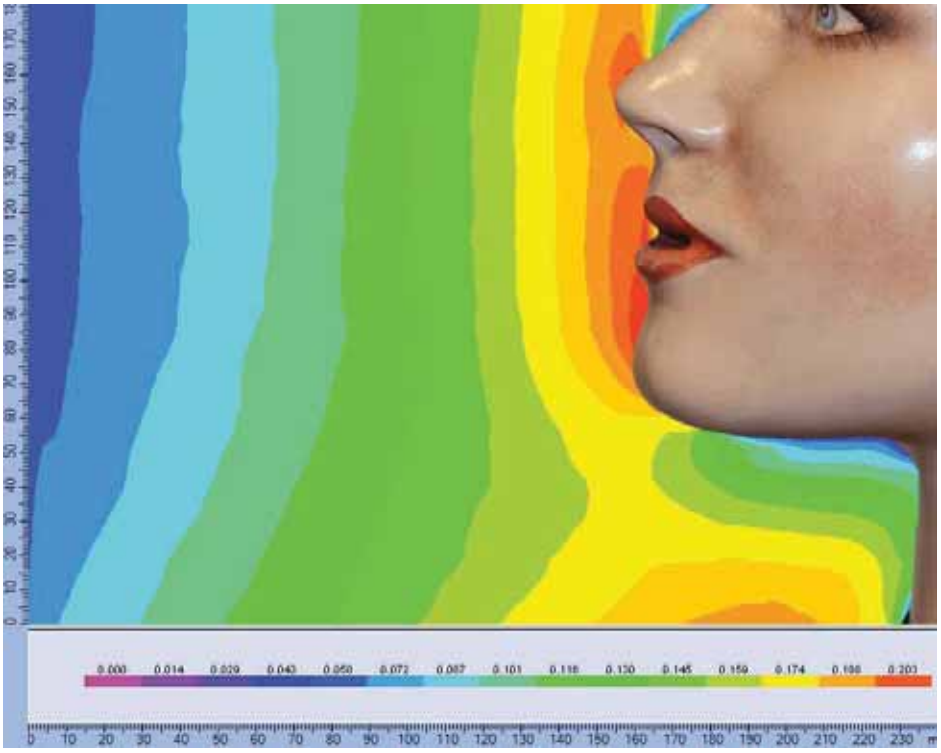

Figure 4.33 *a) Velocity vector diagram showing air direction and b) Contour velocity plot diagram close to the breathing zone of a thermal manikin when heated and manikin 0.012 m backed from table.*

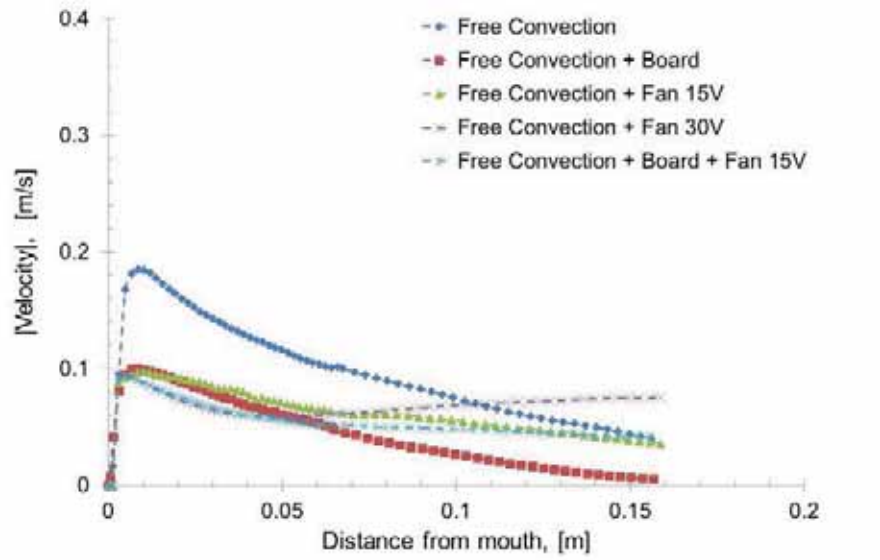

Figure 4.34 *Absolute velocity measured along the plane passing through the middle of the mouth of the breathing thermal manikin at 20°C room temperature when in comfort mode.*

The result of the interaction of the personalized flow and boundary layer was studied when no control was applied. For this purpose the breathing thermal manikin was operated under two modes: when heated and when turned off, i.e. the surface temperature of the manikin was the same as the room temperature (Figure 4.35). In all cases with PV the nozzle was positioned 0.4 m from the breathing zone and slightly from above at an angle of 40° with the horizon. Therefore the PV flow was directed downwards towards the face, i.e. the x and y components of the resultant velocity vector of the personalized flow were negative with respect to the local coordinate system at the mouth center of the manikin. As already mentioned in the following results negative values of the absolute velocity in fact show the dominant direction of the vector itself, downward or upward. A positive velocity means that the free convection flow dominates the complex flow interaction at the breathing zone, while a negative value shows that the forced convection, the PV flow in this case, is dominant. It is clearly seen that with increasing the flowrate from 0 to 8 L/s the PV flow becomes the weighting factor in the complex flow interaction at the breathing zone of the thermal manikin, when it was heated. It is clearly noted from the results that 4 L/s are not enough with this nozzle diameter (d = 0.18 m) to generate high enough velocity to fully penetrate the convection layer. Furthermore the velocity profile when PV air at 4 L/s is supplied toward the face resembles very much the velocity profile when only the free convection layer acts alone. In this case the boundary layer "deflects" the clean PV air away from the face. This in fact explains the low PEE value (PEE_{20C} = 0%) obtained in the tracer gas measurements (Section 4.2, Figure 4.5). Increasing the flow rate to 6 L/s and 8 L/s respectively makes the PV flow strong enough to penetrate the free convection layer and to dominated the flow interaction. Indeed, at 8 L/s personalized flow rate and no control the highest amount of clean air into inhalation PEE_{20C} = 88% was achieved (Section 4.2,

Figure 4.5).

When the manikin was not heated even PV flow at 4 L/s was able to reach the mouth and end up into inhalation. In this case there was no more boundary layer to "cut off" the clean PV air. The velocity at 4 L/s or 6 L/s and close to mouth, when no boundary layer was present around the manikin was comparable to and even higher than that measured at personalized flow of 6 L/s or 8 L/s respectively with heated manikin. In Figure 4.35 b is shown the velocity at the same points as in Figure 4.35 a, but when the manikin was removed. It can be clearly seen that the body of the manikin acting as an obstacle affects the flow interaction in addition to the presence of the free convection layer. When no manikin was present the jet almost retains its initial velocity at the point where the mouth was supposed to be. The decrease in velocity around 0.07 m away from the local coordinate origin (midsection of mouth) is due to the fact that the plane along which the velocity profile was obtained projects out of the jet core and into the entrainment region where the PV flow interacts with the surrounding room air, and this results in fast velocity decay across.

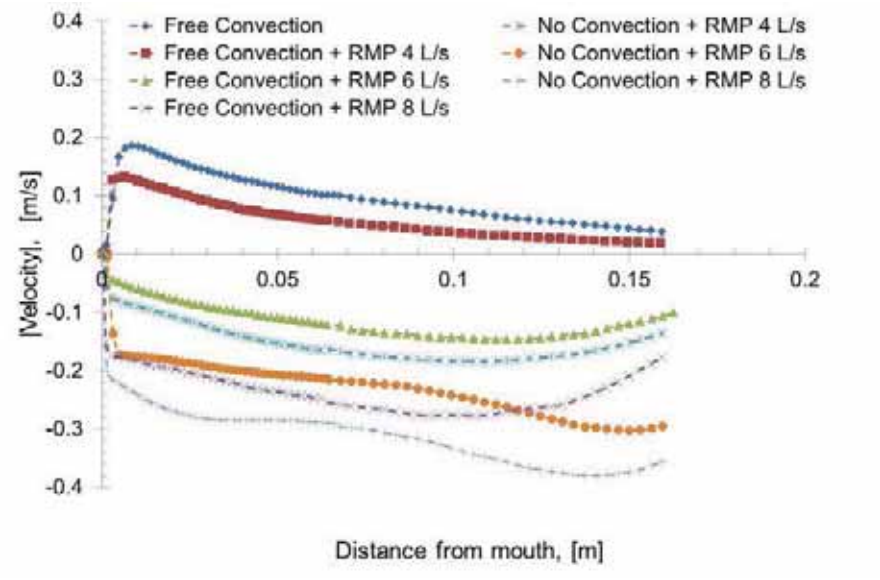

a)

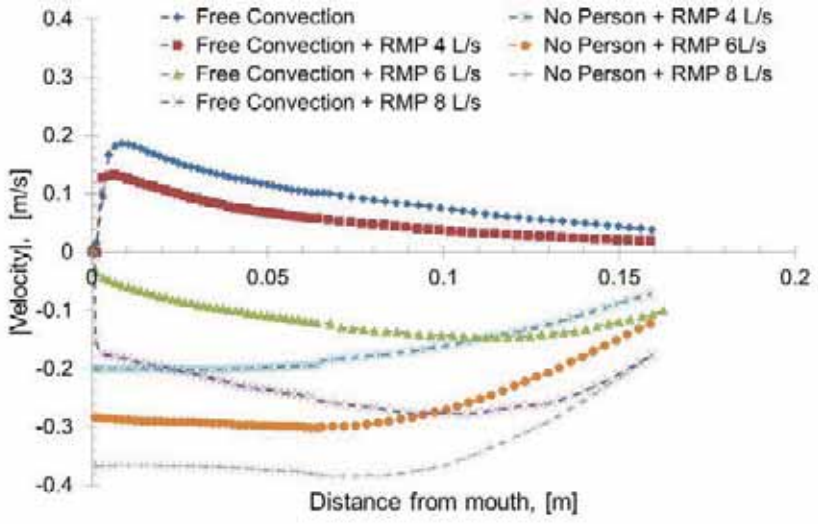

b)

Figure 4.35 *Absolute velocity measured along the plane passing through the middle of the mouth of the breathing thermal manikin at 20 °C room temperature when in comfort mode or a) not heated or b) removed, and when RMP is used to supply clean PV air at three flow rates tested: 4, 6 and 8 L/s.*

Finally the velocity field at the breathing zone resulting from the interaction of the free convection flow and the personalized flow (RMP) when the studied control methods were applied was identified. Some of the obtained velocity profiles are compared in Figure 4.36. All control methods managed to thin enough the convection layer so that the PV air flow managed to penetrate the boundary layer. This was also noticed with the tracer gas measurements. The close magnitude of the velocity of the convection layer and the PV layer at 4 L/s resulted in enhanced mixing and reduced amount of clean air with maximum PEE of 15% when only the straight board was applied (Figure 4.9, Section 4.2.1). The velocity distribution obtained at 4 L/s with any of the studied control methods was close to that when no control and PV supply at 6 L/s. However the corresponding PEE values were different and higher for the latter case (Figure 4.9). The lower PEE at 4 L/s and control could be explained with the enhanced mixing due to the complex interaction close to the thermal manikin as a result from the suction effect of the fans and the difference in the initial velocities at 4 and 6 L/s respectively, resulting in different length of the potential core region of the jet (**Appendix VII**, **Part 1** Figures 14, 17, 20, 23). When increasing the flow rate to 6 L/s and 8 L/s the amount of clean air in inhalation also increased with all control strategies (passive, active and hybrid) and at 6 L/s the PEE was almost the same as when no control was applied and the PV flow rate was 8 L/s. Similar pattern could also be found in the velocity profiles studied.

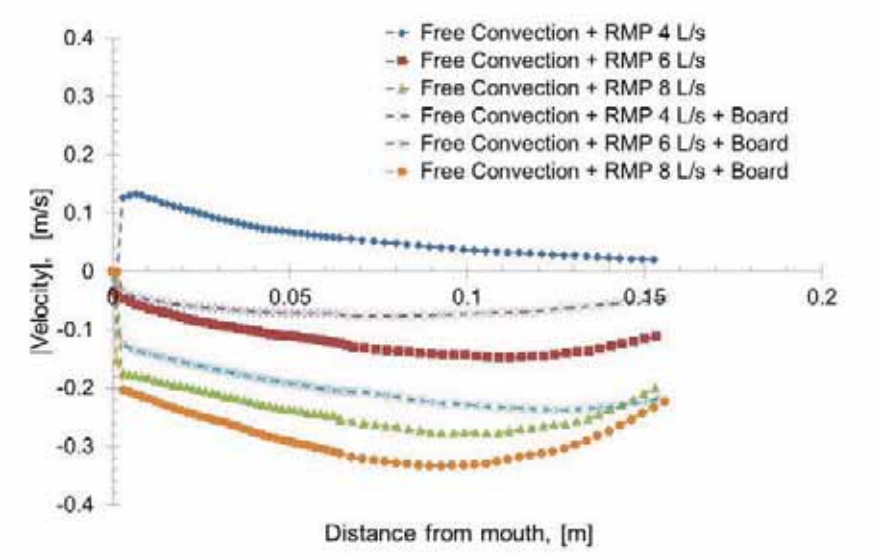
Free Convection + RMP 4 L/s
Free Convection + RMP 6 L/s
Free Convection + RMP 8 L/s
Free Convection + RMP 4 L/s + Board
Free Convection + RMP 6 L/s + Board
Free Convection + RMP 8 L/s + Board
|Velocity|, [m/s]
0.4
0.3
0.2
0.1
0
-0.1
-0.2
-0.3
-0.4
0
0.05
0.1
0.15
0.2
Distance from mouth, [m]

a)

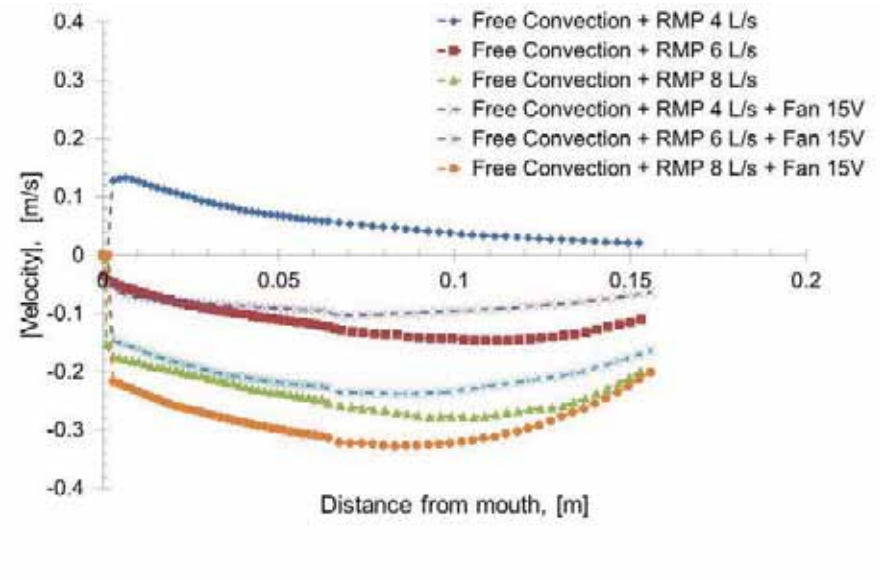
Free Convection + RMP 4 L/s
Free Convection + RMP 6 L/s
Free Convection + RMP 8 L/s
Free Convection + RMP 4 L/s + Fan 15V
Free Convection + RMP 6 L/s + Fan 15V
Free Convection + RMP 8 L/s + Fan 15V
|Velocity|, [m/s]
0.4
0.3
0.2
0.1
0
-0.1
-0.2
-0.3
-0.4
0
0.05
0.1
0.15
0.2
Distance from mouth, [m]

b)

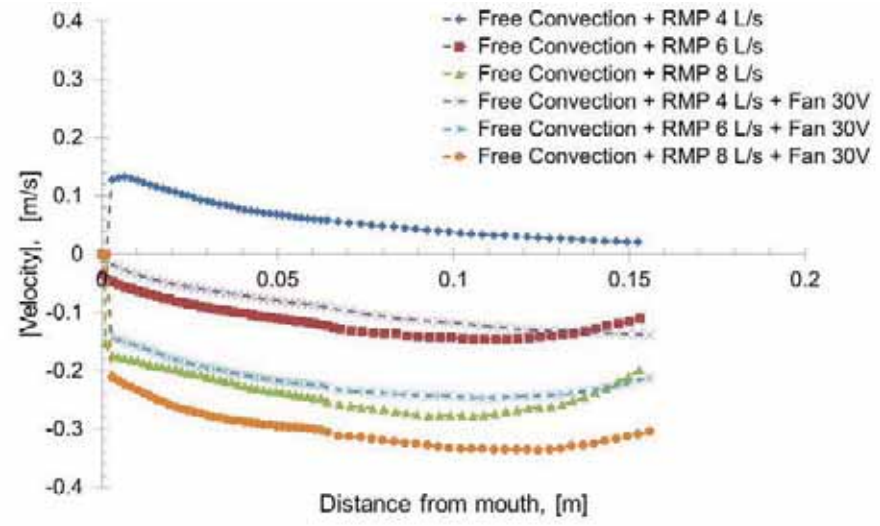

c)

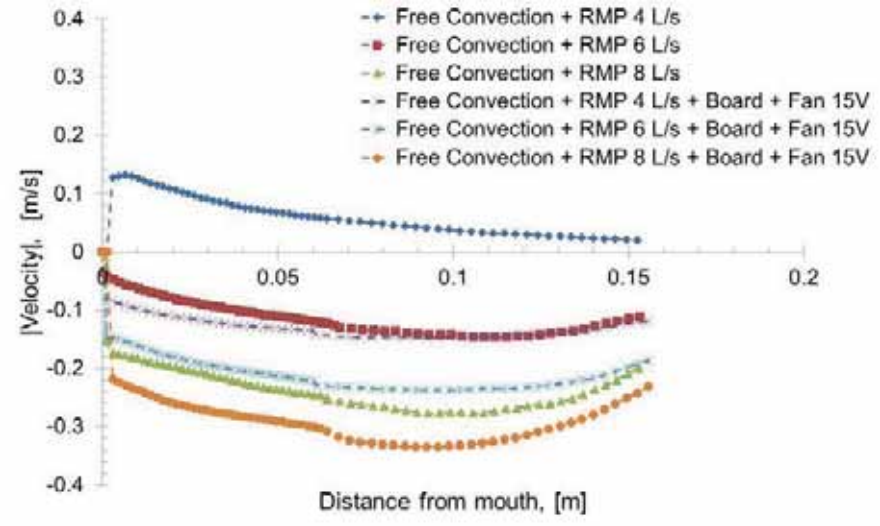

d)

Figure 4.36 *Absolute velocity measured along the plane passing through the middle of the mouth of the breathing thermal manikin at 20°C room temperature when in comfort mode with different control methods over the boundary layer a) board b) fan 15V c) fan 30V d) combination of board and fan at 15V, and when RMP is used to supply clean PV air at the three flow rates tested: 4, 6 and 8 L/s.*

The largest impact of the studied control methods on the airflow interaction at the breathing zone was observed at PV flow rate of 4 L/s. As it can be seen from the results compared

in Figure 4.37 at this flow rate the velocity of the incoming PV flow is not strong enough to "pierce" the free convection layer, when no control is applied. The results also show that all applied control methods weakened the free convection flow to the level to be penetrated by the PV flow. Furthermore, the results show differences in the velocity distribution obtained with the different control method. However these differences appear not to have significant effect in the inhaled air quality since rather low PEE values were obtained with the different control methods (Figures 4.5, 4.7 and 4.9). The most substantial improvement in PEE was noticed at 6 L/s and 20^{o}C temperature when comparing PV without and with control: PEE increased from 32% up to 80 - 92% respectively (Figures 4.5, 4.7 and 4.9). Under these conditions the measured velocity profiles also showed similar trend: all velocity profiles when control was applied were almost identical with downward velocity substantially higher than the velocity measured without control (Figure 4.37b). The difference in PEE ranging from 80% up to 92% could be explained by the suction effect of the fans that pulled down part of the boundary layer already mixed with PV clean air and thus enhancing the mixing (Figure 4.33 and **Appendix VII**, **Part 1**, Figure 18). At 8 L/s the PEE was on average more than 95% (Figures 4.5, 4.7 and 4.9) and all velocity profiles regardless of the control method show same values near the mouth (Figure 4.37c). The results reveal that with the increase of the personalized flow rate above 4L/s the amount of clean air ending in inhalation becomes less dependent on the nature of the control method used to thin down the boundary layer surrounding the human body. Having this in mind and considering the energy utilization the passive method shows up as superior to the other control strategies studied here.

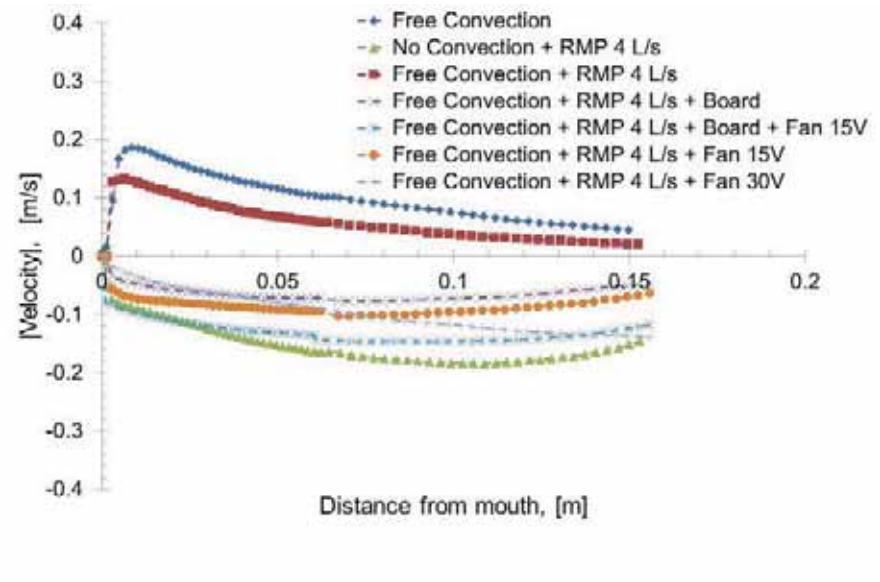

a)

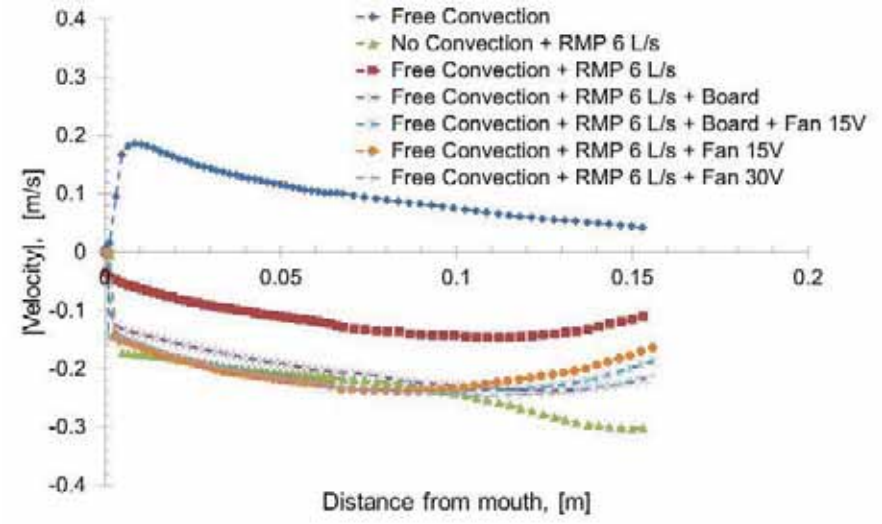

b)

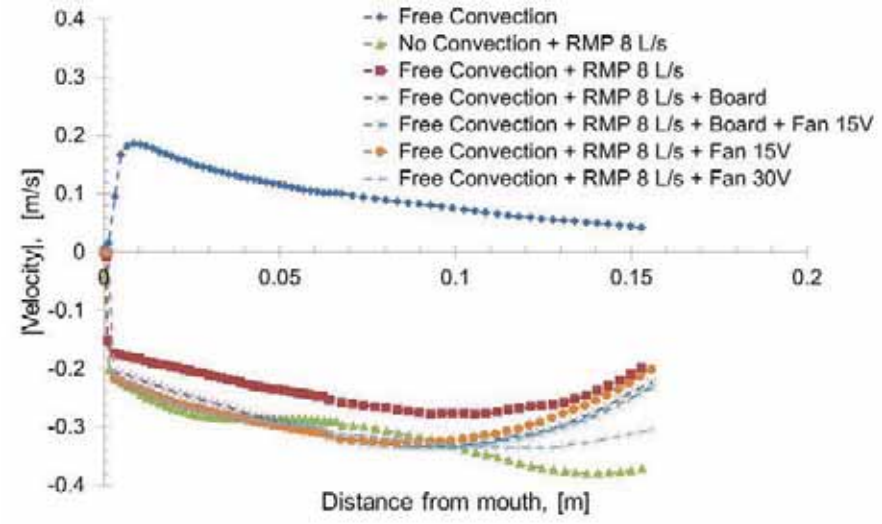

c)

Figure 4.37 *Absolute velocity measured along the plane passing through the middle of the mouth of the breathing thermal manikin at 20°C room temperature when in comfort mode with the four control methods over the boundary layer when RMP is used to supply clean PV air at a) 4 L/s b) 6 L/s and c) 8 L/s.*

4.4.2.2 Control over the Personalized Flow

The PIV measurements for this type of control were done only for the confluent jet box design with the two jets, inner and outer (Chapter 4, Section 4.3) with supply openings 0.06 x 0.5 m

(W x L) and isothermal conditions at 26 °C. Similarly to the control methods over the boundary layer the velocity profiles for the control over the PV flow are made along the same plane starting between the lips and directed away from the breathing thermal manikin (Figure 4.38). The velocities present the length of the resultant vector from the x and y components and are given in absolute value. The same Cartesian coordinate system as mentioned in the previous subsection was adopted for these PIV measurements. The full results are presented in **Appendix VII, Part 2**

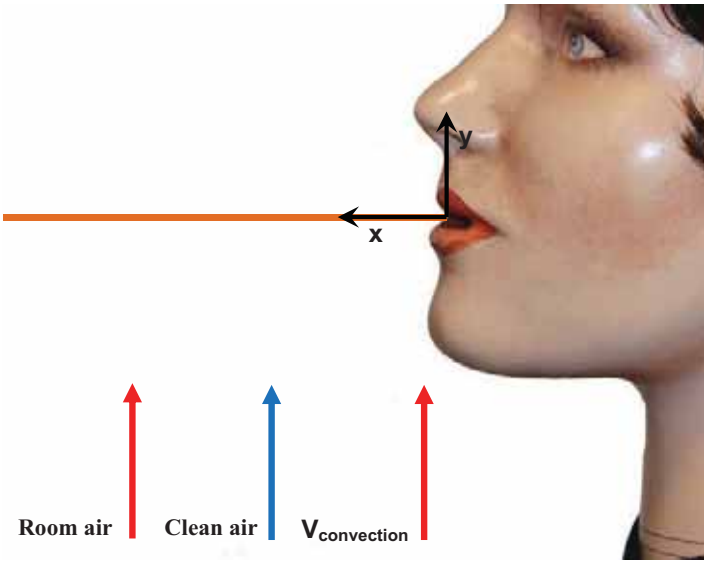

Figure 4.38 *The measurement plane across the mouth of the thermal manikin with the coordinate system shown from the image made with the 35 mm lenses camera for the confluent jet PV.*

The results from the PIV measurements with both slots discharging the same amount of air are presented on Figure 4.39. During the PIV measurement the two slots were supplying room air with glycerol droplets via two axial fans installed close to the TV supply. It can be seen that with the increase of the flow rate, the velocity at the mouth increases as well. However it is noticed that when either 6 or 8 or 10 L/s of air was supplied from both openings 0.06 m away from the moth there was a slight rise in velocity. This is explained with the interaction of the two confluent jets: the inner jet velocity decays faster due to deflection of the boundary layer by the chin and the mandible. The results from the PIV measurements clearly show that the increased amount of clean air into inhalation (tracer gas measurements Section 4.3, Figure 4.18b) results from the increased flow rate. Also the small increase in PEE from 76% for 8 L/s to 85% for 10 L/s could be explained with the enhanced mixing between the two jets.

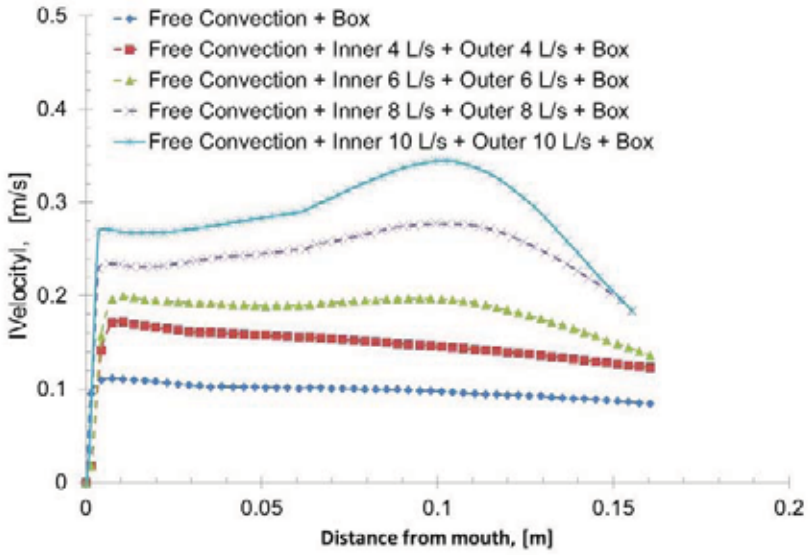

Figure 4.39 *Absolute velocity measured along the plane passing through the middle of the mouth of the breathing thermal manikin at 26 ^{o}C room temperature when in comfort mode with both inner and outer jets supplying the same amount of clean through the opening of width 60 mm.*

The effect of different discharge air flows and hence different initial velocities of the inner and the outer jets was also studied with the width opening of 0.06 m. In these cases the inner jet air flow was equal to, two times or half of the air flow from the outer jet (Figure 4.39). When either inner or outer jet was working alone with clean PV air, the PEE measured was 51% and 47% respectively. Also the velocity of the inner jet was slightly lower than that of the outer jet (Figure 4.40). However, the slightly better performance of the inner jet could be explained with the fact that it was directly "attached" to the manikin body substituting the boundary layer and entrained room air only from its outer side (**Appendix VII**, **Part 2**, Figures 31a and Figure 31b).

The low performance of the inner jet only supplying the PV air at this relatively high flow rate could be explained with the fast velocity decay at the mouth level as a result of the complex body geometry of the breathing thermal manikin closely resembling the one of a real human and the deflection of the clean PV air by the mandible when it meets the chin. In the case of the outer jet supplying clean PV air alone the similar value for PEE shows that in the gap of 0.06 m (in fact the width of the inner jet) room air is pulled from the sides mixing with the clean air as a result of induced under-pressure (**Appendix VII**, **Part 2**, Figure 32a and Figure 32b). Looking at the PEE values obtained from the tracer gas measurements one also notices that the amount of clean air into inhalation when both jets supply 8 L/s or when the inner supplies 8L/s and the outer 4 L/s are identical: 76% and 74% respectively. The presence of the outer jet helps reduce the mixing and "isolates" the clean inner jet from the surrounding polluted room air. Also the velocity of the upcoming clean air in both cases is identical downstream to 0.02 m from the mouth opening and

equal to 0.24 m/s (Figure 4.40). Therefore from energy point of view the latter scenario should be preferred, namely supplying two times lower amounts of air from the outer jet opening.

However when the inner jet has two times lower initial momentum than the outer one the PEE drops down to 33%. The velocity profile from the PIV measurements (Figure 4.40) reveals that this is due to the interaction between the two confluent jets. Moreover, the amount of clean air is even lower compared to when the outer jet supplied the PV air alone (PEE = 47%), despite of the fact that the velocity profiles downstream to 0.01m from the mouth look alike (Section 4.3, Figure 4.20). However from this point downstream the velocities differ: in the case of the outer jet only, the velocity increases, while when in the case of both confluent jets (inner at 4 L/s and outer at 8 L/s) the velocity is almost constant to 0.06 m away from the mouth. In the latter case the inner jet mixes with the outer jet more intensively as both jets were having different initial momentums. In the case of the outer jet only supplying the clean PV air, though present, the mixing was not as intense. The high momentum of the jet at 8 L/s did not allow it to attach to the body (Figure 32, **Appendix VII**, **Part 2**). The velocity of the boundary layer was quite low; in fact the presence of the box itself affected its strength (Section 4.3, Figure 4.20).

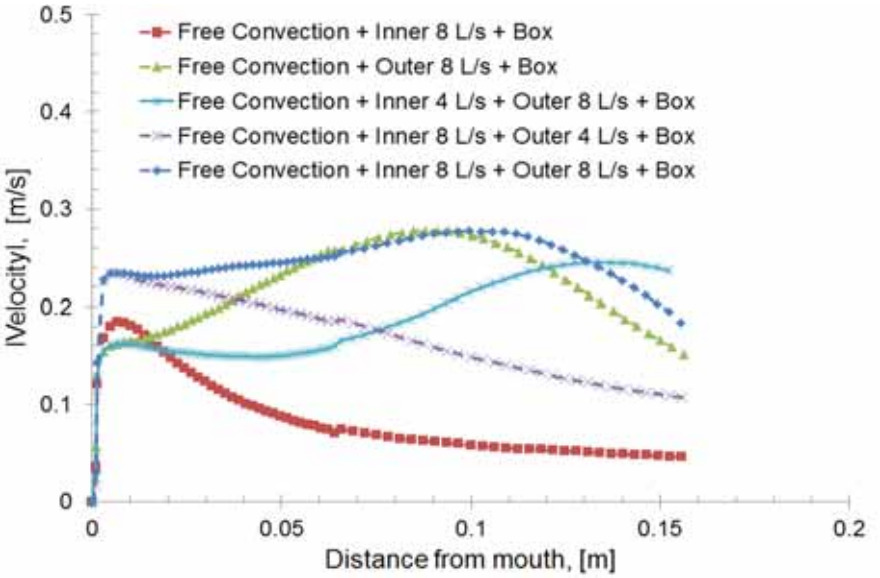

Figure 4.40 *Absolute velocity measured along the plane passing through the middle of the mouth of the breathing thermal manikin at 26°C room temperature when in comfort mode with both inner and outer jets supplying the same or different amount of air through the opening of width 60 mm.*

4.5. Application of the Boundary Layer Theory

The boundary layer theory was applied to describe the free convection flow measured in front of the thermal manikin. In order to be certain in validity of the obtained PIV results the method was applied for a simple classical case of free convection flow over vertical heated plate. The measured velocity distribution over the vertical plate was used to validate the existing

mathematical models for predicting the velocity of the free convection layer which were then applied to approximate the boundary layer of the human body due to its complex geometry.

The breathing thermal manikin was substituted with a flat heated plate (radiator) of 0.01 m thickness and dimensions 0.6 m x 0.7 m (H x L). The lower rim of the radiator was touching the box where the manikin's stomach was supposed to be (0.92 m from floor), Figure 4.41a.

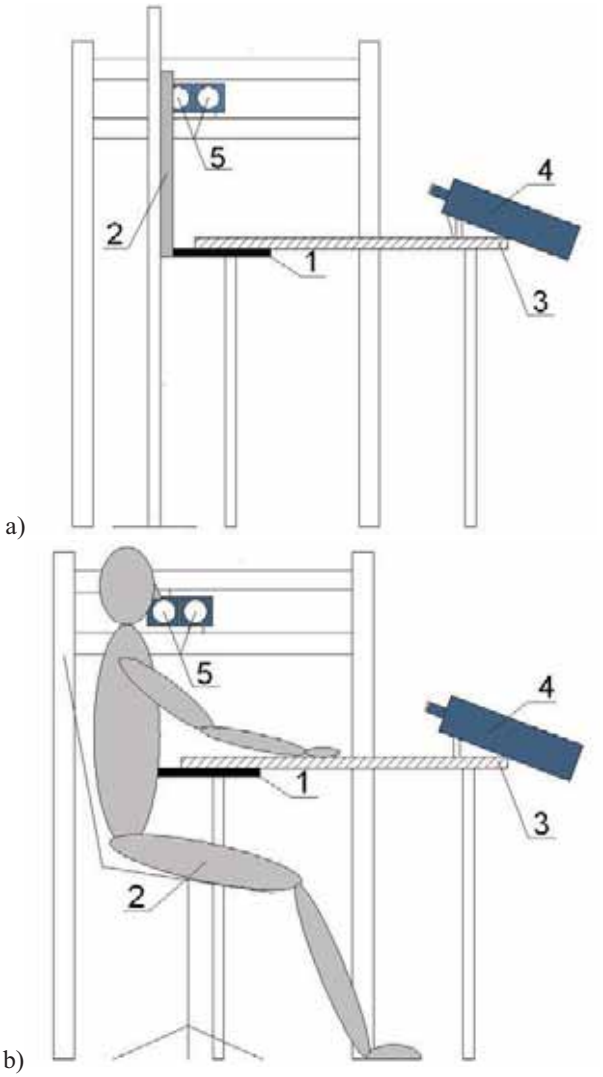

Figure 4.41 *PIV set up with the confluent jet box: 1) confluent jet box; 2) Radiator/ Thermal manikin; 3) table; 4) laser beam generator; 5) CCD cameras.*

The surface temperature of the radiator was adjusted to be the same as the manikin surface temperature (Table 4.7). The radiator temperature was kept constant ±0.1 ^{o}C by means of a water heater and cooler unit placed outside of the measurement chamber.

Table 4.7 *Surface temperature of the clothing of the thermal manikin measured at three heights (in metres) of the body relative to the table surface (in Celsius and Kelvin degrees).*

Height, (m)	Box+Free Convection	Upper jet 8L/s+Free Convection	Upper 4L/s + Lower 8L/s + Free Convection	Lower 8L/s + Free Convection	Lower 4L/s + Free Convection	Lower 4L/s + Upper 8L/s + Free Convection	Free Convection
0.000	31	31	31	30.8	31.2	31.3	30.8
0.093	31.8	31.2	31.8	32.1	32	32	31.9
0.187	32	31.6	32.2	32.3	32.2	32.3	32
Average	**31.6 (304.75)**	**31.3 (304.45)**	**31.7 (304.85)**	**31.7 (304.85)**	**31.8 (304.95)**	**31.9 (305.05)**	**31.6 (304.75)**

The velocity profiles at three positions vertically along the radiator were measured under the same conditions like the manikin with only the free convection layer and when the table was 0.1 m away from it, and when the box with the confluent jets was present but acting as an obstacle (neither of the two jets were used under this experiment), Table 4.8. The PIV measurements were performed at three heights from the edge of the radiator: 0.093 m (middle chest), 0.187 m (upper chest) and 0.365 m (neck region) respectively. During these measurements no jets from the box were applied.

Table 4.8 *Measured conditions with the radiator and the confluent jets. "x" stands for present, "-" stands for not applicable.*

N	Heated plate (radiator)	Convection flow	Inner	Outer	Breathing	Duo Box
1	x	x	-	-	-	-
2	x	x	-	-	-	x

The results from these measurements are shown in Figure 4.42.

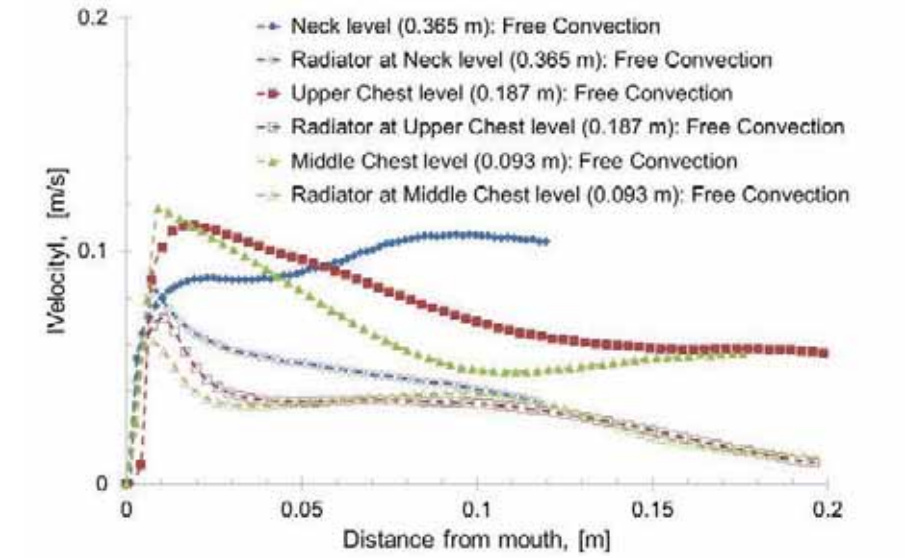

a)

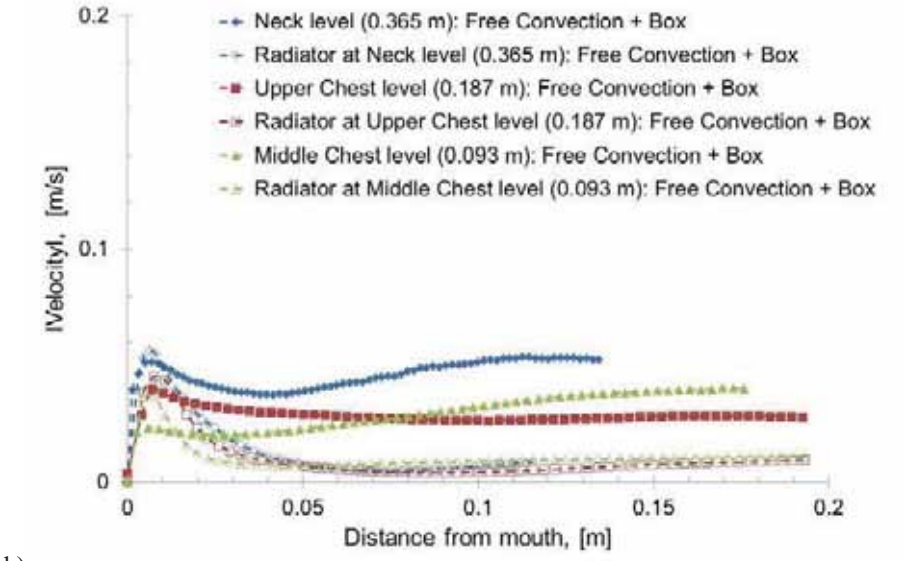

b)

Figure 4.42 *Comparison of the velocity profile at three levels measured with the thermal manikin and the radiator: a) free convection layer (radiator/thermal manikin is 0.12 m back from table); b) the confluent jet box (not supplying air) is pressed against the low edge rim of the radiator/the upper stomach area of the seated thermal manikin, passive control over the convection boundary layer.*

As expected the velocity of the free convection layer developing in front of the radiator having the same surface temperature as the manikin increases with height from the box upwards (Figure 4.42). The same pattern is observed for the manikin as well, but the velocity of the

convection layer at the neck level is lower than at the upper chest. The boundary layer originating at the legs and thighs pulls away from the body the convection layer originating at the groins as the former is stronger, and thus affects the boundary layer development at the neck level of the seated person, resulting in lower velocities compared to those measured at the upper chest (Figure 4.42 a). Also at the neck the boundary layer reduces velocity due to separation at shoulder level. In support to this conclusion, namely that the boundary layer originating from the legs and thighs of a seated person affects the overall development of the convection layer at the upper body of a seated human, the velocities measured at the middle and upper chest are much higher compared to the case with the radiator. Also, the velocities measured with the thermal manikin within the boundary layer decrease with increasing the height, when very close to the body surface, and when there is no blocking effect over the convection layer in front of the body (Figure 4.42 a). As already mentioned this is due to the interaction between the two convection flows (from the legs and thighs and from the groins upwards along the chest) developing around the body of a seated person, and their complex interaction.

On the other hand when the gap is removed by tightly pressing the box against the upper stomach of the manikin the absence of the boundary layer originating from the legs and thighs is no longer an issue, and at the same location of the neck region the convection layer is much stronger than that at the upper and middle chest regions. The velocities measured along the height of the radiator are slightly higher than the velocities measured with the manikin (Figure 4.42 b). The reason for this might be on a molecular level: the clothing has coarser surface than the radiator (polished metal with paint) and affects locally the development of the boundary layer by exerting some friction on the air molecules.

A set of equations are used to approximate the velocity profile for the boundary layer at three different heights corresponding to 0.093, 0.187 and 0.365 m relative to the table surface vertically along the radiator (Table 4.9 and Figure 4.43). The solution is shown using the similarity consideration for a laminar free convection on a vertical surface. The set of the equations, includes:

$$\frac{\partial u}{\partial x} + \frac{\partial v}{\partial y} = 0 \quad , (4.5.1)$$

$$u\frac{\partial u}{\partial x} + v\frac{\partial u}{\partial y} = g\beta(T - T_\infty) + v\frac{\partial^2 u}{\partial y^2} \quad , (4.5.2)$$

$$u\frac{\partial T}{\partial x} + v\frac{\partial T}{\partial y} = \alpha\frac{\partial^2 T}{\partial y^2} \quad , (4.5.3)$$

where,

u and v are mass average fluid velocity components in x and y direction, m/s;
g is the gravitational acceleration, m/s^2;
T temperature in K;
α is the thermal diffusivity in m^2/s;
β is the volumetric thermal expansion coefficient, K^{-1}.

The parameters may be obtained by non-dimensionalizing the governing equations:

$$x^* \equiv \frac{x}{L} \qquad y^* \equiv \frac{y}{L} \quad , (4.5.4)$$

$$u^* \equiv \frac{u}{u_o} \qquad v^* \equiv \frac{v}{u_o} \qquad T^* \equiv \frac{T-T_\infty}{T_s-T_\infty} \quad , (4.5.5)$$

where, L is characteristic length, u_o is an arbitrary velocity defined at L, T is arbitrary temperature defined at L, T_s is the surface temperature of the plate/radiator film and T_∞ is the ambient temperature. The application of this non-dimensionalizing produces the following equations for 4.5.2 and 4.5.3:

$$u^* \frac{\partial u^*}{\partial x^*} + v^* \frac{\partial u^*}{\partial y^*} = \frac{g\beta(T_S-T_\infty)L}{u_o^2} T^* + \frac{1}{Re_L} \frac{\partial^2 u^*}{\partial y^{*2}} \quad , (4.5.6)$$

$$u^* \frac{\partial T^*}{\partial x^*} + v^* \frac{\partial T^*}{\partial y^*} = \frac{1}{Re_L Pr} \frac{\partial^2 T^*}{\partial y^{*2}} \quad , (4.5.7)$$

The first term on the right side of equation 4.5.6 is a result of the buoyancy force. Further by multiplying with $Re_L^2 = (u_o L/\nu)^2$ the Grashof number is introduced into the equation 4.5.6:

$$Gr_L \equiv \frac{g\beta(T_S-T_\infty)L^3}{\nu^2} \quad , (4.5.8)$$

The Grashof number shows the ratio of buoyancy to viscous forces.

To obtain a numerical solution for the similarity consideration of the radiator, the following boundary conditions are assumed for equations 4.5.1 to 4.5.3:

y = 0: u = v = 0 $T = T_s$

$y \to \infty$: $u \to 0$ $T \to T_\infty$

The solution involves transforming variables by introducing the similarity parameters in the form:

$$\eta \equiv \frac{y}{x}\left(\frac{Gr_x}{4}\right)^{1/4} \quad , (4.5.9)$$

Representing the velocity in terms of a stream function yields:

$$\psi(x,y) \equiv f(\eta)\left[4\nu\left(\frac{Gr_x}{4}\right)^{1/4}\right] \quad , (4.5.10)$$

And hence the velocity component along the x axis is:

$$u = \frac{\partial \psi}{\partial y} = \frac{\partial \psi}{\partial \eta}\frac{\partial \eta}{\partial y} = 4\nu\left(\frac{Gr_x}{4}\right)^{\frac{1}{4}} f'(\eta)\frac{1}{x}\left(\frac{Gr_x}{4}\right)^{1/4} = \frac{2\nu}{x} Gr^{\frac{1}{2}} f'(\eta) \quad , (4.5.11)$$

The primed quantities are derivatives with respect to the similarity parameter η. For more details refer to Incropera and DeWitt 1996.

Transition from laminar to turbulent flow in the free convection layer depends on the relative magnitude of buoyancy and viscous forces in the fluid, and is correlated to the Rayleigh

number that is product of Grashof and Prandtl numbers, where Pr = ν/α. For vertical plates the critical number is approximately 10^9.The boundary layer in front of the radiator was laminar at all three heights measured: $Ra_x << 10^9$, which is the critical value showing the effect of the viscous forces in the flow for a heated/cooled plate (Table 4.9).

Table 4.9 *Initial boundary conditions.*

Value	Free Convection	Box+Free Convection
T_{plate}, [K]	304.75	304.75
T_{room}, [K]	299.15	299.15
T_{film}, [K]	301.95	301.95
$Gr_{0.093}$, [-]	282771.44	282771.44
$Gr_{0.187}$, [-]	2298854.67	2298854.67
$Gr_{0.365}$, [-]	17094849.83	17094849.83
$Ra_{0.093}$, [-]	199604.60	199604.60
$Ra_{0.187}$, [-]	1622730.97	1622730.97
$Ra_{0.365}$, [-]	12067027.39	12067027.39

The calculated values are compared with the measured values and shown in Figure 4.43.

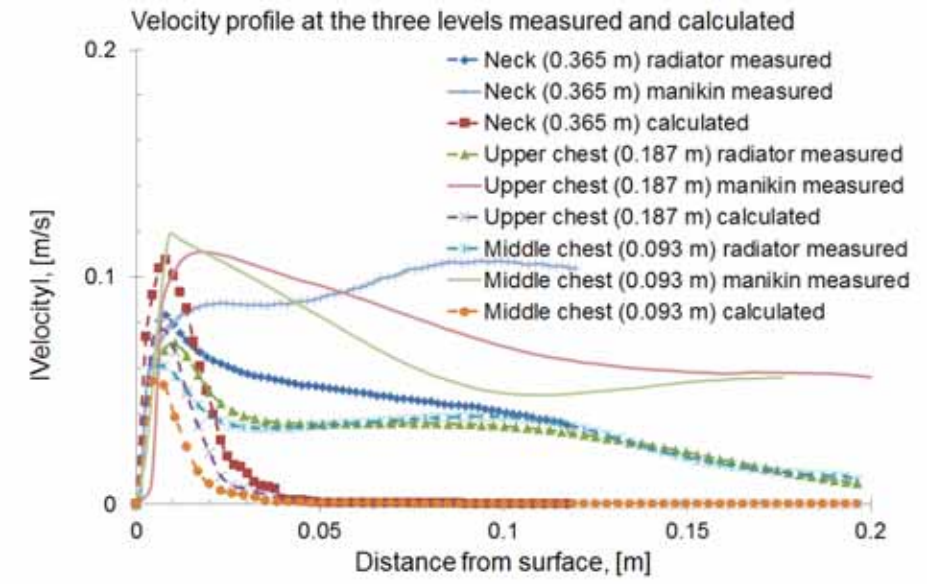

a)

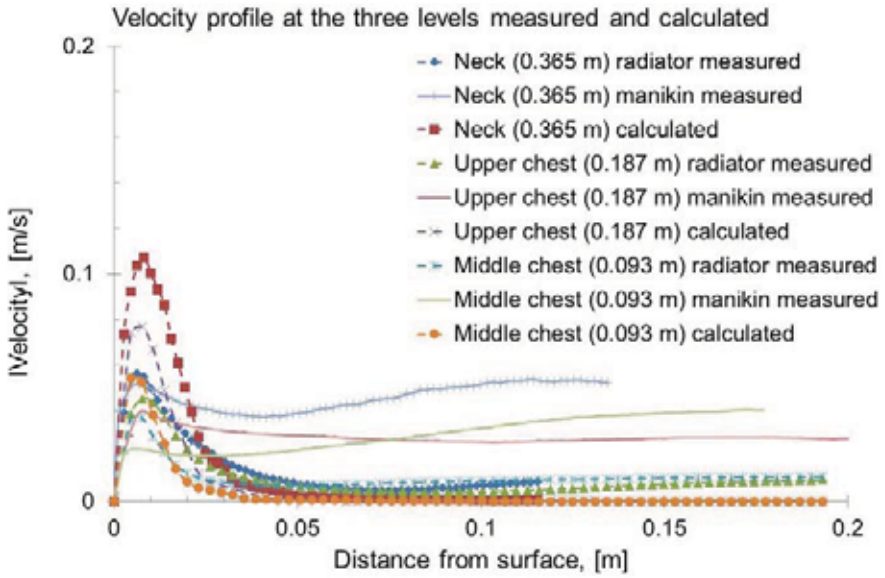

b)

Figure 4.43 *Velocity profiles as measured and calculated at the three heights when there was: a) 0.12 m distance between the table and the radiator/thermal manikin; b) no distance – the confluent jet box was used as a passive control for the convection flow (the two jets inner and outer were not working).*

The theoretical approximation is quite close to the measured velocity profiles within the region close to the radiator surface. The difference is due to the presence of the background ventilation, which causes the "distortion" of the profiles from their theoretical values (Figure 4.43). The boundary layer is quite sensitive to background changes and this affects its width and velocity profile. In the case of the confluent jet box touching the leading edge of the radiator, where the boundary layer started to develop, led to reduction of the resulting velocities. This was because of the effect of the table and the background floor: air from the surroundings was pulled over the table which led to the overall drop in the velocities (**Appendix VII, Part 3**, Figures 38, 40, 41).

From Figure 4.43 it can also be seen that the manikin has quite different velocity distribution measured at the same heights as those for the radiator (**Appendix VII, Part 3**). This is due to the complex body shape as well as the presence of a boundary layer that starts from the feet and joins the secondary boundary layer from groins. Hence, when there was gap between the table and the manikin's body the resultant boundary layer has much higher velocities than the radiator and the calculated theoretical values. In the case when the confluent jet box was used to break the boundary layer much lower velocities were measured, especially at the middle chest (start of the breasts) which led to slight detachment of the flow from the body. The other reason is the presence of clothing which served as additional generator of disturbances on the way of the boundary layer (wrinkles and air niches between the clothing and the body surface).

4.6. Wall Jet and Confluent Jets as PV

The application of the confluent jets incorporated into by the box pressing against the stomach of a seated person resembles the case of a three-dimensional wall jet: the body of the occupant being the vertical surface/wall along which the PV jet spreads.

The theory states that the wall jet has two layers: a turbulent boundary layer close to the wall and an outer shear layer (Baturin 1972). The thickness of the turbulent boundary layer makes the problem quite complicated and could be neglected. In order to calculate the velocity along the axis of the three dimensional wall jet, the jet itself can be assumed as being half of a three-dimensional free jet (Baturin 1972). So the velocity should be calculated for half the width of the discharge opening or $2b = b_o$. Baturin 1972 gives the following equation for the average areal velocity (the flow rate divided by the area) shown in Table 4.10.

Table 4.10 *Relationships for plane jets.*

Axial velocity	Initial Section of the Jet	Main Section of the Jet
$\frac{v_x}{v_0} = \frac{1.2}{\sqrt{(ax/b_o) + 0.41}}$	1	$\frac{v_x}{v_0} = \frac{1.2}{\sqrt{(ax/b_o) + 0.41}}$

The value of a is in the range of 0.09 to 0.12 and the length of the initial section of the jet for this a is s_o/b_o = 8.5 to 11.5, where b_o is half of the initial width of the nozzle opening and s_o is the length of the initial section/core region of the jet (Baturin 1972). The thermal manikin's mouth was 0.36 m above the discharge plane of the box with the 2 confluent jets which makes it within the initial section of the jet (s_o is between 0.51 to 0.69 m; b_o is 0.03 m). Therefore according to theory the axial velocity (maximal in this case) would be equal to the initial velocity up to the mouth. The corresponding velocities for 4 L/s and 8 L/s are 0.13 and 0.26 m/s respectively.

The PIV measured velocity profiles for the radiator and the manikin are presented in Figure 4.44 for three heights, 0.093, 0.187 and 0.365 m, from the discharge surface of the confluent jet PV box corresponding to the middle, upper chest levels (breast level) and neck level. The three heights were chosen to see whether the existing theory for wall jets is compliable to those made for the human body in the region where it is closest to the wall geometry, middle and upper chest, and for the neck where the supplied air flow separates from the body surface and passes by the mandible. The results are plotted in dimensionless form: velocity is divided by the maximum value for each height and the distance is divided by the initial width of the opening. Figure 4.44 presents the results when only the inner or only the outer jet works at 8 L/s for the radiator and the manikin respectively.

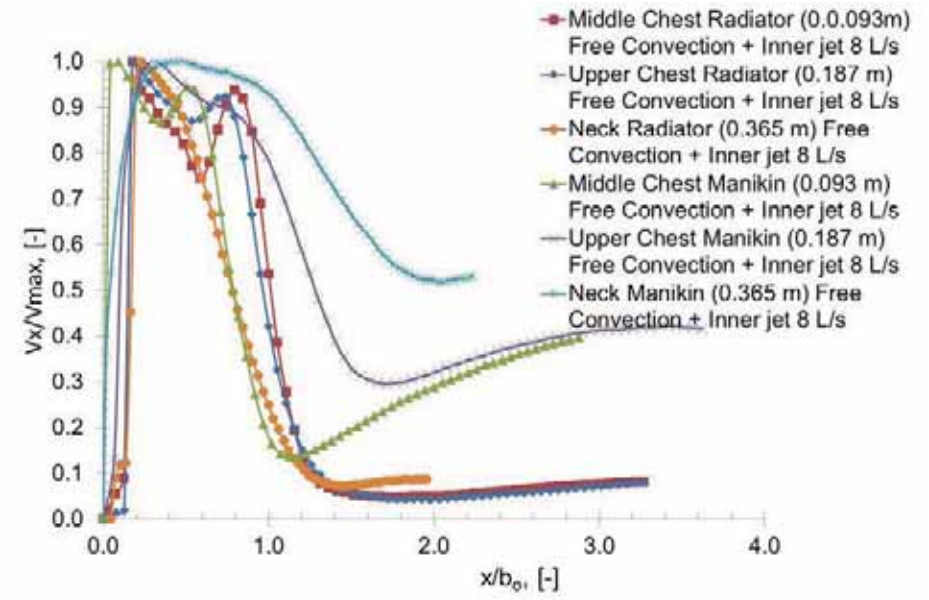

a)

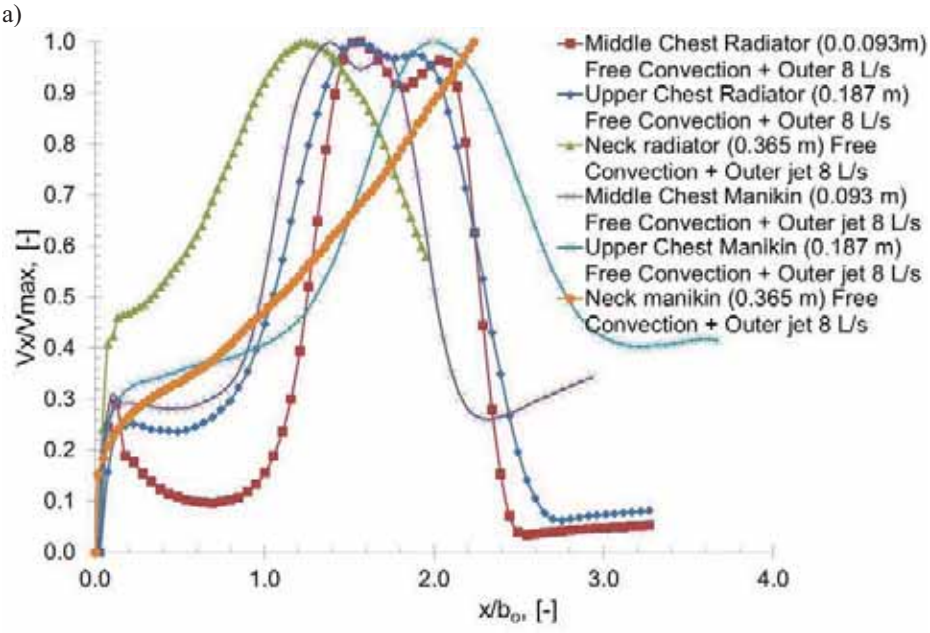

b)

Figure 4.44 *a)Inner jet at 8 L/s and b) Outer jet at 8 L/s for both manikin and radiator at three heights 0.093 m, 0.187 m and 0.365 m.*

The profile of the manikin resembles closely the one received from the radiator but only when the inner jet is working. As a result of the flow interaction (forced convection from PV flow

and TV flow) and body geometry a difference between the velocity profiles for the radiator and the manikin can be observed, that becomes more pronounced with increasing the height. The maximum values for the velocity is given in Table 4.11.

Table 4.11 *Maximum velocity at the three body heights measured.*

[m/s]	0.093 m (middle)	0.187 m (upper)	0.365 m (neck)
Theory v_{max}	0.266	0.266	0.266
Radiator v_{max} Inner jet	0.260	0.258	0.251
Manikin v_{max} Inner jet	0.262	0.262	0.162
Radiator v_{max} Outer jet	0.333	0.330	0.323
Manikin v_{max} Outer jet	0.328	0.318	0.256

The maximum velocities measured by the radiator for only inner jet (**Appendix VII, Part 3**, Figures 41 ÷ 43) are close to the theoretical results and the small difference is due to the fact that in the current experiments there was a background flow that affected the wall jet development. Another reason for the difference is that the radiator was heated and this influenced the length of the initial section of the jet, and also by promoting mixing on molecular level. All these factors contributed to the reduction of the initial (core) section of the jet.

The maximum velocities measured with the manikin at the middle and upper chest are close to the theoretical values. This shows that up to the breast level (upper chest) the theory of wall jets can be applied to approximate the maximum velocity of the jet supplied along the body. However at the neck (0.365 m from table top), the maximum velocity was more than one and a half times smaller than the theoretical and the one measured with the radiator. The reason is that the supplied upwards jet spreads around the neck and then separates from the body for the shoulders project at the base of the neck, which leads to the apparent drop of the velocity measured.

For the outer jet higher velocities were measured both with the radiator and the manikin. The results from the PIV with manikin and radiator show that the jet due to its high initial momentum bends towards the body/heated surface very limitedly and propagates upwards as free plane jet (**Appendix VII, Part 2**, Figure 32 and **Part 3**, Figure 44 ÷ 46)). Even in front of the face the jet is not significantly affected by the proximity of the manikin (Appendix VII, Part 2, Figure32a and 32b). Hence a kind of control via guiding vanes would be beneficial to direct the PV jet towards the face

An interesting case is when both of the jets, i.e. inner and outer work at different velocities. Measurements were done at inner jet supplying the PV air at 4 L/s and outer at 8 L/s and vice versa, inner at 8 L/s and outer at 4 L/s (**Appendix VII, Part 3**, Figures 47 ÷ 52). In this case the interaction of the two jets is quite complicated as it includes three different types of jets, wall jet, confluent free jet and compound jet (jet that is released into an environment at certain background velocity). At the very exit the jet will exhibit a velocity profile with two distinct velocities and due to the difference between the velocities at the side plane where the two confluent jets meet, a shear layer will develop and as a result of the friction the velocity profile downstream was affected.

Figure 4.45 shows the results, when the two jets are used at different velocities. In Figure 4.45a is shown the case when the inner jet (closest to the body) supplies the PV air at 4 L/s and the outer (room air) at 8 L/s, and Figure 4.45b is when inner jet supplies 8 L/s and outer 4L/s. As can be

seen the body shape affects the flow interaction at the vicinity of the manikin. In all cases the transition zone between the two jets is marked by a visible saddle point followed by a secondary peak which is the maximum. The velocity profile measured with the thermal manikin has shifted maximum velocity further away from the manikin as a result of the separation of the inner jet after the upper chest being pulled by the outer jet having the higher momentum. The maximum velocity values are given in Table 4.6.3.

Table 4.6.3. *Maximum velocity at the three body heights measured.*

[m/s]	**0.093 m**	**0.187 m**	**0.365 m**
Radiator v_{max}	0.324	0.322	0.320
Manikin v_{max}	0.331	0.327	0.216

Same tendency of much lower velocity at neck level was noticed at this case as well, when $v_{inner} = 0.5\ v_{outer}$.

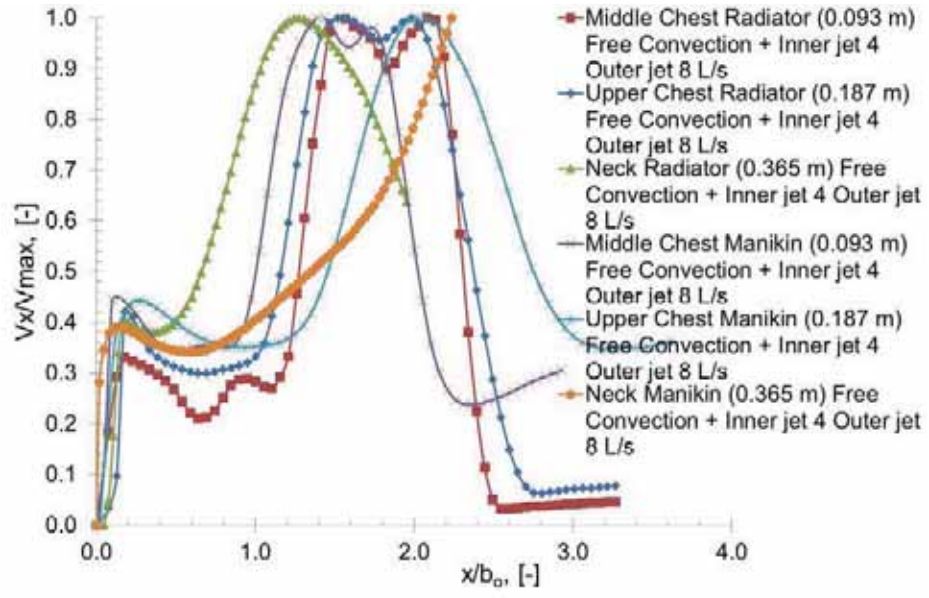

a)

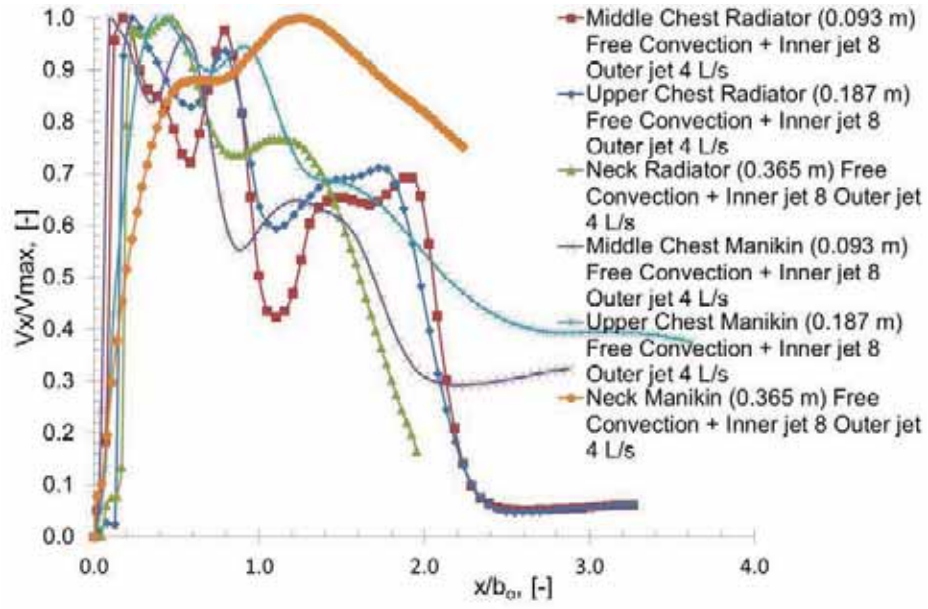

b)

Figure 4.45 *a) Inner jet at 4 L/s and outer jet at 8 L/s and b) inner jet at 8 L/s and outer jet at 4 L/s for both manikin and radiator at three heights 0.093 m, 0.187 m and 0.365 m.*

When the inner jet has twice the velocity of the outer, there is much more enhanced mixing with the outer jet as the inner jet is confound by the torso of the manikin or the radiator (Figure 4.45 b). With height these disturbances are reduced as the velocity starts decreasing. Table 4.12 gives the maximum velocity measured.

Table 4.12 *Maximum velocity at the three body heights measured.*

[m/s]	**0.093 m**	**0.187 m**	**0.365 m**
Radiator v_{max}	0.252	0.252	0.250
Manikin v_{max}	0.268	0.265	0.200

The inner jet affects the velocity distribution at neck level for the manikin. It pulls part of the air away as a result of the spread of the inner jet that pushes the outer one, and thus higher velocities were measured.

4.7. Discussion

All the results obtained in the present study suggest that better understanding of the flow interaction is important in order to fully benefit from the PV jet directing the clean air towards the breathing zone of an occupant. Instead of supplying more air to achieve the penetration of the boundary layer by the PV flow, one can think of a way to control the flow interaction so that more clean air ends up in inhalation at unchanged PV flow rate. This can eventually lead to a substantial decrease in the PV flow rates and better performance. The present results confirm that ppersonalized flow supplied as a free jet with velocity above 0.25 m/s at the target area, i.e. the

breathing zone of the occupant, will be able to penetrate the free convection flow and provide clean air into inhalation (Melikov 2004). In this case it is important to extend the first region of the jet providing the clean air (near the nozzle) to be as long as possible, so as the clean air to be inhaled before mixing with the polluted air. In this way the risk from airborne cross-infection will be reduced and the air quality perception of the occupant will be improved. However, this strategy is not very energy efficient as increased velocity translates into increased volume of air. Hence additional expenses are also implied: more powerful fans, larger ducts, higher demand for heating or cooling of the PV air, depending on the season and temperature difference between the PV air and the room air. Therefore the control over the PV flow should be done meaningfully and should result in lowered energy consumption. At the same time, the air quality performance and individual protection of occupants from airborne diseases should not suffer or be reduced. As already discussed at the start of this Chapter the occupant's inhaled air quality and thermal comfort, when using PV depend on the interaction of the personalized flow with the free convection flow at the breathing zone. It is also important that the target area with clean personalized air, i.e. the area where the head is located, is large enough to accommodate moderate head movement and to ensure high performance of the PV system. Therefore PV nozzles with a relatively large area are recommended for use in practice. However, when large nozzles are used, a high personalized flow rate is needed in order to ensure the minimum velocity needed for penetration of the convection flow. This leads again to the hot topic of energy consumption. Another concern is that the relatively high velocity needed for penetration of the convection flow (above 0.25 m/s) may cause draught discomfort for the PV users, especially at the winter range of room air temperature (20 - 24 ^{o}C) recommended in the standards. However it should be also considered that the user will have control on the supplied flow rate and thus will be able to avoid draught discomfort or to achieve thermal comfort at warm environment. Furthermore, people are more sensitive to high velocities when seated and from the back (around the neck) than at the face, for the contact between the human body and the seat restricts the development of the convection layer at the back. Therefore lower velocities directed towards the back result in increase in heat transfer between the body and the surroundings (Melikov and Zhou 1996). The problem to be solved is to ensure a relatively large target area of clean air at the breathing zone at a reduced flow rate of personalized air, i.e. with low penetration (target) air velocity. In order to solve the problem, control of the airflow interaction at the breathing zone, especially control and weakening the strength of the free convection flow, becomes essential.

This study showed that a mere physical barrier on the upward way of the free convection layer (Chapter 4.2.1) already results in improved performance of the PV unit with respect to air quality at reduced flow rate. The aim of this barrier was to avoid the growth and thickening of the free convection layer around the body of a seated occupant as a result of joining of the convection flow originating at the feet and the one starting at the groins (Homma and Yakiyama 1988, Zukowska et al. 2007). Blocking the free convection layer by as simple method as a board already results in more than 93% of clean air into the inhalation zone of the occupant at 6 L/s (0.23 m/s), an amount earlier achievable only at flow rates above 12 L/s (Bolashikov et al. 2003). The presence of fans, as a way to diminish the free convection layer by exhausting part of it on its way upwards from the legs of the seated human and joining the one starting at the groins, needs to be applied with

caution especially at the flow rates for the PV below 6 L/s. As the PIV measurements have shown (Chapter 4.4.2) for the low flow rate of 4 L/s, though the convection layer at the face of the thermal manikin is weakened and the PV flow can now penetrate it, part of the clean PV air is pulled down by the underpressure generated by the fans (Section 4.2.2 and 4.4.2). The studied methods of control over the boundary layer resulted in rather similar performance. At 6 L/s all methods yielded above 90% of clean air into inhalation, thus providing sufficient evidence to claim that introducing control over the boundary layer at the groins level would result in improved performance in air quality, and also reduced risk from cross infection with regards to desk installed PV supplying the clean air transverse to the weakened boundary layer. Furthermore, the blocking or local suction of the convection layer at the groin level would prevent the pathogen laden airborne particles and odorous substances to be moved upwards from the lower room levels via entrainment towards the breathing zone, which would eventually happen provided a gap exists between the body and the desktop. Although further study on the active method of control is needed, especially with regards, to the importance of the suction flow rate on the development of the boundary layer, it may be suggested that the passive method of control, blocking the free convection flow in front of the human body, may be recommended for practical use. A board installed below the desk top panel and pressed gently against the occupant's abdomen with a simple spring mechanism can be easily and aesthetically applied in practice. The board will follow the backward and forward body movement and thus will break the free convection flow and will improve the performance of PV providing air at a low flow rate. The board can have a straight edge or be shaped to fit tighter to the abdomen, but the results of the present study reveal that the board design is not important for the performance of the control method.

The control of the airflow interaction at the breathing zone by supply of the personalized air from nozzles positioned close to the head might even result in better performance of the PV than in the case of the desk incorporated PV unit such as the RMP (Bolashikov et al. 2003, Bolashikov et al. 2009a, Melikov and Dzhartov 2009) or the co-flow PV nozzle (Khalifa et al. 2008 and Russo et al. 2008). In order to assure better performance with respect to air quality several control strategies were studied with the PV unit incorporated in the headrest of a chair supplying the PV flow from behind transverse to the boundary layer weakened due to the contact of the body with the chair. The results obtained with the reference case, i.e. when only the headrest PV nozzles were used, confirmed previous findings (Jacobs and de Gids 2006, Melikov et al. 2007) that the discharge angle of the personalized flow and its penetration velocity were important factors that determine the performance of the headrest incorporated PV system. Nielsen et al. (2007b) supplied clean air at low momentum to the breathing zone by a neck support (a textile "donut" around the neck) and from the side edge of a chair to make the clean air be taken by the convection layer upward towards the face. The concept of personalized air supply at low initial momentum and from relatively large area around the person resulted in increased initial flow rate. From the tested ATDs the highest PEE of 95% was achieved with the neck support at flow rates above 10 L/s.

The disadvantage of the control strategy based on suction of convection air (control strategy 1) is the required high suction flow rate for better performance of the PV system, i.e. high inhaled quality at low personalized flow rate. In this case, energy will be used to exhaust the air. However, it could still be energy-efficient to use this method due to the low flow rates of PV air

supplied. The energy savings from conditioning less PV air could be enough to cover the energy consumption of extracting the convection air; even energy saving can be realised. Depending on the design used, lower initial costs (ducting, less space, etc.) may add to the effectiveness of the control strategy when applied in practice. This, however, needs to be verified. Nevertheless, this strategy for control of the airflow interaction at the breathing zone leading to improved inhaled air quality may be advantageous for PV applications where the conditioning and cleaning of air is difficult and it is necessary to decrease the supply flow rate of clean air as much as possible, e.g. aircraft cabin. Localized exhaust openings incorporated in aircraft seats (on the headrest or overhead in the privacy divider) have been shown to help evacuate successfully most of the occupant generated pollutants, providing all passengers with air quality better than that in the reference case without localized exhaust openings, when the pollutants were mixed with the cabin air (Dygert and Dang 2009a and b).

The control strategy based on weakening and diluting the convection flow by supply of redirected clean personalized air (control strategy 3) examined in the present study was more efficient at the lower range (20 – 24 ^{o}C) of comfortable room temperatures recommended in the thermal comfort standards and with large nozzles. In this case, a clear advantage was the achievement of a high quality of inhaled air at reduced velocity of the personalized flow by its redirection through the controlled nozzles. For example, a supply of 4 L/s from the large PV nozzles and an additional 3 or 4.5 L/s flow rate of clean air from the control nozzles, i.e. total supply of 7 or 8.5 L/s of clean air, provided inhaled air quality equal to or even better than the case when 8 L/s clean air was supplied only from the PV nozzles. At 20 ^{o}C PEE between 70% and 80% was obtained with a personalized flow of 4 L/s and a control flow of 3 or 4.5 L/s while PEE was 56% when 8 L/s was supplied from the PV nozzles without control flow rate. The strategy of redirecting the personalized air reduced the local velocity in the vicinity of the head and thus draught discomfort as well. For example, the supply of only 4 L/s reduced the initial velocity of the personalized flow from the large nozzles to only 0.17 m/s and this decreased the risk of draught discomfort compared to a supply of 8 L/s at 0.33 m/s initial velocity, while maintaining the same inhaled air quality level. In the same way decrease of the draught risk will be achieved with the studied control strategies when applied with other PV designs providing the personalized flow from the front (Kaczmarczyk et al. 2004, Cermak et al. 2006). The control of the free convection flow leading to a decrease of the personalized flow velocity needed for penetration of the free convection flow will also decrease eye irritation for sensitive occupants, e.g. occupants wearing lenses.

The increase of the room air temperature will decrease the strength of the free convection flow (less difference between the body surface temperature and the air temperature) and thus would make it easier for the personalized flow to penetrate and provide clean air within the breathing zone. Therefore the relative improvement of inhaled air quality at 26^{o}C when the control methods were applied was not substantial (Chapter 4.2).

Control of airflow interaction at the breathing zone by removing the convection flow with opposing flow of polluted room air was not effective due to extensive mixing of the polluted air with the clean air provided close to the breathing zone. Improvement of inhaled air quality by use of the buoyancy force of the convection flow to transport upwards clean air inserted gently between the flow and the upper chest was limited. The inserted flow and the upcoming convection flow were

opposing and counteracting each other and as a result certain mixing was promoted. Therefore the effectiveness (PEE) was higher with the lower flowrates tested.

Two of the strategies studied for control of the airflow interaction at the breathing zone, namely strategy 1 and strategy 3, were shown to be successful and fulfilled several important requirements for design and implementation of PV in practice. Therefore it may be recommended that they could be applied 1) with large air supply devices and at low velocity of the personalized flow, i.e. low flow rate, generating a target area of cleaner air with a size sufficient to accommodate moderate movement of the head; 2) at the lower range of comfortable room air temperatures recommended in the standards (20 – 24 ^{o}C) when risk of draught discomfort is high.

Another way to approach the matter is to provide some control over the PV flow. In the present study this was achieved in two ways. One, by providing additional confluent jet of polluted room air with same aerodynamic and thermal characteristics as the inner (closer to the body) PV jet. In this way friction between the two jets will be avoided and thus the cleaner zone of the PV jet will be preserved for much longer distance on its way to the breathing zone of the occupant. The other way, is to reduce the distance between the PV jet and the breathing zone as much as possible and even immerse the PV nozzle into the free convection layer. This would require very low flow rates and quite smaller outlet concentrated only over the mouth or nose of the occupant.

The method of confluent jets not only assisted the convection layer but in fact replaced it by a clean PV air as the nozzle was incorporated in the board used as passive control over the convection layer. This managed to boost the amount of fresh air into inhalation up to 85% at 10 L/s compared to the similar design suggested by Melikov et al. (2007) where up to 60% of fresh air was at maximum achieved for flow rates over 20 L/s. The reason for the poorer performance of the design studied by Melikov et al. (2007) was a gap between the nozzle and the breathing manikin's body allowing the upcoming boundary layer to dilute and mix more the clean PV air. However, the width of the opening was also found to be an important factor for the effectiveness of the unit in supplying clean air upwards in front of the body into inhalation. The nozzle of width of 0.030 m was able to provide a maximum of 12% of clean PV air into inhalation and at 2 L/s (Chapter 4.3). At the higher flow rates the performance was even lower due to the enhanced mixing and the shorter length of the potential core region of the jet: the region with the initial characteristic of the jet. Regardless of the flow rate and the presence of confluent jet, the amount of clean air into inhalation never exceeded 85%. The reason for this was the pretty complicated geometry of the human body and the separation of the flow at the neck and shoulder level.

The control of the flow interaction by immersing the jet into the free convection layer and thus decreasing the distance between the PV nozzle and the mouth could be expected to provide the best results as the PV jet will be very close to the mouth/nose, and all the clean air supplied should be practically inhaled. All nozzles tested had a cross-sectional area much larger than that of the manikin's mouth of 0.000100 m^2 (100.4 mm^2). Only at the lowest studied velocity (0.2 m/s), the supplied flow rate of the inserted jet was always lower than the inhalation flow rate (0.24 L/s). Nevertheless PEE =1, i.e. the inhaled air to be 100% clean personalized air was not achieved with any of the tested nozzles. During inhalation the air close to the mouth/nose flows from all directions and therefore the amount of free convection air inhaled depends on the area and the shape of the inserted jet at the target spot, i.e. whether it is smaller, equal or overlapping the area of the

mouth/nose. In practice the free area of the mouth changes when people speak. This has to be considered and studied as well. In this respect more research on active control of the characteristics of the inserted jet is needed.

Nevertheless the use of the inserted jet made it possible to obtain similar PEE values to those obtained with the other PV devices, but at lower flow rates reduced more than 10 times. The CFD simulations of a headset PV device (discussed in Chapter 4.3), predicted that over 85% of the inhaled air will be from the air inserted by the jets from either the circular or the elliptical nozzles with an equivalent diameter of 0.030 m when positioned at 0.04 m from the face. Under the same conditions, the present measurements identify that a maximum 62% of the inhaled air will be PV air. In the CFD simulation, the CFD manikin was not breathing and the background velocities were negligible (below 0.01 m/s), and this may be the reason for the higher values obtained; as already discussed, inhaled air enters the mouth from all directions, drawing in also air from the boundary layer mixed with contaminated room air. Furthermore, the initial velocity 0.47 m/s used during the CFD simulations was higher than velocity of 0.4 m/s during the physical measurements. Both the CFD predictions and the present results show very little effect of the shape of the nozzle for the distance of 0.04 m from mouth.

The low flow rate of personalized air makes the headset PV device a feasible solution in crowded places such as trains, buses, aeroplanes, theatres, auditoriums, classrooms, etc., where the device would be used to provide clean air as well as an intelligent means to decrease the risk of airborne cross-infection. The device can be easily manufactured as a “plug and use” unit into a desk, chair/seat hand support, PC (via USB port), etc. in a similar way to the headsets used today for listening to music, radio, etc.

The application of inserted jets in wearable PV units may additionally result in certain energy savings, especially in buildings where the ventilation airflow rate needed for acceptable indoor air quality is higher than the ventilation airflow rate needed for thermal comfort. In this case the supplied indoor air could be 100% recirculated room air for even further energy savings.

4.8. Conclusions

Several methods for control of the airflow interaction at the breathin zone were seggested and their performance with regard to increase of the clean air in inhalation, leading to improved inhaled air quality and decrease risk of airborne cross-infection, was studied. The main conclusion are:

Control of the free convection layer in front of the body:

- Two methods, passive (blocking board) and active (suction fans), for control of the strength of the free convection flow in front of a seated human, and thus for control of its interaction with a personalized flow from the front, proved to be able to enhance the performance of the PV with regard to inhaled air quality at a reduced flow rate of supplied personalized air. At 6 L/s the portion of clean personalized air in the inhaled air was more than 90% and substantially higher than without control of the free convection flow (around 50%);

- Almost no difference was found in the performance of the passive and active method when applied alone. Applying the two methods simultaneously did not show any improvement either; it even led to a slight decrease in the performance of the PV at 6 L/s;
- The design of the board (straight or fitted around the abdomen) had no impact on the control of the free convection flow and thus on inhaled air quality;
- The use of the front or rear fans for active control of the free convection flow showed rather similar result, with slightly better performance when the front fans were used. The impact of the positioning of the fans and the suction flow rate needs to be studied further;
- Improvement of the airflow interaction at the breathing zone by exhausting part of the free convection flow in front of a seated person was found to be effective, especially when personalized air was supplied at low velocity and from larger nozzles installed on the chair headrest. At personalized flow rate of 4 L/s the control of the free convection flow increased the portion of clean air in inhalation to the level obtained without control and a personalized flow rate of 8 L/s;
- Weakening and diluting the convection flow with additional small amounts of personalized air supplied downwards at the upper chest level proved to be effective at a relatively low room air temperature. It improved inhaled air quality at a reduced personalized flow rate, i.e. low supply air velocity. The risk of draught was greatly reduced;
- Control of airflow interaction at the breathing zone by removing the convection flow with an opposing flow of polluted room air was not effective due to extensive mixing of the polluted air with the clean air provided close to the breathing zone;
- Improvement of inhaled air quality by use of the buoyancy force of the convection flow to transport upwards clean air inserted gently between the flow and the upper chest was limited, because the flow of cleaner air was redirected away from the mouth/nose by the lower face (jaws and chin that protrude over the chest vertical plane);
- All methods were tested under isothermal conditions (personalized air temperature equal to the control air temperature). Their potential under non-isothermal condition is recommended to be studied.

Control of the personalized flow:

- The effectiveness of PV jet, supplied upward at the abdominal area of the human body and assisting the free convection flow, with regards to inhaled air quality is limited due to the human body shape: the upward flow gets separated at the neck and shoulder region and only small portion reaches the mouth;
- The use of confluent jet (outer jet) of polluted air to protect the inner jet of clean air (both supplied at the lower chest) increased PEE up to 85% compared to the single jet application (PEE=60%). The change of the amount of air discharged from the outer opening had no effect on the PEE, while the change in the air supplied from the inner jet

resulted in a much worse performance regarding the air quality; 100% clean PV air into the air inhaled are possle to be achieved only when the initial spread of the PV jet issued from the nuzzle covers the inhalation zone around the mouth/noze of the seated person. Therefore the type of nozzle used should have a special geometry to account for increased initial spread, as well as reduced mixing.

- The width of both openings inner (PV) and outer (confluent) jets had effect on the performance of the nozzle. Better perfornce was achieved with the wider openings;
- The posture of the manikin had certain effect on the amount of clean air into inhalation provided by the confluent jets. When bent over the table, slightly better results were achieved compared to the case when the manikin was seated upright;
- The complex body geometry affects the flow interaction around the body of the occupant. Up to the breast level, where the boundary layer becomes turbulent, the existing theory can be applied to approxiate the maxium velocity and obtain good approximations.
- The amount of the clean air supplied by the inserted jet in the boundary layer close to the mouth increased with the increase of the initial jet velocity (i.e. the supply flow rate) and size and with the decrease of the distance between the air supply nozzle and the mouth. More than 80% clean “inserted” air in the inhaled air was measured when the inserted jet with an initial velocity of 0.4 m/s and higher was supplied from a nozzle with an equivalent diameter of 0.030 m (and larger) placed at a distance of 0.040 m (and closer) from the mouth;
- More clean air was inhaled with the inserted jet from the side than from the front and below, when the distance between PV nozzle and face (mouth/nose) exceeded 0.04 m;
- The portion of the clean air into inhalation, when supplied from a nozzle with an elliptical shape, was slightly more than when supplied from a circular nozzle, due to similarity of the geometry of the former with the mouth;
- The use of lobed nozzles changed substantially the characteristics of the inserted jet and thus the portion of clean air in the inhaled air. In this respect, the potential of the lobed jets needs to be studied further;
- The use of inserted jets in practice for PV application has great potential that requires additional research. Wearable PV devices, such as headset incorporated PV ATDs, can be further optimized and used for improvement of inhaled air quality and decrease of the risk from airborne cross-infections in practice, especially in densely occupied places (aeroplanes, trains, buses, theatres, classrooms, hospitals, etc.). The potential energy savings from wearable PV units based on inserted jets, when used in office buildings during different seasons and climates, needs to be explored.
- The existing theoritical approach for calculating the velocities along a heated vertical flat plate cannot be applied when there is “blocking” on the leading edge of the plate, where the boundary layer starts to develop as well as in presence of background velocities. The theory cannot be also applied for a seated human due to the complex development of the resultant boundary layer and the complex human body geometry.

Chapter 5 : Advanced Air Distribution for Reduction of Airborne Cross-infection Due to Coughing in Hospital Wards

Ventilation of infectious hospital wards is used today for decreasing the risk of air-borne cross infection. Dilution of contaminated room air with clean outdoor ventilation air is used. Therefore to enhance the dilution mixing air distribution is most often applied. The minimal air change rate of 12 h^{-1} is recommended in the present standards (ASHRAE 170-2008, DS 2451-9-2003). Even this high air change rate is insufficient to protect completely patients, medical staff and visitors from cross-infection (Chapter 2). Furthermore the method of dilution by high ventilation flow rate is not energy efficient.

This part of the study focuses on the development of new advanced method for air distribution in infectious hospital wards aiming to decrease the risk from cross-infection. The study limits its observations, discussion and conclusions only to cross-infection of pathogens generated due to coughing.

5.1. Flow of coughing

Coughing is the most obvious symptom of a respiratory disease. It is quite rare in healthy individuals. Normally the clearance of the respiratory tract is satisfactorily managed by other mechanisms – the immune and the mucociliary system. When those systems fail, or when they are overloaded by foreign materials or by secretions abnormal in kind or amount, as during respiratory disease, cough is a fast and powerful response (Brain et al. 1977). Coughing is an impulse jet led by a characteristic vortex ring that can penetrate quite far before it dissolves in the surrounding air (Settles 2005, Tang et al. 2009). Information about cough flow rate is available in the literature (Leiner et al. 1966, Singh et al. 1995, Zhu et al. 2006, Gupta et al. 2009). The corresponding peak velocity can vary from 6 m/s to 30 m/s (Edwards et al. 2004, Zhu et al. 2006) with an average of 11.2 m/s. Gupta et al. (2009) found that the medical parameters describing the cough, such as Cough Peak Flow Rate, CPFR, (highest flow rate during cough), Peak Velocity Time, PVT, (time when CPFR is reached as from start of cough) and Cough Expired Volume, CEV, (total amount of air expelled during a single cough) depend mathematically on the personal data such as height, weight and gender. The difference between the maximum and minimum values of CPFR, CEV and PVT for the male subjects was about 200, 300 and 100%, showing the great variety among subjects. They also found that mouth opening area was constant during the whole cough. Therefore a mean mouth opening area to simulate a cough was suggested: 4.00±0.95 cm^2 for male and 3.37±1.40 cm^2 for women.

The total cough volume varies within 0.8–2.2 L with an average of 1.4 L (Zhu et al. 2006), which is the low end according to the results of Mahajan et al. (1994), who observed a variation of up to 5 L with an average of about 3 L. Gupta et al. (2009) identified that CEV ranged from 0.25 to 1.6 L, and was dependent on the subject's sex.

Mahajan et al. (1994) also documented that the cough lasts around 50 ms with the PVT being of the magnitude of a few milliseconds. Singh et al. (1995) reported that PVT also depends on the sex of the coughing person. On average women show higher PVT value due to the larger larynx

compared to men. Gupta et al. (2009) confirmed that the PVT time is sex dependent but shifted by 50 ms compared to the values reported by Mahajan et al. (1994): ranging from 57 to 110 ms.

Usually, when an individual coughs a sequential cough is produced – two coughs in a single set. The flow behavior of the two coughs in the sequential cough is similar to that of single one: the first cough closely follows the behavior of the single cough, while the second one is a scaled down version: 0.5 to 0.6 times the single one (Gupta et al. 2009).

As already mentioned coughing in its nature is aimed to clean the lungs from foreign material or overflow of mucous secretions, and hence is a major contributor of droplets dispersion into the surroundings. Nevertheless, not very precise data on size distribution of generated particles exists in the literature (see Chapter 1 and **Paper I**, **Appendix I**). Recent study of Chao et al. (2009) with Interferometric Mie Imaging (IMI) method with eleven healthy human subjects on cough and speaking showed a geometric mean diameter of the droplets expelled of 13.5 μm and 16 μm respectfully. Up to 2085 droplets with concentration of 5.2 per cm^3 per cough and up to 6720 droplets with concentration of 0.223 per cm^3 for duration of speaking were reported as well. Morawska et al. (2009) implying human subject experiments found that all respiratory activities produced particles at several modes, the predominant one being of diameter below 0.8 μm. The average concentration for the cough is reported to be of the order of 0.57 per cm^3 much lower than that of Chao et al. (2009).

Due to its high initial momentum the cough becomes one of the dominating transport mechanisms indoors for airborne particles generated from a coughing sick individual. The existing ventilation strategies cannot prevent the spread of those particles generated from coughing even if very high ventilation rates are used, especially close to the source: the coughing individual. It becomes clear that new methods are needed to restrict the spread of airborne pathogen laden droplets and thus reduce the risk from airborne cross-infections.

5.2. Advanced method for air distribution: Hospital Bed Integrated Ventilation and Cleansing Unit (HBIVCU)

The need for better control over the air distribution in hospital wards with respect to personal protection of the medical staff and the patients form airborne cross-infection was already discussed (Chapter 2). As already mentioned during coughing a large number of particles are aerosolized and the major number is of size below 0.8 μm (Morawska et al. 2009). These particles after complete evaporation become nuclei of approximately half the size (Nikas et al. 2005), and have high probability of penetrating the lungs of the person who inhales those. One way to control the dispersion of the coughed air is to exhaust it locally close to the mouth of the sick person, where the jet is still less mixed with the surrounding air. In an infectious hospital room most of the time people spend lying in bed. This is especially true during the symptomatic stage of the disease when individuals are highly contagious in case of airborne contagious diseases like measles, small pox, tuberculosis etc. A novel method for reduction the risk of spread and mixing of the coughed air with the room air in infectious hospital wards was proposed. A ventilation unit in close proximity to the head of the sick person guarantees successful evacuation of the largest part of the pathogen laden air from pulmonary activities, purging it (via UVGI or another cleaning method) and directing it e.g. upwards, through one or more horizontal slots, towards the exhaust vents of the total volume

ventilation at elevated velocities (Figure 5.1). The directed thus upwards cleansed air would act as a barrier between the medical staff member, staying close to the bed from one side, and the patient on the other side. Furthermore the discharged air jets (acting as air curtains) will entrain the coughed air and move it upward directly towards the exhaust. Another possibility is to connect via pluggable flexible duct the unit to the TV ventilation exhaust to direct the pathogen laden air out of the room as well as to the TV supply to provide clean air into the room from the horizontal slots, and thus bypass the cleansing section of the unit. The compatibility of the unit would make it quite flexible from energy point of view: it could even be powered by battery unit or plugged into the mains. The expectation is that the unit would have some potential for energy savings. The local extraction of air expelled by the sick individual will lead to reduction in the amount of air from the total volume ventilation, as less air will be needed for dilution. Thus less air would be conditioned to be supplied indoors. The idea is the device to be mobile and easily transported as well as mounted on the patients' beds, following the new concept for hospital appliances, namely "plug and operate". The benefits of such a unit, named Hospital Bed Integrated Ventilation and Cleansing Unit (HBIVCU) are obvious: on the first place is healthier working environment for the medical staff and faster recovery for all patients with reduced risk from nosocomial infections, and second is the potential for energy savings.

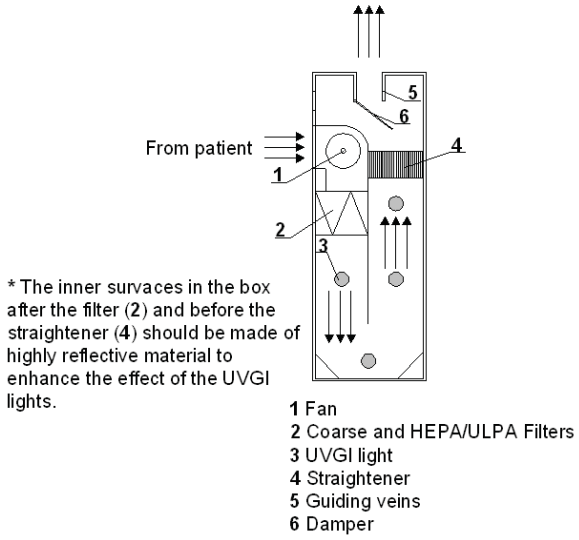

Figure 5.1 *The ventilation and cleansing principle behind the HBIVCU.*

5.3. CFD Prediction

The efficiency of the HBIVCUs with respect to reduction of the transmission of airborne diseases in hospital environment was first examined by CFD simulation with a coughing patient. The objective was to confirm the potential of the novel method in reducing the risk of cross-infection.

5.3.1. Methods

The simulation was performed in a room with dimensions 3.5 m × 4 m × 2.5 m (L x W x H). Two beds were positioned in the room 0.5 m away from the back and side walls and 1 m distance between the beds. Two CFD manikins were used for the current simulation lying in the two beds. The complex shape of the human body, was very similar to a real one, and was adopted to account the impact of the local characteristics of the body shape on the free convection flow at the vicinity of the body. The skin surface area of each CFD human model was 1.46 m^2. The two "patients" were lying in the beds covered with quilts and only their heads were exposed to the ambient room air. The whole room was ventilated by mixing type of total volume ventilation (MV) with flow rate resulting in 6 h^{-1} or 12 h^{-1}. The supply vent was positioned in the center of the room (4 way diffuser 0.5 m x 0.5 m, Table 3) and the two exhaust diffusers (0.5 m x 0.5 m) above the two beds over the head of every patient. The temperature in the room was kept at 22 ^oC.

5.3.2. Cases analyzed

As shown in Table 5.1, 4 cases were studied. In each case, one of the patients was set to do continuous coughing, and the other to do continuous inhalation. In Case1 and 2 (Figure 5.2a), the two beds were without the HBIVCUs installed. In Case 1, the patient lying on one side facing the other patient was assumed cough continuously towards the person lying on his back in the other bed. Opposite to Case 1 in Case 2 the person lying on his back was the one coughing continuously. Case 1 and 2 were considered the reference cases when the HBIVCUs were not incorporated into the bed design. In Case 3, four HBIVCUs were installed at the two beds, two units per bed, from both sides and close to the patient's head (Figure 5.2b). Also in Case 3, the person lying on his side was the one coughing continuously. Coughed air was sucked from the exhaust opening of the HBIVCU and cleaned air was discharged upwards from the top slot opening only from the unit that was installed at the bed of the coughing patient and at that side the coughing patient was lying facing. The only difference between Case 3 and Case 4 was the back head board placed at the two beds (Figure 5.2c). The air change rate was 12 ACH in Cases 1and 2 and 6 ACH in Cases 3 and 4.

Table 5.1Case Analyzed.

Case N	Posture of Coughing person	Discharged airflow per HBIVCU		Sucked air per HBIVCU		Total Volume Ventilation	
		Airflow rate [m^3/h]	Initial velocity. [m/s]	Airflow rate [m^3/h]	Velocity at opening [m/s]	Air Change Rate [h^{-1}]	Velocity at TV supply [m/s]
1	LS	x	x	x	x	12	1.43
2	LB	x	x	x	x	12	1,43
3	LS	200	2,78	200	0.46	6	0,72
4	LS	200	2,78	200	0.46	6	0,72

LB: Person lying on back, LS: Person lying on side.

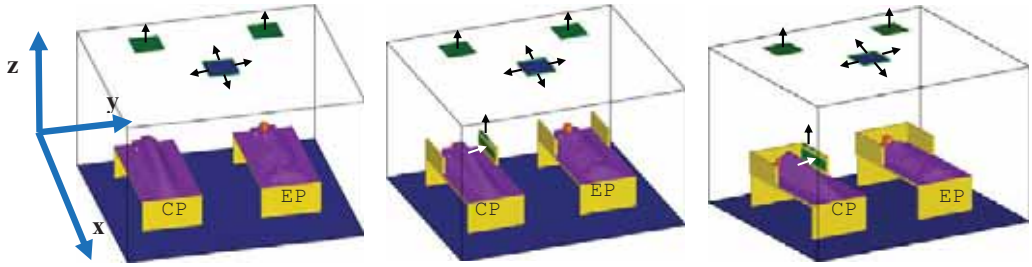

a) In Case 1 and 2* b) In Case 3 c) In Case 4

Figure 5.2 *Room set-up modeled in each of the studied cases. CP – Coughing Patient, EP – Exposed Patient.*

* In Case 2 Figure 5.2a the positions of the patients are switched: The one in the left bed is EP and the one in the right bed is CP.

5.3.3. Grid System

Depending on the case analyzed the grid system varied. In Cases 1 and 2, there were 78,578 triangular surface meshes and 1,065,657 volume cells, in Case 3, the numbers were 81,500 triangular surface meshes and 1,044,290 volume cells, and finally in Case 4, there were 83,936 triangular surface meshes and 1,032,844 volume cells. In each case, in order to account the impact of the local characteristics of the complex shape of the heads, there were 3153 triangular surface meshes for the head of the person lying on one side, and 2518 meshes for the head of the person lying on back. Depending on the case and the position of the simulated person, whether lying on the back or sideways, different number of surface triangular meshes were used for the quilt, the CFD manikin and the pillow (Table 5.2).

Table 5.2 *Number of surface triangular mesh for the quilt, pillow and CFD manikin.*

Case Number	Person Lying Sideways (PS)	Person Lying on Back (PB)
Case 1	13 754	8 658
Case 2	13 754	8 658
Case 3	13 154	8 552
Case 4	12 986	8 389

5.3.4. Contribution Ratio of the Coughed Air

In the simulation, the mouth for coughing was taken as a supplying opening, and the indoor distribution of coughed air was calculated using the mathematical method of SVE4 (Scale Ventilation Efficiency 4; Kato et al. 1992), which was initially developed to evaluate the contribution ratio of a supply opening. SVE4 was defined with the following equation:

$$SVE4(X/mouth) = C(X)/C_0 \quad (5.3.1)$$

where,

$C(X)$ concentration at point X of tracer gas generated at the mouth opening, [ppm];

C_0 concentration of the tracer gas at the mouth opening, [ppm];

$SVE4(X/mouth)$ concentration ratio, [-].

In this simulation, a passive scalar was given at the mouth of the coughing patient with the value of 1. Therefore, a value of 0.09 means that 9% of the air at that point was air exhaled from the coughing patient.

5.3.5. CFD Method and Boundary Conditions

CFD analyses were conducted based on a Standard Reynolds-number type k-ε turbulence model (Launder et al. 1975), together with the implicit SIMPLE algorithm (Patankar 1980). Moreover, the finite volume method with a first-order upwind scheme (UD) was adopted for discretizing the governing equations (Table 5.3). The detailed boundary conditions could be seen in Table 5.4.

Table 5.3 *CFD Methods.*

Turbulence model	Standard Reynolds-number type k-ε turbulence model
Algorithm	SIMPLE
Space Scheme	First order upwind scheme (UD)

Table 5.4 *Boundary Conditions.*

Supply opening of MV		Airflow rate, Velocity, as shown in Table 5.1, Temperature: 22 ºC Turbulence Intensity: 10 %, Turbulence Scale: 0.005 m, Size: 0.04 m×0.5 m (×4)
Exhaust opening		Velocity: free slip, Temperature: free slip, Size: 0.5 m× 0.5 m (×2)
Supply opening at the boards (In case3 and 4)		Airflow rate, Velocity: as shown in Table 5.1, Temperature: 22 ºC, Turbulence Intensity: 10 %, Turbulence Scale: 0.005 m, Size: 0.05 m×0.40 m
Suction openings at the boards (In case3 and 4)		Airflow rate, Velocity: as shown in Table 5.1, Temperature: 22 ºC, Turbulence Intensity: 10 %,Turbulence Scale: 0.005 m, Size: 0.15 m×0.80 m
Wall Boundary		Velocity: Generalized Log-law, Temperature: Generalized Log-law, adiabatic
Human body	Wall surfaces	Velocity: Generalized Log-law, Temperature: Generalized Log-law, convection heat transfer: 33.8 W
	Mouth openings for coughing	Velocity: 22m/s, Temperature of exhaled air: 32 ºC Turbulence Intensity: 10%, Turbulence Scale: 0.01m
	Nostril opening for inhalation	Velocity: 0.8m/s, Temperature: 22 ºC, Turbulence Intensity: 10%, Turbulence Scale: 0.005 m

It was assumed that the human body discharged a total convection heat of 33.8 W (metabolic rate: 0.7 Met, breathing rate: 0.24 L/s). This distribution of convection heat flux was given for quilt, pillow, and head, based on the data obtained through an experiment using a thermal manikin laid down and covered with a blanket (Yang et al. 2001). Except for the above surfaces, the other wall surfaces were assumed to be adiabatic. Moreover, the standard wall function was used for the near wall boundary layer. Continuous inhalation and continuous coughing were simulated by

setting initial velocity at the nose (inhalation) and mouth opening (cough) of each occupant depending on the case (Table 5.4). The concentration distribution of coughed air was calculated by setting a passive scalar uniformly at the mouth opening with an initial value of 1(polluted pathogen laden air of airborne particulate matter < 2 μm in diameter).

5.3.6. Results of simulation

The results are presented as velocity and concentration distributions across several planes:

- Sec.0.2x: Plane across the centers of the mouth of the coughing patient along X-axis (X=0.2m).
- Sec.1.25x: Plane across the center of the inlets of the MV in X-direction (X=1.25m).
- Sec. 0.66z: Plane across the center of the mouth of the person lying on one side in Z-direction (Z=0.66 m height from floor).
- Sec. 1.7z: Plane across the room at height of Z=1.7 m from floor.

In the first case (Case 1) studied the coughing person was turned sideways to the other patient and was continuously coughing. Figure 5.3 shows the velocity and concentration distributions within the hospital room. When the cough reaches the other patient, the velocity decreases to around 1.2 m/s from 22 m/s initial value. The effect of the coughed flow, zone of elevated velocities, is localized mainly in the area concentrated between the two beds around the occupants' heads. At 1 m further down along the X axis (Sec 1.25x) there is no effect of the cough at all on the velocity field in the room.

The highest value of the SVE4 index documented at the mouth of the recipient patient was 0.09 at 12 h^{-1}, i.e. 9% of the air inhaled from that person would be coughed air laden with airborne pathogens. The polluted air hit the wall and then was exhausted by the vent situated above the bed. A zone of polluted room air containing 6% coughed air was formed in the center of the room between the two beds and extending to the recipient patient (Figure 5.3.4 and 5.3.5). It was as a result of the mixing between the room air and the coughed air that hit the opposite to the coughing patient wall initiating a zone of elevated coughed air content between the patient's bed and the wall (Figure 5.3.1, 5.3.3 and 5.3.4).

In Case 2 when the coughing patient was lying on the back, the coughed air was directed upwards towards the exhaust (Figure 5.4). Part of the coughed air hit the neighboring room wall creating a recirculation zone where high concentrations were documented: SVE4 was 7% on average (Figure 5.4.1 and 5.4.3). The spread of the coughed polluted air to the other side, where the recipient patient was lying, was limited due to the clean air coming from the TV supply diffuser pushing the coughed air back and down and limiting the spread further throughout the whole room (Figure 5.4.1 and 5.4.3).

The introduction of the HBIVCU at the sides of the 2 beds even helped to reduce further the concentration of the polluted air at 2 times reduced total volume ventilation rate (corresponding to 6 h^{-1}). However only the HBIVCU facing the coughing patient was working, the other 3 were not operational. This scenario was considered as optimum one, taking into account the energy safe mode of the unit. Via sensor installed (CO_2, infrared temperature sensors etc.) the unit can detect which side of the bed the patient is turned to and activate the corresponding HBIVCU, thus saving additional energy. When the patient lays on the back both units at both sides of the bed can be

turned off. Definitely the presence of local suction helped reduce the concentration of coughed air in the room down to 2% at 6 h^{-1} from 9% at 12 h^{-1} without the unit. In order words the HBIVCU helped reduce the concentration of coughed air 4.5 times by reducing the total volume ventilation by factor of 2. The zone of high concentration was localized very close to the occupant's body (Figure 5.5.4 and 5.5.5).

Adding additional board behind the head of the coughing person (Case 4, Figure 5.6) resulted in slightly worse situation for the exposed patient. Part of the coughed air due to its initial momentum hit the back head board and was mixed into the room, resulting in SVE4 of 3% at the breathing zone of the exposed patient (Figure 5.6.3 and 5.6.5). However, between the bed of the exposed patient and the wall, the concentration of coughed air into the local room air was lowest, only 1%.

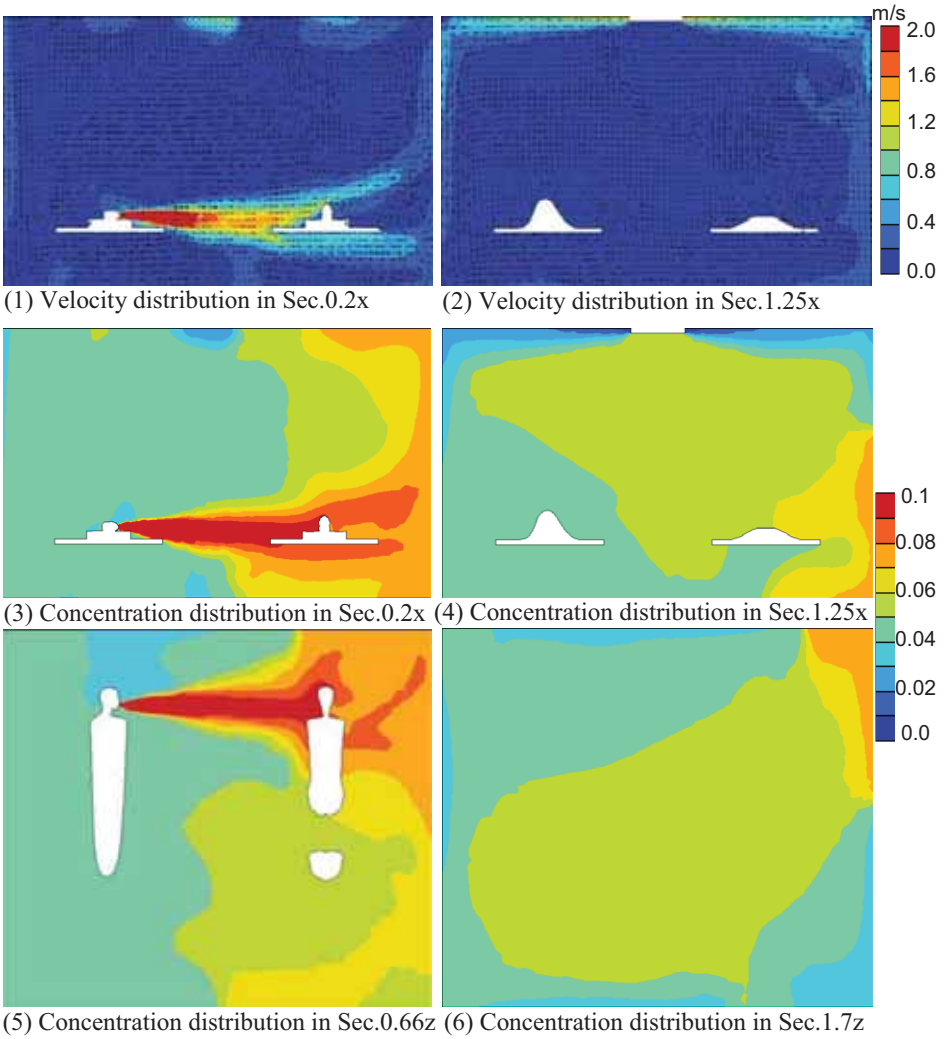

(1) Velocity distribution in Sec.0.2x (2) Velocity distribution in Sec.1.25x

(3) Concentration distribution in Sec.0.2x (4) Concentration distribution in Sec.1.25x

(5) Concentration distribution in Sec.0.66z (6) Concentration distribution in Sec.1.7z

Figure 5.3 *Simulation Results in Case 1.*

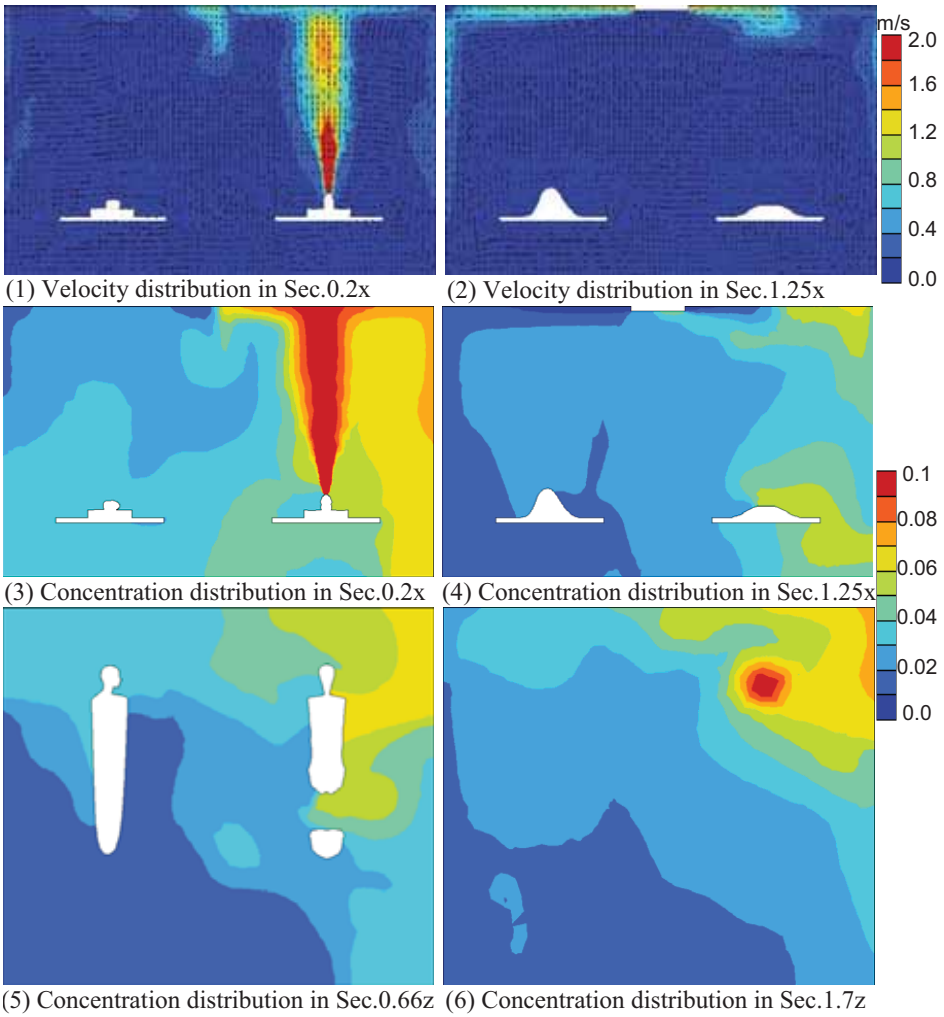

(1) Velocity distribution in Sec.0.2x (2) Velocity distribution in Sec.1.25x

(3) Concentration distribution in Sec.0.2x (4) Concentration distribution in Sec.1.25x

(5) Concentration distribution in Sec.0.66z (6) Concentration distribution in Sec.1.7z

Figure 5.4 *Simulation Results in Case 2*

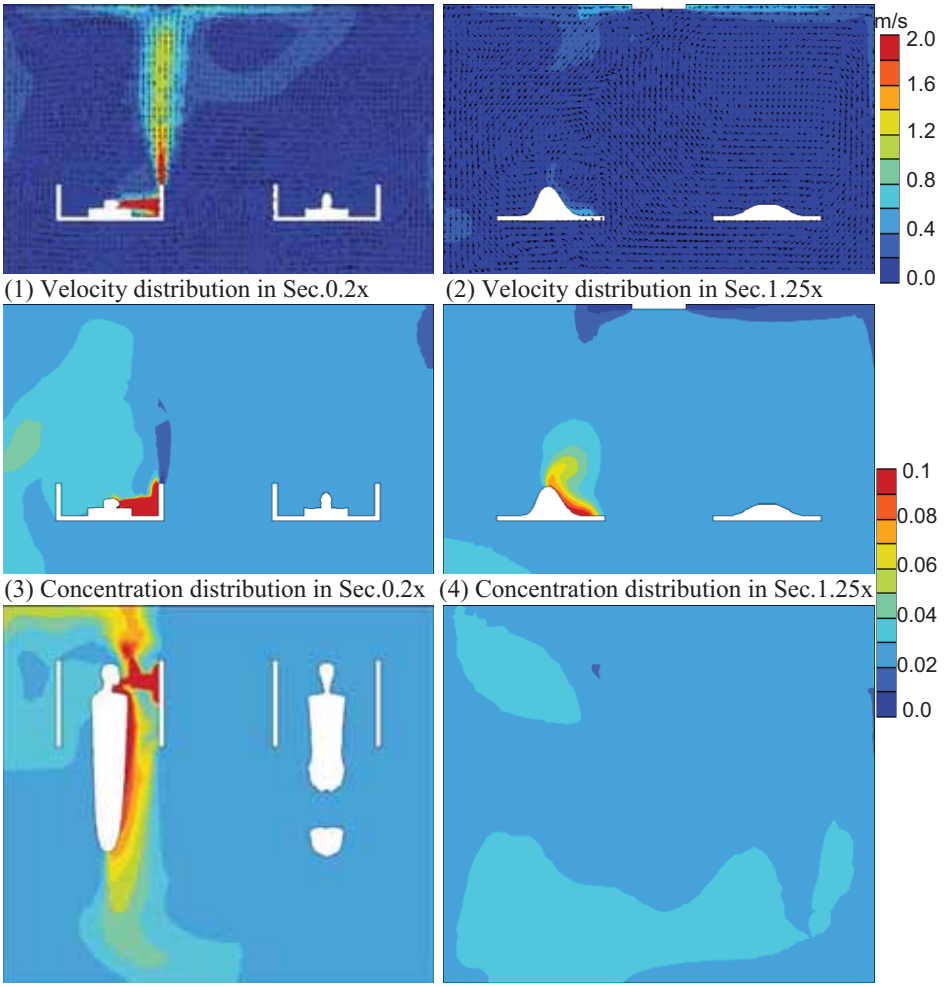

(1) Velocity distribution in Sec.0.2x (2) Velocity distribution in Sec.1.25x

(3) Concentration distribution in Sec.0.2x (4) Concentration distribution in Sec.1.25x

(5) Concentration distribution in Sec.0.66z (6) Concentration distribution in Sec.1.7z

Figure 5.5 *Simulation Results in Case 3.*

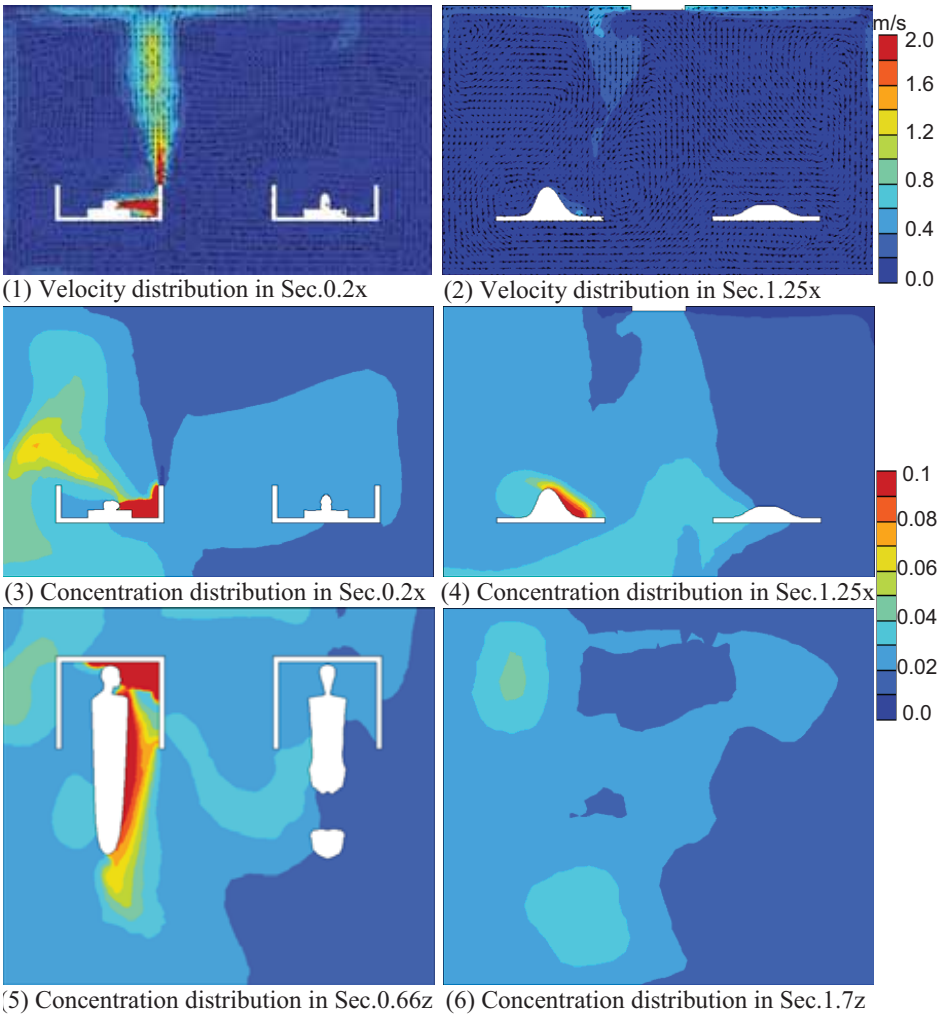

Figure 5.6 *Simulation Results in Case 4.*

5.3.7. Discussion

The results obtained in the current simulation reveal that the direction of the cough strongly influences the room flow distribution and the distribution of pollutants in the room. The elevated flow rate in the room at 12 h^{-1} managed to dilute the coughed air and spread the contamination to a wide zone in the center of the room. However the highest concentration becomes locked within a narrow region between the two patients (Figure 5.3.3 and 5.3.5). The upward directed cough was less mixed and resulted in lower SVE4 index throughout the hospital room (Figure 5.3 and 5.4 Concentration distributions). The reason for this was that the exhaust diffusers were positioned directly above the head of each patient, and this in the case of coughing resulted in

direct extraction of the coughed upwards air (Figure 5.4.3). There was however a small recirculation zone by the wall closest to the coughing patient as a result of the close proximity of the jet to the wall surface and the entrainment of surrounding air. The clean air coming from the supply diffuser also limited the spread of the cough towards the other patient, by pushing it back towards the exhaust and limiting its spread in the other part of the room (Figure 5.4.3). Close to the mouth the SVE4 index was close to the one calculated when the HBIVCU was used, i.e. 3%, but still the ventilation rate in this case was 2 times higher compared to Cases 3 and 4, when the HBIVCU was applied.

The obtained results reveal that the application of the HBIVCU helped to reduce the overall concentration of coughed air in the room; therefore it effectively managed to reduce the risk from airborne cross infection between two patients in a hospital environment. Results showed that 2% of the air inhaled by the exposed patient would be coughed air, when the novel unit is operating, compared to 9% when only TV ventilation functions. Moreover, the close proximity of the suction opening allowed the total volume ventilation to be reduced two times than the recommended in present standards (ASHRAE/ASHE 170-2008, DS 2451-9, 2003) resulting in even better overall performance with regards to contaminant evacuation by the system.

Results also show that when only one HBIVCU was working (Case 3 and 4) not all coughed air was successfully exhausted and some small portions ended up in the room air. Therefore in future experiments and for the future application of the unit, the case when both units at the bed of the coughing person are operational should be considered. This might even lead to further reduction of the total volume ventilation rate associated with increased energy saving.

It should be taken into account the fact that during the simulation the cough was continuously simulated like a free immersed jet with initial velocity of 22 m/s. However in reality this is not the case. The coughed air would behave more like a single transient injection flow with a fast decay of the velocity during release: for 0.5 s the velocity changes from 22 m/s to 0 m/s. Therefore the results presented with the continuous cough have some limitation. In reality the concentration of pollutants introduced by the cough would be lower within the room. Nevertheless the present simulation give some idea about the flow interaction in the occupied place, and justify the application of the new ventilation technique proposed with the HBIVCU.

5.3.8. Conclusions

- In series of CFD simulations, the performance of a novel method, namely the HBIVCU, aiming for evacuating locally the pathogen laden air generated from a coughing sick patient within a hospital environment was studied;
- The position of the coughing patient, when lying in a bed sideways or upwards, results in different distribution of the coughed air into the hospital room. The cough upwards resulted in 3 times reduced coughed air contend in the air inhaled by the other patient than the cough sideways;
- The application of the HBIVCU resulted always in lower concentration of coughed air into the air inhaled; the concentration was reduced as much as 4.5 times. The application of the novel ventilation method based on local evacuation of pollutants via suction helps decrease the exposure to exhaled polluted air from a sick patient

and results in reduced risk from cross infection via the airborne route;

- The use of the HBIVCU led also to a significant reduction of the background ventilation air flow, from 12 h^{-1} down to 6 h^{-1} and has potential for significant energy savings. However this needs to be further studied.

5.4. Experimental validation of HBIVCU method performance

Physical measurements were designed to study the performance of the HBIVCU method under realistic conditions.

5.4.1. Method

5.4.1.1 Full-scale test room

All experiments were performed in a full-scale test room with dimensions 4.65 m x 4.65 m x 2.60 m (W x L x H). Five ceiling-mounted light fixtures (6 W each) provided the background lighting. A hospital room layout consisting of two beds with patients and a standing doctor and two patients facing each other was simulated with the set up (Figure 5.7). The patients were simulated by two heated dummies and the standing doctor with a thermal manikin in the case when doctor was present in room. In the other case, namely when only the patients were in the room, one of the dummies was replaced by the thermal manikin.

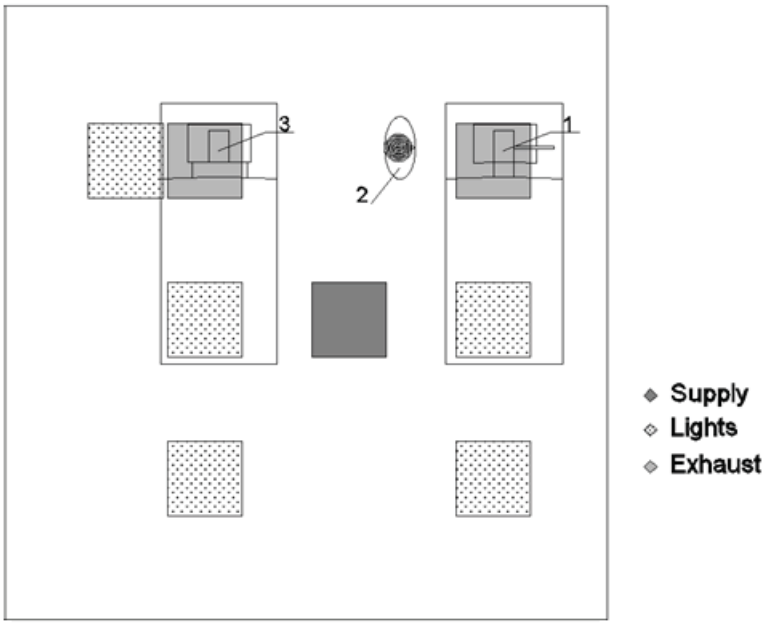

a)

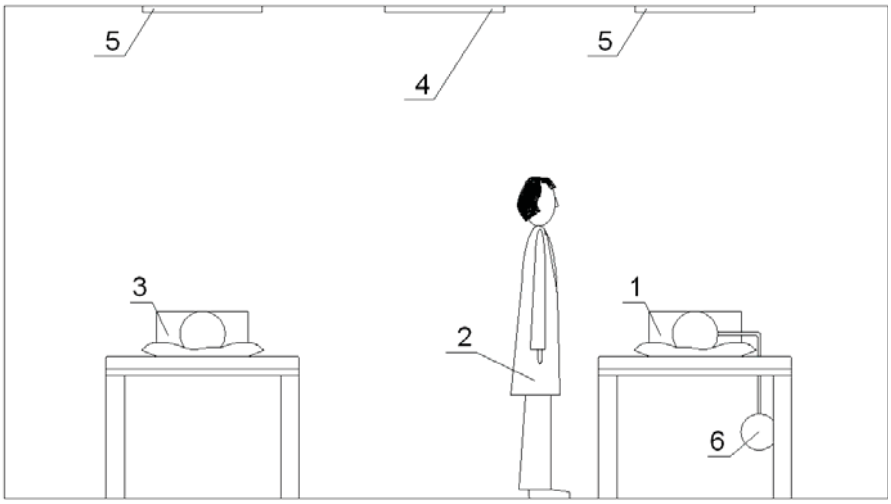

b)

Figure 5.7 *Hospital room layout a) top view, b) side view. 1) coughing sick patient, 2) doctor, 3) exposed patient, 4) TV supply inlet, 5) TV exhaust outlets, 6) coughing generator.*

The test room itself was built in a laboratory hall and raised 0.7 m above the floor. The laboratory hall had a separate ventilation system allowing for temperature control of the environment around the test room where the experiments took place. The walls of the test room were made of particleboard and were isolated with 0.06 m thick styrofoam plates. One of the walls was made of thick single-layer glazing.

5.4.1.2 Total volume ventilation

Mixing type of ventilation was used to condition the air in the test room. The air supply diffuser (a four way diffuser) and two air exhausts (a perforated rectangular diffusers mounted above the two beds above the heads of the patients) were installed on the ceiling (Figure 5.7). The exhaust air was equally balanced between the two diffusers. The supplied air was 100% outdoor (no recirculation was used). A slight under-pressure of 1.6±0.2 Pa, resulting in extra amount of air exhausted was kept during all the experiments in order to avoid a flow of air from the test room to the tall hall. The supply air temperature and the supplied and exhaust air flow rate were continuously controlled to keep the set values defined for each of the tested conditions.

5.4.1.3 System for advanced air distribution at each bed

For the purpose of the experiment, a prototype of the Hospital Bed Integrated Ventilation and Cleaning Unit (HBIVCU) as described in Section 5.2 was made. The prototype used in the experiment at present is a subject of patent approval in Europe (EP 09165736.1) and USA (US 61/226,542). Briefly stated, the HBIVCU is shaped as a box with dimensions of 0.6 m x 0.145 m x 0.60 m (L x W x D). It can be installed at the sides and/or head of a hospital bed. As already described, it helps to exhaust the air from the pulmonary activities of the sick occupant/patient

(breathing, coughing, sneezing etc.), clean that air from the pathogens via UVC light and then discharges it vertically through a horizontal slot at a high initial momentum towards the ceiling, where it is to be exhausted by the total volume ventilation. For the purpose of the present experiments two slots were made on the device suction (0.50 m x 0.14 m, L x W), on the side wall of the box, and a discharge opening (0.54 m x 0.05 m, L x W) on the top (Figure 5.8). It is important to note that in some applications the suction can be used as a supply and the discharge opening as an exhaust opening. These applications claimed in the above mentioned patent application were not studied due to the limited time. To justify the effectiveness of the HBIVCU to capture the coughed/exhaled air from the sick patient, and then cleanse it from any pathogens and subsequently discharge it back into the room, the unit was designed to have two different sections separated from each other by a firm partition, named supply/clean air section and exhaust/capturing section (Figure 5.9). Therefore, for the purpose of this study a separate HVAC system was assigned to supply air isothermally to the supply section of the box, and to exhaust the air from the capturing section of the box at a specific controlled flow rates. The amount of air supplied and exhausted was always the same and was determined by the initial discharge velocity from the top slot (1.4 m/s or 2.8 m/s corresponding to 37.5 L/s and 74.9 L/s). The experiments were performed with either 2 pairs of HBIVCUs installed (one at each side of the two beds) or without any device at all.

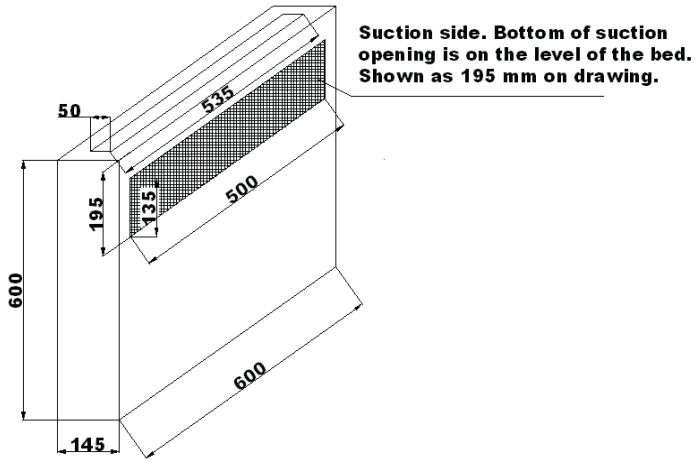

Figure 5.8 *Dimensions of the used Hospital Bed Integrated Ventilation and Cleansing Unit (HBIVCU).Dimensions given in millimeters.*

The HBIVCU units were connected to the HVAC system via flexible ducts. A set of dampers and differential pressure sensors incorporated in both supply and exhaust ducting of each unit, were used to control the supply and exhaust flow rate to and out of each of the boxes (Figure 5.9).

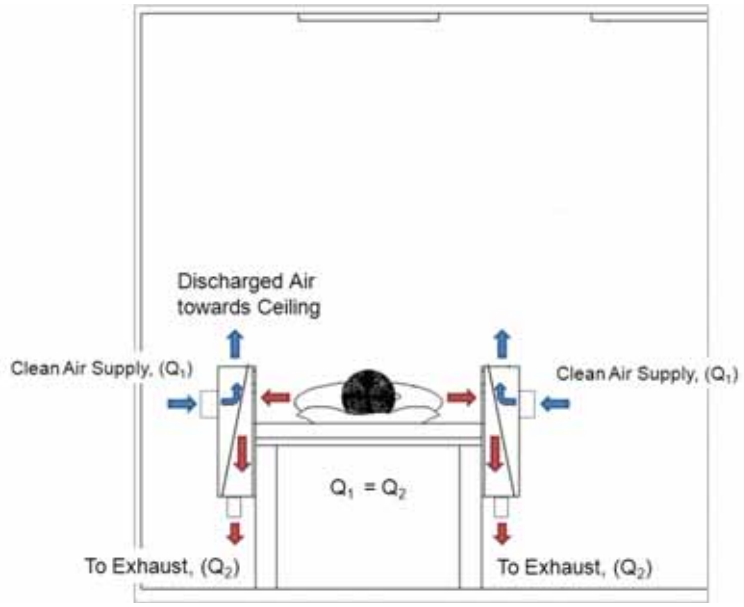

Figure 5.9 *Experimental layout with the HBIVCU connected to a separate HVAC system.*

5.4.1.4 Thermal Manikin

The thermal manikin (described in the Chapter 4) was used to mimic the doctor standing next to the beds of the "sick" occupants or to mimic the patient exposed to the air coughed by the other patient. In none of the experiments the manikin was breathing.

5.4.1.5 Heated Dummies

Two dummies with a simplified human body shape, as shown in Figure 5.10 were used to simulate the sick patients. The dummies consisted of 3 parts – "legs", "torso" and "head". All parts were made from galvanized ducts: The head and legs were made from circular ducts with diameters of 0.2 m and 0.12 m respectively. The torso was a cuboid made from a duct of rectangular cross section with dimensions: 0.6 m x 0.35 m x 0.2 m (H x L x W). The total height of the dummy was 1.65 m. Six bulbs were placed in the torso of a dummy. One was installed in the head, one in the torso and 2 in each leg. Together with the bulbs 1 fan was also installed in the torso to help for homogeneous spread of the air heated by the bulbs throughout the dummy. Totally they produced 80 W of heat power.

Figure 5.10 *Picture of the heated dummy of simplified geometry resembling a human and used to mimic the lying patients in the hospital mock-up environment.*

5.4.1.6 Coughing Machine

One of the dummies was equipped with a specially developed coughing machine. This dummy was used to mimic a "coughing patient". The design of the coughing machine is not disclosed since it is intellectual property. 100% carbon dioxide was used to simulate the flow of coughing. The CO_2 gas was used to simulate airborne droplets with initial diameter of less than 2 μm produced by the coughing "patient", i.e. in this case it was operated as a puffing machine. The mouth was simulated by a circular hole of a diameter of 21 mm. The characteristics of the cough were as follows: volume peak flow – 10 L/s, volume of the cough – 2.5 L, time span of cough – 0.5 s and maximum velocity – 28.9 m/s (Melikov et al. 2009). The time of the cough and the measured voltage by the pressure sensor installed in the coughing machine was recorded by specialized software and saved as a txt format file, which was used to process the data acquired from the CO_2 concentration measurements.

5.4.2. Experimental conditions

The importance of several parameters for the spread of the coughed air in the room and the exposure of the doctor and the second patient to the coughed air were studied with and without HBIVCU. In the following, only the exposure of the doctor and the second patient is discussed. The impact of the following factors is considered: the total volume ventilation flow rate in the occupied space, the location of the doctor with respect to the coughing patient, the distance between the doctor and the coughing patient, the exposure of the second patient, and the exposure of the doctor and the second patient depending on the position of the coughing patient (side coughing or coughing upward toward the ceiling), the operation mode of the HBIVCU, the initial discharge velocity from the HBIVCUs. The total number of experimental conditions based on the parameters studied was 30.

The experiments were performed under isothermal conditions at 22 ^{o}C. Experiments at three airflow rates, namely 46.8, 93.7, 187.4 L/s supplied from the total volume mixing ventilation were performed. These corresponded to air change rates of 3, 6 and 12 h^{-1} respectively. In order to keep the room air temperature constant (22 ^{o} C) the temperature of the supplied air was 16, 18 and 19 ^{o}C respectively. The supplied air was 100% outdoor air (no recirculation was used). Air humidity was not controlled, but was measured to be relatively constant during the experiments (30-35%). The total heat load generated in the test room was 240 W (11.34 W/m^2).

The two dummies were lying in the two beds simulating two patients. They were covered with cotton blankets up to the head. The distance between the beds was set to 1.3 m. The beds (2 x 1m, L x W), with height of 0.8 m, were positioned parallel to each other. One of the dummies was used to simulate "source" patient, i.e. an infected person generating the cough. This dummy was equipped with the puffing machine.

Depending on the simulated case the thermal manikin was used to mimic either the doctor or the "recipient" patient facing the "source" patient. During the measurements when mimicking the doctor the standing manikin was dressed in panties, straight cotton trousers, T-Shirt, calf-length socks, thin soled shoes and medical thick cotton apron (1.02 Clo). When the manikin was mimicking the patient lying in one of the beds, it was dressed in same garment ensemble, but without the apron and the shoes (0.38 Clo).

The impact of the distance (0.55 m, 1.1 m and 2.8 m) between the thermal manikin ("the doctor") and the coughing dummy ("the patient") was also studied. In the case with distance of 2.8 m "the doctor" was standing behind the bed with the second lying dummy ("patient"). These experiments aimed to study cross-infection risk between the sick patient and the doctor. The "doctor", standing between the two beds and "talking" with the two patients while facing both of them was also a case studied as part of the parameters included, namely the position of the doctor relative to the coughing patient (Figure 5.11).

Experiments focused on cross-infection between the two patients were also performed. In this case, the second dummy, which represented the "recipient" patient was replaced with the thermal manikin.

The described layouts of the dummies and the thermal manikin were studied for two postures of the "sick" patient – when the coughing dummy was lying on its back and coughing vertically upward against the ceiling, and when it was lying on its side and facing the doctor/second patient.

The above described experiments were performed as reference cases. When the HBIVCU was installed the importance of the following parameters was studied: the importance of the blocking impact of the HBIVCU, i.e. when installed but not in operation; the importance of positioning of the coughing patient, the importance of the background ventilation flow rate and the impact of discharge velocity from the unit, namely 0, 1.4 and 2.8 m/s. In those experiments both beds were with the HBIVCUs installed.

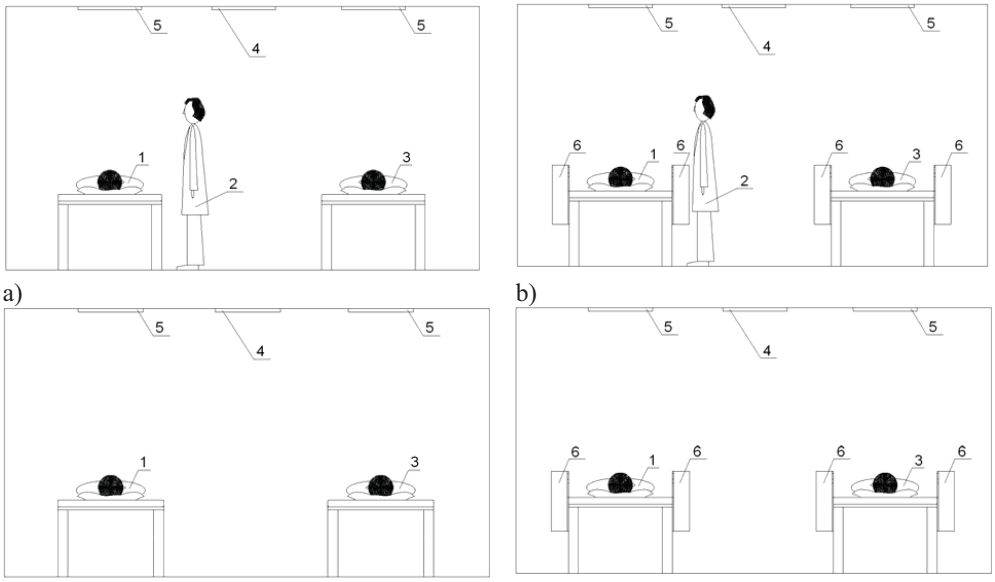

Figure 5.11 *Layout of beds and simulated persons during some of the studied cases: 1) coughing patient turned sideways, 2) doctor, 3) second patient, 4) TV ventilation inlet, 5) TV exhaust outlets, 6) HBIVCU installed on both sides at each bed. a) The doctor is close to the bed of the coughing sick patient, b) Similar to case a) but with HBIVCUs installed at each bed, c) Only the two patients facing each other, d) Similar to case c) but with HBIVCUs installed at each bed.*

5.4.3. Measured parameters and measuring equipment

Tracer gas, carbon dioxide (CO_2), was used to simulate the coughed air caring pathogens. During the measurement the gas was released in the form of a puff from the coughing machine.

The level of the CO_2 within the experimental room was followed by three measuring devices: IAQM PS32, prototype CO_2 monitor PS331 and real-time gas monitor based on the photo-acoustic principle: multi-gas sampler and analyzer 1303 and 1312 INNOVA.

5.4.3.1 CO_2 Sensors – PS32 and PS331

To measure the concentration of CO_2 in the room after the cough was triggered two different sensors were used: Indoor Air Quality Monitor (IAQM) PS32 and PS331.

The IAQM PS 32 is designed for the measurement and recording of carbon dioxide concentration (in range 0 ÷ 5000 ppm), relative humidity, air temperatures (10 ÷ 45 °C) and of barometric pressure (900 ÷ 1100 hPa). A dual beam non-dispersive infrared CO_2 concentration sensor (NDIR) is applied in the system using the attenuation dependence of a specifically defined infrared radiation band of CO_2 concentration. The applied measuring method ensures long-term stability and fast dynamic response. During the measurements the recording time was set to 10 sec. A high quality micro diaphragm gas sampling pump, together with flexible pipes for air sampling was connected to the Monitor (Figure 5.12). After completion of each condition, a specially

designed software enabled for reading the data recorded in the device and saving it in a text file (67 000 records). Four such pairs were used: at the TV supply, TV exhaust, mouth of the manikin (simulating either the "doctor" or the "exposed patient") and a point in the centre of the room at 1.7 m height.

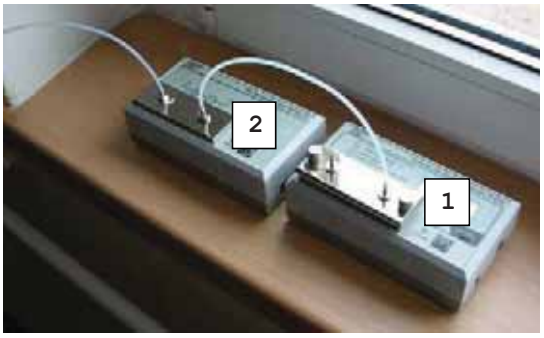

Figure 5.12 *IAQM PS32 (1) connected to the micro diaphragm gas sampling pump (2).*

The second sensor for CO_2 measurement (PS331) used during the experiments was based on the same principle as PS32 but was sampling much faster: every 25 msec. This instrument was a prototype developed for the purpose of the present measurements. Only one such device was used to sample air at the mouth of the thermal manikin. It was able to measure concentrations up to 15 000 ppm.

The CO_2 was sampled by the multi-gas sampler and analyzer at 6 points. The positioning of the 6 sampling points was as follows: the total volume supply, the total volume exhaust, the mouth of the doctor, 2 points on the other patient dummy and the last one in the room at 1.7 m height. These results were also processed and were used as reference to show the background level of CO_2 in the test room and follow it all the time. The concentration measurements at Point 6, positioned at 1.7 m above the floor, were compared with the tracer gas concentration measured at the exhaust and used to justify whether or not good mixing in the room was achieved.

However the measurements taken at the mouth of the manikin with the IAQM PS32 and the multi-gas sampler and analyzer were not used due to the very low sampling frequency of these instruments: 0.1 Hz for the first one and over 0.008Hz for the latter. The readings from these instruments were used to justify the background steady-state CO_2 level reached after the cough was performed.

5.4.3.2 Other parameters measured

The total volume ventilation was controlled based on the differential pressure readings obtained from two orifices installed in the supply and the exhaust ducts (ISO 5221 – 1984 (E)). The readings obtained by pressure transducers were transferred to a control system maintaining the set flow rate value. The supplied flow rate was less than the amount of the air exhausted, in order to achieve under-pressure in the room – 1.6±0.2 Pa. The pressure was monitored by a differential pressure micro-manometer based on the pressure drop in the system with an accuracy of 0.01 Pa ±0.25% of reading.

The amount of air supplied by each HBIVCU was monitored by flow sensors permanently installed into the ducting upstream from each device. Four such pairs were installed: four for the supply system servicing the HBIVCUs and four for the exhaust.

The air temperature in the room, in the supply and exhaust, and the supply ducts of the HBIVCUs was measured by temperature sensors (thermistors) and was recorded. These temperature sensors had an accuracy of ±0.3 ^{o}C.

5.4.4. Data analysis

The PS331 sensor, as well as the procedure for data acquirement, and the following treatment of the data were developed outside the frame of the current project.

The data obtained with the PS331 was exported in the form of a text file and processed in a specially designed for this purpose software. The software used second order polynomial extrapolation to get the initial value of the CO_2 concentration taking into account the instrument characteristics with high accuracy up to 15 000 ppm. Before frequency correction, the signal is interpolated between measured samples, using parabolic interpolation method (Figure 5.13). The reason was to increase 10 times the sampling frequency: from 4Hz to 40Hz. The equations for the two parabolas used for the parabolic interpolation mathematical algorithm are:

$$y_1 = 0.8333x^2 - 2.3333x + 4.625 \quad , (5.4.1)$$

$$y_2 = -1.1458x^2 + 5.1875x - 1.8073 \quad , (5.4.2)$$

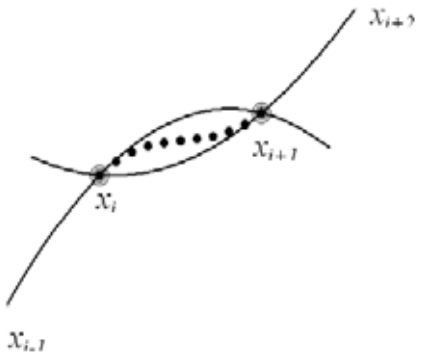

Figure 5.13 *Parabolic interpolation method description.*

Then the frequency corrections were made assuming that the dynamic properties of the CO_2 transducer are like the first order inertial system with time constant found by the step method to be of the order of 0.8 s:

$$Y(s) = \frac{1}{Ts+1} X(s) \quad ,(5.4.3)$$

The above equation yields:

$$X(s) = Y(s)(Ts + 1) \quad ,(5.4.4)$$

It corresponds to a linear differential equation:

$$x = T\frac{dy}{dt} + y \quad ,(5.4.5)$$

It can be solved numerically:

$$x_j = T\frac{y_{j+1} - y_{j-1}}{2\ \Delta t} + y_j \quad ,(5.4.6)$$

The re-sampled with 40 Hz frequency data y_j was used to obtain frequency corrected input data.

The software also compensated for the time the sample needed to travel from the sampling point to the PS331, which was 2.2 s.

5.4.5. Criteria for assessment

For all the experiments the criteria for assessment was the excess concentration of CO_2 with respect to its background level for the day measured at the same point.

Two more parameters are discussed in the following, namely the Peak Concentration Level (PCL) and the Peak Concentration Time (PCT).

PCL is defined as the maximum concentration measured at the mouth of the doctor or the second patient after the cough is generated;

PCT is defined as the time at which the PCL is reached after the cough is generated.

5.4.6. Procedure

The air temperature in the test room and in the laboratory hall was set 24 hours prior to the measurements in order to achieve steady-state conditions. The air temperature in the laboratory hall was kept 22 ^{o}C. At the start of the experiments the thermal manikin and the dummies were switched on. For the experiments with the mixing boxes – they were installed and switched on. The actual flow rate and the supply temperature were adjusted. All measurements commenced after steady-state conditions were achieved. Depending on the air exchange rate the coughing machine was producing:

- one cough every hour at 3 h^{-1};
- one cough every 45 minutes at 6 h^{-1};
- one cough every 30 minutes at 12 h^{-1},

For each of the studied experimental conditions between 15 and 20 coughs were produced. A cough was considered valid if the recorded voltage was between 4.0 and 4.1 Volts. This corresponded to the total flow of 2.5 L for the time of the cough duration of 0.5 s (Melikov et al. 2009). If the voltage was above or below these values the cough was excluded from the analysis and

considered invalid. After that an average cough profile was reconstructed based on the start time of each set of coughs.

5.5. Results

In the following text the results on exposure to coughed air obtained by the applied today st**r**ategy of dilution of contaminated room air by increased ventilation rates and the results based on the measurements with the newly developed and studied HBIVCU are presented separately. Then the results obtained with the two methods are compared and discussed.

All graphs in the following section are presented as excess concentration of CO_2 over the room level measured. The time value of 0 s corresponds to the moment of initiation of the cough by the "sick" patient.

5.5.1. Decreased exposure by dilution of contaminated room air with conditioned total volume ventilation air

All the measured cases discussed in this section were done without any additional ventilation method (HBIVCU) but only mixing type of total volume ventilation.

5.5.1.1 Impact of the background ventilation

The effect of different background ventilation rates (3, 6 and 12 h^{-1}) on the transport of the air coughed by the sick patient to the mouth of the "doctor" was studied and compared. Figure 5.14 compares the CO_2 concentration measured in time at the mouth of the "standing doctor" (a thermal manikin), situated 0.55 m from the mouth opening of the dummy generating the cough. In this case the thermal manikin was facing the coughing dummy and backing the second (not coughing) dummy, lying in the other bed. The coughing dummy was placed lying on one side with mouth opening pointed against the front of the thermal manikin, thus the "puffed" air first hit the manikin in the abdominal area and then acted more or less as an impingent jet over the body of the manikin. It can be assumed, however, that some of the coughed air would glide along the waist of the standing doctor and some would spread upwards (towards the mouth) and downwards (towards the feet). This assumptions need to be further studied and measured through sets of additional experiments.

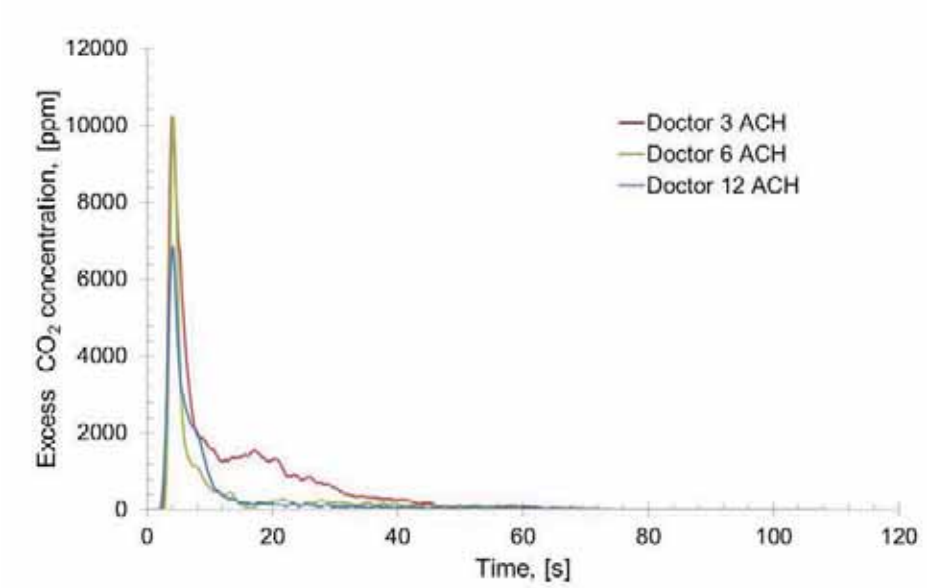

Figure 5.14 *CO_2 concentration change in time at the mouth of the "doctor" standing 0.55 m in front of the "coughing patient" in a hospital mock-up room ventilated at air changes per hour (ACH) - 3, 6 and 12 h^{-1}.*

At this distance the Peak Concentration Time (PCT) time values almost did not depend on the air change rate, due to the high initial discharge velocity of the single coughed air. Around the 7th second the puffed CO_2 cloud reached the breathing zone of the thermal manikin followed by decay in concentration. The Peak Concentration Level (PCL) and the slope of the decay depend on the air change rate in the room: the higher the ventilation rate, the lower the PCL measured and the steeper the slope (faster decay). The decay curve at 3 h^{-1} makes a smaller peak at 20 s after the cough has been initiated and then slowly returns to the background concentration in the room. The incoming cough hits the doctor at the stomach, and then behaves similar to an impingent jet: part of it passes along the waist; part of it flows up and part of it down towards the manikin's feet. There it hits the floor and re-bounces back. The secondary peak at 3 h^{-1} is probably due to the fact that the background velocities are low enough and allow for the free convection layer around the manikin body to restore after the initial impact of the coughed jet, and to recapture part of the re-bounced coughed air and bring it back into inhalation. At 6 h^{-1} and 12 h^{-1} the background velocities are higher and promote enhanced mixing of the cough air with the room air. At 12 h^{-1} the velocities in the room might even be higher than that of the free convection layer surrounding the human body and thus completely peel it off.

At ventilation rate of 12 h^{-1} the PCL is reduced by only 27% compared to that at 3 h^{-1}, when the doctor is close to the bed of the patient, i.e. when the doctor is performing routine medical examination (0.55 m distance measurement). This is true when the medical staff member (doctor or nurse) does not wear any mask. The efficacy of the masks is not 100 percent therefore, the risk of cross-infection remains. Furthermore, even with the mask risk from large droplet contamination

remains, if the eyes are not covered behind protective glasses (Green et al. 2007). Also droplets settle on the clothing and could be subsequently ingested via contact or improper handling.

5.5.1.2 Impact of the distance between the doctor and the coughing patient

The impact of the distance between the coughing patient and the doctor on the exposure of the doctor was studied in three experiments: distance of 0.55 m, 1.1 m and 2.8 m. The CO_2 concentration at the mouth of the doctor facing the coughing patient obtained at the three distances with air change rate of 3, 6 and 12 h^{-1} are shown in Figures 5.14, 5.15 and 5.16. Figure 5.17 compares the impact of the distance at the same background air change rates.

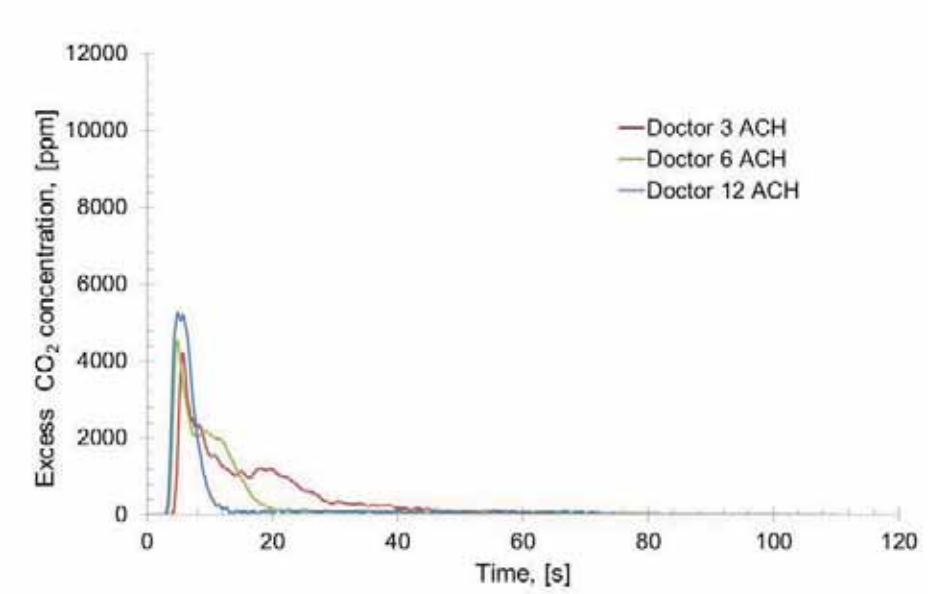

Figure 5.15 *CO_2 concentration change in time at the mouth of the "doctor" standing 1.1 m in front of "coughing patient" in room ventilated at three air changes per hour (ACH) - 3, 6 and 12 h^{-1}.*

It was already discussed, for the results presented at distance of 0.55 m (Figure 5.14), that the PCL at the mouth of the doctor immediately after the cough and the slope of the CO_2 decay depend on the air change rate in the room: the higher the ventilation rate, the lower the PCL and the steeper the slope (faster decay). The results obtained at distance of 1.1 m also show dependence of the PCL on the air change rate. However, as it can be noticed here, opposite to the expectations, the peak concentration at 12 h^{-1} is much higher as compared to 6 and 3 h^{-1}. The reason behind this can be the elevated background velocities at the highest ventilation rate tested. At this flow rate the velocities in the room are high enough to peel off the free convection layer surrounding the human body. At 3 and 6 h^{-1} the background velocities are not that high and the free convection layer is still present. After the cough cloud collides with the boundary layer around the occupant, it restored at 3 and 6 h^{-1} and acted as a barrier for the puffed flow, stopping some of that air to reach the breathing zone of the doctor. Similar results were also found by Wan et al. (2009) and Sze To et al. (2009) in

their measurements of dispersion and deposition of particles, as a result from cough in a mock aircraft cabin. They both also noticed that setting higher supply airflow rates lead to better dilution close to the source (sick coughing patient), but also enhanced the dispersion to expiratory aerosol for those passengers seated further away (two rows upstream) , leading to higher exposures at those locations.

At 2.8 m distance downstream of the cough the dilution becomes even bigger and the peak concentration measured raises just slightly above the background concentration (Figure 5.16). The small peak at 6 h^{-1} is due to the stochastic nature of the cough and the random flow interactions in the room between the background ventilation, the coughed jet and the boundary layer around the lying patients and the doctor.

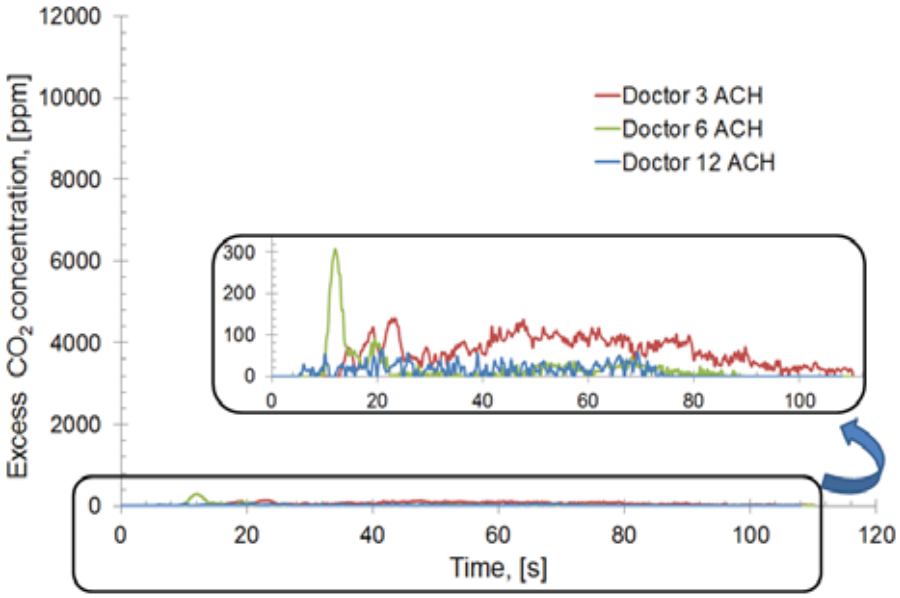

Figure 5.16 *CO_2 concentration change in time at the mouth of the "doctor" standing 2.8 m in front of "coughing patient" in room ventilated at three different air changes per hour (ACH) - 3, 6 and 12 h^{-1}.*

For the three air change rates studied the PCL decreased with the increase of the distance between the doctor and the coughing patient (Figure 5.17). For every air change rate there exists a distance between the doctor and the sick coughing patient beyond which the coughed air jet containing the airborne pathogens is almost completely dissolved by the room air. This, however, needs to be further documented by more detailed measurements. The present experiments show that when the doctor was 2.8 m downstream of the cough the measured concentration of CO_2 at the mouth level was the same as the background level concentration (Figure 5.17).

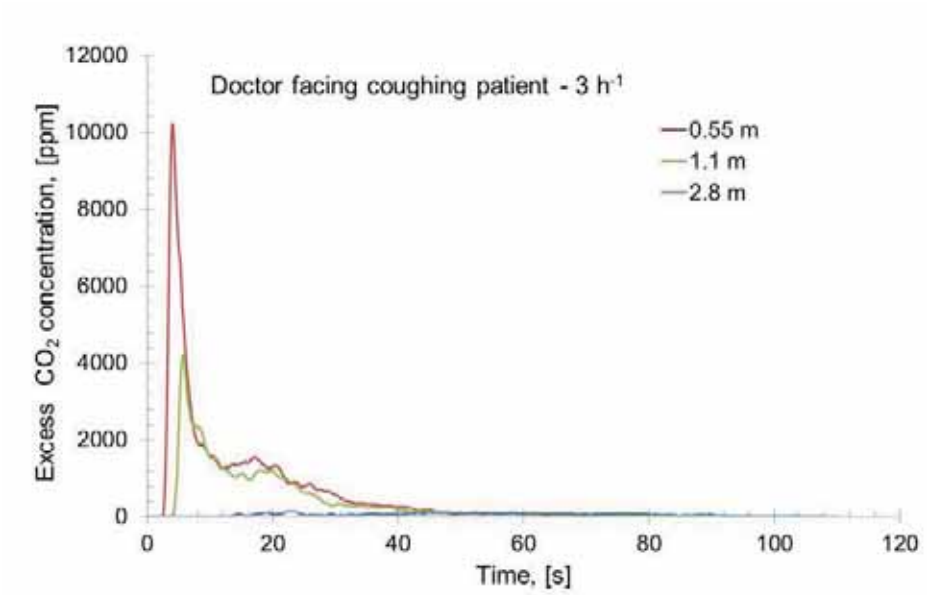
Doctor facing coughing patient - 3 h-1
Excess CO2 concentration, [ppm]
Time, [s]
0.55 m
1.1 m
2.8 m
0
2000
4000
6000
8000
10000
12000
0
20
40
60
80
100
120

a)

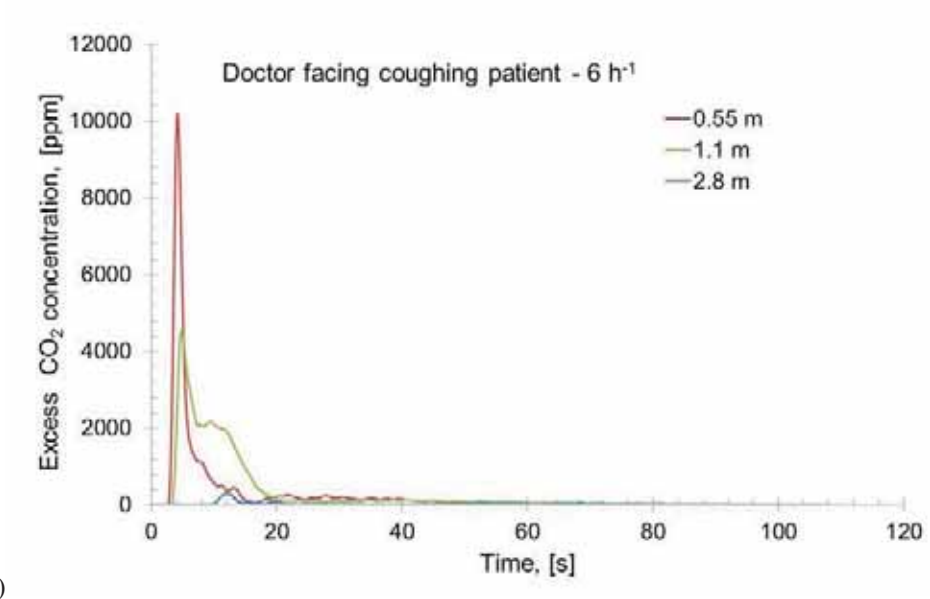
Doctor facing coughing patient - 6 h-1
Excess CO2 concentration, [ppm]
Time, [s]
0.55 m
1.1 m
2.8 m
0
2000
4000
6000
8000
10000
12000
0
20
40
60
80
100
120

b)

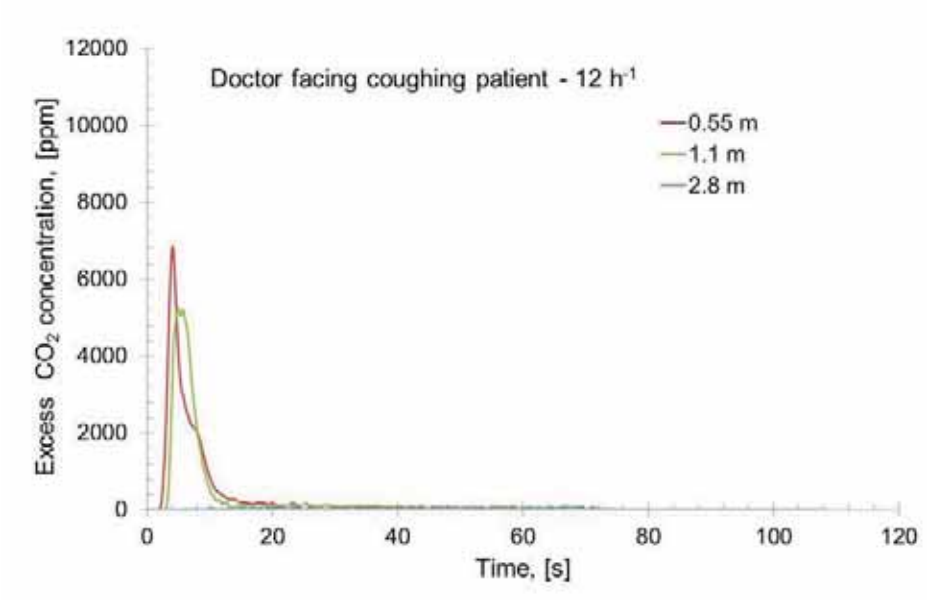

c)

Figure 5.17 *CO_2 concentration change in time at the mouth of the "doctor" standing at three different distances of 0.55 m, 1.1 m and 2.8 m in front of "coughing patient" in room ventilated at three different air changes per hour (ACH) - a) 3 h^{-1}, b) 6 h^{-1} and c) 12 h^{-1}.*

5.5.1.3 Impact of the location of the doctor with respect to the coughing patient and the posture of the coughing patient

As it can be seen from the results discussed so far, the most dangerous spot for the doctor is being right by the bed of the sick patient, who generates the cough, i.e. the exposure increased with the decrease of the distance between the doctor and the coughing patient. These results were obtained with doctor facing the coughing manikin lying on one side. The impact of the position of the doctor with regard to the coughing patient, facing and turned sideways, and the posture of the coughing patient, lying on the back or sideways, was studied as well. In Figure 5.18 the results obtained at different air change rate with coughing patient lying on the back and doctor located at distance of 0.55 m are shown. Unlike in the case when the doctor was facing the coughing patient (Figure 5.14) there is almost no change in the PCL from the room level concentration, suggesting that most of the released by the patient pathogen laden air would move upwards due to the high initial momentum and be directly exhausted there by the TV ventilation. In this case the ventilation rate was not as important as when the patient coughs sideways, towards the face of the doctor, which was the worst case scenario.

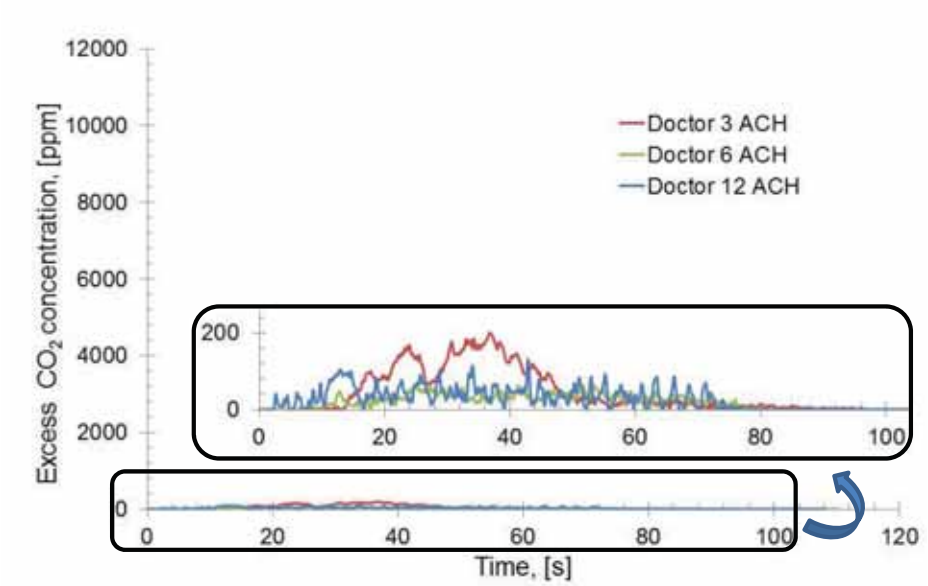

Figure 5.18 *CO_2 concentration change in time at the mouth of the "doctor" standing 0.55 m in front of "coughing patient" lying on back and coughing upwards against the ceiling. Results obtained at three different air changes per hour (ACH) - 3, 6 and 12 h^{-1} are compared.*

The doctor may not face only one of the patients, but as in the case when making visitations he/she may stand by the bed to have view prospective of both patients (defined as "sideways" relative to the coughing patient). This condition was studied only at ventilation rate equal to 6 h^{-1}. The result is shown in Figure 5.19. As can be seen there is only a small change in the concentration measured at the mouth of the doctor after the cough. The reason is that being turned to face both patients, i.e. sideways, the doctor's body does not play the role of an obstacle for the coughed jet. Therefore the high momentum jet just sweeps by the doctor. However small portion from the patient's cough is captured by the boundary layer and brought to the mouth, after longer time compared to the case when doctor is turned, facing only the coughing patient (Figure 5.19).

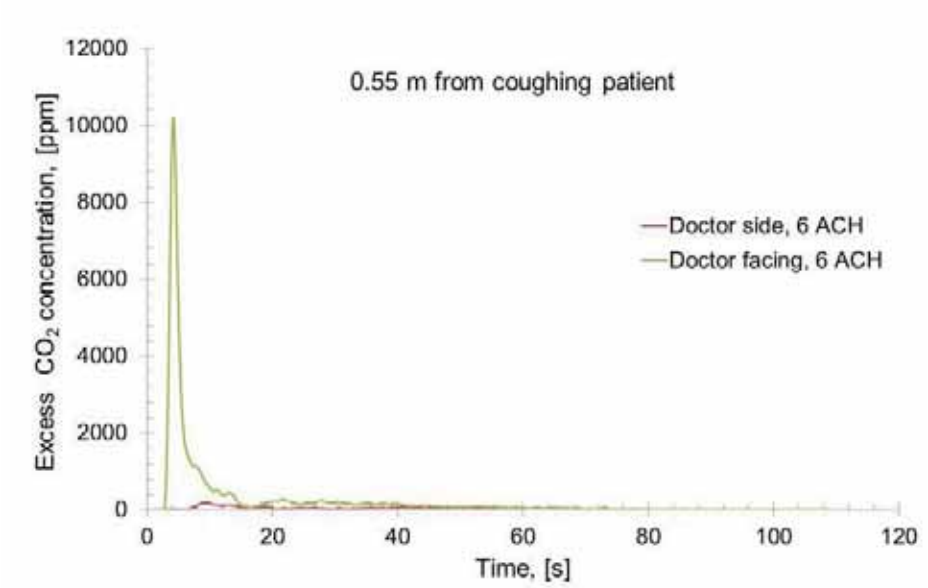

Figure 5.19 *CO_2 concentration change in time at the mouth of the "doctor" standing sideways and viewing the two patients. Coughing patient is lying on one side and coughing against the second patient.*

5.5.1.4 Cross-infection between patients

The effect of cross-transfer among patients was studied in another set of experiments and only when the exposed patient was facing the coughing one. The case when exposed patient was lying on back facing ceiling was not done as the previous measurements showed very low CO_2 concentrations above the room background level.

The thermal manikin was placed in the second bed (instead of the heated dummy) with its head turned facing the coughing dummy. The results of these measurements are shown in Figure 5.20. Due to the high background velocities at 12 h^{-1} by the time the coughed air reached the "exposed" patient the concentration of CO_2 was reduced more than 2 times. The high initial velocity of the coughed CO_2 and the relatively low background velocities at 3 and 6 h^{-1} kept the PCL at the mouth of the exposed patient quite high (Figure 5.20). At 12 h^{-1} the background velocities, a result of the TV ventilation, were relatively high and promoted the enhanced mixing of the room air with the single transient coughed air flow diluting it at a faster rate compared to the cases of 3 and 6 h^{-1} TV ventilation.

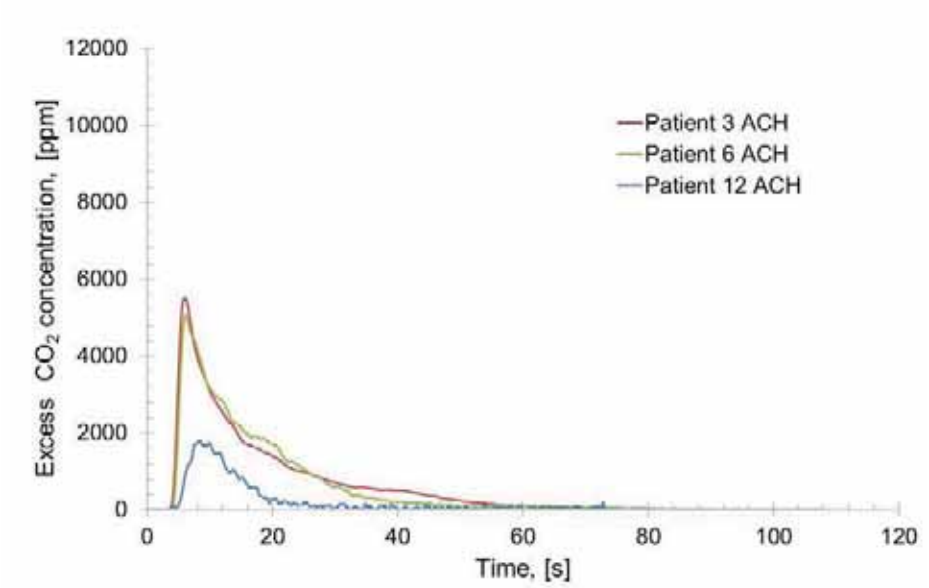

Figure 5.20 *CO_2 concentration change in time at the mouth of the "exposed patient" lying in the second bed and facing the coughing patient lying on one side. Results obtained at three different air changes per hour (ACH) - 3, 6 and 12 h^{-1} are compared.*

5.5.1.5 Exposure to coughed air per unit time

To study the average exposure to coughed air per unit time for the period when CO_2 concentration was above the background level, the area under the excess was calculated applying the trapezoid rule, and then divided by the time interval for which the CO_2 was above the average for the room for each case of 3, 6 and 12 h^{-1}. The obtained thus average concentration was then normalized for the minimum air change tested, e.g. 3 h^{-1} for each condition. Figure 5.21 shows the normalized average exposure per unit time for the three distances between the doctor and the coughing patient (0.55 m, 1.1 m and 2.8 m), when the coughing sick individual was lying sideways and facing the doctor.

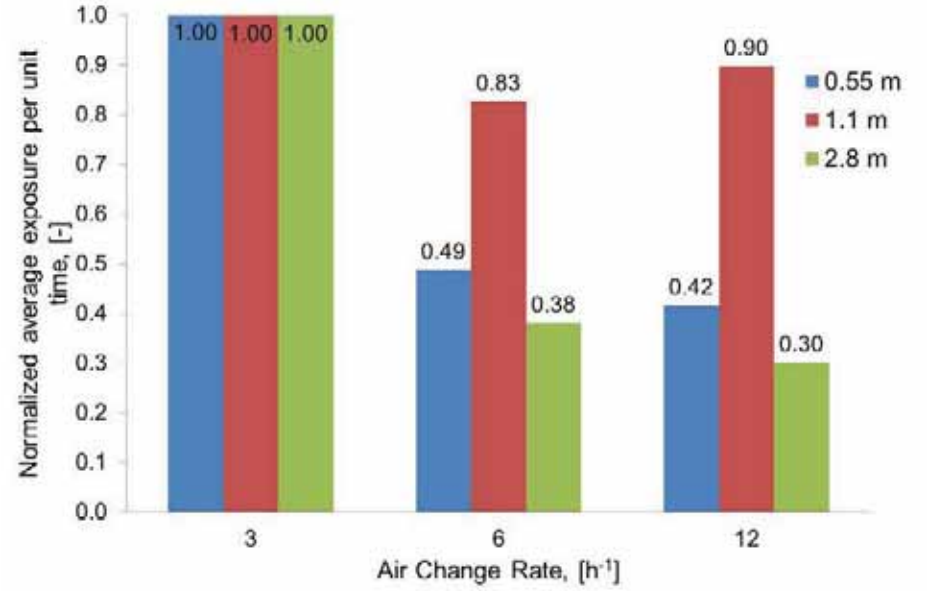

Figure 5.21 *Normalized average exposure per unit time for the three distances tested between the doctor and the coughing patient.*

As can be seen from the data on Figure 5.21, when the doctor is very close to the patient (0.55 m) or far (2.8 m) the exposure to the coughed air decreases more than twice when the background ventilation is set to 6 h^{-1}compared to the reference (3 h^{-1}) case. Further increase in the background ventilation up to 12 h^{-1} almost does not affect the exposure dose. Therefore, increasing the ventilation rates above 6 h^{-1} becomes energy inefficient as the reduction in exposure per unit time is negligible. The doctor is at the same risk at 12 h^{-1} as when the background ventilation is 6 h^{-1}. Same tendency of decreasing the average exposure is also valid for 1.1 m distance. However, the decrease is not as strong as at 0.55 m or 2.8 m. The elevated velocities sweep away the convection layer surrounding the doctor, and as in this case the distance is shorter than 2.8 m, less mixing with the surrounding room air occurred, resulting in higher exposure rates. It should be noted that at 0.55 m distance the doctor gets almost twice as lower exposure as at 1.1 m for 6 and 12 h^{-1}. This is because at 0.55 m the jet has almost unchanged velocity very close to the initial one (29.8 m/s) and sweeps by the body. At 1.1m the velocity is reduced to 3.2 m/s (calculated based on Baturin 1972), part of the air is recaptured by the restored convection layer after the “puff” passes by the body, which acts as an obstacle on the way of the cough.

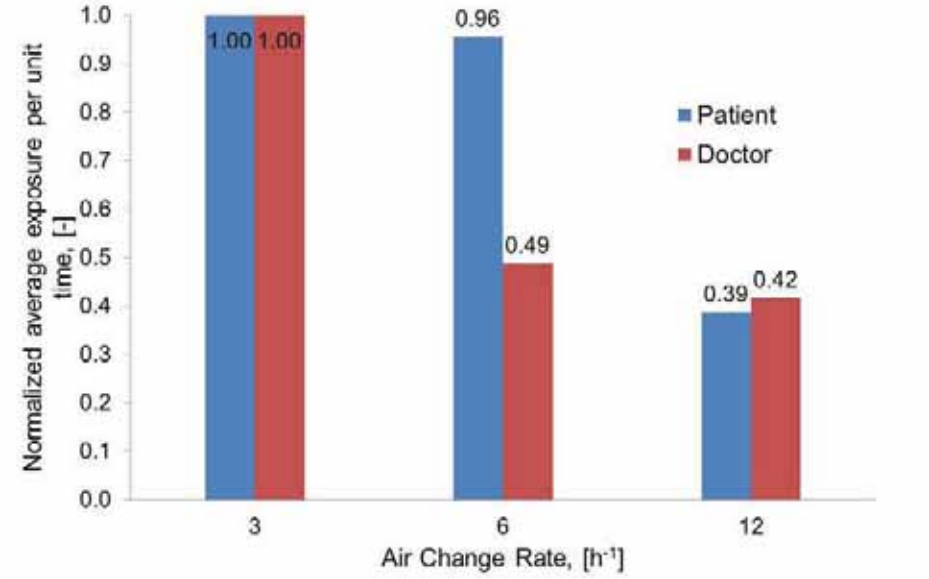

Figure 5.22. *Normalized average exposure per unit time for the doctor when standing at 0.55 m facing the coughing patient compared with the normalized average exposure per unit time for the second patient lying in neighboring bed facing the coughing patient as well.*

Figure 5.22 compares the normalized to 3 h^{-1} averaged exposure per unit time for the other patient lying in the neighboring bed (at 2.2 m distance from mouth of coughing patient) with that for the doctor, when standing close to the bed of the "sick" coughing occupant. No difference is noticed for the patient concerning the exposure over time for 3 and 6 h^{-1}. The increased total volume ventilation at 12 h^{-1} enhances the mixing of the coughed flow and by the time it reaches the lying patient in the neighboring bed the average exposure per unit time drops more than twice resulting in reduced risk from airborne disease contamination (distance between patients exceeds 1m).

5.5.2. Decreased exposure by advanced ventilation (HBIVCU)

In the following, results from experiments on the performance of the HBIVCU are presented and discussed. In section 5.2 it was defined that two set of HBIVCUs were attached to each of the two beds (one HBIVCU on each side, left and right, of the beds). Several experiments were performed to study the decreased risk of exposure for the doctor standing and facing the coughing patient from a distance of 0.55 m and for the second lying patient due to: a) the impact of the HBIVCU as an obstacle (when it was present but not in operation); b) the impact of discharge velocity from the HBIVCU; c) impact of the background ventilation rate on the HBIVCU performance.

5.5.2.1 Impact of the HBIVCU as obstacle

The first test was performed with the boxes being not operational but placed as obstacles

on both sides of the 2 beds (Figure 5.11 b and d). For this reason the suction and discharge opening of the device were both closed. The experiments were performed at 3 and 12 h^{-1}, when the coughing dummy facing the doctor was coughing sideways (CS) and the doctor was 0.55 m distance from the bed of the coughing individual. Then for the 3 h^{-1} the coughing dummy was turned facing the ceiling, so that the puffing was performed upwards (CU). And as a last case measured with the HBIVCU acting as an obstacle, the thermal manikin was placed in the bed of the exposed patient, turned towards the coughing dummy that was facing the manikin as well. Figure 5.23 shows the data from these experiments. The presence of the boxes projecting over the bed (0.42 m) helped reduce the concentration of CO_2 in the breathing zone of the doctor when the patient was coughing sideways (CS) by deflecting the jet upwards towards the ceiling. The PCL for the doctor decreased from 10229 and 6847 without HBIVCU (Figure 5.14) to 498 and 1190 with HBIVCUs present as obstacles for the 3 and 12 h^{-1} respectively (Figure 5.23), and coughing sideways. For the other patient, at 3 h^{-1} the PCL changed from 5518 to 133. The difference in the concentration decay profiles obtained for the doctor at 3 and 12 h^{-1} with coughing patient lying sideways can be explained with the boundary layer surrounding the thermal manikin. At ventilation rate equal to 3 h^{-1} the more gradual decay occurs due to the interaction between the redirected coughed air and the free convection layer. At 12 h^{-1} the free convection flow is destroyed by the background air distribution in the room, which was already discussed before, makes it possible for the coughed air to reach easily the mouth of the doctor. The presence of the free convection layer and its interaction with the deflected jet also affect the PCT for which the PCL is reached at 3 h^{-1}. The PCT is 16 s at 3 h^{-1} and it drops to 8 s at 12 h^{-1}, i.e. two times lower.

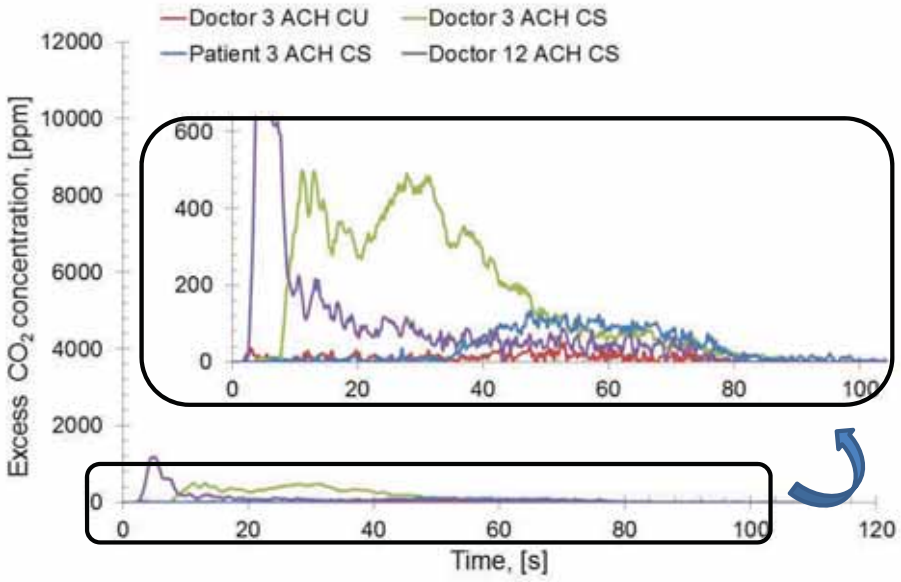

Figure 5.23 *CO_2 concentration change in time at the mouth of the "doctor" standing at distance of 0.55 m from the coughing patient and at the mouth of the other exposed patient, when the HBIVCU were used as obstacles (v=0 m/s). The results obtained at 3 h^{-1} and 12 h^{-1}*

[1] *ACH with manikin coughing sideways (CS) and upward (CU) are compared.*

The results suggest that simple modification of hospital bed design by introducing small partitions on the two bed sides near the head of the patient would help reduce the risk of exposure in hospital rooms. As it can be seen from the comparison shown in Figure 5.24 partitions help to substantially decrease the exposure to the coughed air: at 3 h^{-1} for the doctor and the exposed patient: the PCL decreases from 10229 ppm and 5518 ppm to 498 ppm and 133 respectively. It appears that this inexpensive and simple "passive" control method can be applied easily in practice.

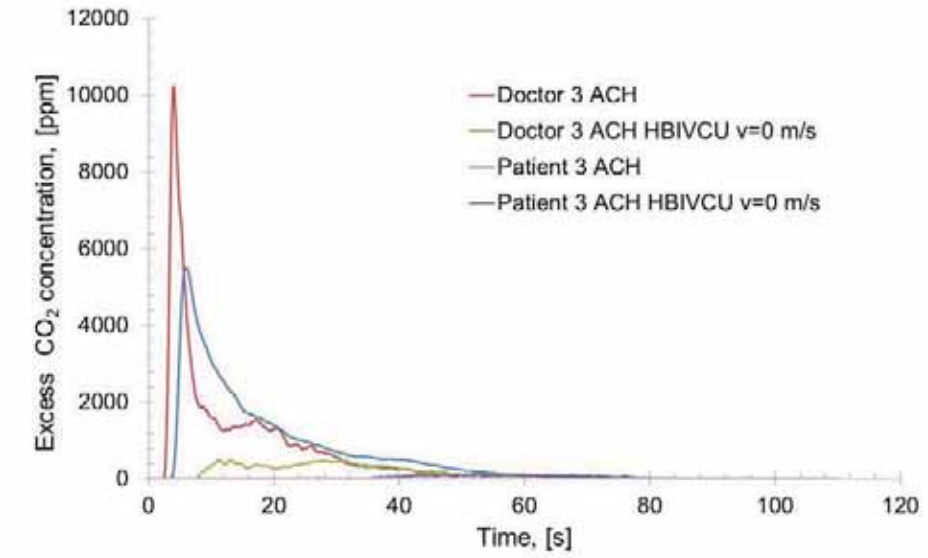

Figure 5.24 *CO_2 concentration change in time at the mouth of the doctor and the "exposed patient" lying in the second bed and facing the coughing patient lying on the side. Results obtained at 3h^{-1} rate are compared for the doctor and the second patient for reference case (no HBIVCU) and with HBIVCU as obstacle (v=0 m/s).*

As already noted, when the sick patient lies on its back and coughs upwards no pollutants reached the breathing zone of the doctor standing at distance of 0.55 m. At the initial velocity of 28.9 m/s and initial diameter of 0.021m the puffed jet did not expand as far out as to reach the boundary layer of the nearby thermal manikin, not at least below the mouth or the nose level (Figure 5.23).

5.5.2.2 Impact of the discharge velocity from the HBIVCUs

The boxes were operated using two different discharge velocities, namely 1.4 and 2.8 m/s. The same amount of air discharged by the HBIVCUs was also sucked by the exhaust opening. The experiments were performed mainly for 3 h^{-1} only. Figure 5.25 compares the results obtained of these measurements with the results obtained during the reference case, i.e. when no HBIVCUs were integrated with the beds.

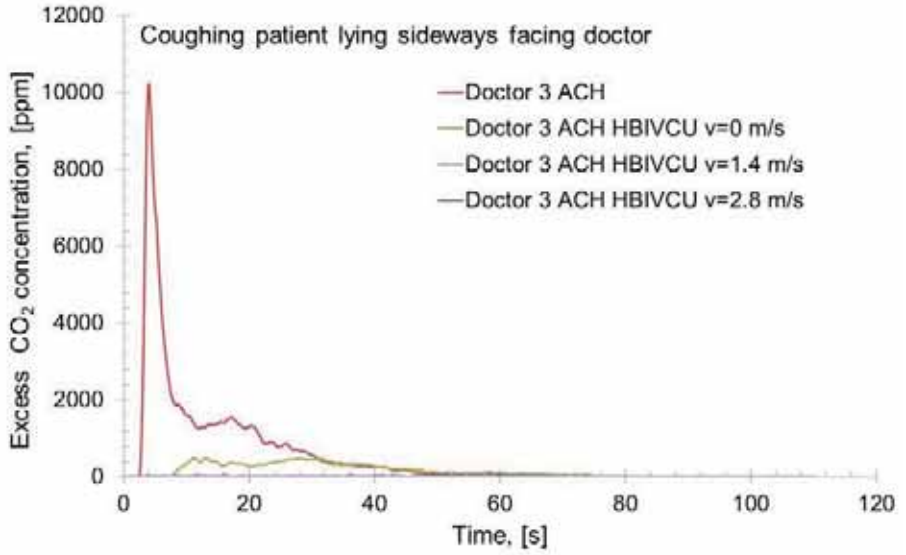
Coughing patient lying sideways facing doctor
Doctor 3 ACH
Doctor 3 ACH HBIVCU v=0 m/s
Doctor 3 ACH HBIVCU v=1.4 m/s
Doctor 3 ACH HBIVCU v=2.8 m/s
Excess CO_2 concentration, [ppm]
Time, [s]
0
2000
4000
6000
8000
10000
12000
0
20
40
60
80
100
120

a)

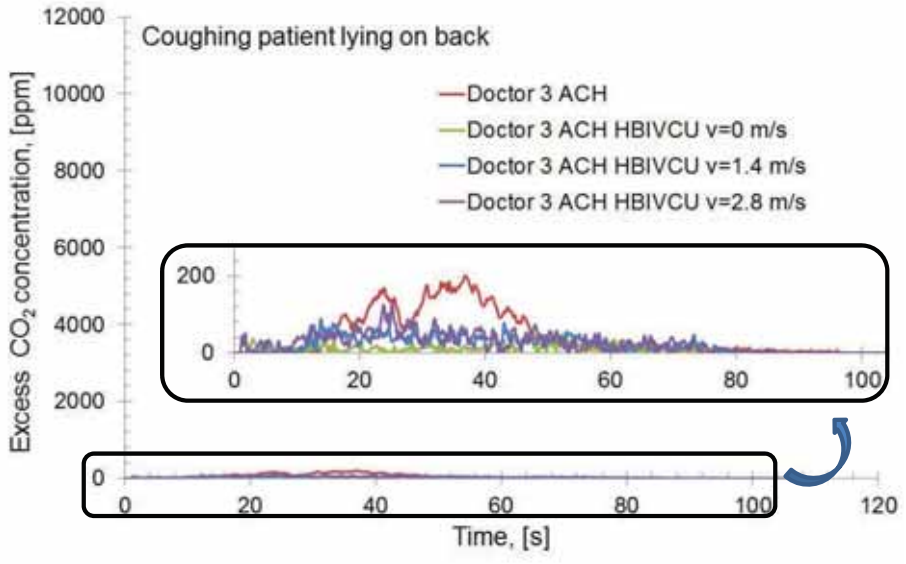
Coughing patient lying on back
Doctor 3 ACH
Doctor 3 ACH HBIVCU v=0 m/s
Doctor 3 ACH HBIVCU v=1.4 m/s
Doctor 3 ACH HBIVCU v=2.8 m/s
Excess CO_2 concentration, [ppm]
Time, [s]
0
2000
4000
6000
8000
10000
12000
200
0
0
20
40
60
80
100
120

b)

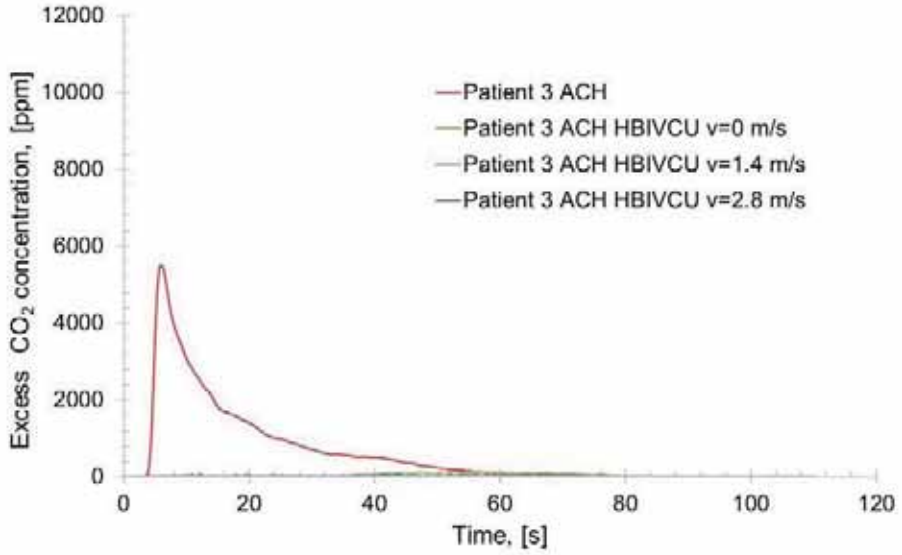

c)

Figure 5.25 *CO_2 concentration change in time at the mouth of the "doctor" standing at distance of 0.55 m from the coughing patient, a) when lying facing the doctor and b) when lying on back and coughing upwards, and c) at the mouth of the exposed patient in the second bed. The results obtained at 3 h^{-1} with the HBIVCU at discharge velocity of 0 m/s (HBIVCU is obstacle), 1.8 m/s and 2.8 m/s and with the reference case without HBIVCU are compared.*

As it can be clearly seen from the results in Figure 5.25 the presence of the HBIVCUs in operation reduced the concentration at the breathing zone of the doctor or the patient back to the background level. Thus the local suction applied close to the coughing patient works in reducing the level of pathogens in the room and provides protection for the medical staff and the other patients. As the performance of the HBIVCUs is the same at 1.4 or 2.8 m/s discharge velocity, the lower velocity is more appropriate as it translates into lower flow rates, and thus lowered energy requirements. However more experiments are needed to find the lowest possible velocity at which the unit will work equally efficiently. The supply and exhaust from the unit were balanced, as already mentioned, to mimic the performance of the future design, i.e. exhaust locally the air, cleanse it from pathogens via UVGI and then discharge it upwards towards the ceiling, where it would be exhausted.

5.5.2.3 Impact of the background ventilation rate on the HBIVCU performance

To acknowledge the performance of the HBIVCU at elevated background ventilation rates some of the above cases were measured at 6 h^{-1}. The results of these experiments are shown in Figure 5.26. The results in the figure reveal that the background ventilation rate does not have impact on the performance efficiency of the HBIVCU.

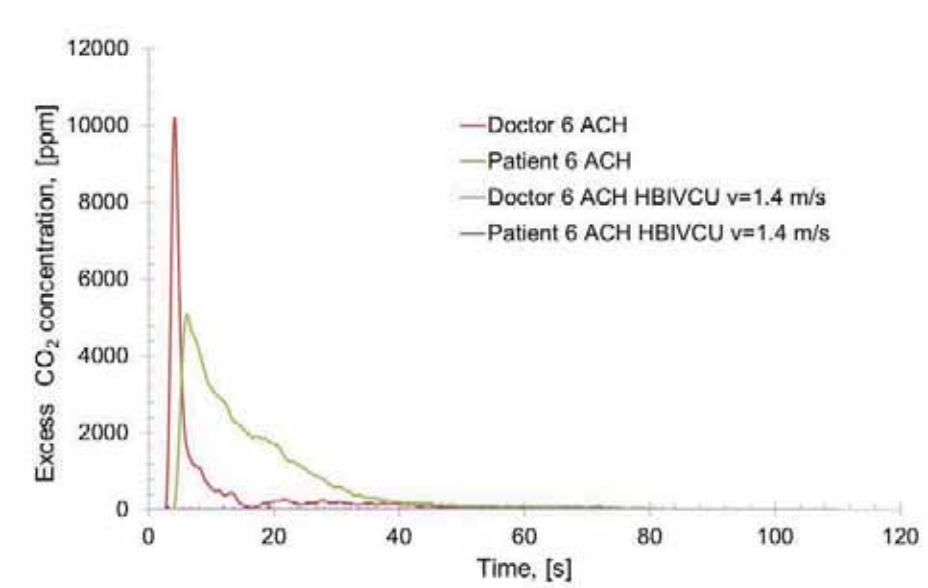

Figure 5.26 *CO_2 concentration change in time at the mouth of the "doctor" standing at distance of 0.55 m from the coughing patient and at the mouth of the exposed patient in the second bed. The coughing patient lies on its side and is facing the doctor and the second patient. The results obtained at 6 h^{-1} with the HBIVCU at discharge velocity of 1.4 m/s and at the reference case without HBIVCU at 6 h^{-1} are compared.*

Figure 5.27 clearly demonstrates that the efficiency of the HBIVCU in protecting the doctor and the second patient from the air coughed by the source patient is not influenced by the total volume ventilation in the room as the ventilation rate changes from 3 to 6 h^{-1}. The PCL measured never rose above the background CO_2 level for the air change rates tested, when the HBIVCU was operated at 1.4 m/s. This was due to the relatively close distance between the mouth of the sick coughing patient and the suction opening of the unit.

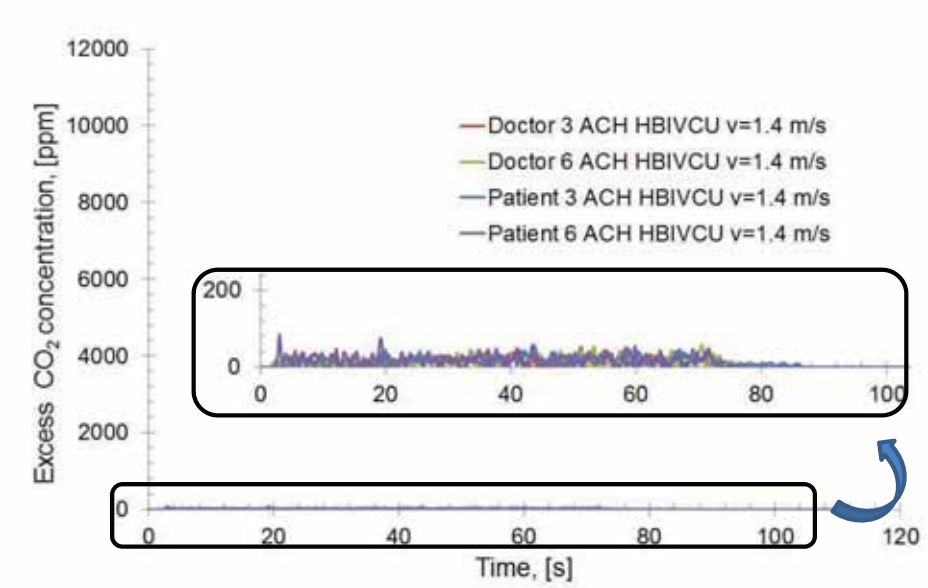

Figure 5.27 *CO_2 concentration change in time at the mouth of the "doctor" standing at distance of 0.55 m from the coughing patient and at the mouth of the exposed patient in the second bed. The coughing patient lies on its side and is facing the doctor and the second patient. The results obtained at 3 h^{-1} and 6 h^{-1} with the HBIVCU at discharge velocity of 1.4 m/s are compared.*

5.6. Discussion

As already discussed, today ventilation rates in infectious hospital wards are kept quite elevated in order to achieve good dilution within the premises, and thus to decrease the risk from airborne cross infections. Ventilation rate as high as 12 h^{-1} is recommended in the present standards and guidelines (ASHRAE 170 2008, CDC guidelines 2005, DS 2451-9 Dansk standard 2003). The high ventilation rate leads to high energy consumption. It also leads to elevated velocity in rooms, which may cause draught discomfort. Therefore the need of improvement of the air distribution in infectious hospital wards is needed. Furthermore, when working in isolation rooms doctors following certain protocols are dressed in disposable environment isolation costumes with incorporated filtration unit. These outfits are expensive and for single use only: after that they are being disposed and the waste is autoclaved at special premises. This is a costly practice, which requires also special facilities to take care of the waste and then autoclave it (an operation that requires high pressure steam at 121° C or more, typically for 15 to 20 minutes depending on the size of the load and the contents prior to waste disposal or incineration). However, during a pandemic it would not be possible for all the members of the medical staff to be equipped with special outfits as it would be expensive. Also the lack of free places in the isolation rooms might require the transformation of other premises into temporary depots, where the sick people might seek help. These places may not be accommodated or fit to host people who are highly contagious, due to lack of specially organized ventilation that would be able to provide the required high ventilation rates.

Even if this is possible, the results from the present study show that the high ventilation rates are as equally dangerous as the low ventilation rates, when the person is close to the source and the velocities either of the air movement generated by the source or the background ventilation are elevated (Chapter 5, Results 5.5, Figure 5.14). The only benefit from the elevated ventilation rates is that the decay of the air coughed in the breathing zone of the person is faster and as a whole the exposure is shorter in time. This result concurs with the result reported by Jensen et al. (2001) on the exposure of a person to air exhaled by another person in a room with mixing ventilation. They concluded that when people are close enough the velocities around them should be low to reduce exposure. The increased background velocities at high background ventilation rate weakened or peeled off the free convection layer around the body. When the person is close to the source this is beneficial as the lack of boundary layer cannot transport a secondary wave of pollutants after the main wave of pathogen laden air passes and the convection layer restores, as in the case with the lower ventilation rates (Chapter 5, Results 5.5, Figure 5.14). However, when the distance between the person and the source downstream of the direction of the cough increases, the absence of powerful free convection boundary layer around the body becomes a factor contributing to the enhancement for the risk of airborne cross infection (Chapter 5, Results 5.5, Figure 5.15). The intensive mixing at 12 h^{-1} due to the elevated velocities brings more polluted air into the breathing zone. As the results of the present study reveal in this case, the presence of the boundary layer at the lower background ventilation rates (3 and 6 h^{-1}) does not allow much of the coughed air to enter into the inhalation.

In a case of pandemic scenario the patient density in an isolation room might be higher than the usual practice of 1-2 people. This is especially true, if the airborne pathogen is highly infectious and causes high mortality and morbidity among the affected population that exceeds the number of healed and recovered patients. With a highly contagious pathogen, transmittable via the airborne route, the increased population density of sick people translates into a higher risk as the generation of pathogens for the same ventilation rate would be increased. Therefore only relying on total volume ventilation as a method to reduce the risk from cross-infection through dilution especially in a worst case scenario such as pandemics is just unthinkable and unreliable.

The effectiveness in purging the pathogens, when applying UVGI in the room depends on factors such as: the air distribution pattern within the space (position of supply and exhaust openings), the position of the sick patient generating the pathogens, irradiation dose and positioning of the UVGI devices (Minki et al. 2009). The room UVGI is positioned close to the ceiling (above 1.8 m) and in louvers to direct the radiation upwards as the UVC light has health adverse effects for humans. The upper room UVGI will not be effective when a healthy individual is close to the source (doctor and patient, Chapter 5, Results 5.5, Figure 5.14).Therefore with the filtration and UVG units incorporated in the HBIVCU the effectiveness could even be increased as the irradiation doze of the UV light can be increased: the UVC source will be incorporated inside the HBIVCU, and the patient will be not directly exposed to its adverse effect (Figure 5.1).

Moreover, the diseases that are usually airborne use the respiratory tract to multiply and are expelled mainly through coughing and sneezing (a way for the respiratory system to clean itself from clotting with sputum and secretions). The corresponding peak velocity can vary from 6 m/s to 30 or higher m/s (Edwards et al 2004, Zhu et al. 2006) with an average of around 11m/s. This

clearly makes the position of the sick person, initiating the cough and the following distribution in a ventilated space, quite important factor. The high initial velocities can sustain the advancement of the flow for quite a long distance. For example assuming the theory of free jets for the initial parameters of the cough used in the present study, namely v_o = 28.9 m/s, which corresponds to the cough peak flow rate of 10 L/s, and initial mouth opening of d = 0.021 m, one can calculate the distance at which the velocity falls to 1 m/s (the velocity of walking), assuming the equation for the velocity decay of free axisymmetric jets given by Baturin (1972):

$$\frac{U_m}{U_o} = \frac{0.48}{(a.x/d+0.145)} \quad , (5.6.1)$$

where

U_m	is the velocity at distance x, [m/s];
U_o	is the initial velocity of the free jet, [m/s];
a	is circular jet constant, which for cylindrical tube is 0.08;
x	is a distance downstream the axis of the jet, [m];
d	is the initial diameter of the jet, [m].

The distance of velocity decay to approximately 1 m/s is calculated to be at distance of 3.6 m. A walking person moves with velocity of approximately 1 m/s (Mund et al. 2001, Halvonova and Melikov 2010). Although quite approximate this result suggests that a person moving downstream of the cough can be affected by the pathogen laden air at quite long distance away from the source.

Furthermore, the coughed air is a single transient injection flow and unlike the submerged free jet the supply velocity is not kept constant over the time, but changes from 28.9 m/s to 0 m/s within 0.5 s for the coughing generator used. All this calculations and assumptions are based on the free jet theory submerged in a still environment. With the presence of background velocity the boundary layer around the free jet would develop faster and will “eat it up” faster (Abramovich 1963).

The newly developed method tested in the current study, namely the HBIVCU, shows great potential of being able to catch the exhaled air close to the source and thus to protect the surrounding people. This ventilation and cleaning unit optimizes the local control via sucking close to the source of the released pathogens, then filtering the captured air, purging the pathogens in it with UVC light, and discharge the cleaned air from slots normal to the suction plane opening. In this case the irradiation in the HBIVCU can be enhanced to the maximum for best effects as the box is closed and the patient cannot experience the adverse effect of the room installed UVGI. For best performance at least two units should be installed: one at the left and one at the right side of the bed. In this way the air expelled by the patient would be “locked” between the two discharged plane jets and guided towards the ceiling. The velocities tested in the present studies were 1.4 and 2.8 m/s. At both velocities tested the unit managed to successfully evacuate the coughed air away from the room and thus provide protection for the health care workers. In a future experiment the impact of the velocity (important for entrainment) and direction of the flow discharged from the box should also be studied.

Both the CFD simulations (Section 5.3) and the physical measurements (Section 5.4) showed similar results: the air was evacuated close to the mouth of the coughing patient, and just very low amount ended up at the other patient thus greatly reducing the risk from airborne cross infection. Detail comparison of the CFD and the measured results is difficult because of differences in the boundary conditions, e.g. in the case of CFD simulation "continuous" coughing was simulated, while during the measurements the coughing was transient.

In the current study the unit was tested only with coughing patient. A new study is needed to provide more information on the effectiveness of the unit to protect the medical staff, when the sick person breathes. In case of exhalation of contaminated air Qian et al. (2006) showed that displacement ventilation performed worse when the source patient was lying face sideways, because the exhalation jet persisted over a very long distance, assisted by the thermal stratification. Therefore in this case applying the HBIVCU with displacement ventilation might be beneficial as it will capture the air or direct it upwards between the two plane jets. The application of the unit with downward ventilation is doubtful. In this case the high speed of the discharged cleansed air will push up the supplied TV ventilation air back to the ceiling. The interaction of the two flows will cause mixing as well.

Another positive issue with the HBIVCU is that it can be made portable and follow the new trend applicable for hospital environment, namely "plug and operate". This versatility would allow the operation at places that are not even designed to take patients, and do not have special ventilation designed. However the effectiveness of the unit with different positioning of the TV supply and exhaust still needs to be studied in the future.

The results from the present study suggest that the application of the novel unit could result in certain energy savings as well as reduced initial and maintenance costs for the building investors. When used the HBIVCU was able to evacuate the coughed from the sick patient air and keep the PCL level at the same level as the room background concentration of CO_2 (Figure 5.24, 5.25), even at the lowest air change rate tested, i.e. for 3 h^{-1}. The application of the HBIVCU will lead to decrease in the established by the standards ventilation requirements for isolation hospital rooms (ASHRAE 170-2008, DS 2451-9-2003) and thus less outdoor air will be conditioned, brought into the patients rooms and the exhausted out. However, the use of many of the HBIVCUs utilizing the plug and operate application might require certain energy consumption. Therefore energy consumption simulations are necessary to study the energy performance of such a unit in a hospital isolation room, working at reduced background ventilation, namely 3 h^{-1}, compared to a hospital isolation room ventilated at 12 h^{-1}, and without the HBIVCU under identical other conditions (heating or cooling loads, number of patients etc.).

As already mentioned the reduced flow rates would also lead to additional savings due to reduced investment and maintenance costs for the hospital management. Reduced ventilation rates would require smaller in diameter ducting, smaller fans and HVAC stations etc. The smaller ducting would require less space to be mounted as well, and smaller servicing areas for the HVAC units and fans. Also the HBIVCU can allow more than two sick individuals from infectious disease to be placed in the same isolation hospital room. Under certain conditions, like epidemics or pandemics when the incidence rate of the infectious disease is high, more people can be treated in this way. This will lead to a reduction in the spread of the disease in a faster and more effective way as more

of the sick individuals will be kept isolated from the healthy population.

5.7. Conclusions

The risk of airborne cross-infection due to pathogens generated during coughing was studied in a full scale mock-up of hospital room with two patients lying in beds and a standing doctor. The following conclusions can be drawn:

- Regardless of the flow rates supplied by the background ventilation in infectious hospital wards there is enhanced risk from airborne cross infection for the medical staff standing in close proximity to a coughing patient;
- Elevated ventilation rates may increase the risk of cross-infection in an occupied place, up to a certain distance downstream of the coughed air, because the high velocities can peel off the boundary layer and leave the person exposed to the coughed flow with high concentration of pathogens. After this distance the higher flowrates result in better dilution and lower risk from cross infection.
- When the distance between the sick person and the HCW increases, the risk from exposure to contaminated coughed air decreases for the same ventilation flow rate due to dilution;
- The posture of the coughing patient and the location of the doctor are important factors: maximal exposure occurs when the HCW is facing the coughing patient; standing sideways of the coughing person decreases substantially the exposure risk. The risk of direct exposure to coughed air is minimal when the coughing persons lies on his/her back;
- Above certain total volume ventilation rate, the averaged exposure level per unit time to the coughed air shows slower decrease with further increase in the total volume ventilation;
- The recommended in the present standards and guidelines air change rate of 12 h^{-1} does not reduce the risk of airborne cross-infection for distances close to coughing sick person. With this respect the mixing air distribution method used today is not efficient.

A novel method, named HBIVCU, for reducing the risk of airborne cross infection by local ventilation at the vicinity of the bed of coughing sick patients in infectious hospital wards was proposed and studied in full-scale mock-up simulating coughing patient in an infectious hospital ward. The following conclusions are made:

- The use of the HBIVCU acts as a protective measure against exposure of people standing closely to the bed of a coughing sick patient;
- The performance of the HBIVCU for the studied conditions is unaffected by the rate of the background ventilation flow (up to 6 ACH);
- With respect to coughed air the background ventilation rate of 12 h^{-1} used today for ventilation of infectious hospital wards can be substantially lowered and the risk of airborne cross-infection reduced, when the novel method of local ventilation is implemented. This strategy may lead to energy savings as well;
- Simple modification of hospital bed design by adding small flat plates on its two sides is inexpensive method for reduction of cross-infection;

- The performance of the developed HBIVCU in case of breathing is recommended to be studied.

References

Abramovich G.N., The theory of turbulent jets, 1963, The M.I.T. Press, Cambridge, Massachusetts.

ANSI/ASHRAE 52.2-2007, Method of Testing General Ventilation Air-Cleaning Devices for Removal Efficiency by Particle Size, ASHRAE Inc., ISSN 1041-2336.

ANSI/AHRAE Standard 55 – 2004, Thermal environmental conditions for human occupancy, American Society of Heating, Refrigerating and Air-Conditioning Engineers, Inc.

ASHRAE/ASHE Standard, 170-2008, Ventilation of Health Care Facilities, American Society of Heating, Refrigerating and Air-conditioning Engineers, Inc. 1791 Tullie Circle NE, Atlanta, GA 30329.

Assar SK, Block SS. Survival of microorganisms in the environment. In: Disinfection, sterilization, and preservation. Lippinkott-Williams; 2000.

Baturin, V. V. Fundamentals of Industrial Ventilation, 1972, Pergamon, Oxford.

Beggs C.B., Kerr K.G., Noakes C.J., Hathway E.A., Sleigh P.A., The ventilation of multiple-bed hospital wards: Review and analysis, American Journal of Infection Control 2008, vol. 36, No. 4, pp. 250-259.

Bjørn E, Mattsson M, Sandberg M, Nielsen V. Displacement ventilation – effects of movement and exhalation. Proceedings of Healthy Buildings 1997:163–8. Washington DC, USA.

Bolashikov ZD, Nikolaev L, Melikov AK, Kaczmarczyk J, Fanger PO. Personalized ventilation: air terminal devices with high efficiency. Proceedings of Healthy Building 2003;2:850–5 [Singapore].

Bolashikov Z.D., Melikov A.K., Methods for air cleaning and protection of building occupants from airborne pathogens, 2009, Building and Environment, vol. 44, pp.1378-1385.

Bolashikov, Z.D., Melikov A.K., Kranek, M., 2009a, Improved Performance of Personalized Ventilation by Control of the Convection Flow around an Occupant's Body, ASHRAE Transactions, Louisville, USA.

Brain J.D., Proctor D.F. and. Reid L.M., Respiratory defense mechanism, 1977, Chapter 2, Cough.

Buttolph JL. Ultraviolet air disinfection in the theater. Journal of the SMPE 1948;51:79–91.

Cano M., Almeida G. and Tavares A., Microbiological Contamination of Air in Hospital "Clean Rooms", 2009, Proceedings of Healthy Buildings, Syracuse, USA, paper 679.

CDC (2005) Guidelines for preventing the transmission of tuberculosis; healthcare settings, 2005. MMWR, 54, 1-141.

CEN CR 1752, 1998. Ventilation for Buildings: Design Criteria for the Indoor Environment.

Cermak R, Melikov AK. Performance of personalised ventilation in a room with an underfloor air distribution system. Proceedings Healthy Building 2003;2:486–91 [Singapore].

Cermak R, Melikov AK. Transmission of exhaled air between occupants in rooms with personalised and underfloor ventilation. Proceedings Roomvent 2004. Coimbra: DEM-FCT, Univ. Coimbra.

Cermak R, Melikov AK, Forejt L, Kovar O. Distribution of contaminants in the occupied zone of a room with personalized and displacement ventilation. Proceedings Roomvent 2004. Coimbr: DEM-FCT, Univ. Coimbra.

Cermak R. and Melikov A.K. Air quality and thermal comfort in an office with underfloor, mixing and displacement ventilation. International Journal of Ventilation 2006;5(3):5.

Cermak, R., Melikov, A.K., Forejt, L. and Kovar, O., 2006, Performance of personalized ventilation in conjunction with mixing and displacement ventilation, International Journal of Heating, Ventilation and Refrigeration Research, vol.12, no.2, pp.295-311.

Cermak R, Melikov AK. Protection of occupants from exhaled infectious agents and floor material emissions in rooms with personalized and under floor ventilation. HVAC&R Research 2007;13(1):23–38.

Chao C.Y.H., Wan M.P., Morawska, L., Johnson G.R., Ristovski Z.D., Hargreaves M., Mengersen K., Corbett S. Li Y., Xie X., Katoshevski D., Characterization of expiration air jets and droplet size

distributions immediately at the mouth opening, 2009, Journal of Aerosol Science, vol. 40, issue 2, pp.122-133.

Cheong K.W.D., Phua S.Y., Development of ventilation design strategy for effective removal of pollutant in the isolation room of a hospital, 2006, Building and Environment, vol.41, pp. 1161-1170.

Ching W.- H., Leung M.K.H., Leung D.Y.C., Li Y., Reducing Risk of Airborne Transmitted Infection in Hospitals by Use of Hospital Curtains, 2008, Indoor and Built Environment; 17; 3, pp. 252-259.

Clark R.P., The role of human micro-environment in heat transfer and particle transport, Ph.D. Thesis, 1973, The City University, London.

Clark R.P., The aerodynamics of warmth and cleanliness, 1974, Clothing Res. J. 2, pp. 5-7.

Clark R.P., 1976, Convection heat loss from the human body, Engl. Med.; 5, 67. (doi:10.1234/EMED_JOUR_1976_005_025_02).

Clark R.P. and Cox R.N., The generation of aerosols from the human body, 1973, Airborne transmission and airborne infection (eds. J:F:P:Hers &K.C: Winker).

Clark R.P and Toy N., 1975, Natural convection around the human head, Journal of Physiology, 244. pp. 283-293.

Clark R.P., de Galcina-Goff M.L., Some aspects of the airborne transmission of infection, 2009, Journal of the Royal Society Interface; 6, S767-S782.

Cole E.C. and Cook C.E., Characterization of infectious aerosols in health care facilities: An aid to effective engineering controls and preventive strategies, 1998, Occupational Health and Industrial Medicine, vol. 39, Issue 5, pp. 213.

Datla B.V. and Glauser M., Flow Measurements in Indoor Office Environment, Proceedings of Healthy Buildings 2009, Syracuse, USA, Paper 809.

Decker J., Evaluation of Isolation Rooms in Health Care Settings Using Tracer Gas Analysis, 1995 Applied Occupational Environmental Hygiene vol. 10 (11), pp.887-891.

Decker M.D. and Schaffner W., Hospital Epidemiology and Infection Control, 2e., Chapter 73, 1999, Lippincott Williams & Wilkins, Philadelphia, USA.

DS 2451-9, Styring af infektionshygiejne i sundhedssektoren – Del 9: Krav til indkøb og vedligehold af teknisk og medicinsk-teknisk udstyr, Dansk Standard – Danish Standards Association, 2003-04-30.

Dygert R.K. and Dang T.Q., 2009a, Mitigation of Cross-Contamination in an Aircraft Cabin via Localized Suction Removal, Proceedings of Roomvent 2009, Busan South, Korea.

Dygert R. K., and Dang T. Q., 2009b, Localized suction-assisted contaminant removal strategies for improved IAQ, Proceedings Helthy Buildings 2009, Syracuse, NY, USA, Paper ID: 217.

Edwards D.A., Man J.C., Brand P., Katstra J.P., Somerer K., Stone H.A., Nardell E., Scheuch G., Inhaling to mitigate exhaled bioaerosols, 2004, PNAS, vol.101, No. 50, pp. 17383-17388.

European Standard 2007. EN 15251 2007. Indoor environmental input parameters for design and assessment of energy performance of buildings addressing indoor air quality. thermal environment. lighting and acoustics. EUROPEAN COMMITTEE FOR STANDARDIZATION. B-1050 Brussels.

Fiegel J, Clarke R, Edwards DA. Airborne infectious disease and the suppression of pulmonary bioaerosols. Elsevier; 2006, vol. 11(1/2). p. 51–7.

Greenwood D, Slack RCB, Peutherer JF. Medical microbiology. 6th ed. Churchill Livingstone; 2002.

Gupta J.K., Lin C.- H., Chen Q., Flow dynamics and characterization of a cough, 2009, Indoor Air; 19, pp. 517-525.

Gupta J.K., Lin C.- H., Chen Q., Characterizing exhaled airflow from breathing and talking, 2010, Indoor Air; 20; pp 31-39.

Gustafson T.L., Lavely G.B., Brawner E.R. Jr., Hutchenson R.H. Jr., Wright P.F. and Schaffner W., 1982, An outbreak of airborne nosocomial varicella, Pediatrics, vol.70 (4), pp. 550-556.

References

Halvoňová, B. and Melikov, A.K., 2008, Displacement ventilation in conjunction with personalized ventilation, In: Proceedings of the 11th International conference on Indoor Air Quality and Climate - Indoor Air 2008, 17-22 August 2008, Copenhagen, Paper ID: 411.

Halvoňová, B. and Melikov, A.K., 2009, Impact of intake positioning height on performance of "ductless" personalized ventilation, In: Proceedings of the 11th International conference on air distribution in Rooms – Roomvent 2009, 24-27 May 2008, Busan, Paper ID: S0131.

Halvoňová B., Melikov A.K., Performance of ''ductless'' personalized ventilation in conjunction with displacement ventilation: Impact of disturbances due to walking person(s), Indoor Air, 2010, v 45, pp. 427-436.

Hatch MT, Wolochow H. Bacterial survival: consequences of airborne state. An introduction to experimental aerobiology. New York: John Wiley and Sons; 1969. p. 267–95.

Hersen G., Moularat S., Robine E., Gehin E., Corbet S., Vabret A., Freymuth F., Impact of Health on Particle Size of Exhaled Respiratory Aerosols: Case-control Study, 2008, Clean - Soil Air Water, vol.36 Issue.7, pp. 572-578.

Hinds W.C., Properties, behavior and measurement of airborne particles, John Wiley & Sons, Inc., 1999.

Homma H. and Yakiyama M., 1988, Examination of free convection around occupant's body caused by its metabolic heat, ASHRAE Transactions 1988, 94 (1), pp. 104-124.

Hyldgaard. C. E. 1994. Humans as a source of heat and air pollution. In: Proc. ROOMVENT '94. 4th Int. Conf. on Air Distribution in Rooms. Krakow. Poland. pp. 414-433.

Incropera F.P. and DeWitt D.P., Introduction to Heat Transfer, 3rd edition, 1996, John Wiley & Sons, ISBN 0-471-30458-1.

Ishida K., Muramatsu H., Iizuka H. and Nobe T., Operating Conditions of a Personal Air-conditioning System in a Hospital, 2009, Proceedings of Healthy Buildings 2009, Syracuse, USA, Paper 602.

ISO 14644-1: 1999, Cleanrooms and associated controlled environments -- Part 1: Classification of air cleanliness, 1999.

ISO, International Standard ISO/DIS/7730, 2005, Moderate Thermal Environments-Determination of PMV and PPD Indices and Specification of the Conditions for Thermal Comfort: International Standard Organization for Standardization, Geneva, Switzerland.

ISO GUIDE 98-3, 2008, International Standard ISO, Guide to the expression of uncertainty in measurement. Geneva: International Organization for Standardization.

Jacobs, P., and de Gids, W.F. 2006. Individual and collective climate control in aircraft cabins, Int. Journal of Vehicle Design, vol. 42, No.1/2, pp. 57-66.

Jensen R.L., Pedersen D.N., Nielsen P.V. and Topp C., Personal exposure between people in a mixing ventilated room, Proceedings of the 4th International Conference on Indoor Air Quality, Ventilation & Energy Conservation in Buildings, IAQVEC 2001, Changsha,Hunan, China, October 2-5, 2001.

Kaczmarczyk J., Melikov A.K., Fanger, P.O., 2004, Human response to personalized and mixing ventilation, Indoor Air 14 (l8), pp. 1-13.

Kaczmarczyk, J., Melikov, A.K., Bolashikov, Z., Nikolaev, L. and P.O. Fanger, 2006, Human response to five designs of personalized ventilation, International Journal of heating, Ventilation and Refrigeration Research 12 (2), pp.367-384.

Kao P.H., Yang R.J., Virus diffusion in isolation rooms, 2006, Journal of Hospital infection, vol 62, pp.338-345.

Kato S., Murakami S. and Kobayashi H., 1992, New scales for evaluating ventilation efficiency as affected by supply and exhaust openings based on spatial distribution of contaminant", In: Proceedings of the ISRACVE'92, Tokyo, Japan, International Symposium on Room Air Convection and Ventilation Effectiveness, 177-186.

References

Kato, S. Murakami, S. and Yoshie R. 1993. Experimental and numerical study on natural convection with strong density variation along a heated vertical plate. Proceedings of the 9th Symposium on Turbulent Shear Flows, Japan, Paper 12-5.

Kaushal V., Saini P.S., Gupta A.K., 2004, Environmental Control Including Ventilation in Hospitals, JK Science, vol.6, No 4, pp. 229-232.

Khalifa H.E., Janos M.I. and Dannenhoffer III J.F., 2009, Experimental investigation of reduced-mixing personal ventilation jets, Building and Environment 44 (2009), pp 1551 – 1558.

Kofoed P., Thermal plumes in ventilated rooms, Ph.D. Thesis, Department of Building Technology and Structural Engineering, Aalborg University, Denmark, 1991.

Kowalski WJ, Bahnfleth WP. Airborne respiratory diseases and mechanical systems for control of microbes. HPAC Engineering July 1998:34–48.

Kowalski WJ, Bahnfleth WP. Effective UVGI system design through improved modeling. ASHRAE Transactions 2000;106(2):4–13.

Kowalski WJ, Bahnfleth WP. UVGI design basics for air and surface disinfection. IUVA News 2001;3(5):4–7.

Kowalski WJ, Bahnfleth WP. Airborne-microbe filtration in indoor environments. The critical aspects of filter sizing and a methodology for predicting a filter's effectiveness against allergens, bacteria, and viruses. HPAC Engineering January 2002:57–69.

Kumar R., Kumar R. and Gupta A., Analysis of the Ventilation System of an Isolation Room for a Hospital, 2008, International Journal of Ventilation, vol. 7, No. 2, pp. 139-149.

Launder BE, Reece GJ, Rodi W. Progress in the development of Reynolds stress turbulence closure. Journal of Fluid Mechanics 1975; 68: 537-66.

Leiner G.C., Abramowitz S., Small M.J. and Stenby V.B., Cough peak flow rate, 1966, Am. J. Med. Sci., 251, pp.211-214.

Lewis H.E., Foster A.R., Mullan B.J., Cox R.N. and Clark R.P., 1967, Aerodynamics of the human microenvironment, The Lancet 1969, Vol. 1, Nr 7609, pp 1273 – 1277.

Lien F.S., Chen W.L. and Leschziner M.A., 1996, Low-Reynolds-number eddy-viscosity modeling based on non-liner stress-strain/vorticity relations, Proceedings of 3rd International Symposium on Engineering Turbulence Modelling and Measurement, Greece, 1-10.

Li Y., Huang H., Yu T.S., Wong T.W., Qian H., Role of air distribution in SARS transmission during the largest nosocomial outbreak in Hong Kong, Indoor Air, 2005, v. 15 (2), pp 83 – 95.

Li Y., Leung G. M., Tang J. W., Yang X., Chao C., Lin J. Z., Lu J. W., Nielsen P. V., Niu J., Qian H., Sleigh A.C., Su H.-J. J., Sundell J., Wong T. W., Yuen P. L., Role of ventilation in airborne transmission of infectious agents in the built environment – a multidisciplinary systematic review, Indoor Air, 2007, v. 17 (1), pp. 2-18 (17).

Li Y., Ching W.H., Qian H., Yuen P.L., Seto W.H., Kwan J.K., Leung J.K.C., Leung M., Yu S.C.T., An Evaluation of the Ventilation Performance of New SARS Isolation Wards in Nine Hospitals in Hong Kong, 2007a, Indoor and Built Environment; 16; 5; pp. 400-410.

Liu L., Li Y., Nielsen P.V., Jensen R.L., Litewnicki M., Zajas J., An Experimental study of Human exhalation during Breathing and Coughing in a Mixing Ventilation Room, Proceedings of Healthy Buildings 2009, Syracuse, USA, Paper 162.

Loudon RG, Roberts RM. Droplet expulsion from the respiratory tract. American Review of Respiratory Disease 1967;95:435–42.

Mahajan R.P., Singh P., Murty G.E. and Aitkenhead A.R., Relationship between expired lung volume, peak flow rate and peak velocity time during a cough manoeuvre, 1994, Br. J. Anaesth. 72, pp. 298-301.

Matsumoto H., Kozaka T., Nakao T. Study on air distribution and ventilation effectiveness in displacement

ventilated rooms with a moving object, Proceedings of Indoor Air, Copenhagen, Denmark, 2008.
Melikov A.K. and Zhou G., Air movement at the neck of the human body, Proc. Indoor Air 1996, Nagoya, Japan, Vol.1, pp.209-214.
Melikov AK, Cermak R, Kovar O, Forejt L. Impact of airflow interaction on inhaled air quality and transport of contaminants in rooms with personalized and total volume ventilation. Proceedings Healthy Building 2003, Vol.2, pp.500–10 [Singapore].
Melikov AK., Personalized ventilation. Indoor Air 2004;14(Suppl. 7):157–67.
Melikov, A.K., 2004a, Breathing thermal manikins for indoor environment assessment: important characteristics and requirements, European Journal of Applied Physiology, vol. 92, number 6, September 2004, pp. 710-713.
Melikov. A.K. and Kaczmarczyk. J., Indoor air quality assessment by a breathing thermal manikin, 2007, Indoor Air 17 (1). pp.50-59.
Melikov AK, Ivanova T, Stefanova G. Seat incorporated personalized ventilation. Proceedings Room Vent 2007:1318.
Melikov A.K., Brand M., Fang L., Reduced exposure to coughed air by advanced air distribution, 2009, Proceedings of Roomvent 2009, Busan, South Korea.
Melikov A.K. and Dzhartov V., 2009, Control of the free convection flow around human body by radiant cooling, Healthy Buildings 2009, Syracuse, USA, Paper ID: 620.
Menzies D., Fanning A., Yuan L., FitzGerald J.M., and the Canadian Collaborative Group in Nosocomial Transmission of TB, Hospital Ventilation and Risk for Tuberculous Infection in Canadian Health Care Workers, 2000 Annals of Internal Medicine, vol 133, issue 10, pp. 779-789.
Menzies D, Popa J, Hanley JA, Rand T, Milton DK. Effect of ultraviolet germicidal lights installed in office ventilation systems on workers' health and wellbeing: double blind multiple crossover trial. The Lancet 2003;362:1785–91.
Meslem A., Nastase I., Abed-Meraim K., 2008, Experimental investigation of the mixing performance of a lobed jet flow. Journal of Engineering Physics and Thermophysics (2008) 81:106-111. August 01. 2008.
Mierzwinski S., Air motion and temperature distribution above a human body in result of natural convection, A4-Serien no. 45, Royal Institute of Technology, Stockholm, 1980.
Minki S., Kato S., Yanagi U., Tanaka T., Ida H., Asai M., Takaki T. and Yanagihara R., Evaluation method on the germicidal effect of Upper Room UVGI system for exhaled air from patients, Proceedings Roomvent 2009, Busan, South Korea, pp. 657-663.
Morawska L. Droplet fate in indoor environments, or can we prevent the spread of infection? Proceedings Indoor Air 2005:9–23.
Morawska L., Johnson G.R., Ristovski Z.D., Hargreaves M., Mengersen K., Corbett S., Chao C.Y.H., Li Y., Katoshevski D., Size distribution and sites of origin of droplets expelled from the human respiratory tract during expiratory activities, 2009, Journal of Aerosol Science, vol. 40, issue 3, pp. 256-269.
Mundt E. Non-buoyant pollutant sources and particles in displacement ventilation. Building and Environment 2001;36:829–36.
Möritz M, Peter H, Nipko B, Ru¨den H. Capability of air filters to retain airborne bacteria and molds in heating, ventilating and air-conditioning (HVAC) systems. International Journal of Hygiene and Environmental Health 2001;203:401–9.
Nastase I., Meslem A., 2006, Experimental investigation on the near and far field behavior of an isothermal lobed jet. WSEAS TRANSACTIONS on FLUID MECHANICS 1, 5 (2006), pp. 414-422.
Nicas M., Nazaroff W.W., Hubbard A., Toward understanding the risk of secondary airborne infection:

emission of respirable pathogens. Journal of Occupational and Environmental Hygiene 2005;2:143–54.

Nielsen P. V. Bjorn E., Brohus H., 2002, Contaminant flow and personal exposure, Journal of Heating, Piping, AirConditioning Engineering, Vol. 74 (8), pp. 40-45+63

Nielsen PV, Jiang H, Polak M., 2007a, Bed with integrated personalized ventilation for minimizing of cross infection. Room Vent 2007:1077.

Nielsen P.V., Bartholomaeussen NM, Jakubowska E, Jiang H, Jonsson OT, Krawiecka K, et al., 2007b, Chair with integrated personalized ventilation for minimizing cross infection. Room Vent 2007:1078.

Nielsen PV, Hylgaard CE, Melikov AK., 2007c, Personal exposure between people in a room ventilated by textile terminals – with and without personalized ventilation. HVAC&R Research 2007;13(4):635–43.

Nielsen P.V., Jensen R.L:, Litewnicki M., Zajas J., Experiments on the Microenvironment and Breathing of a Person in Isothermal and Stratified Surroundings, Proceedings of Healthy Buildings 2009, Syracuse, USA, Paper 374.

Niu J, Gao N, Phoebe M, Huigang Z. Experimental study on chair-based personalized ventilation system. Building and Environmnet 2007;42:913–25.

Noakes C., Fletcher L.A., Sleigh P.A., Booth W.B., Beato-Arribas B., Tomlinson N., Comparison of Tracer Techniques for Evaluating the Behaviour of Bioaerosols in Hospital Isolaion Rooms, 2009, Proceedings of Healthy Buildings, Syracuse, USA, Paper 504.

Omori, T., Yang, J.H., Kato, S. and Murakami, S. 2004. Coupled simulation of convection and radiation on thermal environment around an accurately shaped human body. Proceedings of the 9th International Conference on Air Distribution in Rooms, Portugal, CD-ROM.

Patankar S., Numerical Heat Transfer and Fluid Flow (1980), ISBN 0-89116-522-3.

Peccia J, Werth HM, Miller S, Hernandez M. Effects of relative humidity on the ultraviolet induced inactivation of airborne bacteria. Aerosol Science and Technology 2001;35:728–40.

Popiolek Z., 1981, Problems of testing and mathematical modelling of plumes above human body and other extensive heat sources. A4-Serien no. 54. Royal Inst. of Technology, Stockholm.

Qian H., Li Y., Nielsen P.V., Hyldgaard C.E., Wong T.W., Chwang A.T.Y. Dispersion of exhaled droplet nuclei in a two-bed hospital ward with three different ventilation systems. Indoor Air 2006;16:111–28.

Qian H., Li Y., Nielsen P.V., Hyldgaard C.E., Dispersion of exhalation pollutants in a two-bed hospital ward with a downward ventilation system, 2008, Building and Environment, vol. 43, pp. 344-354.

Riley R., Permut S., Room air disinfection by ultraviolet irradiation of upper air. Air mixing and germicidal effectiveness. Archives of Environmental Health 1955;22:208–19.

Riley R.L., Permut S., Kaufman J.E. Convection, air mixing, and ultraviolet air disinfection in rooms. Archives of Environmental Health 1971;22:200–7.

Riley R.L., Permut S., Kaufman J.E., Room air disinfection by ultraviolet irradiation of upper air. Further analysis of convection air exchange. Archives of Environmental Health 1971a;23:35–9.

Rim D., Novoselac A., Transport of particulate and gaseous pollutants in the vicinity of a human body, 2009, Building and Environment 44 (2009) 1840-1849.

Rudnick SN, Milton DK. Risk of indoor airborne infection transmission estimated from carbon dioxide concentration. Proceedings Indoor Air 2003;13:237–45.

Russo J.S., Dang T.Q. and Khalifa H.E., 2009, Computational analysis of reduced-mixing personal ventilation jets, Building and Environment 44 (2009), pp 1559 – 1567.

Settles G.S., Sniffers: Fluid-Dynamic Sampling for Olfactory Trace Detection in Nature and Homeland Security – The 2004 Freeman Scholar Lecture, 2005, Journal of Fluid Engineering, vol. 127, pp.189-218.

Shah NS, Wright A, Bai G-H, Barrera L, Boulahbal F, Martin-Casabona N, et al. Worldwide emergence of

extensively drug-resistant tuberculosis. Emerging Infectious Diseases 2007;13(3):380–7.

Shih Y.- C., Chiu C.- C., Wang O., Dynamic airflow simulation within an isolation room, 2007, Building and Environment, vol 42, pp. 3194-3209.

Singh P., Mahajan R.P., Murty G.E. and Aithkenhead A.R., Relationship of peak flow rate and peak velocity time during voluntary coughing, 1995, Br. J. Anaesth., 74, pp. 714-716.

Streifel A., Hospital Epidemiology and Infection Control, 2e., Chapter 80, 1999, Lippincott Williams & Wilkins, Philadelphia, USA.

Sze To G. N., Wan M. P., Chao C. Y. H., Fang L. and Melikov A., 2009, Experimental Study of Dispersion and Deposition of Expiratory Aerosols in Aircraft Cabins and Impact on Infectious Disease Transmission, *Aerosol Science and Technology*, Vol. 43, pp. 466–485.

Tanabe, S., Zhang, H., Arens, E.A., Madsen, T.L., Bauman, F.S., 1994, Evaluating thermal environments by using a thermal manikin with controlled skin surface temperature, ASHRAE Transactions 100 (1), pp 39-48.

Tang J. W., Liebner T.J., Craven B.A., Settles G. S., Craven B.A., A Schlieren optical study of the human cough with and without wearing masks for aerosol infection control, 2009, Journal of the Royal Society Interface, Vol.6 Issue. SUPPL. 6, S727-S736

Tellier R. Review of aerosol transmission of influenza a virus. Emerging Infectious Diseases 2006;12(11):1657–62.

Tung Y.- C., Hu S. - C., Tsai T. - I, Chang I - L., An experimental study on ventilation efficiency of Isolation room, 2009, Building and Environment, vol. 44, pp. 271-279.

Tung Y.- C., Shih Y.- C., Hu S.- C., Numerical study on the dispersion of airborne contaminants from an isolation room in the case of door opening, 2009a, Applied Thermal Engineering, vol. 29, pp. 154-1551.

van der Wel, A.M., Orendi, J.M., Hoekstra, J.B.L., Bouwman, J.J.M., van Dijk, Y., Diepersloot, R.J.A., 1996, Nosocomial influenza in a general hospital, The Netherlands Journal of Medicine, vol 48 (5), pp. A94.

Wan MP, Chao CYH. Effect of changing the air distribution system on the dispersion of droplet phase aerosols in an enclosure. Proceedings: Indoor Air 2005:2696–700.

Wan M.P., Sze To G. N., Chao C. Y. H., Fang L. and Melikov A., 2009, Modeling the Fate of Expiratory Aerosols and the Associated Infection Risk in an Aircraft Cabin Environment, *Aerosol Science and Technology*, Vol. 43, pp. 322–343.

Wells WF. On air-born infection. Study II. Droplet and droplet nuclei. American Journal of Hygiene 1934;20:611–18.

Wells WF. Airborne contagion and air hygiene. Cambridge (MA): Harvard University Press; 1955.

Wong K.C. and Leung K.S., Transmission and Prevention of Occupational Infections in Orthopaedic Surgeons, 2004, Journal of Bone & Joint Surgery, American Volume, vol. 86, issue 5, pp.1065-1077.

Xie X, Li Y. How far respiratory droplets move in indoor environments? Proceedings Healthy Buildings 2006:309–14.

Xu P, Kujundzic E, Peccia J, Millie PS, Moss G, Hernandez M, et al. Impact of environmental factors on efficacy of upper-room air ultraviolet germicidal irradiation for inactivating airborne mycobacteria. Environmental Science and Technology 2005;39(24):9656–64.

Yamada K, Yanagi U, Kagi N, Ikeda K. A study about microbes on the surface of air filter in an air conditioning system. Proceedings of Healthy Buildings 2006:443–6.

Yang, J.H., Kato, S., Murakami, S. Kasahara, H. and Hayashi, T. Numerical analysis on air quality of human's inhaled air in room with infiltration, E02-3, Proceedings of the 15th Symposium on Computational Fluid Dynamic, 2001.

References

Yang S, Lee GWM, Chen C-M, Wu C-C, Yu K-P. The size and concentration of droplets generated by Coughingin human subjects. Journal of Aerosol Medicine 2007;20(4):484–94.

Zhu, S.W., Kato, S., Murakami, S. and Hayashi, T. 2004. Study on inhalation region by means of CFD analysis and experiment. Building and Environment, 40(10), 1329-1336.

Zhu S.W., Kato S. and Yang J.H., Investigation into airborne transport characteristics of air-flow due to coughing in a stagnant room environment, 2006, ASHRAE Transactions, 112, pp. 123-133.

Zhu, S.W., Kato, S., Ooka, R. and Sakoi, T. 2007. Development of a computational thermal manikin applicable in a non-uniform thermal environment (Part 1) Coupled simulation of convection, radiation and Smith's human thermal physiological model for sensible heat transfer from a seated human body in radiant environment. ASHRAE HVAC&R Research, 13 (4), 661-679.

Zhu S.W., Bolashikov Z., Melikov A.K., 2008, Examination on performance of headset incorporated personalized ventilation unit using CFD method. Proceedings of Indoor Air 2008. 17-22 August 2008. Copenhagen. Denmark - Paper ID: 1018.

Zukowska D, Melikov A and Popiolek Z, 2007, Thermal plume above a simulated sitting person with different complexity of body geometry. In: Proceedings of the 10th International Conference on Air Distribution in Rooms - Roomvent 2007, Helsinki, Vol. 3, pp. 191-198.

Zukowska D, Popiolek Z and Melikov A., 2007a, Impact of personal factors and furniture arrangement on the thermal plume above a human body. In: Proceedings of the 10th International Conference on Air Distribution in Rooms - Roomvent 2007, Helsinki, Vol. 3, pp. 137-144.

Zukowska D, Melikov A and Popiolek Z., 2008, Impact of Thermal Plumes Generated by Occupant Simulators with Different Complexity of Body Geometry on Airflow Pattern in Rooms. In: Proceedings of the 7th International Thermal Manikin and Modelling Meeting – 7I3M, Coimbra, Portugal, Paper 8

Özcan, O., Mayer, K.E. Melikov, A.K., 2005, A visual description of the convection flow field around the head of a human, Journal of Visualization, Vol. 8, No.1, 23-31.

http://www.merriam-webster.com/dictionary/disease, as of 15th of March 2010.

List of Papers

The thesis is based on the following papers:

Paper I - Bolashikov, Z.D., Melikov A.K., 2009, Methods for air cleaning and protection of building occupants from airborne pathogens, *Building and Environment*, 44 (7), p.1378-1385.

Paper II - Bolashikov, Z.D., Melikov A.K., Krenek, M., 2009, Improved Performance of Personalized Ventilation by Control of the Convection Flow around an Occupant's Body, ASHRAE Transactions 2009, Vol. 115, Part 2, pp 421-431, LO-09-038.

Paper III - Bolashikov, Z.D., Melikov A.K., Krenek, M., 2010, Control of the Free Convection Flow around the Human Body for Enhanced Inhaled Air Quality: Application to a Seat-Incorporated Personalized Ventilation Unit, HVC&R Research, (accepted).

Paper IV - Zhu S.W., Bolashikov Z., Melikov A.K., 2008, Examination on performance of headset incorporated personalized ventilation unit using CFD method. Proceedings of Indoor Air 2008. 17-22 August 2008. Copenhagen. Denmark - Paper ID: 1018.

Paper V - Bolashikov, Z.D., Melikov A.K., Spilak M., 2009, INSERTED JETS APPLIED IN WEARABLE PERSONALIZED UNIT, Building and Environment, Submitted.

Paper VI - Bolashikov Z.D., Nagano H., Melikov A.K., Meyer K.E. and Kato S., Control of the Free Convection Flow within the Breathing Zone by Confluent Jets for Improved Performance of Personalized Ventilation: Part 2 – Inhaled Air Quality, Proceedings Healthy Buildings 2009, Syracuse NY USA, Paper ID: 471.

Abbreviations Used

ACH	Air Changes per Hour
AII	Airborne Infection Isolation
ANSI	American National Standards Institute
ASHRAE	American Society of Heating, Refrigerating and Air Conditioning Engineers
ATD	Air Terminal Device
CCD	Charge Coupled Device
CDC	Centers for Disease Control and Prevention
CEN	European Committee for Standardization or Comité Européen de Normalisation
CEV	Cough Expired Volume
CFD	Computational Fluid Dynamics
CPFR	Cough Peak Flow Rate
CR	Committee Report
CS	coughing sideways
CU	coughing upwards
DNA	Deoxyribonucleic acid
DS	Dansk Standard
EN	European Norm
EP	European Patent
H	Height
HAI	Hospital Acquired Infection
HCW	Health Care Worker
HEPA	High Efficiency Particulate Absorbing
HBIVCU	Hospital Bed Integrated Ventilation and Cleansing Unit
HVAC	Heating Ventilation and Air-Conditioning

Abbreviations Used

IAQM	Indoor Air Quality Monitor
IMI	Interferometric Mie Imaging
ISO	International Organization for Standardization
L	Length
LDA	Laser Doppler Anemometry
LVPV	Low Velocity Personalized Ventilation
MDRSA	Multi-Drug Resistant *Staphylococcus Aureus*
MV	Mixing Ventilation
NDIR	Non-Dispersive Infra-Red
PCO	Photocatalytic Oxidation
PEE	Personal Exposure Effectiveness
PIV	Particle Image Velocimetry
RF	Respiratory Frequency
PCT	Peak Concentration Time
PCL	Peak Concentration Level
ppm	parts per million
PV	Personalized Ventilation
PVT	Peak Velocity Time
RMP	Round Movable Panel
SBS	Sick Building Syndrome
TV	Total Volume
UFAD	Under Floor Air Distribution
ULPA filter	Ultra Low Particulate Filter
US or USA	United States of America
UVGI	Ultra Violet germicidal Irradiation
W	Width

Table of Figures

Table of Tables

Appendixes

Appendixes

Appendix I

Paper I

Bolashikov, Z.D. and Melikov A.K.,

Methods for air cleaning and protection of building occupants from airborne pathogens

Building and Environment 2009, 44 (7), p.1378-1385.

Building and Environment 44 (2009) 1378–1385

Contents lists available at ScienceDirect

Building and Environment

journal homepage: www.elsevier.com/locate/buildenv

Methods for air cleaning and protection of building occupants from airborne pathogens

Z.D. Bolashikov*,[1], A.K. Melikov [1]

International Centre for Indoor Environment and Energy, Department of Civil Engineering, Technical University of Denmark, Nils Koppels Alle, building 402, 2800 Lyngby, Denmark

ARTICLE INFO

Article history:
Received 31 March 2008
Received in revised form 6 August 2008
Accepted 6 September 2008

Keywords:
Pathogen
Generation
Survival
Airborne
Air cleaning
Air distribution

ABSTRACT

This article aims to draw the attention of the scientific community towards the elevated risks of airborne transmission of diseases and the associated risks of epidemics or pandemics. The complexity of the problem and the need for multidisciplinary research is highlighted. The airborne route of transmission, i.e. the generation of pathogen laden droplets originating in the respiratory tract of an infected individual, the survivability of the pathogens, their dispersal indoors and their transfer to a healthy person are reviewed. The advantages and the drawbacks of air dilution, filtration, ultraviolet germicidal irradiation (UVGI), photocatalytic oxidation (PCO), plasmacluster ions and other technologies for air disinfection and purification from pathogens are analyzed with respect to currently used air distribution principles. The importance of indoor air characteristics, such as temperature, relative humidity and velocity for the efficiency of each method is analyzed, taking into consideration the nature of the pathogens themselves. The applicability of the cleaning methods to the different types of total volume air distribution used at present indoors, i.e. mixing, displacement and underfloor ventilation, as well as advanced air distribution techniques (such as personalized ventilation) is discussed.

1. Introduction

Most people live, work and enjoy their leisure activities in densely populated environments, which increase their exposure to many pathogens. The risk of cross-infection is a psychological stress factor as well as a health issue. It reduces the well-being of the population and has a powerful economical impact due to absenteeism and reduced productivity. Human history records many pandemics, e.g. the Spanish influenza epidemic in 1918–1919 (H1N1 virus), which was by far the most lethal flu pandemic of the 20th century, infecting about a quarter of the global population and killing more than 40 million people [1]. Increased mobility permits a rapid dissemination of new diseases and elevates the risk of further pandemics, e.g. of Severe Acute Respiratory Syndrome (SARS), as well as the emergence of old and well-known diseases that have developed resistance to existing drug treatment, e.g. tuberculosis [2]. Another threat imposes the rapid mutation of some microorganisms and their adaptation as a cause of human diseases, e.g. ebola, the H5N1 strain of avian flu, etc. [3].

All these factors increase the importance of making the indoor air as clean from any pathogens, and with high perceived air quality, as the cleanest outdoor air, or even better. Unfortunately, most of our indoor work places are not designed to prevent the spread of airborne pathogens. Furthermore, air distribution systems may even enhance transmission. In order to solve this multidisciplinary problem successfully, knowledge in different fields needs to be combined: the type of pathogen, its generation and survival mechanism before affecting the host, possible disinfection methods to eradicate it, and transmission mechanisms among people. Engineering solutions can be proposed in order to efficiently reduce the pathogen loads released in air, disable their virulence, and make them harmless for healthy inhabitants. The methods applied should be neither life nor health threatening, nor should they reduce in any way occupants' perceived air quality or thermal comfort. They should also be user friendly (if people are to operate them), with low noise emission, energy efficient, highly ergonomic and aesthetic.

The following discussion is limited to the generation, survival and airborne transmission of pathogens, the methods and technologies for removing microorganisms and viruses, from indoor air and their compatibility with existing HVAC practice.

2. Airborne pathogens

2.1. Generation and airborne transmission

Airborne pathogens are those pathogens generated in the respiratory system and released in exhaled air as a way of

* Corresponding author. Tel.: +45 4525 4038; fax: +45 4593 2166.
E-mail address: zdb@mek.dtu.dk (Z.D. Bolashikov).
[1] URL: www.ie.dtu.dk.

0360-1323/$ – see front matter © 2008 Elsevier Ltd. All rights reserved.
doi:10.1016/j.buildenv.2008.09.001

propagation. In her review article Morawska [4] describes the generation mechanism and the sites of pathogens' droplet formation. The factors influencing this process, and the fate of the expelled respiratory droplets are also considered. She concludes that although a great deal is known, more knowledge is needed on the mechanism of pathogen transfer in occupied places. There are 4 parts in the respiratory tract where microorganisms may multiply and be dispersed in exhaled air: nose, oral cavity, throat and lungs. Each provides different habitats to which different pathogens have adapted: tuberculosis in the lungs, *Streptococcus agalactiae* in the throat, etc. Dispersal may take place through the nose and the mouth. Most frequent aerial dispersal takes place from the mouth, when talking, coughing or even sneezing, and involves primarily the saliva [5]. Fiegel et al. [6], on the other hand, identifies the pulmonary region as the main source for deep lung generation of bio-aerosols and the ensuing environmental transport of airborne pathogens. She states that applying "saline therapy" (aerosol approach to immobilize bio-aerosols within the lungs), would reduce airborne pathogen generation, allowing for natural clearing mechanisms. It is clear that the contamination of the generated droplets with pathogens depends on the preferred habitat of the pathogen: coughing will produce droplets with deep lung pathogens, while talking, sneezing, etc., will disperse pathogens inhabiting mainly the mouth, the nose or the throat of the host individual.

According to Tellier [7] the latest medical findings suggest that influenza A virus is more likely to be transferred by the airborne route through aerosolization and to thus penetrate the lower lung region of the exposed occupant. The airborne transmission route has been shown to be predominant for three respiratory diseases: measles, varicella and tuberculosis [8]. When coughing, sneezing, talking or breathing, people generate particles of different sizes and air jets with different initial characteristics. Nicas et al. [9] summarized the scarce data on the particle size distribution of respiratory aerosols. Evaporative water loss was also taken into account. After evaporation is complete the particle retains half of its original diameter. However the authors are skeptical about the existing data on droplet size distribution based on previous experiments. They propose a new fitted mixture model of two log normal distributions to describe the particle size distribution for coughing based on the findings of Loudon and Roberts [10]. According to this model there is a distribution of "small" particles with geometric mean (GM) and geometric standard deviation (GSD) of 9.8 μm and 9.0 μm, respectively, and a distribution of "large" particles with GM of 160 μm and GSD of 1.7 μm. The small particles constitute 71% of all particles emitted by coughing. Particles with a diameter of 10 μm and less are able to penetrate into the lungs [11]. Thus coughed droplets with diameters up to 20 μm should be considered in the case of airborne cross-infection because after full evaporation of the water content in them they attain a diameter of 10 μm or less. If the inhaled particles carry any pathogens the risk of infection is greatly increased. A recent experiment performed by Yang et al. [12] shows that the droplet size distribution is in the range 0.62–15.9 μm. In their experiment they used two methods to identify the size distribution of coughed droplets. In the first method, the droplets expelled by coughing were mixed with clean air with low RH (35%) in a testing column. To avoid interference from the surrounding environment the subjects wore a mask with a P100 filter, which was connected to the testing column. In the second method subjects coughed directly into a sample bag. However, it was found out that more particles were retained in the bag compared to the first method. They also studied the effect of age and gender on droplet generation. In both cases no significance was found ($p > 0.1$). Their findings agree with the conclusions of Nicas et al. [9], but for the small particle range only. This was probably due to the fact that the bigger particles were caught in the filter media or stuck on the walls of the sampling bags. The ambiguity remaining is such that more research is required in the field of droplet generation and size distribution.

A simple physical model proposed by Xie and Li [13] was employed to investigate the coupled evaporation and movement of droplets released during respiratory activities. The effect of droplet size, exhaled air velocity and temperature, and the relative humidity of the ambient air on droplet evaporation and dispersion were all taken into account. The prediction, which applies only to still ambient air, was that expelled droplets move more than 6 m when sneezing (initial velocity of 50 m/s), more than 2 m when coughing (initial velocity of 10 m/s), and less than 1 m when breathing (initial velocity of 1 m/s). Compared to small droplets, large droplets evaporated more slowly and sedimented more rapidly. These processes were strongly dependent on the initial velocity of the respiratory jet: the higher the initial velocity the faster they would evaporate and the faster they would deposit on surfaces. More droplets would be suspended in air at lower initial jet velocities (i.e. talking, laughing etc.). However different air distribution patterns may affect differently the heat and mass transfer from the droplets as well as their dispersion.

Another form of airborne contamination with infectious bio-aerosols could occur when vomiting and when flushing toilets in public premises. Barker et al. [14] showed that a sick person can produce 10^7 viruses per 1 ml of vomit and 10^{12} viruses per 1 g of stool material. So for pathogens that cause vomiting of the host or diarrhea (SARS, *Escherichia coli*, *Neisseria meningitidis* etc.), there is a greatly increased risk of spreading the disease. Rusin et al. [15] found that droplets produced by flushing the toilet could either be inhaled or deposited on surfaces.

The virulence, pathogen generation and the infective dose are other important factors determining the infectivity of a pathogen. Different microorganisms have different methods of overcoming the defence mechanisms of their host and successfully hiding. Also the generation of pathogens is different depending on the stage of the disease (early, advanced or latent). Another point of importance is the infective dose: sometimes a single organism can cause a disease. But this factor is strongly dependent on the immune system and/or age of the host: immuno-compromised people as well as old and very young are more susceptible [16].

2.2. Survival of pathogens in air

In order to be able to reach and infect their host, the airborne pathogens need to survive in the surrounding environment, which makes factors like air temperature and relative humidity important. So far, knowledge on the influence of relative humidity on pathogenic bacteria is scarce and the little data available is for opportunistic representatives (studies were performed on innocuous strains from the same families as the pathogens themselves). In general, mid-range humidity conditions (40–60%) have been shown to be more lethal to non-pathogenic bacteria [17]. Viruses with more lipids tend to be more persistent at lower relative humidity, while viruses with less or no lipid content are more stable at higher relative humidity [18]. Loosli [19] showed that humidity levels of 80–90% for 30 min could render the influenza virus noninfectious to mice, while exposure to lower humidity levels (17–24%) provided the greatest infectivity. Lowen et al. [20] confirmed that the transmission efficiency of influenza A virus is dependent on relative humidity by conducting experiments with guinea pigs in an environmental chamber. The four infected animals were separated from the four healthy ones: each animal was in a cage to avoid any possible contact. Thus the only possible transmission route was airborne. The transmission was highly efficient at low RH (20% or 35%), and less effective at 65%. At 50% only one animal was infected and at 80% RH no transmission of the virus was observed. In all five cases the

temperature was kept constant: 20 °C. The authors suggest that the dry air could desiccate the nasal mucosa, lead to epithelial damage and/or reduction in mucociliary clearance, thus making the host susceptible to respiratory infections. This obviously depends also on the stability of the virus as well as the droplet nuclei formation mechanism: at low RH droplets evaporate faster, shrink and change their size, increasing the possibility of being inhaled if their diameter is less than 10 μm. In other studies the survival of some viruses has been shown to be independent of relative humidity [21]. Harper [22] and Miller and Artenstein [23] showed that picornaviruses and adenoviruses, respiratory disease causatives and members of non-enveloped virus groups, survive better at high relative humidity. Measles and influenza, both enveloped viruses, survive best in aerosols at low relative humidity [24,25].

Studies also report that the effects of relative humidity on virus survival can be influenced either positively or negatively by temperature. At 20 °C human coronavirus (upper respiratory tract diseases) was reported to be most stable at intermediate humidity, but was also relatively stable at low humidity [26]. The same study also found that virus survival at 6 °C and 80% humidity was very similar to the best survival at intermediate humidity. Lower temperatures have also been shown to enhance rhinovirus survival at high relative humidities [27]. Lowen et al. [20] reported that influenza virus transmission is inversely proportional to the temperature. At 5 °C, the transmission of influenza A virus was more effective compared to 20 °C or 30 °C. At 5 °C the infected guinea pigs shed the virus for a longer period compared to the other two conditions and more viable viruses were found in their nose secretions. The authors believed that at low temperature the cooling effect on the cilia slows their beats, reducing mucociliary clearance and diminishing immune defence mechanisms. It was suggested that in cool and temperate climates the predominant route of infection with influenza is airborne, which implies that in tropical and warm environments the direct contact route is dominant. This bold hypothesis may not be true; it is in full contradiction to the findings of Tellier [7] (as already mentioned above). Enveloped viruses and their patterns of survival at different temperatures, [28,29], may not be the same as those of non-enveloped viruses, especially when the viruses are on surfaces [30].

For safety reasons scientists have until now performed studies with non-pathogenic organisms, which have a different structure from their pathogenic relatives [16]. Therefore more research is needed on this topic.

3. Cleaning methods

Chen et al. [31] showed by applying mathematical models (the Well–Riley model, competing-risk model and Von Foester equation), that public health interventions (vaccination, insulation, tracing down of the contacts of infected people etc.) are not enough to stop the outbreak of a disease in a modern society. They concluded that more advanced methods need to be applied to help people fight the diseases, namely engineering techniques combined with public health interventions.

A great effort has been made to find engineering techniques to keep airborne pathogens away from occupants in buildings, or at levels low enough to be unable to cause a disease: dilution, filtration, Ultra Violet Germicidal Irradiation (UVGI), etc. The airborne pathogens might originate from a sick person, from the building itself (infected/polluted HVAC system, infected building materials etc.) or from an intentional release, i.e. a terrorist attack [32,33].

3.1. Dilution

Dilution of room air with clean disinfected air is one of the easiest and best known methods to remove pathogens and to decrease the risk of infections in rooms. Natural, mechanical and hybrid ventilation are often used to supply clean air in rooms. However, this method has its limitations, related to air distribution pattern, occupants' thermal comfort, etc., which is discussed later in this paper. Moreover, if one assumes perfect mixing, a reduction of contaminants' concentration by a factor requires an increase of the air change rate by the same factor.

3.2. Filtration

A method widely used today is the filtration of air in HVAC systems. Classifications and guidelines exist for applying filtration as part of the ventilation system. They are widely used by designers [34,35]. Studies show that filtration is a good method to prevent outside pathogens from penetrating the building envelope through the mechanical ventilation. Kowalski and Bahnfleth [36,37] showed that 80- and 90-per-cent filters can produce air quality improvements that approach those achieved with HEPA filters, but at much lower cost. Another finding is that microorganisms capable of penetrating HEPA filters are predominantly nosocomial infections (HEPA filters remove 99.97% of all particles 0.3 μm or larger in diameter).

Enzyme filters eradicate microbes by attacking the microbial cell membrane, but this assumes that they come into close contact with the microbes. Yamada et al. [38] studied the performance of such an enzyme filter. They used two filters: with and without enzymes, and found out that the performance of the enzyme filter did not differ much from that of a control filter, due to adhesion of particles over time on the filter surface, preventing close contact between the enzymes and any microbes retained by the filter.

3.3. Ultraviolet germicidal irradiation (UVGI)

UVGI light is emitted at wavelength of 253.7 nm by low-pressure mercury vapour arc lamps. UVGI damages the DNA/RNA of pathogens and makes them harmless: they cannot reproduce once they have entered their host. Laboratory research has shown that the germicidal effect of UVGI is primarily a function of two factors: the intensity of the UVGI energy and the duration of exposure [39–42]. These studies also found some influence of pathogen susceptibility, of the presence or absence of a cell wall and its thickness. Since smallpox, influenza and adenovirus lack a cell wall they are more easily inactivated [43], while spores, such as Bacillus anthracis, are the most difficult to inactivate due to their protective cover [44]. There are two ways to use UVGI application in practice: ceiling/wall mounted or in-duct application.

Disinfection of air by ceiling/wall mounted UVGI started in the 30 s in USA [45,46]. The inactivation process occurs when the pathogens enter the UVGI zone: 1.8 m above the floor (the height above which UVGI systems should be installed to avoid any health risks for occupants). The inactivation rate of UVGI in rooms could be enhanced by increasing the intensity of light, by promoting better mixing in rooms, or by generating an upward flow to facilitate the upward transport of pathogens [47–49]. Another important factor for UVGI efficiency is the level of relative humidity. Studies [50,51] show that with increased humidity in the environment the pathogens are more likely to survive the germicidal effect of the UVGI lamp. Xu et al. [51] evaluated the impact of room ventilation rates, UV effluence rates and distribution, airflow patterns, relative humidity, and photoreactivation on the effectiveness of UVGI systems. They suggested that in order to obtain maximum benefit from a ceiling/wall mounted UVGI system, an adequate level of UV radiation of at least 6 W of UV-C per m^3 in the upper zone should be provided. Moreover, the UV radiation should be evenly distributed and good room air mixing should be provided. Room relative humidity should be kept around 50%. Values above 75%

significantly reduce UVGI performance: the effectiveness is reduced by more than 40%. Photoreactivation, a process by which DNA damaged by UV light is repaired by an enzyme that requires light, is not likely to be an issue with any significance for full-scale operation. The amount of photoreactivation has been reported to increase at a high level of relative humidity (RH > 75%). However, there is a threshold dose of UV above which photoreactivation will not occur in airborne bacteria [52].

The adverse health effects of UVGI on humans include a mild form of reddening of the skin (erythema) and painful photokeratitis of the eyes (sensitization to light, as in snowblindness). UVGI lights are therefore mounted in deep louver enclosures to prevent overexposure at eye level or excessive reflection from ceilings, but such casings absorb a large amount of the useful UV energy, making the unit less efficient. Guidelines for upper-room UVGI application are available [53,54]. In buildings with ceilings lower than 2.4 m duct UVGI irradiation must be applied. The problems of direct eye contact or skin contact are not relevant here, so the systems could be operated at even higher intensities. Good mixing and the use of reflective surfaces is an economical way to increase the effectiveness of the in-duct UVGI systems [55,56]. Exposure duration is also important factor. Kujundzic et al. [57] reported that under the same other conditions culturability of the bacteria was reduced by up to 87% and culturability of fungi by 75% at an air stream velocity of 2.2 m/s. The higher velocity (5.1 m/s) rendered the UVGI system ineffective.

3.4. Photocatalytic oxidation

Photocatalysis is the acceleration of a photoreaction by the presence of a catalyst (TiO_2, WO_3, ZnS, etc.). In photogenerated catalysis the photocatalytic activity depends on the ability of the catalyst to create electron–hole pairs, which create free short-lived radicals able to undergo secondary reactions. Photocatalytic oxidation (PCO) could be achieved by either using fluorescent or UV light. PCO is an emerging technology in the HVAC industry, especially in purging airborne bacteria, which is performed by utilizing short-wave ultraviolet light (UVC). The results are somewhat encouraging, since some pathogens are readily destroyed after treatment with a TiO_2 coated PCO unit [58,59]. However only small portion of the pathogens will be absorbed on the catalyst and chemically attacked from a single pass system. Also with time there will be accumulation of "dead" pathogens on contact surface, which will reduce the effectiveness of the method as the UV light will be stopped from activating the catalyst layer. An enhancement of the germicidal effect can be achieved by doping a TiO_2 photocatalyst with Ag^+ ions [60]. On the other hand, a possible problem of the whole PCO approach is that some of the resulting short-lived radicals react to form secondary chemical species (aldehydes, ketones etc.) that reduce the indoor air quality and may reach high unacceptable levels from health point of view [61]. The process of pathogen inactivation by PCO is still under exploration and further research is required [59].

3.5. Desiccant rotor

A new approach to clean volatile organic compounds (VOCs) from indoor air is to apply a dehumidifier with a silica gel desiccant rotor. As reported in Ref. [62], measured levels of VOCs downstream of the rotor indicate efficiency of approximately 94% or higher. This method could be applied to purge airborne pathogens from indoor air, however, this needs to be investigated further.

3.6. Plasmacluster ions

A new technology, plasmacluster ions technology (PCI) that has recently reached the market claims to neutralize 26 kinds of harmful airborne substances. The ion generator uses an alternating plasma discharge (between two electrically charged plates: anode and cathode) to split the airborne molecules of water into positively charged hydrogen (H^+) and negatively charged oxygen (O_2^-). A chemical reaction occurs, and the collision of hydrogen with oxygen ions creates groups of highly reactive OH radicals that react with proteins/polysaccharides in the cell wall or surface structure of the pathogen, thus damaging it and rendering it incapable of causing infection [63]. The molecules of water formed as a result of this reaction are returned back into the air. It is possible that elevated levels of ozone (O_3) may be providing some of these benefits. PCI is a promising method for dealing with harmful airborne substances but it must be further investigated in terms of its effect on human health and on air quality.

3.7. Essential oils

Recent studies have shown that essential oils used in pharmaceutical, cosmetics and food and beverage industries have a strong germicidal effect and could be applied in the ventilation industry. Furthermore, the antimicrobial effect of essential oils' is greater in air than in solution [64–66]. Their application is still under intensive investigation. A hypersensitivity reaction of some occupants to certain essential oils (mint, thyme, oregano etc) and the fact that some of those oils also exhibit cytotoxic activity, i.e. being toxic to human cells as well as to microbial cells may limit the application of essential oils for air cleaning in occupied spaces [66].

3.8. Nanotechnology (silver nanoparticles)

A new method utilizing silver nanoparticles atomized in the air and used to control the viability of pathogens has been suggested [67]. The method was tested by injecting silver nanoparticles together with the aerosolized bacteria in a small glass chamber. Though highly effective (more than 99% of the tested bacteria lost culturability), this methodology still needs further investigations regarding its applicability indoors because of its possible negative effects on health.

4. Protection by ventilation

The current awareness of new emerging diseases serves to emphasise the need to design indoor conditions that prevent cross-infection. A simple way to limit the spread of pathogens is by supplying clean outdoor air, reducing the harmful concentrations indoors. The review article of Li et al. [68] shows strong evidences demonstrating the association between ventilation and the control of airflow directions in buildings and the transmission and spread of infectious diseases. The authors conclude that there is insufficient data on the minimum ventilation requirement for ventilating public premises such as hospital infectious wards, schools, offices, etc. to minimize the spread of airborne infections.

Airflow patterns are of great importance indoors, because they determine the path of the droplet distribution generated from the occupants' respiratory activities. Depending on the airflow pattern, the ventilation process of supplying fresh air indoors may decrease the risk of airborne cross-infection, or it may increase the spread of diseases in occupied volumes. The following discussion, on the importance of airflow distribution in rooms for the airborne transmission of diseases, is limited to mechanically ventilated rooms.

4.1. Total volume air distribution

Two main principles of room air distribution are commonly used in practice: mixing and displacement ventilation. Mixing

ventilation aims to create a homogeneous environment in the occupied zone. The clean air is supplied at high velocity to promote mixing with the room air and thus with the pathogens generated by a sick occupant. In rooms with mixing air distribution the level of exposure to infected air exhaled from another person is independent of the location of the person [69].

Displacement ventilation introduces the clean air at a slightly lower temperature (3–6 °C lower than room temperature), through floor or wall mounted diffusers. The cold air, supplied at relatively low velocity, spreads over the floor and moves upwards, entrained by flows generated from heat sources (people, equipment etc.), and then it is exhausted close to the ceiling from the better-mixed upper region of the ventilated space. Under these conditions airborne cross-infection between occupants (who are not too close to each other) will be low since the warm exhaled air which may carry viruses will rise upward to the ceiling. The problem arises in a dynamic environment, i.e. when people move and cough and the boundary layer around their bodies is disturbed. The airflow pattern is much dependent on local disturbances because air velocity is quite low (except near the floor and in thermal plumes generated by people, office equipment etc.). For example, in a room with a standard height of 2.6 m and an air change rate of unity approximate calculation gives an average upward velocity of $0.7 \times 10–3$ m/s, i.e. the height of the room per hour. A walking person (with speed of 1 m/s) in room with displacement ventilation may cause air mixing close to that of mixing ventilation [70]. Mundt [71] studied particle resuspension at 2 and 4 air changes per hour (ACH) in a room with displacement ventilation. She used talcum powder as a "carpet" in front of the air supply, on which a person walked either normally or vigorously. Data for only three particle size ranges (greater than 0.5 μm, 5 μm and 10 μm) were presented although the particle counter used had four ranges, recording also particles greater than 0.25 μm (one reason might have been that the number of particles smaller than 0.5 μm was low). The size distribution of the talcum powder particles used was not specified. The results in all cases indicated elevated levels of particles in the room and within the convection flow of the heated cylinders used to simulate occupants. It may be concluded that when a person walks in a room with displacement ventilation the dispersion of resuspended particles (with diameter from 0.5 μm to 25 μm) resembles that of mixing ventilation. Settled particles on the floor are resuspended in air and brought by the convection flow into the breathing zone of the occupants. This is valid for those particles for which the settling velocity is smaller than the velocity of the free convection flow. The settling velocities (Stoke's Law) reported by Mundt [71] for talcum powder particles with a density of 2700 kg/m^3 and diameter 0.5 μm, 5 μm and 10 μm was respectively 2×10^{-5} m/s, 2×10^{-3} m/s and 8×10^{-3} m/s. With the density of 1746 kg/m^3 for talcum broken, these velocities will be respectively 1.3×10^{-5} m/s, 1.3×10^{-3} m/s and 5.1×10^{-3} m/s. The diameters of resuspended particles of respiratory origin calculated for these settling velocities and the dry density of nonvolatile species in saliva (Na^+, K^+, Cl^-, lactate and glycoprotein) of 88 kg/m^3 (suggested by Nicas et al. [9]) corresponds respectively to 2.2 μm, 22 μm and 45 μm. The latter two diameters are outside the penetration range for the human lungs (only particles with a diameter less than 10 μm can penetrate the lungs) and are easily resuspended by human activities indoors. Therefore particles of respiratory origin, resuspended from the floor, could increase the risk of infection if they carry viable pathogens.

Denés et al. [72] showed that with mixing ventilation the inlet and outlet positions influence particle deposition, and have an accumulative effect with that of increased airflow velocity. Wan and Chao [73] compared four different types of supply-exhaust positions in regard to dispersion of droplet aerosols indoors: ceiling (supply and exhaust located in the ceiling), floor-return (both supply and exhaust placed in the floor), upward (supply in floor, exhaust in ceiling) and downward (supply in ceiling, exhaust in floor). It was found that the downward system performed best in controlling the transmission of infection by exhaled droplets by achieving the best dilution and reducing lateral dispersion indoors. However, no heat sources were present in the room. The convection flow above heat sources would definitely influence the airflow interaction in the room and the dispersal of droplets indoors.

A comparison of the performance of three ventilation supply systems (mixing, displacement and downward air distribution) was carried out in a hospital environment, to determine which was most capable of protecting patients and health care workers from cross-infection due to the inhalation of droplet nuclei [8]. The downward ventilation performed like the mixing ventilation, due to the counter flow from the free convection around the human body. So although it is recommended for clean rooms, infectious wards and operating theaters, downward air distribution may not always protect people from cross-infection. Displacement ventilation performed worse when patient was lieing face sideways, because the exhalation jet persisted over a very long distance, assisted by the thermal stratification.

Underfloor ventilation has been shown to provide air quality similar to that achieved by displacement ventilation when supplied air was discharged vertically upwards and not horizontally [74]. The inhaled air quality was found to deteriorate when increasing the throw of the supply jet from the floor diffuser. The supply jet promotes mixing close to the floor, which can promote resuspension of particles (including particles carrying pathogens of respiratory origin) from the floor into the air and up into the breathing zone.

Dilution could solve to some extend the problem of controlling the level of pathogens in rooms with total volume ventilation but the limiting factor here would be local thermal discomfort: both mixing and displacement ventilation can cause draught problems. Another issue could be the low cost effectiveness of this approach, due to increased energy use and increased initial costs (bigger ducts, more powerful fans, over-sizing of the HVAC unit etc.). In densely occupied spaces, like theaters, aircraft or vehicle cabins, etc., dilution does help but the risk of transmission of diseases by contact and by droplet transmission, remains high due to proximity of people.

To avoid some of the associated problems of increased dilution, UVGI technology could be used instead. Mounted at the ceiling level, a UVGI unit with louvers would work quite well with mixing ventilation. The enhanced air mixing would transport any pathogens more rapidly to the upper part of the room, where they would be inactivated, but this approach would clearly be less effective when applied to displacement ventilation. Once they had been transported by the warm convection flow around humans, the pathogens would be exhausted close to the ceiling. This would be the case when the gravity forces acting on the droplets are small compared to the velocity of the free convection flow, or they would leave the jet and be deposited in the room. The appropriate UVGI technology here is in-duct installation, provided recirculation is available. This approach is therefore useful for large halls with displacement ventilation, where people spent most of the time seated: theaters, concert halls, offices, etc. [75,76]. Filtration could also be used to control the pathogen levels in such buildings. However filters are not efficient in protecting occupants if pathogens are generated inside the occupied space. In duct installation they are effective at removing the microorganisms or toxins present in the outside air. Sometimes filters themselves can become a source of bacterial growth and thus contribute to high pathogen levels in the respirable range: less than 1.1 μm, especially at elevated humidity, higher than 80% RH [77]. As mentioned above, PCO may generate by-products which can reduce perceived indoor

air quality or in themselves are hazardous. Economy is another important point for consideration: filters need to be regularly changed, as does the catalytic coating of the PCO unit and both types of unit add additional flow resistance to the HVAC system, resulting in a requirement for more powerful fans. In rooms with mixing ventilation an alternative solution can be the usage of chilled-beams or convectors, recirculating part of the room air through a heat exchanger and a local HEPA filter or a UVGI unit.

4.2. Advanced air distribution methods

There is a need for new air distribution systems that reduce to a minimum the airborne route of pathogens in occupied volumes and protect occupants from cross-infection to be developed. One possible solution is personalized ventilation (PV) that provides clean air to the breathing zone of each occupant, and thus improves perceived air quality. Improved thermal comfort, by providing individual control of velocity, temperature and direction of the personalized flow to each occupant, is another benefit of PV. PV may thus increase occupants' satisfaction, decrease SBS symptoms, and increase work performance [78]. When properly applied, PV has greater potential than total volume air distribution to protect occupants from airborne pathogens. Research in this area started only recently but there is already evidence that PV in conjunction with mixing ventilation can protect occupants from airborne pathogens and is superior to mixing air distribution alone [79]. Cermak and Melikov [79] applied the model for prediction of the risk of airborne transmission of diseases suggested by Rudnick and Milton [80] to compare the performance of mixing ventilation, underfloor ventilation and personalized ventilation in conjunction with background mixing ventilation. An air terminal device installed on a movable arm and supplying clean air to the face from in front was used. The comparison was based on the reproductive number calculated for influenza in case of a quantum generation rate of 100 quanta per hour. The reproductive number represents the number of secondary infections that arise when a single infectious case is introduced into a population where everyone is susceptible. The calculation was made when one of 30 persons occupying the same room for eight hours was infected. The results are shown in Fig. 1 and indicate that in the case of mixing ventilation and a supply rate of 10 l/s per person, it is likely that 7 out of 30 occupants will contract influenza in the course of one working day. The number of possibly infected persons decreases to just two (one already infected and one secondarily infected) if either the ventilation rate is increased to 40 l/s per person or an underfloor system (UFAD) with a short throw is employed. The use of PV is shown to reduce the risk of any cross-infection to a very low level.

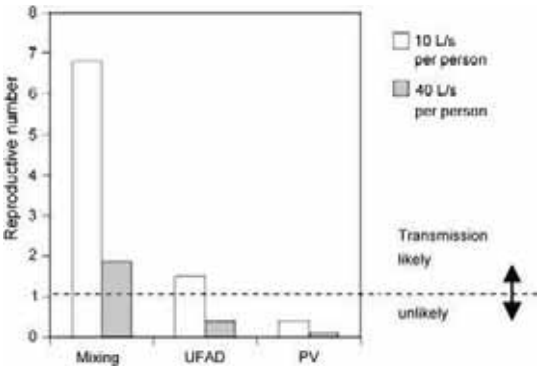

Fig. 1. Reproductive number for influenza, for different ventilation systems and outdoor air supply rates. The normalized concentration was 1, 0.2, and 0.05 in the cases shown from left to right [77].

Apart from protecting occupants, PV may also facilitate the transport of exhaled pathogens, in the case where the host individual uses PV while the other occupants do not use any PV for protection. In rooms with displacement ventilation, PV promotes mixing of the exhaled air with room air [81,84]. This is also true for rooms with underfloor ventilation [79,82–84]. There is therefore a risk of transmission of airborne infections to occupants who are not protected by high efficiency PV, e.g. occupants who are not at their work places. PV has been reported to improve the perceived air quality as well as to protect the user from cross-infection when applied with downward ventilation in rooms with textile air terminals [85].

Most existing PV designs are for desk mounted air supply devices. Bolashikov et al. [86] reported on an air terminal device (named Round Movable Arm, RMP) for installation on a desk, providing nearly 100% clean air for inhalation. A solution that incorporates the PV air supply diffusers into the headrest of the user's chair has recently been proposed [87]. In this case, over 90% of the inhaled air was clean air at PV flow rates above 8 l/s per person. The performance of this system was found to be dependent on the position of the head relative to the diffusers, the angle of the diffusers themselves, the clothing insulation of the occupant, the thermal insulation of the seat and the ambient air temperature. Niu et al. [88] studied a ventilated seat with an adjustable personalized air supply nozzle. Eight different nozzles were studied in terms of their effectiveness in reducing exposure to pollutants and personalized air utilization efficiency (the proportion of actual personalized air in inhaled air to the total supplied personalized air). The best nozzle managed to achieve 80% of clean PV air in the air inhaled. Human subject tests were also performed. People found the air quality better, but at high flow rates (1.6 l/s) they felt draught. Nielsen et al. [89] proposed a low velocity personalized ventilation system (LVPV) discharging supply air at very low velocities (laminar flow) and relying on the entrainment of this clean PV air from the natural convection flow around the human body. Their designs were for a person seated in a chair and included a neck support pillow and a complete seat cover (placed on the seat and backrest of the chair, with the whole surface being the air outlet) and a seat cover which was partially open in areas along the two sides of the seat. The effectiveness of the pillow reached 94% of clean air in the air inhaled and 80% for the seat cover, in both cases for flow rates above 14 l/s.

Among other factors, the performance PV systems installed in desks and chairs depends on their users' activity, body posture and movement. Such designs protect occupants from airborne transmission of infectious agents only when the user is seated at the desk. This narrows their usefulness. Bolashikov et al. [86] used a headset to supply clean air just in front of the mouth and the nose, in order to overcome the disadvantages described above. They achieved up to 80% clean air in inhalation. The close proximity of the Headset supply orifice to the breathing zone makes it applicable in places where there is high occupation density and hence an elevated risk of airborne infection (theaters, cinemas, airplanes etc.).

Low velocity personalized ventilation, based on a ventilated pillow and a ventilated blanket for application in the hospital environment as a way of limiting cross-infection, was studied and reported by Nielsen et al. [90]. The performance of these devices was studied in regard to the patient and not the health care workers or visitors. The efficiency of both devices was found to be dependent on the position of the patient: lying on one side or on the back. The highest efficiency was achieved for a patient lying on his side: almost 95% of the inhaled air was clean PV air. When lying on the back less clean air was able to reach the breathing zone of the

patient. This was due to the low supply velocities: the entrainment rate of the clean PV air by the natural convection flow was low and it was pushed aside before reaching the nose/mouth.

The positive feature of the advanced air distribution methods discussed above is their feasibility and the relatively small flow rates used, as well as their close proximity to the occupant. A HEPA filter or UVGI unit can be included in PV systems that use room air to ensure that each occupant receives air that is clean and free from pathogens. This would further improve the efficiency of the PV system. However field studies are required to evaluate the magnitude of this improvement.

5. Concluding remarks

The concern of airborne transmission of respiratory diseases and the associated risks of epidemics or pandemics increases. The successful solution of the problem requires multidisciplinary research involving epidemiologists, hygienists, engineers and experts in other fields. The knowledge on generation of pathogen laden droplets due to respiratory activities, survivability of the pathogens, their dispersal indoors and their transfer to a healthy person is incomplete. There is need for development of new and efficient technologies for disinfection of air in spaces. Present methods for air distribution indoors are inefficient with regard to decreasing the risk of airborne transmission of diseases. Advanced methods for air distribution indoors are needed for protecting people from cross-infection.

Acknowledgement

The authors would like to thank Dr. David Wyon for his comments and help in editing the manuscript of this article.

References

[1] WHO. Bulletin of the World Health Organization. 2002;80(3):261.
[2] Shah NS, Wright A, Bai G-H, Barrera L, Boulahbal F, Martin-Casabona N, et al. Worldwide emergence of extensively drug-resistant tuberculosis. Emerging Infectious Diseases 2007;13(3):380–7.
[3] WHO. The 40th session of the subcommittee on planning and programming of the executive committee. World Health Organization; 2006.
[4] Morawska L. Droplet fate in indoor environments, or can we prevent the spread of infection? Proceedings Indoor Air 2005:9–23.
[5] Lidwell OM. Aerial dispersal of micro-organisms from the human respiratory tract. Society for Applied Bacteriology Symposium Series 1974;3(0):135–54.
[6] Fiegel J, Clarke R, Edwards DA. Airborne infectious disease and the suppression of pulmonary bioaerosols. Elsevier; 2006, vol. 11(1/2). p. 51–7.
[7] Tellier R. Review of aerosol transmission of influenza a virus. Emerging Infectious Diseases 2006;12(11):1657–62.
[8] Qian H, Li Y, Nielsen PV, Hyldgaard CE, Wong TW, Chwang ATY. Dispersion of exhaled droplet nuclei in a two-bed hospital ward with three different ventilation systems. Indoor Air 2006;16:111–28.
[9] Nicas M, Nazaroff WW, Hubbard A. Toward understanding the risk of secondary airborne infection: emission of respirable pathogens. Journal of Occupational and Environmental Hygiene 2005;2:143–54.
[10] Loudon RG, Roberts RM. Droplet expulsion from the respiratory tract. American Review of Respiratory Disease 1967;95:435–42.
[11] Hinds WC. Aerosol technology. Properties, behaviour, and measurement of airborne particles. 11 respiratory deposition. 2nd ed. John Willey & Sons, Inc; 1999. p. 233–57.
[12] Yang S, Lee GWM, Chen C-M, Wu C-C, Yu K-P. The size and concentration of droplets generated by Coughingin human subjects. Journal of Aerosol Medicine 2007;20(4):484–94.
[13] Xie X, Li Y. How far respiratory droplets move in indoor environments? Proceedings Healthy Buildings 2006:309–14.
[14] Barker J, Stevens D, Bloomfield SF. Spread and prevention of some common viral infections in community facilities and domestic homes. Journal of Applied and Microbiology 2001;91:7–21.
[15] Rusin P, Orosz-Coughlin P, Gerba C. Reduction of faecal coliform, coliform and heterotrophic plate count bacteria in the household kitchen and bathroom by disinfection with hypochlorite cleaners. Journal of Applied Microbiology 1998;85(5):819–28.
[16] Greenwood D, Slack RCB, Peutherer JF. Medical microbiology. 6th ed. Churchill Livingstone; 2002.
[17] Hatch MT, Wolochow H. Bacterial survival: consequences of airborne state. An introduction to experimental aerobiology. New York: John Wiley and Sons; 1969. p. 267–95.
[18] Assar SK, Block SS. Survival of microorganisms in the environment. In: Disinfection, sterilization, and preservation. Lippinkott-Williams; 2000.
[19] Loosli CG, Lemon HM, Robertson OH, Appel E. Experimental airborne influenza infection: I. influence of humidity on survival of virus in air. Proceedings of the Society for Experimental Biology and Medicine 1943;53:205–6.
[20] Lowen AC, Mubareka S, Steel J, Palese P. Influenza virus transmission is dependent on relative humidity and temperature. PLoS Pathogens 2007;3(10):1470–6. e151.
[21] Elazhary MA, Derbyshire JB. Effect of temperature, relative humidity and medium on the aerosol stability of infectious bovine rhinotracheitis virus. Canadian Journal of Comparative Medicine 1979;43(2):158–67.
[22] Harper GJ. Airborne microorganisms: survival tests with four viruses. Journal of Hygiene; Cambridge 1961;59:479–86.
[23] Miller WS, Artenstein MS. Aerosol stability of three acute respiratory disease viruses. Proceedings of the Society for Experimental Biology and Medicine 1967;125:222–7.
[24] de Jong JG, Winkler KC. Survival of measles virus in air. Nature 1964;201:1054–5.
[25] Hemmes JH, Winkler KC, Kool SM. Virus survival as a seasonal factor in influenza and poliomyelitis. Nature 1960;188:430–8.
[26] Ijaz MK, Brunner AH, Sattar SA, Nair RC, Johnson-Lussenburg CM. Survival characteristics of airborne human coronavirus 229E. The Journal of General Virology 1985;66(Pt 12):2743–8.
[27] Karim YG, Ijaz MK, Sattar SA, Johnson-Lussenburg CM. Effect of relative humidity on the airborne survival of rhinovirus-14. Canadian Journal of Microbiology 1985;31(11):1058–61.
[28] Mayhew CJ, Zimmerman WD, Hahon N. Assessment of aerosol stability of yellow fever virus by fluorescent-cell counting. Applied Microbiology 1968;16(2):263–6.
[29] Ehrlich R, Miller S. Effect of relative humidity and temperature on airborne Venezuelan equine encephalitis virus. Journal of Applied Microbiology 1971;22:194–200.
[30] McGeady ML, Siak JS, Crowell RL. Survival of coxsackievirus B3 under diverse environmental conditions. Applied and Environmental Microbiology 1979;37(5):972–7.
[31] Chen SC, Chang CF, Liao CM. Predictive models of control strategies involved in containing indoor airborne infections. Indoor Air 2006;16:469–81.
[32] LaForce FM. Airborne infections and modern building technology. In: Proceedings of the 3rd international conference on indoor air quality and climate. Stockholm, Sweden; 1984. p. 109–27.
[33] Kowalski WJ, Bahnfleth WP. Immune-building technology and bioterrorism defense. HPAC Engineering January 2003:57–62.
[34] ANSI/ASHRAE Standard 52.2-1999. Method of testing general ventilation air cleaning devices for removal efficiency by particle size.
[35] ISO 14644-1. Clean rooms and associated controlled environment – part 1: classification of air cleanliness. 1st ed.; 1999.
[36] Kowalski WJ, Bahnfleth WP. Airborne respiratory diseases and mechanical systems for control of microbes. HPAC Engineering July 1998:34–48.
[37] Kowalski WJ, Bahnfleth WP. Airborne-microbe filtration in indoor environments. The critical aspects of filter sizing and a methodology for predicting a filter's effectiveness against allergens, bacteria, and viruses. HPAC Engineering January 2002:57–69.
[38] Yamada K, Yanagi U, Kagi N, Ikeda K. A study about microbes on the surface of air filter in an air conditioning system. Proceedings of Healthy Buildings 2006:443–6.
[39] Luckiesh M. Applications of germicidal, erythemal and infrared energy. New York: D. Van Nostrand Company; 1946.
[40] Riley R, Knight M, Middlebrook G. Ultraviolet susceptibility of BCG and virulent tubercle bacilli. The American Review of Respiratory Disease 1976;113:413–8.
[41] Chang JC, Osoff SF, Lobe DC, Dorfman MH, Dumais CM, Qualls RG, et al. UV inactivation of pathogenic and indicator microorganisms. Applied and Environmental Microbiology 1985;49:1361–5.
[42] Ko G, First MW, Burge HA. The characterization of upper-room ultraviolet germicidal irradiation in inactivating airborne microorganisms. Environmental Health Perspectives 2002;110:95–101.
[43] Jensen MM. Inactivation of airborne viruses by ultraviolet irradiation. Applied Microbiology 1964;12:418–20.
[44] Knudson GB. Photoreactivation of ultraviolet-irradiated, plasmid-bearing, and plasmid-free strains of *Bacillus anthracis*. Applied and Environmental Microbiology 1986;52:444–9.
[45] Wells WF. On air-born infection. Study II. Droplet and droplet nuclei. American Journal of Hygiene 1936;20:611–8.
[46] Wells WF. Airborne contagion and air hygiene. Cambridge (MA): Harvard University Press; 1955.
[47] Riley R, Permut S. Room air disinfection by ultraviolet irradiation of upper air. Air mixing and germicidal effectiveness. Archives of Environmental Health 1955;22:208–19.
[48] Riley RL, Permut S, Kaufman JE. Convection, air mixing, and ultraviolet air disinfection in rooms. Archives of Environmental Health 1971;22:200–7.
[49] Riley RL, Permut S, Kaufman JE. Room air disinfection by ultraviolet irradiation of upper air. Further analysis of convective air exchange. Archives of Environmental Health 1971;23:35–9.

[50] Peccia J, Werth HM, Miller S, Hernandez M. Effects of relative humidity on the ultraviolet induced inactivation of airborne bacteria. Aerosol Science and Technology 2001;35:728–40.
[51] Xu P, Kujundzic E, Peccia J, Millie PS, Moss G, Hernandez M, et al. Impact of environmental factors on efficacy of upper-room air ultraviolet germicidal irradiation for inactivating airborne mycobacteria. Environmental Science and Technology 2005;39(24):9656–64.
[52] Peccia J, Hernandez M. Photoreactivation in airborne *Mycobacterium parafortuitum*. Applied and Environmental Microbiology 2001;67(9):4225–32.
[53] First MW, Nardell EA, Chaisson WT, Riley RL. Guidelines for the application of upper-room ultraviolet germicidal irradiation for preventing transmission of airborne contagion – part I: basic principles. ASHRAE Transactions 1999;105:869–76.
[54] First MW, Nardell EA, Chaisson WT, Riley RL. Guidelines for the application of upper-room ultraviolet germicidal irradiation for preventing transmission of airborne contagion – part II: design and operational guidance. ASHRAE Transactions 1999;105:877–87.
[55] Kowalski WJ, Bahnfleth WP. Effective UVGI system design through improved modeling. ASHRAE Transactions 2000;106(2):4–13.
[56] Kowalski WJ, Bahnfleth WP. UVGI design basics for air and surface disinfection. IUVA News 2001;3(5):4–7.
[57] Kujundzic E, Hernandez M, Shelly LM. Ultraviolet germicidal irradiation inactivation of airborne fungal spores and bacteria in upper-room air and HVAC in-duct configurations. Journal of Environmental Engineering and Science 2007;6:1–9.
[58] Krishna V, Pumprueg S, Lee S-H, Zhao J, Sigmund W, Koopman B, et al. Photocatalytic disinfection with titanium dioxide coated multi-wall carbon nanotubes. Process Safety and Environmental Protection 2005;83(B4):393–7.
[59] Pal A, Pehkonen SO, Yu LE, Ray MB. Photocatalytic inactivation of gram-positive and gram-negative bacteria using fluorescent light. Journal of Photochemistry and Photobiology A Chemistry 2007;186:335–41.
[60] Vohra A, Goswami DY, Deshpande DA, Block SS. Enhanced photocatalytic disinfection of indoor air. Applied Catalysis B Environmental 2006;65:57–65. Elsevier.
[61] Sæbjörnsson KO, Fang L. Laboratory study on incomplete oxidation of a photocatalytic oxidation air purifier. Healthy Buildings 2006:271–6.
[62] Fang L, Zhang G, Wisthaler A. Experimental investigation of the air cleaning effect of a desiccant rotor on indoor air chemical pollutants. Healthy Buildings 2006:277–82.
[63] Electronics SHARP. Sharp's plasmacluster ions effectively deactivate H5N1 avian influenza virus. Asia Pacific Biotech News 2005;6(11):469.
[64] Hammer KA, Carson CF, Riley TV. Antimicrobial activity of essential oils and other plant extracts. Journal of Applied Microbiology 1999;86:985–90.
[65] Pibiri MC, Seignez C, Roulet CA. Methods to study the effect of essential oils on microbes present in ventilation systems. CISBAT 2003:185–90.
[66] Inouye S, Abe, Yamaguchi H, Asakura M. Comparative study of antimicrobial and cytotoxic effects of selected essential oils by gaseous and solution contacts. The International Journal of Aromatherapy 2003;13:33–41.
[67] Lee BU, Yoon K-Y, Bae G-N, Ji J-H, Hwang J. Airborne silver nanoparticles from an atomizer as an antimicrobial agent against *E. coli* Bioaerosols. Proceedings of Healthy Buildings 2006:345–8.
[68] Li Y, Leung GM, Tang J, Yang X, Chao C, Lin JZ, et al. Role of ventilation in airborne transmission of infectious agents in the built environment – a multidisciplinary systematic review. Indoor Air 2007;17(1):2–18.
[69] Jensen RL, Pedersen DN, Nielsen PV, Topp C. Personal exposure between people in a mixing ventilated room. Proceedings of IAQVEC 2001.
[70] Bjørn E, Mattsson M, Sandberg M, Nielsen V. Displacement ventilation – effects of movement and exhalation. Proceedings of Healthy Buildings 1997:163–8. Washington DC, USA.
[71] Mundt E. Non-buoyant pollutant sources and particles in displacement ventilation. Building and Environment 2001;36:829–36.
[72] Denés T, Abadie M, Limam K, Allard F. Experimental study of fine particle deposition in rooms. Proceedings: Healthy Buildings 2006:469–74.
[73] Wan MP, Chao CYH. Effect of changing the air distribution system on the dispersion of droplet phase aerosols in an enclosure. Proceedings: Indoor Air 2005:2696–700.
[74] Cermak R, Melikov AK. Air quality and thermal comfort in an office with underfloor, mixing and displacement ventilation. International Journal of Ventilation 2006;5(3):5.
[75] Buttolph JL. Ultraviolet air disinfection in the theater. Journal of the SMPE 1948;51:79–91.
[76] Menzies D, Popa J, Hanley JA, Rand T, Milton DK. Effect of ultraviolet germicidal lights installed in office ventilation systems on workers' health and wellbeing: double blind multiple crossover trial. The Lancet 2003;362:1785–91.
[77] Möritz M, Peter H, Nipko B, Rüden H. Capability of air filters to retain airborne bacteria and molds in heating, ventilating and air-conditioning (HVAC) systems. International Journal of Hygiene and Environmental Health 2001;203:401–9.
[78] Melikov AK. Personalized ventilation. Indoor Air 2004;14(Suppl. 7):157–67.
[79] Cermak R, Melikov AK. Protection of occupants from exhaled infectious agents and floor material emissions in rooms with personalized and underfloor ventilation. HVAC&R Research 2007;13(1):23–38.
[80] Rudnick SN, Milton DK. Risk of indoor airborne infection transmission estimated from carbon dioxide concentration. Proceedings Indoor Air 2003;13:237–45.
[81] Melikov AK, Cermak R, Kovar O, Forejt L. Impact of airflow interaction on inhaled air quality and transport of contaminants in rooms with personalized and total volume ventilation. Proceedings Healthy Building 2003;2:500–10 [Singapore].
[82] Cermak R, Melikov AK. Transmission of exhaled air between occupants in rooms with personalised and underfloor ventilation. Proceedings Roomvent 2004. Coimbra: DEM-FCT, Univ. Coimbra.
[83] Cermak R, Melikov AK. Performance of personalised ventilation in a room with an underfloor air distribution system. Proceedings Healthy Building 2003;2:486–91 [Singapore].
[84] Cermak R, Melikov AK, Forejt L, Kovar O. Distribution of contaminants in the occupied zone of a room with personalized and displacement ventilation. Proceedings Roomvent 2004. Coimbr: DEM-FCT, Univ. Coimbra.
[85] Nielsen PV, Hylgaard CE, Melikov AK. Personal exposure between people in a room ventilated by textile terminals – with and without personalized ventilation. HVAC&R Research 2007;13(4):635–43.
[86] Bolashikov ZD, Nikolaev L, Melikov AK, Kaczmarczyk J, Fanger PO. Personalized ventilation: air terminal devices with high efficiency. Proceedings of Healthy Building 2003;2:850–5 [Singapore].
[87] Melikov AK, Ivanova T, Stefanova G. Seat incorporated personalized ventilation. Proceedings Room Vent 2007:1318.
[88] Niu J, Gao N, Phoebe M, Huigang Z. Experimental study on chair-based personalized ventilation system. Building and Environmnet 2007;42:913–25.
[89] Nielsen PV, Bartholomaeussen NM, Jakubowska E, Jiang H, Jonsson OT, Krawiecka K, et al. Chair with integrated personalized ventilation for minimizing cross infection. Room Vent 2007:1078.
[90] Nielsen PV, Jiang H, Polak M. Bed with integrated personalized ventilation for minimizing of cross infection. Room Vent 2007:1077.

Appendix II

Paper II

Bolashikov, Z.D., Melikov A.K., Krenek, M.,

Improved Performance of Personalized Ventilation by Control of the Convection Flow around an Occupant's Body

ASHRAE Transactions 2009, Vol. 115, Part 2, pp 421-431, LO-09-038.

LO-09-038

Improved Performance of Personalized Ventilation by Control of the Convection Flow around Occupant Body

Zhecho D. Bolashikov **Arsen Melikov, PhD** *Fellow ASHRAE* **Miroslav Krenek**

ABSTRACT

This paper deals with methods for control of the free convection flow around the human body, the aim being to improve the quality of the inhaled air for occupants at workstations with personalized ventilation (PV). Two methods of control were developed and explored: passive - blocking the free convection development by modifications in desk design, and active - by local suction below the desk. The effectiveness of the two methods for enhancing the performance of PV was studied when applied separately and combined, and was compared with the reference case of PV alone. The experiments were performed in a full-scale test room with background mixing ventilation. A thermal manikin with realistic free convection flow was used. The PV supplied air from front/above towards the face. All measurements were performed under isothermal conditions at 20 °C (68 °F) and 26 °C (78.8 °F). The air in the test room was mixed with tracer gas, while personalized air was free of it. Tracer gas concentration measurements were used to identify the effect of controlling the free convection flow on inhaled air quality. The use of both methods improved the performance of PV and made it possible to provide more than 90% of clean air for inhalation at a substantially reduced PV supply flow rate.

INTRODUCTION

The aim of personalized ventilation (PV) is to supply clean air to the breathing zone of each room occupant. Together with total volume ventilation, PV can provide superior air quality and can greatly reduce the risk of cross-infection for occupants who spend a relatively long time at their workplace (Cermak and Melikov 2007). Individual control of the flow rate, temperature and direction of the supplied personalized air makes it possible to achieve a preferred microenvironment for each occupant. It has been documented that PV can significantly improve occupants' inhaled air quality and thermal comfort and can significantly decrease SBS symptoms (Kaczmarczyk et al. 2004, 2006).

The performance of PV with regard to occupants' thermal comfort and inhaled air quality depends on the interaction of the flows in the vicinity of the human body, in most cases the personalized airflow, the free convection flow around the human body, the airflow generated by the background total volume ventilation and the flow of exhaled air.

The personalized flow is typically a free jet issued from a circular or rectangular opening or a nozzle. The first region of the jet, known as the potential core region, contains a core with constant velocity, low turbulence intensity and supply air unmixed with the polluted room air. A non-uniform velocity field at the air supply and a high initial turbulence intensity that generates velocity fluctuations increase the mixing of the supplied clean air with the polluted surrounding room air and decrease the length of the potential core (Melikov 2004).

The free convection flow is generated by the difference between the room air temperature and the surface temperature of the human body. The greater the temperature difference, the stronger the free convection flow. The free convection flow develops from laminar, with low velocity at the lower legs, to turbulent, with relatively high velocity at the upper chest and the head region (Clark and Toy 1975). Body shape and posture, room air temperature, clothing insulation, etc. define the mean velocity in the free convection flow, which may be as high as 0.25 m/s (49.21 fpm) at the head region, and the thickness of the boundary layer, which may measure 0.2 m (0.66 ft) or more (Homma and Yakiyama 1988). This flow

Zhecho Bolashikov is a PhD student, **Arsen Melikov** is an associate professor, and **Miroslav Krenek** is a master's student in the Department of Civil Engineering, Technical University of Denmark, Denmark.

induces and transports air (as well as pollutants if present) from lower heights in the room to the breathing zone. Therefore the greater portion of the air that is inhaled by sedentary and standing persons in rooms is from the free convection flow (Brohus and Nielsen 1994).

The background airflow is influenced by the location and type of air supply devices, supply airflow rate and temperature, type and location of heat sources, etc. The flow of exhalation depends on the breathing mode (nose/mouth, mouth/nose, etc.), respiration flow rate (which depends on activity level, body weight), nose and mouth shape (different from person to person), body and head posture, etc.

The interaction of the background flow with the free convection flow is important for the heat loss from the human body. In order to avoid draught discomfort, present indoor climate standards (ISO 7730 2004, ASHRAE 55 2004) recommend low velocity (less than 0.2 m/s (39.37 fpm)) in the occupied zone at the low range of comfortable room air temperature (20 °C (68 °F) – 24 °C (75.2 °F)). Under these conditions, the strength of the free convection flow may be equal to or even stronger than the strength of the background flow. The thermal plume generated above the human body by the free convection flow affects the room air distribution (Homma and Yakiyama 1988, Zukowska et al. 2008). The interaction of the personalized flow with the flow of exhalation determines the spread of bioeffluents and exhaled air between room occupants (Cermak and Melikov 2007).

This study focuses on the performance of PV with regard to inhaled air quality. In this respect the interaction between the free convection flow and the personalized flow is of major importance. The interaction depends on many factors: strength of free convection flow and thickness of its boundary layer, velocity, turbulence intensity, direction and temperature of PV flow, body posture, shape and clothing design, etc. It has been documented that personalized flow directed against the face with a mean velocity higher than 0.3-0.35 m/s (59.06-68.89 fpm) is able to penetrate the free convection flow and provide 100% clean air. This however, may pose draught discomfort, especially at a relatively low room air temperature (Melikov 2004). The risk of draught will decrease when the velocity of the personalized flow decreases, i.e decrease of the personalized flow rate when the air supply terminal device is not changed. This strategy will require a decrease of the strength and the thickness of the free convection flow at the breathing zone to enable its penetration by the personalized flow and to supply clean air for inhalation. However, methods for control of the free convection flow have not yet been developed or studied.

Two methods, passive and active, for controlling the free convection flow at the breathing zone were developed. The effect of these methods on the interaction of the personalized flow with the free convection flow and the resulting improvement of inhaled air quality was studied. The results are presented and discussed in this paper.

METHOD

Full-Scale Test Room

The experiments were performed in a full-scale test room with dimensions 4.70 m × 1.62 m × 2.60 m (15.42 ft x 5.31 ft

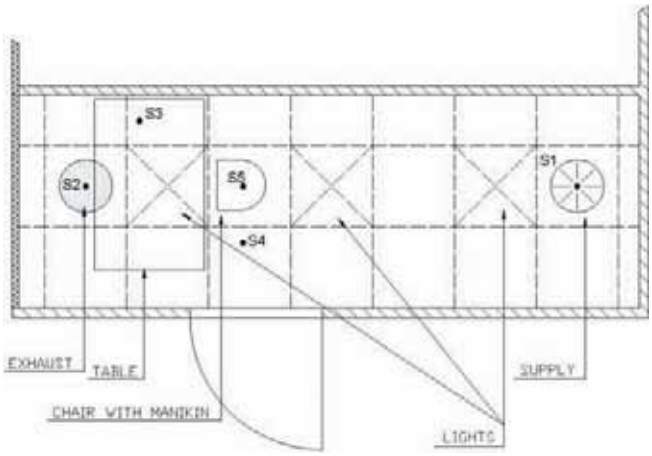

Figure 1 *Floor plan of the test room and positioning of the sampling points: S1—supply air, S2—exhaust air; S3—PV air for RMP; S4—room air; and S5—inhaled air.*

x 8.53 ft) (W×L×H). One workplace consisting of a desk with an air terminal device for PV, a chair and a seated thermal manikin was simulated in the room (Figure 1).

Three fixtures (6 W (20.47 Btu/h) each) located in the ceiling provided the background lighting. The room itself was built in a laboratory hall, 70 cm (2.3 ft) above the floor. The walls of the test room were made of particleboard and were insulated by 6 cm (0.2 ft) thick styrofoam. One of the walls was made from single layer glazing.

Total Volume Ventilation

Mixing type ventilation was used to condition the air in the test room. The air supply diffuser (a rotation diffuser) and the air exhaust diffuser (a perforated circular diffuser) were installed on the ceiling as shown in Figure 1. Supply air temperature and flow rate as well as exhaust flow rate were controlled during the measurements. Air humidity was not controlled but was measured as being relatively constant (30% - 35%). The supplied air was clean (no recirculation was used). The supply flow rate was 12 L/s (25.42 cfm), which corresponded to an air change rate of 2.2 h-1. This flow rate provided good mixing in the room with relatively low velocity.

Personalized Ventilation

The air terminal device of the personalized ventilation, named Round Movable Panel (RMP), was installed on the desk in front of the manikin. The RMP consisted of an arm, which was a lamp-like support enveloped in a flexible duct, and a hollow spherically shaped outlet (ø180 (ø7.1 in)) with a honeycomb straightener at the end. It is described in detail by Bolashikov et al. (2003).

A separate HVAC system was used to supply the personalized air. The temperature and flow rate of the personalized air were controlled. The temperature of the personalized air was maintained constant to the set value by an electrically heated wire, coiled around the supply duct of the personalized air and controlled via a temperature sensor placed in the PV air terminal device. The humidity of the supplied personalized air was not controlled or measured, but was assumed to be close to that in the room (isothermal conditions).

Control Devices

Two control methods, passive and active, were used to reduce the strength and the thickness of the free convection flow at the breathing zone. The passive control device did not require the use of energy, as opposed to the active control device. The two methods are referred to in the following as desk-based designs for control of the convection flow around the occupant's body.

Device for Passive Control

The device for passive control was made of plastic cardboard (10 mm (0.36 in) thick 630 x 360 mm (2.07 ft x 1.18 ft): length x width), placed in front of the manikin to block the gap between the abdomen and the front edge of the desk, and thus to prevent the warm air generated by the lower body (feet, legs, thighs) from moving upwards towards the breathing zone. Two designs were tested, one with a round front edge made to fit around the manikin's abdomen – "cut board" (Fig.2a) and one with a straight front edge – "straight board" (Fig.2b).

Device for Active Control

The device for active control aimed to reduce the convection flow arising from the lower part of the body and prevent it from merging with the flow originating from the lower chest of the manikin. This device consisted of a box with 6 direct current (DC) ordinary PC fans of 1.4 W (4.78 Btu/h) nominal electric power (in 2 rows of 3 fans each). This device, named "suction box" was installed below the desk with its front edge in line with the edge of the table (Figure 3). The front and the rear groups of

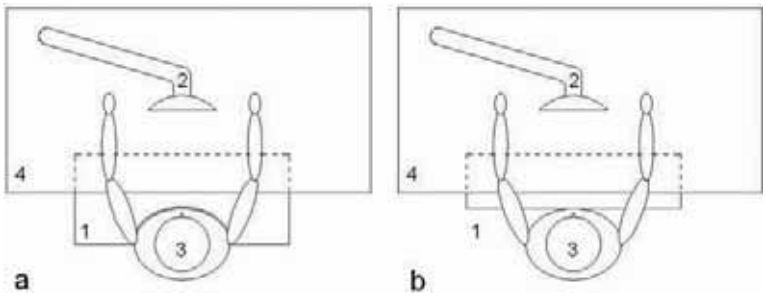

Figure 2 *Desk (4) with personalized ventilation (2) and passive control device (1) installed in front of thermal manikin (3): (a) passive control device with round shape—"cut board"; (b) passive control device with straight front edge—"straight board."*

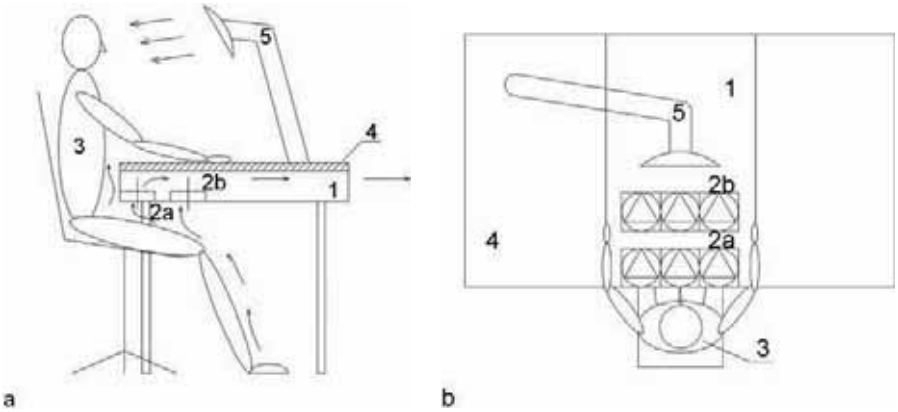

Figure 3 *Desk (4) with personalized ventilation (5), thermal manikin (3), and active control device—"suction box" (1) with front fans (2a) and rear fans (2b) installed below the table: (a) side view and (b) top view.*

fans could be operated separately. The air sucked from the fans was exhausted in the test room more than 1 m (3.28 ft) away from the manikin in order to avoid possible disturbances of the personalized flow and the free convection flow.

Thermal Manikin

A thermal manikin with a surface temperature controlled to be the same as the skin temperature of an average person in a state of thermal comfort was used to resemble an occupant. The manikin's body is shaped to resemble accurately the body of an average Scandinavian woman, 1.7 m (5.58 ft) in height. The manikin is made of a 3 mm (0.12 in) fiberglass coated polystyrene shell and is divided into 23 segments. Each of these segments is equipped with heating and temperature measuring wiring controlled by a computer program so as to maintain a surface temperature equal to the skin temperature of a person in a state of thermal comfort at the actual activity level, and thus realistically to recreate the free convection flow surrounding the human body. The control of the manikin is described by Tanabe et al. (1994).

Experimental Conditions

Experiments were performed under isothermal conditions, i.e. room air temperature equal to the personalized air temperature. The measurements were performed at two air temperatures, 20 °C (68 °F) and 26 °C (78.8 °F), i.e. the lowest and the highest comfortable room air temperature specified in the present thermal comfort standards (ISO 7730 2004, ASHRAE Standard 55 2004).

The manikin, seated on an office chair, was positioned with its abdomen at a distance of 0.1 m (0.33 ft) from the edge of the desk. During the measurements at 20 °C (68 °F) the manikin was dressed in underwear, long elastic trousers, long-sleeved elastic pullover, light socks, leather shoes and light long-sleeved woollen sweater (1.2 clo). At 26 °C (78.8 °F) it was dressed in underwear, shorts, t-shirt, light socks and trainers (0.5 clo). The manikin was wearing a short hair wig just below the ear level.

Most of the experiments were performed at three flow rates of personalized air (4, 6, 8 L/s) (8.47, 12.7, 16.94 cfm). The voltage to the fans in the suction box was controlled to either 15V or 30V by a DC voltage alternator (the flow rate of the exhaust air was not measured). When either of the 2 groups of fans was running (rear or front), the other one was blocked.

In all tested conditions, the RMP was positioned to supply personalized airflow towards the middle of the face of the manikin (the symmetry axis of the outlet was pointing between mouth and nose). The distance between outlet and breathing zone was kept at 40 cm (1.31 ft).

Tracer gas, Freon R134a, was used to simulate pollution in the room air. During the measurements a constant dose of tracer gas was supplied in the duct of the background ventilation system before the ceiling diffuser. After passing the plenum box and the rotation diffuser, the tracer gas was well mixed in the air supplied to the room. The personalized air was free of tracer gas.

The tracer gas sampling and its concentration measurement was performed at 5 points by a real-time gas monitor based on the photo-acoustic principle of measurement. The positioning of the 5 sampling points is indicated in Figure 1. Point S4 was used to assess whether or not good mixing was achieved in the room and was positioned at a height of 1.1 m above the floor. A tube attached at the upper lip of the manikin at a distance of 0.005 m (0.24 in) from the face was used to

sample air for measuring the tracer gas concentration in inhaled air (Figure 1, S5) as recommended by Melikov and Kaczmarczyk (2007).

Prior to the experiment air velocities around the manikin (20 cm (0.66 ft) away) at a height of 0.6 m (1.97 ft) were measured for 3 min with a low velocity thermal anemometer with omnidirectional velocity sensor. All measured velocities were below 0.2 m/s (39.37 fpm). Velocity measurements were performed at several locations and at different heights in the full-scale test room in order to verify the existence of velocities lower than 0.2 m/s (39.37 fpm). The characteristics of the anemometer complied with the requirements specified in the standards (ISO Standard 7726 1998, ASHRAE Standard 113 2005). The accuracy of the velocity (in fact speed) measurement was 0.02 m/s (39.37 fpm) ±1% of the reading in the range between 0.05 and 1 m/s (9,84 and 196.85 fpm).

The personalized airflow rate was measured by a flow sensor based on pressure difference. The pressure was monitored by a differential pressure manometer with an accuracy of 0.01 Pa (4×10^{-5} in of H_2O) ± 0.25% of reading. The flow sensor was installed in the duct of the PV system. The required flow rate was adjusted by a manually operated damper and from the pressure difference readings taken from the manometer.

Criteria for Assessment

The inhaled air quality was assessed by the Personal Exposure Effectiveness index (PEE) introduced by Melikov et al. (2002). The PEE represents the portion of clean personalized air in the air inhaled by an occupant. PEE is equal to 1 (or 100%) when only clean personalized air is inhaled, i.e. best performance of the personalized ventilation; PEE equal to 0 (or 0%) means that the inhaled air is polluted room air. Its value is calculated as:

$$\varepsilon_P = \frac{C_{I,0} - C_I}{C_{I,0} - C_{PV}} \times 100$$

where:

ε_p = personal exposure effectiveness

$C_{I,0}$ = pollution concentration in inhaled air if no PV is used

C_{PV} = pollution concentration in the personalized ventilation air

C_I = pollution concentration in inhaled air when PV is used.

Procedure

The air temperature in the experimental room and the laboratory hall were set up 24 hours prior to the measurements in order to achieve steady-state conditions. The air temperature in the laboratory hall was equal to the temperature in the test room, i.e. either 20 °C (68 °F) or 26 °C (78.8 °F). At the start of the experiments the thermal manikin was switched on, the personalized air temperature and flow rate were adjusted and the dosing of tracer gas started. The measurements were initiated after steady-state conditions were achieved, i.e. constant Freon concentration monitored at the sampling point S4 (Figure 1) and constant heat flux from the manikin.

For each experimental condition, tracer gas concentrations were measured 10 times in all 5 points. The heat flux and the surface temperature for each body segment and the average surface temperature for the whole body of the manikin were recorded for 5 minutes but they are not reported in this paper.

The measurements were performed in this order: 26 °C (78.8 °F), 20 °C (68 °F). The experiments performed at each of the two temperatures (different flow rate, free convection flow control method, etc.) were completely randomised to avoid biasing.

RESULTS

Figure 4 (a and b) shows the PEE obtained with the RMP when the boards with different shapes for passive control of the free convection flow were used. The PEE obtained with the RMP only, i.e. without the blocking effect of the boards, is shown in the figures as well. The PEE obtained with and without board increases with the increase of the flow rate. Comparison of the results obtained at 20 °C (68 °F) and 26 °C (78.8 °F) and at all flow rates studied shows that substantially higher PEE was obtained with the boards than with RMP alone, i.e. the performance of the PV improved when the boards were used. Both at 20 °C (68 °F) and 26 °C (78.8 °F) the maximum increase of the PEE with the board was obtained at 6 L/s (12.7 cfm). At a personalized flow rate of 4 L/s (8.47 cfm) the greater increase was obtained at 26 °C (78.8 °F). The improvement with the boards can be seen at 8 L/s (16.94 cfm) as well (PEE>94%) though the PEE obtained with the RMP alone was also high (88% at 20 °C (68 °F) and 80% at 26 °C (78.8 °F). The impact of the room air temperature on the strength of the free convection flow can be seen from the results in the figures obtained at 4 L/s (8.47 cfm) and 6 L/s (12.7 cfm). The increase of the room temperature to 26 °C (78.8 °F) decreased the strength of the free convection and made its penetration by the personalized flow easier. The differences in the PEE obtained with the two boards at the same personalized flow rate and air temperature were small and could be due to differences in positioning of the boards.

Figure 5 (a and b) shows the results for PEE when the RMP was used together with the suction box with either front fans or rear fans in operation. The PEE obtained with the RMP only, i.e. with the fans off is shown in the figures as well. The results look quite similar to the results obtained with the board. The PEE obtained with and without fans in operation increases with the increase of the flow rate. The comparison of the results obtained at 20 °C (68 °F) and 26 °C (78.8 °F) and at all flow rates studied shows substantially higher PEE obtained with the fans in operation than with RMP alone, i.e. the performance of the PV improved when the suction box was used. Both at 20 °C (68 °F) and 26 °C (78.8 °F) the maximum increase of the PEE is obtained at 6 L/s (12.7 cfm). The effect of the suction box on the PEE is much greater at 20 °C (68 °F) than at 26 °C (78.8 °F). This result is in contrast to what was

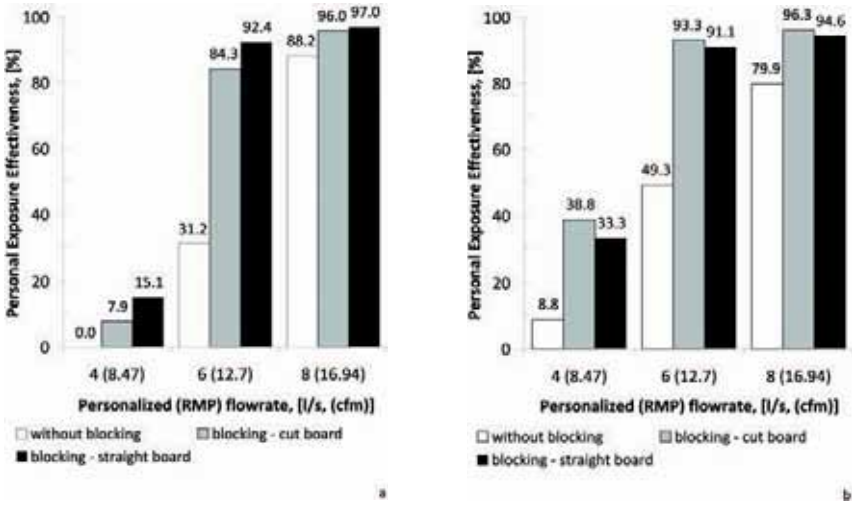

Figure 4 *The effect of the board on PEE of RMP: (a) at 20°C (68°F) and (b) at 26°C (78.8°F).*

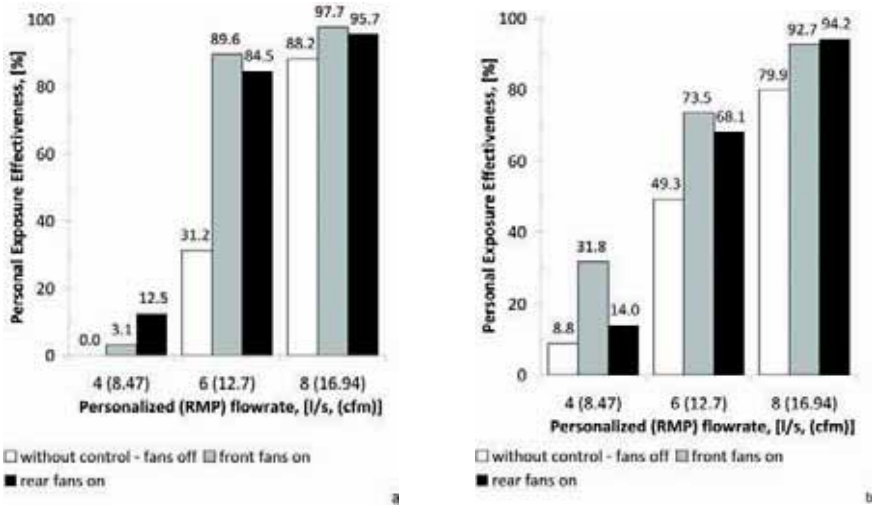

Figure 5 *The effect of the fans on PEE of RMP:(a) at 20°C (68°F) and (b) at 26°C (78.8°F).*

expected and could be due to positioning of the board and the disturbances of the free convection flow due to the suction. This however needs to be further studied. At a personalized flow rate of 4 L/s (8.47 cfm) the greater increase in the PEE was obtained at 26 °C (78.8 °F). An increase of the PEE with the suction box in comparison with the PEE obtained with the RMP alone can be seen at 8 L/s (16.94 cfm) as well (PEE>93%). At this relatively high flow rate the personalized flow was strong enough to penetrate the free convection flow even without use of the suction box (PEE>80%). The impact of the room air temperature on the strength of the free convection flow can be seen from the results obtained at 4 L/s (8.47 cfm) and 6 L/s (12.7 cfm). The increase of the room temperature to 26 °C (78.8 °F) decreased the strength of the free convection and made its penetration by the personalized flow easier, resulting in higher values of the PEE. The effect on the PEE of using only the front fans or only the rear fans was relatively small, though for most of the cases studied better results were achieved with the front fans operating, probably because those were closer to the torso and the thighs where the convection flow was stronger (formed by joining of the flow emerging from the legs and that originating from the groin).

The results obtained with the straight shape board and the cut shape board combined with the suction box with fans are shown in Figure 6 and Figure 7 respectively. At 8 L/s (16.94 cfm) the PEE reached quite high values (above 90%). In almost all cases, the simultaneous use of the fans and the boards did not improve the PEE in comparison with the use of the boards alone. For some of the measurements the use of fans and board at the same time led even to a decrease of the PEE. The reason for these results remains to be studied. The comparison of the results in Figures 6 (a and b) and 7 (a and b) show that for many of the conditions tested the combination of the boards with the front fans in operation performed slightly better than the combination of the boards with the rear fans.

Because of the similarity of the results for the two types of boards used, and also for the two fan arrangements, only one of each was chosen for further comparison. The PEE obtained with the straight shaped board is compared in Figure 8 (a and b) with the results obtained with the front fans in operation. The results obtained with the RMP alone are shown in the figures as well. At 20 °C (68 °F) and 4 L/s (8.47 cfm) and at 26 °C (78.8 °F) and 6 L/s (12.7 cfm) the results are slightly better for the board, but in the other cases studied, the difference in the PEE obtained

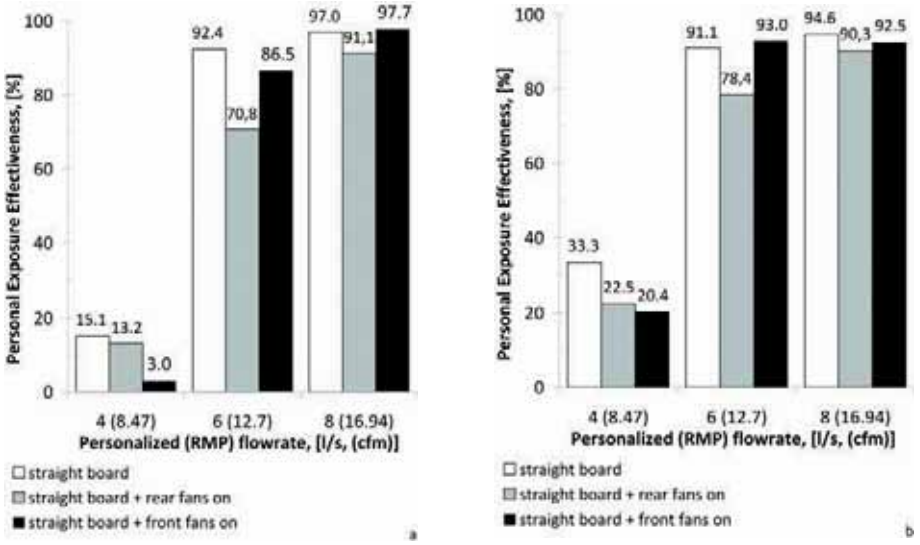

Figure 6 *The effect of use of the suction box with fans together with the straight board on PEE obtained with the RMP: (a) at 20°C (68°F) and (b) at 26°C (78.8°F).*

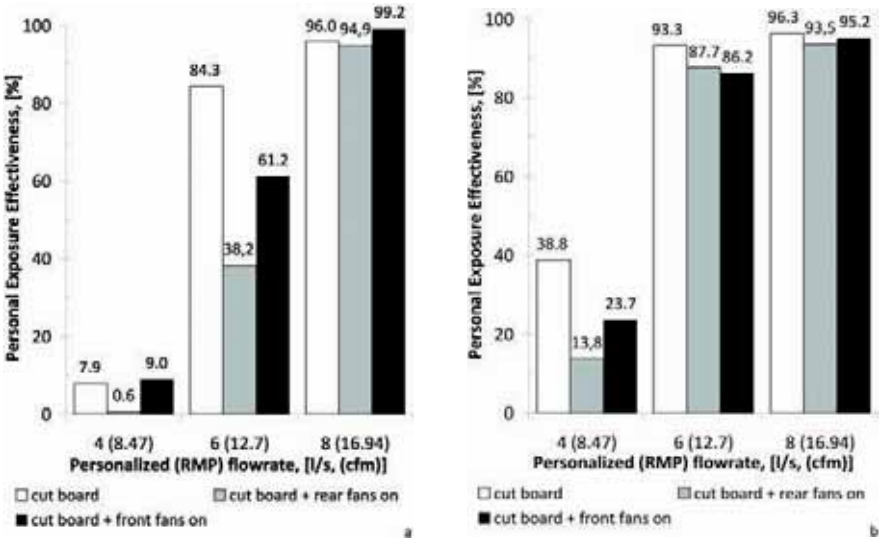

Figure 7 *The effect of use of the suction box with the fans together with the cut board on PEE obtained with the RMP: (a) at 20°C (68°F) and (b) at 26°C (78.8°F).*

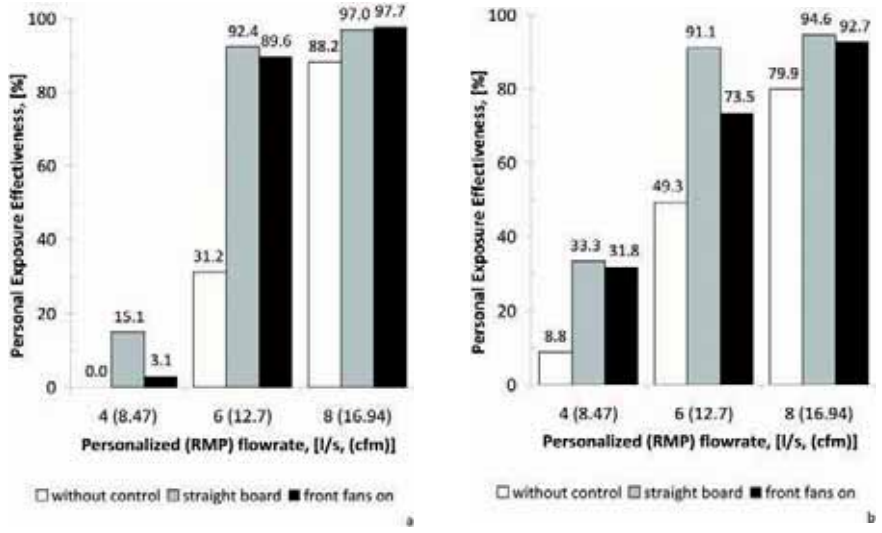

Figure 8 *Comparison of effect of board and fans: (a) at 20°C (68°F) and (b) at 26°C (78.8°F).*

with the board and the fans is hardly noticeable. Generally, the board shows better results than the fans.

The results discussed so far were obtained when the fans were running at half power (15 V). An experiment with the rear fans operating at full power (30 V) at a personalized flow rate of 8 L/s (16.94 cfm) and an air temperature of 26 ^{o}C (78.8 ^{o}F) was also performed. Figure 9 compares the results for the PEE obtained with fans operating at 15 V and 30 V in otherwise identical conditions. The PEE was substantially greater when the fans were operated at half power (15 V) than at full power (30 V). One reason for this result could be that when the fans were operate at full speed, they created quite a strong local suction effect that drew the RMP jet downwards and away from the mouth. The increased suction may enhance the mixing of the personalized air with the room air. A detailed study of the airflow interaction as well as smoke visualization is needed in order to reveal the reason behind the results obtained.

DISCUSSION

It has been shown that poor indoor air quality causes SBS (Sick Building Syndrome) symptoms such as increased prevalence of headache, decreased ability to think clearly, etc., and affects occupant's performance (Wargocki et al. 2002). An increase of the ventilation flow rate up to 25 L/s (52.95 cfm), i.e. substantially above that recommended in present practice, namely 7-10 L/s (14.83-21.18 cfm) per person, has been shown to reduce complaints of SBS symptoms, to improve productivity and to decrease short-term sick leave. However, this strategy is inefficient because it will increase the energy use and the risk of unacceptably high velocities in the occupied zone of rooms. Mixing and displacement room air distribution applied today for providing clean air to occupants in spaces are inefficient because the clean air supplied far from the occupants is more or less polluted and warm by the time it is inhaled. Advanced methods for air distribution need to be developed and applied in practice.

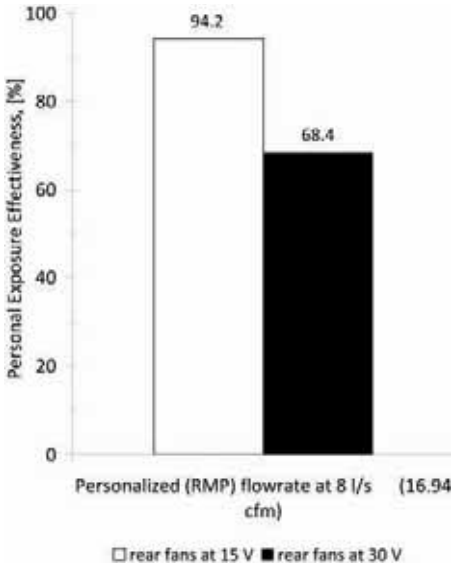

Figure 9 *PEE obtained at 26°C (78.8°F) room air temperature with the RMP when the rear fans in the suction box operate at half (15 V) and full power (30 V), respectively.*

The potential of personalized ventilation for improvement of inhaled air quality and thus improvement of occupants' health comfort and performance has already been discussed in this paper. The importance of airflow interaction in the vicinity of the human body and the need for its control for the optimal performance of PV has been defined. The results of the present study reveal that it is possible by simple methods to control the free convection flow and thus to control the airflow interaction at the breathing zone, resulting in a substantial increase of the inhaled air quality at a decreased flow rate of the personalized air. The control methods studied allow for a decrease in the strength of the convection flow and for its penetration by a personalized flow at lower velocity, thus decreasing the risk of local discomfort due to draught for sensitive people. In the present study, the personalized air was supplied from an air terminal device (RMP) positioned in front of/above the manikin's face. Previous studies with the RMP (Bolashikov et al. 2003, Melikov 2004) have reported more than 90% clean air in inhaled air with this air distribution device at a supply flow rate of 10 L/s (21.18 cfm). The methods for control of the free convection flow applied in the present study made it possible to increase the portion of personalized air in inhaled air to more than 90-95% at a much lower supply flow rate of 6 L/s (12.7 cfm). The maximum PEE obtained in the present study when the RMP was used alone at 6 L/s (12.7 cfm) was less than 50%. Similar low performance with the RMP at 7 L/s (14.83 cfm) has been reported previously (Cermak et al. 2006).

The importance of the airflow interaction at the breathing zone for the inhaled air quality has been reported and discussed before (Melikov et al. 2003, Melikov 2004). It has been shown that a personalized flow of clean air supplied to the breathing zone from the front, i.e. transverse to the upward free convection flow of polluted air, has potential to provide 100% of clean air for inhalation when its strength is sufficient to penetrate the convection flow. A personalized flow of clean air supplied upwards, i.e. assisting the free convection flow, will mix with the convection flow and will dilute the pollution it carries but its potential to provide 100% clean air for inhalation is limited. Melikov et al. (2002) reported that personalized flow supplied from the edge of the desk in front of a seated

thermal manikin and assisting the free convection flow is not able to provide more than 60% clean air for inhalation, even if the supplied flow rate is increased to 20 L/s (42.36 cfm). The results of the present study reveal that control of the free convection flow is an effective strategy for improving the inhaled air quality at a low flow rate of personalized air. The active control method by suction of the free convection flow bellow the desk should be used with caution because it may have a negative impact on the development of the boundary layer in front of the body and its interaction with personalized air, and may result in a decrease of the inhaled air quality.

The energy penalties associated with applying the active method for free convection flow control for improved performance of PV depend on many factors, including the PV system design, the method of coupling of the PV system with the total volume system, the type of total volume system, occupants' activities, etc. Results available from previous experiments performed with different types of fans and the PV air supply device employed in the present study (RMP) were used to demonstrate in a simple way the potential of the active method for control of the free convection flow for energy saving. The use of the three front fans for active control make it possible to achieve PEE in the range 73-89% at a 6 L/s (12.7 cfm) personalized flow rate. At this flow rate, the PEE achieved with the RMP alone was almost twice as low, in the range 31-49%. Previous studies with the RMP used alone (Bolashikov et al. 2003) have identified that a PEE above 80% can be obtained when the supplied flow rate is above 9-10 L/s (19.06-21.18 cfm) (depending on room air and personalized air temperature). A pressure drop of around 10 Pa (0.04 in. of H_2O) has been measured with the RMP at 10 L/s (21.18 cfm). Provided that the PV system has its own fan to transport the air (as recently suggested in the literature (Halvonová B. and Melikov A.K. 2008) 16 W (54.61 Btu/h) of electric power was required to move air at 10 L/s (21.18 cfm) (the fan power depends on the type of fan; the example discussed here is based on previous experiments performed with available fans). The three small fans used in the present study to control actively the free convection flow were computer fans of 1.4 W (4.78 Btu/h) nominal electric power each, giving in total 4.2 W (14.33 Btu/h) of energy consumption. Therefore, applying the active method as a way of control over the convection flow would make it possible to decrease the personalized flow from the RMP from 10 (21.18 cfm) to 6 L/s (12.7 cfm) (without decreasing the inhaled air quality). At this decreased flow rate the pressure drop in the PV system will decrease to 3 Pa (0.012 in. of H_2O) and the air can be moved by a fan with a power consumption of 5 W (17.06 Btu/h). Thus 9.2 W (31.39 Btu/h) in total will be used to achieve the same inhaled air quality as the RMP used alone, i.e. almost twice the energy reduction. This is just an example to demonstrate that energy savings may be achieved with control of the free convection flow. Much more sophisticated analyses need to be made for accurate prediction of the energy saving.

Two methods of control of the free convection flow are presented and discussed in this paper, passive control when the development of the free convection flow in front of the human body is stopped (blocked) and active control when the development of the boundary layer of the convection flow is disturbed by local suction of air. The effectiveness of the two methods when used together was studied as well. Rather similar results were achieved with the two methods of control, i.e. the PEE obtained was similar. Although further study on the active method of control is needed, especially as regards, the importance of the flow rate of the suction flow on the development of the boundary layer, it may be suggested that the passive method of control, blocking the free convection flow in front of the human body, may be recommended for practical use. A board installed below the desk top panel and pressed gently against the occupant's abdomen with a simple spring mechanism can be applied. The board will follow the backward and forward body movement and thus will break the free convection flow and will improve the performance of PV providing air from the front at a low flow rate. The board can have a straight edge or be shaped to fit tighter to the abdomen, but the results of the present study reveal that the board design is not important for the performance of the control method.

The present research focused on improvement of the airflow interaction at the breathing zone by control of the free convection flow, aiming at better inhaled air quality. The inhaled air quality and thus occupants' health, comfort and performance could be improved by simply decreasing the amount of clean personalized air (and also the total ventilation flow rate). Control of the airflow interaction based on the methods described in this paper or on other innovative methods which may be developed in the future, should be considered as an option before increasing the ventilation flow rates above the present requirements as suggested recently in the HVAC literature.

CONCLUSION

Two methods, passive (blocking board) and active (suction fans), for control of the strength of the free convection flow in front of a seated human body, and thus for control of its interaction with a personalized flow from the front, proved to be able to enhance the performance of the PV with regard to inhaled air quality at a reduced flow rate of supplied personalized air. At 6 L/s (12.7 cfm) the portion of clean personalized air in the inhaled air was more than 90% and substantially higher than without control of the free convection flow (around 50%).

Almost no difference was found in the performance of the passive and active method when applied alone. Applying the two methods simultaneously did not show any improvement either; it even led to a slight decrease in the performance of the PV at 6 L/s (12.7 cfm).

The design of the board (straight or fitted around the abdomen) had no impact on the control of the free convection flow and thus on inhaled air quality.

The use of the front or rear fans for active control of the free convection flow showed rather a similar result, with slightly better performance when the front fans were used. The impact of the positioning of the fans and the suction flow rate needs to be studied further.

REFERENCES

ASHRAE. 2004. *ANSI/AHRAE Standard 55 – 2004*, Thermal *environmental conditions for human occupancy, American Society of Heating, Refrigerating and Air-Conditioning Engineers, Inc.*

ASHRAE. 2005. *ANSI/ASHRAE Standard 113-2005, Method of Testing for Room Air Diffusion. American Society of Heating, Refrigerating and Air Conditioning Engineers*, Atlanta, GA.

Bolashikov, Z., Nikolaev, L., Melikov, A.K., Kaczmarczyk, J. and Fanger, P.O., 2003, Personalized ventilation: air terminal devices with high efficiency, *Proceedings of Healthy Buildings 2003, Singapore*, 2, pp. 850-855.

Brohus, H. and Nielsen P., 1994, Personal exposure in a ventilated room with concentration gradients. In: *Proceedings of Healthy Buildings 1994,* Budapest, Volume 2, pp. 559-564.

Cermak, R., Melikov, A.K., Forejt, L. and Kovar, O., 2006, Performance of personalized ventilation in conjunction with mixing and displacement ventilation, *International Journal of Heating, Ventilation and Refrigeration Research*, vol.12, no.2, pp.295-311.

Cermak R., Melikov, A.K., 2007, Protection of occupants from exhaled infectious agents and floor material emissions in rooms with personalized and underfloor ventilation, *HVAC&R Research*, 13(1), pp. 23-38.

Clark R.P and Toy N., 1975, Natural convection around the human head, *Journal of Physiology*, 244. pp. 283-293.

Halvonová B.and Melikov A.K., 2008, "Ductless" personalized ventilation in conjunction with displacement ventilation", Indoor Air 2008, 17-22 August 2008, Copenhagen, Denmark – Paper ID: 411.

Homma H. and Yakiyama M., 1988, Examination of free convection around occupant's body caused by its metabolic heat, *ASHRAE Transactions 1988*, 94 (1), pp. 104-124.

ISO. 1998. *International Standard ISO/DIS/7726: Ergonomics of the Thermal Environment - Instruments for Measuring Physical Quantities*: International Organization for Standardization, Geneva, Switzerland.

ISO. 2004. *International Standard ISO/DIS/7730: Moderate Thermal Environments-Determination of PMV and PPD Indices and Specification of the Conditions for Thermal Comfort*: International Standard Organization for Standardization, Geneva, Switzerland.

Kaczmarczyk J., Melikov A.K., Fanger, P.O., 2004, Human response to personalized and mixing ventilation, *Indoor Air* 14 (l8), pp. 1-13.

Kaczmarczyk, J., Melikov, A.K., Bolashikov, Z., Nikolaev, L. and P.O. Fanger, 2006, Human response to five designs of personalized ventilation, *International Journal of Heating*, *Ventilation and Refrigeration Research* 12 (2), pp.367-384.

Melikov, A.K., 2004, Personalized ventilation*, Indoor Air* 14 (7), pp. 157-167.

Melikov A.K., Cermak R., Majer M., 2002, Personalized ventilation: evaluation of different air terminal devices, *Energy and Buildings* 34, pp 829-836.

Melikov, A.K., Cermak, R., Kovar, O., Forejt, L., 2003, Impact of airflow interaction on inhaled air quality and transport of contaminants in rooms with personalized and total volume ventilation, *Proceedings of Healthy Buildings 2003, Singapore*, 7-1 National University of Singapore, Department of Building, vol. 2, pp. 592-597.

Melikov, A. and Kaczmarczyk, J., 2007, Indoor air quality assessment by a breathing thermal manikin, *Indoor Air* 17 (1), pp.50-59.

Tanabe, S., Zhang, H., Arens, E.A., Madsen, T.L., Bauman, F.S., 1994, Evaluating thermal environments by using a thermal manikin with controlled skin surface temperature, *ASHRAE Transactions 100 (1)*, pp 39-48.

Wargocki P., Sundel J., Bischof W., Brundrett G., Fanger P.O., Gyntelberg F., Hanssen S.O., Harrison P., Pickering A., Seppänen O., Wouters P., 2002, Ventilation and health in non-industrial indoor environments: report from a European Multidisciplinary Scientific Consensus Meeting (EUROVEN), *Indoor Air 12 (2002)*, pp 113-128.

Zukowska D., Melikov A., Popiolek Z., 2008, Impact of thermal plumes generated by occupant simulators with different complexity of body geometry on airflow pattern in rooms, *Proceedings of 7th International Thermal Manikin and Modelling Meeting – University of Coimbra, September 2008, Proceedings CD, Book of abstracts, pp 25-26.*

Appendix III

Paper III

Bolashikov, Z.D., Melikov A.K., Krenek, M.

Control of the Free Convective Flow around the Human Body for Enhanced Inhaled Air Quality: Application to a Seat-Incorporated Personalized Ventilation Unit

HVC&R Research 2010, (accepted)

Control of the Free Convective Flow around the Human Body for Enhanced Inhaled Air Quality: Application to a Seat-Incorporated Personalized Ventilation Unit

Zhecho D. Bolashikov **Arsen Melikov, Ph.D.** *Fellow ASHRAE* **Miroslav Krenek**

ABSTRACT

This paper reports on methods for control of the free convective flow around the human body, with the aim of improving inhaled air quality. The methods were studied with sea-incorporated personalized ventilation (PV): two PV nozzles placed sideways at the head level of a seated occupant supplied the clean air. Another pair of control nozzles below the PV nozzles, the height of the shoulders, either provided an additional amount of clean PV air or exhausted part of the air from the free convective flow. The effectiveness of the methods for enhancing the quality of the inhaled air was studied in full-scale room experiments. A thermal manikin with a realistic free convective flow was used to resemble an occupant in a state of thermal neutrality at sedentary activity level. Numerous experiments comprising different combinations of nozzle sizes, supply and exhaust flow rates, direction of the supplied PV flows and of the control flows, etc., were performed under isothermal conditions at 20°C (68F) and 26°C (78.8F). The methods of control proved to be efficient and made it possible to increase the amount of clean air into inhalation at reduced personalized flow rate and to reduce the risk of draught.

KEYWORDS: Human body, Free convective flow, Personalized flow, Airflow interaction, Control, Inhaled air quality

INTRODUCTION

Personalized ventilation (PV) supplies clean air close to the occupant and directly into the breathing zone, so as to improve the inhaled air quality and to reduce the risk of airborne cross-infection in comparison with total volume (TV) ventilation (Cermak and Melikov 2007). The unique features of PV are the possibility of individual control over the supply flow rate, the temperature, and the direction of the provided clean air.

Thus a microenvironment preferred by each occupant can be achieved. Human subject studies have shown that PV significantly improves the inhaled air quality and the thermal comfort and also significantly decreases SBS symptoms compared to TV ventilation (Kaczmarczyk et al. 2004, 2006).

The performance of PV as regards occupants' inhaled air quality and thermal comfort depends on the interaction of the airflows close to the human body: the personalized airflow, the free convective flow around the human body, the transient flow from exhalation and the airflow generated by the background TV ventilation.

The personalized flow is in most cases a free jet supplied from either a circular or rectangular opening. The first region of such a jet, known as the potential core region, is characterized by constant velocity, low turbulence intensity and hence clean air with a relatively constant temperature, still unmixed with the polluted room air. Non-uniformity of the velocity profile at the air supply, elevated initial turbulence intensity and temperature or density difference between the supplied air and the surrounding air, would enhance the natural process of entrainment and mixing of the supplied clean air with the polluted ambient air and decrease the length of the potential core (Melikov 2004).

The free convective flow around the human body is generated by the difference existing between the room air temperature and the surface temperature of the body. The greater the temperature difference the stronger the free convective flow. The free convective flow originates as laminar, with low velocity at the feet level, and grows into a turbulent flow with relatively high velocity at the upper chest and head region (Clark and Toy 1975). Body shape and posture, room air temperature, clothing insulation, etc. define the mean velocities in the free convective flow that could be as high as 0.25 m/s (0.82 fps) at the head region, with a thickness of 0.2 m (0.66 ft)or even more (Homma and Yakiyama 1988, Melikov and Zhou, 1996, Ozcan et al. 2003, 2005). Most of the air inhaled by a sedentary or a standing (immobile) person in a room with low velocities (below 0.1 m/s (0.33 fps)) originates from the free convective flow (Melikov 2004). This flow entrains and transports air from the room to the breathing zone, and thus brings parts of the polluted room air, as well as body generated bio-effluents into inhalation.

The flow of exhalation depends on the breathing mode (nose or mouth, which determines the initial velocity and direction of the expiration flow), respiration flow rate (which depends on the activity level, body weight, sex and individual differences), nose and mouth shape (different from person to person), body and head posture, etc.

The interaction of the personalized flow with the flow of exhalation determines the spread of bio-effluents and exhaled polluted air between room occupants (Cermak and Melikov 2007). The interaction of the background flow and/or of the personalized flow with the free convective flow is important for the heat loss from the human body (Melikov and Zhou, 1996). In order to avoid draught discomfort, present indoor climate standards (ISO 7730 2005, ASHRAE 55 2004) recommend low background air velocities (lower than 0.2 m/s) in the occupied zone at the low range of comfortable room air temperatures (20°C – 24°C) (68F – 75.2F). Under these conditions, the average velocity of the free convective flow may be equal or even slightly higher than that of the background flow. Therefore, the thermal plume generated above the human body by the free convective flow may affect the room air distribution to a great extent (Homma and Yakiyama 1988, Zukowska et al. 2008).

The interaction between the free convective flow and the personalized flow is of major importance for inhaled air quality. The interaction depends on many factors: the strength and the thickness of the free convective layer, the velocity field, the turbulence intensity, the temperature and the direction of the PV flow relative to the free convective flow, the body posture and shape, the clothing, etc. It has been documented that in the range of comfortable room air temperatures (20-26°C) (68F-78.8F) a personalized flow directed against the face with a mean velocity above 0.3 – 0.35 m/s (0.98 – 1.15 fps) is able to penetrate the free convective flow and result in 100% clean air in inhalation (Bolashikov et al. 2003). This, however, may cause draught discomfort, especially within the lower room air temperature range of 20-24^{o}C, 68F – 75.2F. The risk of draught will diminish when the temperature of the personalized flow increases (Kaczmarczyk et al. 2008) and/or when the target velocity of the personalized flow decreases. The latter strategy will require decrease of the strength and the thickness of the free convective flow at the breathing zone in order to make possible its penetration by the personalized flow. However, methods for control of the free convective flow have not yet been developed and studied.

Unique methods for control of the interaction between the free convective flow and the personalized flow aiming for improved inhaled air quality and decreased risk of draught have been proposed in this study. Four strategies were considered: 1) weakening of the free convective flow at the breathing zone by exhausting part of its air before it reaches the mouth and the nose, and thus making its penetration possible by the personalized flow at reduced flow rate (Figure 1B); 2) supplying a downward flow of polluted room air at the upper chest that will push away the free convective flow at the chest and make it possible for personalized

air to reach the mouth/nose at a reduced flow rate (Figure 1C); 3) supplying part of the clean personalized air in the free convective flow which will be weakened and diluted and then will move upwards towards the face, where it will interact with the rest of the personalized air; in this way it is expected to improve the performance of the personalized flow with regard to inhaled air quality and to reduce the risk from draught due to weakening of the personalized flow (Figure 1D); and 4) inserting the clean personalized air without mixing between the chest and the free convective flow at the upper chest/shoulder level and employing the natural upward motion of the free convective flow to bring the clean PV air into inhalation (Figure 1E). To study the above control methods, a seat-incorporated PV system was chosen. A seat with incorporated PV has already been reported as being efficient in providing a seated occupant with better inhaled air quality in comparison to TV ventilation (Jacobs et al. 2006, Melikov et al. 2007, Nielsen et al. 2007, Niu et al. 2007). The seat-incorporated PV supplies clean air from nozzles positioned at the head level (can be incorporated in the headrest). The personalized flow reaches the person's mouth/nose sideways and from the back. It interacts with the upward free convective flow by pushing it away from the face and spreads it along the cheeks (Figure 1a). The clean air will reach inhalation when the personalized flow is strong enough (i.e. has high enough momentum) to penetrate and peel away the free convective flow at the mouth/the nose. However, high velocities would elevate the risk of draught at the neck and face. Modification of the PV design and its use as shown in Figures 1b, 1c, 1d and 1e will allow for implementation of the control methods discussed above. The effectiveness of the control strategies was studied and the results obtained are reported and discussed in the present paper.

METHOD

Full-scale test room

All experiments were performed in a full-scale test room with dimensions 4.70 m × 1.62 m × 2.60 m, 15.42 ft x 5.32 ft x 8.53 ft, (W×L×H). Three ceiling-mounted light fixtures (6 W, 20.47 Btu/h each) provided the background lighting. A workplace consisting of a desk, an ordinary light office chair (≈ 0.05 Clo based on contact with the manikin), personalized ventilation and a seated thermal manikin was used in the set-up (Figure 2).

The total sensible heat load generated in the test room was 88 W, 300.23 Btu/h (12 W/m^2, 3.84 Btu/h.ft^2). The test room itself was built in a laboratory hall, 0.7 m 2.3 ft above the floor. The laboratory hall

had a separate ventilation system allowing for temperature control. The walls of the test room were made of particleboard and were isolated with 6 cm thick styrofoam plates. One of the walls was made from thick single-layer glazing.

Total volume ventilation

Mixing type of ventilation was used to condition the air in the test room. The air supply diffuser (a rotation diffuser) and the air exhaust vent (a perforated circular diffuser) were installed on the ceiling (Figure 1). The supplied air was 100% outdoor (no recirculation was used) with a flow rate of 12 L/s, 0.42 ft^3/s, which corresponded to an air change rate of 2.2 h^{-1}. This flow rate provided good mixing in the room with relatively low velocities (less than 0.15 m/s, 0.49 fps). The supply air temperature (19 or 25 ^oC, 66.2F or 77F) and flow rate, as well as the exhaust flow rate were controlled during all measurements. Air humidity was not controlled, but was measured to be relatively constant (30-35%).

Personalized ventilation

Two nozzles (PV nozzles) placed at the head level of a seated person (left and right side) supplied the clean PV air (Figure 3). Another pair of nozzles, referred to in the following as control nozzles, was placed just below the PV nozzles, at the height of the shoulders. The control nozzles either supplied air downwards over the upper chest, or sucked it inwards. Both the PV nozzles and the control nozzles were manufactured in two sizes: large and small. They are referred to as such throughout the present paper. The dimensions (supply opening area) of the four nozzles were as follows: 0.08 x 0.15 m (0.012 m^2), 0.26 x 0.49 ft (0.13 ft^2) for the large PV nozzle, 0.08 x 0.08 m (0.0064 m^2), 0.26 x 0.26 ft (0.069 ft^2) for the small PV nozzle, 0.06 x 0.15 m (0.009 m^2), 0.20 x 0.49 ft (0.097 ft^2) for the large control nozzles and 0.06 x 0.08 m (0.0048 m^2), 0.20 x 0.26 (0.052 ft^2) for small control nozzles. All four nozzles were made of steel. The PV nozzles were equipped with aluminium honeycomb grid for minimizing the initial turbulence intensity over the discharge area. The thickness of the used honeycomb was 10 mm, 0.4 in, with a cell width of 6 mm, 0.24 in, and a thickness of the cell walls of 10÷20 μm, $0.04x10^{-2}$÷$0.08x10^{-2}$ in, resulting in a free area ratio of the opening of about 99%. In the final downstream section of the PV nozzles and the control nozzles, a filter material was placed to improve the flow distribution across the outlet.

A separate HVAC system was used to supply the personalized air at a specific controlled temperature and flow rate. The temperature of the supplied PV air was controlled more precisely by an additional

electrically heated wire, coiled around a 1 m, 3.28 ft, section of the supply duct close to the test-room, with a temperature sensor placed in the PV terminal device. The humidity of the supplied personalized air was not controlled but was close to that in the room, i.e. 30 – 35 % RH. The PV pair of nozzles was connected to the PV system via a flexible plastic duct. A set of dampers was used to control the supply flow rate to each of the nozzles.

A flexible plastic duct was used to connect the control nozzles to a second air supply node of the HVAC system for personalized air in those cases when clean air was supplied over the upper chest surface (control strategies 3 and 4, respectively Figures 1d and 1e). In this case both the PV and the control nozzles were using the same clean PV air. For the first and the second control strategies aiming respectively to exhaust part of the convective flow and to destroy the free convective flow by the supply of opposing recirculated room airflow at high momentum (Figures 1b and 1c), the control nozzles were connected to an axial fan that was voltage-controlled. When control strategy 1 was applied the air was exhausted and discharged in the opposite end of the room to avoid influencing in any way the airflow interaction around the manikin. In the case of control strategy 2, room air was supplied through the control nozzles.

Thermal manikin

A thermal manikin with body shape and size of an average Scandinavian woman 1.7 m, 5.58 ft, in height, was used to resemble an occupant. The manikin is made of a 3 mm, 0.12 in, fibreglass-coated polystyrene shell and is divided into 23 segments. Each of these segments is equipped with heating and temperature measuring wiring controlled by a computer program so as to maintain a surface temperature equal to the skin temperature of a person in a state of thermal comfort at the actual activity level, and thus realistically recreate the free convective flow surrounding the human body .The control of the manikin is described by Tanabe et al. (1994).

Experimental conditions

The experiments were performed at two air temperatures, 20^{o}C, 68F and 26^{o}C, 78.8F (the lowest and the highest comfortable room air temperatures recommended in the present thermal comfort standards ISO 7730 2005, ASHRAE Standard 55 2004) and under isothermal conditions, i.e. room air temperature equal to the personalized air temperature. The manikin was positioned with its abdomen at a distance of 0.1 m, 0.33 ft, from the edge of the desk (Figure 3). During the measurements at 20^{o}C, 68F, the manikin was

dressed in underwear, long elastic trousers, long-sleeved elastic pullover, light socks, leather shoes and a light long-sleeved woollen sweater, all giving a clothing thermal insulation of 1.2 clo. At 26^{o}C, 78.8F, it was dressed in underwear, shorts, t-shirt, light socks and trainers (clothing thermal insulation of 0.5 clo). The manikin was wearing a short wig just below the ears during all experiments. The manikin was set to resemble an occupant in a state of thermal comfort at light sedentary activity, namely office work, with the corresponding dry heat loss of 1.2 Met, i.e. 69.8W, 238.02 Btu/h (ISO 7730 2005).

Figure 4 shows the positioning of the PV nozzles (distance and studied angles with relation to the head) and of the control nozzles (distance from the shoulders). The control nozzles when used alone or in conjunction with the headrest PV nozzles were always directed perpendicular to the plane defined by the chest and slightly tilted downward from horizontal to follow the natural inclination of the manikin's shoulders (Figure 4).The suction/discharge area was projecting over the shoulders so as to be within the convective flow.

The nozzles were not attached directly to the chair, but on a separate stand placed immediately behind the chair. In this way it was possible to adjust the nozzles along all the three axes of a Cartesian coordinate system. Rotation of the nozzles (PV and control nozzles) around vertical and horizontal axes was also possible. In all studied cases the PV nozzles were placed above the corresponding control nozzles.

The flow rates reported in this article are total for each pair of nozzles used, i.e. the flow rate from one nozzle is half the value given in the text. Prior to each experiment the supply/exhaust flow rate through the nozzles was adjusted to be identical. Most of the experiments were performed at three flow rates of personalized air (4, 6 and 8 L/s, 0.14, 0.21 and 0.28 ft^3/s). The controlled flow rate in strategy 1 ("suction") mode was 8.5 L/s, 0.30 ft^3/s, and 16 L/s, 0.57 ft^3/s; in the strategies 2 and 3 ("blowing") mode the supplied airflow rate was 3, 4.5, 6 and/or 8.5 L/s, 0.11, 0.16, 0.21 and/or 0.30 ft^3/s. The combination of parameters studied is listed in Table 1.

The strategy of clean personalized air supplied only from the control nozzles (control strategy 4) was studied at two room air temperatures and four flow rates as listed in Table 2. During these experiments the PV nozzles were disassembled from the stand to avoid disturbing the development of the free convective flow around the manikin.

Measurements with only the PV nozzles were performed in order to identify the effect of the personalized flow discharge angle (45^{o} and 90^{o}) on the efficiency of the clean air supply to inhalation. These measurements were performed only at 20^{o}C, 68F, and at 3 flow rates (Table 3).

Measured parameters and measuring equipment

Tracer gas, refrigerant R134a, was used to simulate pollution in the room air. During the measurements a constant dose of tracer gas was supplied in the duct of the background total volume ventilation system before the ceiling diffuser. After passing the plenum box and the rotation diffuser, the tracer gas was well mixed in the air supplied to the room. The personalized air was free of tracer gas.

The tracer gas sampling and its concentration measurement was done at 5 points by a real-time gas monitor based on the photo-acoustic principle of measurement. The positioning of the 5 sampling points is shown in Figure 2. Measurements at Point S4 (Figure 2), positioned at 1.1 m, 3.61 ft above the floor, were used to justify whether or not good mixing in the room was achieved: well mixed was considered the case when the room (S4) and exhaust (S2) readings for the concentration were approximately the same (within 5% difference). A plastic tube attached to the upper lip of the manikin, at a distance of 0.005 m, 0.016 ft, from the face, was used to sample air for measurement of tracer gas concentration in inhaled air (Figure 2, S5) as recommended by Melikov and Kaczmarczyk (2007).

Prior to the experiment, air velocities around the manikin (0.20 m, 0.66 ft, away) at 0.6 m, 1.97 ft, height were measured for 3 min with a low velocity thermal anemometer with an omnidirectional velocity sensor. The characteristics of the anemometer complied with the requirements specified in the standards (ISO Standard 7726, ASHRAE Standard 113 2005). The accuracy of the velocity measurement (in fact speed) was 0.02 m/s ±1% of the reading in the range between 0.05, 0.16 fps, and 1 m/s, 3.28 fps. All measured velocities were below 0.2 m/s, 0.66 fps.

The background total volume ventilation was controlled based on the differential pressure readings obtained from two flow orifices installed in the supply and exhaust ducts (ISO 5221 – 1984 (E)). The readings obtained by pressure transducers were transferred to a control system maintaining the set flow rate value. The supplied flow rate was always equal to the amount of air exhausted. In the case when the PV and/or the control nozzles were supplying extra amounts of outdoor air the exhausted air was increased by the same amount, without changing the total volume air supply.

The personalized airflow rate was measured by a flow sensor based on pressure difference. The pressure was monitored by a differential pressure micromanometer based on the pressure drop in the system with an accuracy of 0.01 Pa, 2.95×10^{-6} inHg ± 0.25% of reading. The flow sensor was installed in the duct of the PV system. The required flow rate was adjusted by a manually operated damper and from the pressure difference readings taken from the micromanometer.

The same type of flow sensor was used to measure and adjust the amount of air exhausted (control strategy 1) or supplied (control strategy 2, 3 and 4) through the two control nozzles.

Criteria for assessment

The inhaled air quality was assessed by the Personal Exposure Effectiveness index (PEE) introduced by Melikov et al. (2002). The PEE represents the portion of clean personalized air in the air inhaled by an occupant and is defined as $PEE = (C_{I,0}-C_I)/(C_{I,0}-C_{PV})$, where $C_{I,0}$ is the pollution concentration if no PV, C_I is the pollution concentration in inhaled air supplied by PV, and C_{PV} stands for pollution concentration in the personalized air supplied by the PV unit. PEE equals 1 (or 100%) when only clean personalized air is inhaled, i.e. best performance of the personalized ventilation. PEE equal to 0 (or 0%) means that the inhaled air is polluted room air.

Procedure

The air temperature in the test room and in the laboratory hall was set 24 hours prior to the measurements in order to achieve steady-state. The air temperature in the laboratory hall was kept equal to the temperature in the test room, i.e. either 20 ^{o}C, 68F, or 26 ^{o}C, 78.8F. At the start of the experiments the thermal manikin was switched on, the personalized air temperature and flow rate (of either the PV nozzles or the control nozzles) were adjusted and the dosing of tracer gas initiated. All measurements commenced after steady-state conditions were achieved, i.e. constant refrigerant concentration monitored at the sampling point S4 (Figure 2) and constant heat flux from the manikin.

For each experimental condition, tracer gas concentrations were measured 10 times at all 5 points and the heat flux, the surface temperature for each body segment, and the average surface temperature for the whole body of the manikin were recorded for 5 minutes.

The measurements were performed in this order: 26 °C (78.8F), 20 °C (68F). The experiments performed at each of the two temperatures (different flow rates, control methods, etc., Table 1, Table 2 and Table 3) were completely randomised to avoid biasing.

During all measurements the temperature conditions were kept constant while the nozzles (small and large) were changed. This might have caused some difference in positioning of the devices relative to the manikin at 20 °C (68F) and 26 °C 878.8), which increased the uncertainty of the measurements.

Uncertainty of measurements

Specially designed experiment was performed to account for the impact of positioning the manikin relative to a PV nozzle on the uncertainty in determination of the normalized PEE index. The same concentration measurement procedure was repeated 3 times in the following order: the manikin was positioned in front of the PV, then after 20 samples it was moved and repositioned again to the same location and new 20 samples were taken. Finally third measurement (n=20 samples) was repeated without changing anything in the set-up. The maximum differenced in the calculated PEE indexes due to the repositioning was calculated to be 2%.

The data were analysed in accordance with ISO guidelines for the expression of uncertainty (ISO 1993). The sample standard uncertainty was calculated as the maximum uncertainty of measurement (random error. The absolute expanded uncertainty with a level of confidence of 95% (coverage factor of 2) is listed in Table 4.

RESULTS

Based on performed pre-tests with the large PV nozzles, two airflow discharge angles, 45° and 90°, relative to the vertical plane bisecting the head and passing through the ears were chosen (Figure 4). At 90° the best inhaled air quality was expected as the clean air provided with the PV nozzles would glide parallel over the facial plane, pushing away the up-coming free convective flow. On the other hand, the 0° angle would yield the worst case for air quality, as the clean PV air would pass over the shoulders and by the face and hardly any of it would end into inhalation; therefore the angle of 45° was chosen. At this angle of PV airflow discharge, the two jets from the pair of nozzles would glide along the cheeks and meet within the breathing zone in front of the face, creating a “shield of clean air” from the surrounding polluted room air. The PEE obtained with the PV nozzles at 20°C, 68F, for the two discharge angles of 45° and 90° is shown in

Figure 5. As expected, at 6 L/s (0.21 ft^3/s) and 8 L/s (0.28 ft^3/s) much better results were achieved at 90^o than at 45^o (at 4 L/s (0.14 ft^3/s) the supplied airflow was not strong enough to penetrate the free convective flow). Despite this result, a 45^o discharge angle was chosen for further investigation because it was considered less disturbing for a seated person; a 90^o position of PV outlets would block the side view too much. The 90^o discharge angle could even prove disturbing for the eyes, especially at increased flow rates causing sensitisation (feeling of dryness). Furthermore, the performance of the PV with nozzles positioned at 90^o would be more sensitive to the movement of the occupant's head, especially forwards and backwards. Nevertheless, this option could be usable in certain applications such as public transportation or in the public services and entertainment sector (cinemas, theatres, auditoriums etc), where restricting the side view is of no concern and head movement is limited.

The PEE obtained with only the PV nozzles in operation at the two temperatures (20 (68) and 26 ^{o}C (78.8F)) and three flow rates with the large and the small pair of PV nozzles is compared in Figure 6. The PEE obtained with the large nozzles increased with the increase of the supply airflow rate (Figure 6a). At 6 L/s (0.21 ft^3/s) and 8 L/s (0.28 ft^3/s) higher PEE was achieved at 26^{o}C (78.8F) rather than at 20^{o}C (68F). This clearly showed the effect of the stronger free convective flow around the body at the lower room temperature as a result of the increased temperature difference between the body surface and the surrounding air. At 4 L/s (0.14 ft^3/s) the portion of clean personalized air in the air inhaled was quite low. It was higher at 20^{o}C (68F), compared to 26^{o}C (78.8F), which may have been caused by minor differences in positioning of the nozzles relative to the manikin's head (discussed above).

Figure 6b shows the results obtained with the small nozzles. At all flow rates, higher PEE was achieved at 26^{o}C (78.8) than at 20^{o}C (68F). The PEE was much higher at 6 L/s (0.21 ft^3/s) than at 4 L/s (0.14 ft^3/s); however, a slight decrease in AQ performance was seen at 8 L/s (0.28 ft^3/s) compared to 6 L/s (0.21 ft^3/s). This may be due to enhanced mixing and entrainment of polluted room air caused by the elevated supply velocities at 8 L/s (0.28 ft^3/s) (about 0.62 m/s, 2.03 fps, discharge velocity).

The results obtained when strategy 1 was applied are presented in Figure 7 (a and b). The PEE obtained at the two temperatures and the three PV supply flow rates when the large PV nozzles were combined with the corresponding large control nozzles under the "suction" mode, is compared in Figure 7a. It can be seen that in all cases the "suction" improved the performance of the PV system considerably compared to the reference case noted as "no suction", i.e. the reference case of only PV air supply. The only case where PEE

was over 90% was at 26°C (78.8), a PV flow rate of 8 L/s (0.28 ft^3/s) and a suction flow rate of 16 L/s (0.57 ft^3/s). At PV flow rate of 4 L/s (0.14 ft^3/s) and a suction of 16 L/s (0.21 ft^3/s), a maximum PEE of about 37% was achieved at 20°C (68F) which, though not as high as at 6 L/s (0.21 ft^3/s) or 8 L/s (0.28 ft^3/s), was still better compared to the case when no suction was provided (12%). A similar trend was noticed for the PEE when the same portion of the free convective air was exhausted by the control nozzles at 26°C (78.8F). For all conditions studied the results were better when suction was at 16 L/s (0.57 ft^3/s) than at 8.5 L/s (0.30 ft^3/s), except at the PV flow rate of 8 L/s (0.28 ft^3/s) and 20°C (68F) (possibly due to inaccurate positioning of the manikin in relation to the nozzles).

Figure 8 (a and b) shows the PEE obtained at the two temperatures and the three PV supply flow rates, when the small PV nozzles were combined with the corresponding small control nozzles under the "suction" mode (control strategy 1). The results reveal that exhausting part of the free convective air enhances its penetration by the personalized air. However, a substantial improvement was observed only at 20°C (68F) and at 4 L/s (0.14 ft^3/s). In this case the PEE improved substantially from 44.4% to 78% when 8.5 L/s (0.30 ft^3/s) were exhausted through the controlled nozzles and 86.2% when 16 L/s (0.57 ft^3/s) were exhausted. By increasing the personalized flow rate to 6 L/s (0.21 ft^3/s) and 8 L/s (0.28 ft^3/s), the improvement due to the use of the control nozzles became less pronounced. The effect of exhausting the free convective flow with the small control nozzles at 26°C (78.8F) was not consistent (Figure 8b). In fact at the PV flow rate of 6 L/s (0.21 ft^3/s) and 26°C (78.8F) the highest PEE was obtained when the control nozzles were turned off, i.e. when the control strategy was not applied. Due to the weak convective flow, the suction may have affected the discharge of the personalized flow. This result needs further investigation. In general, the results with the small nozzles reveal that control strategy 1 was not so efficient for improving inhaled air quality at a high room air temperature and nozzles with a small cross section area. The discharged personalized flow with relatively high velocity (the cross section of the smaller nozzles being almost half as big as the cross section of the large nozzles) was strong enough to penetrate the free convective flow, even without being weakened by the air suction at the shoulder level. Thus the effect of the suction flow of 8.5 L/s (0.30 ft^3/s) and 16 L/s (0.57 ft^3/s) on inhaled air quality improvement with the small nozzles could mainly be seen when the PV flow was weakest (at the lowest flow rate of 4 L/s (0.14 ft^3/s)) and the free convective flow was strongest (at room air temperature of 20 °C (68F)).

Control strategy 2 is aimed at peeling off the free convective flow and thus making it easier for the personalized air to reach the mouth/nose; in this case room air (mixed with tracer gas) was supplied from the control nozzles. Control strategy 3 is aimed at weakening and diluting the polluted free convective flow with a clean personalized airflow supplied from the control nozzles and opposing the upward free convective flow, i.e. supplying part of the PV air at chest level with the control nozzles and the rest from the PV nozzles at head level. In this way, the diluted free convective flow at chest level would add up to the clean air supplied by the PV nozzles and would improve the inhaled air quality. Control strategy 3 could also be advantageous in reducing the risk from draught as the total amount of clean air would be redistributed between the PV and the control nozzles, resulting in a personalized flow with low velocity. The results from pre-tests performed with the large nozzles at 20^{o}C (68F), 8 L/s (0.28 ft^{3}/s) PV flow rate and 8.5 L/s (0.30 ft^{3}/s) supplied from the control nozzles revealed much higher PEE values with control strategy 3, i.e. when clean air was supplied from the control nozzles, rather than with control strategy 2 as can be seen from the comparison in Figure 9. The use of control flow of room air to push down and peel off the free convective flow resulted in a decrease of the PEE from 56.4% without control flow to 47.4% with control flow. The control flow of polluted air supplied at shoulder level with relatively high velocity (0.47 m/s, 1.54 fps, at discharge opening) caused mixing and reduced the ability of the personalized flow with lower initial velocity (0.33 m/s, 1.08 fps) to provide clean air to inhalation. The supply of a controlled flow of clean air caused mixing but also dilution of the polluted free convective flow which resulted in a substantial increase in the PEE, from 56.4% without control flow to 79.7% with the control flow. Therefore it was decided that only control strategy 3 should be studied further. But the amount of clean conditioned air was quite high in this case: 16.5 L/s (0.58 ft^{3}/s) for both PV and control pair nozzles. Therefore in the following up set of experiments, lower flow rates from the control nozzles were selected to further investigate control strategy 3, namely 3 L/s (0.11 ft^{3}/s) and 4.5 L/s (0.16 ft^{3}/s), to reduce the total amount of clean air needed. However, control strategy 2 may prove to be effective as well, especially at lower supply flow rates. This needs to be further studied.

The PEE obtained with the large PV nozzles when clean air was supplied from the large control nozzles (control strategy 3) at 20^{o}C (68F) and 26^{o}C (78.8F) are shown in Figure 10. At 20 ^{o}C (68F), the improvement in the PEE compared to the reference case when clean air was supplied only from the PV nozzles was dramatic. At a PV flow rate of 4 L/s (0.14 ft^{3}/s) about 80% PEE was achieved and at 6 L/s (0.21 ft^{3}/s) PEE it exceeded 90%. In fact this was due to the additional amount of clean PV air supplied by the control nozzles.

As the results in Figure 10 show the relative improvement of the PEE due to the effect of control method 3 decreased with an increase of the supplied flow rate from the PV nozzles, 6 (0.21 ft^3/s) and 8 L/s (0.28 ft^3/s). At 26 ^oC (78.8F) the improvement due to the additionally supplied air from the control nozzles was much smaller (Figure 10b) than at 20^oC (68F). The greatest improvement of the PEE was from almost 0% with a PV flow rate of 4 L/s (0.14 ft^3/s) to 61% when an additional 4.5 L/s (0.16 ft^3/s) was supplied from the controlled nozzles. At the higher PV flow rates studied, the difference in the PEE with and without redistribution of the PV air decreased as the supply velocity of the personalized flow increased, and thus even without "deflecting" and diluting the convective flow with the control flow the PV flow was able to penetrate and reach the breathing zone of the occupant. At 26 ^oC (78.8F) the highest PEE achieved was about 71%. The results were slightly better when discharging 4.5 L/s (0.16 ft^3/s) than 3 L/s (0.11 ft^3/s) from the two control nozzles. The lower PEE at 26^oC (78.8F) compared to 20^oC (68F) might be due to improper positioning of the manikin relative to the control nozzles and the PV nozzles. The buoyancy effect, due to the temperature difference between the supplied PV air and the natural convective flow, was different when the PV air was supplied at 20 ^oC (68F) and 26 ^oC (78.8F) and this together with the different strength of the free convective flow at the two temperatures may have had an effect on the airflow interaction at the breathing zone.

The PEE obtained when control strategy 3 was applied with the small nozzles, i.e. when additional portions of clean air were supplied from the small control nozzles at 20^oC (68F) and 26^oC (78.8F) is shown in Figure 11 for the flow rate combinations studied. At 20^oC (68F) the clean air supplied from the control nozzles against the free convective flow had a positive effect in all flow rates studied (Figure 11a). The PEE increased in comparison with the case of PV air supply only, especially at the low PV flow rate of 4 L/s (0.14 ft^3/s). At 26^oC (78.8F) (Figure 11b) the positive effect was achieved only at the PV flow rate of 4 L/s (0.14 ft^3/s), where PEE increased from 56.2% without control flow to about 75% when the control flow was applied. At PV flow rates of 6 L/s and 8 L/s the PEE was high (above 82%) and no improvement was achieved when the control flow was supplied. In fact the slight decrease in PEE may be due to the enhanced mixing. In all cases studied (except at 20 ^oC (68F) and PV flow rate of 4 L/s (0.14 ft^3/s)) the change of the control flow rate from 3 L/s (0.11 ft^3/s) to 4.5 (0.16 ft^3/s) L/s had almost no impact on the PEE.

The fourth control strategy, namely to insert clean air within the free convective flow and close to the body surface which due to its strength will move it upwards to the breathing zone, required the least possible

mixing of the supplied clean air with the polluted free convective air. In this respect, the initial velocity of the supplied control flow is essential, especially when the free convective flow is weak. This is illustrated in the results shown in Figure 12. During these measurements, the PV flow was switched off. The PEE obtained was only the result of the interaction of the free convective flow with the inserted flow of clean air. Figure 12 shows PEE obtained at 26^{o}C (78.8F), i.e. when the free convective flow was relatively weak and the supplied clean air was warm and light. The results in the figure clearly demonstrate that when the supplied flow rate of the control clean air increases (3, 4.5 and 6 L/s, (0.11, 0.16 and 0.21 ft^3/s)) the portion of clean air in inhalation decreases from 36-44% to 16-18%, depending on the nozzle size. At 3, 4.5 and 6 L/s (0.11, 0.16 and 0.21 ft^3/s) the velocity of the supplied controlled flow was respectively 0.17, 0.25 and 0.33 m/s (0.56, 0.82 and 1.08 fps) for the large nozzles and 0.31, 0.47 and 0.62 m/s (1.02, 1.54 and 2.03 fps) for the small nozzles. The momentum of the inserted flow increased with the increase of the flow rate and enhanced its mixing with the free convective flow. The nozzle size and the shape of the manikin's body (the simulated female shape with large non-uniformity at the chest in comparison with the relatively flat chest of a male body) may play a role as well. The large nozzles covered a larger area of the chest region so the interaction with the convective flow was evenly distributed. With the small control nozzle there may be regions, such as between the breasts, where the interaction was weak and less mixing took place. This complex flow interaction needs to be further studied by more advanced techniques such as PIV and LDA.

DISCUSSION

The insufficiency of the clean outdoor air supply flow rates 4-10 L/s suggested in the present standards (EN 15251 2007, ASHRAE 62.1 2007) to provide building occupants with a healthy, comfortable and stimulating environment has been reported and the supply of clean outdoor air at substantially higher flow rates (up to 25 L/person (5.5 gal/person)) has been proposed (Wargocki et al 2002, Sundell and Levin 2002). However, such a dramatic increase of the supplied outdoor air with the total volume air distribution principles used at present is unrealistic; it will drastically raise the energy use, will increase the initial investments in buildings and HVAC systems (more space and larger ducting, larger air supply diffusers, larger and more powerful air-handling units, etc.) and will generate high velocity in the occupied zone that will increase the risk of thermal discomfort due to draught. Moreover, the present total volume air distribution systems are in most applications inefficient to provide all occupants with clean air and to reduce the risk from airborne transmission of infectious agents (Bolashikov and Melikov 2009). Instead of increasing the supplied outdoor

airflow rate, advanced and energy efficient air distribution methods, such as personalized ventilation (PV), capable of satisfying the individual needs of most occupants with regard to air quality and thermal comfort as well as of reducing the risk from airborne pathogen contamination at reduced flow rates need to be developed.

There are several requirements for optimal performance of personalized ventilation (Melikov 2004). As already discussed in the introduction, the occupants' inhaled air quality and thermal comfort when using PV depend on the interaction of the personalized flow with the free convective flow at the breathing zone. Personalized flow supplied as a free jet with high velocity will be able to penetrate the free convective flow and provide clean air to inhalation. In this case it is important to extend the first region of the jet with clean air (near the nozzle) to be as long as possible so as the clean air to be inhaled before mixing with the polluted air. Khalifa et al (2008) and Russo et al (2008) used a co-flow PV nozzle to control the characteristics and thus the development of the personalized flow. They succeeded to increase substantially the length of the clean air zone of the personalized flow and thus to boost the PV performance with respect to air quality. It is also important that the target area with clean personalized air, i.e. the area where the head is located, is large enough to accommodate moderate head movement and to ensure high performance of the PV system. Therefore PV nozzles with a relatively large area are recommended for use in practice. However, when large nozzles are used, a high personalized flow rate is needed in order to ensure the minimum velocity needed for penetration of the convective flow. This leads to an increase in energy consumption. Another concern is that the relatively high velocity needed for penetration of the convective flow may cause draught discomfort for the PV users, especially at the winter range of room air temperature (20 - 24 ^{o}C)(68 - 75.2F) recommended in the standards. However it should be also considered that the user will have control on the supplied flow rate and thus will be able to avoid draught discomfort or to achieve thermal comfort at warm environment. The problem to be solved is to ensure a relatively large target area of clean air at the breathing zone at a reduced flow rate of personalized air, i.e. with low penetration (target) air velocity. In order to solve the problem, control of the airflow interaction at the breathing zone, especially control and weakening the strength of the free convective flow, becomes essential. Melikov and Dzhartov 2009 affected the strength and thickness of the free convective flow around the human body by using radiant cooling panels. Reducing the body surface temperature, thus boundary layer thickness, by radiation heat exchange allowed the PV jet to reach the breathing zone at reduced supply flow rates.

In the present research, the potential of four strategies for control of airflow interaction at the breathing zone was studied: 1) weakening of the free convective flow at the breathing zone by exhausting part of its air and thus making its penetration possible by a personalized flow with low target velocity as a result of reduced flow rate; 2) removing and "breaking" the upward free convective flow at the breathing zone by supply of an opposing downward flow of polluted room air, making it possible for the personalized air to reach the mouth/nose at reduced flow rate; 3) weakening and diluting the free convective air at the breathing zone by supply of a downward opposing flow of clean personalized air and 4) inserting clean personalized air gently beneath the free convective flow at the upper chest and employing the natural upward motion of the convective flow to bring it into inhalation.

The effectiveness of these control strategies was studied with a seat (headrest) incorporated PV. The results obtained with the reference case, i.e. when only the headrest PV nozzles were used, confirmed previous findings (Jacobs and de Gids 2006, Melikov et al. 2007) that the discharge angle of the personalized flow and its penetration velocity were important factors that determine the performance of the headrest incorporated PV system. The cross section of the large PV nozzles used in the present study was almost twice as large as the cross section of the small nozzles. Therefore, at the same flow rate, the initial velocity of the personalized flow from the large nozzles was almost half as high as the velocity of the flow from the small nozzles. This affected the penetration of the free convection and respectively the inhaled air quality obtained with the two nozzle sizes. For example the velocity (0.33 m/s, 1.08 fps) of the personalized flow supplied at 8 L/s (0.28 ft^3/s) from the large nozzles was too weak to penetrate completely the free convective flow, while at the same flow rate the velocity (0.62 m/s, 2.03 fps) of the personalized flow from the small nozzles could penetrate better the convective flow. This resulted in substantially different PEE: between 56% and 59% with the large nozzle and between 75% and 83% with the small nozzle (Figure 6). At 6 L/s (0.21 ft^3/s) the difference was even greater: with the large nozzles the PEE was between 22.8% and 43.9% and with the small nozzles between 77.8% and 90.4%. Two of the control strategies studied, namely weakening of the free convective flow by suction of part of its air at the breathing zone (control strategy 1) and weakening and diluting the free convective air by clean personalized air (control strategy 3) proved to be efficient. The comparison shown in Figure 13 documents that both strategies improved PEE dramatically: PEE increased from 22.8% without control to 79.5% when suction of 16 L/s (0.57 ft^3/s) was applied and to

92.4% when convective air was diluted by 4.5 L/s (0.16 ft^3/s) clean air. The improvement was higher when the suction and the dilution flows increased.

The disadvantage of the control strategy based on suction of convective air is the required high suction flow rate for better performance of the PV system, i.e. high inhaled quality at low personalized flow rate. In this case, energy will be used to exhaust the air. However, it could still be energy-efficient to use this method due to the low flow rates of PV air supplied. The energy savings from conditioning less PV air could be enough to cover the energy consumption of extracting the convective air; even energy saving can be realised. Depending on the design used, lower initial costs (ducting, less space, etc.) may add to the effectiveness of the control strategy when applied in practice. This, however, needs to be verified. Nevertheless, this strategy for control of the airflow interaction at the breathing zone leading to improved inhaled air quality may be advantageous for PV applications where the conditioning and cleaning of air is difficult and it is necessary to decrease the supply flow rate of clean air as much as possible, e.g. aircraft cabin. Localized exhaust openings incorporated in aircraft seats (on the headrest or overhead in the privacy divider) have been shown to help evacuate successfully most of the occupant generated pollutants, providing all passengers with air quality better than that in the reference case without localized exhaust openings, when the pollutants were mixed with the cabin air (Dygert and Dang 2009a and b).

Nielsen et al. (2007) supplied clean air at low momentum to the breathing zone by a neck support (a textile “donut” around the neck) and from the side edge of a chair to make the clean air be taken by the convective layer upward towards the face. The concept of personalized air supply at low initial momentum and from relatively large area around the person resulted in increased initial flow rate. From the tested performed the highest PEE of 95% was achieved with the neck support at flow rates above 10 L/s (0.35 ft^3/s). The control strategy based on weakening and diluting the convective flow by supply of redirected clean personalized air (control strategy 3) examined in the present study was more efficient at the lower range (20 – 24 ^oC) (68 – 72.2F) of comfortable room temperatures recommended in the thermal comfort standards and with large nozzles. In this case, a clear advantage was the achievement of a high quality of inhaled air at reduced velocity of the personalized flow by its redirection through the controlled nozzles. For example, a supply of 4 L/s (0.14 ft^3/s) from the large PV nozzles and an additional 3 or 4.5 L/s (0.11 or 0.16 ft^3/s) flow rate of clean air from the control nozzles, i.e. total supply of 7 or 8.5 L/s (0.25 or 0.30 ft^3/s) of clean air, provided inhaled air quality equal to or even better than the case when 8 L/s (0.28 ft^3/s) clean air was

supplied only from the PV nozzles. At 20 °C (68F) PEE between 70% and 80% was obtained with a personalized flow of 4 L/s (0.14 ft^3/s) and a control flow of 3 or 4.5 L/s (0.11 or 0.16 ft^3/s) while PEE was 56% when 8 L/s (0.28 ft^3/s) was supplied from the PV nozzles without control flow rate. Redistributing of the clean personalized air between the PV nozzles and the control nozzles reduced the local air velocity and the risk of draught discomfort, as will be discussed in the following. Supply of personalized air close to the human body at the relatively high velocity needed for penetration may cause draught discomfort. Apart from improving inhaled air quality, the two control strategies (strategy 2 and 3) discussed above also decreased the risk of draught due to decreased velocity of the supplied personalized air. For example, the suction of 16 L/s (0.57 ft^3/s) made it possible to obtain with a personalized flow of 6 L/s (0.21 ft^3/s) and an initial velocity of 0.25 m/s (0.82 fps), an inhaled air quality (PEE) value as high as that obtained without suction and a personalized flow of 8 L/s (0.28 ft^3/s) and an initial velocity of 0.33 m/s (1.08 fps). The strategy of redirecting the personalized air reduced the local velocity in the vicinity of the head and thus draught discomfort as well. For example, the supply of only 4 L/s (0.14 ft^3/s) reduced the initial velocity of the personalized flow from the large nozzles to only 0.17 m/s (0.56 fps) and thus decreased the risk of draught discomfort compared to a supply of 8 L/s (0.28 ft^3/s) at 0.33 m/s (1.08 fps) initial velocity, while maintaining the same inhaled air quality level. In practice, the control strategies studied can be applied with other PV designs. For example, supply of the personalized flow from the front (Kaczmarczyk et al. 2004, Cermak et al. 2006). In this case, control of the free convective flow leading to a decrease of the personalized flow velocity needed for penetration of the free convective flow will also decrease eye irritation for sensitive occupants, e.g. occupants wearing lenses.

As expected, the two efficient control strategies discussed performed better at a low personalized flow rate, i.e. at low velocity of the personalized flow. Therefore, the improvement in inhaled air quality (the increase of PEE) was not substantial with the small nozzles (Figure 8a and Figure 11). In this case, supply of airflow at 6 L/s (0.21 ft^3/s) and 8 L/s (0.28 ft^3/s) from the small nozzles generated a personalized flow with a velocity high enough for penetration of the convective flow (respectively 0.47 m/s (1.54 fps) and 0.62 m/s (2.03 fps)) and therefore the benefit from control of the convective flow was not great. Even at the lowest flow rate of 4 L/s (0.14 ft^3/s) (supply velocity of 0.31 m/s (1.02 fps)) the dilution of the convective flow with control clean air of 4.5 L/s (0.16 ft^3/s) (8.5 L/s (0.30 ft^3/s) total supply of clean air to the breathing zone) was beneficial mainly for decreasing the risk of draught since inhaled air quality (PEE) with control (8.5 L/s, 0.30 ft^3/s) and with control (8 L/s, 0.28 ft^3/s) was almost the same.

The increase of the room air temperature will decrease the strength of the free convective flow (less difference between the body surface temperature and the air temperature) and thus would make it easier for the personalized flow to penetrate and provide clean air within the breathing zone. Therefore the relative improvement of inhaled air quality at 26°C (78.8F) when the control methods were applied was not substantial. As the comparison of the results in Figure 14 show, at a PV flow rate of 6 L/s (0.57 ft^3/s) the suction of 8.5 L/s (0.30 ft^3/s) increased the PEE from 22.8% to 42.3% at 20°C (68.8F) and much less, from 43.9% to 55%, at 26°C (78.8F). Similarly, the PEE increase with a suction of 16 L/s (0.57 ft^3/s) was smaller at 26°C (78.8F) (from 43.9% to 81.7%) than at 20°C (68F) (from 22.8% to 79.5%). Nevertheless, in this case, the control of the free convective flow by a suction of 16 L/s (0.57 ft^3/s) increased the portion of clean personalized air in inhalation more than 4 times at 20°C (68F) and almost twice at 26°C (78.8F). Only an isothermal case was reported in this paper, i.e. temperature of the supplied PV and control air equal to the room air temperature. However, a buoyancy effect was still present because of the temperature difference of the free convective flow and the supplied PV and control flow. This had a different impact on the airflow interaction at 20°C (68F) and 26 °C (78.8F). The impact of the buoyancy effect on the complex interaction of the flows at the breathing zone needs to be studied under specially designed experiments.

Control of airflow interaction at the breathing zone by removing the convective flow with opposing flow of polluted room air was not effective due to extensive mixing of the polluted air with the clean air provided close to the breathing zone. Improvement of inhaled air quality by use of the buoyancy force of the convective flow to transport upwards clean air inserted gently between the flow and the upper chest was limited. The inserted flow and the upcoming convective flow were opposing and counteracting each other and as a result certain mixing was promoted. A clear tendency was observed (Figure 12) that a decrease in the PV flow rate, which decreased its velocity and thus the mixing with the convective air, led to an increase in PEE. The supply of personalized air from large nozzles at low velocity and slightly warmer than the room air temperature will minimize the mixing and will help the clean air to be moved more easily upwards to the mouth/nose. Even under these conditions the separation of the clean upward flow at the shoulder-neck region (blocking effect of the jaws) will move away from the part of the clean air supplied for inhalation. A better result may be expected when the inserted flow of clean air can be supplied upwards, i.e. as assisting flow to the convective flow. This needs to be studied.

Two of the strategies studied for control of the airflow interaction at the breathing zone, namely strategy 1 and strategy 3, were shown to be successful and fulfilled several important requirements for design and implementation of PV in practice. Therefore it may be recommended that they could be applied 1) with large air supply devices and at low velocity of the personalized flow, i.e. low flow rate, generating a target area of cleaner air with a size sufficient to accommodate moderate movement of the head; 2) at the lower range of comfortable room air temperatures recommended in the standards (20 – 26 ^{o}C) (68 – 78.8F) when risk of draught discomfort is high. At high room air temperatures the risk of draught discomfort due to personalized flow supplied isothermally and at high velocity needed for penetration of the convective flow, i.e. high inhaled air quality is low.

The strategies studied required the use of additional energy (flow suction) and a special arrangement of the PV system including additional control nozzles. Other control strategies based on a more simplified design that does not require the use of energy (passive control methods) or litte use of energy (active control methods) have been studied and reported (Bolashikov et al. 2009). The passive control method based on blocking the development of the free convective flow at the abdomen by modifications in desk design, and an active control method based on local suction of the free convective flow below the desk by small low-energy consumption fans have shown to be effective with regard to inhaled air quality and more convenient for implementation in office buildings than the control strategies reported in this study. Nevertheless control strategies 1 and 3 studied in this paper can be more easily applied in theatres, concert halls, vehicle cabins (cars, buses, airplanes, etc.), i.e. places where seats are used to support the human body in rest for relatively long periods. The control strategies can also be realised in an office environment. The chair could be either positioned firmly to the floor and then the tables should be able to move or a small battery driven fan can be incorporated into the back of the chair allowing for its mobility. In the latter design the room air will be sucked, filtered, cleansed (in small UVGI chamber) and delivered to the person through two sets of nozzles (control strategy 3). The control strategy based on suction of free convection air through the control nozzles (control strategy 1) can be achieved with the above system. In this case the free convection air will be sucked, cleaned and supplied through the PV nozzles. Another modification can be based on use of two fans, one for supply of the filtered and cleansed room air through the PV nozzles and one for suction of the free convection air. A specially designed set of sensors (pressure sensors into the seat) could activate on or off and glide over the shoulders or retract the controll nozzles to be less intrusive and ergonomic for the user.

The recently suggested concept of ductless PV in conjunction with displacement ventilation (Halvonova and Melikov 2008, 2009, 2009a) can be applied as well. By use of a simple chair incorporated system of ducting and small fan the cliean and cool displacement air spread over the floor can be sucked and transported to the breathing zone. In this way control strategies 1 or 2 can be applied or the cool and clean air can be supplied to the breathing zone only from the PV nozzles.

Only isothermal conditions (personalized air temperature equal to the control air temperature) were investigated in this study. The potential of non-isothermal conditions for improvement of inhaled air quality and thermal comfort is recommended to be explored in the future. Further experiments are needed to understand the complex airflow at the breathing zone affected by several factors, including the buoyancy forces of the interacting flows.

CONCLUSION

The performance of four novel methods for control of airflow interaction at the breathing zone aiming for improved inhaled air quality at a reduced flow rate of personalized air were studied under different conditions.

Improvement of the airflow interaction at the breathing zone by exhausting part of the free convective flow in front of a seated person was found to be effective, especially when personalized air was supplied at low velocity and from larger nozzles. At a personalized flow rate of 4 L/s (0.14 ft^3/s) the control of the free convective flow increased the portion of clean air in inhalation to the level obtained without control and a personalized flow rate of 8 L/s (0.28 ft^3/s).

Weakening and diluting the convective flow with additional small amounts of personalized air supplied downwards at the upper chest level proved to be effective at a relatively low room air temperature. It improved inhaled air quality at a reduced personalized flow rate, i.e. low supply air velocity. The risk of draught was greatly reduced.

Control of airflow interaction at the breathing zone by removing the convective flow with an opposing flow of polluted room air was not effective due to extensive mixing of the polluted air with the clean air provided close to the breathing zone.

Improvement of inhaled air quality by use of the buoyancy force of the convective flow to transport upwards clean air inserted gently between the flow and the upper chest was limited because the flow of

cleaner air was redirected away from the mouth/nose by the lower face (jaws and chin that protrude over the chest vertical plane).

All methods were tested under isothermal conditions (personalized air temperature equal to the control air temperature). Their potential under non-isothermal condition is recommended to be studied.

ACKNOWLEDGMENTS

This research was supported by the Danish Agency for Science, Technology and Innovation, Project No. 274-07-0516.

REFERENCES

ASHRAE. 2004. *ANSI/AHRAE Standard 55 – 2004*, *Thermal environmental conditions for human occupancy, American Society of Heating, Refrigerating and Air-Conditioning Engineers, Inc.*

ASHRAE. 2005. *ANSI/ASHRAE Standard 113-2005, Method of Testing for Room Air Diffusion. American Society of Heating, Refrigerating and Air Conditioning Engineers*, Atlanta, GA.

ASHRAE. 2007. *ANSI/ASHRAE Standard 62.1-2007, Ventilation for Acceptable Indoor Air Quality, American Society of Heating, Refrigerating and Air-Conditioning Engineers, Inc.*

Bolashikov, Z., Nikolaev, L., Melikov, A.K., Kaczmarczyk, J. and Fanger, P.O., 2003, Personalized ventilation: air terminal devices with high efficiency, *Proceedings of Healthy building 2003, Singapore*, 2, pp. 850-855.

Bolashikov, Z.D., Melikov A.K., 2009, Methods for air cleaning and protection of building occupants from airborne pathogens, *Building and Environment*, 44 (7), p.1378-1385.

Bolashikov, Z.D., Melikov A.K., Kranek, M., 2009, Improved Performance of Personalized Ventilation by Control of the Convection Flow around an Occupant's Body, ASHRAE Transactions, (accepted),

Cermak, R., Melikov, A.K., Forejt, L. and Kovar, O., 2006, Performance of personalized ventilation in conjunction with mixing and displacement ventilation, *International Journal of Heating, Ventilation and Refrigeration Research*, vol.12, no.2, pp.295-311.

Cermak R., Melikov, A.K., 2007, Protection of occupants from exhaled infectious agents and floor material emissions in rooms with personalized and underfloor ventilation, *HVAC&R Research*, 13(1), pp. 23-38.

Clark R.P and Toy N., 1975, Natural convection around the human head, *Journal of Physiology*, 244. pp. 283-293

Dygert R.K. and Dang T.Q., 2009a, Mitigation of Cross-Contamination in an Aircraft Cabin via Localized Suction Removal, Proceedings of Roomvent 2009, Busan South, Korea.

Dygert R. K., and Dang T. Q., 2009b, Localized suction-assisted contaminant removal strategies for improved IAQ, Proceedings Helthy Buildings 2009, Syracuse, NY, USA, Paper ID: 217.

European Standard 2007, EN 15251 2007, *Indoor environmental input parameters for design and assessment of energy performance of buildings addressing indoor air quality, thermal environment, lighting and acoustics*, EUROPEAN COMMITTEE FOR STANDARDIZATION, B-1050 Brussels.

Halvoňová, B. and Melikov, A.K., 2008, Displacement ventilation in conjunction with personalized ventilation, *In: Proceedings of the 11th International conference on Indoor Air Quality and Climate - Indoor Air 2008,* 17-22 August 2008, Copenhagen, Paper ID: 411.

Halvoňová, B. and Melikov, A.K., 2009, Impact of intake positioning height on performance of "ductless" personalized ventilation, In: Proceedings of the 11th International conference on air distribution in Rooms – Roomvent 2009, 24-27 May 2008, Busan, Paper ID: S0131.

Halvoňová, B. and Melikov, A.K., 2009a, Performance of “ductless” personalized ventilation in conjunction with displacement ventilation: impact of disturbances due to walking person(s), *Building and Environment*, in press (doi:10.1016/j.buildenv.2009.06.023).

Homma H. and Yakiyama M., 1988, Examination of free convection around occupant,s body caused by its metabolic heat, *ASHRAE Transactions 1988*, 94 (1), pp. 104-124.

ISO 1984. *International Standard ISO 5221* First edition, *Air distribution and air diffusion – Rules to methods of measuring air flow rate in an air handling duct*: International Organization for Standardization, Geneva, Switzerland.

ISO. 1993, *International Standard ISO, Guide to the expression of uncertainty in measurement.* Geneva: International Organization for Standardization.

ISO 1998. *International Standard ISO/DIS/7726: Ergonomics of the Thermal Environment - Instruments for Measuring Physical Quantities*: International Organization for Standardization, Geneva, Switzerland.

ISO 2005. *International Standard ISO/DIS/7730: Moderate Thermal Environments-Determination of PMV and PPD Indices and Specification of the Conditions for Thermal Comfort*: International Standard Organization for Standardization, Geneva, Switzerland.

Jacobs, P., and de Gids, W.F. 2006. Individual and collective climate control in aircraft cabins, Int. Journal of Vehicle Design, vol. 42, No.1/2, pp. 57-66.

Kaczmarczyk J., Melikov A.K., Fanger, P.O., 2004, Human response to personalized and mixing ventilation, *Indoor Air* 14 (l8), pp. 1-13.

Kaczmarczyk, J., Melikov, A.K., Bolashikov, Z., Nikolaev, L. and P.O. Fanger, 2006, Human response to five designs of personalized ventilation, International Journal of heating, *Ventilation and Refrigeration Research* 12 (2), pp.367-384.

Kaczmarczyk, J., Melikov, A., Sliva, D., Avoiding draught discomfort with personalized ventilation used at the low range of comfortable room air temperature, Indoor Air 2008, 17-22 August 2008, Copenhagen, Denmark – Paper 1035.

Khalifa H.E., Janos M.I. and Dannenhoffer, III J.F., 2009, Experimental investigation of reduced-mixing personal ventilation jets, Building and Environment 44 (2009), pp 1551 – 1558.

Melikov, A.K., Zhou, G., 1996, Air movement at the neck of the human body, *Proceedings of Indoor Air 1996*, July 21-26 1996, Nagoya, Japan, vol.1, pp.209-214.

Melikov, A.K., 2004, Personalized ventilation*, Indoor Air* 14 (7), pp. 157-167.

Melikov A.K., Cermak R., Majer M., 2002, Personalized ventilation: evaluation of different air terminal devices, *Energy and Buildings* 34, pp 829-836.

Melikov, A.K., Ivanova, T., Stefanova, G., 2007, Seat incorporated personalized ventilation, *In: Proceedings of the 10th International Conference on Air Distribution in Rooms - Roomvent 2007*, Helsinki, C05, paper 1318.

Melikov, A.K. and Kaczmarczyk, J., 2007, Indoor air quality assessment by a breathing thermal manikin, Indoor Air 17 (1), pp.50-59.

Melikov A.K. and Dzhartov V., 2009, Control of the free convection flow around human body by radiant cooling, Healthy Buildings 2009, Syracuse, USA, Paper ID: 620.

Nielsen P.V., Bartholomaeussen N.M., Jakubowska E., Jiang H., Jonsson O.T., Krawiecka K., Mierzejewski A., Thomas S.J., Trampczynska K., Polak M and Soennichsen 2007, Chair with integrated personalized ventilation for minimizing cross infection, Roomvent 2007, Helsinki, Finland, Paper ID: 1078.

Niu J.L.. Gao. N.P. Ma P.L.Y. and Zuo H.G. 2007. Experimental study on a chair-based personalized ventilation system. Building and Environment. Vol. 42. No. 2. pp. 913-925. 2006(SCI).

Ozcan, O., Meyer, K. E., Melikov, A., 2003, Turbulent and Stationary Convective Flow Field Around the Head of a Human, *Proceedings of International Symposium on Turbulence, Heat and Mass Transfer - THMT-03,* October 12-17, 2003, Antalya, Turkey.

Özcan, O., Mayer, K.E. Melikov, A.K., 2005, A visual description of the convective flow field around the head of a human, Journal of Visualization, Vol. 8, No.1, 23-31.

Russo J.S., Dang T.Q. and Khalifa H.E., 2009, Computational analysis of reduced-mixing personal ventilation jets, Building and Environment 44 (2009), pp 1559 – 1567.

Sundell J. and Levin H., 2007, Ventilation Rates and Health: Report of an Interdisciplinary Review of the Scientific Literature, ASHRAE URP 1443.

Tanabe, S., Zhang, H., Arens, E.A., Madsen, T.L., Bauman, F.S., 1994, Evaluating thermal environments by using a thermal manikin with controlled skin surface temperature, *ASHRAE Transactions 100 (1)*, pp 39-48.

Wargocki P., Sundel J., Bischof W., Brundrett G., Fanger P.O., Gyntelberg F., Hanssen S.O., Harrison P., Pickering A., Seppänen O., Wouters P., Ventilation and health in non-industrial indoor environments: report from a European Multidisciplinary Scientific Consensus Meeting (EUROVEN), *Indoor Air 12 (2002)*, pp 113-128.

Zukowska D., Melikov A., Popiolek Z., 2008, Impact of thermal plumes generated by occupant simulators with different complexity of body geometry on airflow pattern in rooms, *Book of Abstracts of 7th International Thermal Manikin and Modelling Meeting – University of Coimbra, September 2008,* pp 25 – 26, Proceedings on CD.

Figures

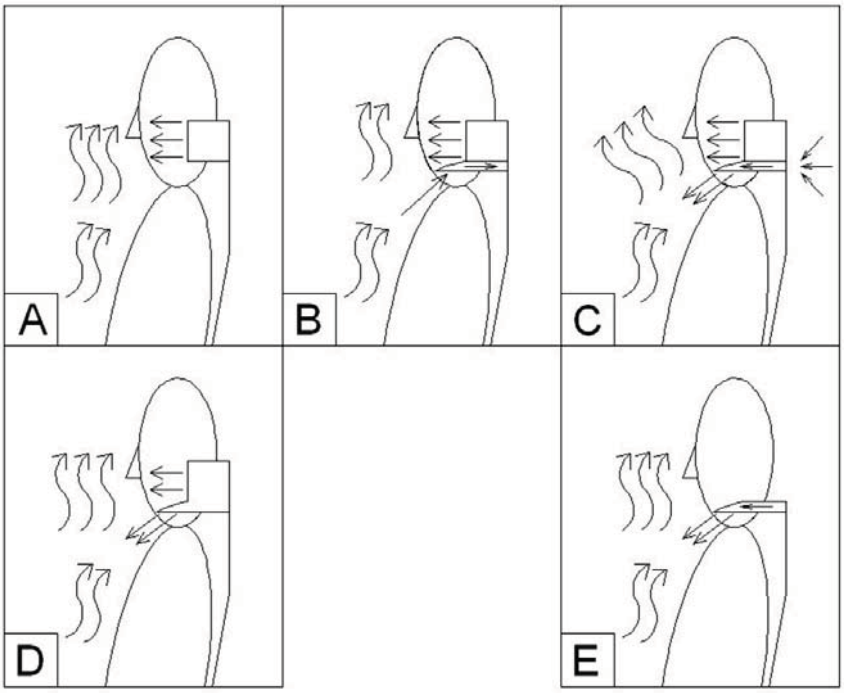

Figure 1. Seat-incorporated personalized ventilation: A) Interaction of the free convective flow with the personalized flow; B) Control of the interaction by exhausting part of the free convective flow air at the upper chest level; C) Control of the airflow interaction by supplying polluted room air to push away the free convective flow at the upper chest/shoulder level; D) Control of the airflow interaction by supplying part of the personalized air at the upper chest/shoulder level to dilute and weaken the free convective flow; E) Control of the airflow interaction by inserting the personalized air without mixing beneath the free convective flow at the chest.

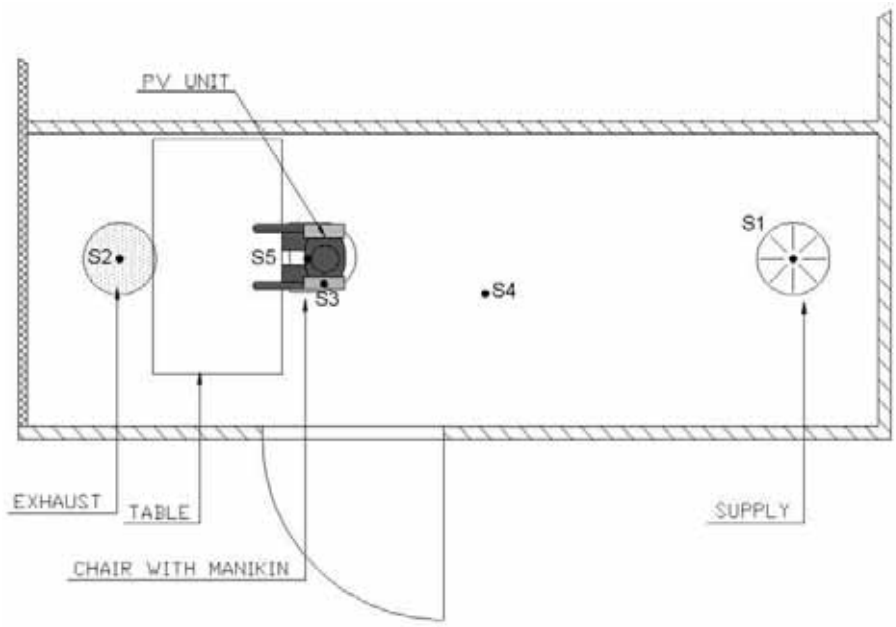

Figure 2. Floor plan of the test room and positioning of the sampling points: S1 – supply air; S2 – exhaust air; S3 – PV air, S4 – room air; S5 – inhaled air.

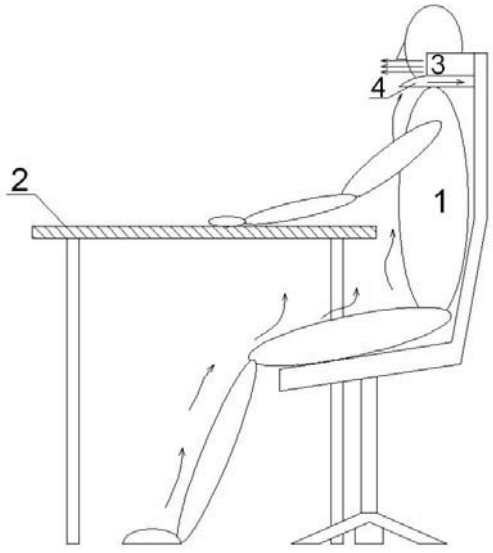

Figure 3. Thermal manikin (1) seated at a table (2) and using a seat-incorporated PV unit (3) with control nozzles (4) exhausting part of the convective flow around the manikin in order to increase the amount of clean air in inhalation (control strategy 1). The same set-up was used when control strategies 2, 3 and 4 (supply of air through the control nozzles) were studied.

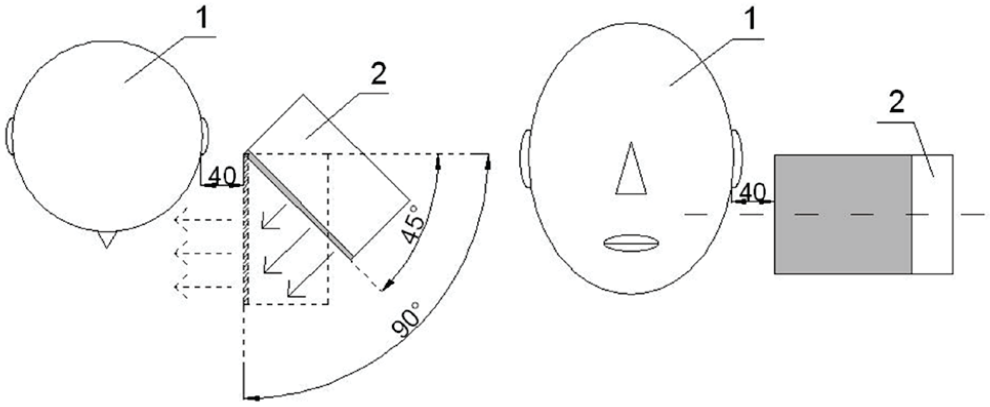

a)

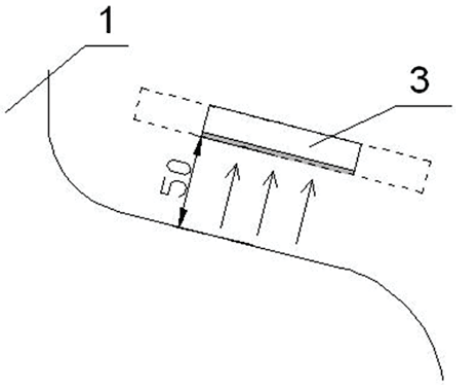

b)

Figure 4. Positioning of the nozzles relative to the head of the breathing thermal manikin (1) a) headrest PV nozzles (2), b) control nozzles(3) above shoulders. All dimensions on the drawing are given in millimetres (1 mm ≈ 0.04 in).

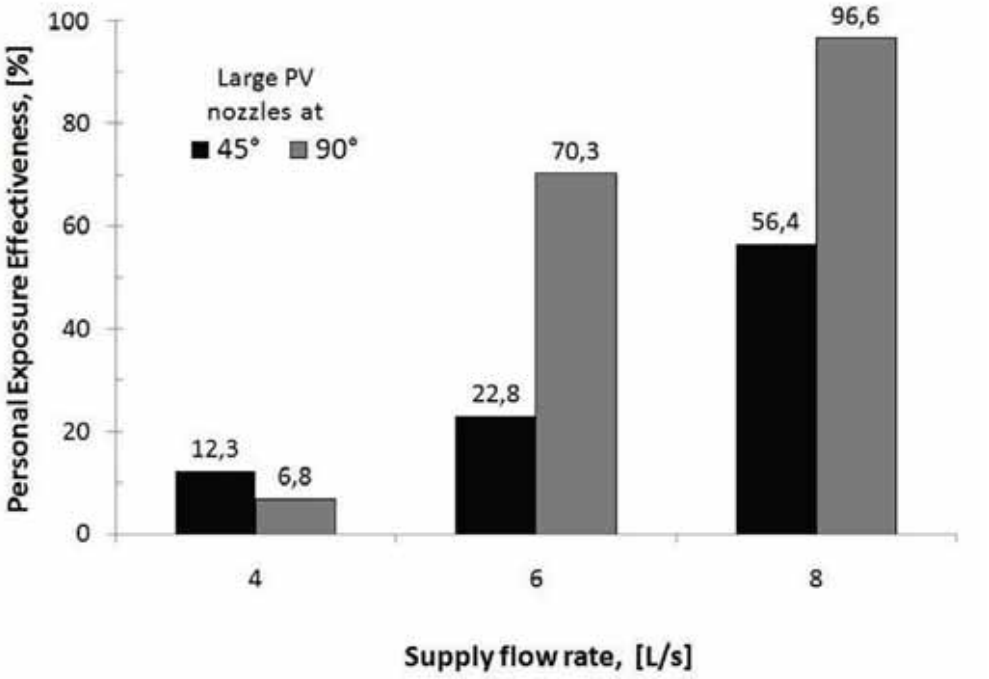

Figure 5. Comparison of PEE for two different angle positioning of the large PV nozzles. Results are obtained at 20°C (68F).

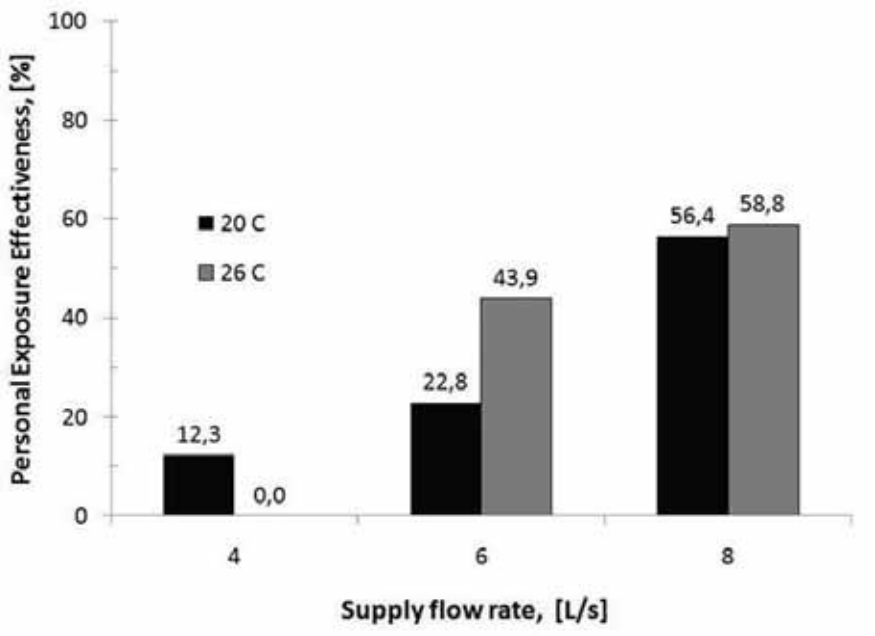

a)

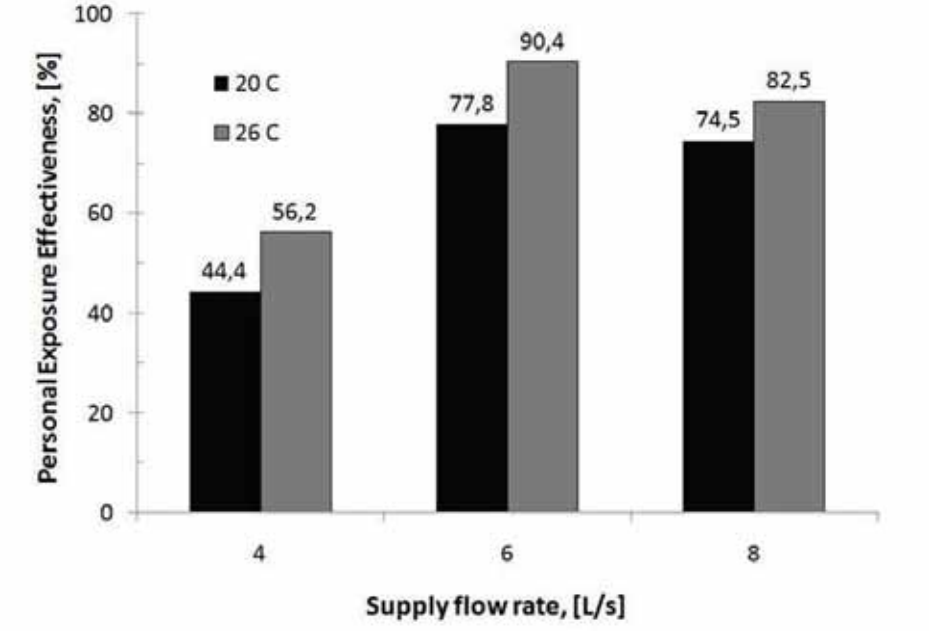

b)

Figure 6. Results for PEE for the reference case of only PV air supply: a) Large PV nozzles; b) Small PV nozzles at 20 (68F) and 26oC (78.8F) isothermal.

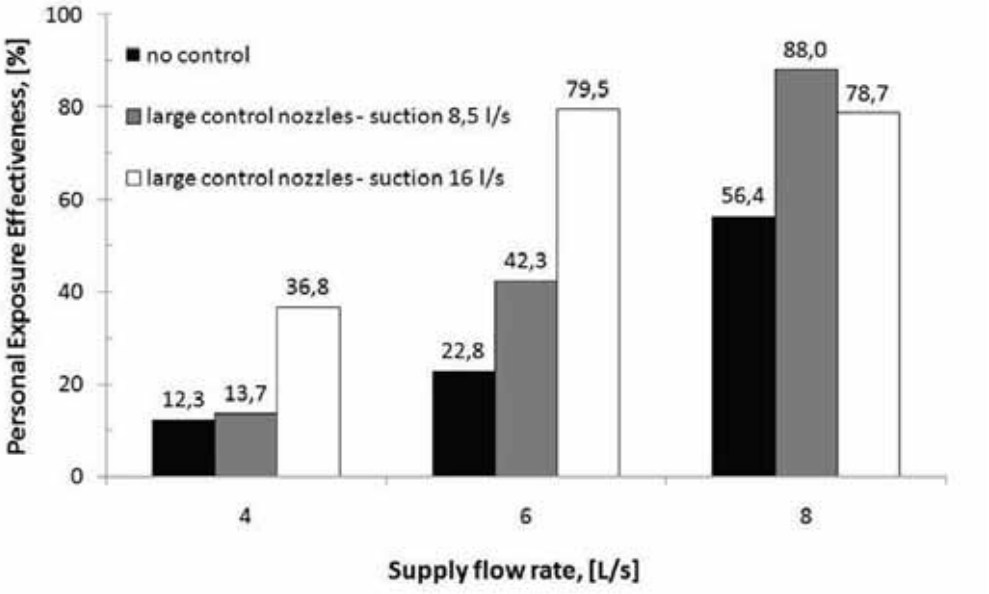

a)

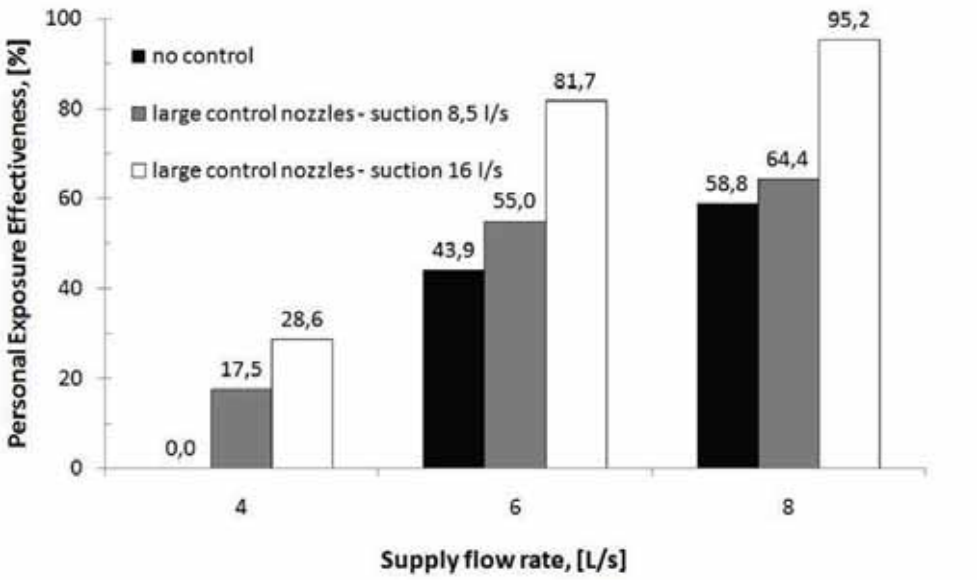

b)

Figure 7. PEE obtained with the large nozzles when control strategy 1 ("suction" mode) was applied: a) at 20°C (68F) and b) at 26°C (78.8F).

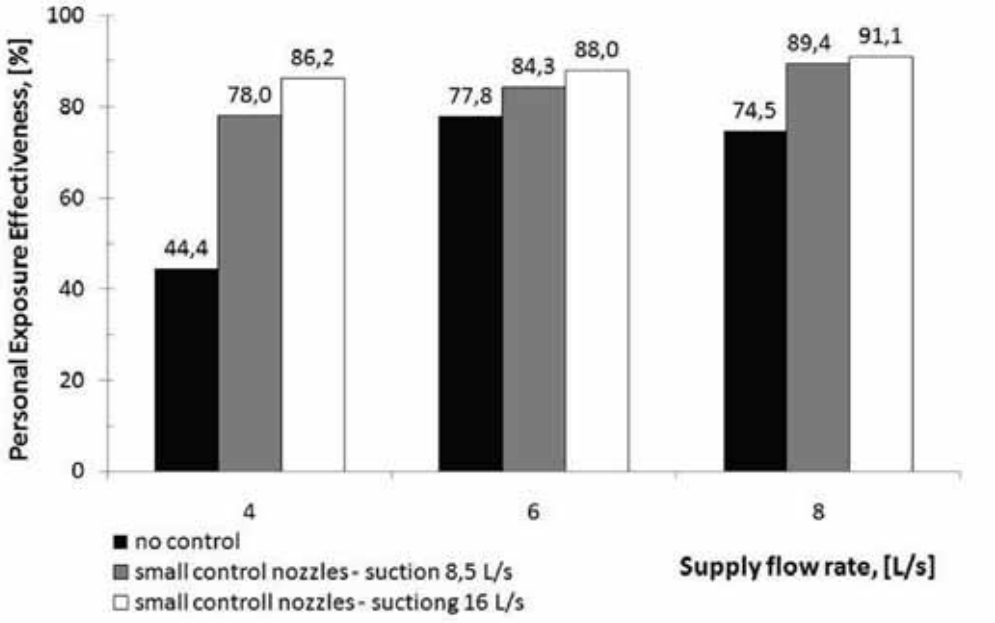

a)

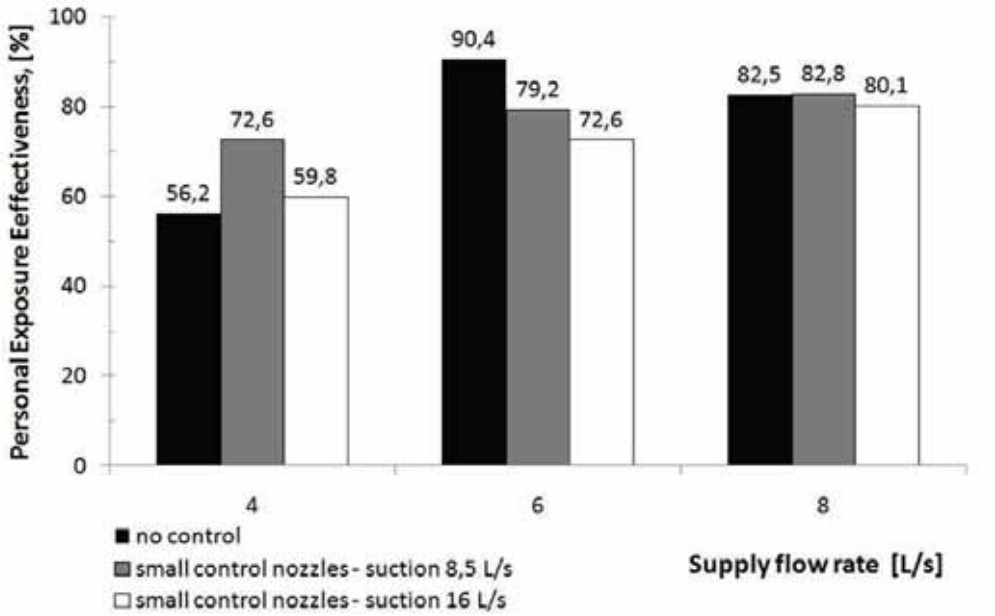

b)

Figure 8. PEE obtained with the small nozzles when control strategy 1 ("suction" mode) was applied: a) at 20 °C (68F) and b) at 26 °C (78.8F).

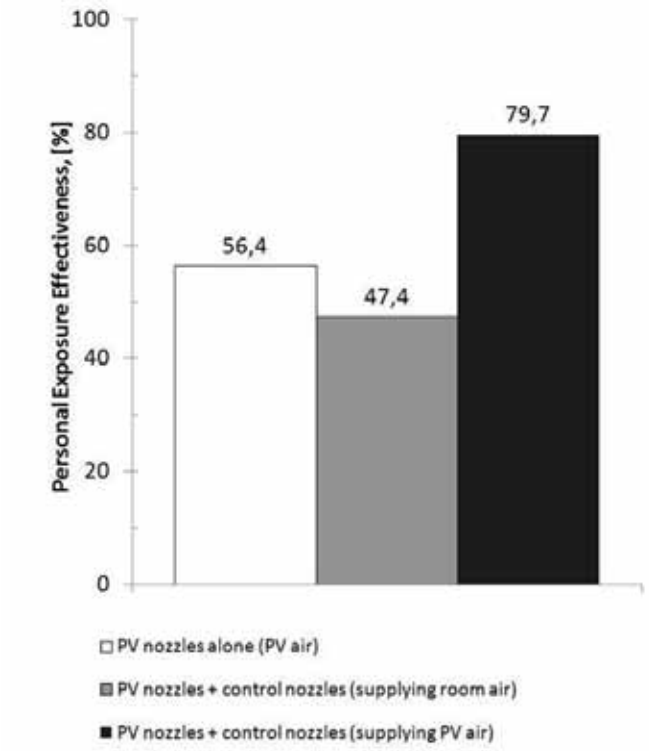

Figure 9. PEE with PV nozzles only for control strategy 2 (to peel off the free convective air by supply of polluted room air) and control strategy 3 (diluting the convective air with clean personalized air supplied from the controlled nozzles). Results obtained with large nozzles, personalized airflow of 8 L/s, airflow supplied from the control nozzle supply 8.5 L/s (0.30 ft^3/s), air temperature 20°C (68F) (isothermal) are compared.

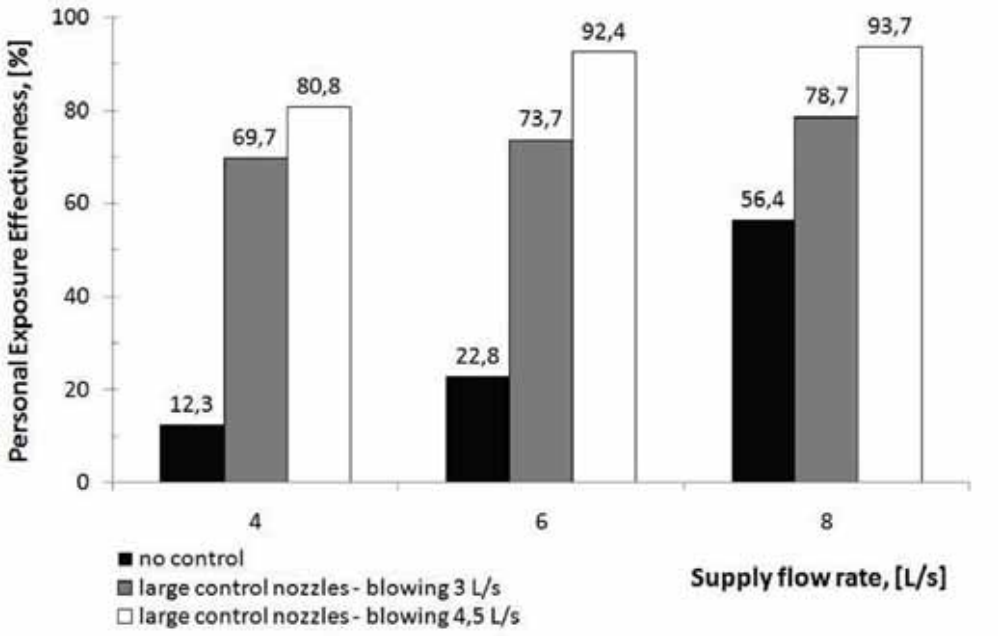

a)

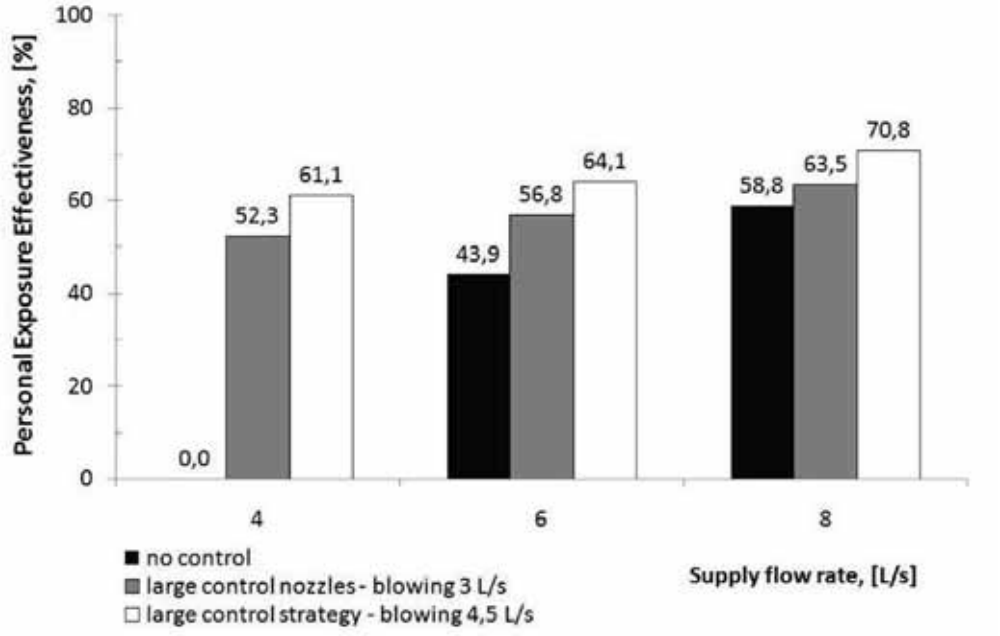

b)

Figure 10. PEE obtained with the large nozzles when control strategy 3 ("blowing" mode) was applied: a) at 20 °C (68F) and b) at 26 °C (78.8F).

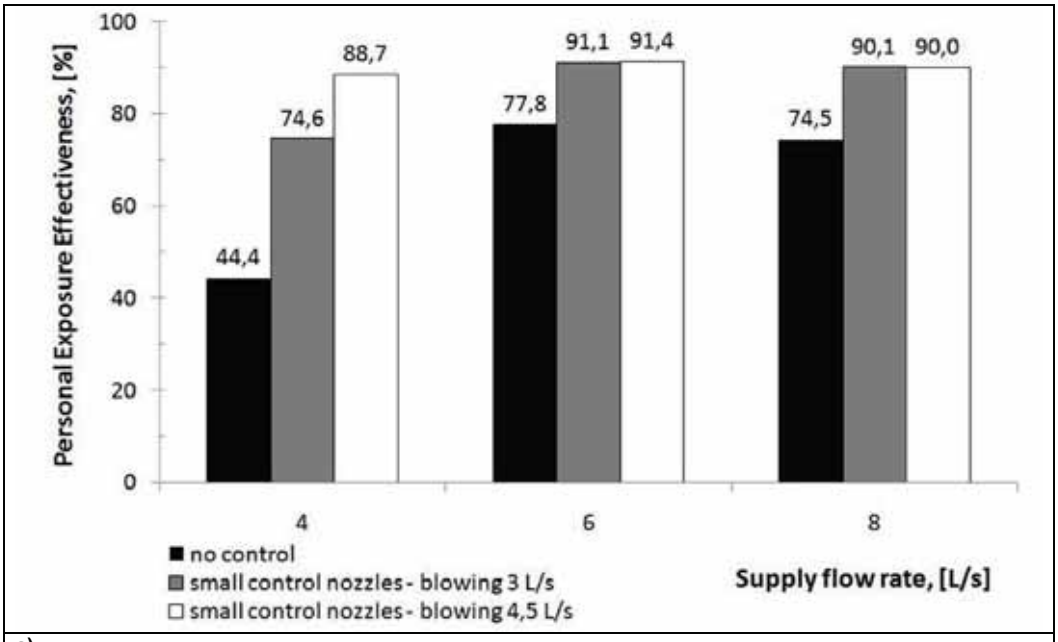

a)

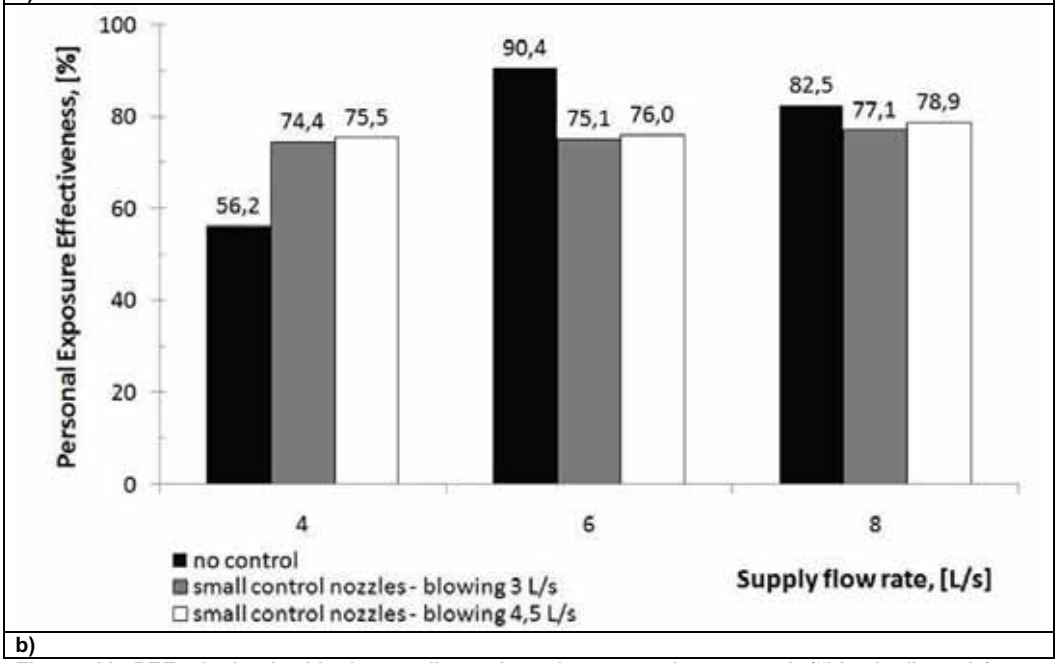

b)

Figure 11. PEE obtained with the small nozzles when control strategy 3 ("blowing" mode) was applied: a) at 20°C (68F) and b) at 26°C (78.8F).

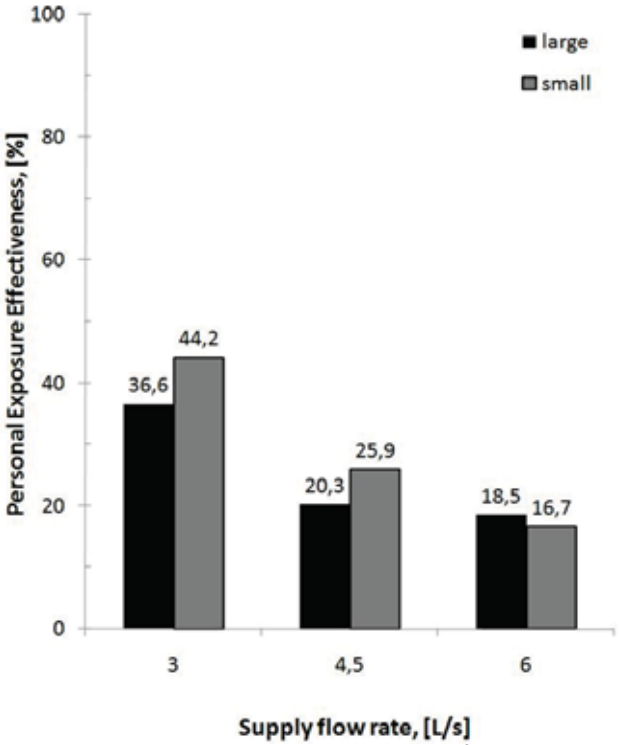

Figure 12. PEE obtained with the large and small nozzles at 26°C (78.8F) when control strategy 4 (supply of clean air beneath the free convective flow) was applied.

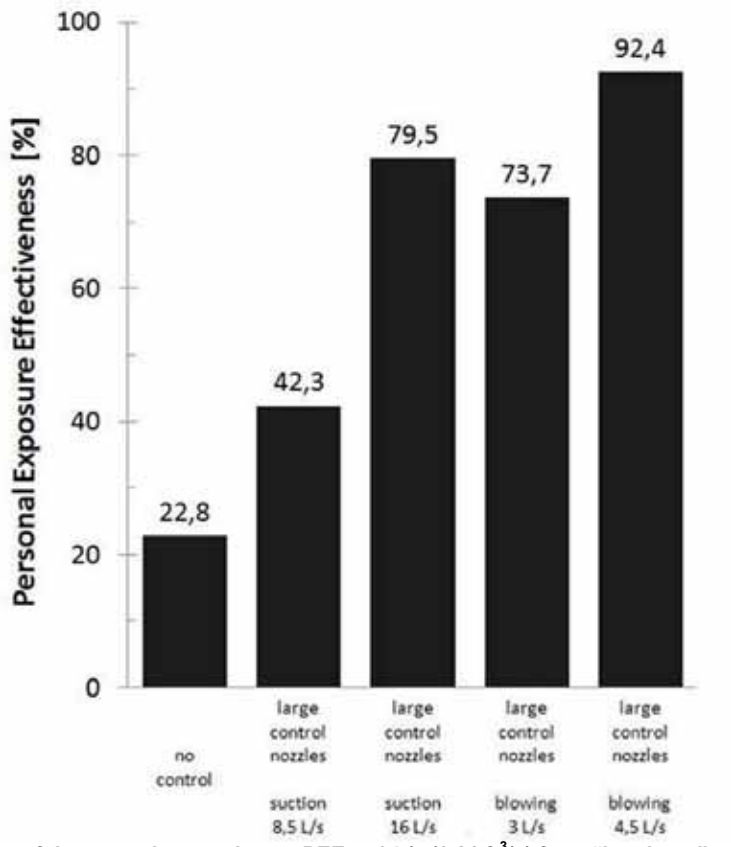

Figure 13. Impact of the control strategies on PEE at 6 L/s (0.21 ft^3/s) from "head rest" type PV nozzle by weakening of the free convective flow (suction) and use of its momentum to transport an additional amount of clean air (blowing), room temperature of 20°C (68F). "Large ATDs" – personalized and control flows with large initial dimensions, i.e. low initial momentum.

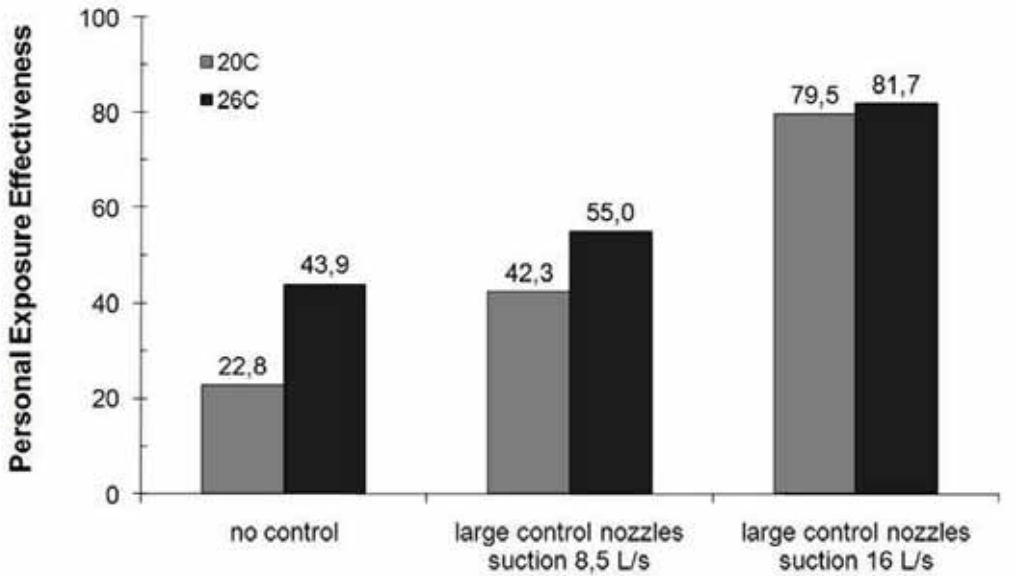

Figure 14. Impact of air temperature on effectiveness of the control strategy of weakening of the free convective flow. PEE obtained at 20°C (68F) and 26°C (78.8F) with PV only at a flow rate of 6 L/s (0.21 ft^3/s) and when a control flow of suction of 8.5 L/s (0.30 ft^3/s) and 16 L/s (0.57 ft^3/s) was employed are compared.

Tables

Table 1: Experimental conditions for control of the free convective flow with chair-incorporated PV for better air quality performance: "v" – tested condition.

	PV nozzles*		Control nozzles*									
20°C, 68F, angle 45°	only supply		suction large, [L/s], [ft^3/s]		suction small, [L/s], [ft^3/s]		blowing large, [L/s], [ft^3/s]			blowing small, [L/s], [ft^3/s]		
supply flow rate, [L/s],[ft^3/s]	large	small	8.5 0.30	16 0.57	8.5 0.30	16 0.57	3 0.11	4.5 0.16	8.5 0.30	3 0.11	4.5 0.16	8.5 0.30
4, 0.14	v	v	v	v	v	v	v	v	v	v	v	v
6, 0.21	v	v	v	v	v	v	v	v	v	v	v	v
8, 0.28	v	v	v	v	v	v	v	v	v	v	v	v
26°C, 68F, angle 45°	only supply		suction large, [L/s], [ft^3/s]		suction small, [L/s], [ft^3/s]		blowing large, [L/s], [ft^3/s]			blowing small, [L/s], [ft^3/s]		
supply flow rate, [L/s], [ft^3/s]	large	small	8.5 0.30	16 0.57	8.5 0.30	16 0.57	3 0.11	4.5 0.16	6 0.21	3 0.11	4.5 0.16	6 0.21
4, 0.14	v	v	v	v	v	v	v	v	v	v	v	v
6, 0.21	v	v	v	v	v	v	v	v	v	v	v	v
8, 0.28	v	v	v	v	v	v	v	v	v	v	v	v

* all suction and supply flow rates tested are total for both nozzles (PV or Control)

Table 2: Tests when clean PV air was supplied only by the control nozzles within the convective flow (control strategy 4); "v" – tested condition, "-" – not available.				
Air discharge from the control nozzles at low momentum				
supply flow rate [L/s], [ft^3/s]	20°C, 68F		26°C, 78.8F	
	Large nozzles	Small nozzles	Large nozzles	Small nozzles
3, 0.11	-	-	v	v
4.5, 0.16	v	v	v	v
6, 0.21	-	-	v	v
8.5, 0.30	v	v	v	-

Table 3: PV nozzle tests at two angles and different supply flow rates: "v" – tested conditions.		
20°C, 68F	only PV air supply	
supply flow rate [L/s], [ft3/s]	Discharge angle: 45°	Discharge angle: 90°
4, 0.14	v	v
6, 021	v	v
8, 0.28	v	v

Table 4: Sampling frequency, duration of data acquisition, and typical values of the uncertainty with a 95% level of confidence.			
Quantity	**Frequency of Data Acquisition**	**Duration of Measurement Period**	**Uncertainty (Conf. Level 95%)**
Concentrations (inhaled and room)	10 min	130 -150 min	1 % of reading
Temperature (room)	5 Hz	1 min	0.3 °C, F
Air velocity (room)	5 Hz	3 min	0.03 m/s, 0.01 fps

Appendix IV

Paper IV

Zhu S.W., Bolashikov Z., Melikov A.K.

Examination on performance of headset incorporated personalized ventilation unit using CFD method.

Proceedings of Indoor Air 2008. 17-22 August 2008. Copenhagen. Denmark - Paper ID: 1018.

Examination on performance of headset incorporated personalized ventilation unit using CFD method

Shengwei Zhu[1,*], Zhetcho Bolashikov[1] and Arsen Melikov[1]

[1]International Centre for Indoor Environment and Energy
Department of Mechanical Engineering, Technical University of Denmark

[*]*Corresponding email: shz@mek.dtu.dk*

SUMMARY
In this study, the performance of a personalized ventilation device with air supply nozzle incorporated in a headset, which can supply clean air directly into the breathing zone, was examined by means of CFD method. The impact of the position of the air supply nozzle on the distributions of velocity, temperature, and personalized air's concentration at the vicinity of the mouth was studied with circular and ellipse-like supply openings, by placing them either in front of, or bellow, or sideways to the mouth. The air discharge area of the nozzle openings was 7cm^2. The distance between the centers of the nozzle opening and the mouth was kept 4cm. In the CFD simulation, a standing computational manikin was used. The personalized air temperature was the same as the room air temperature: 23°C. The personalized air was supplied at a rate of 20 L/min towards the manikin's mouth. Human respiration was not taken into consideration. The results identify that the personalized airflow was able to penetrate the free convection flow around the human body and to provide over 85% of clean air to inhalation. In addition, the performance of the device was little affected by the position and the shape of the air supply nozzle.

KEYWORDS
Indoor air quality, Headset incorporated personalized ventilation unit, Computational Fluid Dynamics, Free ventilation flow

INTRODUCTION
Personalized ventilation (PV) aims at providing clean and cool air to the breathing zone of each occupant to improve his/her inhaled air quality. Indeed, physical measurements have identified a significant decrease of pollution concentration in inhaled air with PV systems in comparison with total volume ventilation (TV) [Faulkner, et al., 1993; Faulkner, et al., 1999; Melikov et al., 2002; Melikov et al., 2003; Cermak et al., 2004, Cermak et al., 2007].

The amount of inhaled personalized air depends not only on the design of supply air terminal device (ATD), its position relative to the occupant, the flow rate and the direction of the personalized airflow, but also on the differences existing between the ambient and PV airflow in terms of temperature and velocity, size of target area, etc [Melikov 2004, Cermak et al., 2006; Kaczmarczyk et al., 2006]. Moreover, since the PV systems are mostly designed for the use at workplaces, their effectiveness also depends on the occupant's activity. Restricted by these factors, the optimal performance for most of the PV systems has not exceeded 50-60% of clean air in each inhalation.

To improve the PV's performance on inhaled air quality, new highly efficient PV systems providing much more clean and cool personalized air in each inhalation for an occupant were developed in recent years [Melikov, et al., 2003; Bolashikov, et al., 2003]. Among these

studies, a headset-incorporated ATD (Headset) with a small rectangular nozzle was proposed to supply clean and cool air directly into the breathing zone, regardless of the occupant's posture, and its performance was examined using a breathing thermal manikin in a climate chamber with piston flow supply. The flow rates of personalized air ranged from 10.8 to 30.0 L/min for the Headset. The much closer distance between air supply nozzle and mouth/nose can greatly decrease the influence of the aforementioned limiting factors on the performance of personalized air, and make the personalized air reach the face before dispersing into the surrounding air. Therefore the Headset supplied up to 80% of personalized air in each inhalation. Although people may be disturbed by the very local impact on the face at high flow rates, it may not be the case when applied at moderate or slightly elevated room air temperatures.

As a part of the second stage in the development of the Headset, we examined the influence of the shape and the positioning of the supply nozzle on the performance of the ATD in this paper. A moderate warm environment of 23°C was considered in the examination and Computational Fluid Dynamics (CFD) method was adopted.

METHODS

Flow field analyzed

A flow field in a room (3m×3m×2.5m) with a naked human body standing at its centre was simulated. The supply nozzle of the Headset was placed close to the mouth. The complex shape of the human body, which was made up of 12,816 surface meshes and very similar to a real one, was adopted to reflect the impact of the local characteristics of the body shape on the free convection flow at the vicinity of the body. Its skin surface area is 1.46m^2. The whole room was ventilated by a very slow constant horizontal isothermal flow (0.01m/s, 23°C) from the whole surface of the wall against the front side of the human body. Therefore, the examination on the performance of the personalized airflow was carried out in a calm ambient environment.

Cases analyzed

In order to examine the impact of the shape and the positioning of the supply nozzle on the performance of the personalized airflow, 6 cases, as listed in Table 1, were conducted. The nozzle opening was circular in cases R1, R2 and R3 or ellipse-like in cases E1, E2 and E3. The air discharge area of the openings was identical for both nozzle types, and equaled to 7 cm^2 with a depth of 2cm. As shown in Figure 1, for both supply nozzle shapes studied, the position was in front of the mouth (Case R1 and E1), bellow the mouth (Case R2 and E2), and sideways relative to the mouth (Case R3 and E3), respectively. Regardless of the position of the supply nozzle, the straight distance between the centres of the mouth and the supply opening was 4 cm in each case. Moreover, the personalized airflow was supplied at an airflow rate of 20 L/min (0.476m/s, 23°C) towards the mouth in each case.

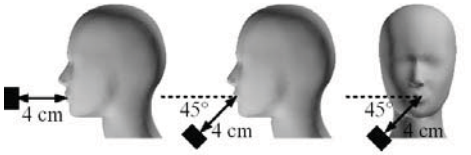

(a) in Case R1 and E1 b) (in Case R2 and E2 (c) in Case R3 and E3

Figure 1. Positions of nozzle in each case.

Table 1 Cases Analyzed

Case	Nozzle type		Position of nozzle		
	circular	ellipse-like	front	below	side
R1	×		×		
R2	×			×	
R3	×				×
E1		×	×		
E2		×		×	
E3		×			×

Grid system

In each case, the flow field simulated was made up of about 34,700 triangular surface meshes and 665,000 fluid cells. Prism-shaped cells were used for the first 4 cell layers placed over the skin surfaces and 5 cell layers placed over the other wall surfaces except for the surfaces of nozzle [Omori, et al, 2004]. y^+, which represents the non-dimensional normal distance (i.e. the wall coordinate) measured from the wall surface to the center of the first fluid cell, was less than 5 over almost all surface [Zhu, et al., 2007]. Previous research on the natural convection from a heated vertical flat board showed that the grid division can ensure sufficient precision for the simulation of the convective flow around the human body [Kato, et al., 1993].

CFD method and boundary conditions

CFD analyses were conducted based on a low-Reynolds-number type k-ε turbulence model [Lien et al, 1996], using the SIMPLE algorithm (Table 2). The detailed boundary conditions can be seen in Table 3. It was assumed that the human body discharged the heat flux due to convection uniformly at a rate of 23.1 W/m^2 (total 33.8 W) [Zhu, et al., 2004]. Except for the human body, the other wall surfaces were assumed to be adiabatic. Human respiration was not taken into consideration. The concentration distribution of personalized air was calculated by setting a passive scalar uniformly at the nozzle opening with an initial value of 1.

Table 2. CFD methods.

Turbulence model	low-Reynolds-number type k-ε turbulence mode
Algorithm	SIMPLE
Space Scheme	First Order Up Wind
Grid System	Spatial cells: 665,000; surface meshes: 34,700

Table 3. Boundary conditions.

Ambient Supplying opening (front wall)	Velocity: 0.01m/s, Temperature: 23°C, Turbulence Intensity: 10 %, Turbulence Scale: 0.05m
Ambient Exhaust opening (back wall)	Velocity: free slip, Temperature: free slip
Supplying opening of nozzle	Velocity: 0.476m/s, Temperature: 23°C, Turbulence Intensity: 10 %, Turbulence Scale: 0.05m
Human body surface	Velocity: no-slip, Uniform heat flux of 23.0W/m^2 (quantity of convective heat loss)
Other walls	Velocity, Temperature: no-slip, adiabatic

RESULTS

Figure 2 shows the distributions of the velocity, air temperature and personalized air's concentration at the vicinity of the human body in Case R1, when the circular nozzle was placed in front of the mouth. Since the differences of these distributions between the cases mostly exist in the area around the face covered or greatly influenced by personalized airflow, and almost same in the remaining part of the room, the corresponding results at the vicinity of the human body for the other 5 cases are not included in this paper. On the other hand, the detailed distributions of velocity, air temperature and personalized air's concentration in the zone around the face are shown in Figure 3, 4 and 5, respectively. The distributions at the vertical section across the middle of the human body and the horizontal section across the centre of the mouth are presented in the figures.

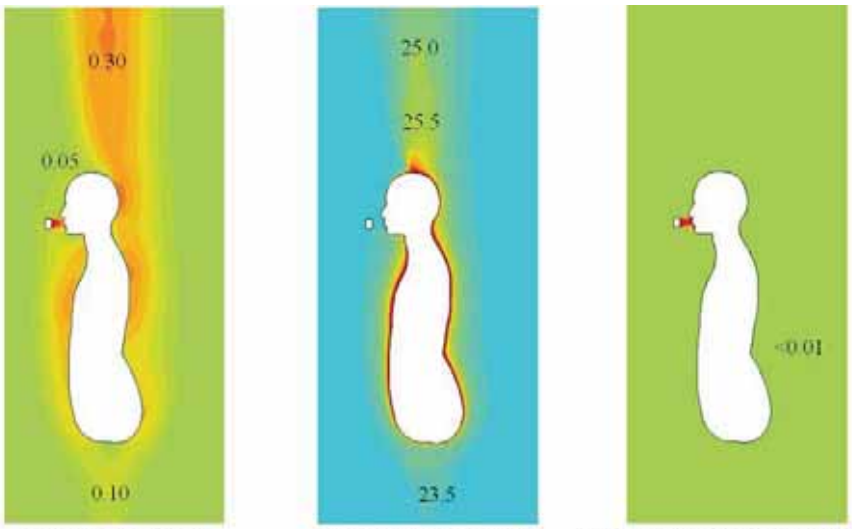

(a) distribution of velocity [m/s] (b) distribution of air temperature [°C] (c) distribution of personalized air's concentration [-]

Figure 2. Simulation results around the human body at the section across the middle of the body in Case R1.

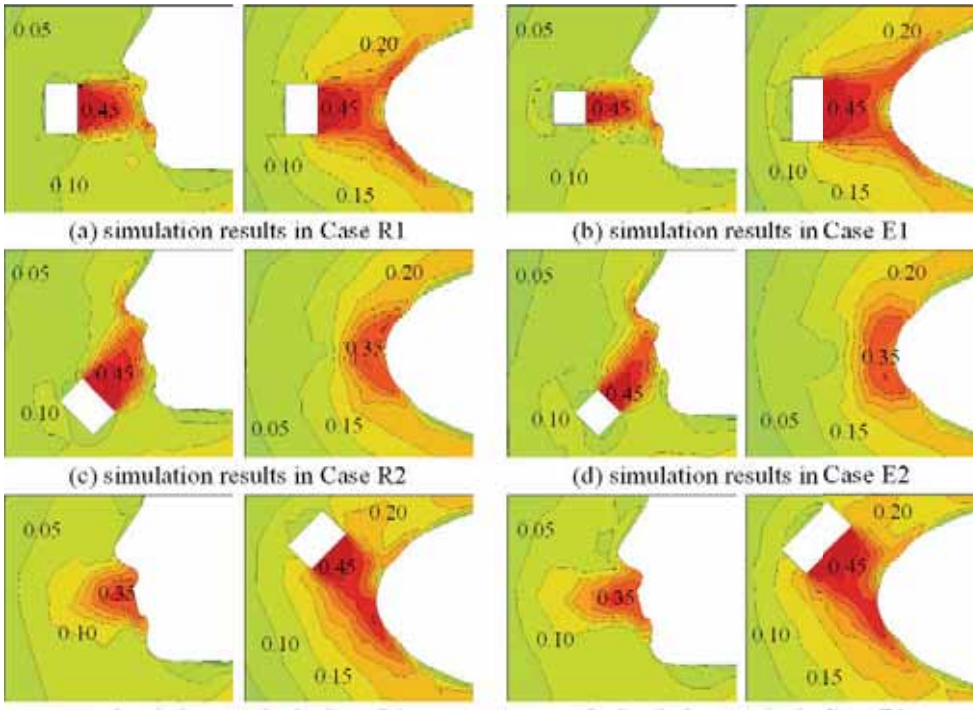

(a) simulation results in Case R1 (b) simulation results in Case E1

(c) simulation results in Case R2 (d) simulation results in Case E2

(e) simulation results in Case R3 (f) simulation results in Case E3

Figure 3. Velocity distribution in the area around the face at the vertical section across the middle of body and the horizontal section across the centre of the mouth in each case [m/s].

Velocity distribution

According to Figure 2(a), a small airflow of less than 0.02m/s was detected in the whole room at the region away from the human body. The free convective airflow can be clearly observed around and above the human body. Although the free convective airflow along the frontal body surface was interrupted and impaired by the personalized airflow, its maximum value reached over 0.3m/s at the top of the head. According to Figure 3, the velocity distribution in the flow field around the face was obviously different depending on the direction of the personalized airflow, i.e. the position of the supply nozzle. In cases R1, E1, R2, and E2, the velocities distributed left-right symmetrically relative to the mouth opening. However, the velocity decreased more slowly above the personalized airflow in cases R2 and E2 when compared to cases R1 and E1. In cases R3 and E3, the velocities distributed left-right asymmetrically, and the velocity decreased more quickly at the side of the nozzle openings. Anyway, in each case, the personalized airflow was weakened quickly by colliding and mixing with the free convection airflow, and the flow field with velocities of higher than 0.25m/s was limited in a very small region between the nozzle opening and the face. Personalized airflow finally impinged over the face focused on the mouth and the nose.

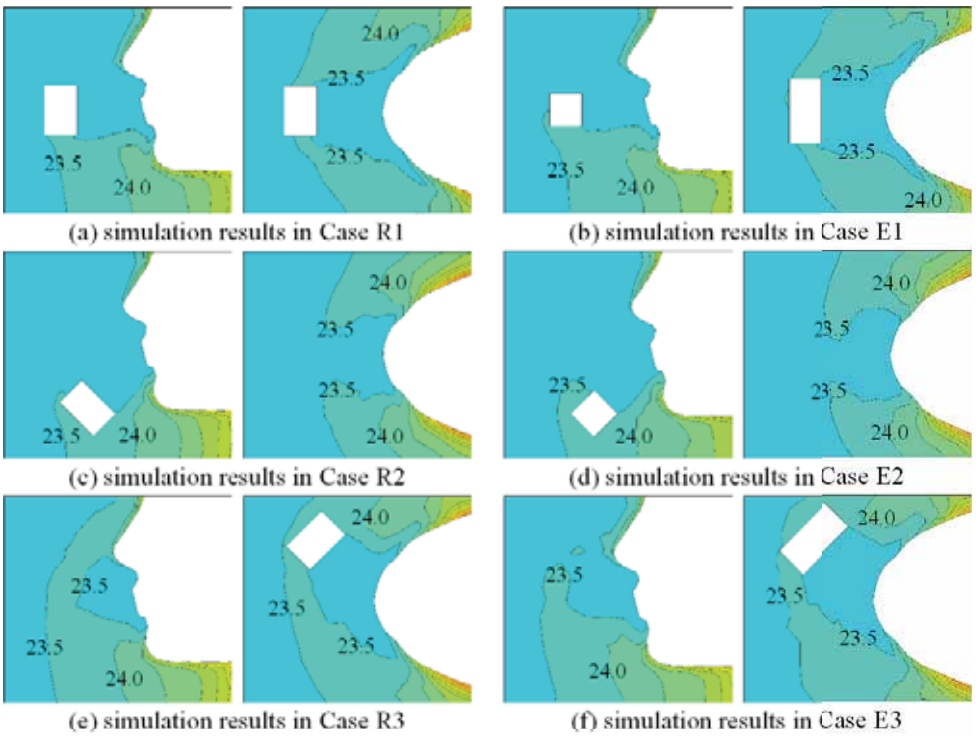

Figure 4. Air temperature distribution in the area around the face at the vertical section across the middle of body and the horizontal section across the centre of the mouth in each case [°C].

Air temperature distribution

According to Figure 2(b), the whole room air was almost kept at a constant air temperature of about 23°C at the region away from the human body. Within the vicinity of the human body, the air was heated and with higher temperature. However, the temperature layer of over 25.5°C was limited in a very narrow region close to the body. According to Figure 4, as well as the velocity distribution, the position of the supply nozzle was also shown to be a crucial

point for the formation of the air temperature distribution in the zone around the face. Since the warm free convection airflow was broken by the cool personalized air of 23 °C, a steep temperature gradient was formed by the interaction of the two airflows. The air temperature was below 24°C in the field around the face except for the temperature boundary layer over the skin surface. Moreover, air temperature distribution around the mouth in the horizontal section was left-right symmetrical in cases R1, E1, R2, and E2, and left-right asymmetrical in cases R3 and E3.

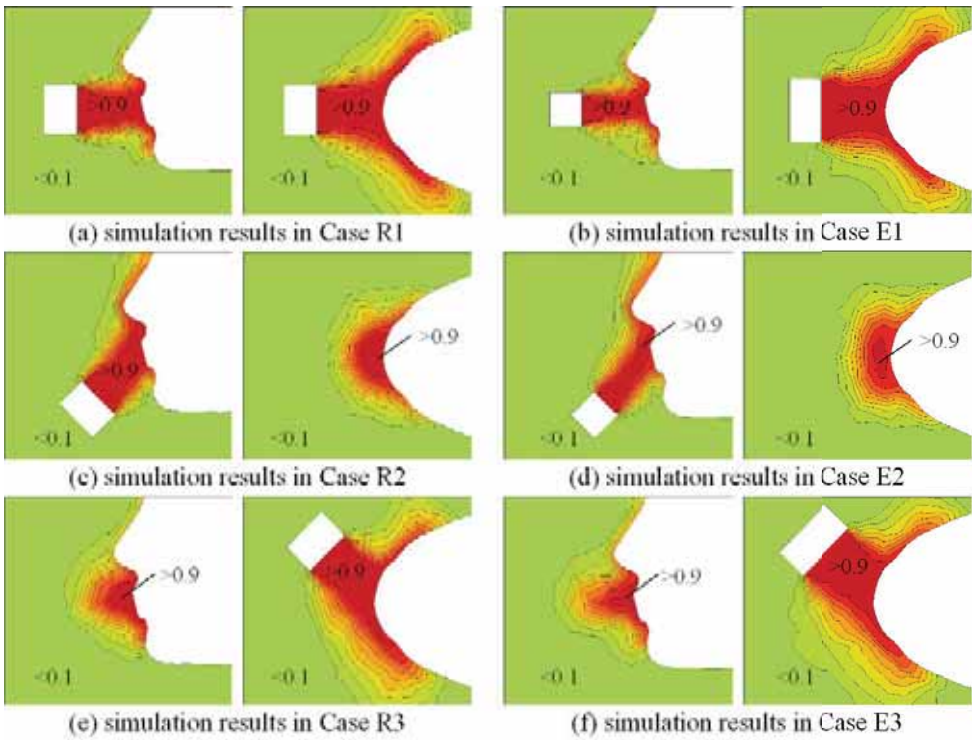

Figure 5. Personalized air's concentration distribution in the area around the face at the vertical section across the middle of body and the horizontal section across the centre of the mouth in each case [-].

Table 4. Personalized air's concentration at the mouth surface [-].

Case	R1	E1	R2	E2	R3	E3
Shape of nozzle	circular	ellipse-like	circular	ellipse-like	circular	ellipse-like
Position of nozzle	in front of the mouth		bellow the mouth		sideways to the mouth	
Concentration	0.969	0.938	0.927	0.856	0.978	0.950

Personalized air's concentration distribution

Figure 2(c) indicates that the personalized air dispersed very fast into the ambient air, and the region with a concentration over 0.1 only existed in a limited area between the nozzle opening and the mouth and the nose. As shown in Figure 5, although the distribution of personalized air's concentration was greatly affected by the position of the supply nozzle, it was almost over 70% around the mouth and nose in each case independent of the position of the supply nozzle. In Table 4, the average concentration of the personalized air at the mouth in each case

is listed. The average concentration at the mouth was over 85% in all studied cases. By comparing the concentration values in the cases using the same supply nozzle (circular or ellipse-like), it was noticed that the value was smallest when the supply nozzle was put bellow the mouth, and largest when the supply nozzle was put sideways to the mouth for the ambient environment considered here.

DISCUSSION

The obtained results reveal that most of the personalized air was distributed in a very small area between the nozzle and the mouth and the nose of the occupant; therefore it effectively improved the inhaled air quality, regardless of the shape and the position of the nozzle. Over 85% of the amount of inhaled air would be clean personalized air. Moreover, although the nozzle was placed in a very small distance of 4 cm away from the mouth, the velocities in the field near the face were around 0.1 m/s. So the risk of draught may not be high.

The shape of the nozzle shows a little influence on the inhaled air quality. Slightly less personalized air was inhaled with the ellipse-like nozzle because due to its smaller height the supplied airflow was more centralized in the vertical direction. At each position, the average concentration of personalized air at the mouth was larger when the circular nozzle was used. It seems that the circular nozzle may have a better performance for improving the inhaled air quality due to the longer potential core region that is generated from this opening.

In this study, the position of the ATD was chosen to be close to the position in which headsets are used in reality. The results identify higher performance when the nozzle was placed in front of and sideways to the mouth. In the case when the nozzle is placed sideways to the mouth at a degree of 45°, the personalized air could “stick” to the face and completely cover the whole mouth surface. However, the performance decreased when the nozzles were positioned bellow the mouth as defined in Table 4 and Figure 4. Nevertheless, it can be concluded that the Headset can ensure its aim of improving the inhaled air quality in reality.

CONCLUSIONS

In this paper, the influence of the nozzle’s shape and position on its performance was examined by means of CFD simulation. According to the results, the personalized air was able to penetrate the free convective airflow around the human body and provide over 85 % of clean air to inhalation. The circular nozzle had a slightly better performance of improving the inhaled air quality than the ellipse-like nozzle. Moreover, the performance of the device was slightly affected by the position of the supply nozzle.

In future, in order to develop a practical headset-incorporated personalized ventilation unit, we would examine its performance in diverse ambient ventilation conditions, such as in under-floor ventilated indoor environment, constant back/side airflow, non-isothermal environment, etc. Moreover, the influence of the personalized air’s characteristics, such as airflow rate, temperature, velocity, direction, etc would also be examined in different ambient conditions, as well as the nozzle opening’s area. Besides the CFD simulation, corresponding experiments would be conducted to verify the simulation results and confirm the effect of the headset incorporated personalized ventilation unit on real people’s inhaled air quality perception.

ACKNOWLEDGEMENT

It was supported by Hans Christian Ørsted Postdoc Programme of Technical University of Denmark. Kato’s Laboratory, Institute of Industrial Science, the University of Tokyo offered its CFD resources for the CFD simulation in this study.

REFERENCES

Bolashikov, Z., Nikolaev, L., Melikov, A.K., Kaczmarczyk, J. and Fanger, P.O. 2003. Personalized ventilation: air terminal devices with high efficiency. *Proceedings of Healthy building 2003*, Singapore, 2, 850-855.

Cermak, R. and Melikov, A.K. 2004. Transmission of exhaled air between occupants in rooms with personalized and underfloor ventilation, *Proceedings of Roomvent 2004*, Portugal, CD-ROM.

Cermak, R., Melikov, A.K., Forejt, L. and Kovar, O. 2006. Performance of personalized ventilation in conjunction with mixing and displacement ventilation. *HVAC&R Research*, 12(2), 295-311.

Cermak, R. and Melikov, A.K. 2007. Protection of occupants from exhaled infectious agents and floor material emissions in rooms with personalized and underfloor ventilation. *HVAC&R Research*, 13(1), 23-38.

Faulkner, D., Fisk, W.J. and Sullivan, D.P. 1993. Indoor airflow and pollutant removal in a room with desktop ventilation, *ASHRAE Transactions*, 99, 750-758.

Faulkner, D, Fisk, W.J., Sullivan, D.P. and Wyon, D.P. 1999. Ventilation efficience of desk-mounted task/ambient conditioning systems, *Indoor Air*, 9, 273-281.

Kaczmarczyk, J., Melikov, A.K., Bolashikov, Z., Nikolaev, L. and Fanger, P.O. 2006, Human response to five designs of personalized ventilation, *International Journal of heating, Ventilation and Refrigeration Research*, 12(2), 367-384.

Melikov, A.K., Cermak, R. and Mayer, M. 2002. Personalized ventilation: Evaluation of different air terminal devices. *Energy and Buildings*, 34, 829-836.

Melikov, A.K., Cermak, R., Kovar, O. and Forejt, L. 2003. Impact of airflow interaction on inhaled air quality and transport of contaminant in rooms with personalized and total volume ventilation. *Proceedings of Healthy building 2003*, Singapore, 2, 592-597.

Melikov, A.K. 2004. Personalized ventilation. *Indoor Air*, 14, (suppl 7), 157-167.

Kato, S. Murakami, S. and Yoshie R. 1993. Experimental and numerical study on natural convection with strong density variation along a heated vertical plate. *Proceedings of the 9th Symposium on Turbulent Shear Flows*, Japan, Paper 12-5.

Lien, F.S., Chen, W.L. and Leschziner, M.A. 1996. Low-Reynolds-number eddy-viscosity modeling based on non-liner stress-strain/vorticity relations. *Proceedings of 3rd International Symposium on Engineering Turbulence Modelling and Measurement*, Greece, 1-10.

Omori, T., Yang, J.H., Kato, S. and Murakami, S. 2004. Coupled simulation of convection and radiation on thermal environment around an accurately shaped human body. *Proceedings of the 9th International Conference on Air Distribution in Rooms*, Portugal, CD-ROM.

Zhu, S.W., Kato, S., Murakami, S. and Hayashi, T. 2004. Study on inhalation region by means of CFD analysis and experiment. *Building and Environment*, 40(10), 1329-1336.

Zhu, S.W., Kato, S., Ooka, R. and Sakoi, T. 2007. Development of a computational thermal manikin applicable in a non-uniform thermal environment (Part 1) Coupled simulation of convection, radiation and Smith's human thermal physiological model for sensible heat transfer from a seated human body in radiant environment. *ASHRAE HVAC&R Research*, 13 (4), 661-679.

Appendix V

Paper V

Bolashikov, Z.D., Melikov A.K., Spilak M.

INSERTED JETS APPLIED IN WEARABLE PERSONALIZED UNIT

Building and Environment 2009, Submitted.

INSERTED JETS APPLIED IN WEARABLE PERSONALIZED UNIT

Z. D. Bolashikov[†], A. K. Melikov[1], M. Spilak[1], A. Meslem[2] and I. Nastase[3]

[1]*International Centre for Indoor Environment and Energy, Department of Civil Engineering, Technical University of Denmark, 2800 Lyngby, Denmark, www.ie.dtu.dk;*

[2]*LEPTIAB, University of La Rochelle, 17000 La Rochelle, France;*

[3]*Building Services Department, Technical University of Civil Engineering, 021414 Bucharest, Romania.*

[*] Zhecho Bolashikov, Ph. D. Student: *Tel: + 45 2826 8654, Fax: + 45 4593 2166*
e-mail address: zdb@byg.dtu.dk

INSERTED JETS APPLIED IN WEARABLE PERSONALIZED UNIT

Z. D. Bolashikov[†], A. K. Melikov, M. Spilak, A. Meslem and I. Nastase

ABSTRACT

A way to improve the inhaled air quality and to reduce the risk from airborne disease contamination by supplying small portions of clean air within the free convective flow surrounding the human body close to the mouth/nose is reported. Experiments at 23°C were performed in a full-scale test room with a breathing thermal manikin resembling a seated occupant in a state of thermal neutrality, with a realistic free convective flow and a normal breathing cycle. The air in the room was mixed with tracer gas. Inserted jets supplied isothermally the clean air from circular, elliptical and lobed nozzles with different diameters (equivalent diameters ranging from 0.025 to 0.035 m) positioned within the boundary layer and at the height of the mouth. The enhancement of the inhaled air quality by changing the initial velocity (0.2 – 0.6 m/s), the distance between the nozzles and the mouth (0.02 – 0.06 m) and the direction of the inserted jets (from front, side and below) was studied. The control over the interaction between the inserted jet and the free convective flow proved to be efficient. It made it possible to increase up to 94% the portion of the clean air into the inhaled air. The application of inserted jets in the design of wearable personalized ventilation devices and their use in buildings and heavily occupied spaces (aeroplanes, trains, buses, theatres, hospitals, etc.) for improvement of inhaled air quality and decreasing the risk of airborne cross-infection at reduced energy use is discussed.

KEYWORDS:

Air quality, personalized ventilation, inserted jet, free convective flow, airflow interaction, headset

INTRODUCTION

Nowadays people live, work, travel and spend their leisure time in close proximity. This increases the risk of potential spread and epidemics or even, pandemics of contagious diseases. The reemergence of well-known pathogens such as tuberculosis, avian flu, swine flu, etc, but in a mutated form and resistant to medication

[*] Zhecho Bolashikov, Ph. D. : *Tel: + 45 2826 8654, Fax: + 45 4593 2166*
e-mail address: zdb@byg.dtu.dk

puts big pressure on mankind. So far no reliable measures exist to protect people fully indoors from becoming infected with airborne commutable pathogens. The “old way” of ventilating spaces and thus diluting the indoor air contaminated with pathogens with fresh outdoor air as much as possible is not efficient, especially now, when the associated energy costs to support increased air-change rates are extremely high [1]. Draught discomfort due to elevated velocity resulting from increased ventilation rates is another serious problem with the present total volume air distribution techniques. Moreover, the total volume ventilation used today provides all occupants with the same conditions, so those who are young, old or immuno-compromised are at the highest risk. However, when speaking of human lives and well-being, the stakes are high and no compromises should be allowed. Clearly, new and alternative solutions are needed to provide people with acceptable air indoors. The air supplied should be clean, fresh and free from pathogens or health-hazardous matter. A new way to deliver the clean air is the personalized ventilation [2]. It aims to supply clean air close to/within the breathing zone of each individual, so that it is inhaled before being mixed with the polluted room air. The PV concept shows great potential for improving occupants’ comfort and work performance, reducing Sick Building Syndrome (SBS) symptoms, and diminishing the risk from airborne cross-infection ([3], [4]).

Different desk-top installed air terminal devices (ATDs) have been developed and studied over the last 10 years with focus on inhaled air quality ([3], [5] – [10]). Personalized flow with a large cross-section area, i.e. from large ATDs, will cover better the user’s face and the amount of inhaled clean air will be less affected by an occupant’s movement. However, this will result in higher flow rates in order to ensure the minimum velocity the personalized flow needs to penetrate the free convective flow. Bolashikov et al. [11] reported on a desk-installed ATD capable of providing 100% clean air in inhalation. The ATD of a circular shape and a diameter 0.18 m supplies the personalized air at low initial turbulence intensity and reduces mixing with the surrounding polluted room air when the user’s face is located at a distance of up to 2-3 ATD diameters downstream. Nevertheless, a personalized flow rate of 10 L/s is needed to generate the minimum velocity of approx. 0.3 m/s at the facial area of the occupant in order to penetrate the free convective flow. The same velocity can be obtained at a reduced flow rate when ATDs with small supply areas are used. This, however, will decrease the cross-section of the personalized flow in the target area. Such PV may perform well provided that the positioning of the PV air supply nozzle relative to the mouth/nose of the user does not change. However, restraining the head from moving is seldom the case in practice. Chair-incorporated PV

nozzles supplying air sideways and from behind [12] or textile permeable diffusers formed as a neck support [13] have been studied as well. As it will be discussed in the following, these designs perform well only at supply flow rate higher than 8-10 L/s.

The positioning of the PV ATD in relation to mouth/nose will remain unchanged if it is attached to the user's head (similar to a headset microphone). A PV ATD located just a few centimeters away from the mouth will also be energy-efficient because of the rather low personalized flow rates required, compared to the flow rate (4 - 10 L/s per person) used with conventional total volume ventilation systems. A sedentary person at a low activity level inhales on average 0.24 L/s [14], which is just 10% from the lowest flow rate of 2.5 L/s per person for offices recommended in the present ventilation standard ASHRAE 62.1 [15], and 6% from that suggested in EN 15251 [16] i.e. 4 L/s per person. Bolashikov et al. [11] reported on personalized ventilation with a supply nozzle installed in the microphone casing of a headset unit. As much as 80% of the air inhaled by an occupant equipped with such a unit was clean unpolluted PV air. The efficiency of the headset unit in supplying clean air was found to be independent of the breathing mode (mouth or nose) and to increase by reducing the distance from the mouth/nose or by increasing the flow rate supplied (maximum flow rate tested was 0.5 L/s).

Niu et al. [17] used nozzles with relatively large supply cross section positioned at some distance bellow the chin and suppled the personalised flow upward. The Re number calculated based on the data provided in their paper was in the range ($1.6x10^3$ – $4x10^3$). At this Re number the potential core of the jet is short and remains away from the mouth because of the positioning of the nozzle: microphone positioning. Thus the mouth will be exposed mostly to the polluted air in the mixing region of the jet around the potential core. This can be clearly seen from the results reported by the authors: the fraction of personalized air in the inhaled air will never reach 100% regardless of the increase of the supply flow rate.

Zhu et al. [18] examined, by means of computational fluid dynamics (CFD) simulation, the influence of the shape (circular and elliptic with an opening area of 0.0007 m^2, d = 0.03 m) and the positioning (front, side and below at a distance of 40 mm) of a headset-incorporated PV nozzle on the air quality performance of the PV ATD. A moderate warm environment of 23°C was considered. The personalized air was supplied at a rate of 0.33 L/s and directed towards the manikin's mouth. In the CFD model no human respiration was simulated. The results identify that the personalized airflow was able to penetrate the free convective flow

around the human body and to provide more than 85% of clean air into inhalation. The authors reported that the performance of the device, with regard to the clean air supplied into inhalation, was only slightly affected by the position relative to the mouth (front, side and below) and the shape of the air supply nozzle.

From a fluid mechanics point of view, the supply of personalized air from a headset-installed PV nozzle refers to a jet (personalized flow) inserted in a transverse flow (the upward free convective flow). The amount of clean personalized air provided into inhalation will depend on the interaction between the inserted jet and the free convective flow. The interaction depends on the characteristics of the inserted jet and the free convective flow as well as on the direction of the inserted flow. As defined in [9] personalized flow can be supplied horizontally, upward or downward, i.e. transverse, opposing and assisting the upward boundary layer flow. The characteristics of the free convective flow (strength, thickness, etc.) depend on factors such as: the difference between the surface body temperature and the room air temperature, the body shape and its posture, and the clothing ensemble etc. ([2], [19] – [23]). Within the room air temperatures of 20 - 24 °C (the lower range of comfortable room air temperatures) the maximum velocity in the free convective flow at the face region can be as high as 0.25 m/s. The characteristics of the personalized flow depend on the design, size and shape of the air supply nozzle (circular, elliptical, rectangular, etc.). Khalifa et al. [24] and Russo et al. [25] used a co-flow PV nozzle to control the characteristics and thus the development of the personalized flow. They succeeded in increasing substantially the length of the clean air zone of the personalized flow. The initial velocity and turbulence intensity profile can affect significantly the characteristics of free air jets. As reported in the literature ([26], [27], [38]), lobed free jets from nozzles with lobes integrated in the design geometry have completely different characteristics (distribution of velocity, spread of the flow, entrainment ability, etc.) which can be controlled by change the shape, size, etc. of the lobes. The lobed lip edges allow the increase of the shear boundary between the primary and the secondary flows. Then, jet induction boundary increases whereas effective injection area is kept constant. Furthermore, the lobed lip edge of the nozzle generates large streamwise structures known as responsible for jet induction phenomenon ([26], [27], [38]). Therefore, the use of lobed jets as personalized flow may be efficient for improving the performance of PV in general and in particular the performance of PV based on inserted jets, such as the headset PV: a smaller nozzle would be able to cover a larger area around the mouth (the inhalation hemisphere region).

Previous research [11, 18] as discussed shortly above has revealed the high potential of inserted jets for controlling the air quality performance of the PV. However, the results have been obtained under limited conditions with limited control over the characteristics of the personalized flow and thus the airflow interaction at the breathing zone. Therefore a study was designed to identify the effect of the initial velocity, the distance from and the positioning relative to the face as well as the size and the shape of the outlet (circular, elliptical or lobed) of the inserted jets and their ability to provide clean air to inhalation. Some of the results obtained are presented in this paper.

METHODS

Experimental set-up

The experiment was designed and performed in a full-scale test room with dimensions 4.70 m × 1.62 m × 2.60 m (W×L×H). Three ceiling-mounted light fixtures (6 W each) provided the background lighting. A workplace consisting of a desk with a seated breathing thermal manikin, an ordinary light office chair (≈ 0.05 Clo based on contact with the manikin) and different personalized ventilation ATDs that generated the inserted personalized jet, were used in the set-up (Figure 1).

The test room itself was built in a laboratory hall, 0.7 m above the floor. The laboratory hall had a separate ventilation system allowing for temperature control and hence reduced heat transfer (the air temperature of the laboratory hall was kept the same as that of the test room itself). The walls of the test room were made of particleboard and were insulated with 0.06 m thick styrofoam plates. One of the walls was made from thick single-layer glazing (the non-hatched area on Figure 1a).

Total volume ventilation

Mixing type ventilation was used to condition the air in the test room. The air supply diffuser (a rotation diffuser) and the air exhaust diffuser (a perforated circular diffuser) were installed on the ceiling (Figure 1). The supplied air was 100% outdoor (no recirculation was used) with a flow rate of 15 L/s, which corresponded to an air change rate of 2.7 h^{-1}. This flow rate provided good mixing in the room with relatively low velocities (less than 0.15 m/s). A slight under-pressure of 1.4 Pa, resulting in 30 L/s at the exhaust, was kept during all the experimental conditions in order to avoid a flow of air from the test room to the tall hall.

The supply air temperature (21 ^{o}C) and flow rate (15 L/s), as well as the exhaust flow rate were controlled during all the measurements.

Personalized ventilation

A separate HVAC system was used to supply the personalized air at a specific controlled temperature and flow rate. The temperature of the supplied PV air was controlled by an electric heater installed downstream of the main fan with a temperature sensor placed close to the PV ATD. The humidity of the supplied PV air was not controlled, but was close to that in the room due to the fact that the PV air was supplied at the same temperature as the room air, and both were 100% outdoor air. Because of the high pressure loss generated in the PV system three fans with similar characteristics were connected in series with more than 1 m distance between them to minimize the pressure fluctuations. To avoid excessive heating of the supplied PV air due to the high resistance of the system, a T connection with 2 dampers were set downstream of the fans in order to control the amount of air supplied towards the nozzle. The excess air was always led out into the laboratory hall.

Nine headset nozzles were chosen to be tested: three with a circular initial cross-section of diameters 0.025 m, 0.030 m and 0.035 m respectively, three nozzles with an elliptic initial cross-section and equivalent diameters of 0.025, 0.030 and 0.035 m (Figure 2a) and three lobed jet nozzles with circular, four-leafed clover and six-edged star shapes with a free area equal to the free area of a circular jet of a diameter of 0.025 m (Figure 2b). The circular and elliptic nozzles had the shape of a cone with a slope angle of 7^{o} and a fine mesh at the end. This was done in order to distribute the flow more homogeneously across the discharge surface and at low turbulence intensity and also to obtain maximal length of the potential core region of the generated jet. The cones were made of copper sheet of thickness 0.005 m. The lobed nozzles were cut on a plastic hemisphere with a diameter of 0.045 m and a wall thickness of 0.002 m. The particular shape of the lobed jets used was chosen based on results of previous studies on lobed orifice jets ([27], [38] – [42]). For aesthetics aspect, the lobed orifices are integrated in this study on hemispherical instead of on a flat plane. The hemispherical nozzle with circular orifice (widely used for ventilation air supply), was chosen as a reference for the other two lobed nozzles as well as for comparing the cone nozzle with circular exit. Flexible pipe was used to transport the personalized air to the nozzles. A specially designed mechanism was used to secure firm positioning of the nozzles. The mechanism was attached to a traverse that allowed for

fine adjustment in all three planes of a Cartesian coordinate system relative to the facial plane of the manikin on the X (forth and back 0.20 m), Y (left and right 1.50 m) and Z (up and down 0.22 m) axes. The set-up of the nozzles and the coordinate system are defined in Figure 1b.

Breathing thermal manikin

A breathing thermal manikin with body shape and size of an average Scandinavian woman 1.7 m in height, was used to resemble a seated occupant. The manikin is made of a 0.003 m fibreglass-coated polystyrene shell and is divided into 23 segments. Each of these segments is equipped with heating and temperature measuring wiring controlled by a computer program so as to maintain a surface temperature equal to the skin temperature of a person in a state of thermal comfort at the actual activity level, and thus realistically recreate the free convective flow surrounding the human body. The control of the manikin is described by Tanabe et al. [28].

The artificial lung of the breathing thermal manikin simulated the breathing cycle of an average healthy person performing light physical work: 2,5 s inhalation, 2,5 s exhalation and 1,0 s break with a respiration flow rate 0,24 L/s [14]. The air exhaled by the manikin was warmed to give 33.6°C at the mouth, in order to ensure a density close to that of air exhaled by a human being (1.14 kg/m^3).

Different breathing modes can be simulated with the artificial lung [29]. During these experiments the breathing mode was set to inhalation through mouth exhalation through nose. Inhalation and exhalation through the mouth may be common for many people when talking. However, breathing only through the mouth was not used because due to the design of the airway system the uncertainty in measurement of the gas concentration in inhaled air was relatively high. An exhalation through the nose creates two jets at an angle of 45^o with the horizon and an intervening angle of 30^o. The two jets with an initial velocity of about 1.85 m/s will diffuse as two separate jets in the surrounding air [14]. When the exhalation is through the mouth only one jet (with initial velocity of 2.4 m/s for the mouth opening of the used manikin) will result. In both cases the exhaled jets will disturb the inserted jet due to the close positioning of the PV nozzle with respect to the mouth/nose. This, however, will not affect the ability of the inserted jet to provide air to the inhalation because it is recovered during the 1 s break between exhalation and inhalation (study not published yet).

Experimental conditions

The total heat load generated in the test room was 88 W (12 W/m^2). The experiments were performed at an air temperature of 23 ^oC (as it is the boundary between winter and summer comfortable room air temperatures recommended in the present thermal comfort standards [30], [31]) and under isothermal conditions, i.e. room air temperature equal to the personalized air temperature. The manikin was positioned with its abdomen at a distance of 0.1 m from the edge of the desk. During the measurements the manikin was dressed in underwear, t-shirt, cotton trousers, light socks and trainers (clothing thermal insulation of 0.6 clo). The manikin was wearing a short wig just below the ears during all experiments. The manikin was set to resemble an occupant in a state of thermal comfort at light sedentary activity, namely office work, with the corresponding dry heat loss of 1.2 Met, i.e. 69.8W [30].

The personalized airflow rate was chosen to provide an initial jet velocity of 0.2, 0.4 and 0.6 m/s. The lowest velocity chosen was 0.2 m/s to be able to withstand and oppose the free convective flow at the facial plane of the occupant. Velocity lower than 0.2 m/s might result in full deflection of the jet upwards even though the nozzle is inside the boundary layer. The velocity of 0.6 m/s was substantially higher than the velocity of the convective flow. Higher velocity could result in an unpleasant sensation and draught for the user, i.e. “too localised effect”, as reported by Kaczmarczyk et al. [10]. The experimental combinations are summarised in Table 1.

The distance between the face of the manikin and the nozzles (0.02, 0.04, 0.06 m) was one of the parameters studied during the experiments as well.

For the headset circular nozzle of diameter 0.030 m, additional measurements were performed that studied the effect of positioning the device relative to the face of the manikin, namely from front, below and side (Figure 3)

Tracer gas, Freon R134a, was used to simulate pollution/airborne pathogens laden nuclei (d < 2 μm) in the room air. During the measurements a constant dose of tracer gas was supplied in the duct of the background total volume ventilation system upstream of the ceiling diffuser. After passing the plenum box and the rotation diffuser, the tracer gas was well mixed with the air supplied into the room. The personalized air was free of tracer gas. The air exhaled by the manikin was outdoor clean air with no tracer gas in it. The air inhaled by the manikin, after being analysed, was exhausted in the TV exhaust system so as to avoid pollution of the tall hall where the climate chamber was situated. During all the measurements the lungs were situated outside of the experimental chamber.

Measured parameters and measuring equipment

The tracer gas was sampled at 5 points and its concentration was measured by a real-time gas monitor based on the photo-acoustic principle of measurement. The positioning of the 5 sampling points is shown in Figure 1. Measurements at Point S3 (Figure 1), positioned at 1.1 m above the floor, were used to justify whether or not good mixing in the room was achieved, i.e. when the concentration in the supply, in the exhaust and at the point S3 was close and within 2 to 4 % difference.

The personalized airflow rate was measured with the help of a Venturi tube with an outer diameter of 0.025 m and inner diameter of 0.008 m [32]. The Venturi tube was calibrated prior to the experiments using a linear Fleish pneumotachograph for spirometry medical manipulations with a sampling frequency of 100 Hz and an accuracy of ± 5% when in the operating range for the flow rate of 0.02 to 16 L/s [33]. To avoid incorrect readings from the Venturi tube, a straight PVC pipe section of 12 diameters was placed upstream and downstream the measuring device. The pressure difference at the Venturi tube was measured with a differential pressure micromanometer (accuracy of 0.01 Pa ± 0.25% of reading). The flow sensor with a diameter of 0.08 m was installed in the duct of the PV system close to the nozzles. The required flow rate was adjusted by a manually operated damper according to the pressure difference readings taken from the micromanometer.

Criteria for assessment

The inhaled air quality was assessed by the Personal Exposure Effectiveness index (PEE) introduced by Melikov et al. [8]. The PEE represents the portion of clean personalized air in the air inhaled by an occupant and is defined as PEE = $(C_{I,0}-C_I)/(C_{I,0}-C_{PV})$, where $C_{I,0}$ is the pollution concentration in inhaled air without PV, C_I is the pollution concentration in inhaled air with PV, and C_{PV} stands for pollution concentration in the personalized air supplied by the PV unit. PEE equals 1 (or 100%) when only clean personalized air is inhaled, i.e. best performance of the personalized ventilation. PEE equal to 0 (or 0%) means that the inhaled air consists of 100% polluted room air.

Procedure

The air temperature in the test room and in the laboratory hall was set 24 hours prior to the measurements in order to achieve steady-state. The air temperature in the laboratory hall was kept equal to the temperature in the test room. At the start of the experiments the thermal manikin and the artificial lung were switched on, the personalized air temperature and flow rate were adjusted and the dosing of tracer gas initiated. All measurements commenced after steady-state conditions were achieved, i.e. constant Freon concentration monitored at the sampling point S3 (Figure 1) and constant heat flux from the manikin.

For each experimental condition, tracer gas concentrations were measured 20 times at all 5 points and the heat flux, the surface temperature for each body segment, and the average surface temperature for the whole body of the manikin were recorded for 5 minutes.

The experiments performed at the air temperature of 23 ^{o}C (different flow rates, nozzles, etc., Table 1) were completely randomised to avoid biasing. During all measurements the temperature conditions were kept constant. A laser beam level meter was used to align the nozzles when changed in order to minimize the difference in position of the nozzles and thus to minimise the uncertainty of the measurements.

Uncertainty of measurements

The measured data were analysed in accordance with ISO guidelines for the expression of uncertainty [34]. The sample standard uncertainty was calculated as the maximum uncertainty of measurement (random error). The absolute expanded uncertainty with a level of confidence of 95% (coverage factor of 2) is listed in Table 2.

RESULTS

In Figure 4 the results obtained for the PEE with the inserted jet supplied from the nozzles with equivalent diameter of 0.025 m at initial velocities of 0.2, 0.4 and 0.6 m/s (Table 1), and at the three distances from the mouth, 0.020, 0.040 and 0.060 m, are compared. The results were obtained with nozzles positioned in front of the face and towards the mouth, i.e. with the inserted jets against the face of the manikin transverse to the free convective layer around the body. The closer the nozzle to the mouth and the higher the velocity, the higher the PEE value. The results clearly showed the importance of control of the characteristics of the PV flow for the inhaled air quality. The PEE achieved with the lobed jet of clover nozzle geometry was the lowest and only little or no change in PEE was documented, regardless of the distance of the nozzle from the face and the supplied flow rate. As will be discussed later in the paper, this low performance resulted from the

“closing” of the orifice centre. In fact, this centre-closed geometry does not allow forwarding clean air on the breathing zone. The PEE obtained with the star lobed jet was better than the jet from the clover nozzle but still not as high as the PEE values obtained with the circular or the elliptical nozzles when positioned at distance 0.02 m = 0.8D from the mouth. However, at 0.04 m = 1.6D and 0.06 m = 2.4D and velocity of 0.4 m/s (Re_0= 667) the six-star lobed jet performed equally well compared to the circular and elliptic jet, and at 0.6 m/s (Re_0= 1000) it became even superior in air quality performance. An explanation of the six-star lobed jet results will be given later in the paper through analysis of vortex dynamics generated by the lobed orifice shape. The results in Figure 4 clearly point out the hemisphere nozzle with circular exit jet as the one performing best with highest PEE values for the highest supply flow rate and largest distance from the face. This particular result remains to be analyzed by detail measurement of velocity distribution fields since the diameter of the potential core (non-mixed air jet) at the interest position (0.06 m) depends on the inlet Reynolds number and other parameters such as the initial turbulence level, the momentum thickness and the shape factor of the jet boundary layer. Furthermore, the Kelvin-Helmholtz vortex ring and streamwise structure development which control entrainment phenomenon [27], [42[) and thus in this case jet mixing with pollutant ambient air, also depend on the previous parameters.

Figure 5 shows the impact of the initial diameter of the inserted jet on the PEE index. The results in the figure were obtained with the circular shaped headset nozzles with three different diameters (D = 0.025, 0.030 and 0.035 m), at the three distances and the three velocities tested. The inserted jets were generated with nozzles positioned horizontally towards the manikin’s face, i.e. with the geometric center of the PV orifice aligned with the center of the manikin’s mouth. All the circular nozzles showed the same trend of increasing the amount of clean PV air in inhalation with the increment of the supply velocity. Both the initial diameter of the nozzle, the initial velocity and the distance of the nozzle from the face were parameters that influenced the PEE index. The greater the diameter, the more air was supplied to achieve the same initial velocity, and hence more cleaner air into inhalation resulting in a maximum PEE value of 0.92 achieved with the circular nozzle of diameter 0.035 m, initial velocity of 0.6 m/s and a distance of 0.020 m frontally towards the mouth. The distance was another important factor: the further the nozzle was moved from the mouth the lower the PEE value. The mixing of the PV jet with the free convective flow entraining polluted room air on its way upwards towards the mouth resulted in a PEE below 100% even when the nozzle was just 0.020 m away from the mouth and the supply velocity was as high as 0.6 m/s.

In Figure 6 results obtained with the elliptical nozzles under similar conditions as those in Figure 5 are shown. The PEE values increase either with the increase of the initial velocity (0.2, 0.4 and 0.6 m/s) of the inserted jet, or with the increase of the initial equivalent diameter of the nozzle (0.025, 0.030 and 0.035 m) or with the decrease of the distance between the nozzles and the mouth (0.060, 0.040 and 0.020 m). The maximum PEE=94% was achieved with the largest nozzle (diameter of 0.035 m) at 0.6 m/s initial velocity and 0.020 m frontal distance from the mouth.

As the performance of the round jet with a diameter of 0.030 m was slightly better than that of the elliptical jet (Figure 5 and Figure 6), the former nozzle was chosen for investigating further the effect of the direction on the inserted jet performance to supply clean air to inhalation. Results of these tests are compared in Figure 7. Only the personalized flow with an initial velocity of 0.4 m/s, able to penetrate the free convective flow at the face region (with a velocity of approximately 0.2 m/s) without causing discomfort due to draught and “dry” eyes”, was studied. In Figure 7 the PEE values are compared for the tested round nozzle when positioned to generate inserted jet of personalized air from the front, from the side and from below. For the shorter distances of 0.020 and 0.040 m studied, the direction of insertion of the jet had almost no effect on the overall air quality performance. However, at the distance of 0.060 m the best performance was obtained when the inserted jet was directed from the side. The reason might be that the side positioning allowed a larger section of the potential core of the personalized flow to cover better the mouth of the manikin. When supplied from the side, the potential core of the inserted jet (positioned longitudinal to the mouth) covered a larger area of the mouth compared to the other two cases, from front and from below. This was clearly seen with the increase of the distance between the nozzle and the mouth. The cross section area of the potential core of the jet reaching the mouth decreased with the increase of the distance and this caused decrease in the amount of clean air in the total inhaled air. Furthermore the personalized jet, when supplied from the side, attached to the cheek and followed the natural curvature of the face over the cheekbone and ending up at the mouth (“Coanda effect”). This result remains to be studied by detail measurement of velocity distribution filed at the mouth (for example by Particle Image Velocimetry).

DISCUSSION

In the present study, the use of inserted jets as an efficient strategy for design of personalized ventilation was examined. The possibility of clean air supplied into inhalation by control over the personalized flow and its interaction with the boundary layer at low flow rates, was explored. The initial characteristics of the inserted personalized flow were changed by utilizing nozzles of different shapes and sizes. The importance of initial velocity and size of the inserted jet, the distance between the air supply nozzle and the mouth and the direction of introducing the inserted flow into the boundary layer was studied, based on the amount of clean air in the air inhaled by the breathing thermal manikin. The results revealed that the initial size, velocity and direction of the inserted jet, as well as the distance between the nozzle and the mouth of the manikin, are important parameters affecting the flowinteraction close to the face of a seated occupant. The PEE index increased with the increase of the initial velocity (i.e. with the flow rate of the supplied personalized air), with the size of the inserted jet opening, or with the decrease of the distance between the nozzle and the mouth (Figures 4, 5 and 6). When the distance between the face and the inserted jet increased above 0.040 m, the direction of the inserted jet when supplied transverse to the free convective flow from front or side (tangentially) or from below relative to the face, had an effect on the amount of clean air in the inhaled air (Figure 7). When supplied from the side the jet followed the natural extension of the mouth and thus covered better the inhalation region around the mouth and resulted in better air quality performance.

Of all nozzles tested, the circular and the elliptical performed equally well in supplying clean air into inhalation (Figure 5 and Figure 6). However, the elliptical resulted in a slightly higher PEE value for the largest equivalent diameter tested (0.035 m). Though the areas of the ATDs were the same (Table 3), the major diameter of the ellipse (0.040 m) was greater than the equivalent diameter (0.035 m), and it covered better the inhalation region around the mouth, resulting in larger amounts of clean air inhaled. It is important to note that the distance between the nozzles and the mouth was kept bellow 2.4 equivalent diameters. In the case of the elliptical jet the distance was less than 1.5 major nozzle diameters, i.e. the region in the elliptic jet where its major diameter propagation direction remained almost unchanged [35]. Zhu et al. [18], based on CFD simulations of a headset PV device (discussed in the introduction), predicted that over 85% of the inhaled air will be from the air inserted by the jets from either the circular or the elliptical nozzles with an equivalent diameter of 0.030 m when positioned at 0.04 m from the face. Under the same conditions, the present measurements identify that a maximum 62% of the inhaled air will be PV air. Differences in the initial velocity 0.47 m/s for the CFD simulations and 0.4 m/s for the measurements and in the boundary conditions

(shape of the face, free convection flow, etc.) can explain this result. Both the CFD predictions and the present results show very little effect of the shape of the nozzle for the distance of 0.04 m from mouth (Figure 7).

The possibility of controlling the characteristics of the inserted jet by introducing a lobed nozzles design was explored in the present study as well. It has been reported that lobed geometry nozzles have wider initial spread and increased mixing compared to the free circular jet ([27], [38] – [42]). For the close distances between the lobed nozzles and the face, studied in the present measurements, the initial side spread was considered beneficial, because the inserted jet would better cover the mouth and the adjacent inhalation zone, resulting in higher PEE. The results, however, did not validate this expectation. The lowest PEE obtained was with the four-leafed lobed nozzle (Figure 4). The six-edged star lobed jet performed equally well compared to the circular and the elliptical nozzles for the distance of 0.04 m and 0.06 m from the mouth and velocity of 0.4 m/s. At the higher velocity of 0.6 m/s the six-edged star lobed jet performed better than the tapered circular jet and the elliptic jet.

In order to analyze the phenomena at the origin of the important difference between 6 star lobed jet performance and the 4 clover lobed jet, we performed flow visualization in the interest zone between X=1De and X=3D (Figure 8). The flows were considered as free and the initial Reynolds number was taken equal to 700. This value falls between the values of 667 and 1000 previously used for the PV lobed nozzles. All the three values of Reynolds number fall in the transitional regime. Since these Reynolds number values are very close, the free flow development should be the same. In order to facilitate the observation of the involved phenomena, the nozzles were considered on flat surface (i.e. orifices on plates having a thickness of 0.002 m); 4 clover lobed nozzle and 6 lobed nozzle star were compared with a circular reference nozzle.

The first observation which we can make on these visualizations, is the presence of an axis switching phenomenon in both lobed jets (Figure 8 b and c), which is characteristic of orifice lobed jets ([27], [38], [42]). Contrary to the circular jet which preserves the initial shape (Figure 8 a), the lobed jet undergoes a geometrical transformation which produces an effect of an apparent jet rotation. Lobes develop in orifice troughs at the same time as the progressive disappearance of the initial lobes (Figures 8 a, 8 c). In 6 star lobed jet, this phenomenon appears earlier than in 4 clover lobed jet. The second important observation is the behaviour of the 4 clover lobed jet. On the visualization images the jet flow is coloured in grey and the black colour indicates the absence of jet flow, i.e. the background air. In the interest zone of the jet for

headset PV (X<3 D), the 4 clover lobed jet forms a central core without jet flow (Figure 8 b). Consequently, this centre-closed geometry does not allow forwarding clean air to the breathing zone. That explains the weakness of its performance.

The axial velocity evolution (Figure 9) confirms the previous observation. Besides, the results suggest that the 4 clover lobed jet could become integrated advantageously into desk-mounted PV units where the distance between the breathing zone of the occupant and the orifice will exceed 7 equivalent diameters. Indeed, from the axial distance of 7D, the central flow deficit disappears. Nevertheless, the speed in the centre of the jet is lower than in the circular reference jet until X = 20 D where both speeds become equal. This characteristic will avoid an unpleasant sensation and draught for the user, though the air mixed with the room air will be less clean. Furthermore, the axial component of rotational field obtained with the PIV measurements shows a double crown of counter-rotative vortices (Figure 10 b) generated by the double line of shear due to the central closing of the orifice. In the absence of a central closing, a single crown of counter-rotative vortices exists (Figure 10 c). The double crown of counter-rotative vortices of 4 clover lobed jet reduces the mixing with the surrounding polluted room air, increasing the length of the clean air zone. This second characteristic will favour the quality of inhaled air when the PV system is placed relatively far from the breathing zone. Thus, in our future works it should be interesting to evaluate this geometry in desk-mounted PV configuration.

Concerning the 6 star lobed jet, the axis-switching phenomenon comes along with a strong entrainment which reaches 2.5 times that of the circular jet at the axial distance X = 1 D [38]. This fact would explain the low value of Personal Exposure Effectiveness index when this jet is used close to the face (0.02 m = 0.8 D and 0.04 m = 1.6 D). Beyond X=2D, the entrainment is on average 50 % higher to that of the reference circular jet [38]. However, as revealed by streamwise axial velocity of 6 lobed star jet compared with that of the circular reference jet (Figure 9), the dilution of the lobed jet remains peripheral and the jet centre core is less mixed than that of the circular jet. This is also visible on jet flow visualizations (Figure 8 a and c). In fact, in the circular jet at X=3 D the Kelvin-Helmholtz vortex ring (Figure 8 a) is large in size in comparison to the jet core size. This Kelvin-Helmholtz vortex ring assures ambient air engulfment toward the jet core which is harmful for inhaled air quality. In the 6 star lobed jet, the Kelvin-Helmholtz structures are very small [38] and the flow is dominated by 6 large scale streamwise structures which assure ambient air entrainement continuously. At X=3De the 6 star lobed jet non-mixed core (Figure 8 c) is larger then the circular jet non-

mixed core region (Figure 8 a). This characteristic would explain the slightly better performance observed previously for 6 star lobed jet for a distance of 0.6m=2.4D. This behaviour (strong entrainment with a weak mixed central core) was observed the first time for a cross shaped orifice jet [39]. It was shown in particular that the strong entrainment and the fast decrease of mean velocity (the mean velocity is given by the ratio between the jet flow rate and the jet flow area at each streamwise position) in comparison to the circular reference jet, is concomitant with an inverse tendency for the streamwise axial velocity evolution: axial velocity decrease is not as fast in the lobed jet as in the circular jet.

The result on the high performance of the six-edged star lobed jet obtained in the present study is important. It reveals the potential application of lobed jet for personalised ventilation, as an extension to the global room ventilation application ([39]). Further measurements by optical techniques such as LDA, LIP or PIV are needed for in-depth analyses of the structure of this flow, in particular when the flow is close to the manikin face.

All nozzles tested had a cross-sectional area much larger than that of the manikin's mouth of 0.000100 m^2 (100.4 mm^2) [30], (Table 3). Moreover, at the lowest studied velocity (0.2 m/s), the supplied flow rate of the inserted jet was always lower than the inhalation flow rate (0.24 L/s). Therefore relatively low PEE values were obtained. In this case the strength/momentum of the inserted jet was also insufficient to completely penetrate the free convection flow. Velocity measurements performed by Particle Image Velocimetry on the convective layer surrounding the seated thermal manikin (not discussed in this paper) revealed that at a room air temperature of 20 ^oC the maximum velocity (0.18 m/s) in the boundary layer at the face occurs at a distance of approx. 0.006 m frontally from the mouth and it is at maximum 0.25 m/s at distance of 0.010 m. Due to the lower velocities of the inserted jet compared to those of the free convection and their transverse direction, intensive mixing is promoted at 0.2 m/s. In contrast, much higher PEE values were measured with the nozzle with an equivalent diameter of 0.025 m when the initial velocity was 0.4 and 0.6 m/s. Yet, 100% clean air in inhalation was not achieved, even in the case when the distance was 0.02 m and the velocity was 0.6 m/s. As already mentioned, during inhalation the air close to the mouth/nose flows from all directions and therefore the amount of free convective air inhaled depends on the cross-section and the shape of the inserted jet at the target area, i.e. whether it is smaller, equal or overlapping the area of the mouth/nose. Furthermore, the free area of the mouth changes when people speak. This has to be considered and studied as well. In this respect more research on active control of the characteristics of the inserted jet is needed. A

possible way to improve the air quality performance of the inserted jet is to reduce the strength of the free convective flow in order to make its penetration easier. Further improvement can be achieved by use of the headset device in conjunction with displacement ventilation because the cleaner air close to the floor will be naturally brought upwards by the boundary layer. However, this concept needs to be further investigated.

The importance of the initial characteristics of the inserted jet on its interaction with the free convective flow and thus on the inhaled air quality was clearly demonstrated in the present study by the results obtained with the two circular jets tested: the circular jet from the tapered (conical) nozzle and the circular jet from the hemispherical nozzle (Figure 4 – respectively “circular tapered” and “circular hemispherical nozzle”). The circular jet from hemispherical nozzle with circular opening performed much better than the circular jet from the tapered/conical nozzle. The portion of clean air in the air inhaled with the hemispherical nozzle with circular exit was almost twice as much as with the tapered circular nozzle. This result shows the potential for control of the jet by changes in the geometry of the nozzle. One advantage of the application of inserted jets for personalized ventilation is that inserting the clean air jet into the free convective flow at the breathing zone will result in reduced amounts of PV air supplied. Figure 11 compares the PEE values as a function of the supplied flow rate obtained in the present study with the circular and elliptic nozzles (diameter of 0.035 m) when placed at a distance of 0.06 m from the mouth, with results obtained from several other PV designs previously reported in the literature. The use of the inserted jet made it possible to obtain similar PEE values to those obtained with the other PV devices, but at lower flow rates reduced more than 10 times. Bolashikov et al. [11] supplied the clean air transverse to the convective flow and far from the face (0.40 m) with an ATD with an initial diameter of 0.18 m. As can be seen in the figure, reduction of the distance between the face and the air supply nozzle, as applied in the present study, resulted in a substantial decrease in the supplied airflow rate needed to obtain the same amount of clean air into inhalation as compared to other designs. Melikov et al. [12] supplied the PV air also transverse to the free convective flow but from the headrest of a chair. This resulted in higher performance of the unit due to the closer positioning of the nozzles at the breathing zone (95% of the inhaled air was clean PV air). Yet, the PV flow rate supplied was relatively high (10 L/s). Bolashikov et al. [37] added to the chair design additional control nozzles that inserted gently small amounts of additional clean air (3 L/s) within the free convective flow, resulting in enhanced air quality and improved personal protection from airborne pathogens, but this strategy also increased the demand for clean PV air. Nielsen et al. [13] “injected” the clean air at low momentum within the free convective flow with a PV

unit designed as a textile “doughnut” around the neck (named “neck support”). The device achieved 95% of clean air into the air inhaled only for flow rates above 8 L/s.

The localized inserted flow will not affect the whole body thermal sensation of users. However, it may cause local discomfort when the initial velocity is high. Kaczmarczyk et al. [10] in human subject experiments used a rectangular nozzle incorporated in a headset that generated a flow with an initial velocity of 1.7 m/s. At this speed some human subjects who participated in the experiments reported an unpleasant sensation at the mouth. In the present study, the maximum initial velocity of the studied inserted jets was 0.6 m/s, i.e. almost three times lower. It may be expected that such a velocity will not be felt as unpleasant.

It may be expected that from an aesthetical point of view a headset PV with an inserted jet nozzle and an elongated shape following the natural profile of the mouth will be preferred rather than a bulky circular end. Aesthetics is another factor for studying with inserted jets with nozzles of different geometry. The low flow rate of personalized air makes the headset PV device a feasible solution in crowded places such as trains, buses, aeroplanes, theatres, auditoriums, classrooms, etc., where the device would be used to provide clean air as well as an intelligent means to decrease the risk of airborne cross-infection. The device can be easily manufactured as a “plug and use” unit into a desk, chair/seat hand support, PC (via USB port), etc. in a similar way to the headsets used today for listening to music, radio, etc.

The application of inserted jets in wearable PV units may additionally result in certain energy savings, especially in buildings where the ventilation airflow rate needed for acceptable indoor air quality is higher than the ventilation airflow rate needed for thermal comfort. In this case the supplied indoor air could be 100% recirculated room air for even further energy savings.

CONCLUSIONS

A novel method for control of the airflow interaction at the breathing zone by inserting clean air into the free convective flow of polluted air, aiming at improved inhaled air quality and protection from airborne disease contamination at a reduced supply flow rate, was studied under isothermal conditions with a breathing thermal manikin.

The amount of the clean air supplied by the inserted jet in the inhaled air increased with the increase of the initial jet velocity (i.e. the supply flow rate) and size and with the decrease of the distance between the air supply nozzle and the mouth. More than 80% clean “inserted” air in the inhaled air was measured when the

inserted jet with an initial velocity of 0.4 m/s and higher was supplied from a nozzle with an equivalent diameter of 0.030 m (and larger) placed at a distance of 0.040 m (and closer) from the mouth.

More clean air was inhaled with the inserted jet from the side than from the front and below when the distance between PV nozzle and face (mouth/nose) exceeded 0.04 m.

The portion of the clean air into inhalation, when supplied from a nozzle with an elliptical shape, was slightly more than when supplied from a circular nozzle, due to similarity of the geometry of the former with the mouth.

The use of lobed hemispherical and circular hemispherical nozzles changed substantially the characteristics of the inserted jet and thus the portion of clean air in the inhaled air. In this respect, the potential of the lobed jets needs to be studied further.

The use of inserted jets in practice for PV application has great potential that requires additional research. Wearable PV devices, such as headset incorporated PV ATDs, can be further optimized and used for improvement of inhaled air quality and decrease the risk from airborne cross-infections in practice, especially in densely occupied places (aeroplanes, trains, buses, theatres, classrooms, hospitals, etc.). The potential energy savings from wearable PV units based on inserted jets, when used in office buildings during different seasons and climates, needs to be explored in details.

ACKNOWLEDGEMENT

This research was supported by the Danish Agency for Science Technology and Innovation. Project No. 09-064227.

REFERENCES

[1] Bolashikov. Z.D.. Melikov A.K.. 2009a. Methods for air cleaning and protection of building occupants from airborne pathogens. *Building and Environment*. 44 (7). p.1378-1385.

[2] Melikov. A.K.. 2004. Personalized ventilation. Indoor Air 14 (7). pp. 157-167.

[3] Kaczmarczyk J., Melikov A.K., Fanger. P.O., 2004. Human response to personalized and mixing ventilation. *Indoor Air* 14 (I8). pp. 1-13.

[4] Cermak R.. Melikov. A.K.. 2007. Protection of occupants from exhaled infectious agents and floor material emissions in rooms with personalized and underfloor ventilation. *HVAC&R Research*. 13(1). pp. 23-38.

[5]

[6] [7] Faulkner D., Fisk W. J., Sullivan D. P., Lee S. M., 2002 – ”*Ventilation Efficiencies of a Desk-Edge-Mounted Task Ventilation System*”, Proceedings of Indoor Air 2002, Monterey, California, June 30-July 5, 2002.

[8] Melikov A.K., Cermak R., Majer M., 2002, Personalized ventilation: evaluation of different air terminal devices. *Energy and Buildings* 34. pp 829-836.

[9] Melikov, A.K., Cermak, R., Kovar, O., Forejt, L., Impact of airflow interaction on inhaled air quality and transport of contaminants in rooms with personalized and total volume ventilation, *Proceedings of Healthy Buildings* 2003, Singapore, 7-1 National University of Singapore, Department of Building, vol. 2, pp. 592-597.

[10] Kaczmarczyk, J., Melikov, A.K., Bolashikov, Z., Nikolaev, L. and P.O. Fanger, 2006, *Human response to five designs of personalized ventilation*, International Journal of heating, Ventilation and Refrigeration Research 12 (2), pp.367-384.

[11] Bolashikov. Z.. Nikolaev. L.. Melikov. A.K.. Kaczmarczyk. J. and Fanger. P.O.. 2003. Personalized ventilation: air terminal devices with high efficiency. *Proceedings of Healthy building 2003. Singapore*. 2. pp. 850-855.

[12] Melikov, A.K., Ivanova, T., Stefanova, G., 2007, Seat incorporated personalized ventilation, In: Proceedings of the 10th *International Conference on Air Distribution in Rooms - Roomvent* 2007, Helsinki, C05, paper 1318.

[13] Nielsen P.V., Bartholomaeussen N.M., Jakubowska E., Jiang H., Jonsson O.T., Krawiecka K., Mierzejewski A., Thomas S.J., Trampczynska K., Polak M and Soennichsen 2007, Chair with integrated personalized ventilation for minimizing cross infection, Proceedings of the 10th *International Conference on Air Distribution in Rooms - Roomvent* 2007, Helsinki, Finland, Paper ID: 1078.

[14] Hyldgaard. C. E. 1994. *Humans as a source of heat and air pollution*. In: Proc. ROOMVENT '94. 4th Int. Conf. on Air Distribution in Rooms. Krakow. Poland. pp. 414-433.

[15] ASHRAE. 2007. *ANSI/ASHRAE Standard 62.1-2007. Ventilation for Acceptable Indoor Air Quality. American Society of Heating. Refrigerating and Air-Conditioning Engineers. Inc.*

[16] European Standard 2007. EN 15251 2007. *Indoor environmental input parameters for design and assessment of energy performance of buildings addressing indoor air quality. thermal environment. lighting and acoustics*. EUROPEAN COMMITTEE FOR STANDARDIZATION. B-1050 Brussels.

[17] Niu J, Gao N, Phoebe M, Huigang Z. Experimental study on chair-based personalized ventilation system. Building and Environmnet 2007;42:913–25.

[18] Zhu S.W., Bolashikov Z., Melikov A.K., 2008, Examination on performance of headset incorporated personalized ventilation unit using CFD method. Proceedings of Indoor Air 2008. 17-22 August 2008. Copenhagen. Denmark - Paper ID: 1018.

[19] Lewis H.E., Foster A.R., Mullan B.J., Cox R.N. and Clark R.P., 1967, Aerodynamics of the human microenvironment, *The Lancet 1969*, Vol. 1, Nr 7609, pp 1273 – 1277.

[20] Homma H. and Yakiyama M.. 1988. Examination of free convection around occupant.s body caused by its metabolic heat. *ASHRAE Transactions 1988*. 94 (1). pp. 104-124.

[21] Melikov, A.K., Zhou, G., 1996, Air movement at the neck of the human body, *Proceedings of Indoor Air 1996*, July 21-26 1996, Nagoya, Japan, vol.1, pp.209-214.

[22] Özcan, O., Meyer, K. E., Melikov, A., 2003, Turbulent and Stationary Convective Flow Field Around the Head of a Human, *Proceedings of International Symposium on Turbulence, Heat and Mass Transfer - THMT-03,* October 12-17, 2003, Antalya, Turkey.

[23] Özcan, O., Mayer, K.E. Melikov, A.K., 2005, A visual description of the convective flow field around the head of a human, Journal of Visualization, Vol. 8, No.1, 23-31.

[24] Khalifa H.E., Janos M.I. and Dannenhoffer III J.F., 2009, Experimental investigation of reduced-mixing personal ventilation jets, Building and Environment 44 (2009), pp 1551 – 1558.

[25] Russo J.S., Dang T.Q. and Khalifa H.E., 2009, Computational analysis of reduced-mixing personal ventilation jets, Building and Environment 44 (2009), pp 1559 – 1567.

[27] El Hassan M. and Meslem A., 2010, Time-resolved stereoscopic particle image velocimetry investigation of the entrainment in the near field of circular and daisy-shaped orifice jets, 2010, Physics of Fluids, 22, doi:10.1063/1.3358465.

[28] Tanabe. S., Zhang. H., Arens. E.A., Madsen T.L., Bauman. F.S., 1994. Evaluating thermal environments by using a thermal manikin with controlled skin surface temperature. *ASHRAE Transactions 100 (1)*. pp 39-48.

[29] Melikov. A. and Kaczmarczyk. J. 2007. Indoor air quality assessment by a breathing thermal manikin. Indoor Air 17 (1). pp.50-59.

[30] ISO. 2005. International Standard ISO/DIS/7730: Moderate Thermal Environments-Determination of PMV and PPD Indices and Specification of the Conditions for Thermal Comfort: International Standard Organization for Standardization. Geneva. Switzerland.

[32] ISO 1984. International Standard ISO 5221 First edition, *Air distribution and air diffusion – Rules to methods of measuring air flow rate in an air handling duct: International Organization for Standardization*, Geneva, Switzerland.

[33] Vitalograph UK. http://www.vitalograph.co.uk/

[34] ISO GUIDE 98-3, 1995, International Standard ISO, *Guide to the expression of uncertainty in measurement. Geneva*: International Organization for Standardization.

[35] Ho C-M and Gutmark E., 1987, Vortex induction and mass entrainment in a small-aspect-ratio elliptic jet, J. Fluid Mech., vol. 179, pp. 383-405.

[36] Gutmark E.J. and Grinstein F.F., 1999, FLOW CONTROL WITH NONCIRCULAR JETS, Annu. Rev. Fluid Mech.. vol. 31, pp. 239-272.

[37] Bolashikov. Z.D.. Melikov A.K. and Krenek M. 2009b. Improved Performance of Personalized Ventilation by Control of the Convection Flow around an Occupant's Body by Optimized Furniture Design, Proc. of Roomvent 2009, Busan, South Korea, Paper N: S0275.

[38] Nastase, I. and A. Meslem, 2008, Vortex dynamics and entrainment mechanisms in low Reynolds orifice jets. Journal of Visualization, 2008. 11(4).

[39] Meslem A., Nastase I., and Allard F., 2010, Passive mixing control for innovative air diffusion terminal devices for buildings. Building and Environment, 2010. 45 (2679-2688)

[42] Nastase, I., A. Meslem, and P. Gervais, 2008, Primary and secondary vortical structures contribution in the entrainement of low Reynolds number jet flows. Experiments in Fluids, 2008. 44(6): p. 1027-1033.

FIGURE 1

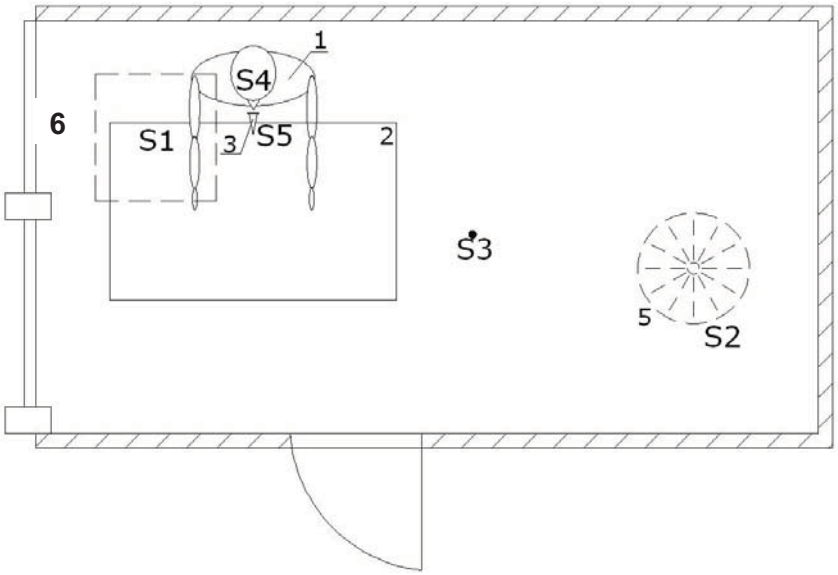

a) Top View

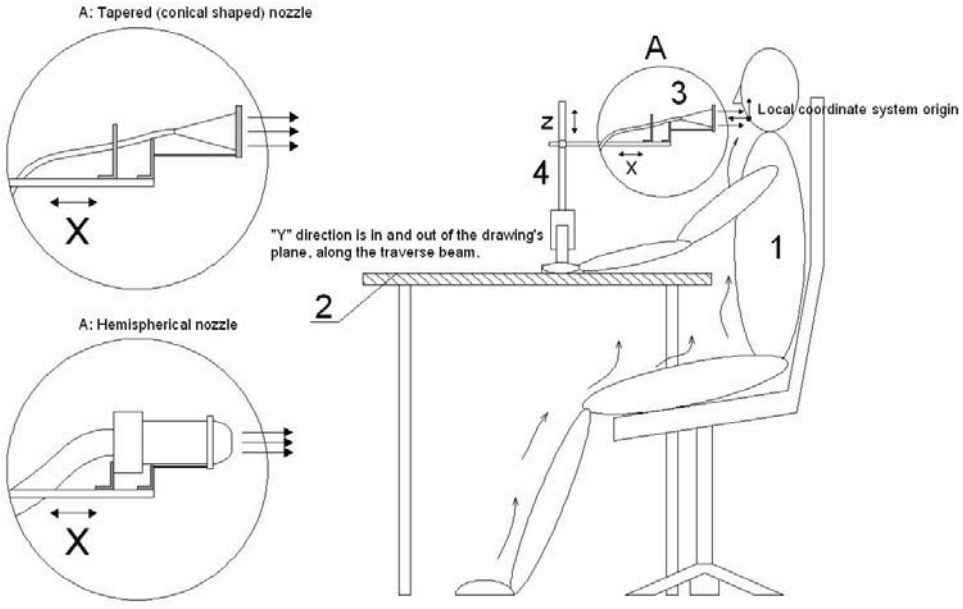

b) Side View

Figure 1 Experimental set-up: 1 – breathing thermal manikin; 2 – desk; 3 – PV with nozzle ATDs; 4 – traverse mechanism; 5 – supply ATD; 6 – exhaust ATD. Tracer gas sampling positions: S1- Supply air; S2 – Exhaust air; S3 – Room; S4 – Artificial lungs; S5 – Personalized air.

FIGURE 2

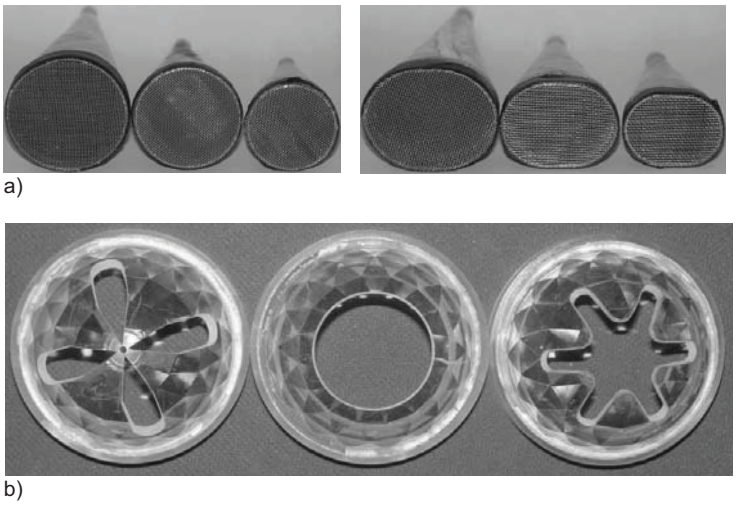

a)

b)

Figure 2. The circular and the elliptical nozzles of the three sizes of 0.035, 0.030 and 0.025 m (a) and the lobed nozzles of 0.025 m equivalent diameter (b).

FIGURE 3

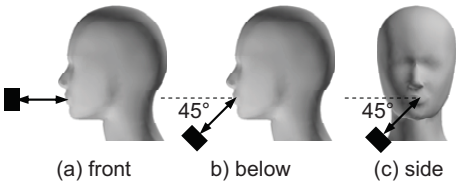

Figure 3. Positioning of the circular nozzle of diameter 0.03 m relative to the manikin's face: a) front, b) below, c) side.

FIGURE 3

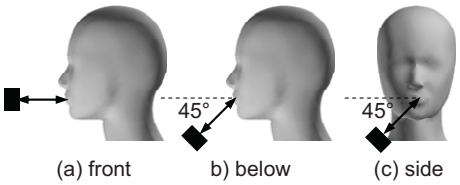

Figure 3. Positioning of the circular nozzle of diameter 0.03 m relative to the manikin's face: a) front, b) below, c) side.

FIGURE 4

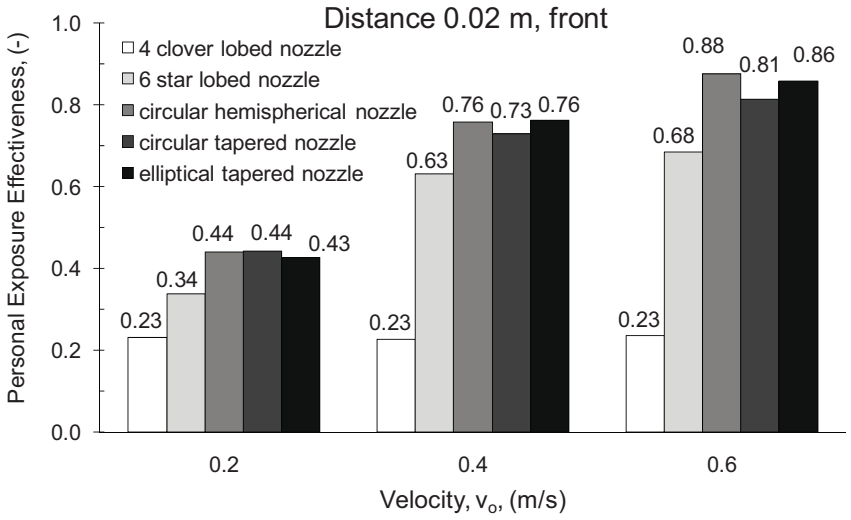
Distance 0.02 m, front
4 clover lobed nozzle
6 star lobed nozzle
circular hemispherical nozzle
circular tapered nozzle
elliptical tapered nozzle
Personal Exposure Effectiveness, (-)
1.0
0.8
0.6
0.4
0.2
0.0
0.23
0.34
0.44
0.44
0.43
0.23
0.63
0.76
0.73
0.76
0.23
0.68
0.88
0.81
0.86
0.2
0.4
0.6
Velocity, v_o, (m/s)

a)

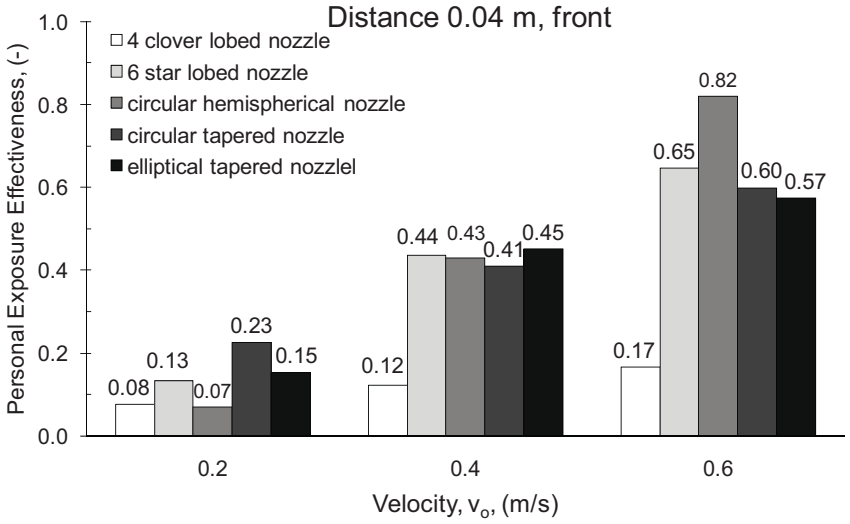
Distance 0.04 m, front
4 clover lobed nozzle
6 star lobed nozzle
circular hemispherical nozzle
circular tapered nozzle
elliptical tapered nozzlel
Personal Exposure Effectiveness, (-)
1.0
0.8
0.6
0.4
0.2
0.0
0.08
0.13
0.07
0.23
0.15
0.12
0.44
0.43
0.41
0.45
0.17
0.65
0.82
0.60
0.57
0.2
0.4
0.6
Velocity, v_o, (m/s)

b)

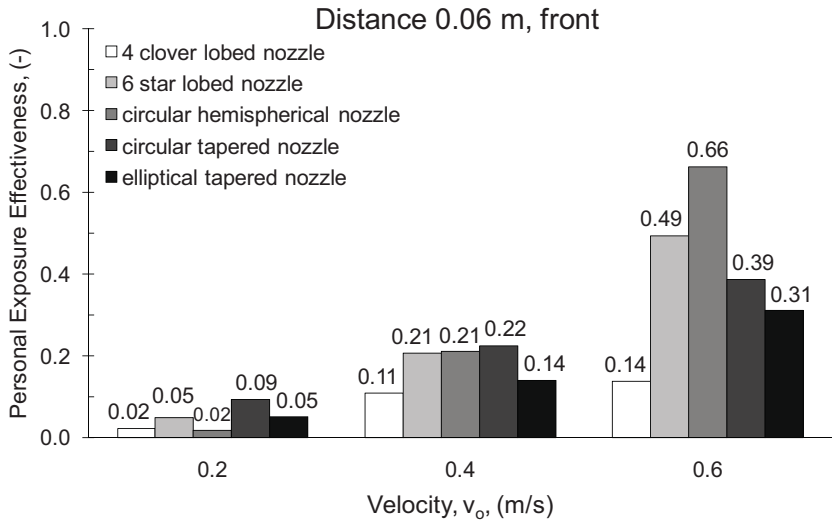

c)

Figure 4. Comparison of air quality performance of the tested PV headset nozzles (diameter 0.025 m) for the three different distances and from front relative to the facial plane: a) 0.020 m, b) 0.040 m, c) 0.060 m.

FIGURE 5

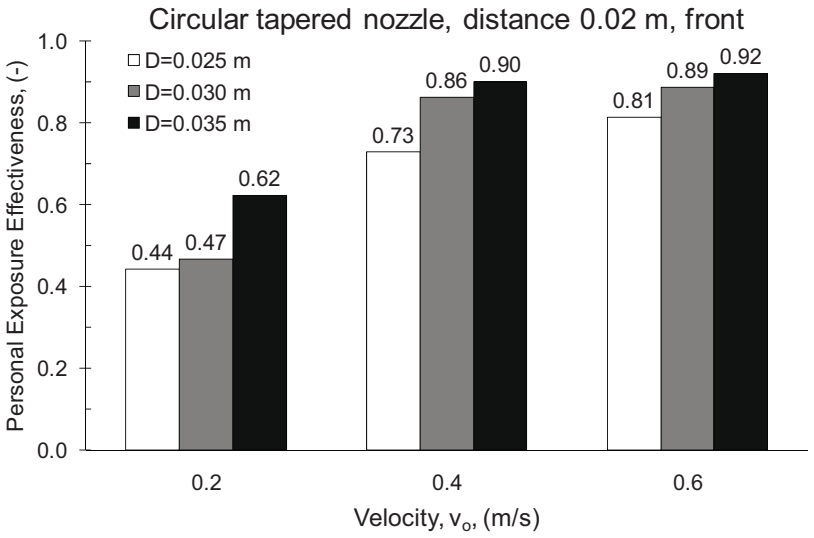
Circular tapered nozzle, distance 0.02 m, front
Personal Exposure Effectiveness, (-)
1.0
0.8
0.6
0.4
0.2
0.0
D=0.025 m
D=0.030 m
D=0.035 m
0.44
0.47
0.62
0.73
0.86
0.90
0.81
0.89
0.92
0.2
0.4
0.6
Velocity, v_o, (m/s)

a)

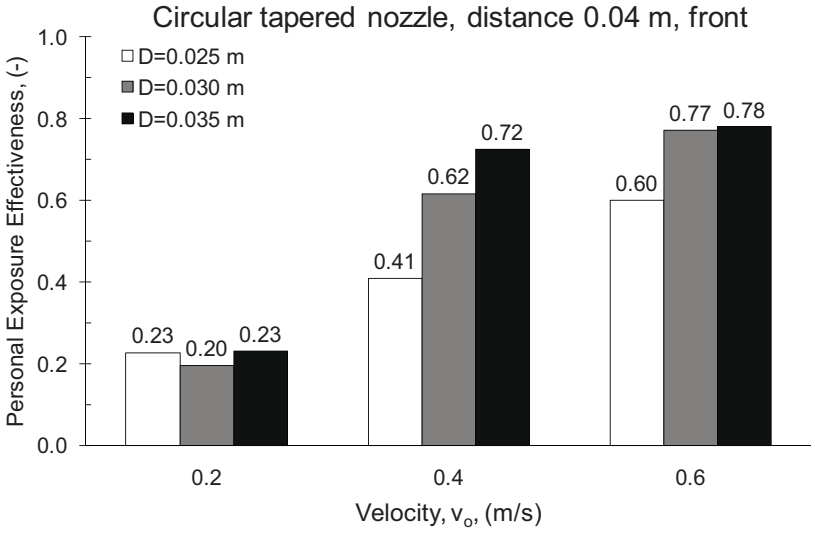
Circular tapered nozzle, distance 0.04 m, front
Personal Exposure Effectiveness, (-)
1.0
0.8
0.6
0.4
0.2
0.0
D=0.025 m
D=0.030 m
D=0.035 m
0.23
0.20
0.23
0.41
0.62
0.72
0.60
0.77
0.78
0.2
0.4
0.6
Velocity, v_o, (m/s)

b)

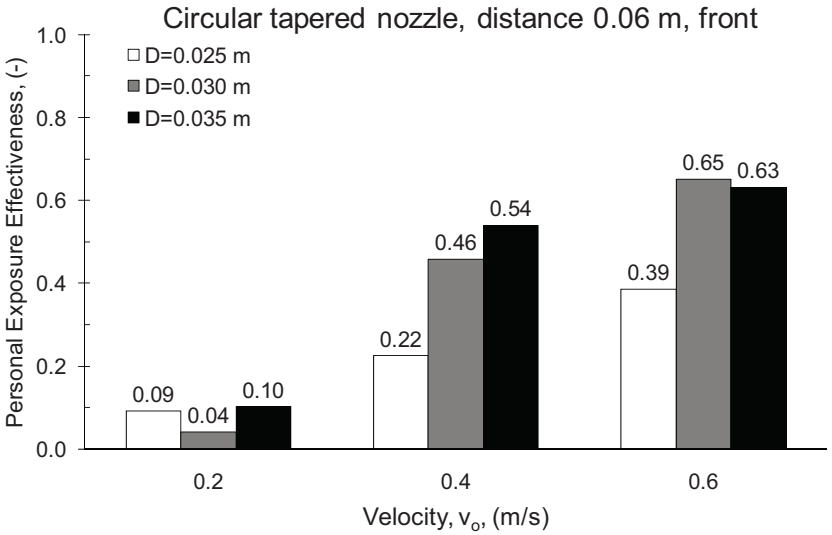

c)

Figure 5. Air quality performance of the circular PV headset nozzles (0.025, 0.030 and 0.035 m diameters) at the three different distances tested and from front relative to the facial plane: a) 0.020 m, b) 0.040 m, c) 0.060 m.

FIGURE 6

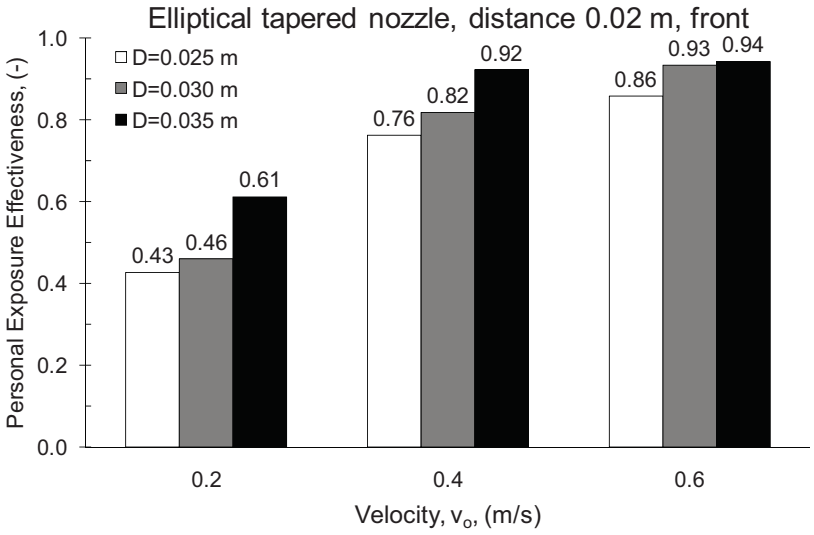
Elliptical tapered nozzle, distance 0.02 m, front
Personal Exposure Effectiveness, (-)
1.0
0.8
0.6
0.4
0.2
0.0
D=0.025 m
D=0.030 m
D=0.035 m
0.43
0.46
0.61
0.76
0.82
0.92
0.86
0.93
0.94
0.2
0.4
0.6
Velocity, v_o, (m/s)

a)

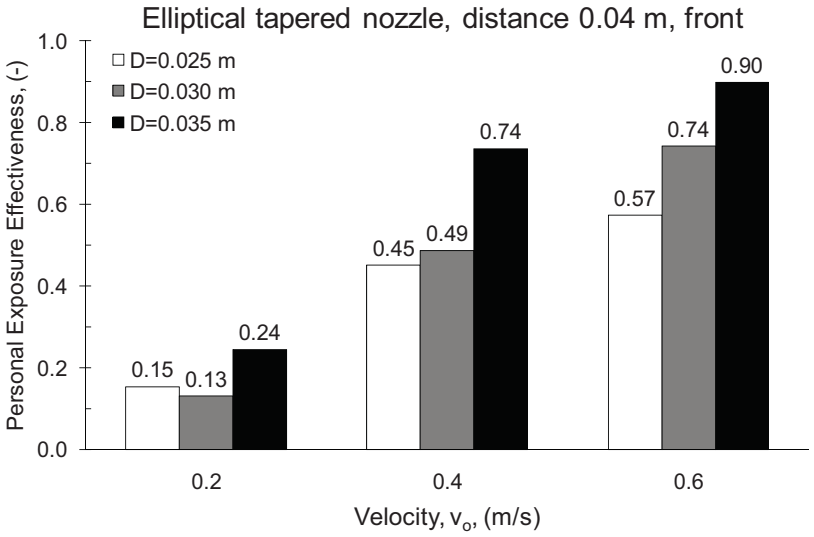
Elliptical tapered nozzle, distance 0.04 m, front
Personal Exposure Effectiveness, (-)
1.0
0.8
0.6
0.4
0.2
0.0
D=0.025 m
D=0.030 m
D=0.035 m
0.15
0.13
0.24
0.45
0.49
0.74
0.57
0.74
0.90
0.2
0.4
0.6
Velocity, v_o, (m/s)

b)

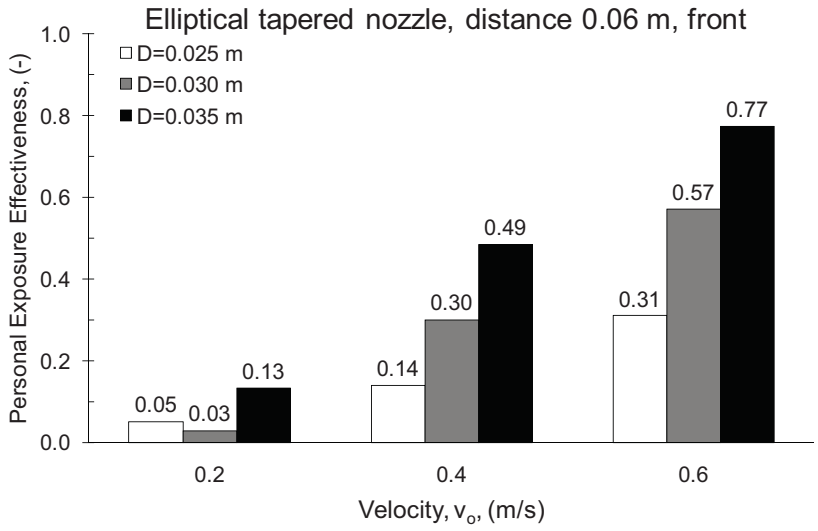

c)

Figure 6. Air quality performance of the elliptical PV headset nozzles (0.025, 0.03 and 0.035 m diameters) at the three different distances tested and from front relative to the facial plane: a) 0.02 m, b) 0.04 m, c) 0.06 m.

FIGURE 7

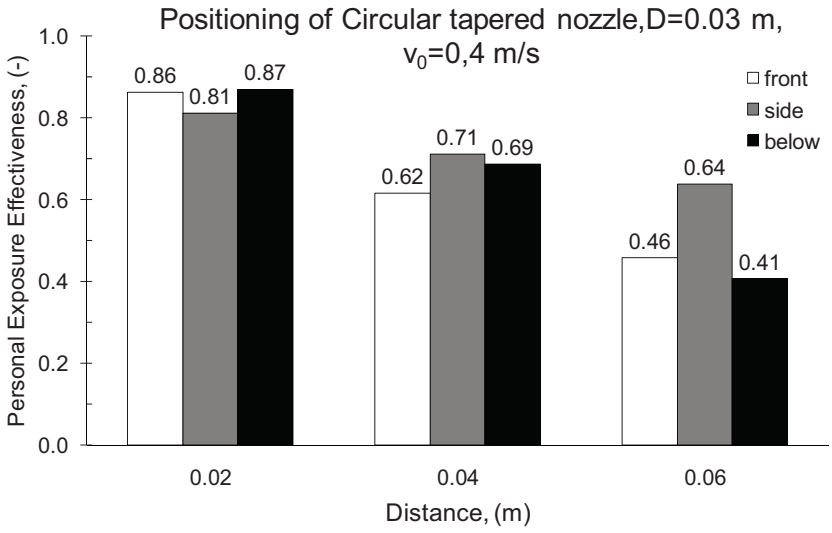

Figure 7. Comparison of the air quality performance of the circular PV nozzle (D=0.030 m), for the three directions of the headset relative to the facial plane, front, side and below.

FIGURE 8

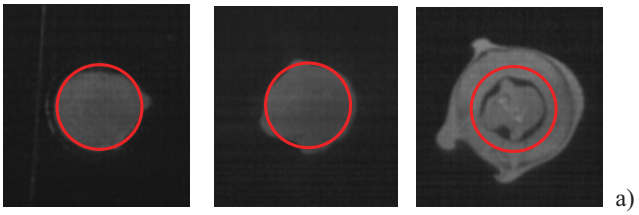

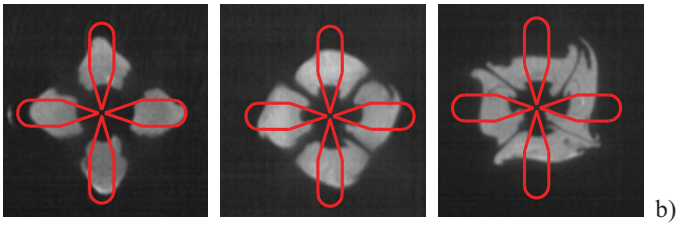

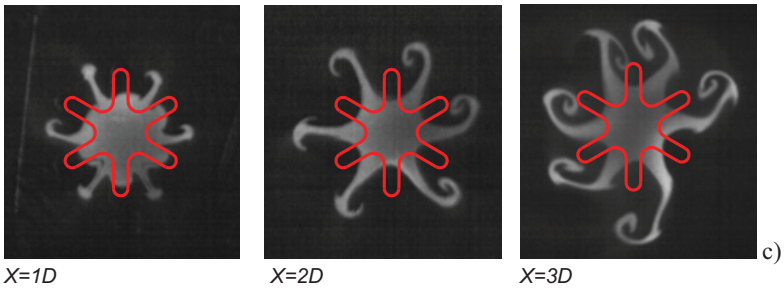

Figure 8: Flow visualization in jet transverse plane: a) circular jet, b) 4 clover lobed jet, c) 6 star lobed jet

FIGURE 9

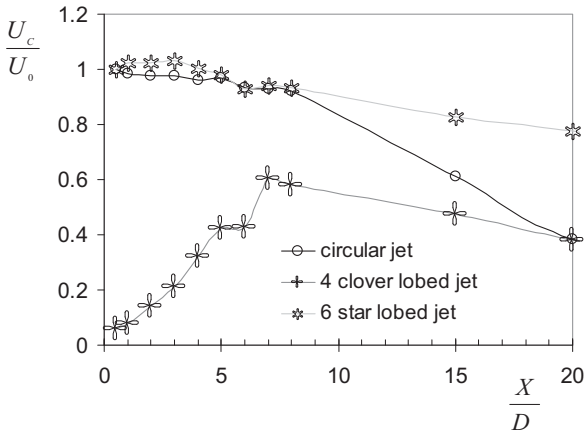

Figure 9: Streamwise evolution of jet axial velocity

FIGURE 10

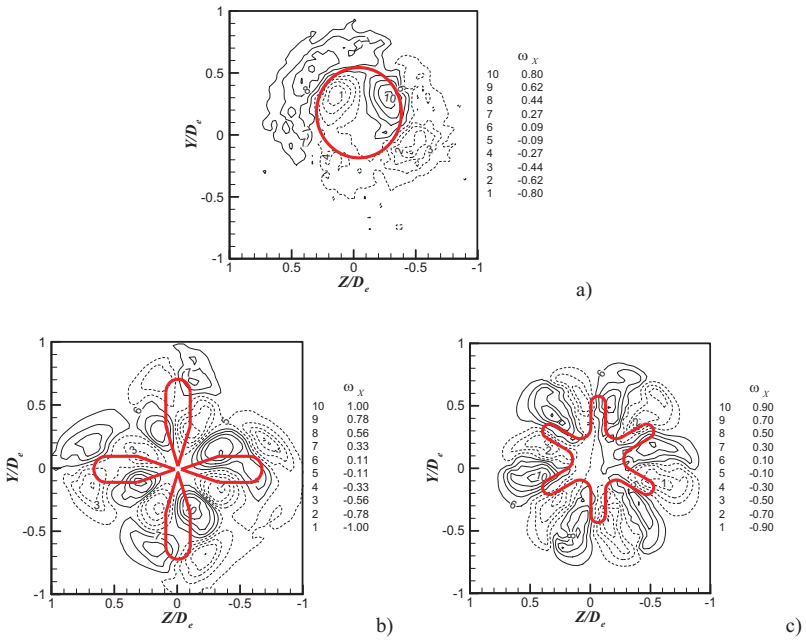

Figure 10 : Streamwise rotational component at *X=1D* : a) circular jet, b) 4 clover lobed jet, c) 6 star lobed jet, $\omega_x = \frac{D_e}{U_0}\left(\frac{\partial W}{\partial Y} - \frac{\partial V}{\partial Z}\right)$

FIGURE 11

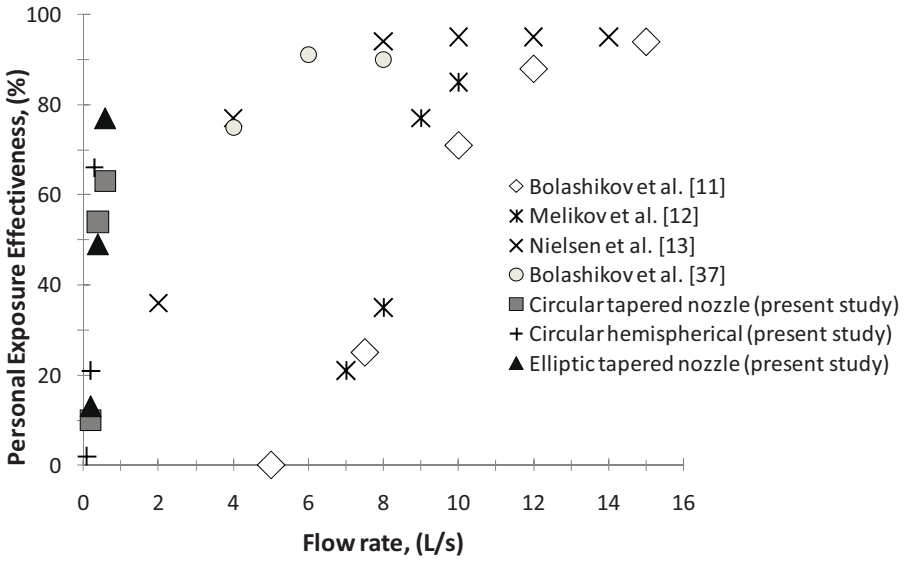

Figure 11. Air quality performance of the circular and elliptical tapered/conical PV nozzles of 0.035 m diameter and at a distance 0.06 m from mouth and the hemispherical nozzle with circular exit of 0.025 m diameter at distance of 0.06 m from mouth compared to three other PV units. Bolashikov et al. [11] – desk mounted round shape ATD; Melikov et al. [12] – two rectangular ATD mounted on seat headrest; Nielsen et al. [13] – air supplied from neck support; Bolashikov et al. [37] – two rectangular seat headrest ATD with two additional control nozzles.

TABLE 1

Nozzle type	**Unit**	**Lobed:** Circular Clover 4 Star 6	**Circular**	**Elliptic** **(a, b)*** **a: major d** **b: minor d**
Diameter (equivalent)	m	0.025	0.025 0.030 0.035	0.025 (0.029, 0.020) 0.030 (0.034, 0.025) 0.035 (0.039, 0.030)
Initial velocity for primary jet v_o	m/s	0,2/0,4/0,6	0,2/0,4/0,6	0,2/0,4/0,6
Distance from manikin's face	m	0.020 0.040 0.060	0.020 0.040 0.060	0.020 0.040 0.060
Direction of the headset	-	front	front front/below/side*	front
TV ventilation supply air flow	L/s	15	15	15
TV ventilation diffuser air temperature	°C	21	21	21
TV ventilation exhaust air flow	L/s	30	30	30
TV ventilation exhaust temperature	°C	23	23	23

*tested for Circular nozzle of diameter 0.03 m only

Table 1: PV nozzle tests.

TABLE 2

Quantity	Frequency of Data Acquisition	Duration of Measurement Period	Uncertainty (Conf. Level 95%)
Concentrations (inhaled and room)	10 min	130 -150 min	1 % of reading
Temperature (room)	5 Hz	1 min	0.3 °C
Air velocity (room)	5 Hz	3 min	0.03 m/s

Table 2. Sampling frequency, duration of data acquisition, and typical values of the uncertainty with a 95% level of confidence

TABLE 3

Type	Size [m]	Area [m^2]	Initial velocity 0.2 m/s			Initial velocity 0.4 m/s			Initial velocity 0.6 m/s		
			Flow rate [L/s]	Re [-]	PEE [-]	Flow rate [L/s]	Re [-]	PEE [-]	Flow rate [L/s]	Re [-]	PEE [-]
0.020 m											
Circular	0.035	0.000962	0.192	463	0.62	0.385	927	0.90	0.577	1 389	0.92
	0.030	0.000707	0.141	397	0.47	0.283	794	0.86	0.424	1 191	0.89
	0.025	0.000491	0.098	331	0.44	0.196	662	0.73	0.295	993	0.81
Elliptic	0.035	0.000962	0.192	463	0.61	0.385	927	0.92	0.577	1 389	0.94
	0.030	0.000716	0.143	397	0.46	0.286	794	0.82	0.430	1 191	0.93
	0.025	0.000494	0.099	331	0.43	0.198	662	0.76	0.296	993	0.86
0.040 m											
Circular	0.035	0.000962	0.192	463	0.23	0.385	927	0.72	0.577	1 389	0.78
	0.030	0.000707	0.141	397	0.20	0.283	794	0.62	0.424	1 191	0.77
	0.025	0.000491	0.098	331	0.23	0.196	662	0.41	0.295	993	0.60
Elliptic	0.035	0.000962	0.192	463	0.24	0.385	927	0.74	0.577	1 389	0.90
	0.030	0.000716	0.143	397	0.13	0.286	794	0.49	0.430	1 191	0.74
	0.025	0.000494	0.099	331	0.15	0.198	662	0.45	0.296	993	0.57
0.060 m											
Circular	0.035	0.000962	0.192	463	0.10	0.385	927	0.54	0.577	1 389	0.63
	0.030	0.000707	0.141	397	0.04	0.283	794	0.46	0.424	1 191	0.65
	0.025	0.000491	0.098	331	0.09	0.196	662	0.22	0.295	993	0.39
Elliptic	0.035	0.000962	0.192	463	0.13	0.385	927	0.49	0.577	1 389	0.77
	0.030	0.000716	0.143	397	0.03	0.286	794	0.30	0.430	1 191	0.57
	0.025	0.000494	0.099	331	0.05	0.198	662	0.14	0.296	993	0.31

Table 3 Table of initial flow rates and PEE for Round and Elliptical nozzles at distance 0.02, 0.04 and 0.06 m from the mouth.

Appendix VI

Paper VI

Bolashikov Z.D., Nagano H., Melikov A.K., Meyer K.E. and Kato S.

Control of the Free Convection Flow within the Breathing Zone by Confluent Jets for Improved Performance of Personalized Ventilation: Part 2 – Inhaled Air Quality

Proceedings Healthy Buildings 2009, Syracuse NY USA, Paper ID: 471.

Control of the Free Convection Flow within the Breathing Zone by Confluent Jets for Improved Performance of Personalized Ventilation: Part 2 – Inhaled Air Quality

Zhecho D. Bolashikov[1,*], Hideaki Nagano[1,2], Arsen K. Melikov[1], Knud Erik Meyer[1] and Shinsuke Kato[2]

[1]Technical University of Denmark, Dept. of Civil Engineering, 2800 Kgs. Lyngby, Denmark
[2]University of Tokyo, Institute of Industrial Science, Tokyo, Japan
[*]*Corresponding email: zdb@byg.dtu.dk*

SUMMARY
A unique method for inhaled air quality improvement by personalized ventilation by control of the free convection flow and its interaction with the clean air based on confluent jets was studied. The confluent upward jets were generated close to the front of the human body by openings at the front edge of a desk board pressed against the abdominal area. The inner jet supplied clean air, while the assisting outer jet supplied polluted room air. Comprehensive experiments were performed under isothermal conditions (26^{o}C) in a full-scale room with a typical workstation and a thermal manikin simulating realistically human body shape and the generated free convection flow. Tracer gas measurements were performed to identify the impact of the control method on inhaled air quality. Results showed improved air quality at the breathing zone, but the benefit was limited due to flow separation at shoulder-neck region.

KEYWORDS
Confluent jet, personalized ventilation, control, free convection flow, air quality

INTRODUCTION
Much attention has been paid to the personalized ventilation (PV) within the last decade, especially at improving the design for providing better inhaled air quality, perceive air quality, thermal comfort and personal protection from airborne pathogens (Melikov 2004, Kaczmarczyk et al., 2004, Melikov et al. 2007). Most of the present research has concentrated on the application of single axisymetric free jets with a long potential core region and a low initial turbulence that benefit the occupant by providing clean personalized air at considerable distances: up to 5 initial diameters of the supply nozzle (Melikov 2004). Another advantage of the axisymetric jet is its air quality performance independence on positioning relative to the human face: from top, left, right or from above (Melikov et al. 2007). All these techniques imply that the PV jet is transverse to the free convection flow at the breathing zone with at least 0.3 m/s target velocity so as to penetrate it and result in improved air quality (Melikov 2004). PV jets discharging upward air at the abdominal area and thus assisting the free convection flow have also been reported (Melikov et al. 2002). The performance of such jets is limited to a maximum of 60% clean air in the air inhaled at flow rates higher than 15 L/s.

The present paper shows a way to improve the performance of the assisting PV jet by simply replacing the convection flow in the front plane of the body starting at the abdominal area and protecting this clean jet by an additional jet (confluent jets) of recirculated room air from the outer surface (facing the room). This would prevent the PV air entrain with polluted room air and keep it unmixed for a longer distance. The result would be an increase in the amount of clean air into the air inhaled resulting in better perceived air quality, health and protection of occupants from airborne diseases at reduced PV flow and thus a reduced risk from draught.

The impact of the method of confluent jets on occupants' thermal comfort at warm environment was studied in Part 1 (Nagano et al. 2009).

METHODS

The experiments were performed in a full-scale test room with dimensions 4.70 m × 2.40 m × 2.60 m (W×L×H). A workplace consisting of a desk with confluent jet device for PV, a light office chair (0.1 Clo) and a seated thermal manikin (0.5 Clo) was simulated in the room. Three fixtures (6 W each) located in the ceiling provided the background lighting. The room itself was built in a laboratory hall, 70 cm above the floor. The walls of the test room were made of particleboard and were insulated by 6 cm thick styrofoam. One of the walls was made from single thick layer glazing.The mixing type ventilation used to condition the air in the test room to 26^{o}C supplied 100% clean air (no recirculation) with an air change rate of 2.2 h^{-1}. This flow rate provided good mixing in the room at low velocity (below 0.2 m/s within the occupied zone). A rotation type air supply diffuser and and a perforated circular air exhaust diffuser were installed on the ceiling. Air humidity was not controlled but was measured as being relatively constant (30% - 35%).

The air terminal device of the personalized ventilation, generating the two confluent jets, consisted of two plenum boxes nested in each other and placed below the desk top. The two boxes were having the discharge slots (60 mm x 500 mm, width x length) attached with no distance between and pressed firmly against the abdominal area of the thermal manikin. Each box had a separate supply fan to drive the air trough the boxis. The jet closer to the manikin supplied always clean PV air (inner jet) while the outer jet (close to table board rim) discharged room air. The fan of the outer jet that was used to drive room air was placed in the tes-room at the opposite corner relative to the manikin at a distance of more than 2.5 m (along the width of the room).The temperature of the personalized air was maintained constant to the set value of 26^{o}C (same as that of the room) by an electrical heater installed in the PV supply system and a temperature sensor placed in the ducting before the PV supply box (inner jet). The temperuture of the outer jet was not controlled but was measured to be on average with 0.5^{o}C higher than the room air temperature due to the heat generated from the fan motor. The humidity of the supplied personalized air was not controlled or measured, but was assumed to be close to that in the room, 30 - 35% (isothermal conditions).

Tracer gas, Freon R134a, supplied at constant dose in the duct of the background ventilation system before the ceiling diffuser, was used to simulate pollution in the room air. The personalized air supplied through the inner jet was free of tracer gas. A tube attached at the upper lip of the manikin at a distance of 0.005 m from the face was used to sample air for measuring the tracer gas concentration in inhaled air as recommended by Melikov and Kaczmarczyk (2007). The airflow rates from the inner and outer jets were measured by two flow sensor based on pressure difference measured by manometer with an accuracy of 0.01 Pa ± 0.25% of reading. The required flow rate was adjusted by a manually operated damper.

The inhaled air quality was assessed by the index known as Personal Exposure Effectiveness (PEE) introduced by Melikov et al. (2002). The PEE calculates the portion of clean personalized air in the air inhaled by an occupant and is given as; $PEE=(C_{I,0}-C_I)/(C_{I,0}-C_{PV})$ where $C_{I,0}$ is the pollution concentration if no PV, C_I is the pollution concentration in inhaled air and C_{PV} stands for pollution concentration in personalized air. PEE is equal to 1 (or 100%) when only clean personalized air is inhaled, i.e. best performance of the personalized ventilation. PEE equal to 0 (or 0%) means that the inhaled air is the polluted room air.

RESULTS

The results for the air quality performance of the confluent jet PV boxes design at different supply flow rates are shown in Figure 1. Both boxes discharged same amount of air: the inner one supplied only clean PV air while the outer was operated with recirculated room air.

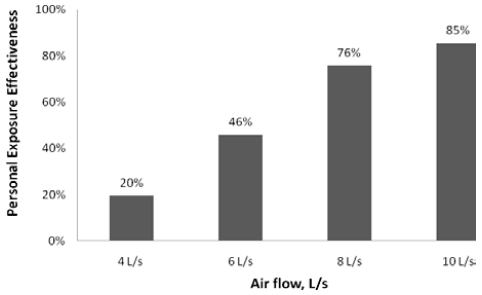

Figure 1. Personal Exposure Effectiveness as a function of flow rate. Both inner (PV air) and outer (room air) jets provide same amount of air.

As can be clearly seen from the graph, the inhaled air quality improves with the increase of the supplied flow rate. Already at 8 L/s the PEE reaches a value of 76% and 85% at 10 L/s.

The effect of different discharge air flows of the inner and the outer jets on PEE was studied when the inner jet air flow was equal to, two times larger or half of the air flow from the outer jet (Figure 2). Figure 3 also shows the case when the inner jet supplied clean air alone with no "protection" from outer jet as a reference.

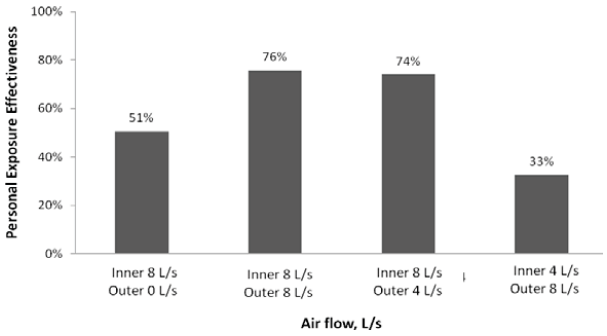

Figure 2. Personal Exposure Effectiveness as a function of the difference in the discharge amount of air (air velocity) of the inner and the outer jets.

As could be seen reducing two times the velocity of the outer jet has no effect on the PEE (74% PV air was inhaled), while the opposite (reducing 2 times the air flow of the inner jet) is not true: the amount of clean air in inhalation drops almost 2.5 times. The assisting effect of the outer jet increased the PEE from 51% to 76%.

DISCUSSION

Previous research on PV jets supplied from the front edge of desk and assisting the convection flow achieved a maximum PEE of 60% at minimum flow rate of 10 L/s (Melikov et al. 2002).

Further increase in the flow rate resulted in no change of the amount of fresh air into the air inhaled. Even the reduction of the discharge area by 50%, i.e. increase of the supply velocity did not result in improvement the performance in regard to inhaled air quality. The use of confluent jets at isothermal conditions of 26^{o}C increased the amount of clean air in the inhaled air up to 85% at flow rate of 10 L/s and up to 76% at flow rate of 8 L/s. Thus, using the outer jet to protect the clean inner jet from mixing with its surroundings was beneficial. However better performance was expected as there was no friction between the two jets and hence no mixing. One reason for the lower performance was the separation of the upcoming clean jet at the neck- shoulder region of the body. Some amount of the clean air managed to overcome the blocking effect of the jaws and reached the inhalation zone. Another reason could be that the outer jet heated by the fan was slightly warmer (with maximum 1 ^{o}C) of the room temperature, and this might have promoted some mixing of the two jets.

Different discharge flow rates were also tested with the confluent jets resulting in difference in velocities of the upcoming flows. When the velocity of the outer jet is equal or half of that of the inner jet the performance of the confluent jets with regard to air quality was the same: around 76% clean air into the air inhaled. PEE decreased drastically (33%) when the flow rate of the clean air supplied by the inner jet was reduced two times compared to the outer jet. The reason might be due to the higher momentum of the outer jet.

CONCLUSIONS

The effectiveness of PV jet, supplied upward at the abdominal area of the human body and assisting the free convection flow, with regards to inhaled air quality is limited due to the human body shape: the upward flow gets separated at the neck and shoulder region and only small portion reaches the mouth. The use of confluent jet (outer jet) of polluted air improved PEE (up to 85%) compared to the single jet application (60%). The change of the amount of air discharged from the outer opening had no effect on the PEE, while the change in the air supplied from the inner jet resulted in a much worse performance regarding the air quality.

ACKNOWLEDGEMENTS

This research was supported by the Danish Agency for Science, Technology and Innovation, Project No. 274-07-0516.

REFERENCES

Kaczmarczyk J., Melikov A.K., Bolashikov Z., Nikolaev L. and Fanger P.O., 2006, Human response to five designs of personalized ventilation, *International Journal of Heating, Ventilation and Refrigeration Research* 12 (2), pp.367-384.

Melikov A.K., 2004, Personalized ventilation*, Indoor Air* 14 (7), pp. 157-167.Engineering, Fanger P.O. 1970. *Thermal Comfort*. Copenhagen: Danish Technical Press.

Melikov A.K., Cermak R., Majer M., 2002, Personalized ventilation: evaluation of different air terminal devices, *Energy and Buildings* 34, pp 829-836.

Melikov A.K. Pavlov G., Dimitrov N., 2007, Personalized ventilation: impact of airflow direction at the breathing zone on inhaled air quality, *Proceedings of Clima 2007 WellBeing Indoors*.

Melikov, A. and Kaczmarczyk, J., 2007, Indoor air quality assessment by a breathing thermal manikin, *Indoor Air* 17 (1), pp.50-59.

Nagano, H., Bolashikov, Z.D., Melikov, A.K., Kato, S., Meyer, K.E., 2009, Control of the free convection flow within the breathing zone by confluent jets for improved performance of personalized ventilation: Part 1 – Thermal influence, *Proceedings of Healthy Buildings 2009.*

Appendix VII

Contents

Table of Figures

Part 1

a)

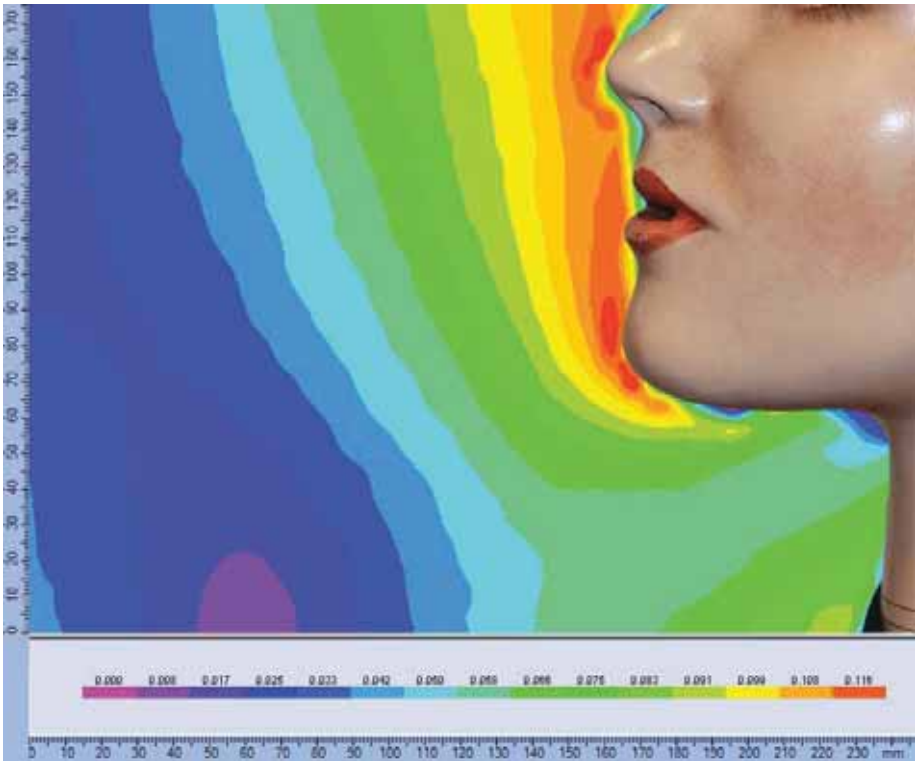

b)

Figure 1 *a) Velocity vector diagram showing air direction and b) Contour velocity plot diagram close to the breathing zone of a thermal manikin when heated and with straight board (passive control method) pressed at stomach level.*

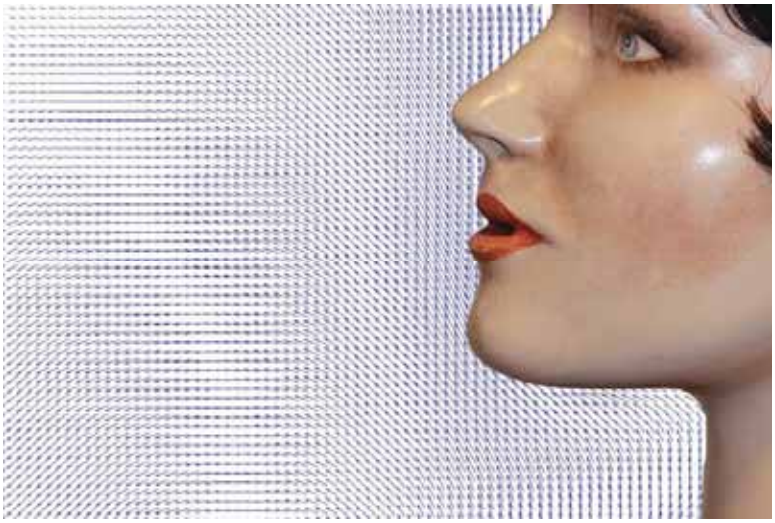

a)

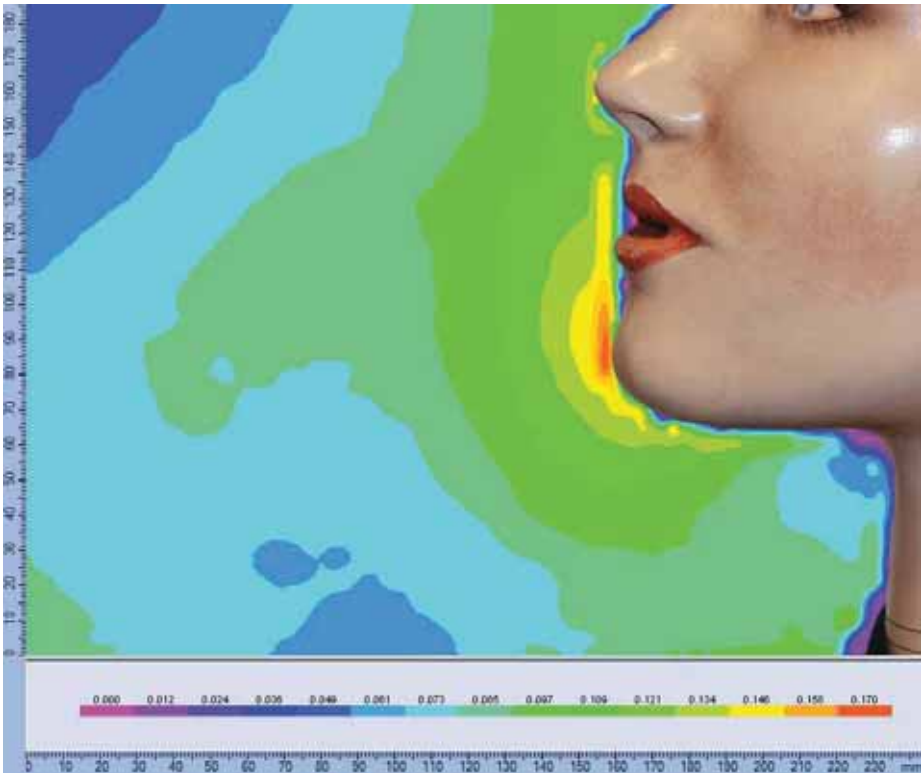

b)

Figure 2 *a) Velocity vector diagram showing air direction and b) Contour velocity plot diagram close to the breathing zone of a thermal manikin when heated and with active control method when front row of 3 fans is working at 15V each.*

a)

b)

Figure 3 *a) Velocity vector diagram showing air direction and b) Contour velocity plot diagram close to the breathing zone of a thermal manikin when heated and with active control method when front row of 3 fans is working at 30V each.*

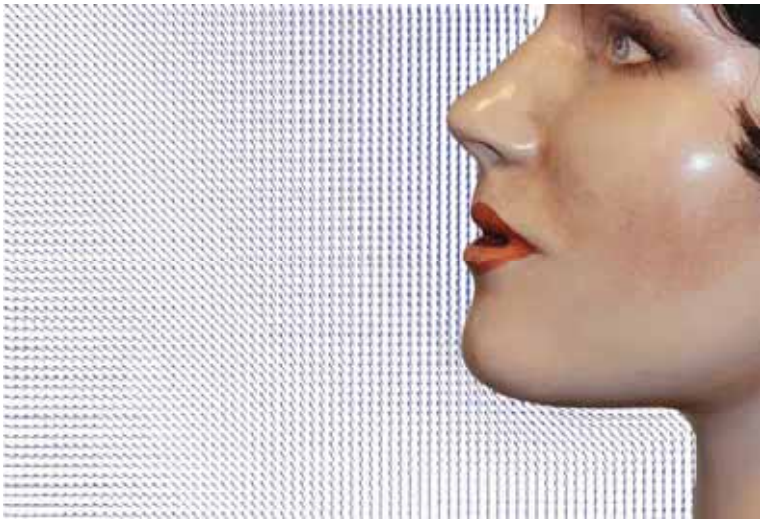

a)

b)

Figure 4 *a) Velocity vector diagram showing air direction and b) Contour velocity plot diagram close to the breathing zone of a thermal manikin when heated and with combination of active control method when front row of 3 fans is working at 15V each and straight board pressed against stomach (passive control method).*

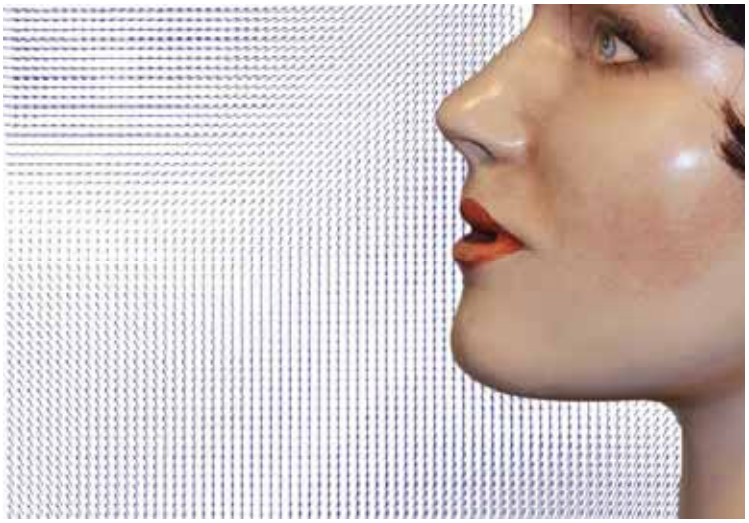

a)

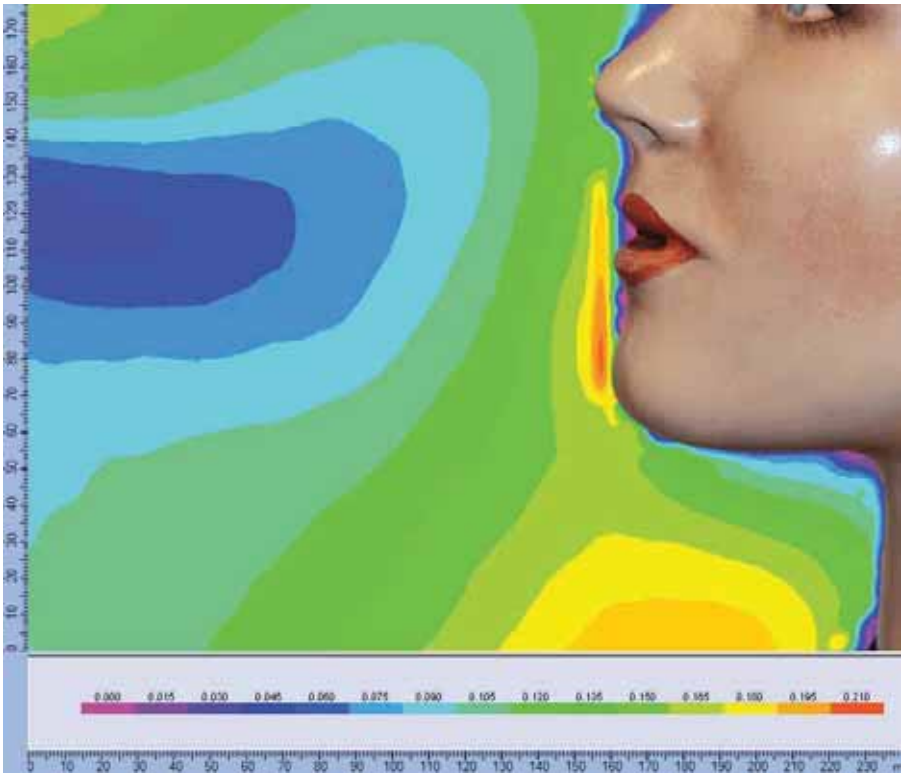

b)

Figure 5 *a) Velocity vector diagram showing air direction and b) Contour velocity plot diagram close to the breathing zone of a thermal manikin when heated and RMP supplying 4L/s at 0.4m frontally slightly from above.*

a)

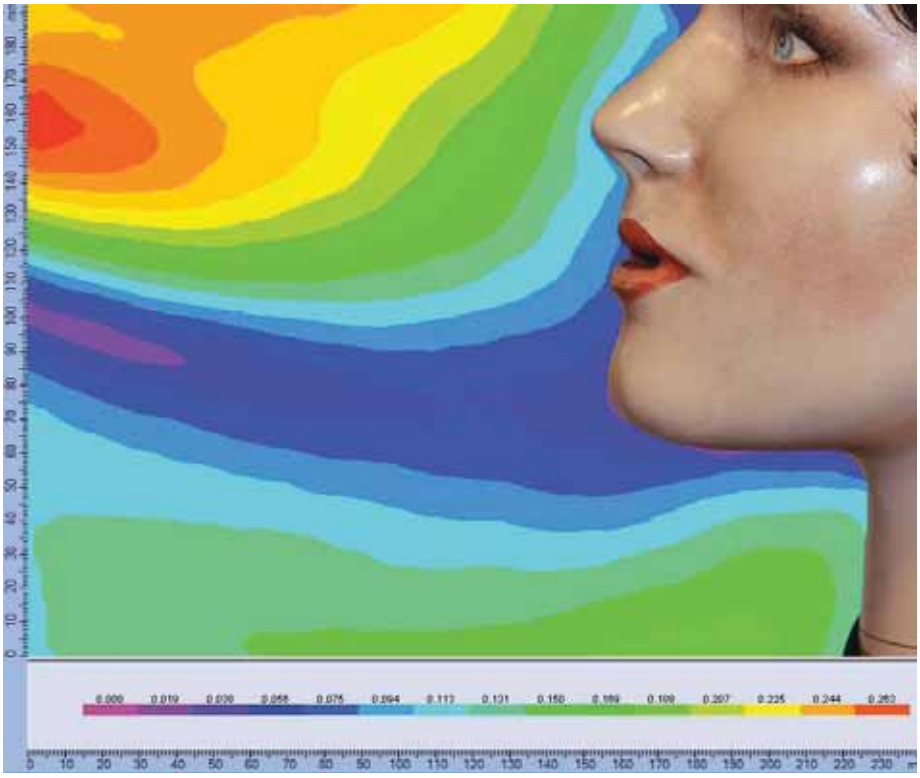

b)

Figure 6 *a) Velocity vector diagram showing air direction and b) Contour velocity plot diagram close to the breathing zone of a thermal manikin when heated and RMP supplying 6L/s at 0.4m frontally slightly from above.*

a)

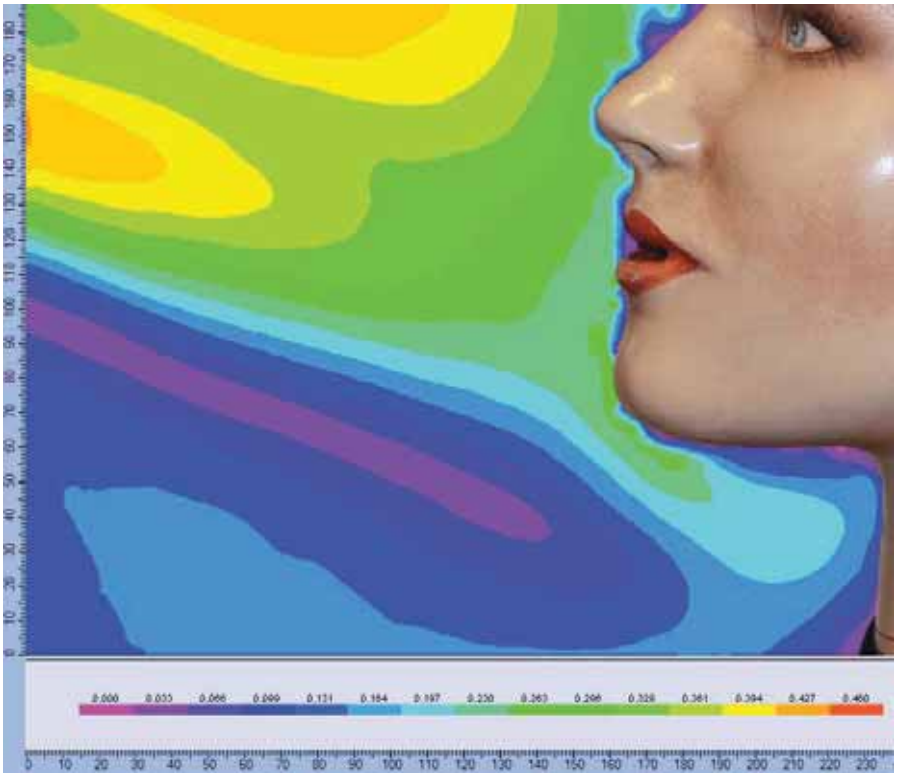

b)

Figure 7 *a) Velocity vector diagram showing air direction and b) Contour velocity plot diagram close to the breathing zone of a thermal manikin when heated and RMP supplying 8L/s at 0.4m frontally slightly from above.*

a)

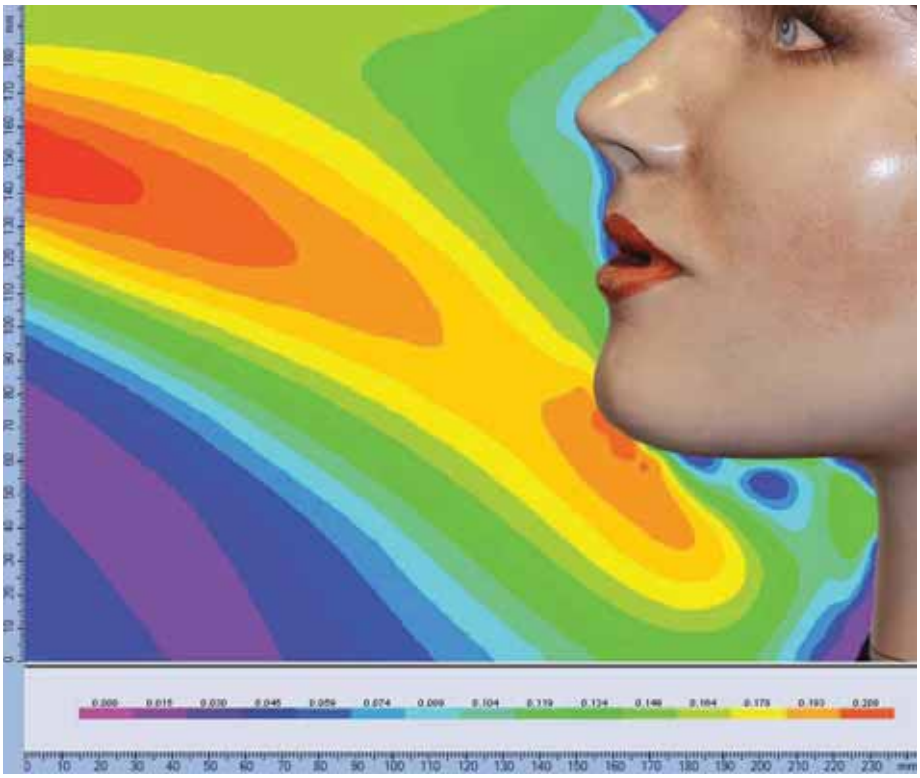

b)

Figure 8 *a) Velocity vector diagram showing air direction and b) Contour velocity plot diagram close to the breathing zone of a thermal manikin not heated and RMP supplying 4L/s at 0.4m frontally slightly from above.*

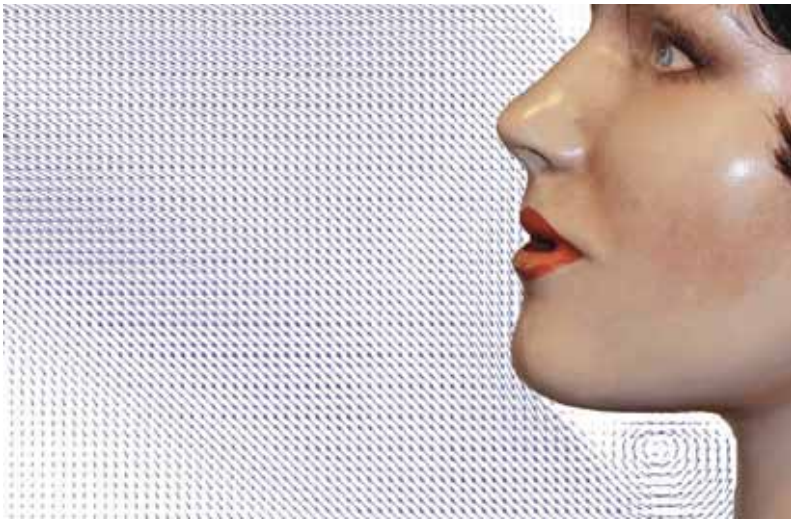

a)

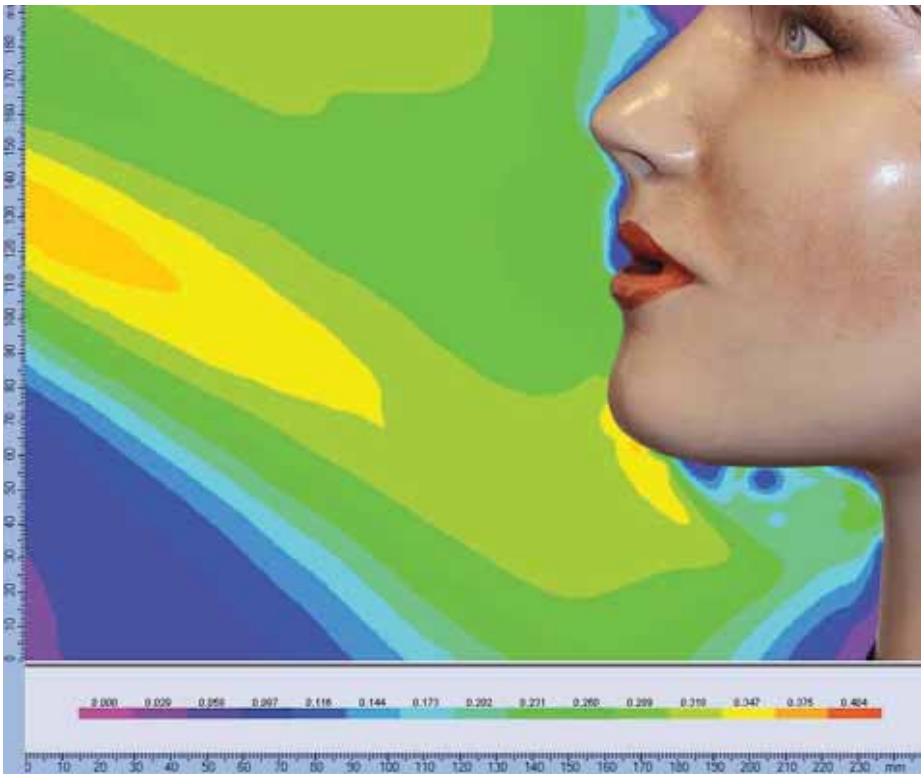

b)

Figure 9 *a) Velocity vector diagram showing air direction and b) Contour velocity plot diagram close to the breathing zone of a thermal manikin not heated and RMP supplying 6L/s at 0.4m frontally slightly from above.*

a)

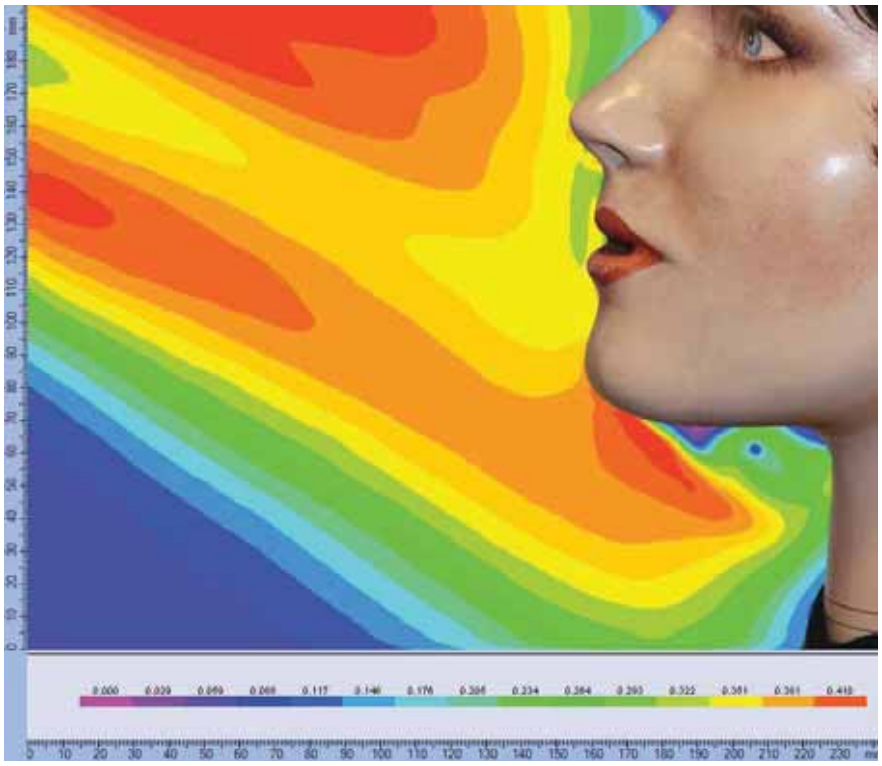

b)

Figure 10 *a) Velocity vector diagram showing air direction and b) Contour velocity plot diagram close to the breathing zone of a thermal manikin not heated and RMP supplying 8L/s at 0.4m frontally slightly from above.*

a)

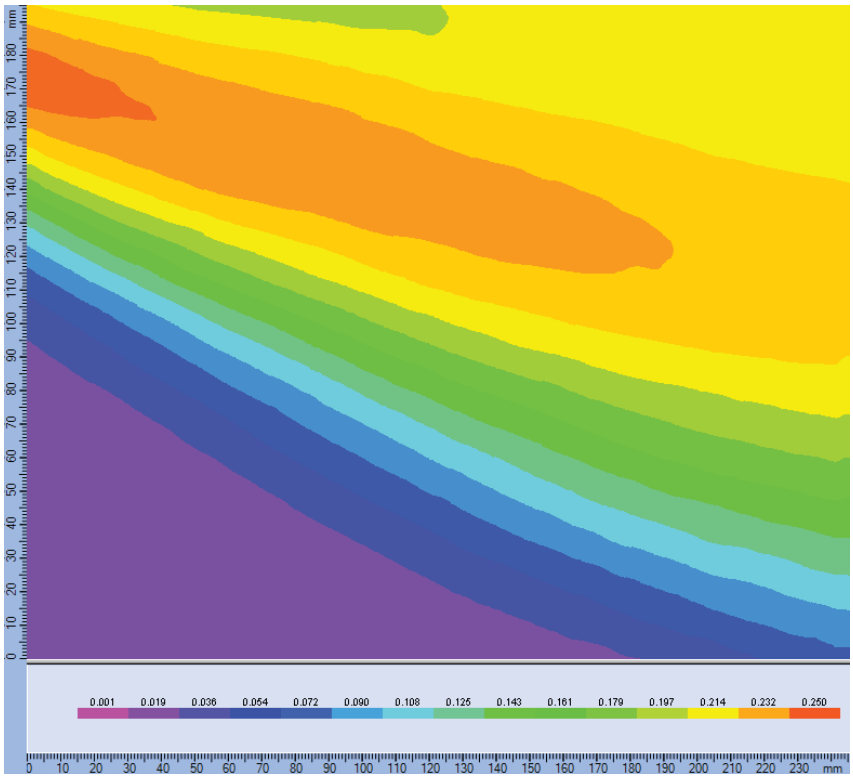

b)

Figure 11 *a) Velocity vector diagram showing air direction and b) Contour velocity plot diagram of the RMP supplying 4L/s without the thermal manikin being present.*

a)

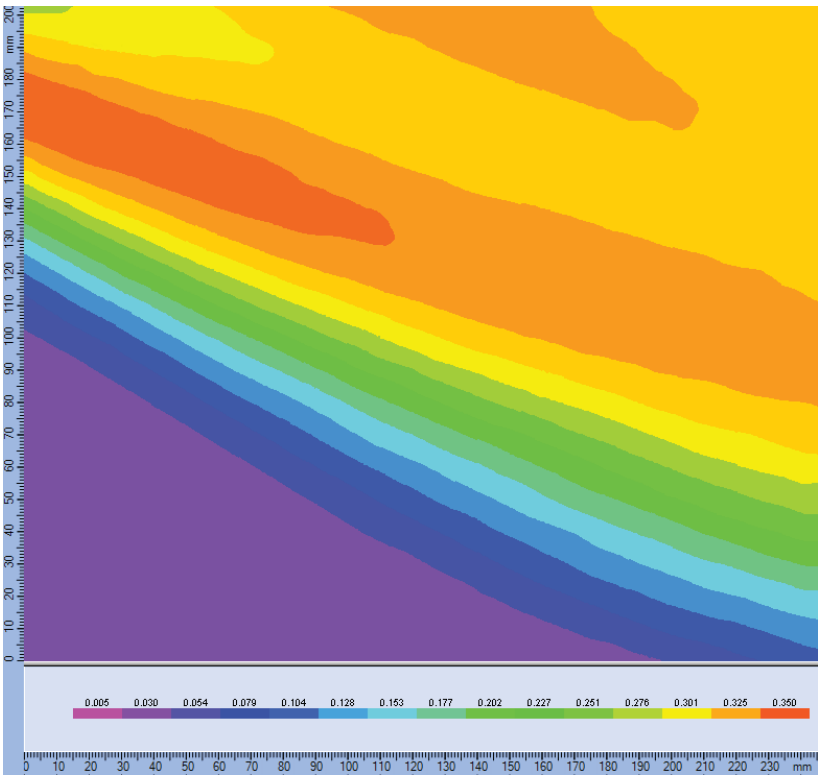

b)

Figure 12 *a) Velocity vector diagram showing air direction and b) Contour velocity plot diagram of the RMP supplying 6L/s without the thermal manikin being present.*

a)

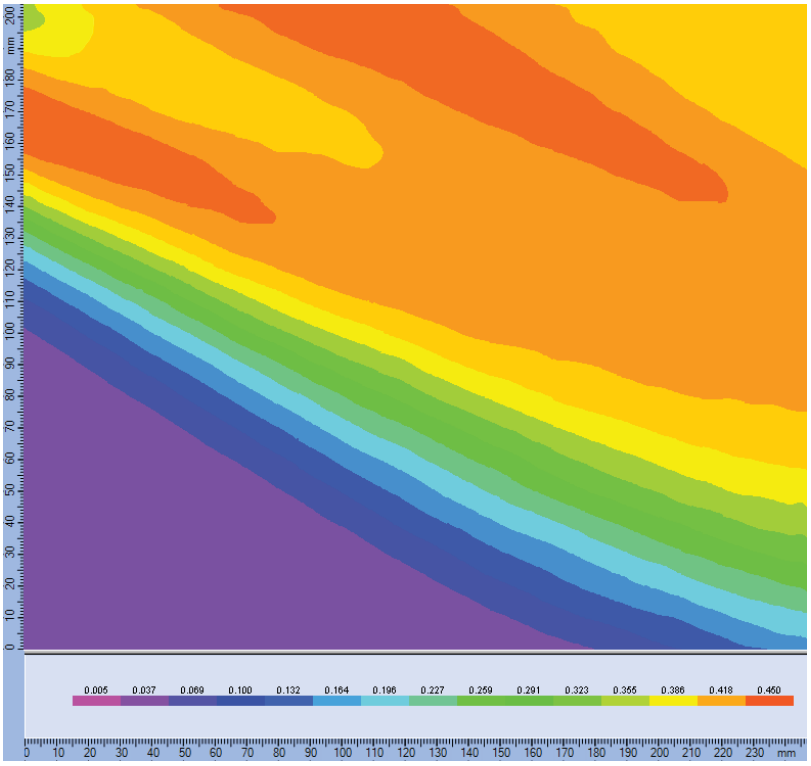

b)

Figure 13 *a) Velocity vector diagram showing air direction and b) Contour velocity plot diagram close of the RMP supplying 8L/s without the thermal manikin being present.*

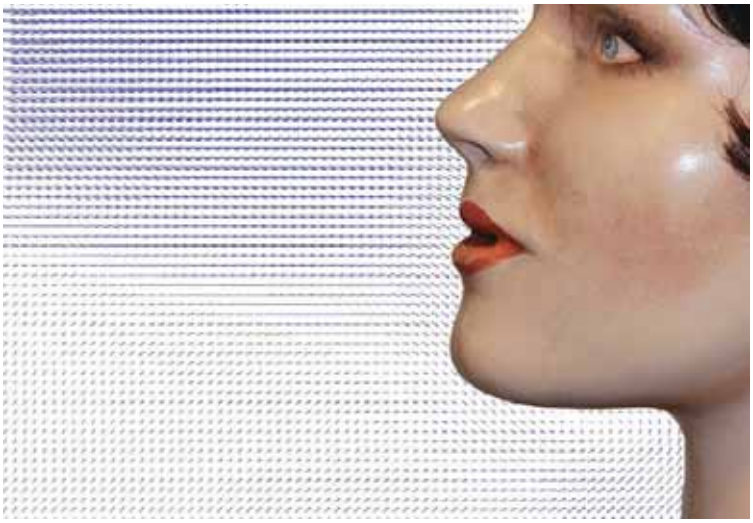

a)

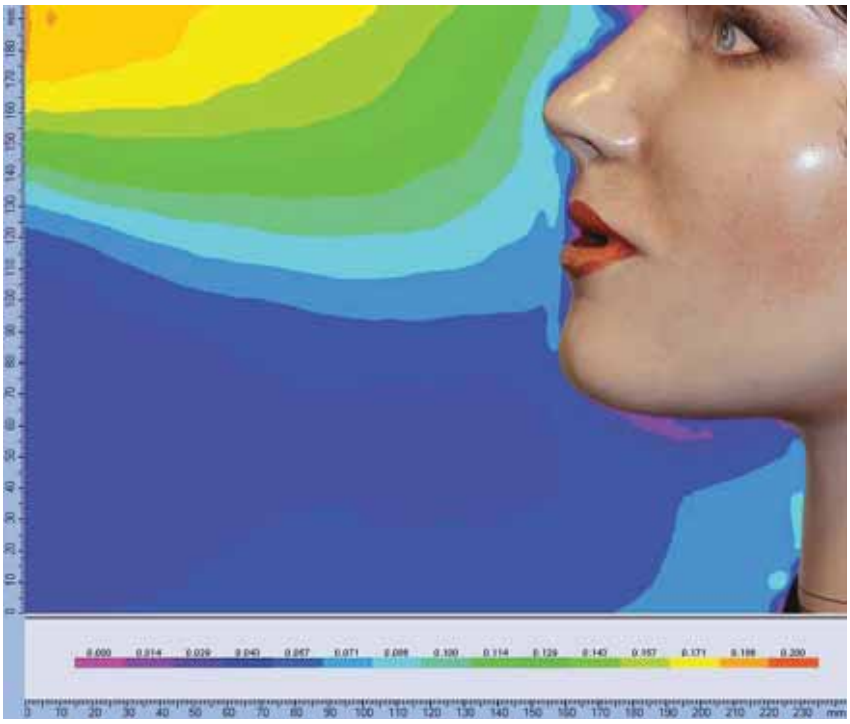

b)

Figure 14 *a) Velocity vector diagram showing air direction and b) Contour velocity plot diagram close to the breathing zone of a thermal manikin when heated, with straight board (passive control method) pressed at stomach level and the RMP supplying 4L/s at 0.4m frontally slightly from above.*

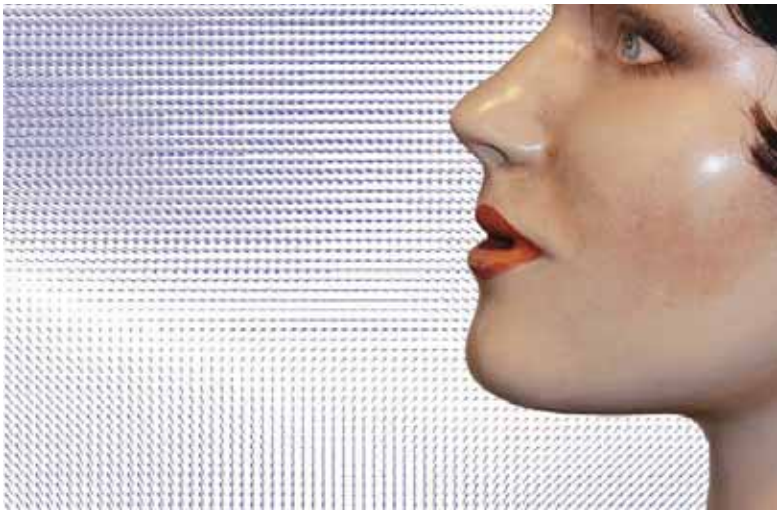

a)

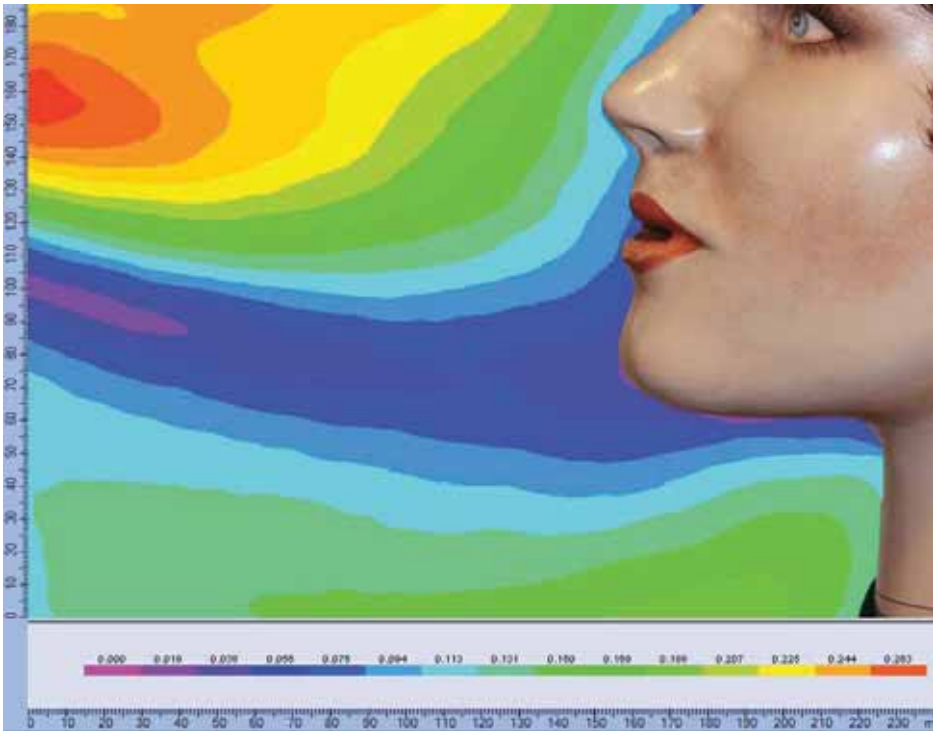

b)

Figure 15 *a) Velocity vector diagram showing air direction and b) Contour velocity plot diagram close to the breathing zone of a thermal manikin when heated, with straight board (passive control method) pressed at stomach level and the RMP supplying 6L/s at 0.4m frontally slightly from above.*

a)

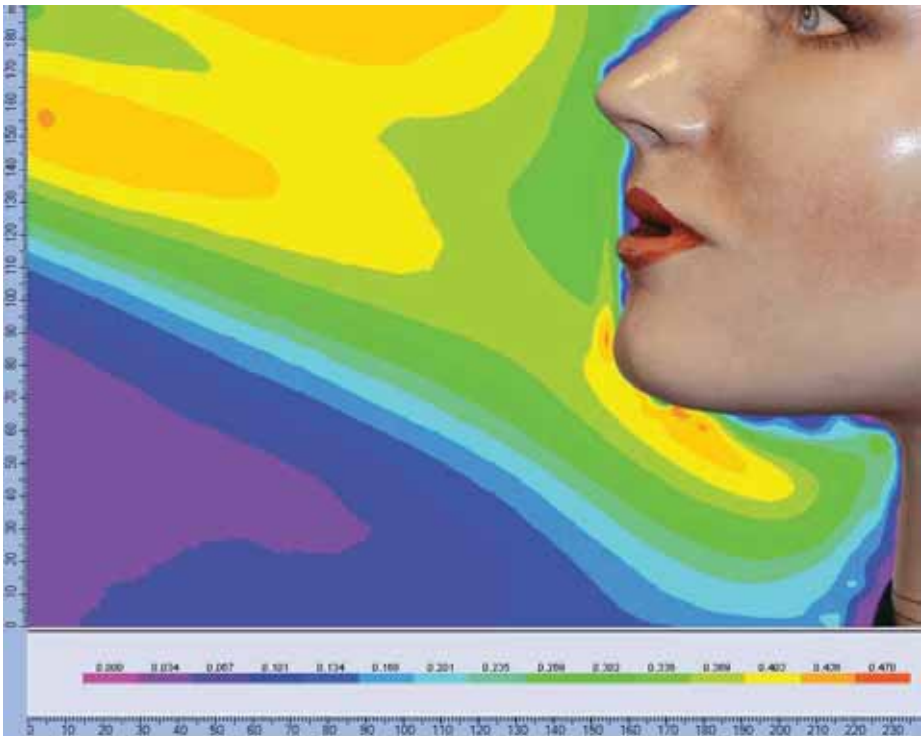

b)

Figure 16 *a) Velocity vector diagram showing air direction and b) Contour velocity plot diagram close to the breathing zone of a thermal manikin when heated, with straight board (passive control method) pressed at stomach level and the RMP supplying 8L/s at 0.4m frontally slightly from above.*

a)

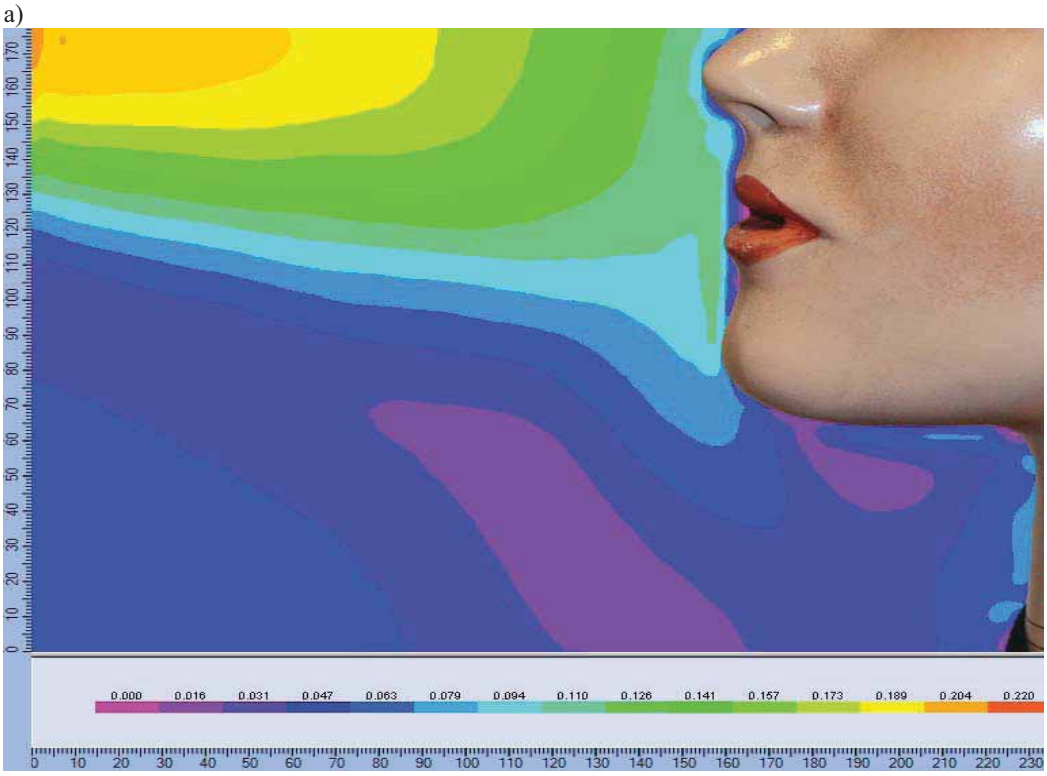

b)

Figure 17 *a) Velocity vector diagram showing air direction and b) Contour velocity plot diagram close to the breathing zone of a thermal manikin when heated, with active control method when front row of 3 fans is working at 15V each and the RMP supplying 4L/s at 0.4m frontally slightly from above.*

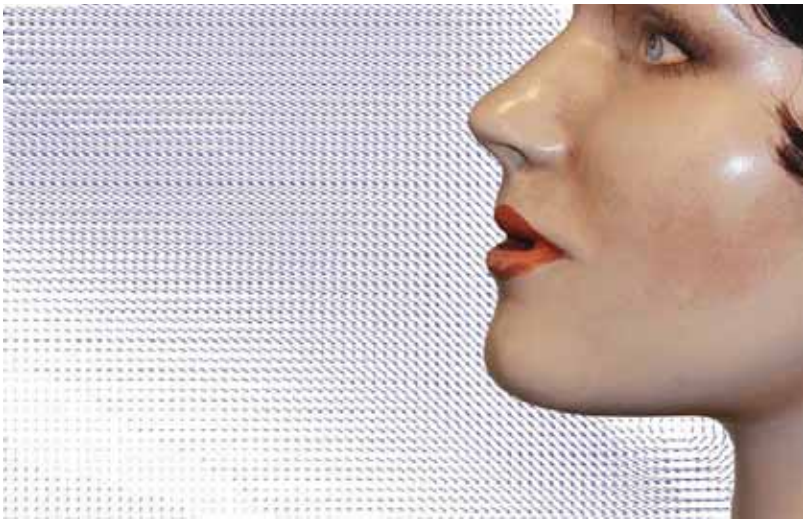

a)

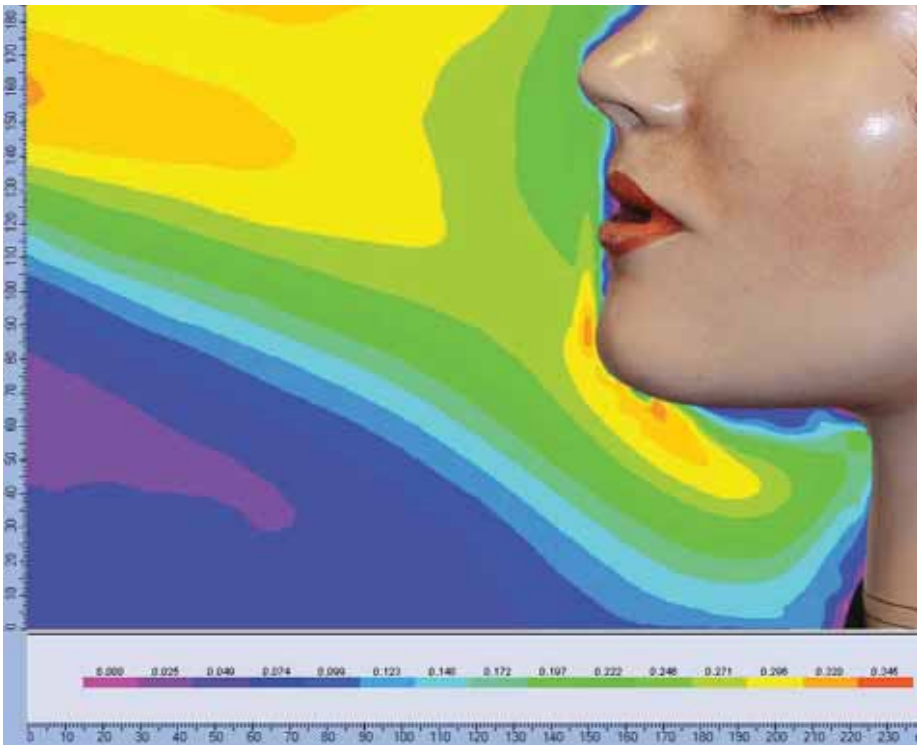

b)

Figure 18 *a) Velocity vector diagram showing air direction and b) Contour velocity plot diagram close to the breathing zone of a thermal manikin when heated, with active control method when front row of 3 fans is working at 15V each and the RMP supplying 6L/s at 0.4m frontally slightly from above.*

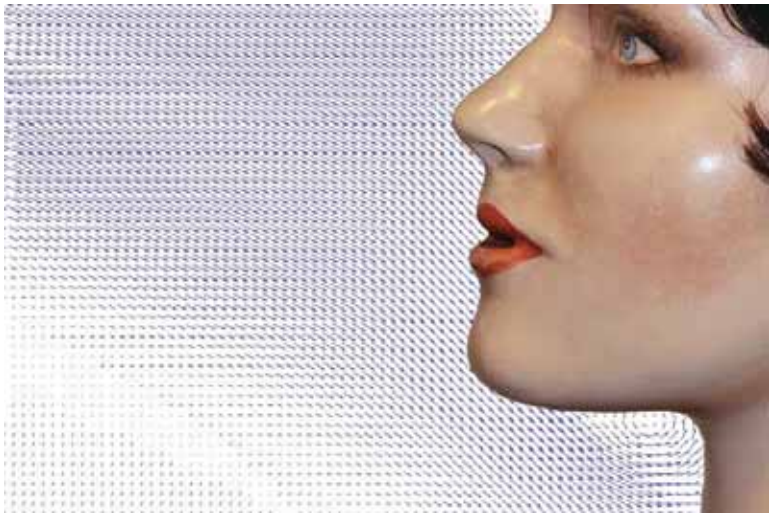

a)

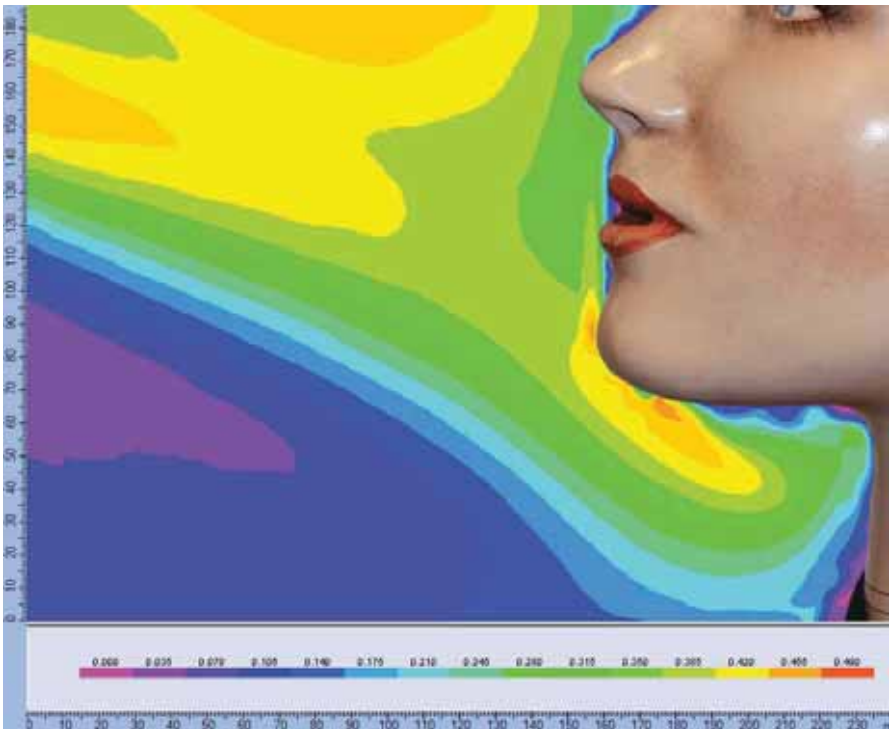

b)

Figure 19 *a) Velocity vector diagram showing air direction and b) Contour velocity plot diagram close to the breathing zone of a thermal manikin when heated, with active control method when front row of 3 fans is working at 15V each and the RMP supplying 8L/s at 0.4m frontally slightly from above.*

a)

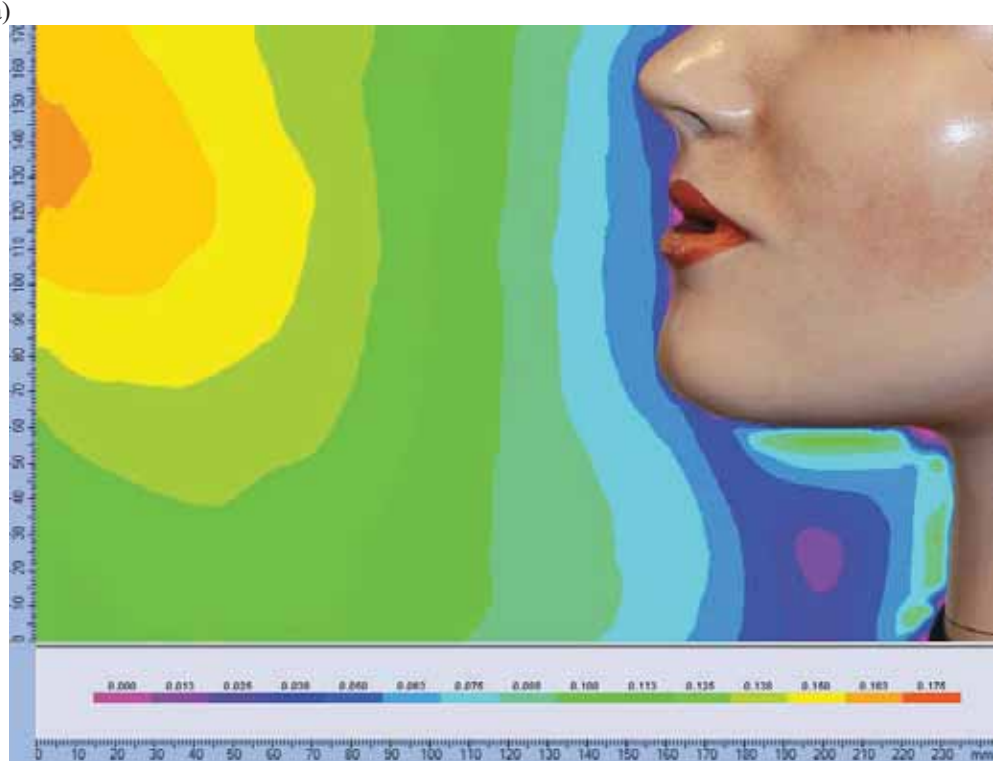

b)

Figure 20 *a) Velocity vector diagram showing air direction and b) Contour velocity plot diagram close to the breathing zone of a thermal manikin when heated, with active control method when front row of 3 fans is working at 30V each and the RMP supplying 4L/s at 0.4m frontally slightly from above.*

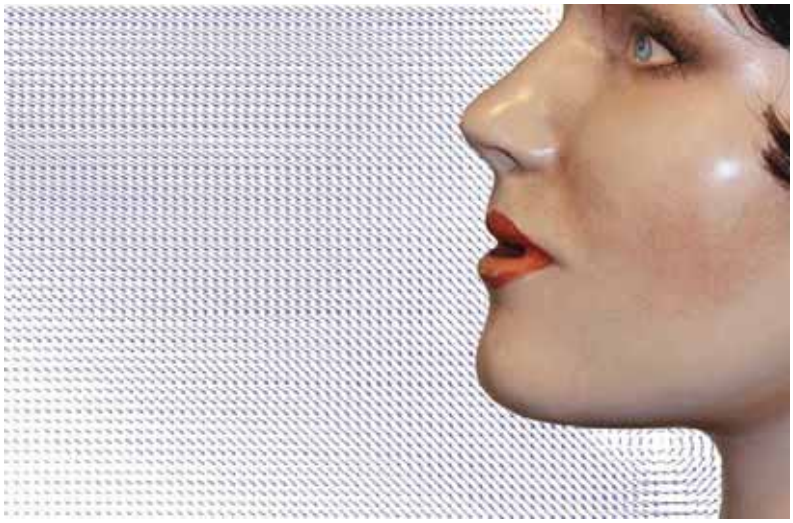

a)

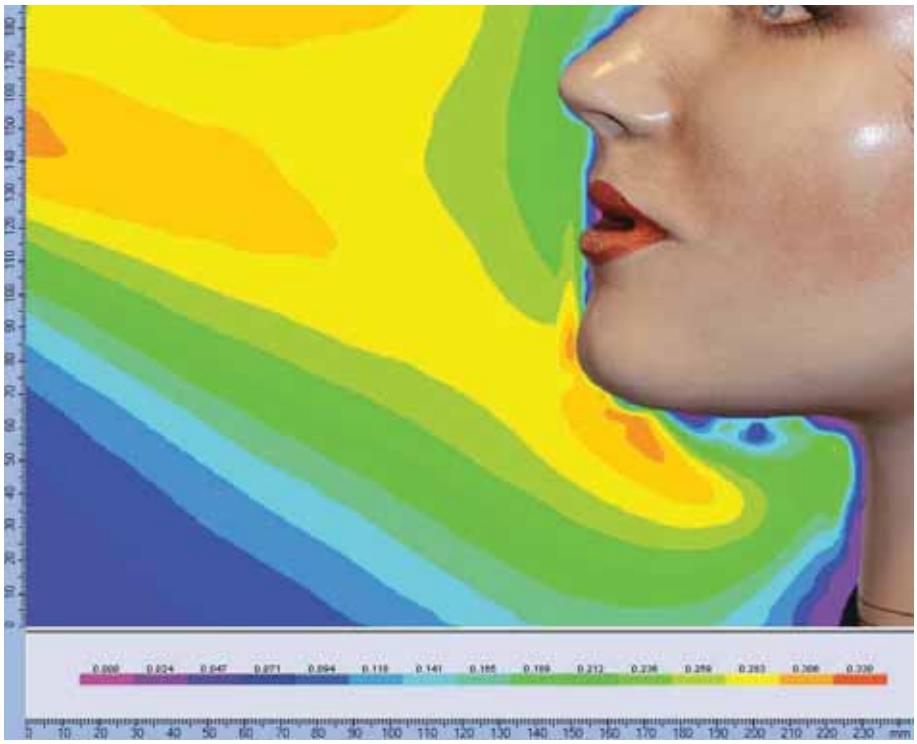

b)

Figure 21 *a) Velocity vector diagram showing air direction and b) Contour velocity plot diagram close to the breathing zone of a thermal manikin when heated, with active control method when front row of 3 fans is working at 30V each and the RMP supplying 6L/s at 0.4m frontally slightly from above.*

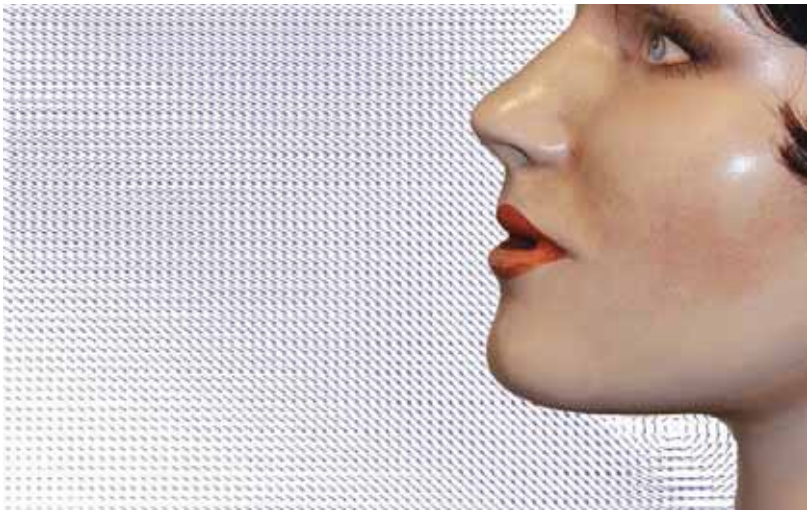

a)

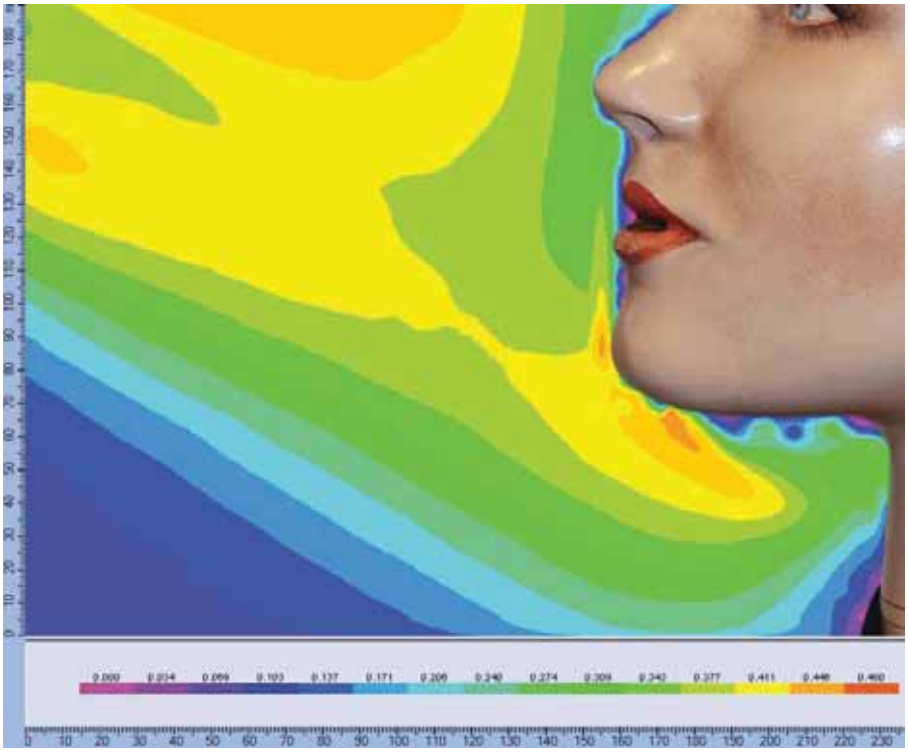

b)

Figure 22 *a) Velocity vector diagram showing air direction and b) Contour velocity plot diagram close to the breathing zone of a thermal manikin when heated, with active control method when front row of 3 fans is working at 30V each and the RMP supplying 8L/s at 0.4m frontally slightly from above.*

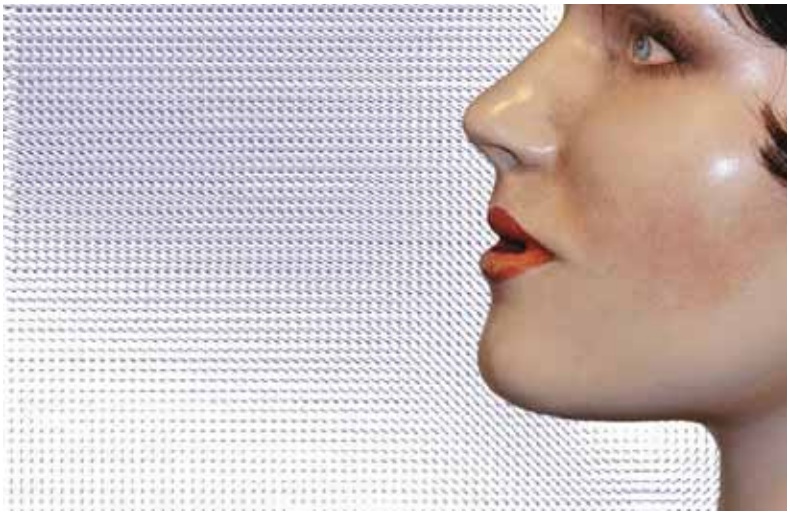

a)

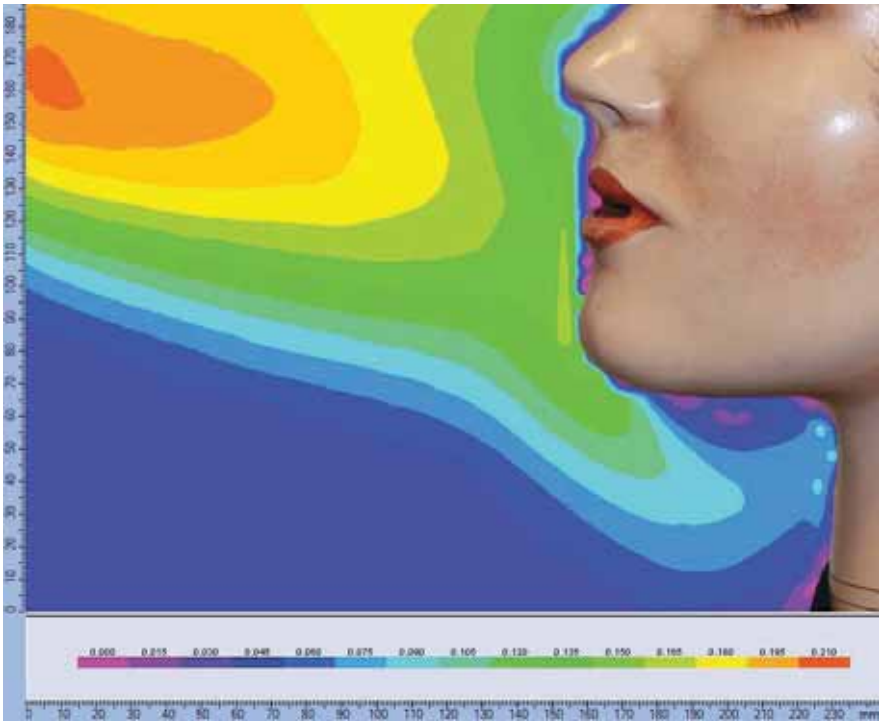

b)

Figure 23 *a) Velocity vector diagram showing air direction and b) Contour velocity plot diagram close to the breathing zone of a thermal manikin when heated, and combined passive control – straight board pressed against stomach with active control method when front row of 3 fans is working at 15V each and the RMP supplying 4L/s at 0.4m frontally slightly from above.*

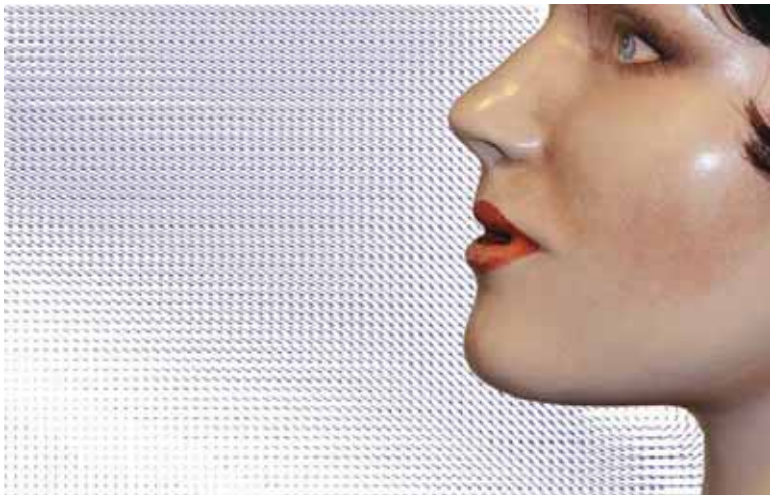

a)

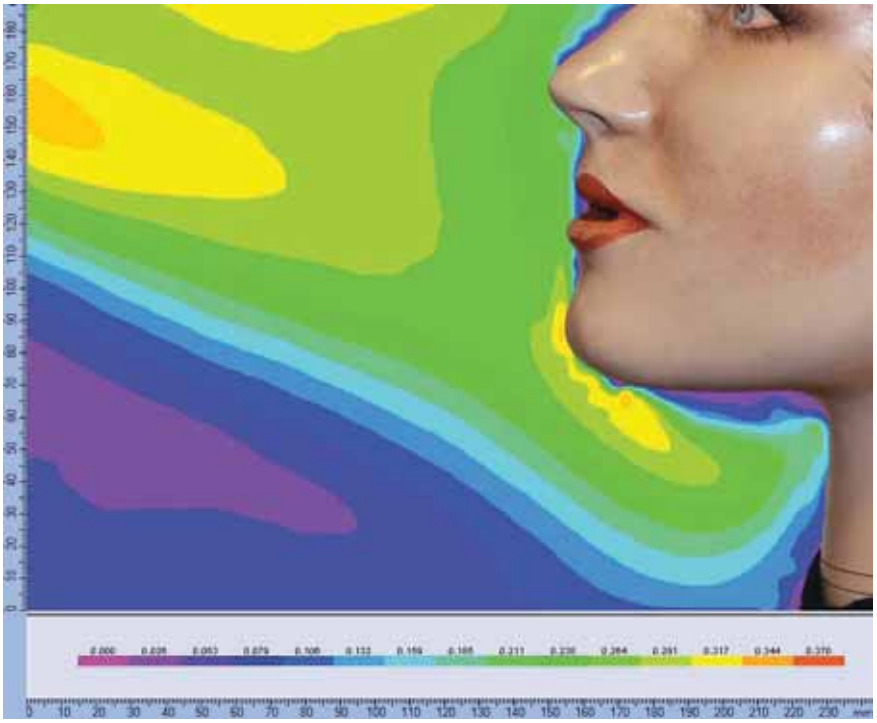

b)

Figure 24 *a) Velocity vector diagram showing air direction and b) Contour velocity plot diagram close to the breathing zone of a thermal manikin when heated, and combined passive control – straight board pressed against stomach with active control method when front row of 3 fans is working at 15V each and the RMP supplying 6L/s at 0.4m frontally slightly from above.*

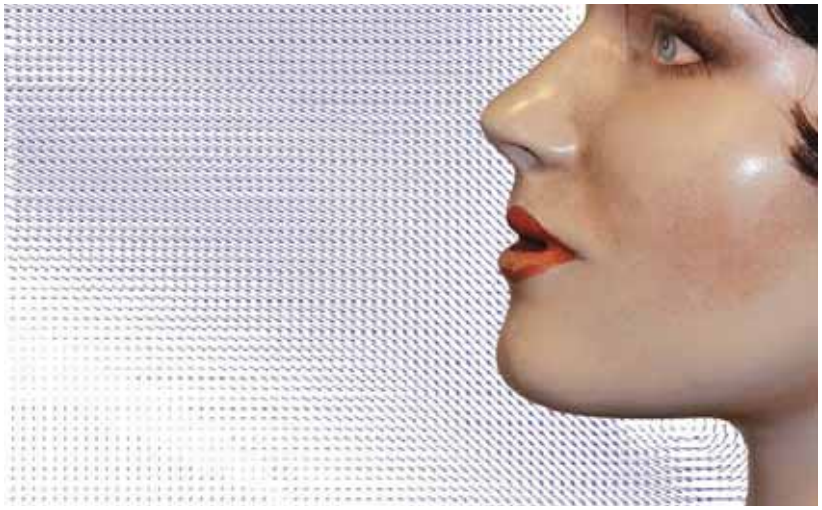

a)

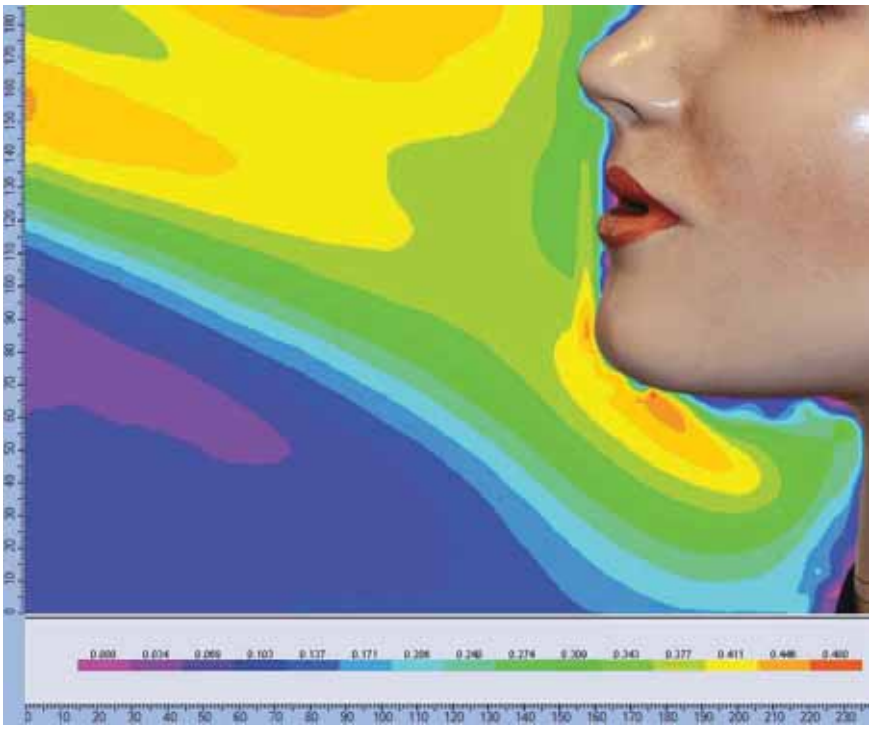

a)

Figure 25 *a) Velocity vector diagram showing air direction and b) Contour velocity plot diagram close to the breathing zone of a thermal manikin when heated, and combined passive control – straight board pressed against stomach with active control method when front row of 3 fans is working at 15V each and the RMP supplying 8L/s at 0.4m frontally slightly from above.*

Part 2

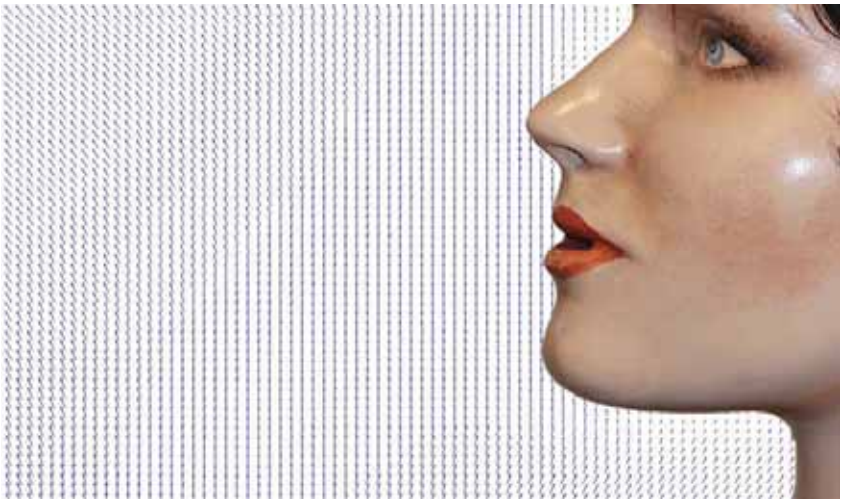

a)

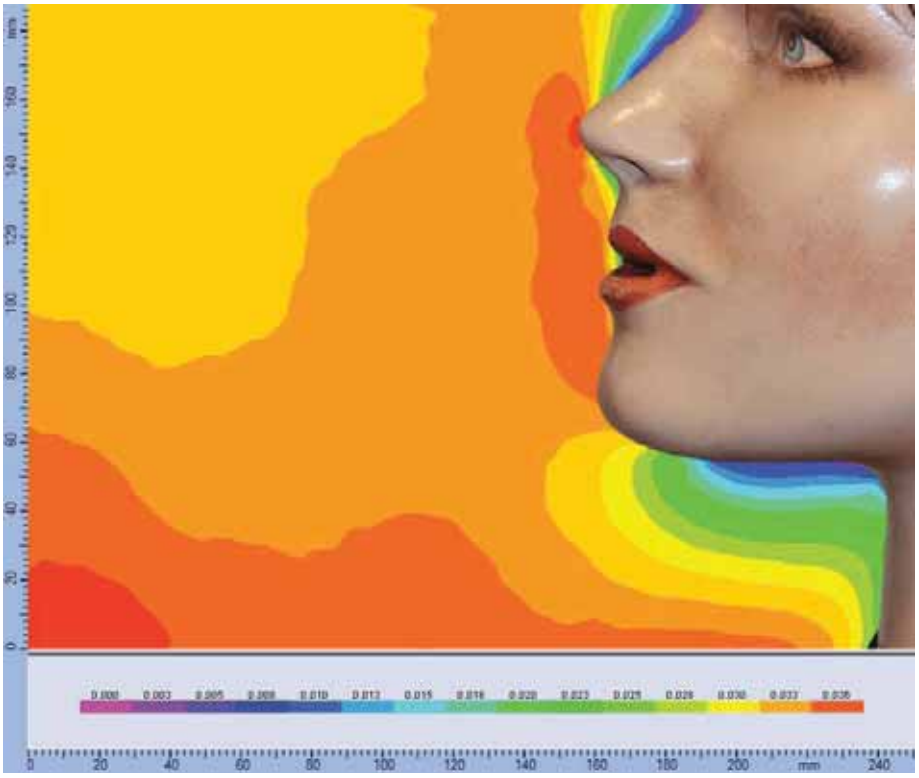

b)

Figure 26 *a) Velocity vector diagram showing air direction and b) Contour velocity plot diagram close to the breathing zone of a thermal manikin when heated and box with integrated confluent jets (jets not on).*

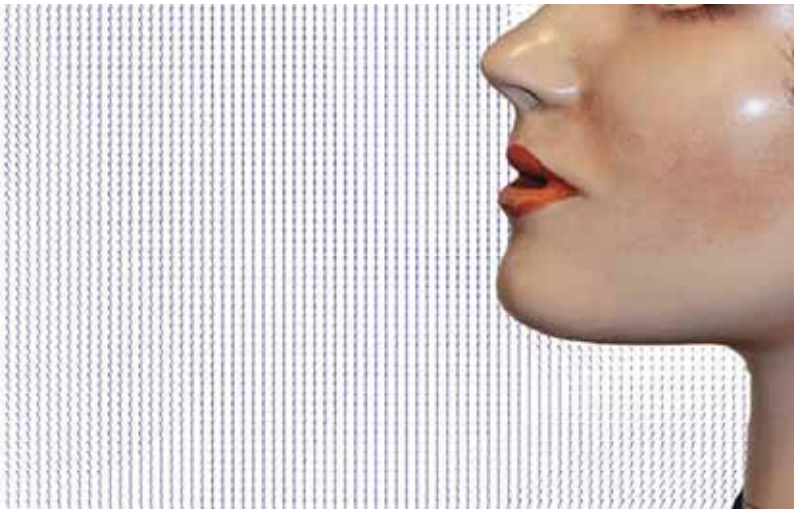

a)

b)

Figure 27 *a) Velocity vector diagram showing air direction and b) Contour velocity plot diagram close to the breathing zone of a thermal manikin when heated and box with integrated confluent jets when both inner and outer supply 4L/s.*

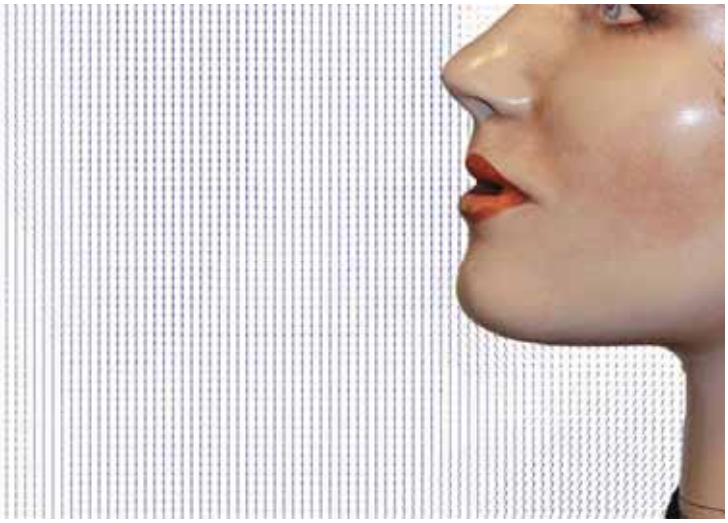

a)

b)

Figure 28 *a) Velocity vector diagram showing air direction and b) Contour velocity plot diagram close to the breathing zone of a thermal manikin when heated and box with integrated confluent jets when both inner and outer supply 6L/s.*

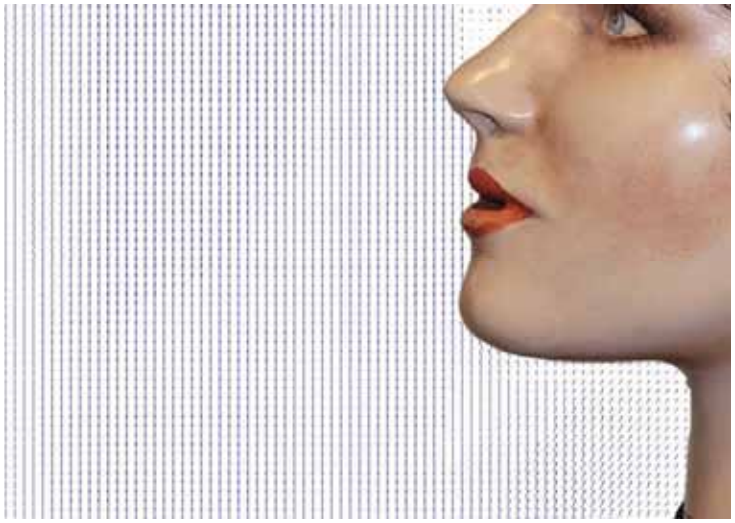

a)

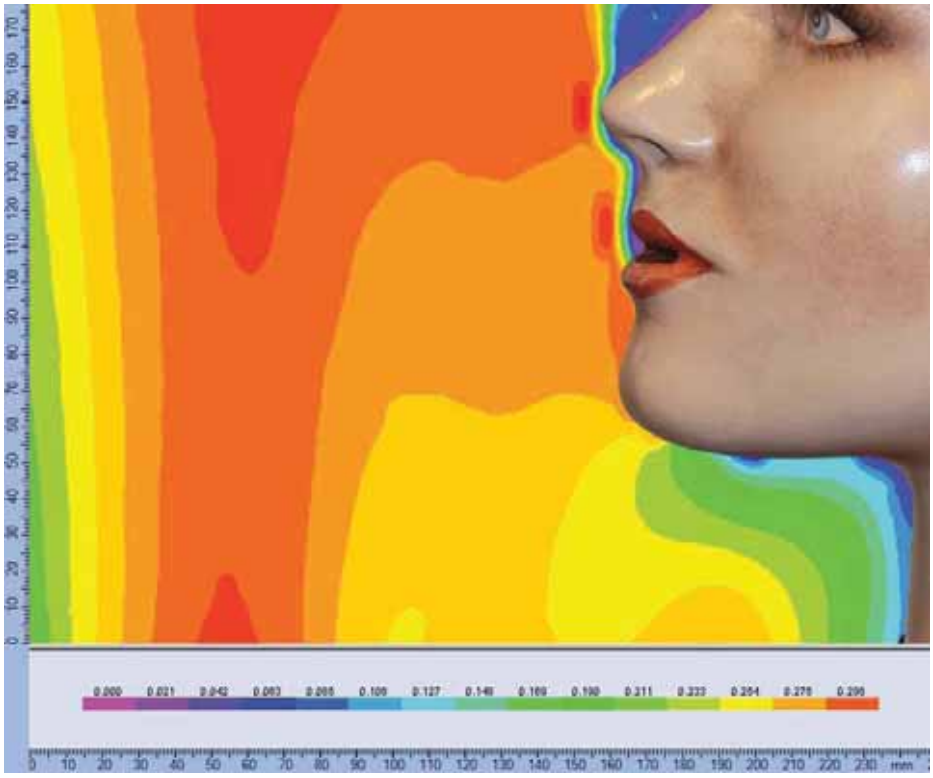

b)

Figure 29 *a) Velocity vector diagram showing air direction and b) Contour velocity plot diagram close to the breathing zone of a thermal manikin when heated and box with integrated confluent jets when both inner and outer supply 8L/s.*

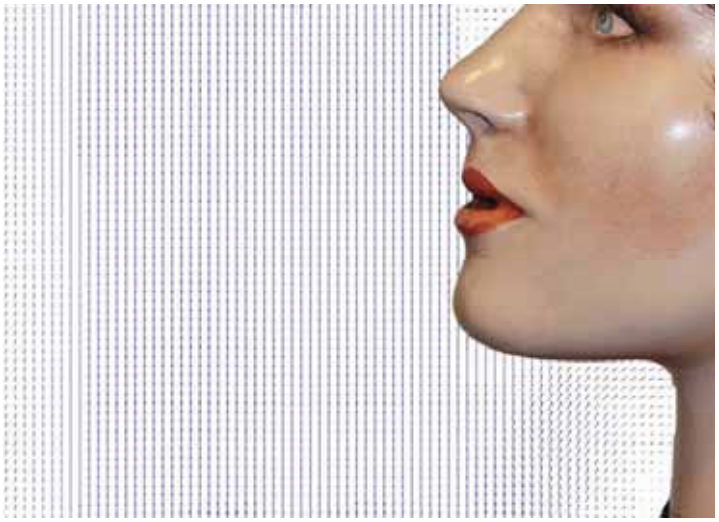

a)

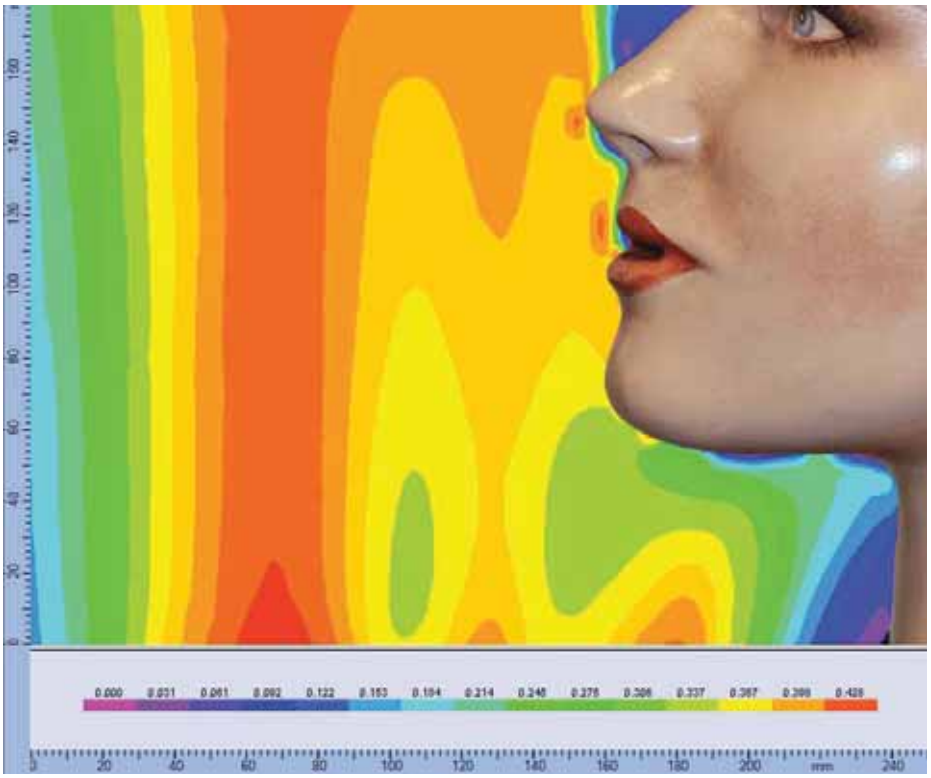

b)

Figure 30 *a) Velocity vector diagram showing air direction and b) Contour velocity plot diagram close to the breathing zone of a thermal manikin when heated and box with integrated confluent jets when both inner and outer supply 10L/s.*

a)

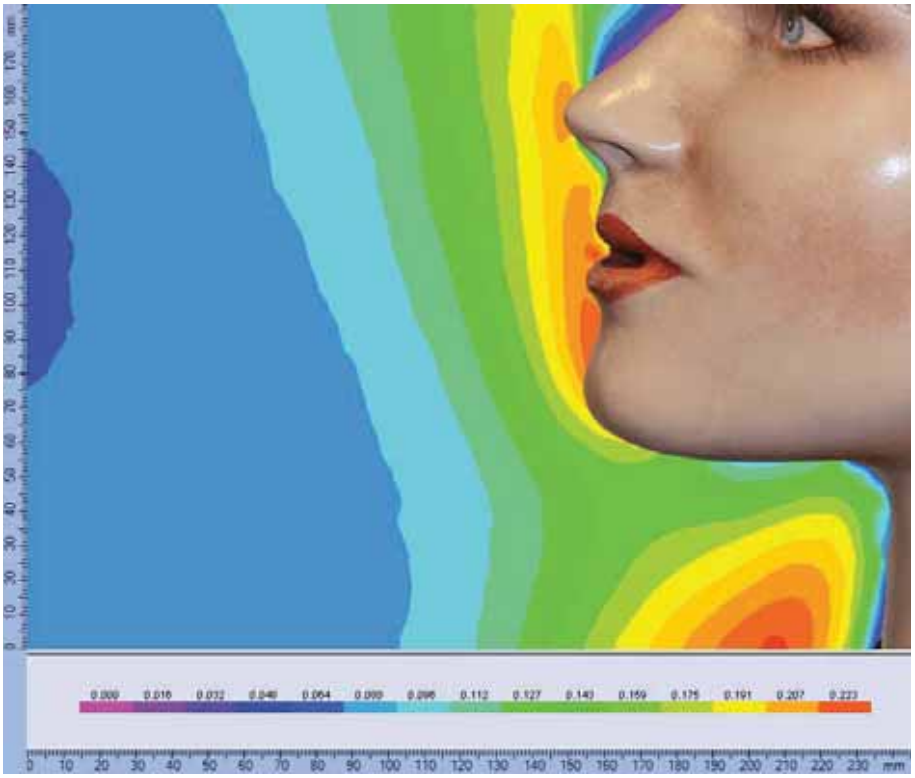

b)

Figure 31 *a) Velocity vector diagram showing air direction and b) Contour velocity plot diagram close to the breathing zone of a thermal manikin when heated and box with integrated confluent jets when only inner jet supplies 8L/s.*

a)

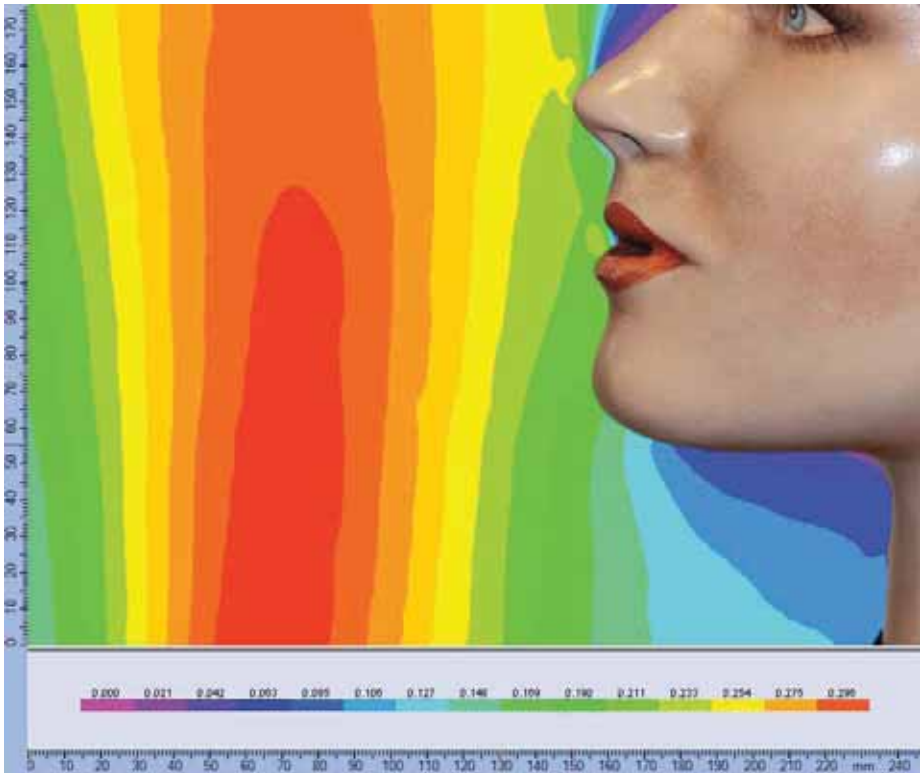

b)

Figure 32 *a) Velocity vector diagram showing air direction and b) Contour velocity plot diagram close to the breathing zone of a thermal manikin when heated and box with integrated confluent jets when only outer jet supplies 8L/s.*

a)

b)

Figure 33 *a) Velocity vector diagram showing air direction and b) Contour velocity plot diagram close to the breathing zone of a thermal manikin when heated and box with integrated confluent jets when inner jet supplies 4L/s and outer jet supplies 8L/s.*

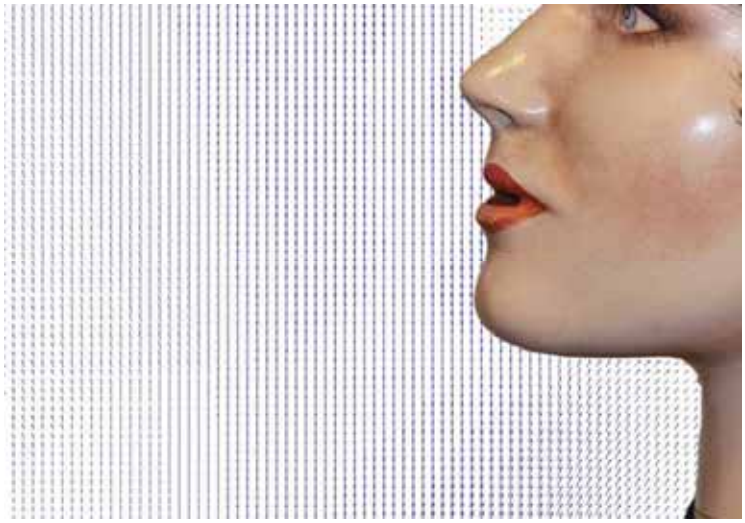

a)

b)

Figure 34 *a) Velocity vector diagram showing air direction and b) Contour velocity plot diagram close to the breathing zone of a thermal manikin when heated and box with integrated confluent jets when inner jet supplies 8L/s and outer jet supplies 4L/s.*

Part 3

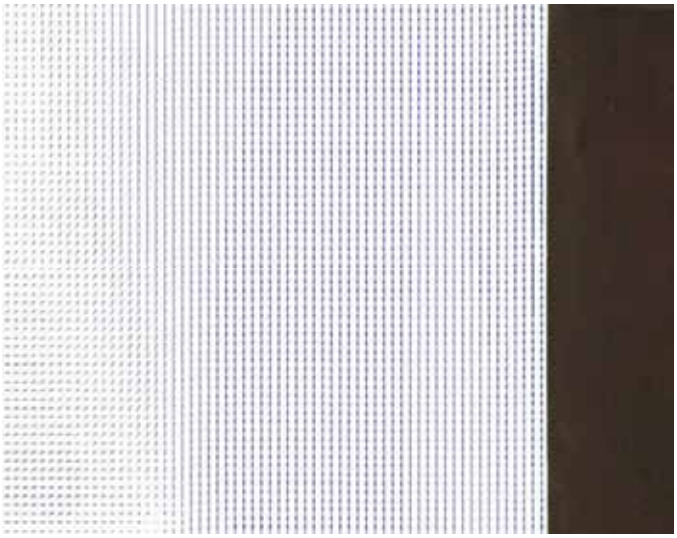

a)

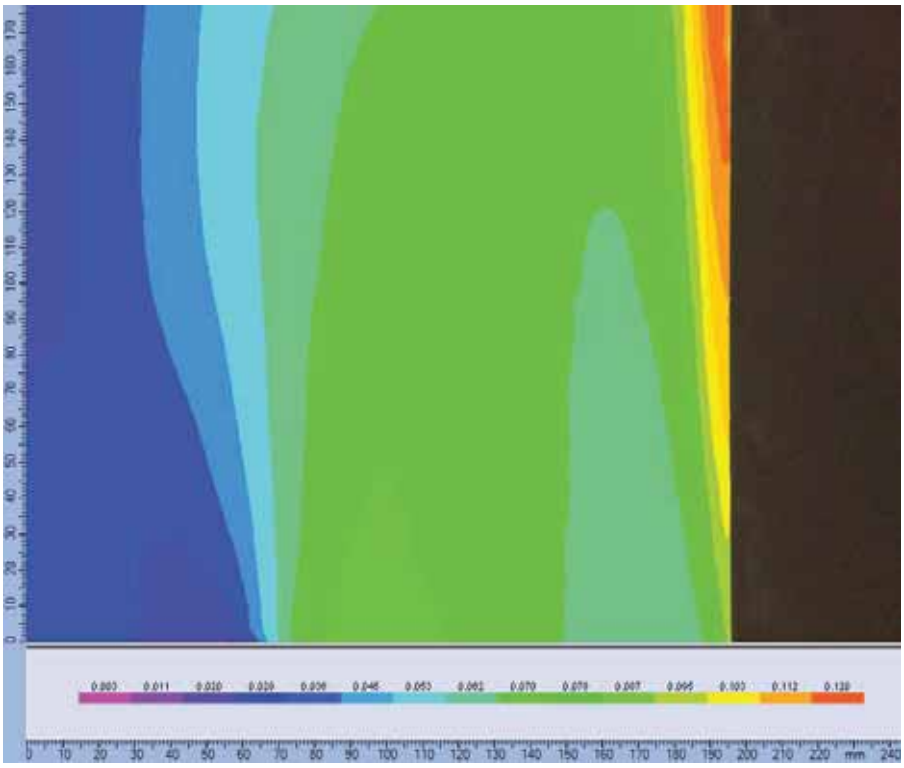

b)

Figure 35 *a) Velocity vector diagram showing air direction and b) Contour velocity plot diagram close to the heated radiator surface when distance between radiator and table was 0.12 m.*

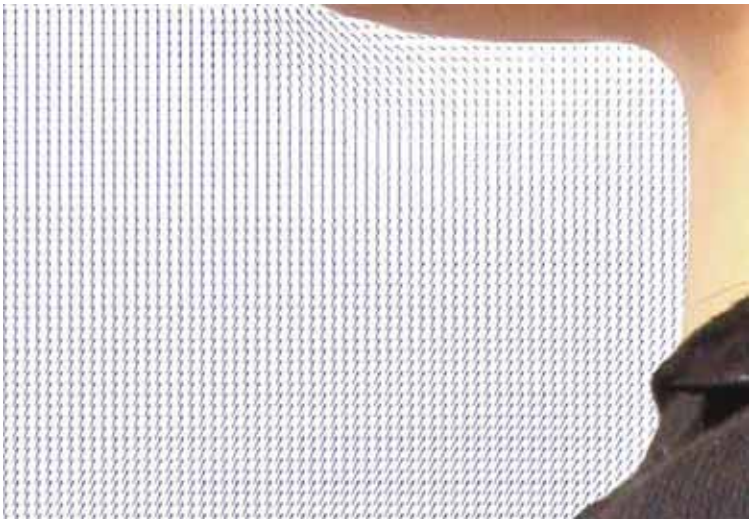

a)

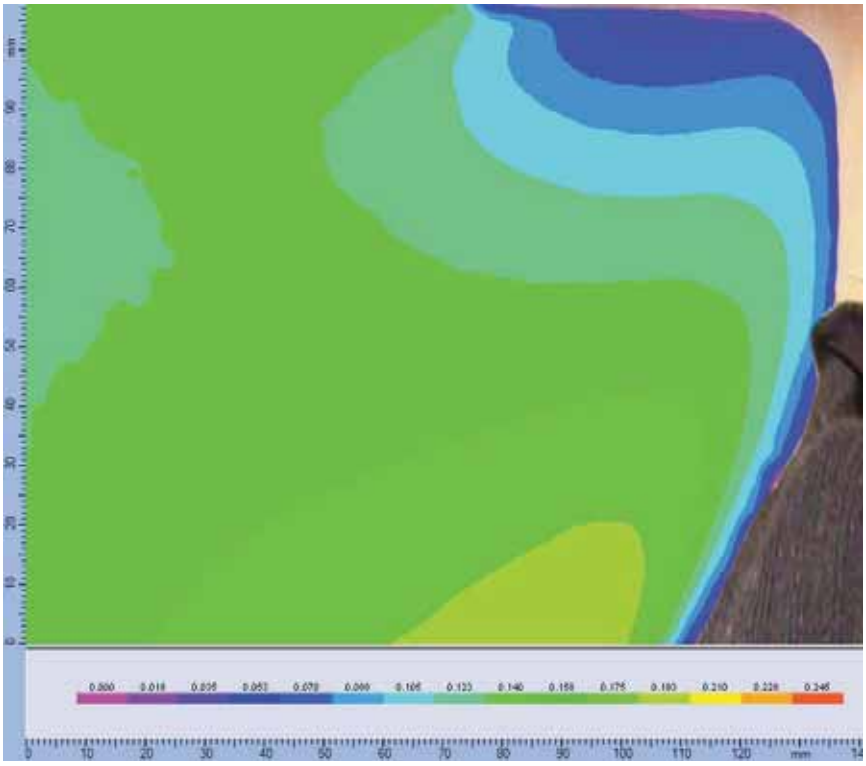

b)

Figure 36 *a) Velocity vector diagram showing air direction and b) Contour velocity plot diagram close to the heated manikin (neck) when distance between manikin and table was 0.12 m.*

a)

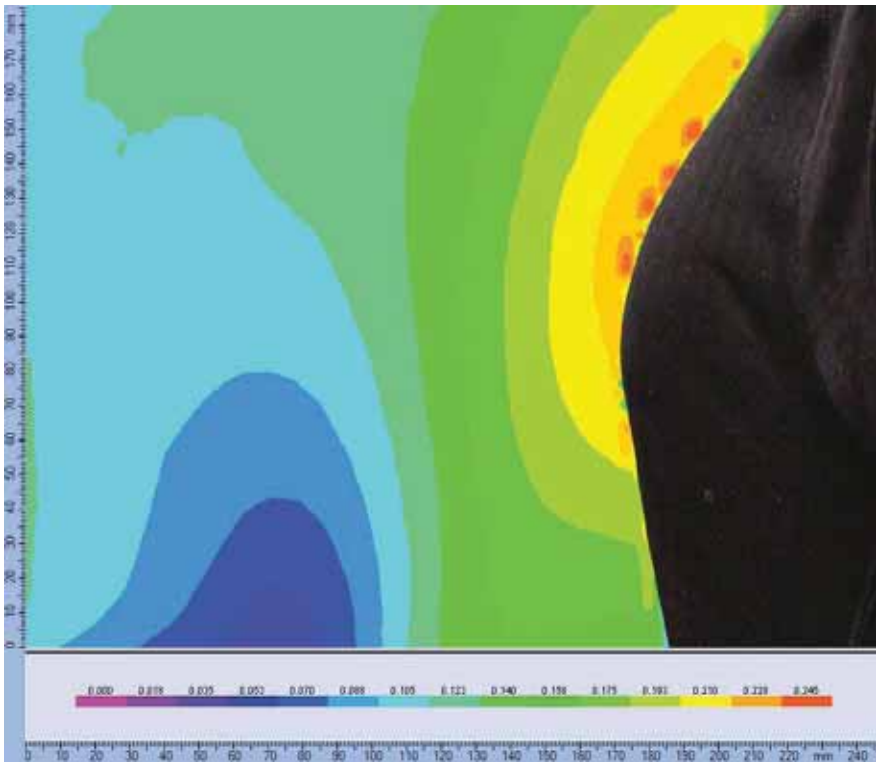

b)

Figure 37 *a) Velocity vector diagram showing air direction and b) Contour velocity plot diagram close to the heated manikin (chest) when distance between manikin and table was 0.12 m.*

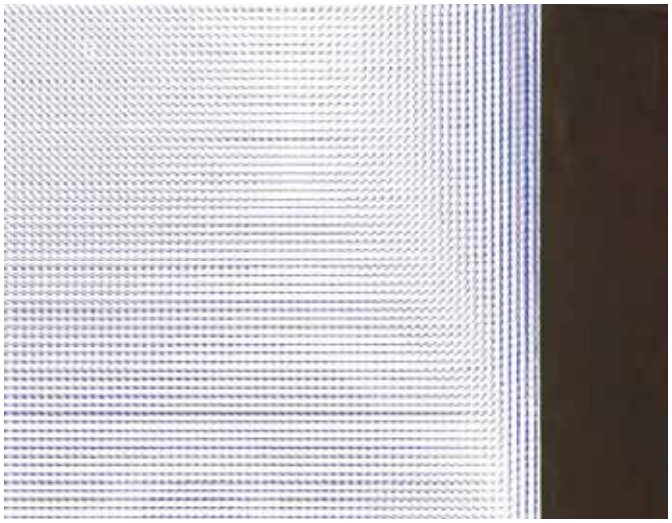

a)

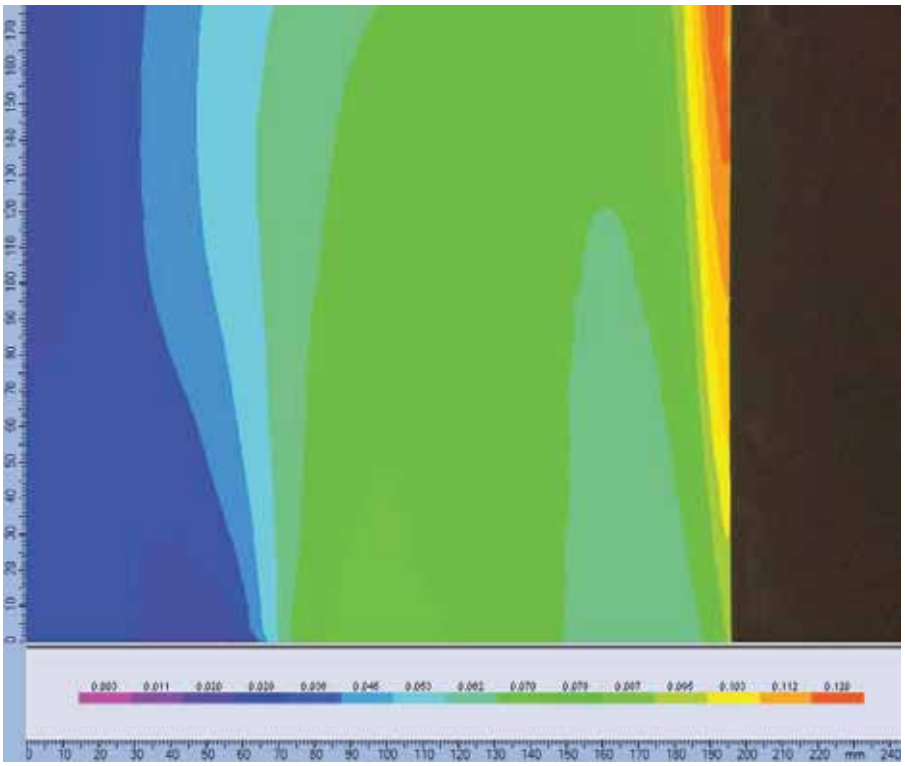

b)

Figure 38 *a) Velocity vector diagram showing air direction and b) Contour velocity plot diagram close to the heated radiator surface when box with integrated confluent jet is not working.*

a)

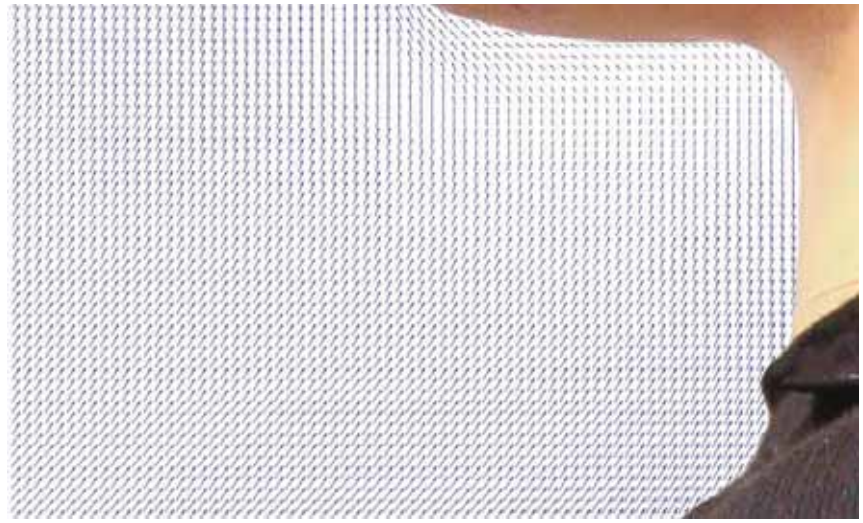

b)

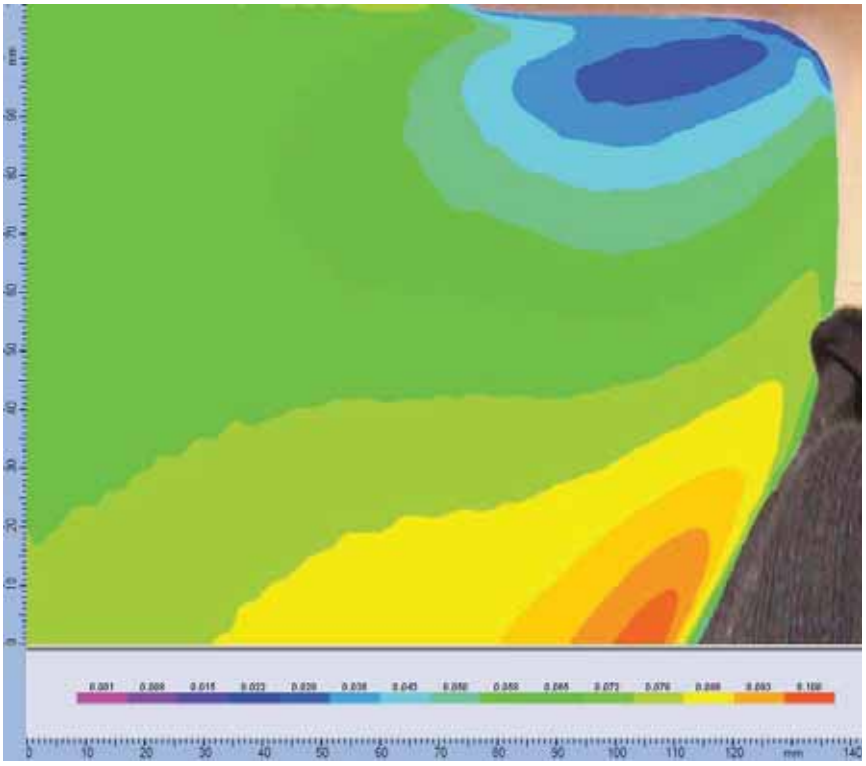

Figure 39 *a) Velocity vector diagram showing air direction and b) Contour velocity plot diagram close to the heated manikin (neck) when box with integrated confluent jet is not working.*

a)

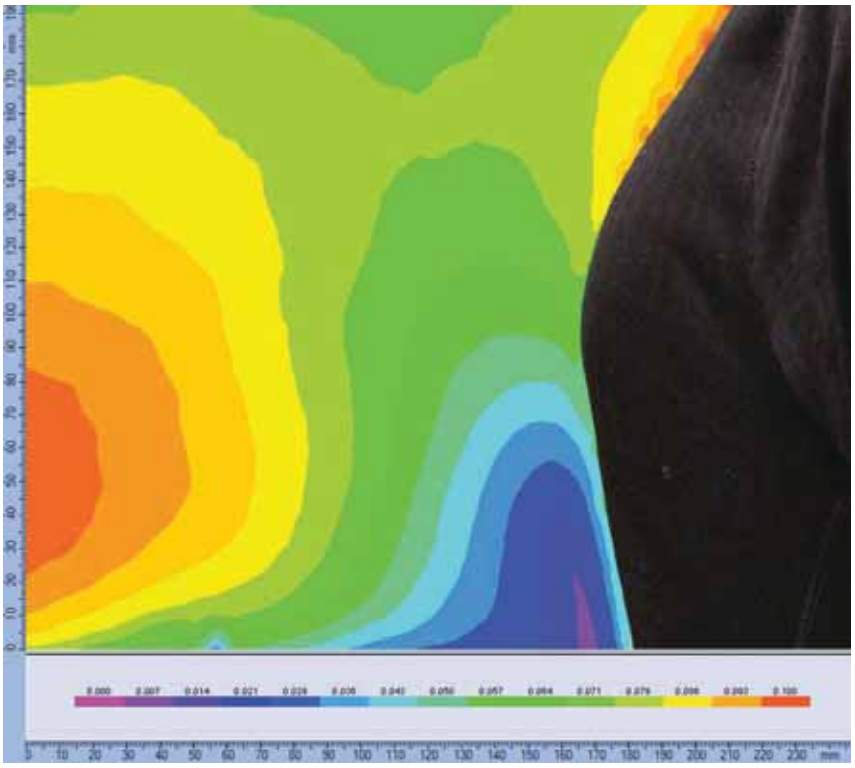

b)

Figure 40 *a) Velocity vector diagram showing air direction and b) Contour velocity plot diagram close to the heated manikin (chest) when box with integrated confluent jet is not working.*

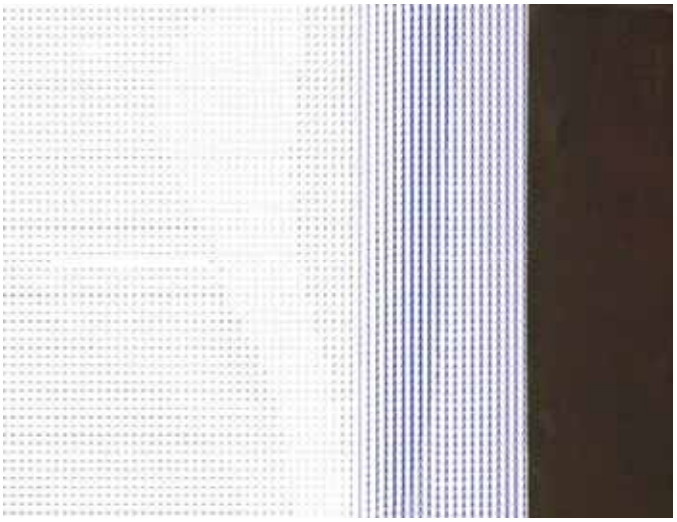

a)

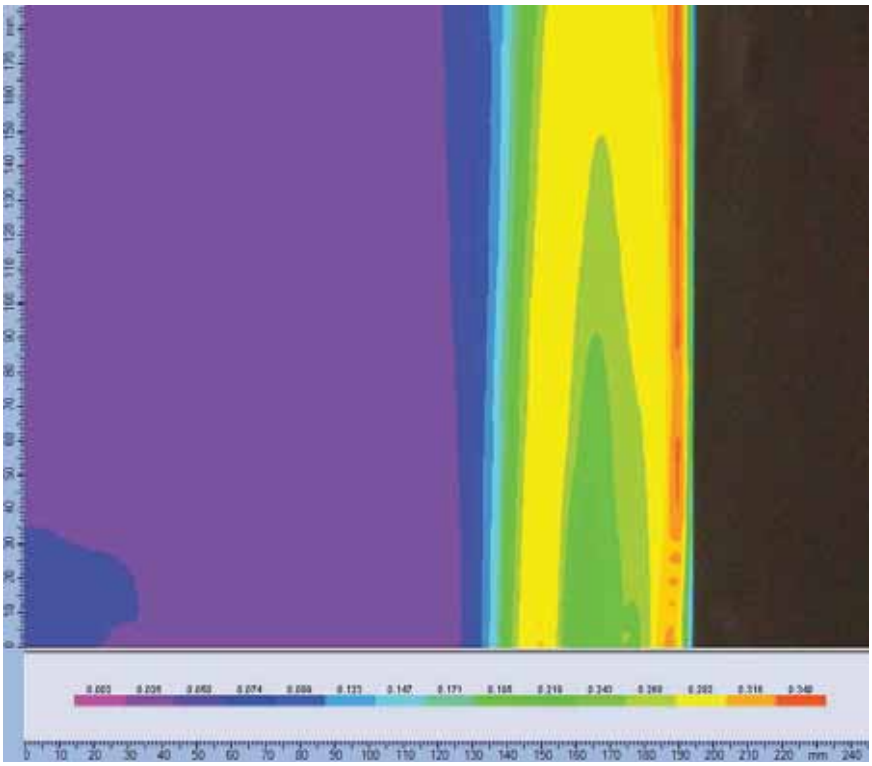

b)

Figure 41 *a) Velocity vector diagram showing air direction and b) Contour velocity plot diagram close to the heated radiator surface and box with integrated confluent jets when only inner jet supplies 8L/s.*

a)

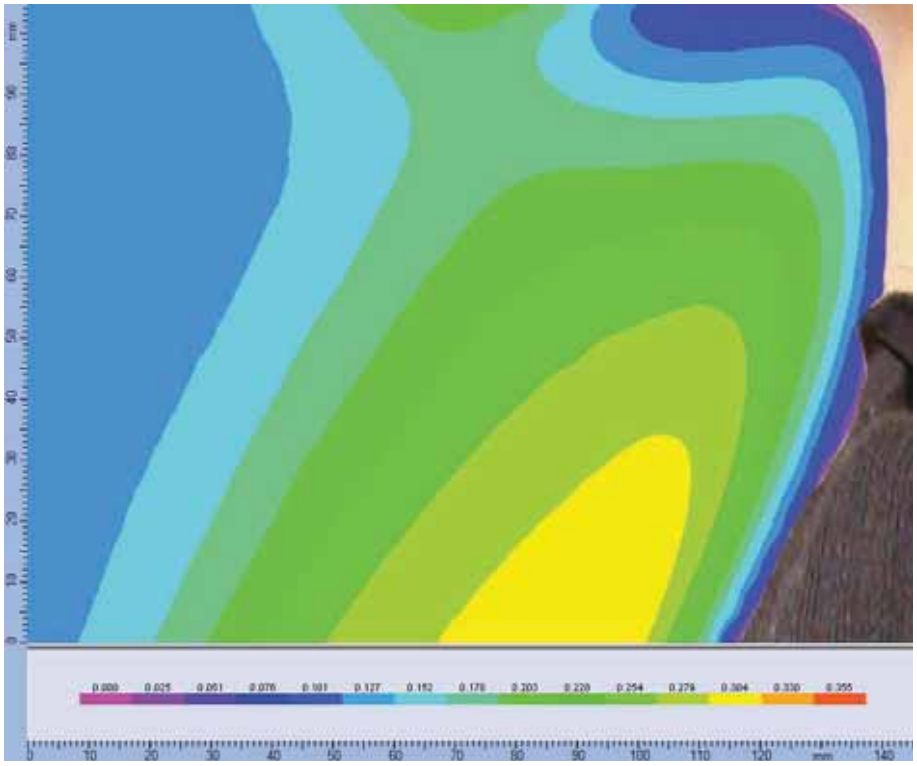

b)

Figure 42 *a) Velocity vector diagram showing air direction and b) Contour velocity plot diagram close to the heated manikin (neck) and box with integrated confluent jets when only inner jet supplies 8L/s.*

a)

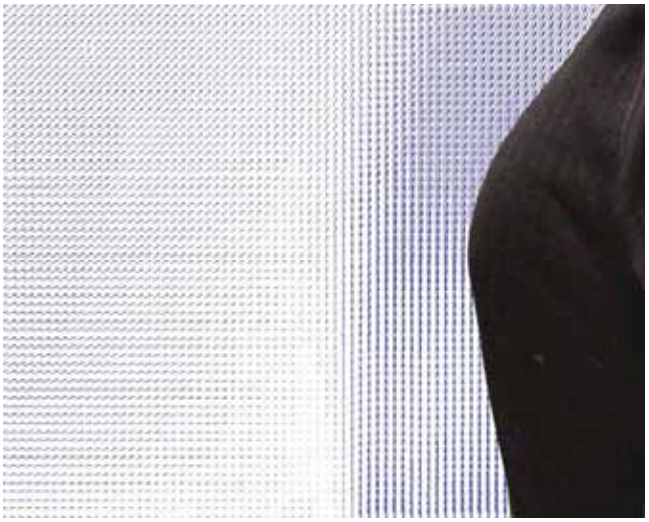

b)

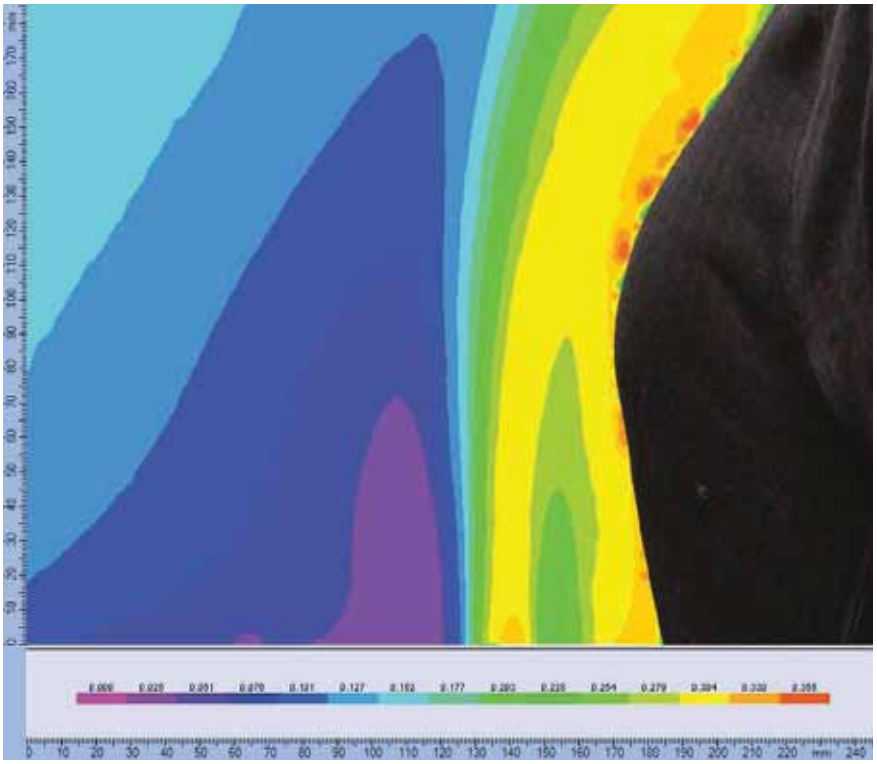

Figure 43 *a) Velocity vector diagram showing air direction and b) Contour velocity plot diagram close to the heated manikin (chest) and box with integrated confluent jets when only inner jet supplies 8L/s.*

a)

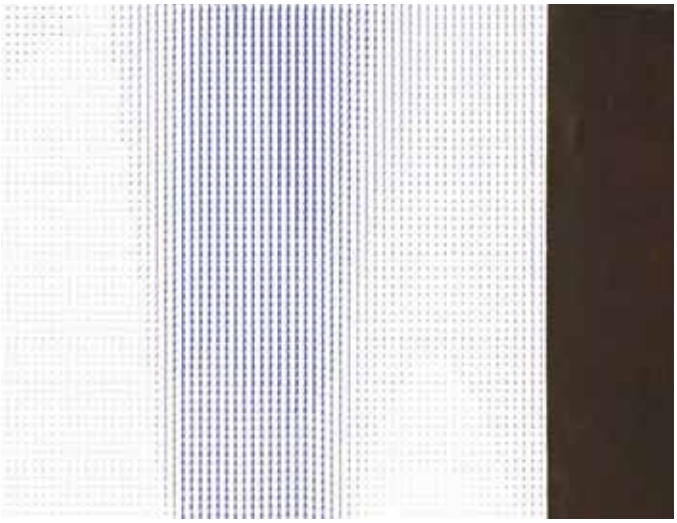

b)

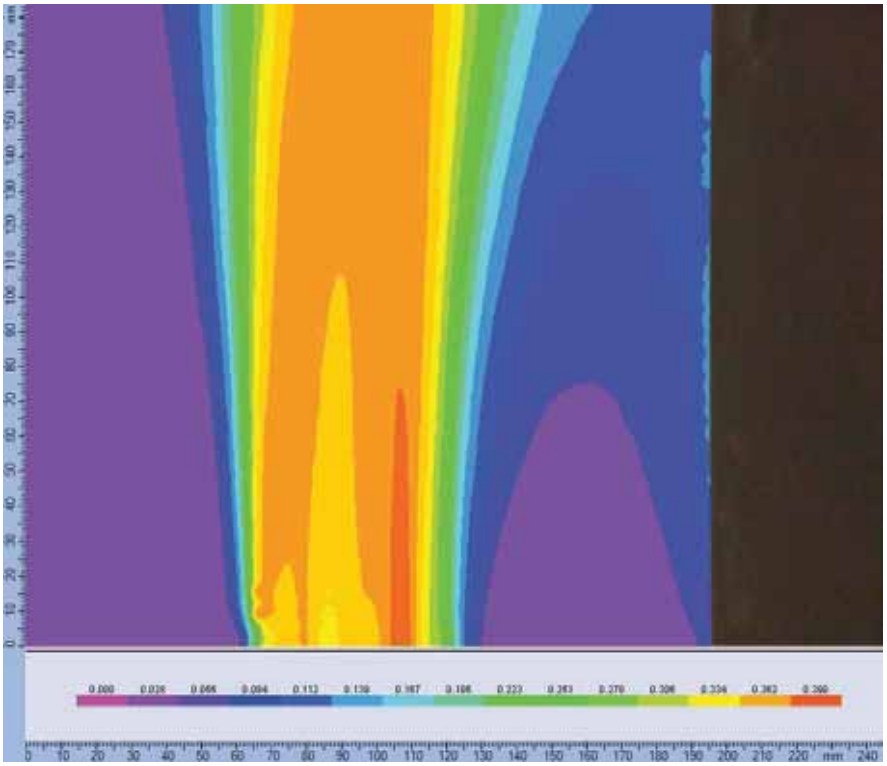

Figure 44 *a) Velocity vector diagram showing air direction and b) Contour velocity plot diagram close to the heated radiator surface and box with integrated confluent jets when only outer jet supplies 8L/s.*

a)

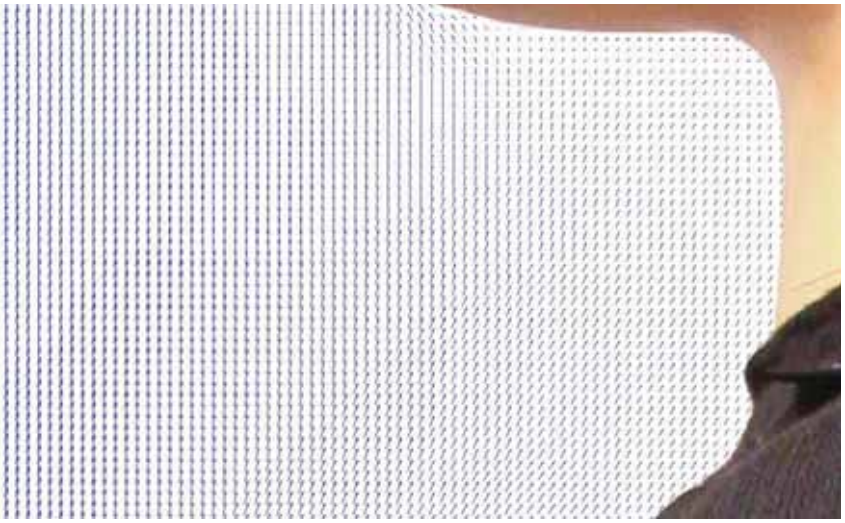

b)

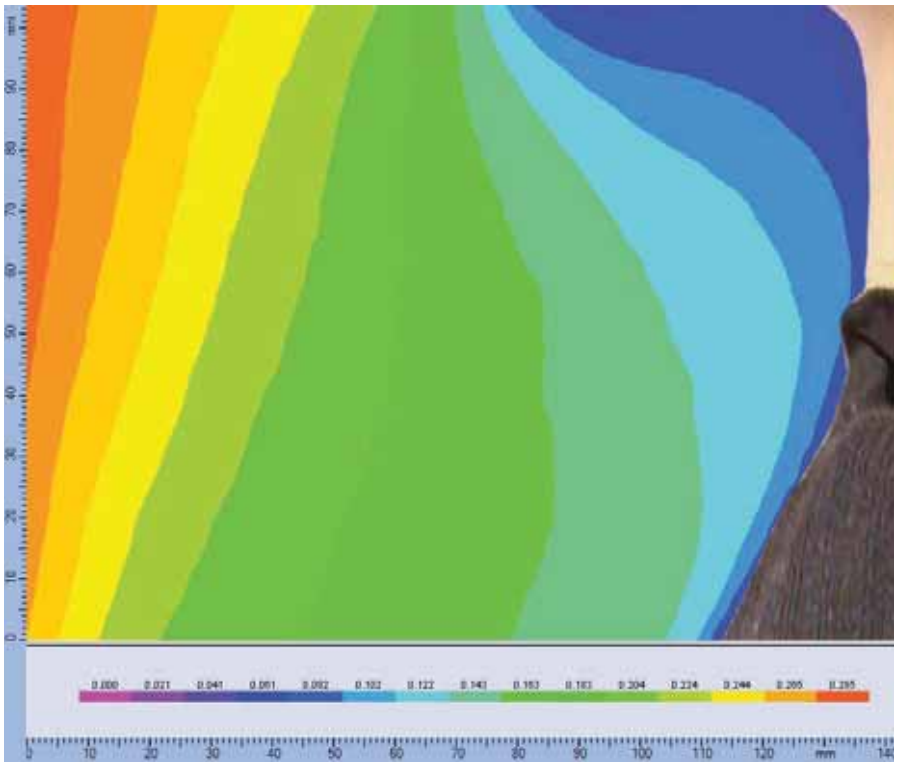

Figure 45 *a) Velocity vector diagram showing air direction and b) Contour velocity plot diagram close to the heated manikin (neck) and box with integrated confluent jets when only outer jet supplies 8L/s.*

a)

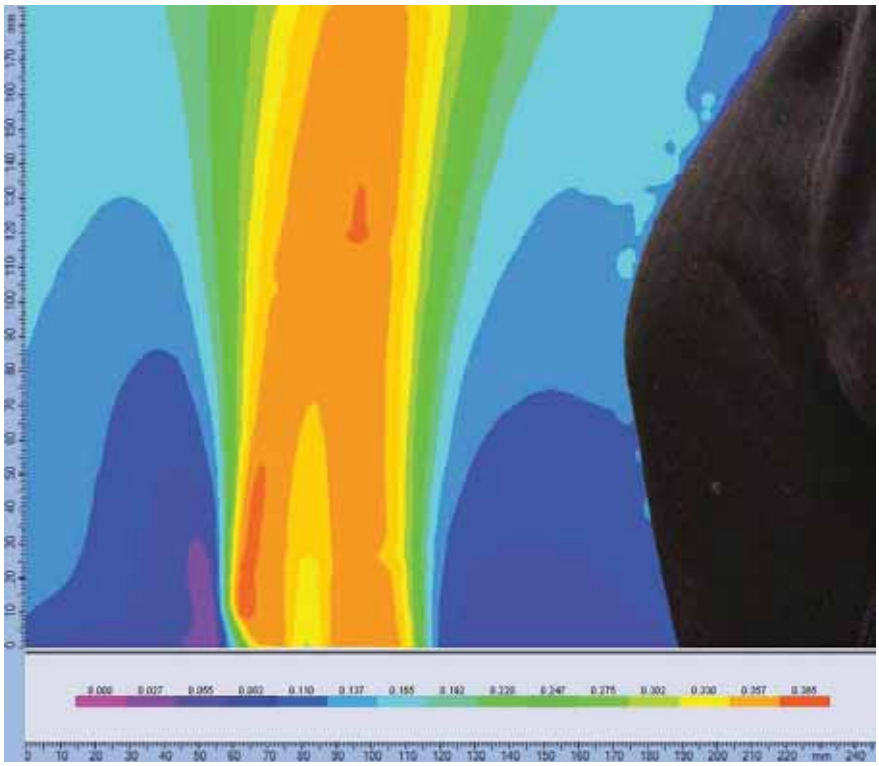

b)

Figure 46 *a) Velocity vector diagram showing air direction and b) Contour velocity plot diagram close to the heated manikin (chest) and box with integrated confluent jets when only outer jet supplies 8L/s.*

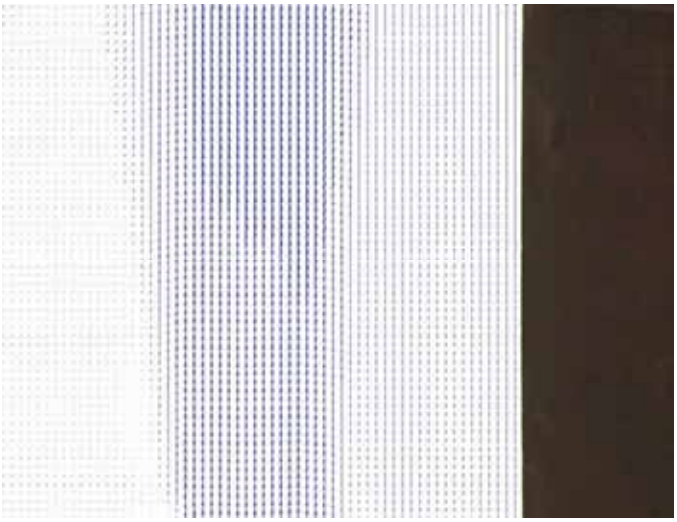

a)

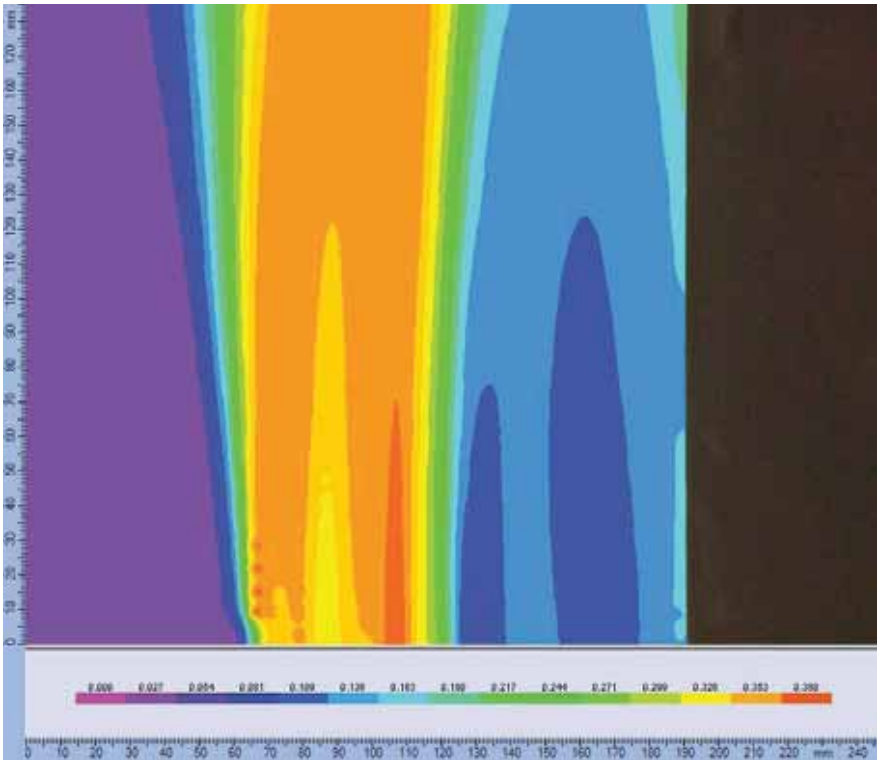

b)

Figure 47 a*) Velocity vector diagram showing air direction and b) Contour velocity plot diagram close to the heated radiator surface and box with integrated confluent jets when inner jet supplies 4 L/s and outer jet 8L/s.*

a)

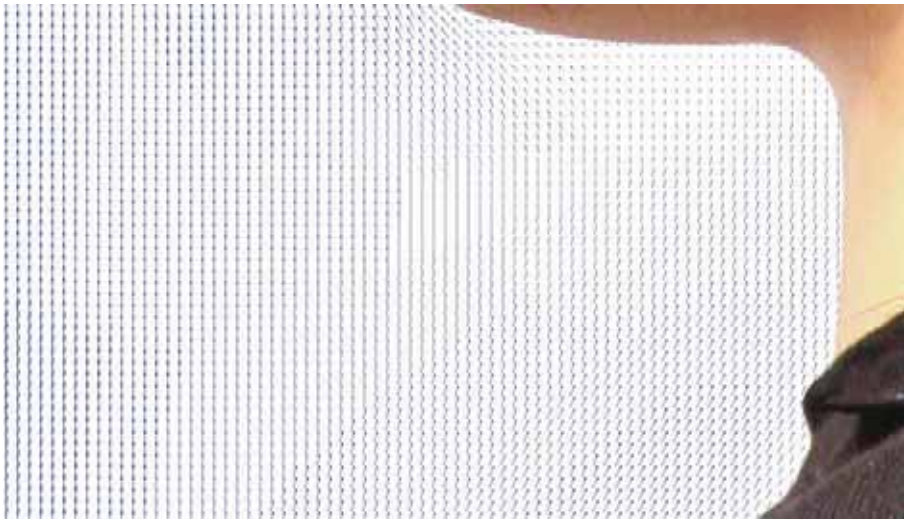

b)

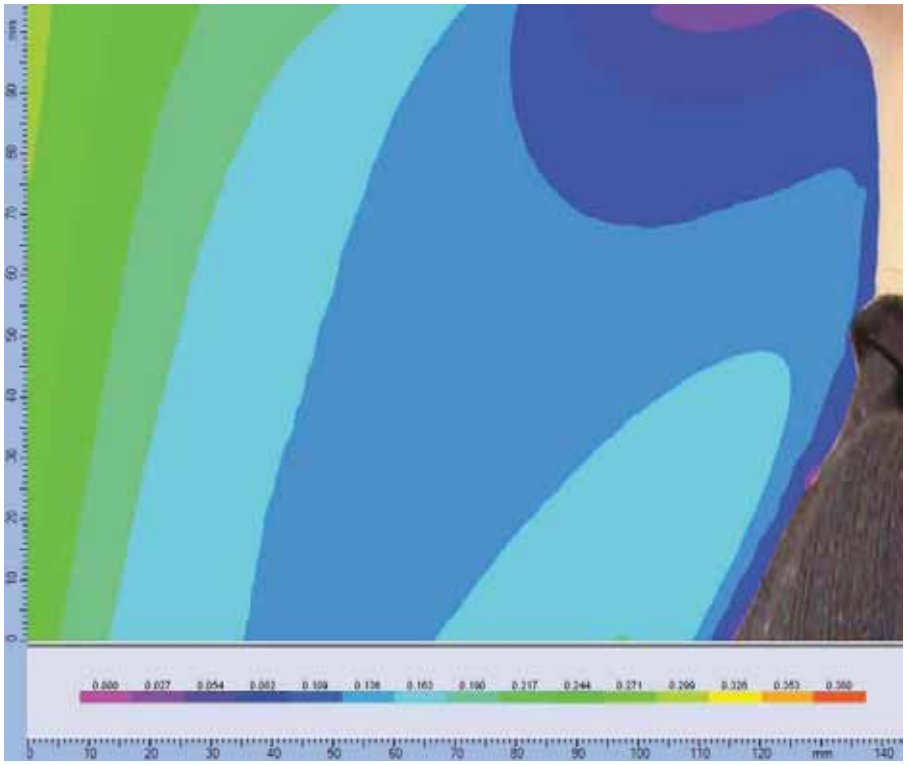

Figure 48 *a) Velocity vector diagram showing air direction and b) Contour velocity plot diagram close to the heated manikin (neck) and box with integrated confluent jets when inner jet supplies 4 L/s and outer jet 8L/s.*

a)

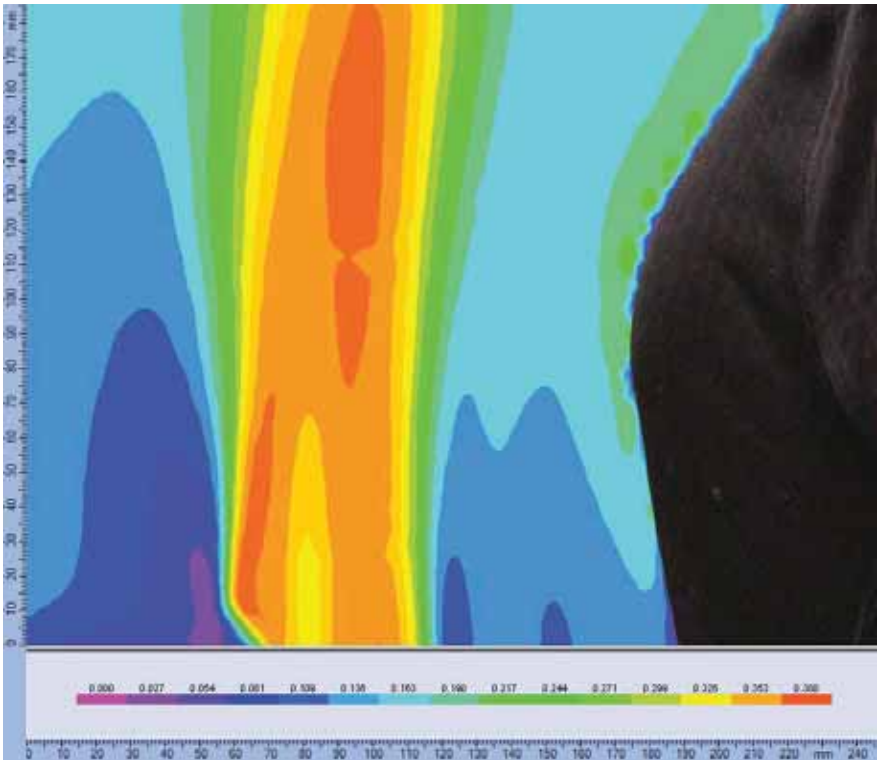

b)

Figure 49 *a) Velocity vector diagram showing air direction and b) Contour velocity plot diagram close to the heated manikin (chest) and box with integrated confluent jets when inner jet supplies 4 L/s and outer jet 8L/s.*

a)

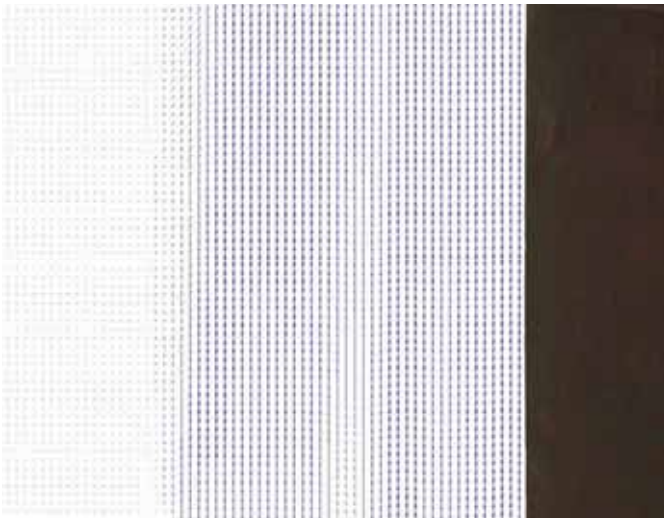

b)

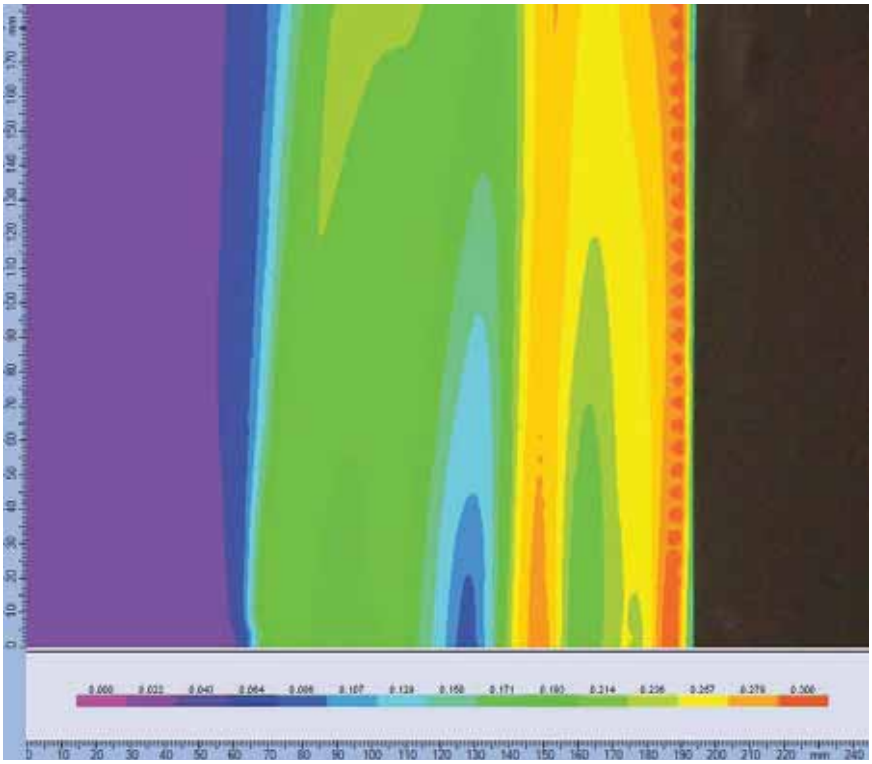

Figure 50 *a) Velocity vector diagram showing air direction and b) Contour velocity plot diagram close to the heated radiator surface and box with integrated confluent jets when inner jet supplies 8 L/s and outer jet 4L/s.*

a)

b)

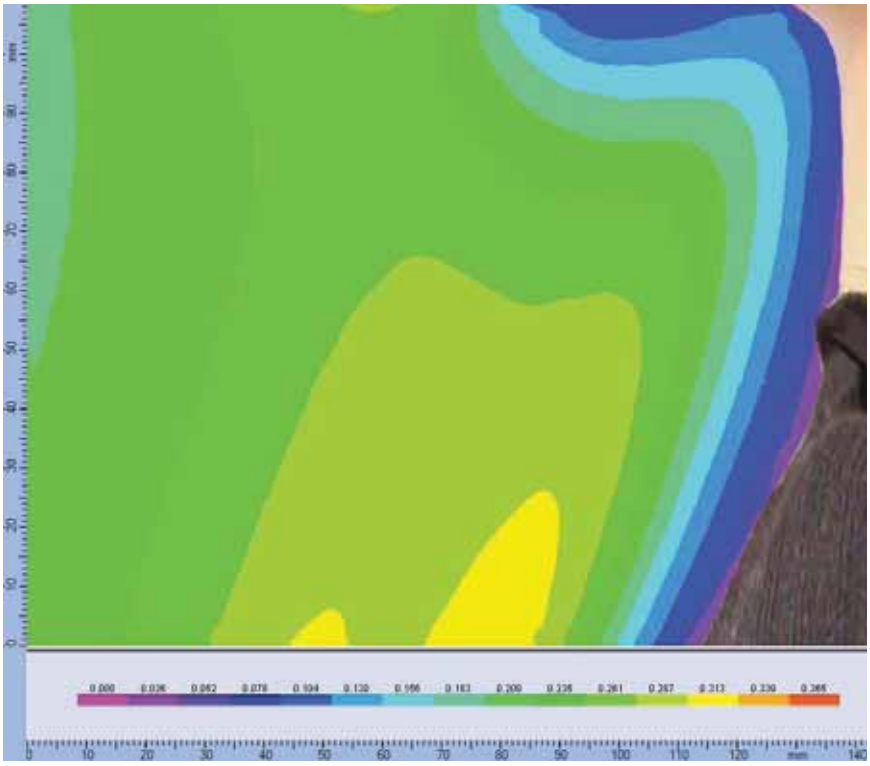

Figure 51 *a) Velocity vector diagram showing air direction and b) Contour velocity plot diagram close to the heated manikin (neck) and box with integrated confluent jets when inner jet supplies 8 L/s and outer jet 4L/s.*

a)

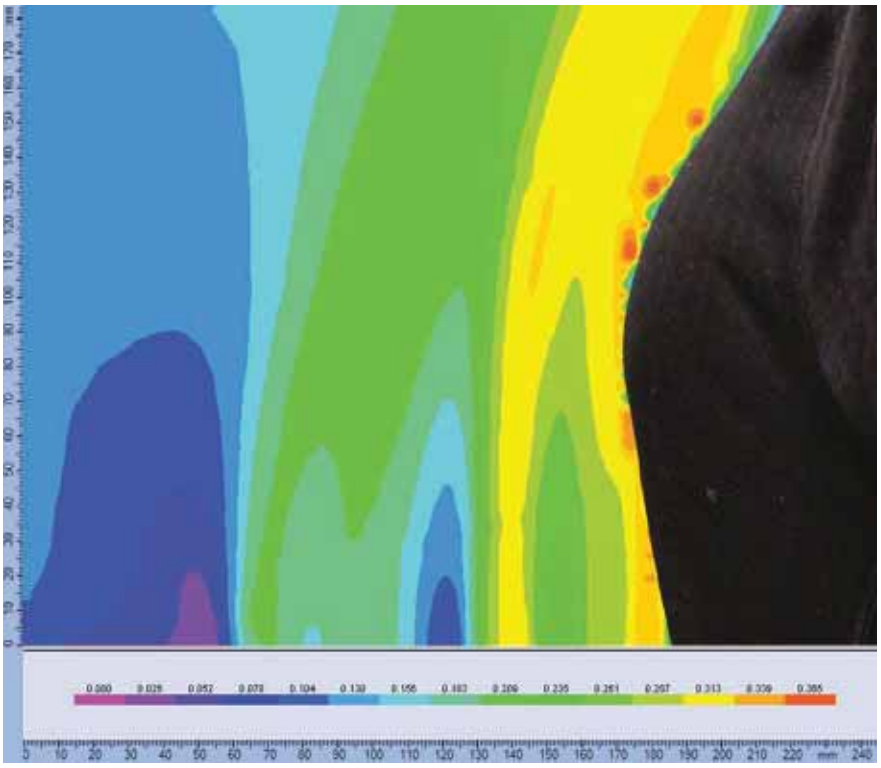

b)

Figure 52 *a) Velocity vector diagram showing air direction and b) Contour velocity plot diagram close to the heated manikin (chest) and box with integrated confluent jets when inner jet supplies 8 L/s and outer jet 4L/s.*

Advanced methods for distribution of clean ventilation air in office and hospital environment are studied. Effective strategies for enhancement the performance of the methods by control of the airflow interaction at the vicinity of human body are developed. The ability of the novel air distribution methods in providing increased amounts of clean air to each occupant and in reducing the risk of airborne cross-infection compared to the used at present total volume ventilation is documented.

Method and device for advanced ventilation in hospitals at the location of patients' bed is subject to a DTU patent (EP 09165736.1and US 61/226,542).

DTU Civil Engineering
Department of Civil Engineering
Technical University of Denmark

Brovej, Building 118
2800 Kgs. Lyngby
Telephone 45 25 17 00

www.byg.dtu.dk

ISBN: 9788778773180
ISSN: 1601-2917